DOE/ORP-2000-24
Rev. 0

Hanford Immobilized Low-Activity Waste Performance Assessment: 2001 Version

F.M. Mann, R.J. Puigh II,
S.H. Finfrock, E.J. Freeman, Jr., R. Khaleel,
D.H. Bacon, M.P. Bergeron, B.P. McGrail, and S.K. Wurstner

Ken Burgard, CHG Project Manager (2000, 2001)
W.R. Root, CHG Project Manager (1998, 1999, 2000)
P.E. LaMont, DOE Project Manager

August 2001

DOE/ORP-2000-24
Rev. 0

F.M. Mann
CH2M Hill Hanford Group, Inc. (CHG)

R.J. Puigh II
Fluor Federal Services

S.H. Finfrock
Fluor Federal Services

E.J. Freeman, Jr.
Pacific Northwest National Laboratory

R. Khaleel
Fluor Federal Services

D.H. Bacon
Pacific Northwest National Laboratory

M.P. Bergeron
Pacific Northwest National Laboratory

B.P. McGrail
Pacific Northwest National Laboratory

S.K. Wurstner
Pacific Northwest National Laboratory

C.T. Kincaid, peer reviewer
Pacific Northwest National Laboratory

M.I. Wood, peer reviewer
Fluor Hanford, Inc.

Ken Burgard
CHG Project Manager

G.L. Parsons
CHG Manager, Immobilized Waste

C.A. Babel
DOE/OPR PA Project Manager

P.E. LaMont
DOE/ORP Project Manager

EXECUTIVE SUMMARY

The *Hanford Immobilized Low-Activity Waste Performance Assessment* examines the long-term environmental and human health effects associated with the planned disposal of the vitrified low-activity fraction of waste presently contained in Hanford Site tanks. The tank waste is the byproduct of separating special nuclear materials from irradiated nuclear fuels over the past 50 years. This waste is stored in underground single- and double-shell tanks. The tank waste is to be retrieved, separated into low-activity and high-level fractions, and then immobilized by vitrification. The U.S. Department of Energy (DOE) plans to dispose of the low-activity fraction in the Hanford Site 200 East Area. The high-level fraction will be stored at the Hanford Site until a national repository is approved.

This report provides the site-specific long-term environmental information needed by the DOE to modify the current Disposal Authorization Statement for the Hanford Site[1] that would allow the following:

- Construction of disposal trenches
- Filling of these trenches with ILAW containers and filler material with the intent to dispose of the containers.

The original Disposition Authorization Statement was based on the 1998 version[2] of this performance assessment, which was conditionally accepted by DOE.[3] There were two conditions for DAS approval. The first condition required the submittal of results of glass testing that occurred after the submittal of the performance assessment and the second condition was addressing of minor concerns in the next (i.e., this) performance assessment. A report on glass testing has been submitted[4] to DOE; and this document (the 2001 ILAW PA) addresses the concerns raised in the second condition.

---

[1] "Disposal Authorization Statement for the Hanford Site Low-Level Waste Disposal Facilities," Memorandum from J.J. Fiore, DOE/HQ and M.W. Frei, DOE/HQ, to R.T. French, DOE/ORP, and K.A. Kline, DOE/RL, Washington, D.C., October 25, 1999.

[2] F. M. Mann, R. J. Puigh II, P. D. Rittmann, N. W. Kline, J. A. Voogd, Y. Chen, C. R. Eiholzer, C. T. Kincaid, B. P. McGrail, A. H. Lu, G. F. Williamson, N. R. Brown, and P. E. LaMont, *Hanford Immobilized Low-Activity Tank Waste Performance Assessment*, DOE/RL-97-69, Rev. 0, U.S. Department of Energy, Richland, Washington, March 1998.

[3] Conditional Acceptance of the Immobilized Low-Activity Tank Waste Disposal Facility Performance Assessment and the Hanford Site 200 Plateau Composite Analysis, Memorandum from James J. Fiore and Mark W. Frei to Richard French and Keith A. Klein, U.S. Department of Energy, Washington, D.C., October 20, 1999.

[4] "Initial Data Package from the Tank Focus Area on 55 Test Glasses for Hanford Immobilized Low-Activity Waste (ILAW) Studies," memorandum to Mark W. Frei, 00-DPD-018, Office of River Protection, U.S. Department of Energy, Richland, Washington, March 10, 2000.

Four major changes have occurred since the issuance of the 1998 performance assessment: the design of the disposal facility has been changed from underground concrete vaults to trenches, all of the low-level fraction will be disposed in a new facility rather than just 90 percent, a class of glasses (termed low-temperature glasses) has been chosen (although a final composition is still not available), and site-specific and waste-form-specific data have been collected. This performance assessment addresses each of these changes individually.

This report also analyzes the long-term performance of the planned disposal system as a basis to perform the following:

- Set requirements for the waste form and the facility design that will protect the long-term public health and safety and protect the environment

- Demonstrate that the requirements can be met.

The calculations in this performance assessment show that a "reasonable expectation" exists that the disposal of the immobilized low-level fraction of tank waste from the Hanford Site can meet environmental and health performance objectives. As shown by the sensitivity studies, this conclusion remains valid despite the conceptual designs of the disposal facility and the ILAW packaging having undergone changes.

The performance assessment activity will continue beyond this assessment. The activity will collect additional data on the geotechnical features of the disposal sites, the disposal facility design and construction, and the long-term performance of the waste form. This activity also will perform analyses to determine the impact of these new data or information collected from other programs. Better estimates of long-term performance will be produced and reviewed regularly. Performance assessments supporting closure of filled facilities will be issued seeking DOE approval of those actions necessary to conclude active disposal facility operations.

ES1 BACKGROUND

DOE and its predecessor agencies have used the Hanford Site in south-central Washington State extensively for producing defense materials. Over the last 50 years, radioactive and mixed waste from materials production and related activities have been stored and disposed on the Hanford Site. The largest fraction (in terms of activity) is stored in underground single- and double-shell tanks in 18 tank farms.

As part of the Hanford Site's environmental restoration and waste management mission, DOE is proceeding with plans to retrieve to the maximum extent possible, the waste from the tanks, some of which have already leaked part of their contents. The mission is to accomplish the following:

- Separate the waste into a small quantity of high-level waste and a much larger quantity of low-activity waste

- Immobilize both waste streams

- Store the immobilized high-level waste until it can be sent to a federal geologic repository

- Dispose of the immobilized low-activity waste on Site in near-surface low-activity waste disposal facilities.

This plan is based on Revision 6 of the *Hanford Federal Facility Agreement and Consent Order* (Tri-Party Agreement)[5] and on the *Record of Decision for the Tank Waste Remediation Systems, Hanford Site, Richland, Washington*[6]. More than 200,000 m^3 (7,000,000 ft^3) of immobilized low-activity waste will be disposed under this plan. This large volume will contain one of the largest inventories of long-lived radionuclides in the DOE complex to be disposed in a near-surface, low-activity waste facility.

By source definition, most of the waste in the Hanford Site tanks is considered high-level radioactive waste. However, the staff of the U.S. Nuclear Regulatory Commission (NRC) has indicated that the low-level fraction would be considered "incidental waste" if DOE follows its program plan for separating and immobilizing the waste to the maximum extent that is technically and economically practical, if the waste meets the Class C standards of Title 10 *Code of Federal Regulations* (CFR) Part 61[7], and if the performance assessments continue to indicate that public health and safety would be protected to standards comparable to those established by the NRC for the disposal of low-level waste.[8] Therefore, disposal of the ILAW as incidental waste does not fall under the licensing authority of the NRC.

The current program plan is to construct new trench facilities for ILAW disposal. An earlier program to dispose of the tank waste built four large concrete subsurface vaults with a total usable volume of about 15,000 m^3. These vaults will be kept in reserve and may be used for storage or disposal of various Hanford Site waste types. ILAW production is scheduled to continue until 2024, with closure of the ILAW disposal facilities later in the decade.

---

[5]Ecology, DOE, and EPA, 1996, *Hanford Facility Agreement and Consent Order*, Sixth Amendment, Washington State Department of Ecology, United States Environmental Protection Agency, United States Department of Energy. The document is available from any of the parties.

[6]62 FR 8693, "Record of Decision for the Tank Waste Remediation System, Hanford Site, Richland Washington," *Federal Register*, Volume 62, page 8693, February 26, 1997.

[7]10 CFR 61, Section 55, "Licensing Requirements for the Land Disposal of Radioactive Waste," *Code of Federal Regulations*, as amended.

[8]C.J. Paperiello, *Classification of Hanford Low-Activity Tank Waste Fraction*, letter to Jackson Kinzer, Assistant Manager, Office of Tank Waste Remediation System, dated June 9, 1997. Director, Office of Nuclear Material Safety and Safeguards, U.S. Nuclear Regulatory Commission, Washington, D.C.

DOE and its contractors are currently obligated to meet the DOE order on radioactive waste management, currently DOE O 435.1.[9] Before a new low-level radioactive waste disposal facility can be constructed or the waste can be disposed, DOE-Headquarters must issue a Disposal Authorization Statement. The issuance of a Disposal Authorization Statement is predicated on many analyses, including the performance assessment, which investigates the disposal system's ability to provide long-term environmental, public health, and safety protection. DOE and its contractors also will meet the requirements of the Washington State regulations for dangerous waste. As noted, DOE has issued a Disposal Authorization Statement to the Hanford Site for the disposal of ILAW packages in underground concrete vaults.

ES2 APPROACH

This performance assessment has been written for a waste form (vitrified low-level fraction) that doesn't exist yet and for a disposal facility that has not been fully designed yet. Therefore, due to the possible variability of waste composition and the likelihood of different disposal facility designs, this performance assessment takes the following three-step approach:

1. Understand the important principles, data, and requirements
2. Set requirements based on long-term environmental and human health impacts
3. Demonstrate that the requirements can be reasonably expected to be met.

The first step is to understand the important principles, data, and requirements of this disposal action that impact the public and the environment. Running a base analysis case and numerous sensitivity cases develops such an understanding on how the system will perform as various conditions or parameters are changed. Based on applicable regulations and earlier performance assessments, performance objectives were established[10] to protect the following:

The general public	The inadvertent intruder
Groundwater resources	Surface water resources
Air resources.	

The quantitative values for the performance objectives are provided later in this executive summary where the results are compared to the performance objectives.

The protection level for Hanford Site workers is assumed to be the same as that for the general public.

---

[9]DOE O 435.1, "Radioactive Waste Management," U.S. Department of Energy, Washington, D.C., July 9, 1999.

[10]F. M. Mann, *Performance Objectives for the Hanford Immobilized Low-Activity Waste (ILAW) Performance Assessment*, HNF-EP-0826, Revision 3, Fluor Daniel Northwest, Inc., Richland, Washington August 1999.

The performance objectives included not only the peak impact that would be acceptable, but also the time period ("time of compliance") over which the impacts would be determined. Following DOE standards, the time of compliance for protecting the general public as well as groundwater, surface water, and air resources is 1,000 years, in contrast with the 10,000 years used in the 1998 analyses. However, this analysis also compares estimated impacts at 10,000 years to the impact limits. Data and models were selected based on earlier Hanford Site studies.

The second step involved using this understanding to set requirements on the disposal facility design and on the ILAW product quality. Finally, to show, with reasonable expectation, that public health and the environment will be protected, this document shows that the requirements are likely to be met.

As more data are collected through performance assessment activity data collection, tank retrieval sampling, ILAW production experience, disposal facility operating history, and other research, this performance assessment will be modified. Because of the requirements of DOE O 435.1 and to follow good business practices, this performance assessment will be revised to reflect our growing knowledge and understanding.

This commitment to iterative analysis is demonstrated by noting that this performance assessment is actually the fourth set of environmental analyses performed for the program. The first set[11] provided the background for disposal facility conceptual design and waste form quality. The second set, the *Hanford Low-Level Tank Waste Interim Performance Assessment*[12], provided a set of analyses based on the previous DOE order on radioactive waste management and showed that the disposal of ILAW would likely meet its performance objectives based on DOE's current plans and on current knowledge. The third set, the 1998 performance assessment, built on the analyses presented in the interim performance assessment. The fourth set is this document report, which relies on much new data and many improved methods developed since the last performance assessment.

The data are summarized and the assumptions are listed in Table ES-1. The data used in this performance assessment are documented in *Data Packages for the Hanford Immobilized Low-Activity Tank Waste Performance Assessment: 2001 Version*.[13] Analyses of likely conditions, along with sensitivity scenarios, provide the range of impacts to be expected.

---

[11]F. M. Mann, C. R. Eiholzer, N. W. Kline, B. P. McGrail, and M. G. Piepho, *Impacts of Disposal System Design Options on Low-Level Glass Waste Disposal System Performance*, WHC-EP-0810, Revision 1, Westinghouse Hanford Company, Richland, Washington, September 1995.

[12]F. M. Mann, C. R. Eiholzer, A. H. Lu, P. D. Rittmann, N. W. Kline, Y. Chen, B. P. McGrail, G. F. Williamson, J. A. Voogd, N. R. Brown, and P. E. LaMont, *Hanford Low-Level Tank Waste Interim Performance Assessment*, HNF-EP-0884, Revision 1, Lockheed Martin Hanford Company, Richland, Washington, September 1997.

[13] F. M. Mann and R. J. Puigh II, *Data Packages for the Hanford Immobilized Low-Activity Tank Waste Performance Assessment: 2001 Version*, HNF-5636, Revision 0A, Fluor Federal Services, Richland, Washington, February 2001.

Disposal will occur in the southern part of the 200 East Area of the Hanford Site in a previously unused area. This disposal facility is expected to consist of a series of large trenches based on similar trenches presently being used by the Hanford Site Waste Management Project. Current planning for the disposal facilities includes installing a RCRA-compliant surface cover to minimize the flow of water or other potential intrusions into the facility and a sand-gravel capillary barrier to divert water around the waste form.[14]

Table ES-1. Major Sources of Information for the Base Analysis Case

Data Type	Major Source	Reference
Location	The new facilities are just southwest of the PUREX Facility (in the 200 East Area).	[15]
Waste form	Waste package design based on early BNFL, Inc. documentation and River Protection Project planning.	[16], also App. I of [13]
Inventory	Based on Best Basis Inventory estimates (calculated from modeling Hanford Site production reactors corrected for off-site transfers, and discharges to the ground and biased to tank measurements). **ASSUMED** separations into high- and low-activity fractions, and off-gas generation.	[17], also App. H of [13]
Long-term waste form performance	Based on data collected on relevant glass formulations.	[18], also App. K of [13]

[14] *Preliminary Closure Plan for the Immobilized Low Activity Waste Disposal Facility*, RPP-6911, Revision 0, CH2M Hill Hanford Group, Inc., Richland, Washington, August 2000. This plan was approved by the DOE/ORP Field Manager in memorandum to Carolyn L. Huntoon (Assistant Secretary), "U.S. Department of Energy (DOE), Office of River Protection (ORP) Approval of the Hanford Site Transmittal of the Immobilized Low-Activity Waste (ILAW) Disposal Facility Preliminary Closure Plan," 00-PRD-63, Office of River Protection, U.S. Department of Energy, Richland, Washington, September 22, 2000.

[15] W.A. Rutherford (Director, Site Infrastructure Division), letter 97-SID-285 to H.J. Hatch (President of Fluor Daniel Hanford, Inc.), "Contract DE-AC06-96RL113200 - Approval of Tank Waste Remediation System Complex Site Evaluation Report," dated July 10, 1997, U.S. Department of Energy, Richland, Washington.

[16] R. J. Puigh II, *Disposal Facility Data for the Hanford Immobilized Low-Activity Tank Waste*, HNF-4950, Rev. 1, Fluor Federal Services, Richland, Washington, December 1999.

[17] D. W. Wootan, *Immobilized Low Activity Tank Waste Inventory Data Package*, HNF-4921, Revision 0, Fluor Daniel Northwest, Inc., September 1999.

[18] B. P. McGrail, J. P. Icenhower, W. L. Ebert, P. F. Martin, H. T. Schaef, M. J. O'Hara, J. L. Steele, and E. A. Rodriguez, *Waste Form Release Data Package for the 2001 Immobilized Low-Activity Waste Performance Assessment*, PNNL-13043, Revision 2, Pacific Northwest National Laboratory, Richland, Washington, January 2001.

Table ES-1. Major Sources of Information for the Base Analysis Case

Data Type	Major Source	Reference
Disposal facility design	**ASSUMED** from preconceptual ideas for the remote-handled trench and preliminary design for the concrete vault.	[14], also App. I of [13]
Recharge	Estimates were derived from lysimeter and tracer measurements collected by the ILAW PA activity and by other projects combined with a modeling analysis.	[19], also App. J of [13]
Geotechnical	Taken from geotechnical measurements studies of ILAW site borehole and other locations in the Hanford Site 200 East Area.	[20], [21], and [22]; also App. L, M, and N of [13]
Exposure	Taken from past Hanford Site documents and experience and DOE O 435.1 direction.	[23], also App. O of [13]

DOE = U.S. Department of Energy
ILAW = immobilized low-activity waste
PA = performance assessment
PUREX = Plutonium-Uranium Extraction (Facility)

Site-specific geologic, hydraulic, geochemical, and water infiltration data were obtained for this analysis.[18, 19, 20, 21] Additional disposal site-specific data are being collected and through integration with other projects like the Hanford Groundwater/Vadose Zone Integration Project additional related geotechnical data are being collected. The inventory[16] of contaminants in the waste form is based on estimates for the tank waste inventory and uses a conservative estimate to project the low-level fraction of radionuclides immobilized in the waste form after the separation

---

[19] M. J. Fayer, *Recharge Data Package for the Immobilized Low-Activity Waste 2001 Performance Assessment*, PNNL-13033, Pacific Northwest National Laboratory, Richland, Washington, December 1999.

[20] R. Khaleel, *Far-Field Hydrology Data Package For The Immobilized Low-Activity Waste Performance Assessment*, HNF-4769, Revision 2, Fluor Federal Services, Richland, Washington, December 1999.

[21] P. D. Meyer and R. J. Serne, *Near Field Hydrology Data Package for the Immobilized Low-Activity Waste 2001 Performance Assessment*, PNNL-13035, Revision 1, Pacific Northwest National Laboratory, Richland, Washington, December 1999.

[22] D. L. Kaplan And R. J. Serne, *Geochemical Data Package For The Immobilized Low-Activity Waste Performance Assessment*, PNNL - 13037, Pacific Northwest National Laboratory, Richland, Washington, December 1999.

[23] P. D. Rittmann, *Exposure Scenarios And Unit Dose Factors For The Hanford Immobilized Low-Activity Tank Waste Performance Assessment*, HNF-SD-WM-TI-707, Revision 1, Fluor Federal Services, Richland, Washington, December 1999.

and immobilization processes. The tank waste inventory estimate is based on a synthesis of actual tank waste measurements and of computer simulations of the production reactor history and the known reprocessing histories. It is estimated that a wide range of tank waste compositions are presently contained within the Hanford site underground storage tanks.

The release rates of contaminants from the waste form are based on simulations. The low-activity glass LAWABP1 is used because it has an extensive experimental database and is in the expected composition envelope. The base case analysis assumed the dimensions as of early 2000. A sensitivity study shows that that the use of the current planning basis[24] for the dimensions and packing of the ILAW packages do not change the conclusions of the analyses.

A sand-gravel capillary barrier is included in the best-estimate case. However, because of the uncertainty of the final design parameters for a barrier, the more conservative case of not including a barrier was chosen for the base case. A wide variety of sensitivity cases (using different inventories, glass compositions, models, and parameter values) also were studied.

ES3 RESULTS OF COMPUTER SIMULATIONS

ES3.1 Introduction

A large number of simulations were run in this analysis. Details are provided in the following documents:

Waste Form Release Calculations for the 2001 Immobilized Low-Activity Waste Performance Assessment[25]

Near Field, Far –Field, and Estimated Impact Calculations for the Hanford Immobilized Low-Activity Tank Waste Performance Assessment: 2001 Version[26]

Groundwater Transport Calculations Supporting the Immobilized Low-Activity Waste Disposal Facility Performance Assessment[27]

---

[24] D. A. Burbank, R. K. Biyani, and L. F. Janin, *Preliminary Closure Plan for the Immobilized Low Activity Waste Disposal Facility*, RPP-6911, Revision 0, CH2M Hill Hanford Group, Inc., Richland, Washington, August 2000.

[25] D. H. Bacon and B. P. McGrail, *Waste Form Release Calculations for the 2001 Immobilized Low-Activity Waste Performance Assessment*, PNNL-13369, Pacific Northwest National Laboratory, Richland, Washington, February 2001.

[26] S. H. Finfrock, E. J. Freeman, R. Khaleel, and R. J. Puigh, *Near Field, Far Field, and Estimated Impact Calculations for the Hanford Immobilized Low-Activity Tank Waste Performance Assessment: 2001 Version*, RPP-7463, Fluor Federal Services, Richland, Washington, December 2000.

[27] M. P. Bergeron and S. K. Wurstner, *Groundwater Transport Calculations Supporting the Immobilized Low-Activity Disposal Facility Performance Assessment*, PNNL-13400, Pacific Northwest National Laboratory, Richland, Washington, December 2000.

These reports are combined in *Simulations for the Hanford Immobilized Low-Activity Waste Performance Assessment: 2001 Version.*[28]

Because of the potential for variable recharge rates at the top of the disposal site, two-dimensional simulations of the moisture flow into the disposal facility were made. Using this moisture flow, one-dimensional simulations were run of the glass corrosion, contaminant release, and resulting contaminant transport in the disposal facility. Two-dimensional simulations then were made of the subsequent vadose zone moisture flow and contaminant transport, using the output of the preceding models. The Hanford Site groundwater model and a site-specific submodel derived from it were used to calculate groundwater flow and transport. The results from the codes were combined with inventory and dosimetry data to provide radionuclide concentrations in groundwater and dose rates.

Explicit calculations were conducted to 100,000 years after disposal. For inadvertent intruder analyses, a spreadsheet was used with calculations extending from 100 to 1,000 years.

Because of the very slow predicted release of contaminants from the waste form (hundreds of thousands of years), the estimated concentration of radionuclides in the groundwater shows a broad plateau rather than a peak (for an example, see the beta/photon drinking water dose rate shown in Figure ES-1). This result contrasts with most other environmental assessments, where the contaminant release time is short compared to the contaminant travel time, resulting in a peaked response.

Figure ES-1. Beta/photon drinking water dose rates for the base analysis case at a well 100 meters downgradient from the disposal facility.

The performance objective is less than 4.0 mrem in a year for the first 1,000 years.

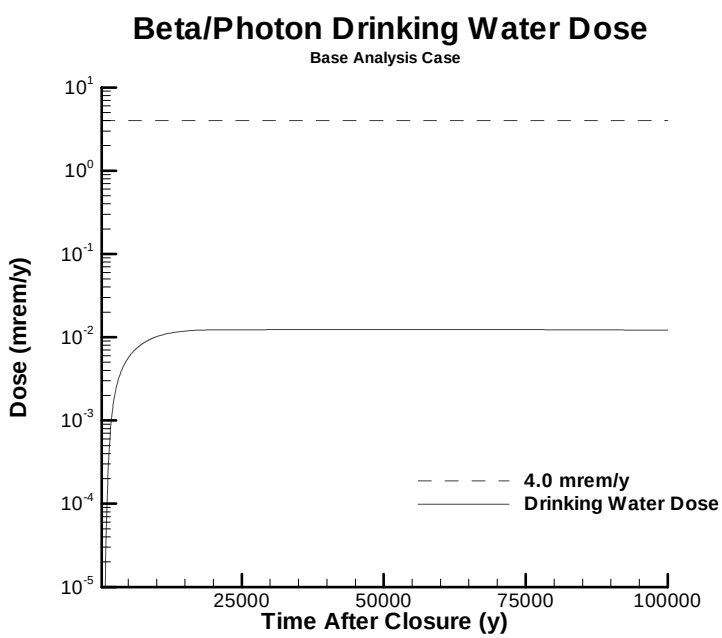

[28] R. J. Puigh and F. M. Mann, *Simulations for the Hanford Immobilized Low-Activity Tank Waste Performance Assessment: 2001 Version,* RPP-7464, Fluor Federal Services, Richland, Washington, February 2001.

The base analysis case assumes a natural recharge rate. This case allows simpler, more flexible cases to be run while providing results very similar to, but slightly higher than, the case that explicitly considers the effect of a surface barrier whose properties change over time. A best estimate case, which includes the effect of a subsurface, sand–gravel capillary barrier, also was run.

ES3.2 Protection of the General Public

Table ES-2 compares the performance objectives for protecting the general public with the results from both the base analysis case and the best estimate case calculations. The estimated all-pathways doses are significantly lower than the performance objectives. The sensitivity cases show that these results are very robust. To invalidate the results, the inventory of key contaminants (^{99}Tc, ^{129}I, uranium isotopes, and ^{237}Np) would have to be orders of magnitude higher and/or the waste release must increase by a large amount.

During the first 1,000 years (the period of compliance), the estimated doses are insignificant. Even for a period of 10,000 years, the estimated all-pathways dose for the base analysis case is over 300 times smaller than the 25 mrem/year goal. The best estimate case is smaller still. The results for this analysis are significantly below that of the 1998 analysis because of newer data (better knowledge of waste form release, groundwater flow, inventory) and methods (explicit calculation of waste form release), as will be discussed in Section ES6. Technetium-99 is estimated to contribute 71 percent of this dose at 1,000 years, declining to 38 percent at 10,000 years as the uranium and neptunium isotopes become more important. The all-pathways dose is estimated to increase during the 100,000 years explicitly calculated, reaching 0.59 mrem in a year at 100,000 years. For these long times, ^{237}Np and uranium and its daughters are the main contributors.

The other two performance measures (all-pathways including other actions at the Hanford Site and a design that produces doses as low as reasonably achievable [ALARA]) are not expected to exceed the performance objectives of 100 mrem in a year or 500 person-rem per year at any time.

Impacts from chemicals also were investigated. The chemicals investigated were based on a data quality objectives process.[29] The impacts from these chemicals were found to be very small (see section 4.3.6). Using nominal estimates for the hazardous chemicals that may be in the waste form, the estimated impacts at 1,000 years were more than a factor of 100,000 less than the performance goals for groundwater concentrations at a well 100 meters downgradient from the disposal facility.

---

[29] K. D. Wiemers, M. E. Lerchen, M. Miller, K. Meier, *Regulatory Data Quality Objectives Supporting Tank Waste Remediation System Privatization Project*, PNNL-12040, Rev. 0., Pacific Northwest National Laboratory, Richland, Washington, 1998.

Table ES-2. Comparison of Estimated Impacts with Performance Objectives for Protecting the Public.
The DOE time of compliance is 1,000 years. The point of compliance is a well 100 meters downgradient of the facility.

Performance Measure	Performance Objective[10]	Estimated Impact at 1,000 y	Estimated Impact at 10,000 y	
			1998 ILAW PA	Present Results
All-pathways [mrem in a y]	25.0			
Base Analysis Case		0.000078	6.4	0.070
Best Estimate Case		1.7×10^{-10}	nc*	1.3×10^{-6}

* nc = "not calculated" in the 1998 ILAW PA

ES3.3 Protection of Inadvertent Intruders

Table ES-3 compares the estimated impacts to the performance objectives for protecting the inadvertent intruder. A one-time dose (an acute exposure) scenario and a continuous exposure scenario (a chronic exposure) are defined. Both performance objectives are met.

The acute dose, estimated by assuming that a person drills a well through the disposal facility, is much less than the performance objective. The continuous dose, which includes the ingestion of contaminated food and water, the inhalation of air, and direct radiation exposure, is over a factor of 3 lower than the performance objective. At the time of compliance, 500 years, ^{126}Sn contributes more than 82 percent of the dose. Doses for later times to 1,000 years are smaller.

Table ES-3. Comparison of Estimated Impacts with Performance Objectives for Protecting the Inadvertent Intruder.
The time of compliance is 500 years.

Performance Measure	Performance Objective[10]	Estimated Impact at 500 y	
		1998 ILAW PA	Present Results
Acute exposure [mrem]	500.0	5.5	0.76
Continuous exposure [mrem in a year]	100.0	27.5	10.2

ES3.4 Protection of Groundwater Resources

Table ES-4 compares the estimated impacts to the performance objectives for protecting the groundwater resources. These performance objectives are based on the federal drinking water standards. The time of compliance is 1,000 years and the point of compliance is at a well 100 meters downgradient of the disposal facility. The estimated impact from beta emitters for the base analysis case at 1,000 years is a factor of over four orders of magnitude less than the performance objective and the estimated impact from alpha emitters (including radium) is insignificant. At 10,000 years, the estimated impact for the base analysis case from beta emitters remains small (still a factor of almost 400 below the 4 mrem in a year goal). The estimated impact from alpha emitters at 10,000 years is significantly larger than at 1,000 years, but still is a factor of over 400 below the goal of 15 pCi/L. The maximum impact is seen around 76,500 years, reaching a peak of 0.13 mrem in a year. Values for the best estimate case are many of orders of magnitude smaller in each case.

Impacts from chemicals also were investigated and again were found to be very small. The margins found for the protection of groundwater are similar to those found for protection of the general public. The most important drivers for determining peak groundwater concentrations are the inventory of technetium-99 for beta/photon emitters and neptunium for alpha emitters, the release rate from the waste form, and the amount of mixing in the aquifer.

For the most part, other geotechnical data (water infiltration rate, hydraulic parameters, and geochemical factors) are less important because they mainly affect the time at which the plateau is reached. The two exceptions are as follows.

For the base analysis case, the beta/gamma drinking water dose rate reaches a plateau of about 0.012 mrem in a year at about 15,000 years, which extends to the end of the explicit calculation at 100,000 years.

The concentration of alpha emitters slowly increases during the 100,000 years explicitly calculated, reaching a maximum of 0.54 pCi/L at 100,000 years.

Table ES-4. Comparison of Estimated Impacts with Performance Objectives for Protecting Groundwater Resources.

The DOE time of compliance is 1,000 years. The point of compliance is a well 100 m downgradient of the facility.

Performance Measure	Performance Objective[10]	Estimated Impact at 1,000 years	Estimated Impact at 10,000 years	
			1998 ILAW PA	Present Results
Beta/photon emitters [mrem in a y]	4.0	0.000021	2.0	0.0102
Alpha emitters [pCi/L]	15.0	1.0×10^{-16}	1.7	0.034
Radium [pCi/L]	5.0	0.0	<0.001	<0.001

ES3.5 Protection of Surface Water Resources

Table ES-5 compares the estimated impacts to the performance objectives for protecting the surface water resources. The time of compliance is 1,000 years and the point of compliance is at a well intersecting the groundwater just before the groundwater mixes with the Columbia River. The estimated impacts for the base analysis case are many orders of magnitudes lower than the performance objectives. The results for the best estimate case are far lower yet. The calculations indicate that the impacts never reach the values given as performance objectives. Because of the large flow of the Columbia River, mixing occurs in the river and the predicted impacts actually would be far lower than the performance objectives.

Table ES-5. Comparison of Estimated Impacts with Performance Objectives for Protecting Surface Water Resources.

The DOE time of compliance is 1,000 years. The point of compliance is a well located just before the groundwater mixes with the Columbia River.

Performance Measure	Performance Objective[10]	Estimated Impact at 1,000 y	Estimated Impact at 10,000 y	
			1998 ILAW PA	Present Results
Beta/photon emitters [mrem in a y]	1.0	2.0×10^{-6}	0.07	0.00095
Alpha emitters [pCi/L]	15.0	1.0×10^{-17}	0.058	0.0032
Radium [pCi/L]	0.3	0.0	<0.001	<0.001

ES3.6 Protection of Air Resources

Table ES-6 compares the estimated impacts to the performance objectives for protecting air resources. (The values of these performance objectives are given in federal clean air regulations.) The time of compliance is 1,000 years and the point of compliance is just above the disposal facility. The estimated impacts are significantly lower than the values prescribed in the performance objectives.

Table ES-6. Comparison of Estimated Impacts with Performance Objectives for Protecting Air Resources.

The DOE time of compliance is 1,000 years. The point of compliance is just above the disposal facility.

Performance Measure	Performance Objective[10]	Estimated Impact	
		1998 ILAW PA	Present Results
Radon [pCi m^{-2} s^{-1}]	20.0	<0.001	<0.96
Other radionuclides [mrem in a year]	10.0	$<10^{-8}$	$<6 \times 10^{-3}$

ES4 SETTING REQUIREMENTS

A major purpose of a performance assessment in the DOE system is a source of technical information for the setting of requirements on design, construction, and operation of the disposal facility. In past DOE PAs, the major requirements have been restrictions on the total amount of each significant radionuclide that could be disposed in the facility. Because this performance assessment deals with one type of waste, because the release rate from that waste form also drives the calculated impacts, and because the analyses are being done so early in the design cycle, this analysis can affect more functions and be more useful than previous PAs.

Based on the computer simulations, relatively simple requirements on disposal facility design and operation and on waste form characteristics can be set. The requirements are more complex than those normally set, but they are similar. To achieve more assurance during the design process that the final objectives will be met, the performance objectives used in the performance assessment were replaced with the more conservative values displayed in Table ES - 7. Because the impacts are increasing quickly at 1,000 years, the time of applicability was increased to 10,000 years for the all-pathways and drinking water doses. Protection of air and surface water are not considered because the estimated results from the base analysis case were shown to be so small.

Protection of the homesteader translates into limiting the contaminant inventory in the ILAW package multiplied by the stack height in the disposal facility. Besides these restrictions, the RPP Immobilized Waste Program also has decided to place additional restrictions on waste concentrations. To satisfy the NRC[7] in their determination that the immobilized low-activity waste is not high-level waste, the concentration of all radionuclides will be below the Class C limits set in 10 CFR 61.[7]

Table ES-7. Performance Goals for Requirement Cases.

Performance Measure	Requirement Point	Performance Objective	Performance Goal
Continuous inadvertent intruder dose	Disposal facility	100 mrem/year @ 500 years	100 mrem/year @ 500 years
All-pathways dose	Well 100 m downgradient	25 mrem/year @ 1,000 years	5 mrem/year @ 10,000 years
Beta/gamma drinking water dose	Well 100 m downgradient	4 mrem/year @ 1,000 years	1 mrem/year @10,000 years
Alpha emitter concentration	Well 100 m downgradient	15 pCi/L @ 1,000 years	5 pCi/L @ 10,000 years

The DOE also has mandated[30] concentration limits for strontium-90, technetium-99, and cesium-137 for the first phase of waste form production. To provide maximum flexibility in future decisions, these contract limitations are not placed on this analysis of waste disposed in the new disposal facilities.

The waste to be disposed must meet both the NRC Class C limits and the requirements set by this analysis. A few isotopes (mainly actinides) may be more restricted by this analysis than by the NRC restriction. Note that the radioisotope of greatest concern for intruder protection (^{126}Sn) is not addressed by the NRC regulation.

Protection of groundwater translates into limits on the release rate from all of the ILAW packages and on the amount of smearable contamination on the ILAW package surfaces. As expected from the results used in the comparison to performance objectives, the restrictions placed on inventory (I) and waste form release rate (R) are not great. Although it is the product (IR) that is important, using the current inventory, the contaminant release rate from the waste form less than should be less than 137 ppm/year. The present analysis estimates that the release rate will be less than 0.7 ppm/year for the base analysis case and 0.0003 ppm/year for the best estimate case at 10,000 years after facility closure.

The isotopes facing the greatest restrictions relative to the expected performance are technetium-99, iodine-129, and neptunium-237. This is not surprising because these are the most mobile, because most of the uranium and transuranic elements have been separated from the low-activity waste form, and because other fission products (e.g., carbon-14 and tritium) found to be important in other waste forms are volatile and are not captured in this waste form.

The limits for smearable contamination found from this analysis are quite high and are orders of magnitude less restrictive than those in the contract with the treatment vendor.[30]

Most of the requirements imposed by the performance assessment analysis are on the waste form. However, a few are imposed on the disposal facility. The major facility requirements deal with subsidence, recharge rate, layout, interactions with the waste form, and intruder protection.

The performance assessment assumes that subsidence is small based on the slow degradation of the waste form and the use of filler materials to minimize voids in the disposal facility. This means that the facility must be constructed without significant void space (i.e., empty space between packages). Similarly, the ILAW packages must have a minimum of empty space inside them to minimize subsidence. At present, such a requirement on the ILAW packages is part of the waste treatment plant contract.[30] In addition, after waste is placed inside the facility, the spaces between the waste containers must be filled with a dry material. The estimated impacts from a 1 m subsidence in the remote-handled trench facility located 10 m from

---

[30] Contract with Bechtel, National, Inc., *Design, Construction, and Commissioning of the Hanford Tank Waste Treatment and Immobilization Plant*, Contract number DE-AC27-01RV141376, U.S. Department of Energy, Office of River Protection, Richland, Washington, December 2000. Web reference: http://www.hanford.gov/orp/contracts/de-ac27-01rv14136/index.html.

the RCRA cap apex are factors of 500 and 1,000 times larger for the alpha concentration and beta/photon drinking water dose, respectively, than the estimated impacts for the best estimate case at 10,000 years after facility closure. Facility performance enhancements associated with the RCRA cap and the capillary break are effectively lost locally if subsidence occurs. For the subsidence case analyzed, the estimated impacts still are less than the estimated impacts for the base analysis case.

Because the waste form releases contaminants so slowly, the time-dependence curve for exposure shows more of a plateau structure than a peaked shaped. The major effects of the recharge rate are to slow the waste form release rate and delay the arrival of contaminants to the groundwater. If the recharge rate is large and the second group of contaminants (i.e., those having K_d = 0.6 mg/L, such as uranium) arrive before 10,000 years, the all-pathways dose performance objective could be violated and restrictions would have to be placed on the recharge rate. The base analysis case shows that achieving a moisture infiltration rate into the disposal facility equal to or less than the natural recharge rate (4.2 mm/year) is sufficient to meet the performance objectives. If a subsurface sand-gravel capillary barrier is used, the infiltration rate could be far lower.

The requirement for groundwater protection actually is on the disposal system. The designers of the disposal structures must ensure that materials are not used that would accelerate waste form degradation. Alternatively, the designers can add components (for example, hydraulic diverters, getters) to minimize the requirements on the waste form.

Designers of the engineered system may wish to add components to provide greater defense in depth. The major components would be an improved surface barrier to reduce the recharge rate, a hydraulic barrier to divert moisture from the waste, the addition of concrete material to trap uranium, and other getter materials to trap important radionuclides such as technetium. The recharge rate is the main driving function for the system. Having a surface barrier that could reduce this rate would lengthen the time the contaminants take to reach the groundwater. Diverting water away from the waste would likely reduce the contaminant release rate from the waste form and also would create a greater moisture shadow under the disposal system that also would delay contaminant travel. Concrete is known to highly retard uranium isotopes, thus reducing their impact during the time of compliance. If an inexpensive getter could be found for technetium, such a material also could have important impacts.

ES5 COMPLIANCE

The cases used to compare estimated performance of the disposal facility with the performance objectives are basically the same as the base analysis or best estimate cases. The major difference is that the dimensions of the ILAW package and the number of such packages would change. However, because of the large margin, such a change is not significant for the protection of the public, groundwater resources, and surface water resources. The consequence to the inadvertent intruder can be mitigated through operational controls based on projected waste container inventories. The operational controls will be better defined as the project matures.

ES6 SUMMARY OF THE IMPACT OF DIFFERENCES BETWEEN THE 1998 ILAW PA AND THIS DOCUMENT

Of the three types of scenarios (groundwater, air, and inadvertent intruder) studied in the 1998 ILAW PA[2] and in this document, only the results for the groundwater scenario are significantly different. Five major differences occur in inputs between the 1998 ILAW PA and this document that affect the peak values of estimated impacts for scenarios that contaminate groundwater:

Time of compliance

Inventory of mobile constituents

Disposal facility design

Waste form performance

Groundwater dilution.

Other new data (such as recharge rates, geochemistry, and hydrology) affect the time that the peak occurs or the estimated impacts through one of the last four inputs cited above.

The 1998 ILAW PA used 10,000 years as the time of compliance. Because of new DOE guidance, the present time of compliance is 1,000 years. However, because of the slow travel time in the vadose zone, even the mobile constituents do not reach the groundwater in any significant quantity in only 1,000 years.

To make comparisons with the 1998 ILAW PA easier, Table ES-8 summarizes the differences in estimated impacts at 10,000 years for the beta/gamma drinking water dose.

The facility design effect is associated with areal distribution of the waste. For the remote-handled trench disposal concept, the areal footprint for the facility is 124,800 m^2. For the 1998 ILAW PA, the Concept 1 disposal facility had an areal footprint of 51,000 m^2. The larger areal distribution of the waste leads to a dilution factor of 0.41 associated with the contaminant concentration entering the aquifer.

The impact at 10,000 years of changing the inventory of the mobile constituents is a factor of 0.34 (0.26 * 1.32). This results because of two changes, the change in the ^{99}Tc inventory (the most important radionuclide in either analysis) and the change of inventories of other mobile radionuclides. The 1998 ILAW PA assumed that 80 percent of the technetium in the tanks would end up in ILAW, while this document assumes, based on the contract between the treatment vendor and DOE, that only 20 percent of the technetium in tanks will go into ILAW. The remaining slight difference in technetium inventory results from a small change in tank inventory.

Table ES-8. Effect of Updated Model Inputs on the Estimated Beta/Gamma Drinking Water Dose at 10,000 Years.
(1998 ILAW PA estimated this dose as 2.0 mrem/y.)

Updated Model Input	Beta/gamma drinking water dose
	Ratio 2001 ILAW PA to 1998 ILAW PA
Facility design	0.41
Technetium inventory	0.26
Other mobile contaminants (1)	1.32
Technetium dose factor	0.83
Waste form release rate/ vadose zone transport	0.30
Groundwater dilution	0.14
All inputs	0.0049

(1) based on updated K_d values for selenium, iodine, and neptunium.

Based on disposal site-specific geochemical measurements, the determination of which contaminants are mobile has changed somewhat. Technetium-99 still is the most important mobile contaminant. In the 1998 ILAW PA, selenium-79 was assumed to be mobile because no Hanford Site-specific data were available that indicated otherwise. Since then, it has been learned that the half-life of selenium-79 is longer than believed and disposal-site specific information has shown that selenium transport in the vadose zone is chemically retarded. However, iodine and neptunium, which were treated as relatively immobile in the 1998 ILAW PA, are now known through disposal-site specific information to be more mobile. Thus, whereas technetium-99 was 75 percent of the drinking water dose in the 1998 ILAW PA, it is only 50 percent in this document. Therefore, the relative contribution from other mobile contaminants has increased to 1.32 (0.75/0.57). Finally, the new DOE Order 435.1 requires the use of the EPA dose factors; the dose factor for technetium-99 was a factor of 0.83 of the dose factor used in the 1998 ILAW PA. In the 1998 ILAW PA, the release from the vaults was assumed to be that given in the request for proposal for treatment services (4.0×10^{-6}/year).[31] At 10,000 years after facility closure the contaminant flux to the aquifer was 2.0×10^{-6}/year. In this document, the release from the remote-handled trench is calculated by simulating the waste form

[31] *Request for Proposals (RFP) No. DE-RP06-96RL13308*, letter from J.D. Wagoner to Prospective Offerors, Department of Energy, Richland, Washington, February 20, 1996.

release (rate = 0.8 x 10^{-6}/year at 10,000 years after facility closure) from LAWABP1 glass and performing the transport of contaminants through the vadose zone resulting in a contaminant flux of 0.7 x 10^{-6}/year at 10,000 years after facility closure. This results in a 30 percent decrease in the contaminant flux to the aquifer when compared to the 1998 ILAW PA values.

The disposal site is now realized to be over the old channel of the Columbia River. Also, the base analysis case used a recharge rate of 3 mm/year in the 1998 ILAW PA and a rate of 4.2 mm/year in this analysis. The hydraulic conductivity of the unconfined aquifer is higher, resulting in greater dilution, by about a factor of 7.

Combining these factors (inventory of mobile constituents, disposal facility design, waste form performance, and groundwater dilution), the overall effect is a reduction by about a factor of 200 from the 1998 ILAW PA.

ES7 CONCLUSIONS

This performance assessment analyzed the long-term environmental and human health impact of disposing of immobilized low-activity waste from Hanford Site tanks. This analysis confirms the conclusions of the 1998 ILAW PA that an understanding of ILAW contaminant transport exists and that a base case can meet the performance objectives using a trench disposal concept. Based on this expectation, requirements for waste acceptance and disposal facility performance were established. The final analysis of this performance assessment shows a “reasonable expectation” that these requirements will be met.

Contents

Contents i
List of Tables xii
List of Figures xvi
List of Acronyms xx

1.0 INTRODUCTION 1-1
1.1 PURPOSE 1-1
1.2 BACKGROUND 1-2
1.3 GENERAL DESCRIPTION OF THE FACILITY 1-4
1.4 IMMOBILIZED WASTE PROGRAM 1-5
1.5 RELATED DOCUMENTS 1-9
1.5.1 Other Relevant Hanford Site Environmental Assessments 1-9
1.5.1.1 Previous Work Related to the Proposed Disposal Action. 1-9
1.5.1.2 Other Hanford Site Project-Specific Performance Assessments. 1-11
1.5.2 Regulatory Agreements and Documents 1-13
1.5.3 Guidance Documents 1-13
1.6 PERFORMANCE OBJECTIVES 1-14
1.6.1 Summary 1-14
1.6.2 Regulations and Other Performance Assessments 1-18
1.6.2.1 Introduction. 1-18
1.6.2.2 Protection of the General Public. 1-19
1.6.2.3 Protection for Workers. 1-20
1.6.2.4 Protection of the Inadvertent Intruder. 1-20
1.6.2.5 Protection of Groundwater Resources. 1-21
1.6.2.6 Protection of Surface Water Resources. 1-22
1.6.2.7 Protection of Air Resources. 1-22
1.6.2.8 Chemical Objectives. 1-22
1.6.3 Programmatic Requirements 1-23
1.6.4 Public Involvement 1-23
1.7 APPROACH AND MAJOR DATA SOURCES 1-23
1.8 STRUCTURE OF THIS PERFORMANCE ASSESSMENT 1-26

2.0 DISPOSAL FACILITY DESCRIPTION 2-1
2.1 OVERVIEW 2-1
2.2 HANFORD SITE CHARACTERISTICS 2-1
2.2.1 Geography of the Hanford Site 2-1
2.2.2 Location of Disposal Sites 2-4
2.2.3 Demography 2-4
2.2.4 Land and Water Use 2-6
2.2.4.1 Socioeconomics. 2-7
2.2.4.2 Past and Future DOE Activities at the Hanford Site. 2-7
2.2.4.3 Future Hanford Use. 2-8
2.2.5 Climate and Meteorology 2-10
2.2.5.1 Summary. 2-10
2.2.5.2 Current Data. 2-10
2.2.5.3 Historical Data. 2-12
2.2.5.4 Long-Range Forecasts. 2-12
2.2.5.5 Severe Weather. 2-13
2.2.5.6 Climate Summary. 2-13
2.2.6 Ecology and Biotic Conditions 2-13
2.2.7 Regional Geology 2-15
2.2.7.1 Overview. 2-15
2.2.7.2 Topography and Physiography. 2-16
2.2.7.3 Stratigraphy. 2-19
2.2.7.4 Soils. 2-22
2.2.7.5 Earthquakes. 2-23
2.2.7.6 Volcanology. 2-26
2.2.8 Geology of the Proposed Immobilized Low-Activity Tank Waste Disposal Facility Locations 2-26
2.2.8.1 Previous Studies. 2-26
2.2.8.2 Site Stratigraphy. 2-26
2.2.8.3 Columbia River Basalt Group. 2-35
2.2.8.4 Ringold Formation. 2-35
2.2.8.5 Hanford Formation. 2-38
2.2.9 Regional Hydrology 2-41
2.2.9.1 Surface Hydrology. 2-41
2.2.9.2 Flooding. 2-43
2.2.9.3 Groundwater Hydrology. 2-44
2.2.9.4 Natural Recharge Rates. 2-48
2.2.10 Geochemistry 2-49
2.2.11 Natural Resources 2-51

2.2.12 Regional Background Contamination and Hanford Site Monitoring 2-52
2.2.12.1 Soil Background Levels. 2-52
2.2.12.2 Groundwater Background Levels. 2-52
2.2.12.3 Radiation Background Levels. 2-55
2.3 WASTE CHARACTERISTICS 2-56
2.3.1 Overview 2-56
2.3.2 Underground Tank Storage 2-56
2.3.3 Tank Waste Retrieval 2-57
2.3.4 Separations 2-57
2.3.5 Immobilization of the Low-Activity Waste 2-59
2.3.6 Packaging and Certification 2-62
2.3.7 Transportation and Waste Emplacement 2-62
2.4 DISPOSAL TECHNOLOGY 2-63
2.4.1 Current Remote-Handled Trench Planning 2-63
2.4.1.1 Preconceptual Design. 2-63
2.4.1.2 Trench Fill Material. 2-67
2.4.1.3 Disposal Unit Closure. 2-68
2.4.1.4 Disposal Site Closure. 2-68
2.4.2 ILAW Concrete Vault Design—Alternative Concept 2-68
2.4.3 Possible Future Disposal Concepts 2-69

3.0 ANALYSIS OF PERFORMANCE 3-1
3.1 OVERVIEW 3-1
3.2 INVENTORY SOURCE 3-1
3.2.1 Relevant Contaminants of Concern 3-1
3.2.1.1 Radioactive Contaminants. 3-2
3.2.1.2 Chemical Contaminants. 3-3
3.2.2 Decay Data 3-3
3.2.3 Inventory 3-3
3.2.4 Release Rate from Waste Form 3-13
3.3 PATHWAYS AND SCENARIOS 3-14
3.3.1 Selection Criteria 3-14
3.3.2 Pathways 3-14
3.3.2.1 Release Mechanism. 3-14
3.3.2.2 Future Land Use. 3-15
3.3.2.3 Land-Use-Driven Scenarios. 3-16
3.3.2.3.1 Unconfined Aquifer Contamination. 3-16
3.3.2.3.2 Surface Water. 3-18
3.3.2.3.3 Air Resources. 3-18
3.3.2.4 Natural Event Scenarios. 3-18

3.3.3 Contaminant Release Scenario....3-19
3.3.3.1 General Description. 3-19
3.3.3.2 Contaminant Release Based on Glass Corrosion. 3-19
3.3.4 Contaminant Transport....3-20
3.3.4.1 Moisture Movement. 3-20
3.3.4.2 Advective, Dispersive, and Diffusive Transport....3-21
3.3.4.3 Vapor Transport. 3-22
3.3.4.4 Solid Transport....3-22
3.3.5 Exposure Scenarios 3-22
3.4 VALUES AND ASSUMPTIONS 3-22
3.4.1 Selection Criteria....3-22
3.4.2 Key Assumptions 3-24
3.4.3 Site 3-25
3.4.3.1 Location and Stratigraphy. 3-25
3.4.3.2 Vadose Zone Hydrologic Parameters. 3-26
3.4.3.2.1 Near-Field Hydrology Data. 3-28
3.4.3.2.2 Far-Field Hydrology. 3-29
3.4.3.3 Geochemical Retardation Factors. 3-30
3.4.3.4 Unconfined Aquifer Properties and Boundaries. 3-36
3.4.3.4.1 Hydrogeologic Framework. 3-36
3.4.3.4.2 Recharge and Aquifer Boundaries. 3-38
3.4.3.4.3 Flow and Transport Properties. 3-39
3.4.3.4.4 Groundwater Sensitivity Cases. 3-41
3.4.4 Waste Package 3-41
3.4.4.1 Waste Package Geometry. 3-41
3.4.4.2 Waste Form Release Rate. 3-42
3.4.4.3 Waste Form Data Used in this PA. 3-44
3.4.4.4 Sensitivity Cases. 3-50
3.4.5 Disposal Facility....3-50
3.4.6 Infiltration Rate 3-51
3.4.7 Exposure Parameters....3-53
3.5 PERFORMANCE ASSESSMENT METHODOLOGY 3-55
3.5.1 Integration 3-55
3.5.1.1 Strategy. 3-55
3.5.1.2 Base Analysis Case. 3-57
3.5.1.3 Best Estimate Case. 3-58
3.5.1.4 Sensitivity Cases. 3-58

3.5.2 Computer Codes....3-59
3.5.2.1 General Selection Criteria for Computer Codes. 3-61
3.5.2.2 Calculation of the Contaminant Release Rate from Glass....3-62
3.5.2.2.1 Selection. 3-63
3.5.2.2.2 Code Description. 3-63
3.5.2.2.3 Code History. 3-63
3.5.2.2.4 Verification. 3-63
3.5.2.3 Calculation of Water Flow and Contaminant Transport in the Vadose Zone. 3-64
3.5.2.3.1 Selection. 3-64
3.5.2.3.2 Code Description. 3-64
3.5.2.3.3 Code History. 3-64
3.5.2.3.4 Verification. 3-64
3.5.2.4 Calculation of Water Flow and Contaminant Transport in the Unconfined Aquifer. 3-64
3.5.2.5 Integration of Results. 3-65
3.5.2.6 Spreadsheets. 3-66
3.5.3 Computer Models....3-66
3.5.3.1 Waste Form Release. 3-66
3.5.1.1.1 Waste Form Release Model. 3-66
3.5.3.1.2 Waste Form Release Model for Trenches. 3-68
3.5.3.1.3 Waste Form Release Model for Concrete Vaults. 3-69
3.5.3.2 Disposal Facility Barrier and Vadose Zone. 3-69
3.5.3.2.1 Disposal Facility Barrier Model. 3-69
3.5.3.2.2 Far-Field Model. 3-71
3.5.3.3 Groundwater Model. 3-71
3.5.3.3.1 Simulation of Site-Wide Steady-State Flow Conditions. 3-72
3.5.3.3.3 Local-scale Model Development and Description. 3-75
3.5.3.3.4 Grid Design. 3-75
3.5.4 Input Data....3-78
3.5.4.1 Contaminant Release Data. 3-78
3.5.4.2 Vadose Zone Data. 3-78
3.5.4.3 Aquifer Modeling. 3-78
3.5.4.3.1 Hydraulic Properties. 3-78
3.5.4.3.2 Transport Properties. 3-82
3.5.4.3.3 Base Case: Areal Sources Representing New Facility Disposal Concept. 3-82
3.5.4.4 Integration of Results. 3-82
3.5.5 Sensitivity Cases. 3-86
3.5.5.1 Scenario-Dependent Sensitivity Cases. 3-86
3.5.5.2 Inventory-Dependent Sensitivity Cases. 3-87
3.5.5.3 Infiltration-Dependent Sensitivity Cases. 3-87

3.5.5.4 Geology-Dependent Sensitivity Cases. 3-88
3.5.5.5 Facility-Dependent Sensitivity Cases. 3-88
3.5.5.6 Facility Degradation-Dependent Sensitivity Cases. 3-89
3.5.5.7 Hydraulic Parameter-Dependent Sensitivity Cases. 3-89
3.5.5.8 Waste Form-Dependent Sensitivity Cases. 3-89
3.5.5.9 Geochemical-Dependent Sensitivity Cases. 3-91
3.5.5.10 Exposure Parameter-Dependent Cases. 3-91
3.5.5.11 Location/Layout of the Facility. 3-91

4.0 RESULTS OF ANALYSES 4-1
4.1 INTRODUCTION 4-1
4.2 Comments On Calculations 4-2
4.2.1 Presentation of Results 4-2
4.2.2 Calculational Accuracy and Stability 4-3
4.3 RESULTS OF GROUNDWATER SCENARIOS, BASE ANALYSIS AND BEST ESTIMATE CASES 4-3
4.3.1 Overview 4-3
4.3.2 Base Analysis Case: Moisture Flow Into Disposal Facility 4-4
4.3.3 Base Analysis Case: Waste Form Release 4-4
4.3.4 Base Analysis Case: Moisture Flow And Contaminant Transport in the Vadose Zone 4-9
4.3.5 Base Analysis Case: Moisture Flow And Contaminant Transport in Groundwater 4-15
4.3.6 Base Analysis Case: Conversion into Dose 4-20
4.3.7 Best Estimate Case: Moisture Flow Into Disposal Facility 4-28
4.3.8 Best Estimate Case: Waste Form Release 4-30
4.3.9 Best Estimate Case: Moisture Flow And Contaminant Transport in the Vadose Zone 4-30
4.3.10 Best Estimate Case: Moisture Flow And Contaminant Transport in Groundwater 4-32
4.3.11 Best Estimate Case: Conversion into Dose 4-32
4.4 Sensitivity Cases: Moisture Flow Into Disposal Facility 4-33
4.5 Sensitivity Cases: Waste Form Release 4-35
4.5.1 Overview 4-35
4.5.2 Forward Rate of Reaction 4-35
4.5.3 Glass Dissolution Rate 4-37
4.5.4 Effect of Infiltration Rate 4-38
4.5.5 Effect of Materials Surrounding ILAW Packages 4-38
4.5.5.1 Effect of Filler Material on Glass Dissolution. 4-39
4.5.5.2 Steel Containers. 4-40
4.5.5.3 Conditioning Layer. 4-41
4.5.6 Effect of Type of Disposal Facility 4-41

4.5.7 Effect of Waste Loading and Other Glass Compositions 4-42
4.5.8 Effect of Waste Package Design 4-45
4.5.9 Other Calculations.....4-46
4.6 Sensitivity Cases: Vadose Zone Moisture Flow And Contaminant Transport.....4-53
4.6.1 Overview 4-53
4.6.2 Recharge.....4-53
4.6.3 Vadose Zone Properties 4-55
4.6.4 Waste Form Release or Disposal Facility Time Dependence.....4-59
4.7 Sensitivity Cases: Groundwater Flow And Contaminant Transport 4-59
4.7.1 Overview 4-59
4.7.2 Disposal Facility Layouts and Location.....4-60
4.7.3 Pumping Rates at the Well Retrieving the Contaminated Water.....4-62
4.7.4 Hydraulic Conductivities Beneath the Site 4-62
4.7.5 Regional Influences.....4-63
4.8 Sensitivity Cases: Other Factors.....4-65
4.8.1 Overview 4-65
4.8.2 Inventory 4-65
4.8.3 Land Use 4-67
4.8.4 Dosimetry Parameters 4-67
4.8.5 Facility Location 4-68
4.8.6 Ignored Processes and Conditions 4-68
4.9 Sensitivity Cases: Extreme Cases.....4-69
4.9.1 Overview 4-69
4.9.2 Instantaneous Waste Form Release.....4-69
4.9.3 Instantaneous Vadose Zone Travel 4-73
4.9.4 Bathtub Effect 4-74
4.10 Cumulative Impacts from Hanford Site Activities 4-75
4.10.1 Introduction 4-75
4.10.2 Hanford Site Composite Analysis.....4-75
4.10.3 Results from 1998 ILAW PA.....4-76
4.11 Summary of Groundwater Pathway Cases 4-78
4.12 Effects of Releases To Air.....4-79
4.12.1 Upward Diffusion of Radionuclides 4-79
4.12.2 Mechanisms Affecting the Diffusion Flux.....4-83
4.12.2.1 Atmospheric Pressure. 4-83
4.12.2.2 Atmospheric Temperature. 4-83
4.12.2.3 Wind.....4-83
4.12.2.4 Rainfall.....4-84
4.12.3 Consequences and Comparison with Performance Objectives.....4-84
4.13 Effects FROM Biotic Pathways 4-85
4.14 Effects of Catastrophic Events 4-85
4.15 ALARA Analysis 4-85
4.15.1 Past ALARA Activities.....4-86

4.15.2 Future ALARA Activities 4-87

5.0 RESULTS FOR AN INADVERTENT INTRUDER SCENARIO 5-1
5.1 Overview 5-1
5.2 Inadvertent Intruder Scenarios 5-1
5.3 Facility Description And Assumptions For The Inadvertent Intruder Analysis....5-2
5.4 Inadvertent Intruder Analysis Results 5-4
5.4.1 Driller Scenario 5-4
5.4.2 Homesteader Scenario....5-5
5.4.3 Uncertainties 5-7
5.4.3.1 Waste Loading. 5-7
5.4.3.2 Stability of Waste Form. 5-7
5.4.3.3 Area of Homesteader Garden....5-9
5.4.3.4 Size of the Hole Drilled. 5-9
5.4.3.5 Average Areal Distribution of the Waste....5-9
5.4.3.6 Other Factors....5-10
5.5 Summary Of The Inadvertent Intruder Scenario 5-11

6.0 INTERPRETATION OF RESULTS 6-1
6.1 Overview 6-1
6.2 Integration of Results 6-1
6.3 Verification of Performance Assessment Results 6-4
6.4 Basis for Waste Acceptance Limits....6-5

7.0 PERFORMANCE EVALUATION 7-1
7.1 OVERVIEW....7-1
7.2 COMPARISON OF ESTIMATED IMPACTS TO PERFORMANCE....7-1
7.2.1 Protection of General Public 7-1
7.2.2 Protection of Inadvertent Intruders 7-2
7.2.3 Protection of Groundwater Resources 7-3
7.2.4 Protection of Surface Water Resources....7-3
7.2.5 Protection of Air Resources 7-4
7.2.6 Summary 7-4
7.3 PERFORMANCE SENSITIVITY TO KEY PARAMETER UNCERTAINTIES.7-5
7.3.1 Disposal Facility Design And Layout....7-5
7.3.2 Waste Form Performance....7-5
7.3.3 Groundwater Flow 7-6
7.3.4 Inventory 7-6
7.3.5 Other Factors....7-7
7.4 Conservatisms and Caveats 7-7
7.4.1 Conservatisms 7-7
7.4.2 Caveats 7-8

7.5 UNCERTAINTIES REGARDING GLASS PERFORMANCE 7-9
7.6 REQUIREMENTS SET BY PERFORMANCE ASSESSMENT 7-13
7.6.1 Introduction 7-13
7.6.2 Requirement Development Based on Inadvertent Intruder Protection. 7-14
7.6.3 Requirement Development Based on Groundwater Protection 7-18
7.6.3.1 Waste Inside ILAW Package. 7-18
7.6.3.2 Smearable Contamination. 7-20
7.6.4 Waste Form Restrictions 7-22
7.6.4.1 Concentration. 7-22
7.6.4.2 Release Rate. 7-22
7.6.4.3 Smearable Contamination. 7-22
7.6.5 Disposal Facility Requirements 7-22
7.6.6 Likelihood of Meeting Requirements 7-23
7.6.6.1 Inadvertent Intruder Compliance Case. 7-24
7.6.6.2 Groundwater Protection Compliance Case. 7-24
7.6.6.3 Smearable Contamination Compliance Case. 7-25
7.7 SUMMARY OF THE IMPACT OF DIFFERENCES BETWEEN THE 1998 ILAW PA AND THIS DOCUMENT 7-25
7.8 FURTHER WORK 7-27
7.8.1 Future Performance Assessments 7-28
7.8.2 Waste Form Data Collection and Model Development 7-28
7.8.3 Interactions with Disposal Facility Designers 7-30
7.8.4 Geotechnical Data Collection and Model Development 7-30
7.8.5 ILAW Inventory 7-31
7.8.6 Other Data Collection 7-31
7.9 CONCLUSION 7-32

8.0 PREPARERS AND MAJOR REVIEWERS 8-1

9.0 REFERENCES 9-1

Appendix A LFRG Comments on Performance Assessment for Hanford Immobilized Low-Activity Tank Waste, 7/27/99. ..... A-1
3.1.1 PA is Complete A-1
3.1.2. PA is Thorough and Technically Supported A-18
3.1.3. PA Conclusions Are Valid and Acceptable A-33
Appendix B Dosimetry Dose Factors B-1
Appendix C Governing Equations Used in Major Codes C-1
C.1 Introduction C-1
C.2 Flow and Transport C-1
C.2.1 Overview C-1

C.2.2 Moisture Flow C-1
C.2.3 Advective and Diffusive Transport C-3
C.2.4 Vapor Transport C-5
C.3 Waste Form C-6
C.3.1 Mass Conservation of Aqueous Solutes C-6
C.3.2 Texture Dynamics C-7
C.3.3 Contaminant Release Rate From Glass C-8

Appemdix D Detailed Results For Estimated Impacts D-1
D.1 Introduction D-1
D.2 Waste Form Calculations D-1
D.3 Vadose Zone Calculation D-1
D.4 Groundwater Calculations D-1
D.5 Estimated Impacts D-2
Facility Cases D-3
Waste Form Release D-3
Vadose Zone Cases D-4
Groundwater Cases D-5
Inventory Cases D-6
Dosimetry Cases D-7
Other Sensitivity Cases D-7
D.6 Outline for Compact Disk Files D-9

Appendix E "A Strategy to Conduct an Analysis of the Long-Term Performance of Low-Activity Waste Glass in a Shallow Subsurface Disposal System at Hanford" E-1
E-1.0 INTRODUCTION E-1
E-2.0 DISPOSAL SYSTEM DESCRIPTION E-3
E-2.1 WATER INFILTRATION E-3
E-2.2 FACILITY DESCRIPTION E-4
E-3.0 MODELING APPROACH E-6
E-3.1 GLASS CORROSION PROCESS E-6
E-3.1.1 Importance of Secondary Phases E-6
E-3.1.2 Effect of Ion Exchange E-7
E-3.2 GLASS CORROSION MODEL E-8
E-3.2.1 Rate Law for Hydrolysis and Dissolution E-8
E-3.2.1.1 Experiments for Kinetic Rate Law Parameters. E-9
E-3.2.1.2 Experiments for Affinity Term Parameters. E-10
E-3.2.2 Rate Law for Ion Exchange E-11
E-4.0 LABORATORY TESTING E-13
E-4.1 SINGLE-PASS FLOW-THROUGH TEST E-14

E-4.1.1 Well-Mixed Batch Reactor E-14
E-4.1.2 Packed Bed Reactor E-14
E-4.1.3 Fluidized Bed Reactor E-15
E-4.1.4 SPFT Testing Strategy E-15
E-4.2 VAPOR HYDRATION TEST E-16
E-4.3 PRODUCT CONSISTENCY TEST E-17
E-4.4 PRESSURIZED UNSATURATED FLOW TEST E-19
E-4.5 OTHER TEST METHODS E-22
E-4.5.1 Soxhlet Tests E-22
E-4.5.2 MCC-1 Test E-22
E-4.5.3 MCC-3 Solubility Test E-23
E-4.5.4 Periodic Replenishment Tests E-23
E-4.5.5 Unsaturated or “Drip” Test E-24
E-4.5.6 Accelerated Dissolution Test E-25
E-4.6 REQUIRED TESTS WITH RADIOACTIVE GLASSES E-25
E-4.7 MATERIALS INTERACTION TESTS E-26
E-4.8 ROLE OF NATURAL ANALOGS E-27
E-4.9 LABORATORY TESTING STRATEGY SUMMARY E-29
E-5.0 FIELD TESTING E-30
E-6.0 MODELING THE DISPOSAL SYSTEM E-32
E-6.1 SUBPROCESS MODEL DEVELOPMENT E-33
E-6.1.1 Adaptive Reaction Network E-33
E-6.1.2 Composition-Dependent Hydraulic Property Model E-33
E-6.2 NUMERICAL METHODS E-34
E-6.3 DISPOSAL SYSTEM SIMULATIONS FOR THE PERFORMANCE ASSESSMENT E-35
E-7.0 CONCLUSION E-38
E-8.0 REFERENCES E-39

F. QUALITY ASSURANCE F-1
F.1 Overview F-1
F.2 CH2M Hill Hanford Group, Inc. F-1
F.3 Pacific Northwest National Laboratory F-1
F.4 Other Contractors F-2
F.5 Hanford Environmental Dose Overview Panel F-2
F.6 Technical Reviews of Supporting Documents F-2
F.7 Review of the Performance Assessment F-2

List of Tables

Table 1-1. Schedule for ILAW Disposal Facilities. 1-6
Table 1-2. Schedule for Performance Assessment Activities. 1-8
Table 1-3. Radiological Performance Objectives....1-16
Table 1-4. Performance Goals for Inorganic and Organic Materials. 1-17
Table 1-5. Major Sources of Information for the Base Analysis Case....1-25

Table 2-1. Stratigraphy of the200 East Area. 2-19
Table 2-2. Approximate Probability of Exceeding Given Ground Motions During Selected Time Periods. 2-25
Table 2-3. Semiquantative Estimates of Minerals in Selected Sediments from ILAW Borehole. 2-50
Table 2-4. Activity of Radionuclides in Hanford Sitewide Background Data Set 2-52
Table 2-5. Background Values for Hanford Site Groundwater. [a] 2-53
Table 2-6. Summary of Phase 1 and Phase 2 ILAW Package Production. 2-62
Table 2-7. Trench Packing Characteristics....2-67

Table 3-1. ILAW Inventories and Concentrations for Important Constituents....3-4
Table 3-2. Inventory Estimate Changes from 1998 ILAW PA. 3-11
Table 3-3. Best-Estimate Hydraulic Parameter Values For Near-Field Materials. 3-28
Table 3-4. Best-Estimate Hydraulic Parameter Values For Far-Field Layers. 3-29
Table 3-5. Best-Estimate K_d Values For The Far-Field Sand Sequence. 3-32
Table 3-6. Other Important Geochemical Values. 3-35
Table 3-7. Summary of Best Estimate Rate Law Parameters for LAWABP1 and HLP-31 Glasses at 15°C. 3-45
Table 3-8. Recharge Rate Estimates 3-52
Table 3-9. Annual Unit Dose Factors for Post-Intrusion Resident. 3-53
Table 3-10. Total Annual Unit Dose Factors for Low-Water Infiltration Cases. 3-54
Table 3-11. Base Analysis Case Input Data for the Disposal Facility. 3-79
Table 3-12. Elemental Compositions of LAWABP1 and HLP31....3-91
Table 3-13. List of Sensitivity Cases....3-93

Table 4-1. Inventory-Normalized Contaminant Release to the Vadose Zone for Various Times for the Base Analysis Case. 4-8
Table 4-2. Well Intercept Factors. 4-19
Table 4-3. Estimated Impacts from the Base Analysis Case for a Well 100 m Downgradient from the Disposal Facility....4-21
Table 4-4. Major Radionuclide Contributors at 1,000 Years and 10,000 Years to the Estimated Beta/Photon Drinking Water Dose at a Well 100 m Downgradient from the Disposal Facility. 4-22

Table 4-5. Major Radionuclide Contributors at 1,000 Years and 10,000 Years to the Estimated All-Pathways Dose at a Well 100 m Downgradient from the Disposal Facility. ...4-23
Table 4-6. Major Radionuclide Contributors at 10,000 Years to the Estimated Concentration of Alpha Emitters at a Well 100 m Downgradient from the Disposal Facility. 4-24
Table 4-7. Estimated Impacts at 1,000 Years from the Base Analysis Case for a Well at Various Locations Downgradient from the Disposal Facility. 4-25
Table 4.8. Impacts from Chemicals at 1,000 Years and 10,000 Years at a Well 100 m Downgradient from the Disposal Facility. 4-25
Table 4-9. Impacts from Chemicals at 1,000 Years and 10,000 Years at a Well Just Before Entering the Columbia River. 4-26
Table 4-10. Estimated Impacts From The Best Estimate Case For A Well 100 Meters Downgradient From The Disposal Facility. 4-32
Table 4-11. Summary of Near-Field Hydraulic Sensitivity Calculations. 4-34
Table 4-12. Summary of Waste Form Sensitivity Calculations.. 4-36
Table 4-13. Travel Times and All-Pathways Doses for the Various Vadose Zone Sensitivity Cases. 4-54
Table 4-14. Estimated Impacts from Sensitivity Case Where All Radionuclides are Assumed Mobile Compared to the Base Analysis Case for a Well 100 m Downgradient from the Disposal Facility. 4-58
Table 4-15. Estimated Impacts from Clastic Dike Simulation Compared to the Base Analysis Case for a Well 100 m Downgradient from the Disposal Facility.....4-58
Table 4-16. Ratio of Well Intercept Factors for the Various Groundwater Sensitivity Cases. 4-60
Table 4-17. Sensitivity of Variables to Key Radioisotope Inventories.....4-66
Table 4-18. All-Pathways Doses for Three Other Exposure Pathways for Points Located Near the Disposal Facility. 4-67
Table 4-19. Effect on Estimated Impacts Assuming All Contaminants Release at Once.....4-70
Table 4-20. Major Radionuclide Contributors at 1,000 Years and 10,000 Years to the Estimated Beta-Photon Drinking Water Dose at a Well 100 m Downgradient from the Disposal Facility for Instantaneous Release. 4-71
Table 4-21. Major Radionuclide Contributors at 1,000 Years and 10,000 Years to the Estimated All-Pathways Dose at a Well 100 m Downgradient from the Disposal Facility for Instantaneous Release. 4-72
Table 4-22. Major Radionuclide Contributors at 10,000 Years to the Estimated Concentration of Alpha Emitters at a Well 100 m Downgradient from the Disposal Facility for Instantaneous Release. 4-72
Table 4-23. Estimated Impacts Assuming Instantaneous Vadose Zone Travel. 4-74
Table 4-24. Effect On The All-Pathways Dose When Instantaneous Vadose Zone Travel Occurs For The Most Important Radioisotopes. 4-74
Table 4-25. Mixing Factors from Other Sources for a Well 100 m Downgradient of the Low-Level Tank Waste Disposal Site. 4-77
Table 4-26. Calculation Summary for ^{3}H and ^{14}C Air Releases 4-80

Table 5-1. Facility Dimensions and Waste Volume Exhumed. 5-4
Table 5-2. Driller Intruder Dose at Various Intrusion Times.....5-12
Table 5-3. Homesteader Intruder Dose at Various Intrusion Times 5-14

Table 6-1. Important Radioisotopes in Groundwater Pathway. 6-2
Table 6-2. Important Radioisotopes in Homesteader Inadvertent Intruder Scenario.....6-2

Table 7-1. Comparison of Estimated Impacts with Performance Objectives for Protecting the Public. 7-2
Table 7-2. Comparison of Estimated Impacts with Performance Objectives for Protecting the Inadvertent Intruder.. 7-2
Table 7-3. Comparison of Estimated Impacts with Performance Objectives for Protecting Groundwater Resources. 7-3
Table 7-4. Comparison of Estimated Impacts with Performance Objectives for Protecting Surface Water Resources. 7-4
Table 7-5. Comparison of Estimated Impacts with Performance Objectives for Protecting Air Resources.. 7-4
Table 7-6. Performance Goals for Requirement Cases. 7-13
Table 7-7. Types of Operation Parameters to be Restricted by PA. 7-14
Table 7-8. Restrictions Based on Protecting Inadvertent Intruder. 7-16
Table 7-9. Restrictions Based on Protecting Groundwater - ILAW Package.. 7-20
Table 7-10. Restrictions Based on Protecting Groundwater - Smearable Contamination.. 7-21
Table 7-11. Comparison of ILAW Inventory Concentrations to Allowed Limits. 7-24
Table 7-12. Effect of Updated Model Inputs on the Estimated Beta/Gamma Drinking Water Dose at 10,000 Years. 7-26
Table 7-13. Beta-Gamma Drinking Water Dose.....7-26

Table B-1. Radionuclides to be Considered and Their Half Lives. B-1
Table B-2. Decay Chains Actually Computed. B-5
Table B-3. No Water Infiltration Case: Intruder. B-7
Table B-4. No Water Infiltration Case: Post-Intrusion Resident. B-10
Table B-5. Low Water Infiltration Case: All Pathways Farmer.....B-13
Table B-6. No Water Infiltration Case: Intruder. B-16
Table B-7. Low Water Infiltration Case: HSRAM Industrial. B-19
Table B-8. Low Water Infiltration Case: HSRAM Residential. B-22
Table B-9. Low Water Infiltration Case: HSRAM Agricultural. B-25
Table B-10. Low Water Infiltration Case: Native American Subsistence Resident. B-28
Table B-11. Low Water Infiltration Case: Columbia River Population. B-31
Table B-12. Ratio of Total Dose to Drinking Water Dose. B-34
Table B-13. Ingestion Dose Factors. B-37
Table B-14. Inhalation Dose Factors.....B-41
Table B-15. External Dose Rate Factors. B-44

Table D-1. Summary of Estimated Impacts for 2001 ILAW PA. D-3
Table D-2. Cross-reference for Sensitivity Cases and Output Files from Waste Form, Vadose Zone, and INTEG Calculations for the 2001 ILAW PA. D-10

Table E-4.1. Master Test Matrix for Long Term Performance Evaluation of a Glass..... E-29

Table F-1. Data Package External Reviewers. F-3

List of Figures

Figure 1-1. The Hanford Site and its Location in Washington State. 1-3
Figure 1-2. RH Trench Preconceptual Design 1-4
Figure 1-3. Activities Diagram for the Immobilized Low-Activity Waste Project.....1-7

Figure 2-1. Hanford Site in Washington State. 2-2
Figure 2-2. Hanford Site Map Showing Public Highways and Future Site Boundary. 2-3
Figure 2-3. Activities in the 200 Areas. 2-5
Figure 2-4. Population Centers Within an 80-km Radius of the Hanford Site. 2-6
Figure 2-6. Divisions of the Intermontane Physiographic and Adjacent Snake River Plains Provinces. 2-18
Figure 2-7. Map Showing the Location of Earthquakes Detected From 1969 to 1999. 2-24
Figure 2-8. Total Mean Seismic Hazard for 200 Area Plateau, Hanford Site.....2-25
Figure 2-9. Map Showing Borehole Locations in the New ILAW Disposal Site.....2-27
Figure 2-10. Fence Diagram of the ILAW Disposal Site and Vicinity.....2-28
Figure 2-11. Summary Diagram of a West to East Cross-Section for the ILAW Disposal Site. 2-29
Figure 2-12. West to East (Southern Section) Cross-Section for the ILAW Disposal Site. 2-30
Figure 2-13. West to East (Northern Section) Cross-Section Across the ILAW Disposal Site. 2-31
Figure 2-14. Alternate West to East Cross-Section Across the New ILAW Disposal Site. 2-31
Figure 2-14. Alternate West to East Cross-Section Across the New ILAW Disposal Site. 2-32
Figure 2-15. Southwest to Northeast Cross-Section Across the ILAW Disposal Site.....2-33
Figure 2-16. Alternate Southwest to Northeast Cross-Section Across the ILAW Disposal Site. 2-34
Figure 2-17. Isopach Map of the Ringold Formation at the ILAW Disposal Site. 2-36
Figure 2-18. Structural Contour Map on the Surface of the Ringold Formation. 2-37
Figure 2-19. Isopach Map of the Hanford Formation at the New ILAW Disposal Site. 2-38
Figure 2-20. Hydrologic Basins Designated for the Washington State Portion of the Columbia Plateau.....2-42
Figure 2-21. Hindcast Water Table Map of the Hanford Site, January 1944.....2-46
Figure 2-22. Hanford Site Water Table Map, June 1989. 2-47
Figure 2-23. Averages for Natural and Human-Produced Sources of Radiation.....2-55
Figure 2-24. Ternary Diagrams Depicting Compositional Variability for ILAW Glasses.....2-60
Figure 2-25. Comparison of VHT and PCT-A Test Performance of ILAW Glasses with Respect to DOE Product Acceptance Specifications 2-61
Figure 2-26. Layout of ILAW Disposal Facility.....2-64
Figure 2-27. RH Waste Trench Conceptual Model.....2-65
Figure 2-28. RH Waste Trench Liner Details. 2-65

Figure 3-1. Predicted Groundwater Flowlines for Post Hanford Conditions.....3-17
Figure 3-2. Comparison of Generalized Geology and Hydrostratigraphic Columns.....3-37
Figure 3-3. Hydraulic Conductivity Distribution Obtained for the Uppermost Unconfined Aquifer from Inverse Calibration for 1979 Conditions. 3-40

Figure 3-4. Forward Reaction Rate as a Function of Temperature and Solution pH for Several Borosilicate Glasses. 3-47
Figure 3-5. Plot of Dissolution Rate at 90ºC Versus Mixed Al-Si Activity Product.. 3-47
Figure 3-6. Excess Sodium Release via Ion Exchange as a Function of Temperature for LAWABP1 Glass at pH(25°C)=9. 3-48
Figure 3-7. Normalized Release Rates in PUF Test with LAWABP1 Glass. 3-49
Figure 3-8. Comparison of PCT Solution Concentration Data with the Solution Composition Calculated with the EQ3/6 Code. 3-49
Figure 3-9. Predicted Paragenetic Sequence of Alteration Phases Formed During the Reaction of LAWABP1 Glass in Deionized Water. 3-50
Figure 3-10. Eight Sequential Steps for the Groundwater Pathway. 3-56
Figure 3-11. Modeling Strategy for Assessing ILAW Disposal System. 3-60
Figure 3-12. Material Zones for Remote Handled Trench Waste Form Release Simulations. 3-68
Figure 3-13. Material Zones for New ILAW Vault Waste Form Release Simulations. 3-69
Figure 3-14. Predicted Water Table for Post-Hanford Conditions for Assumed Steady-State Conditions (as Simulated after 350 Years). 3-73
Figure 3-15 Predicted Water Table for Post-Hanford Conditions for Assumed Steady-State Conditions between ILAW Disposal Facility and Columbia River (as Simulated after 350 Years). 3-74
Figure 3-16. Finite Element Grid Used in Local –Scale Model. 3-76
Figure 3-17. Three-Dimensional Distribution of Major Hydrogeologic Units in the Local-Scale Model. 3-76
Figure 3-17. Three-Dimensional Distribution of Major Hydrogeologic Units in the Local-Scale Model. 3-77
Figure 3-18. Distribution and Hydraulic Conductivities of Major Hydrostratigraphic Units in Local-scale Model. 3-83

Figure 4-1. Moisture Content Inside the Disposal Facility for Various Recharge Rates. The base analysis case uses 4.2 mm/year. 4-5
Figure 4-2. pH inside the Disposal Facility for Base Analysis Case. 4-6
Figure 4-3. Waste Form Dissolution as a Function of Time and Space Inside the Disposal Facility. 4-7
Figure 4-4. Relative Contaminant Flux to the Vadose Zone from the Disposal Facility (Assuming Unit Concentration Initially) for the Base Analysis Case and Other Infiltration Rates. 4-8
Figure 4-5. The Estimated Moisture Content for the Far-Field Zone for the Base Analysis Case. 4-10
Figure 4-6. Darcy Velocity at the Top of the Far Field (Bottom of the Disposal Facility). 4-11
Figure 4-7. Inventory-Normalized Mobile Contaminant Concentration at the Bottom of the Disposal Facility at 1,000 years. 4-12
Figure 4-8. Mobile Contaminant Concentration Just Prior to Entering the Groundwater at 10,000 Years. 4-13
Figure 4-9. Inventory-Normalized Contaminant Flux Summed Over Horizontal Distance as a Function of Time and K_d Bin (Linear Scale). 4-13
Figure 4-10. Inventory-Normalized Contaminant Flux Summed Over Horizontal Distance as a Function of Time and K_d Bin (Logarithmic Scale). 4-14

Figure 4-11. Water Table Elevation Predicted by the Hanford Site Groundwater Model for Steady-State Conditions After Hanford Site Operations. 4-15
Figure 4-12. Base Analysis Case Contaminant Groundwater Plume at the Water Table, Showing the Contaminant Concentration Values. 4-16
Figure 4-13. Vertical Distribution of the Groundwater Plume Along the Line A-A', Which Is Near the Centerline of the Plume. 4-17
Figure 4-14. Well Intercept Factor for Wells at 100 m and 1,000 m as a Function of Time for the Base Analysis Case. 4-18
Figure 4-15. Asymptotic Areal Distribution of the Contaminant Groundwater Plume for Large Distances. 4-19
Figure 4-16. Time History of Groundwater Concentrations At The Greater Distances. 4-20
Figure 4-17. Time Dependence of the Estimated Beta/Photon Drinking Water Dose at a Well 100 m Downgradient from the Disposal Facility. 4-22
Figure 4-18. Time Dependence of the Estimated All-Pathways Dose at a Well 100 m Downgradient from the Disposal Facility. 4-23
Figure 4-19. Time Dependence of the Concentration of Alpha Emitters Dose at a Well 100 m Downgradient from the Disposal Facility. 4-24
Figure 4-20. Volumetric Moisture Content With The Sand-Gravel Capillary Barrier Atop The Disposal Facility. 4-29
Figure 4-21. Total Inventory-Normalized, Mobile, Contaminant Flux to the Groundwater for the Base Analysis and Best Estimate Cases as a Function of Time. 4-31
Figure 4-22. Comparison of Total Inventory-Normalized Contaminant Flux Leaving the Disposal Facility and Entering into the Groundwater for the Best Estimate Case for K_d = 0 and 0.6 mL/g as a Function of Time. 4-31
Figure 4-23. Inventory-Normalized Contaminant Flux to the Vadose Zone for Different Glass Dissolution Models. 4-37
Figure 4-24. Contaminant Flux to the Vadose Zone Assuming Different Surrounding Materials. 4-39
Figure 4-25. Contaminant Flux to the Vadose Zone Assuming Different Surrounding Materials. 4-40
Figure 4-26. Contaminant Flux to the Vadose Zone for Vault Simulations. 4-42
Figure 4-27. VHT Corrosion Rate as a Function of Waste Loading (from Vienna [2000]). 4-43
Figure 4-28. Dependence of HLP-31 Glass Dissolution Rate on Concentration of Silicic Acid. 4-44
Figure 4-29. Inventory-Normalized Contaminant Flux to the Vadose Zone for Different Glass Formulations. 4-45
Figure 4-30. pH for RH Trench Simulation Extended to Water Table 4-48
Figure 4-31. TcO_4^- for RH Trench Simulation Extended to Water Table. 4-49
Figure 4-32. TcO_4^- For Fully-Saturated RH Trench Simulation With No Flow. 4-50
Figure 4-33. Total Water Mass Per Node for Fully-Saturated RH Trench Simulation With No Flow. 4-51
Figure 4-34. Inventory-Normalized Contaminant Flux to the Vadose Zone for One-Dimensional and Two-Dimensional Simulations. 4-52
Figure 4-35. Total Inventory-Normalized Contaminant Flux to the Groundwater as a Function of Recharge Rate (No Capillary Barrier). 4-55

Figure 4-36. Total Inventory-Normalized Contaminant Flux to the Groundwater Assuming the Vadose Zone is All Sand or All Gravel (No Capillary Barrier - Recharge = 4.2 mm/year). 4-56
Figure 4-37. Inventory-Normalized Contaminant Flux Entering the Groundwater Assuming All Contaminants Release from the Waste Form at Once. 4-70

Figure 5-1. Inadvertent Intruder Results for the Driller Scenario - Base Intruder Case. 5-5
Figure 5-2. Inadvertent Intruder Results for the Homesteader Scenario - Base Intruder Case. ..5-6
Figure 5-3. Predicted Driller Doses for Different Availability of Radionuclides for Ingestion and Inhalation. 5-8
Figure 5-4. Predicted Homesteader Doses for Different Availability of Radionuclides for Ingestion and Inhalation. 5-8

Figure 7-1. Radial Distribution Plot of 200°C VHT Corrosion Rates for HLP Series of ILAW Glasses. 7-10
Figure 7-2. Cumulative Distribution Plot of 200°C VHT Corrosion Rates for HLP Series of ILAW Glasses. 7-11
Figure 7-3. Comparison of Glass Corrosion Rate in PUF Tests at 99°C and 2 mL/d. 7-12
Figure 7-4. Comparison of Glass Corrosion Rate in PUF Tests at 99°C and VHT Tests at 200°C. 7-12

Figure E-2.1. Schematic of ILAW Disposal System. E-4
Figure E-3.1. Links Among Glass Tests and Modeling E-8
Figure E-3.2. Excess Sodium Release via Ion Exchange as a function of Temperature for LAWABP1 Glass at pH(25 ^{o}C)=9. ....E-12
Figure E-4.1. Schematic of a Typical Batch Flow Through Cell. E-14
Figure E-4.2. SPFT Test Results for Various ILAW Glasses. E-16
Figure E-4.3. Schematic of VHT Test. E-16
Figure E-4.4. PUF Apparatus. E-19
Figure E-4.5. Normalized Release Rates in PUF Tests with LAWABP1 Glass. E-21
Figure E-6.1 Modeling Strategy for Assessing ILAW Disposal System. E-37

List of Acronyms

ADT	accelerated dissolution test
AEA	Atomic Energy Act
ALARA	as low as reasonably achievable
ALT	accelerated leach test
ANL	Argonne National Laboratory
ANS	American Nuclear Society
ANSI	American National Standards Institute
ASME	American Society of Mechanical Engineers
AREST-CT	Analyzer of Radionuclide Source Term with Chemical Transport
ASTM	American Society for Testing and Materials
BBI	best basis tank-by-tank inventory
BHI	Bechtel Hanford, Inc.
BNFL	British Nuclear Fuels, Ltd.
CEC	cation exchange capacity
CERCLA	Comprehensive Environmental Response, Compensation, and Liability Act
CFEST	coupled fluid, energy, and solute transport (code)
CFR	code of Federal regulations
CHARIMA	commercial surface water hydrology and sediment transport model
CPU	central processing unit
DLT	dynamic leach test
DOE	U. S. Department of Energy
DNFSB	Defense Nuclear Facilities Safety Board
DQO	data quality objectives
Ecology	Washington State Department of Ecology
EDE	effective dose equivalent
EIS	environmental impact statement
EM-50	Environmental Management organization dealing with science and technology development
EMSP	Environmental Management Science Program
EP	the probability of exceedence over the performance life
EPA	U. S. Environmental Protection Agency
ERDF	Environmental Remediation Disposal Facility
FFTF	Fast Flux Test Facility
GIS	geographic information systems
GFLOPS	10^9 floating point operations per second
HDPE	high-density polyethylene
HFSUWG	Hanford Future Sites Uses Working Group
HLW	high level waste
HLP	product acceptance
HMS	Hanford Meteorology Station
HSRAM	Hanford Site risk assessment methodology
IHLW	immobilized high level waste
ILAW	immobilized low-activity waste
INVERTS	inverse reactive transport simulator

IR	inventory release rate
ISO	International Standards Organization
K	potassium
K_d	distribution coefficient
LAW	low-activity waste
LAWABP1	sample name of glass used in analysis
1LDL	lower detectability limit
LDR	land disposal restriction
LFRG	Low-Level Waste Disposal Facility Federal Review Group
LLW	low-level waste
MCC-1	Materials Characterization Center static leach test
MCC-3	Materials Characterization Center agitated powder leach test
MCC-5	Materials Characterization Center Soxhlet test
MIIT	materials interface interaction Test
NA	not available
NC	not calculated
NEPA	National Environmental Policy Act
NLLWMP	National Low-Level Waste Management Program
NRC	Nuclear Regulatory Commission
ORP	Office of River Protection
PA	performance assessment
PCT	product consistency test
PDE	partial differential equations
PNNL	Pacific Northwest National Laboratory
ppb	part per billion
PUF	pressurized unsaturated flow test
PUREX	Plutonium-Uranium Extraction (facility)
RCRA	Resource Conservation and Recovery Act
REDOX	Reduction-Oxidation (facility)
rem	roentgen equivalent man (unit used for measuring effective dose of radiation
RFP	request for proposals
RH	relative humidity
RH	remote-handled
RHO	Rockwell Hanford Operations
RI/FS	remedial investigation/feasibility study
RL	Richland Operations Office
RMW	radioactive mixed waste
RPP	River Protection Project
RWTSP	radioactive waste technical support program
SPFT	single pass flow-through (test)
STOMP	a nonisothermal, multiphase flow simulator
STORM	subsurface transport over reactive multiphases
S/V	surface area-to-solution volume ratio
TFA	tank focus area
TIG	tungsten-inert gas
TOX	total organic halides

TWRS	Tank Waste Remediation System
TWRSO&UP	Tank Waste Remediation System Operation and Utilization Plan
VAM3D	variably saturated analysis model code
VHT	vapor hydration test
VSL	Vitreous State Laboratory
WAC	Washington administrative code
WHC	Westinghouse Hanford Company
WIF	well intercept factor
WIPP	Waste Isolation Pilot Plan
WNP	Washington Nuclear Plant

1.0 INTRODUCTION

1.1 PURPOSE

This performance assessment examines the long-term environmental and human health effects of the planned Hanford Low-Level Tank Waste Disposal Facility to support the continuation of the Disposal Authorization Statement issued by the U.S. Department of Energy (DOE) (DOE 1999a) as required by DOE O 435.1, *Radioactive Waste Management* (DOE 1999b). This document also fulfills the requirement for a new performance assessment in fiscal year (FY) 2001 as stated in, DOE/ORP-2000-01, *Maintenance Plan for the ILAW Performance Assessment* (DOE/ORP 2000a).

This performance assessment updates DOE-97-69, *Hanford Immobilized Low-Activity Tank Waste Performance Assessment* (Mann 1998a), which is commonly known as the 1998 ILAW PA. The 1998 ILAW PA was submitted to the Low-Level Waste Disposal Facility Federal Review Group (LFRG) for review and action. The LFRG has completed their review (DOE 1999c). Based on this review, the DOE accepted the ILAW Performance Assessment (DOE 1999d) and issued the Disposal Authorization Statement. This acceptance is contingent on the following actions:

- Providing the LFRG with documentation of the near-term glass test results to assure DOE that the glass performance assumed in the performance assessment can actually be achieved

- Addressing the secondary issues identified by the review team in future revisions to the performance assessment.

The LFRG reviewed the documentation on relevant glass performance that was provided (French 1999 and French 2000a) and determined that the assumed glass performance can be achieved (DOE 2000). The secondary issues identified by the LFRG are addressed in this version of the ILAW PA (see Appendix A).

The major advances in understanding or programmatic changes since the 1998 ILAW PA have been the following:

- Waste form release data from vendor-relevant glass formulations
- ILAW site specific geologic, chemical, and hydraulic data from a new borehole
- New groundwater model
- Expanded understanding to extrapolate laboratory measurements to field conditions
- Selection of a different disposal facility conceptual design (Taylor 1999a).

The approach used to prepare this performance assessment document is to

- Limit its length (the supporting data summarized in this document are fully described in Mann/Puigh (2000a) while the analysis cases and simulations that are summarized in this document are fully described in Puigh 2001),
- Tier from other documents (see, for example, the discussion in Section 1.5.2 on earlier Hanford Site performance assessments and environmental impact statements), and
- Include detailed results and lengthy technical information in appendices.

1.2 BACKGROUND

The Hanford Site, in south-central Washington State (Figure 1-1), has been used extensively for producing defense materials by DOE and its predecessors, the U.S. Atomic Energy Commission and the U.S. Energy Research and Development Administration. Starting in the 1940's, Hanford Site operations were dedicated primarily to producing nuclear weapons materials. In the 1960's, operations were expanded to producing electricity from a dual-purpose reactor, conducting diverse research projects, and managing waste. In the late 1980's, the Site's original mission ended. This mission left a large inventory of radioactive and mixed waste (~55 million gallons) stored in underground single- and double-shell tanks in the Hanford Site 200 Areas.

Today, the Site's missions are environmental restoration, energy-related research, and technology development. As part of its environmental restoration mission, DOE is proceeding with plans to permanently dispose of the waste stored on site. These plans are based on Revision 6 of the *Hanford Federal Facility Agreement and Consent Order* (Tri-Party Agreement) (Ecology 1998-1) and the *Record of Decision for the Tank Waste Remediation Systems Environmental Impact Statement* (DOE 1997b). These documents call for the waste to be retrieved from the tanks, then treated to separate the low-level fraction (now called the low-activity fraction) from the high-level/transuranic fraction. Both fractions will then be immobilized.

The two products (the small volume of high-level immobilized waste and the much larger volume of ILAW) will be disposed in different locations. The high-level waste will be stored on the Hanford Site until it is sent to a federal geologic repository. The ILAW will be buried in a near-surface disposal system on the Hanford Site. Over 200,000 m^3 (7,000,000 ft^3) of low-activity immobilized waste will be disposed under this plan. This is among the largest amounts of waste in the DOE Complex (DOE 1997) and has one of the largest inventories of long-lived radionuclides at a low-level waste disposal facility.

The DOE is procuring services to treat and immobilize the tank waste. The first immobilized waste should be delivered in 2008. The first phase of the effort would extend for about a decade. The contract for the second phase, in which most of the waste will be processed, will be awarded in the second half of this decade.

Figure 1-1. The Hanford Site and its Location in Washington State.

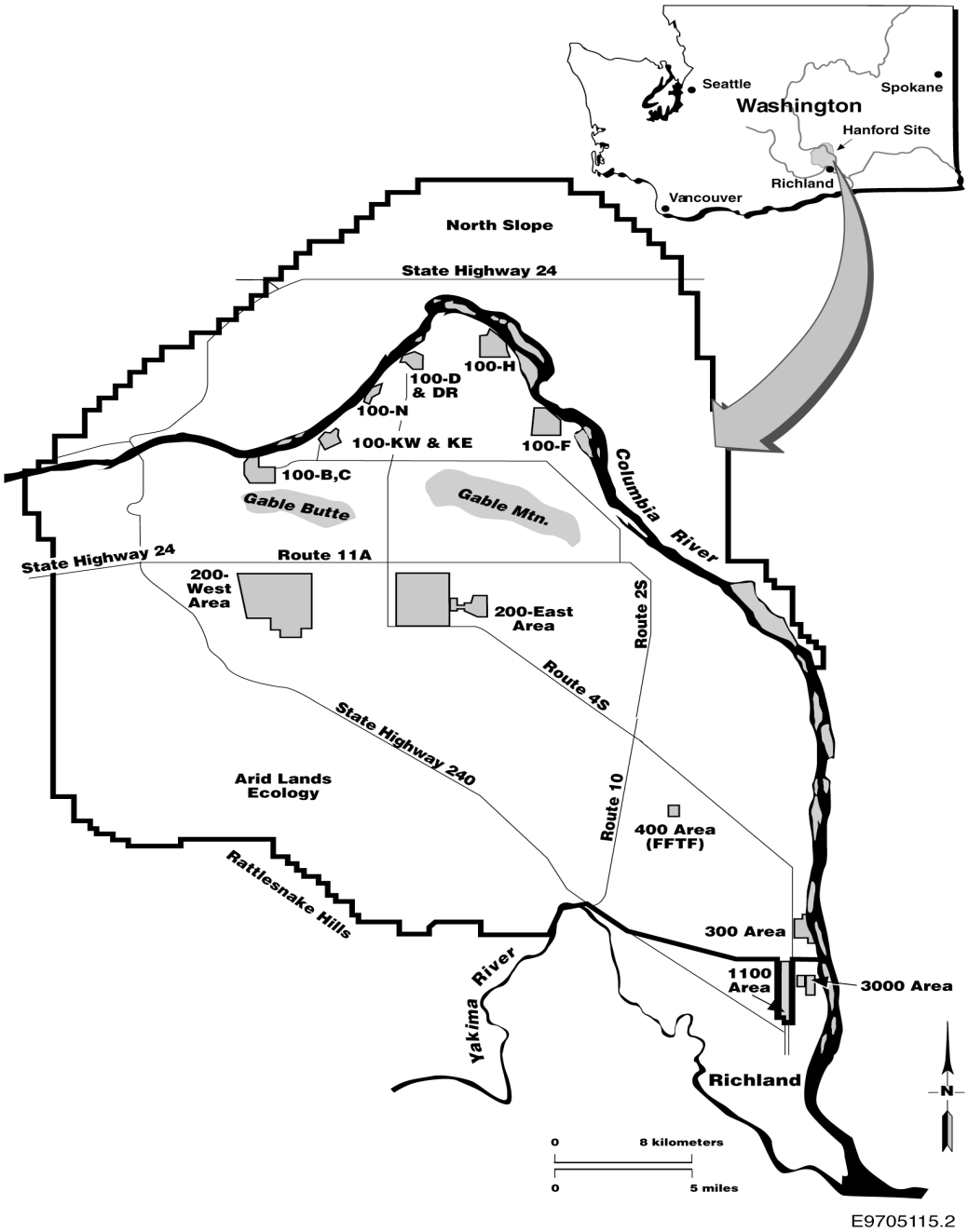

1.3 GENERAL DESCRIPTION OF THE FACILITY

This section provides a general description of the disposal facilities. Section 2.1 describes the geology, hydrology, and geochemistry of the Hanford Site and the 200 East Area where the disposal facility will reside. Section 2.3 provides much more information including figures showing the conceptual and preconceptual designs.

It was assumed in the 1998 ILAW PA that the waste would be disposed in underground concrete vaults. The current plan (Taylor 1999a) of DOE's Office of River Protection (ORP) is to dispose of the immobilized waste in trenches that are similar in design to those used to dispose of radioactive mixed waste at the Hanford Site. A major purpose of this version of the ILAW PA is to obtain DOE Headquarters' approval for this new disposal facility design.

Under the ILAW disposal planning described in the following paragraphs, the disposal facility is a *Resource Conservation and Recovery Act of 1976* (RCRA)-compliant landfill (i.e., a double-lined trench with leachate collection system). Many operational aspects and ancillary activities of the landfill (e.g., leachate collection and disposition, storm water control, installation of surface barrier at closure, etc.) would be similar to that incorporated into the radioactive mixed waste burial trench. However, operational activities related to ILAW package receipt and emplacement in the trench would be modified to accommodate the specific ILAW package size.

The design concept layout (Puigh 1999) of the trenches within the ILAW disposal site is shown schematically in Figure 1-2. The trench side slopes at a ratio of 3:1. This design concept will evolve as the design for the ILAW disposal trench is developed.

Figure 1-2. RH Trench Preconceptual Design (dimensions are in meters).

RH TRENCH CONCEPTUAL MODEL

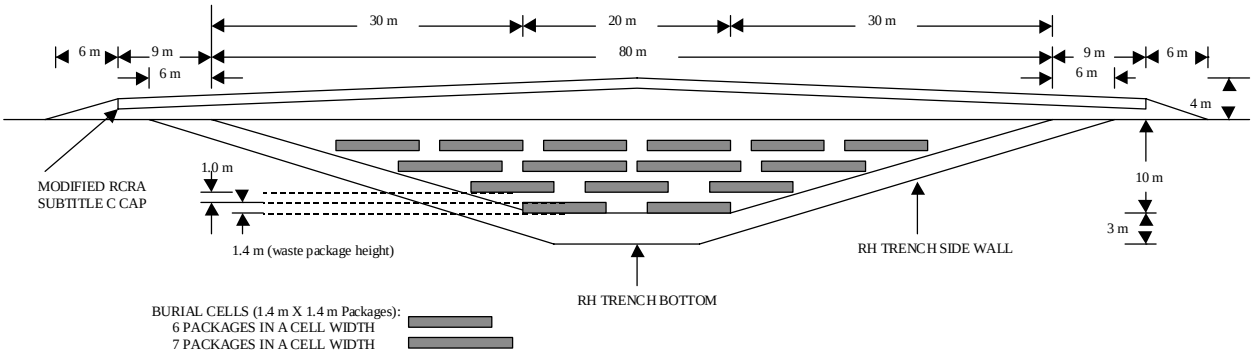

A cell is defined as a contiguous group of waste packages in a given layer. In the base case analysis, the waste package is a cube with each side of the cube being 1.4 m (DOE/BNFL 1998 - contract modification 10) (see Section 3.4.3). Although this is not the current design, the results for a sensitivity case using the new design are similar. Using this packing density, approximately six trenches are needed to accommodate the entire total ILAW production.

The disposal system will include a set of barriers. The exact nature will be determined during the design effort before closure. The present conceptual design consists of both subsurface and surface barriers. Subsurface sand-gravel capillary barriers would be placed over the cells to divert water around the cells to minimize infiltration. A surface barrier (presently seen as a modified RCRA Subtitled C barrier) to minimize water, plant, animal, and human intrusion would cap each disposal facility.

1.4 IMMOBILIZED WASTE PROGRAM

The ORP is the DOE organization at the Hanford Site responsible for the safe underground storage of the liquid waste from previous Hanford Site operations presently stored in the Hanford Site tank farms, the retrieval of this waste, the treatment of this waste into immobilized waste forms, the storage and disposal of the immobilized tank waste, and the closure of the underground tanks. The contractors working for the ORP form the River Protection Project (RPP). As part of the RPP, the Immobilized Waste Program is responsible for the following:

- Designing the facilities for disposal of the immobilized low-activity tank waste
- Obtaining necessary permits and regulatory approvals
- Constructing the disposal facilities
- Operating the disposal facilities
- Closing the disposal facilities
- Designing, constructing, using, and decommissioning of the facilities for storing the immobilized high-level waste until it is shipped to a federal geologic repository.

PA team is actively involved with all aspects of the Immobilized Waste Program

Table 1-1 presents the schedule for the disposal facilities. Figure 1-3 illustrates the current baseline planning logic for the Immobilized Low-Activity Disposal Project within the Immobilized Waste Program. The performance assessment activity is closely connected with other parts of the Immobilized Waste Program.

Table 1-1. Schedule for ILAW Disposal Facilities.

Description	Date
Issue engineering studies (Done)	October 1997
Issue conceptual design	September 2001
Issue Part B RCRA Permit Application to state regulatory authority	August 2002
Issue detailed design for first set of facilities	September 2004
Start construction of first set of facilities	April 2005
Complete construction of first set of facilities	July 2006
Start use of first set of facilities	March 2008
Fill first set of facilities	September 2018
Construct and use additional disposal facilities	...
Receive last container of waste	September 2026
Close last disposal facility	September 2028

The Immobilized Waste Program has established a performance assessment team of leading Hanford Site geotechnical and waste-form experts. The team is supported by Site staff (including the Pacific Northwest National Laboratory), as well as scientists and engineers from around the DOE complex (particularly from the Argonne National Laboratory). The leader of the performance assessment team has been on the decision board for preconceptual design studies and interacts with the engineering and architect-engineering staff on the design. In addition, the team is cooperating closely with the ORP group waste treatment services. Current specifications for the waste form are based heavily on performance assessment results. Future modifications to the waste form specifications, if necessary, will be based on what is learned in the performance assessment activity. Finally, the performance assessment team is closely involved in characterizing the waste inventory.

The performance assessment activity supports design, use, and closure of the disposal facilities. Thus, the schedule for producing performance assessment documents is iterative (see Table 1-2). Maintenance of the ILAW performance assessment is based on DOE guidance (DOE 1999e) and is documented in the *Maintenance Plan for the ILAW Performance Assessment* (DOE/ORP 2000a). This document was approved by the ORP field manager and sent to the LFRG as required (French 2000b).

Figure 1-3. Activities Diagram for the Immobilized Low-Activity Waste Project.

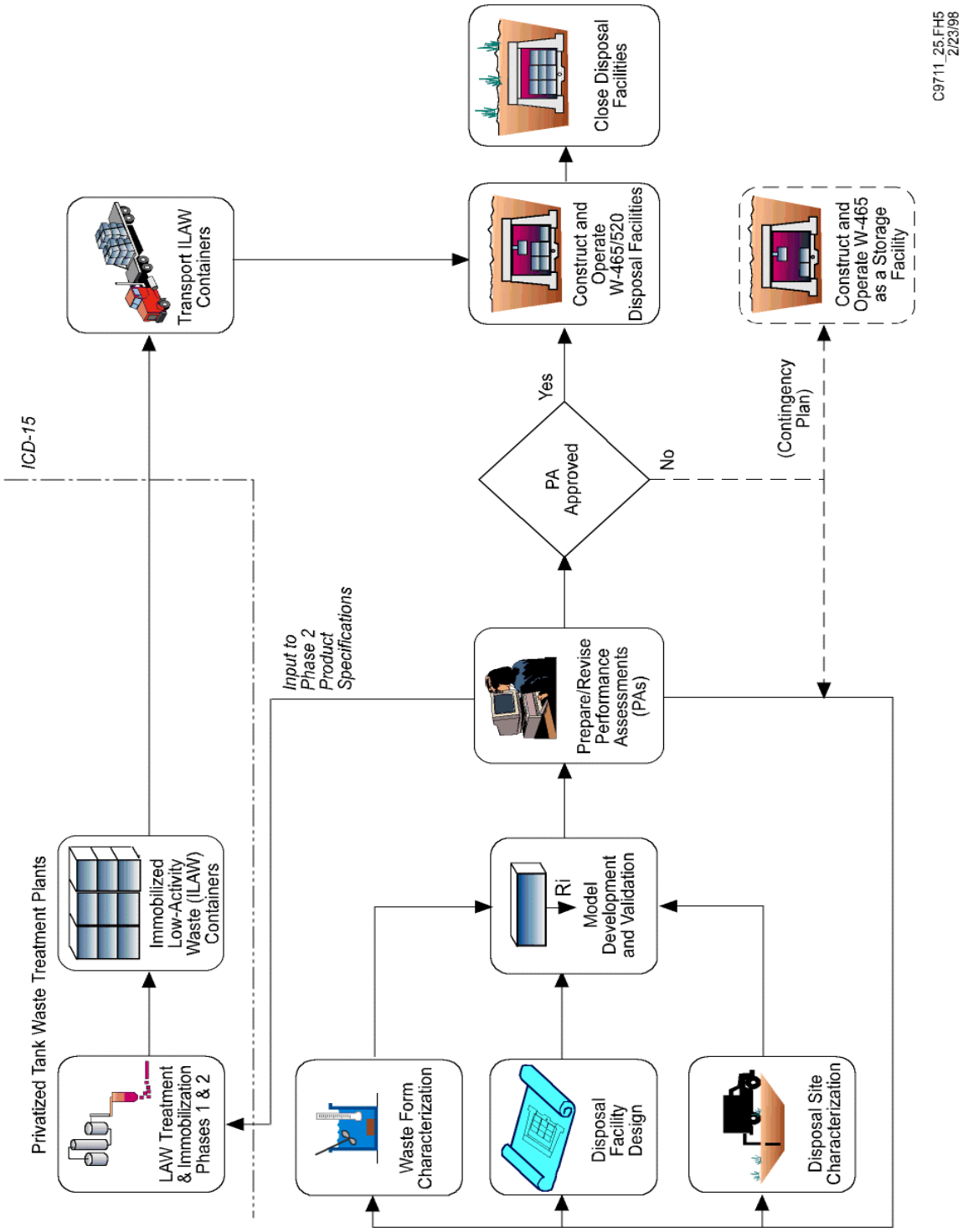

Table 1-2. Schedule for Performance Assessment Activities.

Revision	Purpose	Date of Issue
Interim Performance Assessment		
Rev. 0	Document potential impacts as early in project's life as possible.	September 1996
Rev. 1	Revise Rev. 0 based on comments, especially those of an external advisory board.	September 1997
Performance Assessment		
Rev. 0	Support application for Disposal Authorization Statement to modify existing disposal facilities, use existing disposal facilities, construct the first generation of new disposal facilities, and use the new disposal facilities.	March 1998
	Received conditional approval from the Low-Level Waste Disposal Facility Federal Review Group and a Disposal Authorization Statement from DOE.	October 1999
Rev. 1 (This document)	Update Rev. 0 based on results of waste form performance testing and simulations, geotechnical data collection and analysis, new facility design, and the RPP Standard Inventory effort.	March 2001
Rev. 2	Update Rev. 1 based on additional performance assessment activity data collection and analysis (just before start of operations).	September 2005
Rev. 3	Update Rev. 2 based on using actual inventories disposed in the existing facilities, additional data collection (especially waste performance of production samples), and engineering studies investigating the use of other Site facilities.	September 2010
Rev. 4	Update Rev. 3 using new data.	September 2015
Rev. 5	Update Rev. 4 using new data.	September 2020
Rev. 6	Update Rev. 5 using new data.	September 2025
Rev. 7	Update Rev. 6 to support closure of all immobilized low-activity waste disposal facilities.	September 2028

DOE = U.S. Department of Energy

As required by the maintenance plan, new site-specific, waste-form specific, and facility-specific data have been collected (Mann/Puigh 2000a). A *White Paper Updating the Conclusions of the 1998 ILAW Performance Assessment*, DOE/ORP-2000-07 (Mann 2000b) based on these new data was issued. The white paper determined that the conclusions of the 1998 ILAW PA were still valid, but that they were conservative. Based on the conclusions of the white paper, the ILAW PA annual summary (Mann 2000c) also was issued as required by the maintenance plan and by DOE guidance (DOE 1999f).

The goals of this performance assessment are to determine impacts from the following sources:

- Changes in disposal facility design
- Different waste form compositional space
- New geotechnical and other data.

The goals of the next ILAW PA version (scheduled for 2005) are to determine the impacts from new data so that these impacts can be considered before actual disposal operations begin. Even later performance assessments will focus on determining impacts before closure of individual trenches and before final closure.

1.5 RELATED DOCUMENTS

This section discusses the most important environmental assessments completed for the Hanford Site, as well as the documents used to provide guidance for preparing this document.

➔➔➔ See Sections 3.2 and 3.4 for documents justifying data used in this document.

➔➔➔ See Section 1.6 for documents supporting the setting of performance objectives.

1.5.1 Other Relevant Hanford Site Environmental Assessments

This document builds on earlier Hanford Site environmental assessments.

Many environmental assessments have been performed at the Hanford Site. They can be classified as documents pertaining to the disposal of immobilized low-activity tank waste, as documents fulfilling the requirements DOE O 435.1, or as more general documents.

1.5.1.1 Previous Work Related to the Proposed Disposal Action. A number of reports have been published on environmental aspects of ILAW disposal. As noted in Section 1.1, the 1998 ILAW PA was conditionally approved by the LFRG (DOE 1999d) and a Disposal Authorization Statement was issued (DOE 1999a). As required by the Disposal Authorization Statement, a maintenance plan for the ILAW PA was issued (DOE/ORP 2000a) and approved (French 2000b).

Monitoring (Horton 2000) and closure plans (Burbank 2000) were also issued and approved (Boston 2000a and Boston 2000b).

To support the 2001 version of the ILAW performance assessment, two auxiliary documents (*Data Packages for the Hanford Immobilized Low-Activity Tank Waste Performance Assessment: 20001 Version* [Mann/Puigh 2000a] and *Simulations for the 2001 ILAW PA* [Puigh 2001]) have been issued. Based on the data packages, a preliminary analysis of the ILAW disposal system performance was issued as *White Paper Updating the Conclusion of the 1998 ILAW Performance Assessment* (Mann/Puigh 2000b). This analysis was combined with other data required by the ILAW PA maintenance plan and issued as *Annual Summary of Immobilized Low-Activity Tank Waste (ILAW) Performance Assessment* (DOE/ORP 2000b) and sent to DOE/EM (French 2000c).

The 1998 ILAW PA (Mann 1998a) was described in Section 1.1. It used geotechnical data typical of the area in which the disposal facility will be located and waste form data based on procurement documents. The 1998 ILAW PA showed that a reasonable expectation exists that the public and the environment would be protected.

The first performance assessment on this disposal action was *Hanford Low-Level Tank Waste Interim Performance Assessment*, WHC-EP-0884, Rev. 0 (Mann 1996a) and WHC-EP-0884, Rev. 1 (Mann 1997a). These documents were designed to provide the best available analysis given limited project-specific data. The revision (Mann 1997a) was based on comments received on the initial interim performance assessment (Mann (1996a).

Data Packages for the Hanford Low-Level Tank Waste Interim Performance Assessment (Mann 1995a) and *Definition of the Base Analysis Case of the Interim Performance Assessment* (Mann 1995b) define the data used in the interim performance assessments. These document covering the data packages document (Mann 1995a) justify the values used in the analysis. The definition document (Mann 1995b) defines all data to be used in the interim performance assessment and the sensitivity cases studied.

Revisions 0 (Rawlins 1994) and 1 (Mann 1995d) of *Impacts of Disposal System Design Options on Low-Level Glass Waste Disposal System Performance* provided sensitivity analyses of the long-term environmental impact based on various design features for the low-level tank waste disposal facility. The first analysis was updated based on better data and on the comments received on Revision 0. Neither report is as comprehensive as a performance assessment.

1.5.1.2 Other Hanford Site Project-Specific Performance Assessments. This document also builds on the previous performance assessments prepared for the Hanford Site. These performance assessments were prepared under the requirements of the DOE Order 5820.2A, *Radioactive Waste Management* (DOE 1988a) for other Hanford Site disposal actions. All performance assessments prepared under DOE Order 5820.2A were reviewed for technical adequacy by the Peer Review Panel (established by the order). This panel performed a preliminary review, a completeness review, and a final review for each performance assessment. Then, DOE-Headquarters reviewed the documents and could approve the disposal action if the performance assessment satisfied the requirements of the DOE Orders.

The *Long-Term Performance Assessment of Grouted Phosphate/Sulfate Waste from N-Reactor Operations*, PNL-6512 (Stewart 1987), forms the basis of the environmental assessment (DOE 1986a) for the disposal of low-level radioactive waste generated by decontamination operations and other activities associated with N Reactor operations. The grouted phosphate-sulfate performance assessment predates the DOE approval process for performance assessments. The DOE review was conducted by reviewing the environmental assessment.

The *Performance Assessment of Grouted Double-Shell Tank Waste Disposal at Hanford* (Kincaid 1995) dealt with disposing of low-level liquid waste from the double-shell tanks. The waste was to be combined with cement, fly ash, and clay to form a grout that would cure and solidify in large subsurface vaults located to the east of the 200 East Area. The grout performance assessment was approved in principle by the Peer Review Panel (Wilhite 1994). DOE (Lytle 1995) found that the analysis performed in Kincaid (1995) was "technically adequate and provides reasonable assurance that the selected performance objectives would be met." However, noting that the grout project had been canceled, DOE also stated that a new or revised performance assessment would be needed for routine disposal of waste in the Grout Disposal Facility.

The *Performance Assessment for the Disposal of Low-Level Waste in the 200 West Area Burial Grounds* (Wood 1995a) dealt with the solid waste from operations at the Hanford Site and other DOE sites. This waste is placed into trenches in the western part of the 200 West Area then covered with a barrier. The Peer Review Panel found the performance assessment to be technically acceptable. The 200 West Area performance assessment has been "conditionally accepted" by DOE-Headquarters (Cowan 1996). The "conditions" referred to added documentation.

The *Performance Assessment for the Disposal of Low-Level Waste in the 200 East Area Waste Burial Grounds* (Wood 1996) addresses waste that is similar to that addressed in the 200 West Area performance assessment. However, the disposal trenches for this waste are in the northern part of the 200 East Area. The final performance assessment for this action also has been conditionally approved by DOE-Headquarters (Frei 1997).

A maintenance plan for these two performance assessments has been written. Annual summaries also have been submitted to LFRG. In addition, to satisfy a conditional requirement specified in the disposal authorization statement, a review of solid waste characterization

practices has been completed and accepted by the LFRG. The review was conducted to determine if these practices were adequate to support the evaluation of disposal facility performance relative to compliance with performance objectives. Waste characterization practices were found to be adequate and a report was issued to DOE Headquarters in June 2000.

The *Environmental Remediation Disposal Facility Performance Assessment* (Wood 1995b) was written to support disposal of waste generated by the cleanup of the Hanford Site. Most of this waste is expected to be contaminated soil. Trenches are planned to be the main means of disposal at the facility. Because the Environmental Remediation Disposal Facility is regulated under the *Comprehensive Environmental Response, Compensation, and Liability Act of 1980* (CERCLA), this performance assessment was not submitted to the Peer Review Panel. However, *A Remedial Investigation and Feasibility Study Report for the Environmental Restoration Facility*, DOE-RL-93-99 (DOE/RL 1994a), was written. A cross walk between this report and the requirements of DOE O 435.1 has recently been submitted for LFRG approval.

1.5.1.3 More General Hanford Site Environmental Assessments. A series of general environmental assessments also has been written for Hanford Site activities. These assessments look at the Hanford Site as a whole or address environmental impacts in a more general manner.

The *Composite Analysis for Low-Level Waste Disposal in the 200-Area Plateau of the Hanford Site*, PNNL-11800 (Kincaid 1998), was prepared in response to Recommendation 94-2 of the Defense Nuclear Facilities Safety Board to the Secretary of Energy (DNFSB 1994). The recommendation noted the need for a risk assessment that investigates the environmental impacts of all radioactive waste disposal actions or leaks at a DOE site. The authors of the composite analysis are working with the authors of the previous performance assessments to maximize consistency in data and methods. The first version of this analysis was reviewed along with the 1998 ILAW PA. The LFRG also conditionally approved the Composite Analysis in "Disposal Authorization Statement for the Hanford Site Low-Level Waste Disposal Facilities" (DOE 1999a) with comments more fully documented in *Low-Level Waste Disposal Facility Federal Review Group Manual* (DOE 1999c).

The *Environmental Impact Statement for the Tank Waste Remediation System* (TWRS EIS) (DOE 1996b) analyzed various options to manage the Hanford Site's tank waste with the record of decision issued shortly thereafter (DOE 1997b). Because of the scope of the TWRS EIS, the analyses relied on data less complete and less project-specific than this performance assessment. The record of decision covers the disposal of ILAW in the Hanford Site 200 Areas. The TWRS EIS was preceded by the Hanford Defense Waste EIS, *Final Environmental Impact Statement: Disposal of Hanford Defense High-Level Transuranic and Tank Wastes*, DOE/EIS-0113 (DOE 1987).

The *Draft Hanford Remedial Action Environmental Impact Statement and Comprehensive Land Use Plan*, DOE/EIS-0222-D (DOE 1996c), analyzed the potential impacts associated with establishing future land-use objectives for the Hanford Site. These impacts will come primarily from remediation activities. The document also proposes a land-use plan for near-future activities. TWRS activities were not extensively considered because they were part

of the EIS and land-use plan. Based on comments, the draft EIS was rewritten and issued as a land use plan EIS (DOE 1999h) with an associated record of decision (DOE 1999i).

1.5.2 Regulatory Agreements and Documents

The Tri-Party Agreement (Ecology 1998) is an agreement between DOE, the U.S. Environmental Protection Agency (EPA), and the Washington State Department of Ecology (Ecology) concerning the cleanup of the Hanford Site. The Tri-Party Agreement has legally enforceable milestones, some of which (the M90 series) cover the Immobilized Waste Program. Milestone M-90-05T (due in March 2002) was met when DOE submitted a copy of the 1998 ILAW performance assessment to Ecology for comment at the same time that DOE submitted the document to DOE Headquarters for approval.

The DOE has written the *Hanford Site Ground Water Protection Management Plan*, DOE-RL-89-12, Rev. 2 (DOE/RL 1995c), with Ecology's approval. However, the current version of the management plan does not address long-term protection of the groundwater resource.

1.5.3 Guidance Documents

The main documents guiding this performance assessment are as follows:

- *Format and Content Guide for U.S. Department of Energy Low-Level Waste Disposal Facility Performance Assessments and Composite Analyses* (DOE 1999e)
- *Maintenance Plan for the Immobilized Low-Activity Waste Performance Assessment Activity* (DOE/ORP 2000b)
- Comments on the 1998 ILAW PA by the Low-Level Waste Disposal Facility Federal Review Group (DOE 1999c)

The following additional documents also were used as guidance in preparing this performance assessment:

- *Critical Assumptions for Department of Energy Low-Level Waste Disposal Facility Assessments* (Alm 1997)
- *Issuance of Low-Level Waste Performance Assessment Guidance* (Frei 1996)
- *Performance Assessment Review Guide for Low-Level Radioactive Waste Disposal Facility*, DOE/LLW-93 (Dodge 1991)
- *Proceedings of the Department of Energy Performance Assessment Briefing, Denver, Colorado, October 29, 1991*, DOE/LLW-138 (NLLWMP 1992)
- *Performance Assessment Task Team Progress Report*, Revision 1, DOE/LLW-157 (Wood 1994)

- *A Compilation of DOE Performance Assessment Peer Review Panel Review Comments and Recommendations*, DOE/LLW-216 (RWTSP 1994).

- "DOE Headquarters Review of the *Performance Assessment of Grouted Double-Shell Tank Waste at Hanford*" (Lytle 1995)

- *Implementation Plan, Defense Nuclear Facilities Safety Board Recommendation 94-2, Compliance with Safety Standards at Department of Energy Low-Level Nuclear Waste Sites* (DOE 1996a)

Performance assessments from other DOE sites and the comments on those studies also are reviewed to understand different approaches and methods.

1.6 PERFORMANCE OBJECTIVES

1.6.1 Summary

The DOE's requirements for waste disposal (DOE 1999a) can be summarized as follows:

- Protect public health and safety
- Protect the environment.

The requirements for this performance assessment are the same as for the 1998 ILAW PA, except that comparisons at 1,000 years for the groundwater pathway and for non-radioactive hazardous compounds (hereafter referred to as chemicals in this Performance Assessment) have been added.

> The performance objectives are the same as for the 1998 ILAW PA. Time of compliance is 1,000 years for groundwater pathways, rather than 10,000 years. However, a comparison will be also be made at 10,000 years. In addition, this analysis includes chemicals.
>
> Most restrictive performance objectives are as follows:
>
> 1) Groundwater ($\beta\gamma$): 4 mrem in a year for 10,000 years
> 2) Intruder (continuous): 100 mrem in a year after 500 years

For this performance assessment, the following methods were used to establish the quantitative performance objectives as explained in *Performance Objectives of the Tank Waste Remediation Systems Low-Level Waste Disposal Program*, HNF-EP-0826 (Mann 1999a):

- Investigate all potentially applicable regulations, as well as interpretations made by the Peer Review Panel and the LFRG (Section 1.6.2)

- Work with Immobilized Waste Project management to establish their needs (Section 1.6.3)

- Work with the Hanford Site stakeholders to understand the values of residents in the Pacific Northwest (Section 1.6.4).

The manual (DOE 1999g –1) for DOE O 435.1 (DOE 1999b) provides performance objectives for a performance assessment as

(1)(a) "25 mrem in a year total effective dose equivalent from all exposure pathways"

(1)(b) "10 mrem in a year total effective dose equivalent " via the air pathway

(1)(c) "Release of radon shall not exceed 10 mrem in a year total effective dose equivalent"

(2)(g) "Include an assessment of impacts to water resources"

(2)(h) "The intruder analysis shall use performance measures for chronic and acute exposures, respectively, of 100 mrem in a year and 500 mrem in a year total effective dose equivalent."

(2)(b) "The point of compliance shall correspond to the point of highest projected dose or concentration beyond a 100 meter buffer zone surrounding the disposal waste."

(2) "Include calculations for a 1,000 year period after closure"

The proposed disposal action will also require concurrence from the U.S. Nuclear Regulatory Commission (NRC) on the waste classification of ILAW and a RCRA Part B permit. Therefore, additional constraints were considered in the establishment of the performance objectives used in the ILAW PAs.

The NRC has indicated that the ILAW would be considered "incidental waste" (Paperello 1997) if the following three conditions are met:

- DOE follows its program plan for separating and immobilizing the waste to the maximum extent possible that is technically and economically possible
- The wastes meet Class C standards of 10 *Code of Federal Regulations* (CFR) 61
- The performance assessments continue to indicate that public health and safety would be protected to standards comparable to those established by the NRC for the disposal of low-level waste.

The first two conditions are built into the current contract for the immobilization of LAW. Also, the 1998 ILAW performance assessment has shown that the public and safety are protected. As "incidental waste," the ILAW would not fall under the licensing authority of the NRC. This position does require the assessment of estimated impacts at 10,000 years after disposal site closure to make comparisons to standards established by the NRC.

Specifically, the RCRA concerns bring in the impacts of hazardous waste. The inorganic chemicals selected are based on a data quality objectives (DQO) process, while the organics are based on having the largest number of analytical detects from those organics identified in the DQO process (Wiemers 1998).

Therefore, as documented in Mann (1999a), these requirements have been merged into a unified set of performance objectives for the ILAW PA. Table 1-3 presents the performance objectives for radionuclides. Table 1-4 presents the performance objectives for chemicals identified as most important.

Table 1-3. Radiological Performance Objectives.

Protection of General Public and Workers [a, b]	
All-pathways dose from only this facility	25 mrem in a year [d, h]
All-pathways dose including other Hanford Site sources	100 mrem in a year [e, i]
Protection of an Inadvertent Intruder [c, f]	
Acute exposure	500 mrem
Continuous exposure	100 mrem in a year
Protection of Groundwater Resources [b, d, j]	
Alpha emitters	
^{226}Ra plus ^{228}Ra	5 pCi/L
All others (total)	15 pCi/L
Beta and photon emitters	4 mrem in a year
Protection of Surface Water Resources [b, g]	
Alpha emitters	
^{226}Ra plus ^{228}Ra	0.3 pCi/L
All others (total)	15 pCi/L
Beta and photon emitters	1 mrem in a year [k]
Protection of Air Resource [b, f, l]	
Radon (flux through surface)	20 pCi m^{-2} s^{-1}
All other radionuclides	10 mrem in a year

[a] All doses are calculated as effective dose equivalents; all concentrations are in water taken from a well. Values given are in addition to any existing amounts or background.

[b] Evaluated for 1,000 and 10,000 years, but calculated to the time of peak or 10,000 years, whichever is longer.

[c] Evaluated for 500 years, but calculated to 1,000 years.

[d] Evaluated at the point of maximum exposure, but no closer than 100 meters (328 feet) from the disposal facility.

[e] Evaluated at the 200 East Area fence (assumed future boundary of the DOE site).

[f] Evaluated at the disposal facility.

[g] Evaluated at the Columbia River, no mixing with the river is assumed.

[h] Main driver is DOE Orders on *Radioactive Waste Management* (DOE 1999b/g)

[i] Main driver is DOE Order 5400.5, *Radiation Protection of the Public and the Environment* (DOE 1993).

[j] Main driver is National Primary Drinking Water Regulations (40 CFR 141).

[k] Main driver is Washington State Surface Water Standards (WAC 173-201A)

[l] Main driver is National Emission Standards for Hazardous Air Pollutants (40 CFR 61H and 40 CFR 61Q).

Table 1-4. Performance Goals for Inorganic and Organic Materials.
(See Mann 1999a for Source of Performance Goals.)

Inorganics		
Chemical	Groundwater	Surface Waters
Ammonia (NH_3)	(a)	4.0 mg/L
Antimony (Sb)	0.006 mg/L	0.006 mg/L
Arsenic (As)	0.00005 mg/L	0.05 mg/L
Barium (Ba)	1.0 mg/L	2.0 mg/L
Beryllium (Be)	0.004 mg/L	0.004 mg/L
Cadmium (Cd)	0.005 mg/L	0.00077 mg/L
Chlorine (Cl)	250 mg/L	230 mg/L
Chromium (Cr)	0.05 mg/L	0.011 mg/L
Copper (Cu)	1.0 mg/L	0.0078 mg/L
Cyanide (CN)	0.2 mg/L	0.0052 mg/L
Fluoride (F-)	4.0 mg/L	4.0 mg/L
Iron (Fe)	0.3 mg/L	(a)
Lead (Pb)	0.05 mg/L	0.0015 mg/L
Manganese (Mn)	0.05 mg/L	(a)
Mercury (Hg)	0.002 mg/L	0.000012 mg/L
Nickel (Ni)	(a)	0.115 mg/L
Nitrate as N (NO_2)	10 mg/L	10 mg/L
Nitrite as N (NO_3)	1.0 mg/L	1.0 mg/L
Nitrite plus Nitrate	10 mg/L	10 mg/L
Selenium (Se)	0.01 mg/L	0.005 mg/L
Silver (Ag)	0.05 mg/L	(a)
Sulfate (SO_4)	250 mg/L	(a)
Thallium (Tl)	0.002 mg/L	(a)
Zinc (Zn)	5.0 mg/L	0.072 mg/L

Table 1-4. Performance Goals for Inorganic and Organic Materials. (See Mann 1999a for Source of Performance Goals.)

Organics			
CAS #	Constituent (a)	Groundwater	Surface Waters
56-23-5	Carbon tetrachloride	0.0003 mg/L	0.005 mg/L
67-66-3	Chloroform	0.007 mg/L	(a)
71-43-2	Benzene	0.001 mg/L	0.005 mg/L
71-55-6	1,1,1-Trichloroethane	0.003 mg/L	0.2 mg/L
75-09-2	Dichloromethane (Methylene Chloride)	0.005 mg/L	0.005 mg/L
79-00-5	1,1,2-Trichloroethane	0.005 mg/L	0.005 mg/L
79-01-6	1,1,2-Trichloroethylene	0.005 mg/L	0.005 mg/L
95-47-6	o-Xylene	0.7 mg/L	0.7 mg/L
100-41-4	Ethyl benzene	0.1 mg/L	0.1 mg/L
106-46-7	1,4-Dichlorobenzene	0.004 mg/L	0.075 mg/L
108-88-3	Toluene	1.0 mg/L	1.0 mg/L
127-18-4	1,1,2,2-Tetrachloroethene	0.005 mg/L	0.005 mg/L

(a) No entry in a cell indicates that no limit was found

1.6.2 Regulations and Other Performance Assessments

1.6.2.1 Introduction. Several Federal and State regulations potentially apply to how well the public health and safety and the environment must be protected. The following categories of requirements were reviewed for relevance to this proposed disposal action:

- Protection of the general public
- Protection for workers
- Protection of the inadvertent intruder
- Protection of groundwater resources
- Protection of surface water resources
- Protection of air resources.

Appendix B of Mann (1999a) lists the regulations that were reviewed and judged to be potentially relevant to this proposed disposal action. Some regulations and general environmental acts were judged not relevant to the performance assessment activity for one or more of the following reasons:

- Requirements are the responsibility of other participants in the Immobilized Waste Program (for example, ensuring compliance with the *National Environmental Policy Act* [NEPA]).

- Requirements are for different environmental actions (for example, the CERCLA).

- Requirements deal with general environmental concerns such as the protection of endangered species that are thought to be adequately covered for the long-term by the regulations presented here.

- Requirements are only at a preliminary stage and are likely to change, {e.g., the "Radiation Site Cleanup Regulation" [proposed Title 40 CFR Part 196] and "Environmental Radiation Standards for Management and Disposal of Low-Level Waste" [proposed 40 CFR Part 193] from the EPA}. The development of these requirements will be closely followed and the requirements will be incorporated as appropriate.

Performance assessments of low-level waste disposal in the DOE complex were reviewed also to identify any regulations relevant to this proposed disposal action. These assessments provide "case law" interpretations. Appendix C of Mann (1999a) lists the other performance assessments in the DOE complex, as well as their performance objectives.

In their review of the Interim Performance Assessment (Mann 1997a), in "Classification of Hanford Low-Activity Tank Waste Fraction," the staff of the NRC (Paperiello 1997) indicated that meeting the performance objectives in that performance assessment (which are the same as the ones in this document) would meet the performance objectives of the NRC regulations (10 CFR 61-3).

1.6.2.2 Protection of the General Public. For this assessment, the performance objective for the protection of the general public is 25 mrem (effective dose equivalent [EDE]) in a year. This value is used consistently in the regulations (DOE 1999b and 10 CFR 61-3) and was used in the past performance assessments. Although other methods are available for determining body dose, the EDE method was selected because regulations normally use this method. The location for compliance is at the point of maximal exposure, but not less than 100 m (328 ft) from the disposal facility (DOE 1999g).

The Defense Nuclear Facilities Safety Board (DNFSB 1994) noted that a member of the public could receive exposures from several sources at a DOE site. Guidance from DOE Headquarters (DOE 1996a) is that protection of the general public from multiple sources should be based on *Radiation Protection of the Public and the Environment*, DOE Order 5400.5 (DOE 1993-1). This order sets a limit of 100 mrem in a year from all sources. The interpretation of DOE Order 5400.5 places the point of compliance at the fence line of the future site. For the Hanford Site, this is considered to be a fence surrounding the present Hanford Site 200 Areas. The *Composite Analysis for Low-Level Waste Disposal in the 200-Area Plateau of the Hanford Site* (Kincaid 1998) shows compliance with this requirement.

Little guidance is provided on interpreting the as low as reasonably achievable (ALARA) guidance. The Immobilized Waste Program is integrating design and safety, including environmental considerations, into a single program to optimize the design and operation of the ILAW disposal facility. The iterative approach uses environmental and safety analyses of preconceptual designs (see Mann 1996a), followed by preliminary and detailed designs using the results of those analyses, followed by more complete environmental and safety analysis, such as successors to this document. Disposal facility components will be incorporated into the design whenever their inclusion significantly adds protection to human health or the environment.

As directed by DOE guidance, the compliance time for this performance assessment is 1,000 years. (The compliance time is the time starting 100 years from the present over which the predicted dose must remain below the performance objectives.) However, explicit comparisons also are made at 10,000 years to show compliance with NRC guidance. In addition, the calculation was carried out to 100,000 years for the base analysis case and to 20,000 years for the other sensitivity cases.

1.6.2.3 Protection for Workers. For this performance assessment, as for others performed under the DOE orders on radioactive waste management, no distinction is made between performance objectives for workers and for the general public. Because the protection requirements for the general public are more restrictive than those for the workers, the workers will be adequately protected. Protection for workers during construction and operations will be addressed in the safety analysis report that will be written for the Immobilized Waste Program.

1.6.2.4 Protection of the Inadvertent Intruder. The exposure limits for protecting a hypothetical inadvertent intruder are consistent with the regulations (DOE 1999b and 10 CFR 61-3) and with earlier performance assessments. (Appendix Tables B-2 and C-2, respectively, in Mann [1999a] give details). These limits are 500 mrem (EDE) for a one-time (acute) exposure and 100 mrem (EDE)/year for a continuous exposure. These limits are used in this performance assessment.

The compliance time for protecting an inadvertent intruder is defined differently from the compliance time for protecting the general public or the environment. The inadvertent intrusion compliance time differs slightly between regulations. Current DOE guidance (Alm 1997) is that active institutional control shall occur for at least 100 years, but notes that longer times can be used if justified. DOE intends to control the Hanford Site 200 Areas as long as necessary to protect the public. U.S. Department of Energy, Richland Operations Office (RL) directive 5820.2A (DOE/RL 1993) allowed a compliance time of 500 years if passive barriers and markers are used. The Hanford Site grout performance assessment (Kincaid 1995-1) used the 500-year compliance time based on the assumption that passive barriers and markers would be present. The performance assessments for the disposal of solid radioactive waste on the Hanford Site (Wood 1995a and Wood 1996) also use a compliance time of 500 years. This is consistent with the NRC requirement for Class C waste that inadvertent intruders be protected for 500 years (10 CFR 61-1).

Following the precedent of the other Hanford Site performance assessments, the 500-year compliance time was used in this assessment because passive barriers and markers are planned

for this proposed disposal action. Therefore, protection of an inadvertent intruder shall be considered met if the exposure limits are met at 500 years after closure. Calculations were run and results shown from 100 years to 1,000 years after the time of disposal to obtain the doses as a function of time.

1.6.2.5 Protection of Groundwater Resources. The protection level for groundwater is the most complicated requirement to determine. The level of protection for groundwater usually is based on its intended use. However, predicting future groundwater use is highly subjective given the long time frames involved in a performance assessment. The type of quantities being limited (decay rate and dose) differs in the various regulations. Moreover, different regulatory agencies approach protecting groundwater resources using different metrics. In addition, earlier DOE performance assessments have taken different approaches. The guidance under DOE O 435.1 is to use the Site groundwater protection management plan. However, the Hanford Site plan (DOE/RL 1995c) is silent on long-term protection of groundwater.

Previous performance assessments have generalized the requirements from the "National Primary Drinking Water Regulations," 40 CFR 141, for determining whether the disposal action met the groundwater protection requirement. The scenario used is based on a public drinking water system serving at least 25 people and located at least 100 m (328 ft) downstream from the disposal facility. The previous performance assessments set a limit for the total exposure at less than 4 mrem (EDE) in a year from all radionuclides for an individual drinking the water. The "National Primary Drinking Water Regulations," however, use the limit of 4 mrem in a year, not for all radionuclides, but for just beta and gamma emitters. The distance of 100 m from the disposal facility is given in *Manual for DOE O 435.1*, DOE M 435.1 (DOE 1999g), the DOE manual implementing DOE O 435.1. Four mrem (EDE) in a year was chosen for two reasons. First, the value corresponds to the risk-based limit found in the "National Primary Drinking Water Regulations." Also, for most of the radionuclides, the value is more restrictive (see Table B-3 of Mann 1999a) than the decay rate concentration limits specified in the Washington State regulations (WAC 173-200).

The requirements for alpha emitters are the same in both the Washington State (WAC 173-200) and Federal (10 CFR 141) regulations. Both regulations limit alpha emitters by decay rate concentration limits, not annual dose. In addition, both sets of requirements limit the same subsets of alpha emitters (^{226}Ra, total radium, and other) and set the same quantitative limits. These decay rate concentration limits (Table 1-3) are used for this performance assessment.

Washington State's requirements for beta emitters are based on screening levels previously used by the EPA. These screening levels were selected because the requirements are easily verified in the field. (The current EPA regulations are based on risk limitation.) The current state screening level ensures that, even for beta emitters emitting high-energy gamma radiation, the dose limit will be met. However, for low-energy beta emitters, the state screening level is overly conservative by a factor of about 100. This high degree of conservatism exists for radionuclides, such as ^{99}Tc, that are important in this performance assessment.

For this performance assessment, the Federal standards are used. This means that the current EPA regulation governing drinking water (40 CFR 141) is used to protect groundwater. The "National Secondary Drinking Water Standards" (40 CFR 143) were not used because they are stated only as goals. This follows the precedent set in the TWRS EIS (DOE 1996b), a joint publication of the Ecology and DOE. Thus, the performance objective is an EDE of 4 mrem in a year for beta and photon emitters and a concentration of 15 pCi/L for alpha emitters. Although uranium is not restricted by the regulations, for this analysis it is included under other alpha emitters. The values are displayed in Table 1-3. A dose of 4 mrem (EDE) in a year for 70 years corresponds to an incremental health risk of 0.0001 (EPA 1989b).

To ensure compliance with the intent of Federal and State groundwater regulations, the limits shown in Table 1-3 are applied to a well 100 m downgradient from the disposal facility for 10,000 years after closure, the same time of compliance as for protection of the general public. The hypothetical well from which the water is drawn is sized to be the minimum public drinking water system to serve 25 people. Further information is given in Section 3.4.7.2. The effects of placing the well at other locations (including the Hanford Site 200 Area fence line) also are determined.

1.6.2.6 Protection of Surface Water Resources. The thrust is the same of both the Federal (10 CFR 141) and State requirements (WAC 173-201A) for protecting surface water resources. The point of compliance is where the groundwater is predicted to reach the Columbia River. The concentration of radionuclides in the groundwater at the point where it enters the Columbia River should meet all the standards listed in Table 1-3.

The 1.0 mrem (EDE) dose in a year (one quarter of the EPA drinking water standard) value is selected because it meets the Washington State regulation while minimizing reporting requirements. The Washington State regulation (WAC 173-201A) mandates a dose limit that is the lesser of the EPA drinking water standard and the explicit limits for each radionuclide contained in the State regulation. For the major radionuclides of interest, the explicit limits (when converted to dose) are greater than 1.3 mrem in a year. Therefore, using 1.0 mrem in a year for the sum of all beta and photon emitters is restrictive in meeting this standard.

The compliance time for protecting surface water resources is selected as 1,000 years, the same compliance time as for protecting groundwater resources. However, the calculations are carried out to 10,000 years or to the time of maximum impact, if the peak occurs after 10,000 years.

1.6.2.7 Protection of Air Resources. Air emissions limits were taken from Parts H and Q of the "National Emissions Standards for Hazardous Air Pollutants" (40 CFR 61H and 40 CFR 61Q). These limits are more restrictive than the Washington State requirements (WAC 173-480 and WAC 246-247). Based on these standards, emissions (except radon) are limited to 10 mrem (EDE) in a year with radon emissions limited to 20 pCi/m^{2}s.

1.6.2.8 Chemical Objectives. The DOE O 435.1 (DOE 1999b) and its associated manual (DOE 1999g) cover only the management of radioactive waste. However, Chapter 1, Section 1, item 10 of the manual notes that mixed waste also is subject to the RCRA as amended. Because ILAW

may contain some materials regulated under RCRA and because the RCRA Part B permit for the disposal facility will be based on this analysis, performance objectives for chemicals were established. The 1998 ILAW PA did not address chemicals.

The determination of chemical objectives followed the same process as for radiological objectives (see Mann 1999a). That is, all relevant regulations were reviewed and the most restrictive limits were used. The chemicals included are ones based on the those identified by a data quality objectives (DQO) process (Wiemers 1998). This DQO process included Ecology.

1.6.3 Programmatic Requirements

The Immobilized Waste Program also has established other requirements. The project mandated that all waste to be disposed or stored in the facility shall meet NRC Class C concentration limits (10 CFR 61-2). This restriction will satisfy the NRC determination that the immobilized low-activity waste is not high-level waste and can be disposed as “incidental” waste (Paperiello 1997).

1.6.4 Public Involvement

Giving Hanford Site stakeholders an opportunity to affect the performance objectives of this proposed disposal action is important. The performance objectives and scenarios (WHC 1994a) were summarized for the stakeholders. The summary was sent to each member and alternate of the Hanford Advisory Board, to selected Hanford Site contractor employees, and to selected members of the DOE’s Peer Review Panel and Performance Assessment Task Team.

We received feedback from the stakeholders and have responded to their concerns. Copies of the performance objectives document (WHC 1994a) were sent to all who requested it. All comments received on either the summary or the performance objectives have been documented as an internal file. These comments and corresponding responses are available for review (Murkowski 1995).

A member of the Hanford Advisory Board, Todd Martin, also was a member of the external review board (see Appendix F.1 of Mann 19996a) that commented on the interim performance assessment and the performance assessment activity.

1.7 APPROACH AND MAJOR DATA SOURCES

This performance assessment is being performed early in the project life. Therefore a three-step approach is being taken:

- Perform forward calculations using a series of cases to understand the behavior of the disposal system
- Perform backward calculations using the best current data to establish requirements for the waste form and the disposal facility

- Perform forward calculations to show that such requirements can be "reasonably expected" to be met without heroic efforts.

The first set of calculations is built around a base analysis case that reasonably describes our understanding of the system components and how they will interact. This step starts with the known conditions and estimates the impacts from those conditions (i.e., a forward calculation). These calculations are supplemented by simulations built on a series of sensitivity cases to determine the robustness of the results from the base analysis case and to develop an understanding of the important features and parameters of the disposal system.

Based on this understanding, a set of relatively simple equations can be derived (See Section 7.6) that represents the important quantities of the system which drive the environmental and human impacts. The second set of calculations then back calculates these equations to set restrictions on the most important parameters involved in waste form performance and facility design.

Having such requirements then allows a final set of calculations to show whether engineered solutions exist that can meet these requirements. Because this performance assessment is being done early in the life of the program, the actual engineered solutions may differ, but the engineered solutions actually used should be better (e.g., more cost effective, perform better) than the ones used here to show compliance.

Because of the long time frames involved in this analysis, estimates of impacts require computer simulations, rather than direct observations. The models used in the analyses are very flexible and should be adequate to describe the evolving features of the disposal system. However, because this analysis is performed early in the project life, many of the data are taken from related Hanford Site projects.

The major sources of information for the base analysis case are present in Table 1-5. Sensitivity cases (See Section 3.5.5) were performed to determine the impact of uncertain data. Among the most important uncertain data were the following:

- Contaminant release from waste form,
- Facility layout and design
- Groundwater flows
- Infiltration.

➔➔➔ See Section 3.3.5 for the definition of sensitivity cases.

Table 1-5. Major Sources of Information for the Base Analysis Case. (Significant differences with the 1998 ILAW PA are shown in italics.)

Data Type	Major Source	Data Base Reference
Location	The new facilities are just southwest of the PUREX Facility (in the 200 East Area).	Rutherford 1997
Waste Form	Waste package design based on early BNFL, Inc. documentation and River Protection Project planning.	Puigh 1999; also in Mann/Puigh 2000a Appendix I
Inventory	*Based on best basis **i**nventory estimates (calculated from modeling Hanford Site production reactors corrected for offsite transfers, and discharges to the ground and biased to tank measurements).* ***ASSUMED** separations into high- and low-activity fractions, and off-gas generation.*	*Wootan 1999; also in Mann/Puigh 2000a Appendix H*
Long-term waste form performance	*Based on data collected on BNFL, Inc. relevant glass formulations.*	*McGrail 2001; McGrail 1999; also in Mann/Puigh 2000a and 2001 as Appendix K*
Disposal facility design	***ASSUMED** from preconceptual ideas for the remote handled trench and conceptualy design for the concrete vault.*	*Puigh 1999; also in Mann/Puigh 2000a Appendix I*
Recharge	Estimates were derived from lysimeter and tracer measurements collected by the ILAW PA activity and by other projects combined with a modeling analysis.	Fayer 1999; also in Mann/Puigh 2000a Appendix J
Geotechnical	*Taken from geotechnical measurements studies of ILAW site borehole and other locations in the Hanford Site 200 East Area.*	*Khaleel 1999, Meyer 1999, and Kaplan 1999; also in Mann/Puigh 2000a Appendices L, M, and N, respectively*
Exposure	Taken from past Hanford Site documents and experience and DOE O 435.1 direction.	Rittmann 1999; also in Mann/Puigh 2000a Appendix O

Table 1-5. Major Sources of Information for the Base Analysis Case. (Significant differences with the 1998 ILAW PA are shown in italics.)

Data Type	Major Source	Data Base Reference

DOE = U.S. Department of Energy
ILAW = immobilized low-activity waste
PA = performance assessment
PUREX = plutonium-uranium extraction (facility)

Future performance assessments will be issued as new information about the waste form, its inventory, the design of the disposal facility, and site characterization is collected and as these factors are better understood.

1.8 STRUCTURE OF THIS PERFORMANCE ASSESSMENT

This performance assessment is divided into nine chapters and eight appendices. The appendices provide additional detailed information about topics presented in the chapters. This section summarizes the contents of each of chapter and appendix.

- Chapter 2 describes the Hanford Site environment, the waste characteristics, and the waste disposal system.
- Chapter 3 covers the methods used to assess system performance, including the radionuclide transport pathways and exposure scenarios. It also discusses the assumptions used in modeling system performance.
- Chapter 4 presents and integrates results from the transport and exposure models used to estimate the potential consequences of long-term contaminant release from the disposal vaults.
- Chapter 5 presents the results from the inadvertent intruder analyses.
- Chapter 6 interprets disposal facility performance with respect to the performance objectives defined in Chapter 1, sets waste acceptance criteria and disposal facility requirements, shows that these requirements can be “reasonably expected” to be met, and discusses further work associated with the performance assessment activity.
- Chapter 7 outlines the quality assurance procedures used in the performance assessment activity.
- Chapter 8 contains brief resumes of contributors to the document.
- Chapter 9 lists the cited references.

- Appendix A contains the LFRG comments on the 1998 ILAW PA and their resolution.
- Appendix B contains dosimetry data factors used in the analysis.
- Appendix C contains the equations used in the major codes.
- Appendix D presents detailed results of the analysis.
- Appendix E contains the program plan to establish the expected long-term contaminant release rates from vendor-supplied waste forms.
- Appendix F contains quality assurance information.

2.0 DISPOSAL FACILITY DESCRIPTION

2.1 OVERVIEW

This chapter explains the expected environment within the region and around the immobilized low-activity tank waste disposal facilities, probable waste retrieval and immobilization methods, and likely design, operating, and closure concepts for the disposal facilities. It covers the following topics.

Hanford Site Characteristics (Section 2.2). Regional and local geography; demography, including future land use; climate, geology, hydrology, soils, ecological and biotic conditions; and natural background radiation.

Waste Characteristics (Section 2.3). Current waste storage in underground tanks and plans for retrieving the waste, separating it into high- and low-activity fractions, and immobilizing the low-activity fraction, including packaging and certification.

Disposal Technology (Section 2.4). The current concepts on disposal units, waste handling and interim storage operations, waste emplacement, disposal unit closure and stabilization, and site closure.

Disposal site-specific information has been collected since the last ILAW performance assessment (Mann 1998a). This information has been compiled into a database (Mann/Puigh 2000a) used for the analyses to be provided in this revision of the ILAW performance assessment. Some summary information has been included in this document. For a more complete description of this new information, the reader should review Mann/Puigh (2000a).

2.2 HANFORD SITE CHARACTERISTICS

This section describes the regional and local environment in which the immobilized low-activity tank waste disposal facilities will be located. Extensive research has been done on the physical characteristics of the Hanford Site. In addition, significant new data have been accumulated since the last ILAW PA (Mann 1998a) for the ILAW disposal sites (Mann/Puigh 2000a).

2.2.1 Geography of the Hanford Site

The Hanford Site is a 1450-km^2 (560-mi^2) area of semiarid land located in south-central Washington State. The Hanford Site is owned by the U.S. Government and restricted to uses approved by the DOE. Figure 2-1 shows the Hanford Site in relation to the rest of the state. It also identifies the major cities in the region, Seattle, Portland, and Spokane, all of which are over 160 km (100 mi) from the Hanford Site.

Figure 2-1. Hanford Site in Washington State.

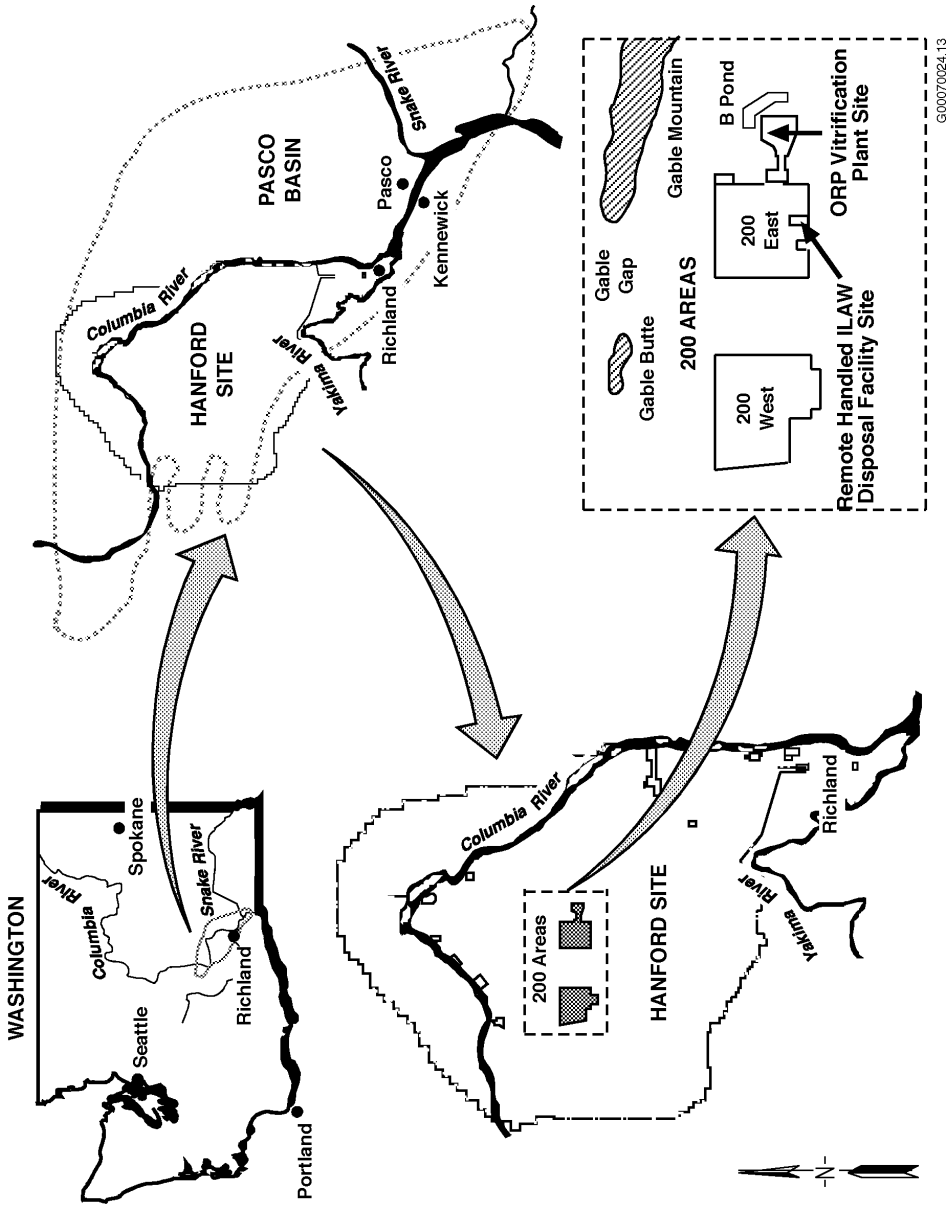

The major features of regional geography are the nearby rivers and mountains. The Columbia River, which forms the eastern boundary of the Hanford Site, is an important source of water and hydroelectric power for the region. Other important rivers near the Hanford Site are the Yakima River to the southwest and the Snake River to the east. The Cascade Mountains, which are about 160 km (100 mi) to the west, have an important effect on the climate of the area, which is discussed in Section 2.2.5.

Figure 2-2 shows the Hanford Site. The DOE is planning to release some of the Hanford Site land for uses found in the *Final Hanford Comprehensive Land-Use Plan Environmental Impact Assessment* (DOE 1999h) and its associated record of decision (DOE 1999i). The areas planned for release are the area north of the Columbia River and the Fitzner/Eberhardt Arid Lands Ecology Reserve southwest of State Highway 240. This land now is part of the Hanford Reach National Monument (Clinton 2000).

Figure 2-2. Hanford Site Map Showing Public Highways and Future Site Boundary.

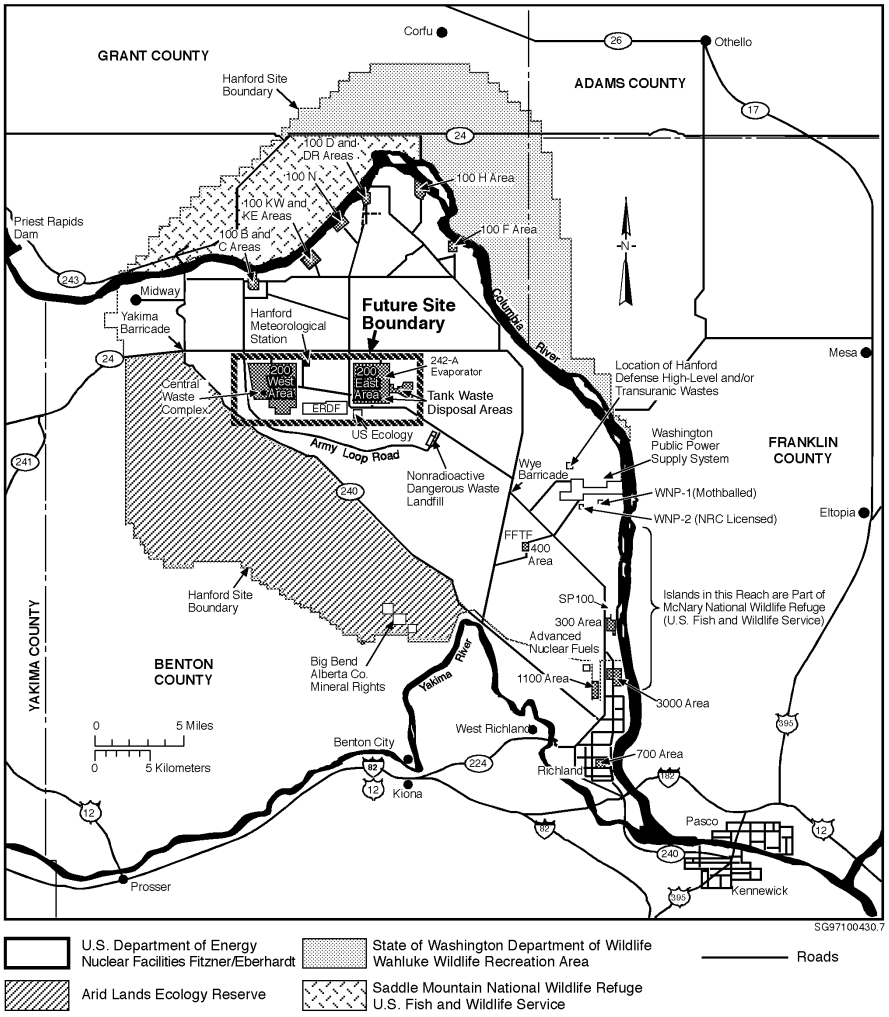

The 200 Areas, where the tank waste is located, are in the center of the Hanford Site. Just south of the 200 Areas is land used by U.S. Ecology, Inc., for commercial low-level radioactive waste disposal.

As discussed more fully in Section 2.2.4.3, the *Final Hanford Comprehensive Land Use Plan Environmental Impact Statement* (DOE 1999h) has defined the future site boundaries as just outside of the 200 Area boundaries, as shown in Figure 2-2.

2.2.2 Location of Disposal Sites

The ILAW Disposal Area is in the south central part of the 200 East Area of the Hanford Site.

Historically, two sites have been considered for disposal of immobilized low-activity tank waste (ILAW) (Shade 1997): the four existing TWRS disposal vaults, and the ILAW disposal site (Rutherford 1997). Figure 2-3 shows the two potential disposal areas. The four existing TWRS disposal vaults are located at the eastern edge of the Hanford Site 200 East Area (Burbank 1996, Burbank 1997). The vaults are just east of the AP Tank Farm and at the western edge of the Tank Waste Vitrification Area. These vaults originally were constructed for the disposal of double-shell tank waste in a grouted waste form. New facilities are located in the south-central part of the 200 East Area between existing office structures and the PUREX fuel reprocessing facility. The location of the new facilities was chosen (Rutherford 1997) for the following three reasons (Shord 1995):

- The location is near existing tank farms
- Unused land is available
- The location is inside the fence line of the 200 Areas.

The current planning (Taylor 1999a) is to use the ILAW disposal site for the disposal of all ILAW waste. The ILAW Disposal program also may use the existing disposal vaults, if needed.

2.2.3 Demography

Demographic data are used in a performance assessment to help set the scenarios and select the dosimetry parameters. This section describes the current population database, area socioeconomics, past and planned DOE activities, and the results of an investigation of future uses conducted by the Hanford Future Site Uses Working Group.

Figure 2-3. Activities in the 200 Areas. The plan area for ILAW disposal is located in the south central part of the 200 East Area and is labeled "New Disposal Area".

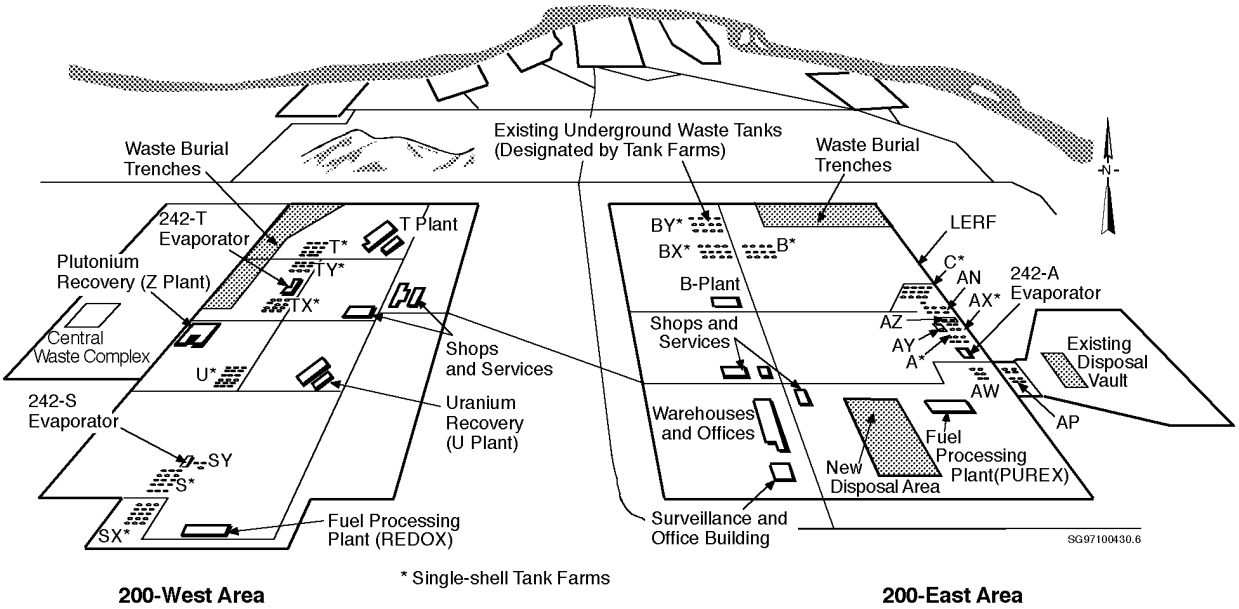

The major population centers within 80 km (50-mi) of the Hanford Site are identified in Figure 2-4, along with populations based on the 1990 U.S. Bureau of Census estimates (DOC 1991). This radius is centered on the Hanford Meteorology Station (HMS), located between the 200 East and 200 West Areas. The Tri-Cities (Richland, Kennewick, and Pasco), southeast of the Site, is the largest population center close to the Hanford Site. Other major population centers include Yakima and the Yakima Valley towns and Moses Lake in Washington to the west and north, respectively, and Umatilla and Hermiston in Oregon to the south. The cities of Ellensburg and Walla Walla, Washington lie just beyond the 80 km (50-mi) radius. Portions of Benton, Franklin, Adams, Grant, Kittitas, Yakima, Klickitat, and Walla Walla counties in Washington and Morrow and Umatilla counties in Oregon lie within the 80 km (50-mi) radius.

The year 2000 population estimates for Washington State (OFM 2000), as summarized in *Hanford Site National Environmental Policy Act (NEPA) Characterization* (Neitzel 2000-1), are used. The population in Benton County was approximately 140,000 in 2000, compared to 112,560 in 1990. Approximately 37,190 people reside in Richland; 53,270 people reside in Kennewick; and 15,235 people reside in West Richland, Benton City, and Prosser. The approximate population in the unincorporated portions of the county is 35,005. The estimated population of Franklin County was 45,900 in 2000, compared to 37,473 in 1990, with 27,370 people living in Pasco, 15,110 people living in other incorporated areas, and 17,600 people living in unincorporated areas. Benton and Franklin Counties accounted for approximately 3 percent of Washington State's population (OFM 1999).

Figure 2-4. Population Centers Within an 80-km Radius of the Hanford Site. Populations shown are based on 1990 census (DOC 1991).

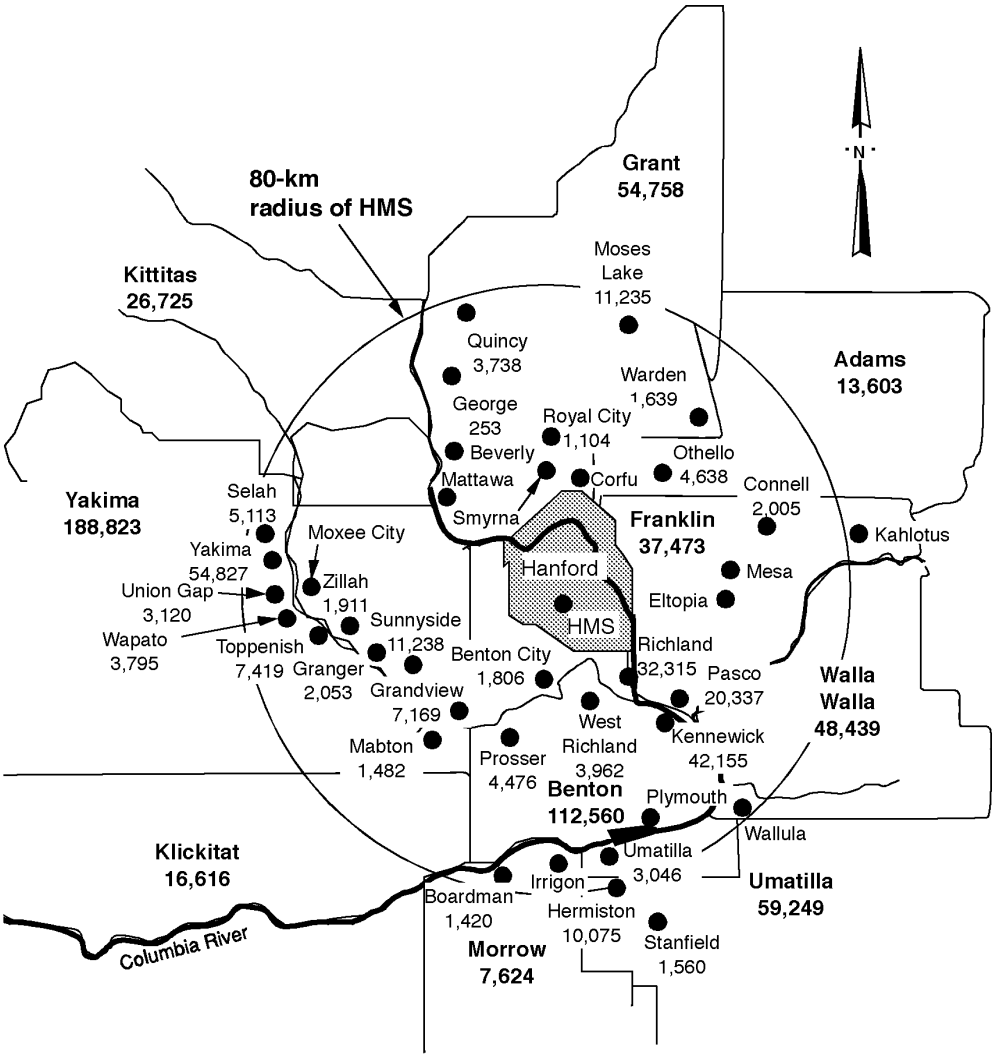

2.2.4 Land and Water Use

Land and water use information are used in a performance assessment to help set the scenarios and select the dosimetry parameters. This section describes area socioeconomics, past and planned DOE activities, and the results of an investigation of future uses conducted by the Hanford Future Site Uses Working Group.

2.2.4.1 Socioeconomics. The major employers in the Tri-Cities area since 1970 have been the DOE and the Hanford Site contractors; Energy Northwest (formerly the Washington Public Power Supply System), which operates a nuclear power plant; agriculture; and a large food-processing industry; plus several smaller industrial operations. Other than DOE activities, agriculture and food processing are the dominant industries. The socioeconomics of the area surrounding the Hanford Site are more fully described in Section 4.6 of Neitzel (2000-2).

The land use classification around the Hanford Site varies from urban to rural. Most of the land south of the Hanford Site is urban, including the Tri-Cities, while much of the land to the north and east is irrigated crop land. Most of the irrigation water comes from the Bureau of Reclamation's Columbia Basin Project, which uses the water behind Grand Coulee Dam as the primary water source. The water is transported via canals to the areas north and east of the Columbia River. The land to the west of the Hanford Site is used for irrigated agriculture near the Yakima River and dry-land farming at the higher elevations.

The area rivers are used as sources of irrigation and drinking water, as major sources of power production for the western United States, as primary salmon spawning grounds as well as for recreation. The Hanford Reach was designated as a national monument in 2000 (Clinton 2000).

2.2.4.2 Past and Future DOE Activities at the Hanford Site. In 1943, the U.S. Army Corps of Engineers created the Hanford Site from small farming areas along the Columbia River to locate facilities used to produce nuclear weapon materials for fighting World War II. Since then, the major activities on the Hanford Site have been controlled by the DOE and its predecessors, the U.S. Atomic Energy Commission (1945-1975), and the Energy and Research Development Administration (1975-1976). Current major programs at the Hanford Site are dedicated to waste management, environmental restoration, long-term stewardship, and research and development.

The DOE nuclear facilities occupy about 6 percent of the Site's total available area. The major operating areas, as shown in Figure 2-2, are identified by numbers: 100 Areas, 200 Areas, 300 Area, and 400 Area. The activities conducted in these areas are described in the following paragraphs.

100 Areas. The 100 Areas, directly bordering the Columbia River (Figure 2-2), contain nine graphite-moderated plutonium production reactors, eight of which were shut down by the early 1970's. The ninth is the N Reactor, the first dual-purpose reactor built in the United States. N Reactor began operating in 1963 and was shut down in 1986.

200 Areas. Fuel reprocessing, plutonium and uranium separation, plutonium finishing, and waste management, including treatment, storage, and disposal activities, were conducted in the 200 Areas. Waste from the research and development activities and fuel fabrication activities in the 300 Area, reactor operation programs conducted in the 100 Areas, and the Fast Flux Test Facility (FFTF) in the 400 Area is sent to the 200 Areas for storage and disposal. Waste management activities are scheduled to continue until the mid 21st century. Waste management facilities are located in the 200 Areas, which are surrounded by security fencing (Figure 2-2). The following major facilities are located in the 200 Areas (see Figure 2-3):

- Burial trenches
- Eighteen underground storage tank farms (the A, AN, AP, AW, AX, AY, AZ, B, BX, BY, C, S, SX, SY, T, TX, TY, and U tank farms)
- Very large fuel processing and recovery facilities (B, T, U, and Z Plants and the Reduction-Oxidation [REDOX] and Plutonium Uranium Extraction [PUREX] facilities)
- Tank waste water evaporator facilities (the 242-A, -S, and -T Evaporators)
- Office and warehouse buildings.

Many of these facilities are inactive. The Canister Storage Building was built recently just west of B Plant to store spent nuclear fuel from N Reactor. The Canister Storage Building will also be outfitted to store the immobilized high-level tank waste fraction.

Between and just south of the 200 East and West Areas is the Environmental Remediation Disposal Facility (ERDF) (see Figure 2-2). This trench system will hold most of the contaminated soil and materials from facility decontamination and decommissioning and Hanford Site remediation.

A 3.9 km^2 (1.5-mi^2) parcel located between the 200 West and East Areas is leased to Washington State. A portion of this land is subleased to U.S. Ecology, Inc., a private company, for the disposal of commercially generated low-level radioactive waste.

400 Area. The Fast Flux Test Facility (FFTF) is located in the 400 Area. This facility contains a liquid-metal cooled fast reactor previously used for testing breeder reactor fuels, materials, and components. The FFTF operated until 1992 and now is in standby mode.

A 4.4 km^2 (1.7 mi^2) parcel northeast of the 400 Area is leased to Energy Northwest (formerly the Washington Public Power Supply System) for commercial nuclear power reactors. The Columbia Generating Station (CGS), a boiling-water reactor, currently is the only operating nuclear reactor on the Hanford Site. Construction of two pressurized-water reactors (WNP-1 and WNP-4) will not be completed.

300 Area. Originally, the 300 Area was dedicated to fabricating fuel for Hanford Site reactors. Now, the 300 Area laboratories constructed over the last 30 years are used for research programs.

2.2.4.3 Future Hanford Use. In 1992, DOE, EPA, and Ecology gathered a group of stakeholders to study potential future uses for the Hanford Site land. This Hanford Future Site Uses Working Group issued a summary (HFSUWG 1992a) and a detailed report (HFSUWG 1992b) of its findings. The *Final Hanford Comprehensive Land Use Plan Environmental Impact Statement* (DOE 1998h) is heavily based on the work of the Hanford Future Site Uses Working Group. However, DOE's land use planning extends for only 50 years instead of the 100 years forecast by the working group.

HFSUWG (1992a-1) contains the following statement about near-term use of the 200 Areas, called the Central Plateau in the report.

> *"The presence of many different types of radionuclides and hazardous constituents in various forms and combinations throughout the site poses a key challenge to the Hanford cleanup. To facilitate cleanup of the rest of the site, wastes from throughout the Hanford site should be concentrated in the Central Plateau waste storage, treatment, and disposal activities in the Central Plateau should be concentrated within this area as well, whenever feasible, to minimize the amount of land devoted to, or contaminated by, waste management activities. This principle of minimizing land used for waste management should specifically be considered in imminent near-term decisions about utilizing additional uncontaminated Central Plateau lands for permanent disposal of grout."*

The report continues on the subject of future use options (HFSUWG 1992a-2),

> *"In general, the Working Group desires that the overall cleanup criteria for the Central Plateau should enable general usage of the land and groundwater for other than waste management activities in the horizon of 100 years from the decommissioning of waste management facilities and closure of waste disposal areas."*

Based on conversations of the working group, they could not agree on a definition of "general use." For the "foreseeable future" the working group developed options involving waste treatment, storage, and disposal of DOE low-level radioactive waste. The differences among the options are whether offsite waste (radioactive and/or hazardous) would be allowed to be disposed on the Hanford Site.

Finally (HFSUWG 1992a-3) says

> *"The working group identified a single cleanup scenario for the Central Plateau. This scenario assumes that future uses of the surface, subsurface and groundwater in and immediately surrounding the 200 West and 200 East Areas would be exclusive. Surrounding the exclusive area would be a temporary surface and subsurface exclusive buffer zone composed of at least the rest of the Central Plateau. As the risks from the waste management activities decrease, it is expected that the buffer zone would shrink commensurately."*

For nearer term land use planning, the record of decision (DOE 1999i) for the *Final Hanford Comprehensive Land-Use Plan Environmental Impact Statement* (DOE 1999h) identifies near-term land uses for the Hanford Site. The record of decision proscribes the use in the 200 Areas as exclusively industrial (primarily waste management) with much of the surrounding land having the use of preservation or conservation. In the past year, the Hanford Reach National Monument (Clinton 2000) was established along the river corridor as well in lands at the northern and western edges of the site.

However, no formal land use planning is expected to be accurate over the hundreds to hundreds of thousands of years covered in this analysis.

2.2.5 Climate and Meteorology

The information in this section is taken from *Hanford Site National Environmental Policy Act (NEPA) Characterization*, PNNL-64415, Rev. 12, Section 4.1 (Neitzel 2000-3.)

2.2.5.1 Summary. Local and regional climate patterns and projections must be considered when estimating the effect of water on the disposal system. Both total precipitation and seasonal frequency are important. Potential long-term climatic conditions must be projected to evaluate future climate changes that might cause higher precipitation rates or glaciation. Climate also affects the potential for flooding.

The climate of the Pasco Basin (where the Hanford Site is located) can be classified as midlatitude semiarid or midlatitude desert, depending on the climatological classification system being used. Large diurnal temperature variations are common, resulting from intense solar heating and nighttime cooling. Summers are warm and dry with abundant sunshine. Daytime high temperatures in June, July, and August can exceed 40 °C (104 °F). Winters are cool with occasional precipitation that makes up about 44 percent of the yearly total. During the winter, outbreaks of cold air associated with modified arctic air masses can reach the area and cause temperatures to drop below -18 °C (0 °F). Overcast skies and fog occur during the fall and winter months.

The Cascade Mountain Range greatly affects the temperature, wind, and precipitation in the region. Air masses that reach the Pasco Basin are changed as they pass over the region's relatively complex topography. The mountains limit the Pacific Ocean's maritime influence, making the climate of Eastern Washington drier with greater temperature extremes than the coast. In addition to this rain shadow effect, the Cascades are a source of cold air drainage, which has a considerable effect on the Site's wind regime.

The rest of this section summarizes the modern climate patterns in the Hanford Site area, the regional climate patterns of the recent past, and the possible future changes.

2.2.5.2 Current Data. Climatological data are available from the Hanford Meteorological Station (HMS), located between the 200 East and 200 West Areas at about 215 m (705 ft) elevation (See Figure 2-2). Data have been collected at this location since 1945. Temperature and precipitation data also are available from nearby locations for the period from 1912 through 1943. Data from the HMS are representative of the general climatic conditions for the region and describe the specific climate of the 200 Areas. The most recent summary is *Hanford Site Climatological Data Summary 1999 With Historical Data*, PNNL-13117 (Hoitink 2000).

Daily maximum temperatures vary from a normal maxima of 2°C (35°F) in late December and early January to 35°C (95°F) in late July. On the average, 52 days during the summer months have maximum temperatures of 32°C (90°F) or higher and 12 days with maxima

of 38°C (100°F) or higher. From mid-November through early March, minimum temperatures average ≤0°C (32°F), with the minima in late December and early January averaging -6°C (21°F). During the winter, on average, 3 days have minimum temperatures of -18°C (~0°F) or lower; however, only about 1 winter in 2 experiences such temperatures. The record maximum temperature is 45°C (113°F), and the record minimum temperature is -31°C (-23°F). The highest winter monthly average temperature at the HMS was 6.9°C (44°F) in February 1958, while the record lowest average temperature was -11.1°C (12°F) during January 1950. The record maximum summer monthly average temperature was 27.9°C (82°F) in July 1985, while the record lowest average temperature was 17.2°C (63°F) in June 1953.

Between 1946 and 1998, annual precipitation at the HMS averaged 16 cm (6.3 in.) and varied between 7.6 cm and 31.3 cm. The wettest season on record was the winter of 1996-1997 with 141 mm (5.4 in.) of precipitation; the driest season was the summer of 1973 when only 1 mm (0.03 in.) of precipitation was measured. Most precipitation occurs during the winter, with more than half of the annual amount occurring from November through February. Days with more than 13 mm (0.5 in.) precipitation occur on average less than once each year. Rainfall intensities of 13 mm/h (0.5 in./hr) persisting for 1 hour are expected once every 10 years. Rainfall intensities of 25 mm/h (1 in./hr) for 1 hour are expected only once every 500 years.

About 38 percent of the precipitation during December through February falls as snow. Winter monthly average snowfall ranges from 0.8 cm (0.3 in.) in March to 13.5 cm (5.3 in.) in January. Only one winter in four is expected to accumulate as much as 15 cm (5.9 in.) of snow on the ground. During these winters, four days, on average, have 15.2 cm (6.0 in.) or more of snow on the ground. However, the 1964-1965 winter had 35 days with snow on the ground, 32 of which were consecutive. That winter also provided one of the deepest accumulations, with 31 cm (12 in.) of snow occurring in December 1964. The record accumulation of snow is 62.2 cm (24.5 in.) in February 1916.

Prevailing wind directions on the 200 Area Plateau are from the northwest in all months of the year. Secondary maxima occur for southwesterly winds. Summaries of wind direction indicate that winds from the northwest quadrant occur most often during the winter and summer. During the spring and fall, the frequency of southwesterly winds increases with a corresponding decrease in northwest flow. Winds blowing from other directions (e.g., northeast) display minimal variation from month to month. Monthly average wind speeds are lowest during the winter months, averaging 10 to 11 km/hr (6 to 7 mi/hr), and highest during the summer, averaging 13 to 15 km/hr (8 to 9 mi/hr). Wind speeds that are well above average are usually associated with southwesterly winds. However, the summertime drainage winds are generally northwesterly and frequently reach 50 km/hr (30 mi/hr). These winds are most prevalent over the northern portion of the Hanford Site.

This climate profile suggests opportunities for moisture infiltration or recharge. This infiltration is centered around the frequency of precipitation during the winter months when evaporation is low and plant uptake and transpiration are minimal.

2.2.5.3 Historical Data. Historical climate data can provide insights into how future and current climate patterns may differ. Information exists on climate for the past few centuries and, in less detail, for the last 10,000 years.

Cropper and Fritts (Cropper 1986) derived a 360-year regional reconstruction of seasonal and annual variations in temperature and precipitation from statistical relationships between meteorological records from Columbia Basin stations and tree-ring data from western North America. They calibrated the relationship between Columbia Basin weather records and a network of 65 tree-ring chronologies. The results suggest that the average temperature of the Columbia Basin for the past 3 centuries was slightly higher by 0.09 °C (0.16°F) and more variable (4 percent higher standard deviation) than in the twentieth century. The increase was primarily attributed to warmer winters. This reconstruction also suggests that the past 3 centuries were wetter on the average by 0.8 cm (0.3 in.), primarily in the autumn. Furthermore, droughts were apparently more frequent starting in the second half of the seventeenth century and lasted longer than twentieth century droughts. Gramulich (1987) also used multiple regression models to reconstruct precipitation in the Pacific Northwest. The results indicate that the average precipitation in the eighteenth and nineteenth centuries was the same as the average precipitation in the twentieth century.

Chatters (1991) and Chatters and Hoover (Chatters 1992) summarized proxy evidence for climatic change in the Columbia Basin for the past 10,000 to 13,000 years. They identify an environment for about 13,000 years ago that was kept cool and dry by masses of ice and glacial meltwater, supporting a mosaic of isolated plant and animal communities. This was followed between 10,000 and 8,500 years ago by a period of warmer than modern summers, colder than modern winters and low, but spring-dominant, precipitation. This climate supported extensive grasslands and their associated fauna. By 8,000 years ago, summers and winters were both relatively warm, and precipitation was at least 33 percent below current levels. This climate pattern resulted in reduced stream flows, with late spring flow maxima, and extensive development of shrub-steppe vegetation throughout most of the region. Between 4,500 and 3,900 years ago, the climate evolved to wetter and cooler conditions. Rivers flooded frequently and forests expanded into steppe zones. From 3,900 to 2,400 years ago the climate was cool in the summer and cold in the winter, with winter-dominant precipitation at least 30 percent above current levels. Warmer, drier conditions returned between 2,400 and 2,000 years ago, reducing vegetation density and renewing flooding.

2.2.5.4 Long-Range Forecasts. Future long-range forecasts of climate are uncertain. Climatologists universally accept that global climates have undergone significant variation in the past and that such natural variations are expected to continue into the future. Berger (1991) reviewed 7 models of different complexity developed to predict the global climate for the next 10,000 to 100,000 years. All the models are in relatively good agreement. Without human disturbances, the long-term cooling trend that began some 6,000 years ago is expected to continue for the next 5,000 years. This trend should be followed by a stabilization at about 15,000 years, a cold interval centered at approximately 25,000 years, and finally a major glaciation at about 55,000 years. Although human disturbances (such as the green-house effect) could occur, their main effect will be to delay the onset of these trends.

2.2.5.5 Severe Weather. Severe weather events are not significant to the Hanford Site. According to the records of the Hanford Meteorological Station and the National Severe Storms Forecast Center's database, only 24 separate tornados have occurred between 1916 to 1994 within 160 km (100 mi) of the Hanford Site. Only one of these tornadoes was observed within the boundaries of the Hanford Site (at the extreme western edge), and no damage resulted. The estimated probability of a tornado striking a point at the Hanford Site is 9.6×10^{-6}/y. Hurricanes do not reach the interior of the Pacific Northwest.

Severe winds are associated with thunderstorms or the passage of strong cold fronts. The greatest peak wind gust was 130 km/h (81 mi/h), recorded at 15 m (50 ft) above ground level at the Hanford Meteorological Station. Extrapolations based on 35 years of observation indicate a return period of about 200 years for a peak gust in excess of 145 km/hr (90 mi/hr) at 15 m above ground level.

2.2.5.6 Climate Summary. The analyses of present and future climatic conditions at the Hanford Site and in the surrounding region suggest that conditions similar to the current climate will prevail for at least 10,000 years and probably considerably longer. However, because of the uncertainty inherent in any analysis of climate, wetter conditions and associated higher recharge or infiltration rates also will be considered. Scientists generally accept that, at about 50,000 years from now or later, major glaciation will occur, followed by possible flooding similar to what occurred near the end of the last glacial stage. Although considerable uncertainty is associated with future glaciation, some simulations in this performance assessment examined human health impacts associated with a resident population following flooding and redeposition after 50,000 years.

2.2.6 Ecology and Biotic Conditions

The information in this section is taken from *Hanford Site National Environmental Policy Act (NEPA) Characterization*, PNNL-64415, Rev. 12, Section 4.4 (Neitzel 2000-4).

This section summarizes the ecology of the Hanford Site, emphasizing plant and animal activities that may affect exposure pathways. The primary impact would be through roots penetrating and animals burrowing through barriers into a disposal facility. Secondarily, the types of plants and animals and their density can affect net groundwater recharge, which is

greatly influenced by surface vegetation and burrowing. Neitzel (2000-4) details both the terrestrial and aquatic ecology of the Hanford Site and presents extensive listings of plant and animal species. This section considers only terrestrial ecological effects because the proposed immobilized low-activity tank waste disposal facility sites are not located near significant aquatic ecological systems.

The Hanford Site consists of mostly undeveloped land. Chemical processing facilities, shut down nuclear reactors, and supporting facilities occupy only about 6 percent of the site. Most of the Hanford Site has not experienced tillage or agricultural grazing since the early 1940's.

The Hanford Site is characterized as a shrub-steppe ecosystem that is adapted to the region's mid-latitude semiarid climate. Such ecosystems are typically dominated by a shrub overstory with a grass understory. In the early 1800's, dominant plants in the area were big sagebrush (*Artemisia tridentata*) and an understory consisting of perennial Sandberg's bluegrass (*Poa sandbergii*) and bluebunch wheatgrass (*Pseudoregneria spicata*). Other species included threetip sagebrush, bitterbrush, gray rabbitbrush, spiny hopsage, bluebunch wheatgrass, needle-and-thread grass, Indian ricegrass, and prairie Junegrass.

With the advent of settlement, livestock grazing and agricultural production contributed to colonization by non-native vegetation species that currently dominate portions of the landscape. Although agriculture and livestock production were the primary subsistence activities at the turn of the century, these activities ceased when the Site was designated in 1943. Range fires that historically burned through the area during the dry summers eliminate fire-intolerant species (e.g., big sagebrush) and allow more opportunistic and fire resistant species to establish. Of the 590 species of vascular plants recorded for the Hanford Site, approximately 20 percent are non-native. The dominant non-native species, cheatgrass, is an aggressive colonizer and has become well established across the Site. Over the past decade, several knapweed species also have become persistent invasive species in areas not dominated by shrubs.

The plant community at the two ILAW disposal sites is shrub-steppe dominated by big sagebrush, Sandberg's bluegrass, and cheatgrass. Most of the new ILAW Disposal Site has this cover, but the existing disposal site has a significant fraction of area where disturbance occurred during vault construction. Appendix F of Fayer (1999) describes some of the data collected recently to characterize the plant community at these two sites.

Approximately 300 species of terrestrial vertebrates have been observed on the Hanford Site, including approximately 40 species of mammals, 246 species of birds, 4 species of amphibians, and 9 species of reptiles. Terrestrial wildlife include Rocky Mountain elk, mule deer, coyote, bobcat, badger, deer mice, harvest mice, grasshopper mice, ground squirrels, voles, and black-tailed jackrabbits. The most abundant mammal on the Site is the Great Basin pocket mouse. Bird species commonly found in the shrub-steppe habitats at the Hanford Site include the western meadowlark, horned lark, long-billed curlew, vesper sparrow, sage sparrow, sage thrasher, loggerhead shrike, and burrowing owls.

Butterflies, grasshoppers, and darkling beetles are among the more conspicuous of the approximately 1,500 species of insects that have been identified from specimens collected on the Hanford Site. The actual number of insect species living on the Hanford Site may reach as high as 15,000.

The side-blotched lizard is the most abundant reptile species that occurs on the Hanford Site. Short-horned and sagebrush lizards are reported, but occur infrequently. The most common snake species includes gopher snake, yellow-bellied racer, and Pacific rattlesnake. The Great Basin Spadefoot Toad, Woodhouse's Toad, Pacific tree frog, and bullfrogs are the only amphibians found on the Site.

Wildlife species observed at the two ILAW disposal sites include mule deer, black-tailed jackrabbits, cottontail rabbits, coyotes, side-blotched lizards, gopher snakes, sage sparrows, shrikes, meadowlarks, and horned larks.

Wildfires are frequent on the Hanford Site. Three large wildfires in the past 2 decades have burned over 15 percent of the site. However, because of fire-control measures, no fire has been on the ILAW disposal sites for at least 50 years.

No farming has occurred on the Hanford Site since the government took control of the Site. However, the Hanford Site has all the components that favor successful irrigated farming Constraints to agricultural development are political and social, not economic or technical. A report prepared by Washington State University for this performance assessment, *Evaluation of the Potential for Agricultural Development at the Hanford Site* (Evans 2000), provides many details on potential agricultural activities on the Site.

2.2.7 Regional Geology

The information in this section is based on *Geologic Data Packages for 2001 Immobilized Low-Activity Tank Waste Performance Assessment*, HNF-SD-WM-TI-707 (Reidel 1999).

2.2.7.1 Overview. Knowledge of the thickness and lateral distribution of the sediments and other geologic characteristics is required for the following reasons:

To define a conceptual model for the flow of water and the transport of contaminants from a disposal facility through the vadose zone (the zone between the surface and the groundwater that is not saturated with water) and from the unconfined aquifer (the uppermost groundwater layer) to the human environment

To define hydraulic parameters

To interpret modeling results.

The geology of the Hanford Site includes thick sequences of water-derived sediments varying in texture from cobbles and coarse gravels to fine silts and clays. These sediments

overlay thick basalt flows. The top sequence or surface soil has been modified by wind. An unconfined aquifer exists in the lower part of the sedimentary sequence overlaying the uppermost basalt flow. This relatively thin aquifer is considered the primary contaminant pathway for evaluating exposure scenarios. The aquifer intercepts infiltration from the vadose (unsaturated) zone above it, providing a pathway for water and contaminant transport to users or ultimately the Columbia River.

The geological and physical settings of the Hanford Site have been extensively characterized. This section summarizes the physical geology and environmental setting of the Hanford Site and of the proposed disposal site. Emphasis is on the sedimentary sequence, which is the pathway to the groundwater. More detailed discussions of the geology of the Northwest and the Hanford Site are found in *Final Environmental Impact Statement: Disposal of Hanford Defense High-Level Transuranic and Tank Wastes* DOE (1987-1), *Consultation Draft Site Characterization Plan* DOE (1988b), *Geologic Studies of the Columbia Plateau: A Status Report*, RHO-BWI-ST-4 (Myers 1979), *Subsurface Geology of the Cold Creek Syncline*, RHO-BWI-ST-14 (Myers 1981), "Volcanism and Tectonism in the Columbia River Flood-Basalt Province" (Reidel 1989), and *Geology and Hydrology of the Hanford Site: A Standardized Text for Use in WHC Documents and Reports*, WHC-SD-ER-TI-003 (Delaney 1991).

2.2.7.2 Topography and Physiography. The proposed disposal facilities are on the Hanford Central Plateau, a Pleistocene flood bar most commonly referred to as the 200 Areas Plateau, near the center of the Hanford Site. The Hanford Central Plateau is approximately 198 m (650 ft) to 229 m (750 ft) above mean sea level. The plateau decreases in elevation to the north, northwest, and east toward the Columbia River. The plateau escarpments have elevation changes of 15 m to 30 m (50 to 100 ft).

The Hanford Site is situated within the Pasco Basin of south-central Washington State (Figure 2-5). The Pasco Basin is one of many topographic depressions located within the Columbia Intermontane Province (Figure 2-6), a broad basin located between the Cascade Range and the Rocky Mountains. The Columbia Intermontane Province is the product of Miocene continental flood, basalt volcanism, and regional deformation. The Pasco Basin is bounded on the north by the Saddle Mountains; on the west by Umtanum Ridge, Yakima Ridge, and the Rattlesnake Hills; on the south by the Horse Heaven Hills; and on the east by the Palouse Slope (Figure 2-5).

The physical geography of the Hanford Site is dominated by the low-relief plains of the Pasco Basin and anticlinal ridges of the Yakima Folds physiographic region. The surface topography of the Hanford Site is the result of the following events:

- Uplift of anticlinal ridges
- Pleistocene cataclysmic flooding
- Holocene eolian activity.

Uplift of the ridges began in the Miocene epoch (starting about 17 million years ago) and continues to the present. This uplift is occurring on geologic time scales (i.e., over tens of millions of years). The uplift is not incorporated into our conceptual model of the immobilized

low-activity tank waste disposal facilities, which addresses a time scale of tens of thousands of years.

Glacier-related flooding has had a major impact on the physical geography. Cataclysmic flooding occurred when ice dams in western Montana and northern Idaho were breached, allowing large volumes of water to spill across eastern and central Washington. The last major flood occurred about 13,000 years ago, during the late Pleistocene Epoch. Interconnected flood channels, giant current ripples, and giant flood bars are among the landforms created by the floods. These formations resulted in heterogeneous and discontinuous characteristics for sediments ranging in size from silts to coarse gravels. These sediments yield a wide range of vadose zone hydraulic properties.

Figure 2-5. Geologic Structures of the Pasco Basin and the Hanford Site.

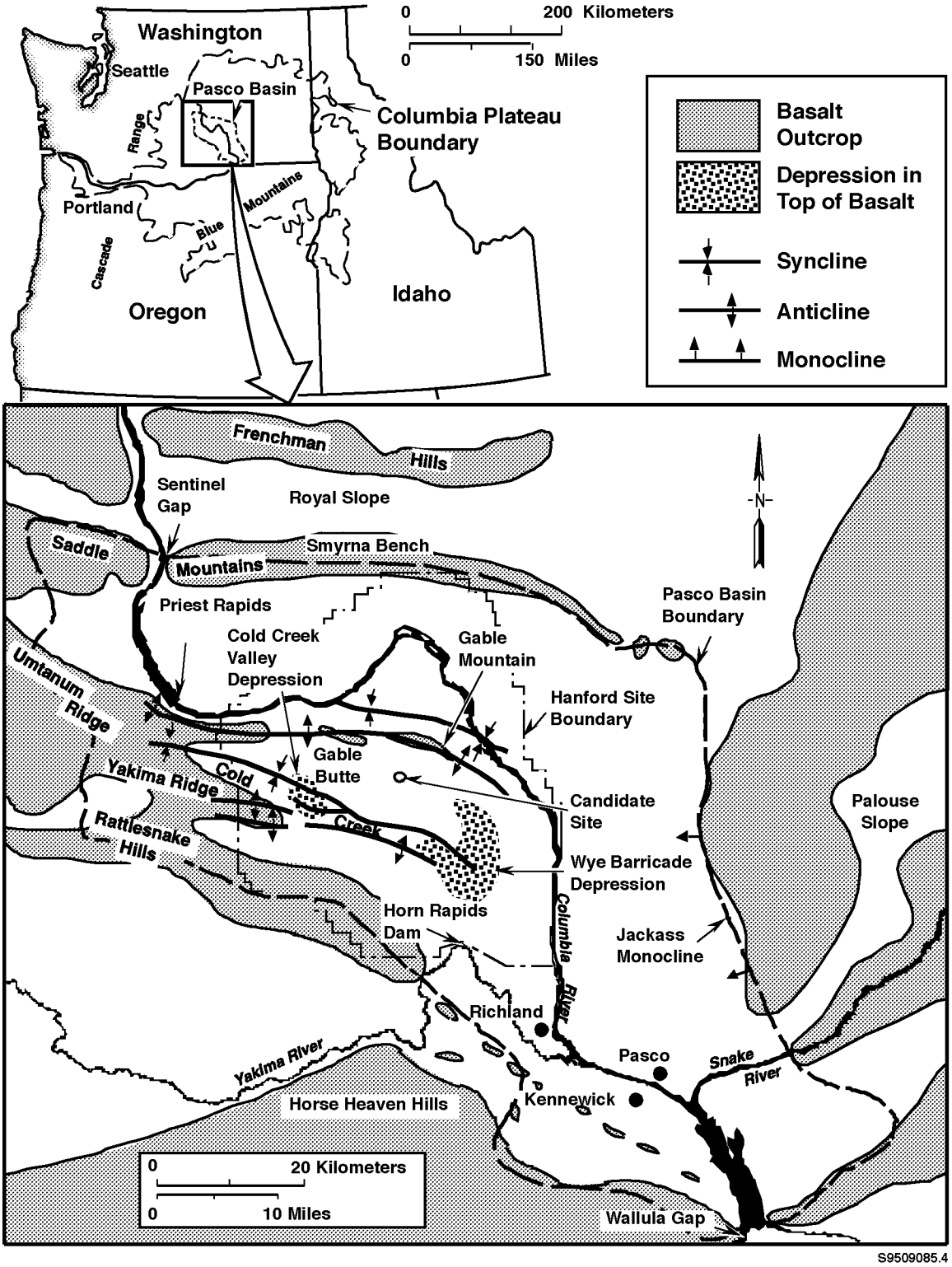

Figure 2-6. Divisions of the Intermontane Physiographic and Adjacent Snake River Plains Provinces.

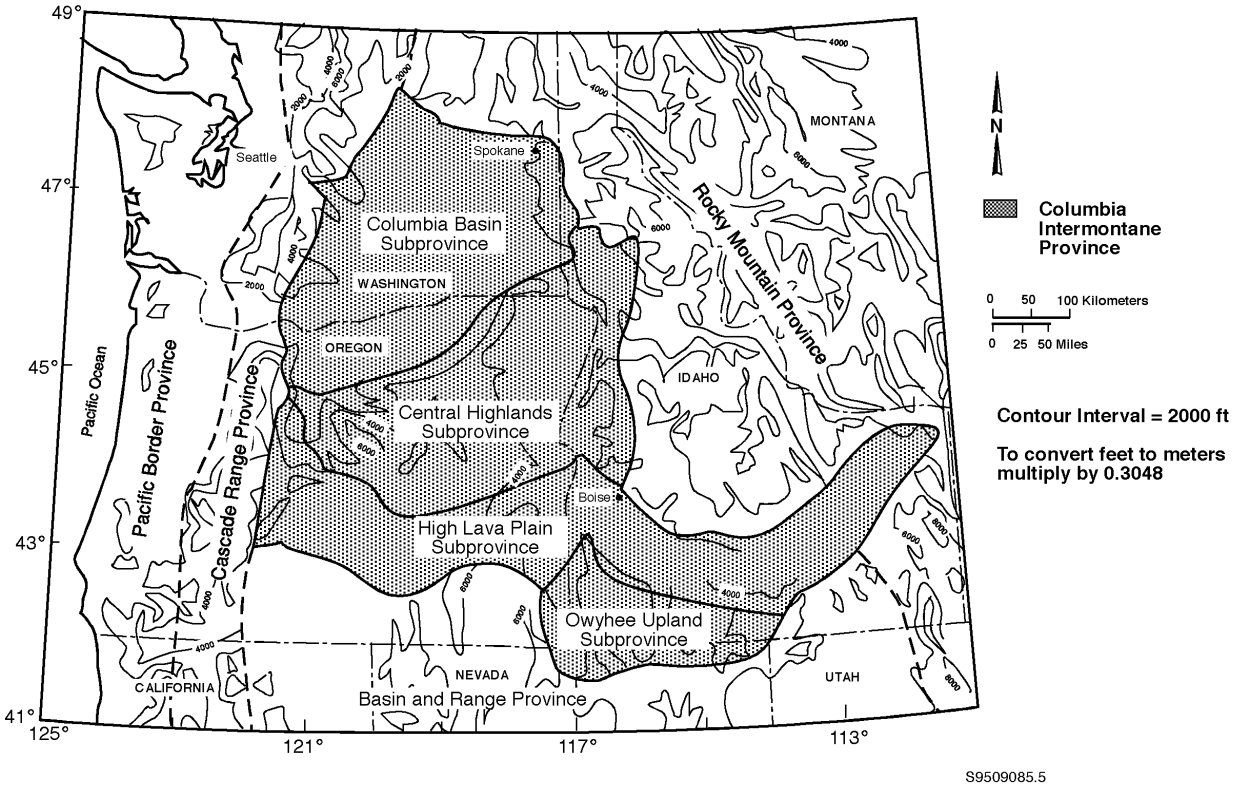

Landslides have had a limited effect on physical geography. Previous landslide activity in the area generally is limited to the White Bluffs area east of the Hanford Site and Rattlesnake Mountain, on the western edge of the Hanford Site. No landslide activity is observed in the Hanford Central Plateau.

During the Holocene Epoch (the last 11,000 years), winds have locally reworked the flood sediments. The winds deposited dune sands in the lower elevation and loess (very fine wind-blown silts) around the margins of the Pasco Basin. Generally, anchoring vegetation has stabilized sand dunes. However, they have been reactivated where vegetation has been disturbed. Most sand dunes on the Hanford Site are located southeast of the 200 East Area and are stabilized by vegetation.

The location of the Hanford Site in an intermontane basin helps maintain a semiarid climate with low recharge. Most topographical surface features that could disturb the near-surface hydraulic characteristics affecting recharge, such as sand dunes and landslides, are not found at the location of the immobilized low-activity tank waste disposal facilities. Moreover, sand dunes are indicators of past, cumulative wind directions. Their location approximately downwind of the new disposal facility site suggests that future dune formation over the facility is not likely.

2.2.7.3 Stratigraphy. The stratigraphy or geologic layering is not extremely complex in the Hanford Site region. Late Miocene to Pleistocene suprabasalt sediments (2 to 5 million years old) and Miocene-aged basalt (16 to 17 million years old) of the Columbia River Basalt Group lie beneath the Hanford Site. Miocene-aged basalt is exposed at some locations, including Gable Mountain and Gable Butte. The basalts and sediments thicken into the Pasco Basin and generally reach maximum thickness in the Cold Creek syncline, which is southwest of the disposal facility sites. Cenozoic (25 to 65 million years old) sedimentary and volcaniclastic rocks underlying the basalts are not exposed at the surface near the Hanford Site.

Table 2-1 delineates the general stratigraphy of the suprabasalt sedimentation that makes up the vadose zone sediments beneath the locations of the disposal facilities. This table illustrates the degree of heterogeneity and discontinuity in the sediments. The sedimentation is composed largely of Ringold Formation and Hanford formation sediments, with the Hanford formation above the Ringold Formation. At the disposal facility sites, the Hanford formation makes up most of the vadose zone.

Table 2-1. Stratigraphy of the200 East Area.

Nomenclature Used in this Report		Equivalent of Lindsey (1994a), Lindsey (1996), and Reidel (1992)	Equivalent of Reidel (1994a, 1994b)
Eolian			Qd
Hanford formation		H	Qfs and Qfg
Sandy Sequence	Layer 3	H2	Qfs_3
	Layer 2	H2	Qfs^2
	Layer 1	H2 and HZA	Qfs_1(?)
Basal Gravel Sequence		H3	Qfs_1(?)
Ringold Formation, Member of Wooded Island		Ringold Formation, Member of Wooded Island	P_L~~M~~
	Unit E	Unit E	P_L~~M~~cg
	Lower Mud	Lower Mud	P_L~~M~~c
	Unit A	Lower A	P_L~~M~~cg

? indicates an uncertain assignment
P_L relates to Pleistocene era
~~M~~ relates to Miocene

The suprabasalt sedimentary sequence at the Hanford Site is about 230 m (750 ft) thick in the west central Cold Creek syncline. This sedimentary sequence pinches out against the Saddle Mountains anticline, Gable Mountain/Umtanum Ridge anticline, Yakima Ridge anticline, and Rattlesnake Hills anticline. The suprabasalt sediments are dominated by laterally extensive deposits assigned to the late Miocene- to Pliocene-aged Ringold Formation and the Pleistocene-aged Hanford formation (Table 2-1). Locally occurring strata assigned to the informally defined Plio-Pleistocene unit and pre-Missoula gravels compose the remainder of the sequence.

The following sections describe the geology of the Ringold Formation and the Hanford formation sediments in some detail. These sediments are the basis for determining vadose zone hydraulic and geochemical properties for contaminant transport modeling.

2.2.7.3.1 Ringold Formation. The Ringold Formation varies in thickness throughout the Hanford Site. It is up to 183 m (600 ft) thick in the deepest part of the Cold Creek syncline south of the 200 West Area and 170 m (560 ft) thick in the western Wahluke syncline near the 100 B Area. It pinches out against the Gable Mountain, Yakima Ridge, Saddle Mountains, and Rattlesnake Mountain anticlines (Figure 2-5). It is mostly absent in the northern and northeastern parts of the 200 East Area and adjacent areas to the north near West Pond.

The Ringold Formation consists of fluvial and lacustrine sediments deposited by the ancestral Columbia and Clearwater-Salmon river systems between about 3.4 and 8.5 million years ago. Lindsey (1996) described the Ringold Formation in terms of three informal members: the member of Wooded Island, the member of Taylor Flat, and the member of Savage Island. Of these, only the member of Wooded Island is present beneath the 200-East Area.

The member of Wooded Island consists of five separate units dominated by fluvial gravels (conglomerate). The gravels are designated (from bottom to top) as units A, B/D, C, and E. Fine-grained deposits typical of overbank and lacustrine environments separate the gravel units. The lowermost of the fine-grained sequences is designated the lower mud unit. Only gravel units A and E are present beneath the 200-East Area and the Ringold Formation is entirely absent beneath the north and northeast parts of the 200-East Area (Lindsey 1992, 1994b).

The Ringold Formation conglomerate is a variably indurated clast- and matrix-supported, pebble to cobble gravels with a fine to coarse sand matrix (Lindsey 1996). The most common lithologies are basalt, quartzite, and intermediate to felsic volcanics. Interbedded lenses of silt and sand are common. Cemented zones within the gravels are discontinuous and of variable thickness. In outcrop, the gravels are massive, planer bedded, or cross-bedded. Lying above the Ringold gravels are silts and sands of the upper Ringold, the member of Taylor Flats, which is not generally present beneath the 200-East Area.

2.2.7.3.2 Hanford Formation. The Hanford formation (an informal designation) is up to 64 m (210 ft) thick in the Cold Creek bar near the 200 Areas. It is absent on ridges approximately 360 m (1,180 ft) above sea level.

The Hanford formation overlies the Ringold Formation. The Hanford formation consists of glaciofluvial sediments deposited by cataclysmic floods from Glacial Lake Missoula, Pluvial Lake

Bonneville, and ice-margin lakes. Hanford formation sediments resulted from at least four major glacial events and were deposited between about 1 million years and 13 thousand years ago. The formation consists of pebble to boulder gravel, fine- to coarse-grained sand, and silt to clayey silt. These deposits are divided into three facies: gravel-dominated facies, sand-dominated facies, and silt-dominated facies (Reidel 1992; Lindsey 1992, 1994a, 1994b). These facies are referred to as coarse-grained deposits, plane-laminated sand facies, and rhythmite facies, respectively, in Bjornstad (1987) and Baker (1992). The Hanford formation is present throughout the Hanford Site and is as much as 380 ft (116 m) thick (Delaney 1991).

Gravel-Dominated Facies. This facies generally consists of coarse-grained basaltic sand and granule to boulder gravel. These deposits display an open framework texture, massive bedding, plane to low-angle bedding, and large-scale planar cross bedding in outcrop. Silt content is variable and local interbedded silt and clay have been observed in outcrop. Clay and silt have been found as coatings on clasts but generally not filling open spaces between clasts. The gravel-dominated facies was deposited by high-energy floodwaters in or immediately adjacent to the main cataclysmic flood channelways.

Sand-Dominated Facies. This facies consists of fine- to coarse-grained sand and granule gravel. The sands typically have high basalt content and are commonly referred to as black, gray, or salt-and-pepper sands (Lindsey 1992). They may contain small pebbles and rip-up clasts, pebble-gravel interbeds, and silty interbeds less than 1 m (3 ft) thick. The silt content of the sands varies, but where it is low, a well-sorted and open framework texture is common. The sand facies was deposited adjacent to main flood channelways during the waning stages of flooding. The facies is transitional between the gravel-dominated facies and the silt-dominated facies.

Silt-Dominated Facies. This facies consists of thin bedded, plane-laminated, and ripple cross-laminated silt and fine- to coarse-grained sand. Beds are typically a few centimeters to several tens of centimeters thick and commonly display normal grading (Myers 1979; Bjornstad 1987; DOE 1988b). Local clay-rich beds occur in the silt-dominated facies and paleosols have been observed in cores from the 200-East Area. Sediments of this facies were deposited under slack water conditions and in back flooded areas (DOE 1988b).

2.2.7.3.3 Clastic Dikes. Clastic dikes are vertical to subvertical sedimentary structures that cross cut normal sedimentary layering and could effect the vertical movement of water and contaminants. Clastic dikes are a common geologic feature of Pleistocene flood deposits of the Hanford formation although they also have been found in the underlying Ringold Formation and in Columbia River Basalt Group and intercalated sedimentary interbeds. Clastic dikes on the Hanford Site have been described in detail by Fecht (1998).

Clastic dikes typically occur in swarms and occur as regularly shaped polygonal patterns; irregularly shaped polygonal patterns; preexisting fissure fillings; and random occurrences. Regular polygonal networks resemble 4- to 8-sided polygons. Dikes in irregular-shaped polygon networks generally are crosscutting in both plane and cross-section, resulting in extensive segmentation of the dikes. Clastic dikes often occur in zones of preexisting weakness.

Clastic dikes typically show a wide range in widths, depths, and lengths. The vertical extent of clastic dikes has been observed to range from 30 cm to greater than 55 m. Clastic dike widths ranges from about 1 mm to greater than 2 m and their length varies from as little as 0.3 m to more than 100 m.

In general, a clastic dike is composed of an outer skin of clay with coarser infilling material. Clay linings are commonly 0.03 mm to 1.0 mm thick, but linings up to about 10 mm are known. The clay skins may have a great influence on transport both within and adjacent to the clastic dikes. The width of individual infilling layers range from as little as 0.01 mm to more than 30 cm and their length can vary from about 0.2 m to more than 20 m. Infilling sediments are typically poor to well-sorted sand, but may contain clay, silt, and gravel.

Clastic dikes have been noted in the Hanford formation sand sequence in the existing disposal site (Lindberg 1993) and are suspected to occur but have not been identified at the new disposal site. At the existing disposal site, clastic dikes have not been mapped and their number and distribution are not known. Clastic dikes have been found in numerous locations on the 200 Area plateau where they occur primarily in polygonal networks with dimensions ranging from 30 to 240 m (Fecht 1998). The total depth of the clastic dikes in the existing disposal site also is unknown, but they extend below the bottom of the excavations for the former Grout Treatment Facility (Lindberg 1993).

2.2.7.3.4 Surficial Deposits. Holocene surficial deposits consist of silt, sand, and gravel that form a veneer less than 4.9 m (16 ft) thick atop much of the Hanford Site. These sediments were deposited by wind and local flood processes.

2.2.7.4 Soils. Hajek (1966) lists and describes the 15 different soil types on the Hanford Site, varying from sand to silty and sandy loam. The following soils are found in the south-central part of the 200 East Area:

Burbank Loamy Sand. This soil is dark-colored, coarse-texture soil underlain by gravel. Surface soil is usually about 40 cm (16 in.) thick but can be 76 cm (30 in.) thick. Gravel content of the subsoil ranges from 20 to 80 percent.

Ephrata Sandy Loam. The surface is dark colored and subsoil is dark grayish-brown medium-texture soil underlain by gravelly material, which may continue for many feet.

Rupert Sand. This soil is brown to grayish brown coarse sand grading to dark grayish-brown at about 90 cm (35 in.). Rupert sand developed under grass, sagebrush, and hopsage in coarse sandy alluvial deposits that were mantled by wind-blown sand.

2.2.7.5 Earthquakes. Seismic events can accelerate the degradation of a disposal facility and of the waste form.

2.2.7.5.1 Faults and History of Earthquakes. The Hanford Site lies in the Pasco Basin near the eastern limit of the Yakima Foldbelt. The Site is underlain by basalt of the Columbia River Basalt Group, which is covered by up to 213 m (700 ft) of relatively stiff sediments. It is in an area of low-magnitude seismicity and is under north-south compressional stress, which is reflected in the deformation of the Yakima folds. The following sources are major contributors to the seismic hazard in and around the Hanford Site:

Fault sources related to the Yakima folds

Shallow basalt sources that account for the observed seismicity within the Columbia River Basalt Group and are not associated with the Yakima Folds

Crystalline basement source region

Cascadia Subduction Zone earthquakes.

Earthquake activity at the new and existing disposal sites is typical of the Hanford Site. Figure 2-7 shows the location of earthquakes that have occurred near the 200-East Area since monitoring began at the Hanford Site in 1969. Most of the earthquakes have been less than coda magnitude 3.0. Coda magnitude is a local magnitude and is an estimate of the Richter magnitude. Thirty-three percent of the earthquakes shown on 2-7 occurred in the Columbia River Basalt Group. Sixteen percent were in the subbasalt sediments and 51 percent were in the crystalline basement.

The principal geologic structures described in *Geologic Map of the Richland 1:100,000 Quadrangle, Washington*, Open File Report 94-8 (Reidel 1994a), are reproduced in Figure 2-7. Comparing the location of earthquakes to the geologic structures shows no apparent pattern.

The largest historical earthquake in the Columbia Plateau occurred in 1936 near Milton-Freewater, Oregon, approximately 90 km (54 mi) east of the site. The earthquake had a magnitude of 5.75 and was followed by a number of aftershocks. The ground motion from this event is estimated to have been less than 0.03 g at the Hanford Site.

A seismic monitoring network has been operated in and around the Site since 1969. The network, operated by DOE, can locate all earthquakes of magnitude 1.5 and larger on or near the Hanford Site, and those of magnitude 2.0 and larger throughout south-central and south-eastern Washington State. The largest recorded earthquake on the Hanford Site had a magnitude of 3.8 near Coyote Rapids in 1971 and was felt in the 100 N Area.

Figure 2-7. Map Showing the Location of Earthquakes Detected From 1969 to 1999.

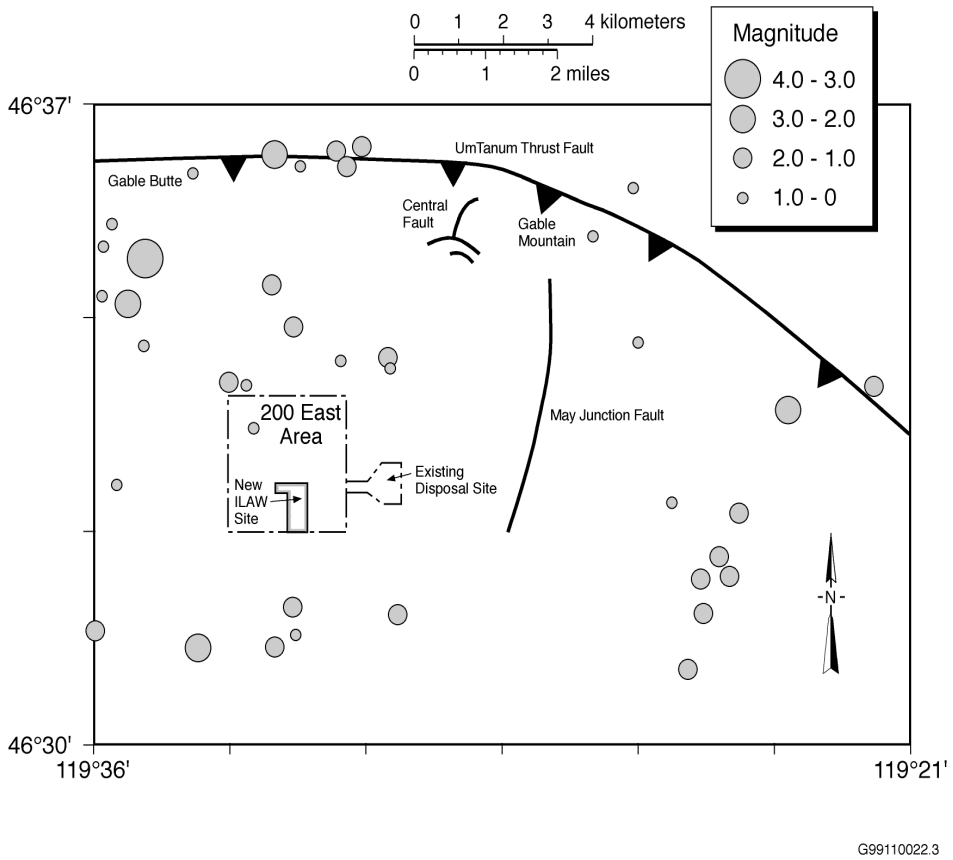

2.2.7.5.2 Seismic Hazard Assessment. This section explains the earthquake ground motions that the facility is expected to experience during the performance period. Deformation and cracking from earthquake ground motion may physically degrade the engineered system.

A probabilistic seismic hazard analysis was recently completed for the Hanford Site (Geomatrix 1996). Previous seismic hazard analyses were done for Energy Northwest's WNP-1/4 and WNP-2, which also are located on the Hanford Site (Power 1981). Woodward Clyde Consultants (WCC 1989) later applied the Energy Northwest study to the Hanford Site areas under DOE control. The mean seismic hazard curves for the 200 West, 200 East, and 400 Areas are shown in Figure 2-8. The 200 West Area ground motion values are shown for the selected time period in Table 2-2. (See Geomatrix [1996] for details including response spectra).

Table 2-2. Approximate Probability of Exceeding Given Ground Motions During Selected Time Periods.

Ground Motion (g)		Return Period (Years)	Annual Probability of Exceedence (p)	Exceedence Probability (EP)[a] over 50 years (%)	EP over 1,000 years (%)	EP over 10,000 years (%)
Horizontal	Vertical					
0.19	0.11	1,000.0	1×10^{-3}	5.0	63	100
0.26	0.16	2,000.0[b]	5×10^{-4}	2.0	39	99
0.37	0.25	5,000.0	2×10^{-4}	1.0	18	86
0.48	0.33	10,000.0	1×10^{-4}	0.5	10	63

[a] $EP = 1-(1-p)^n$ where

p = the annual probability of exceedence,
n = the performance life
EP = the probability of exceedence over the performance life.

[b] Performance Category 3, DOE Order 5480.28.

Figure 2-8. Total Mean Seismic Hazard for 200 Area Plateau, Hanford Site.

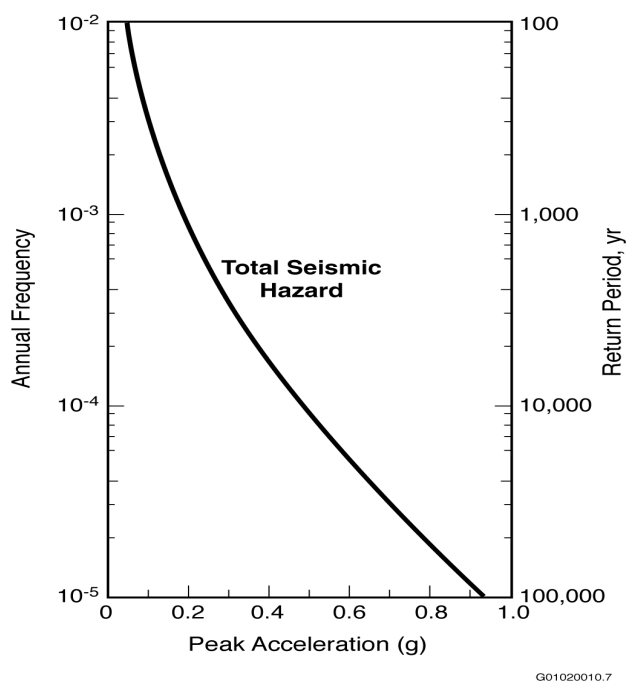

2.2.7.6 Volcanology. Several major volcanoes are located in the Cascade Range, west of the Hanford Site. The nearest volcano, Mount Adams, is about 160 km (100 mi) from the Hanford Site. The most active volcano, Mount St. Helens, is located approximately 220 km (136 mi) west-southwest of the Hanford Site. Because of the distance from the range, volcanic flows are not expected; the only effect of an eruption would be ash fall. The impacts of any such ash fall are not expected to have any long-term significance to contaminant movement.

2.2.8 Geology of the Proposed Immobilized Low-Activity Tank Waste Disposal Facility Locations

The information in this section is based on *Geologic Data Packages for 2001 Immobilized Low-Activity Tank Waste Performance Assessment*, HNF-SD-WM-TI-707 (Reidel 1999).

2.2.8.1 Previous Studies. The ILAW disposal site is an area where no previous construction or disposal sites exist so no major geologic studies have been carried out there. Studies relevant to the site are summarized in Tallman (1979), DOE (1988b), Lindsey (1992, 1994a, 1994b, 1996), and Reidel (1998a, 1998b). The first major activity was drilling borehole 299-E17-21 in 1998 at the southwest end of the site and obtaining the first high-quality data from the area [Reidel 1998a and Reidel 1998b].

2.2.8.2 Site Stratigraphy. The stratigraphy at the ILAW disposal site consists of the Hanford formation and Ringold Formation overlying the Columbia River Basalt Group. Surfacial sediments are mainly eolian deposits consisting of reworked Hanford formation sands and silts.

The stratigraphy and the stratigraphic model developed for this study is based on the boreholes depicted in Figure 2-9 and summarized in Table 2-1 and Figures 2-10, 2-11, and 2-12. This diagram is based on more detailed cross sections (Figures 2-13 through 2-16). Figure 2-11 represents a summary diagram for stratigraphy, west to east, across the middle southern part of the disposal site (between boreholes 299-E-18-1 and 299-E24-17 (see Figure 2-9). Figure 2-13 represents a summary diagram for stratigraphy, northwest (NW) to southeast (SE), across the northern part of the disposal site (between boreholes 299-E33-1 and 299-E24-17 (see Figure 2-9).

Figure 2-9. Map Showing Borehole Locations in the New ILAW Disposal Site.

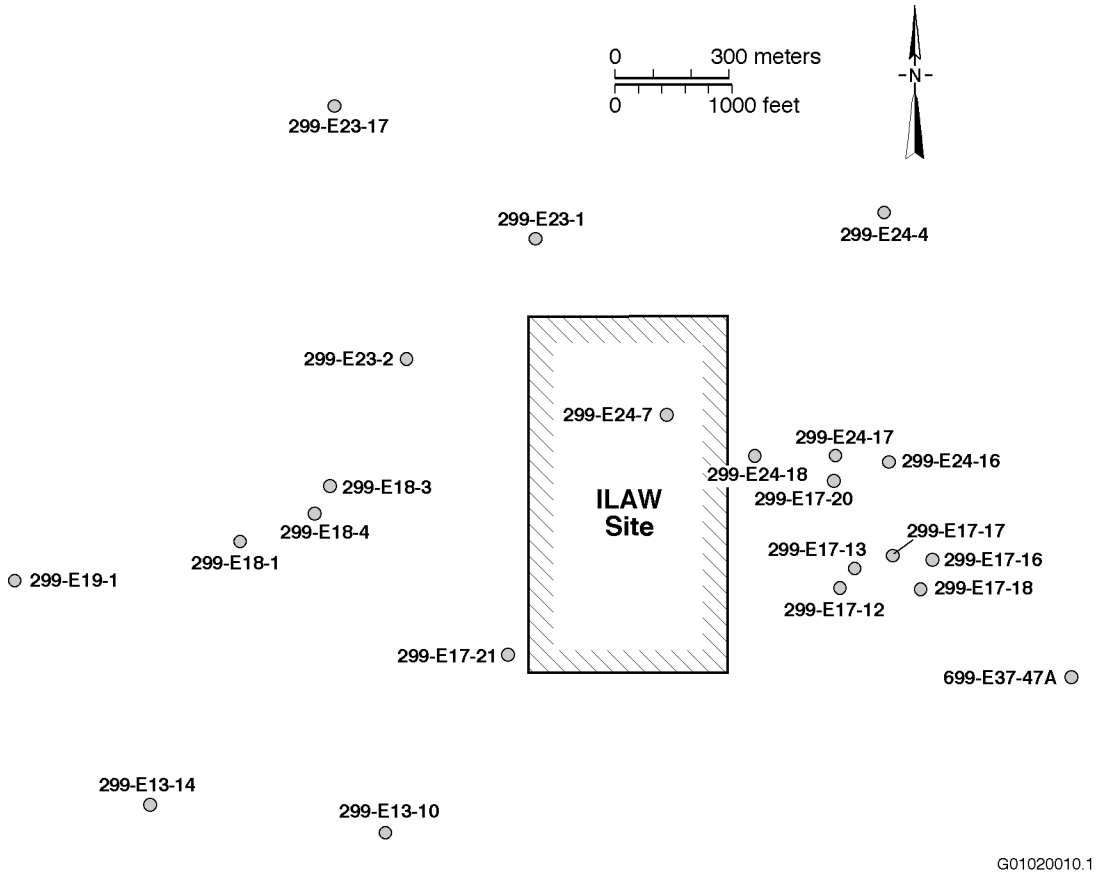

Figure 2-10. Fence Diagram of the ILAW Disposal Site and Vicinity.

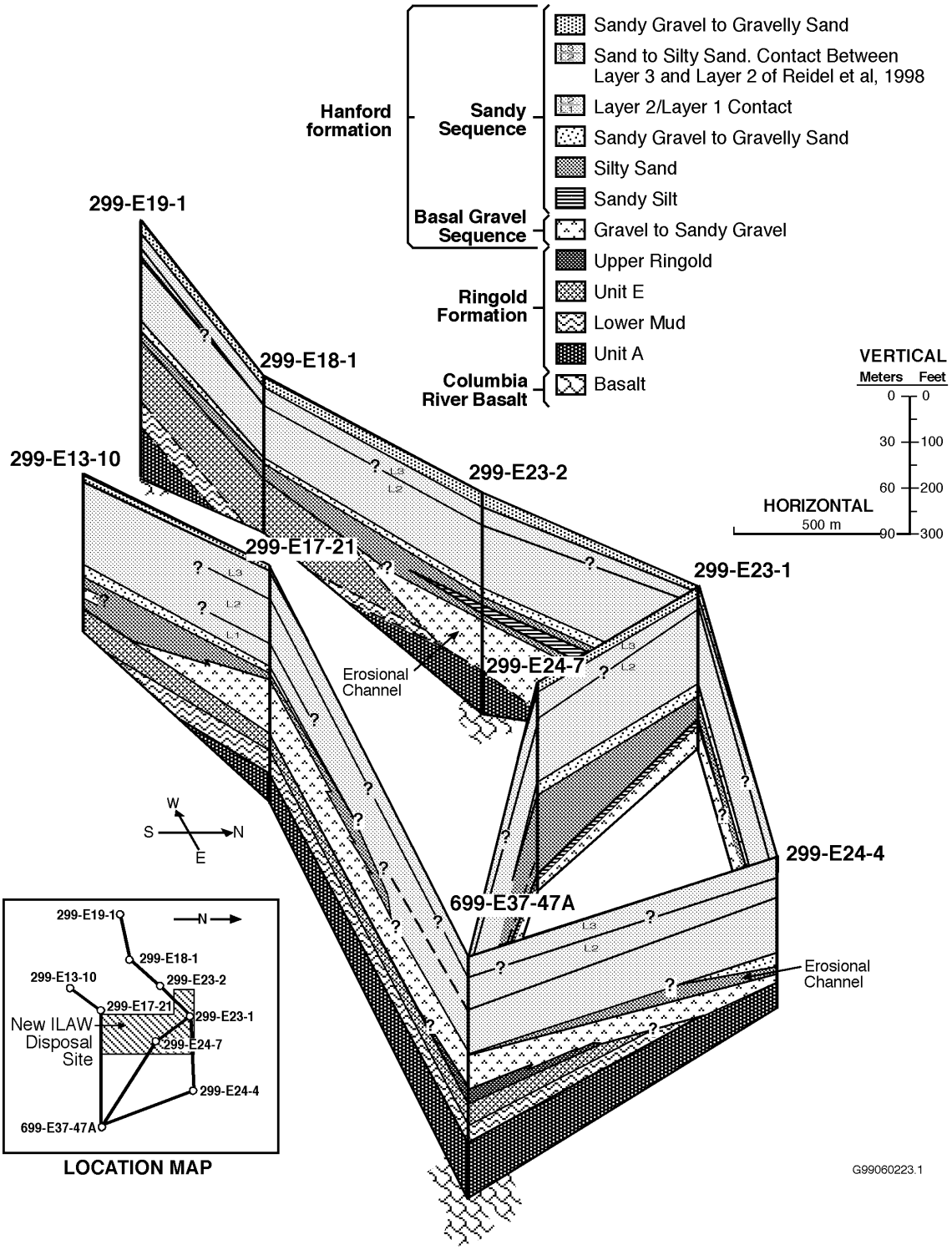

Figure 2-11. Summary Diagram of a West to East Cross-Section for the New ILAW Disposal Site.

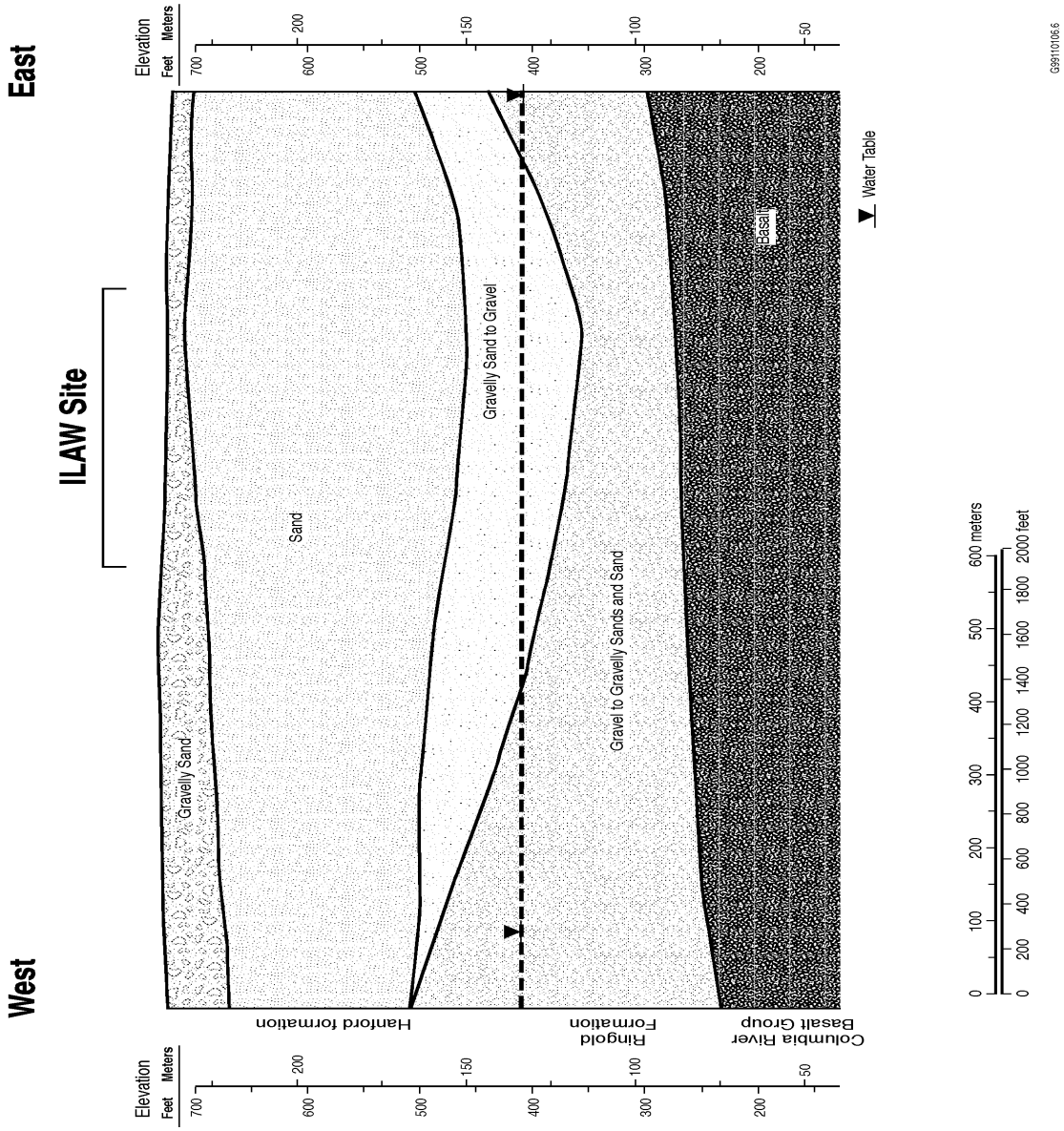

Figure 2-12. West to East (Southern Section) Cross-Section for the ILAW Disposal Site.

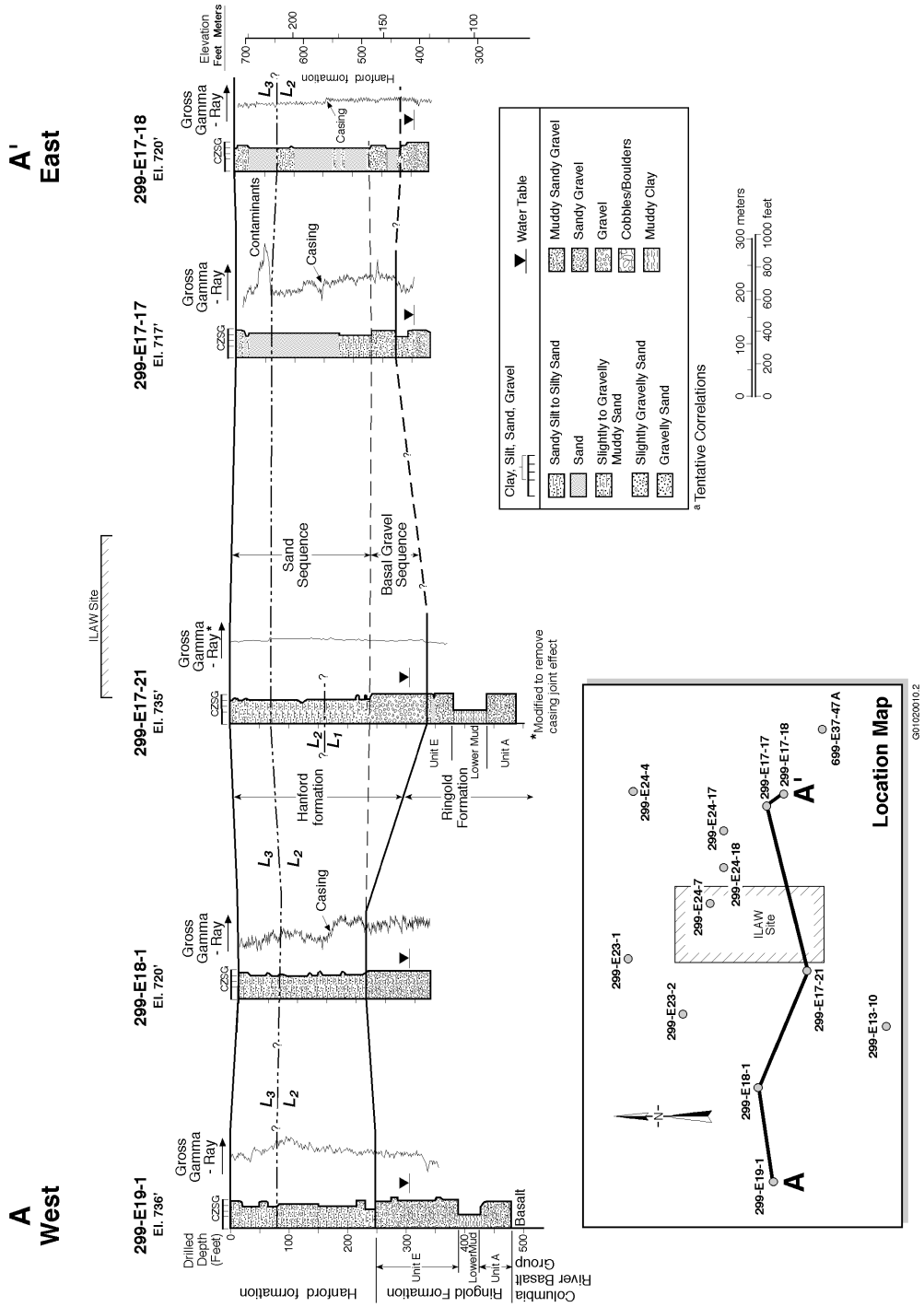

Figure 2-13. West to East (Northern Section) Cross-Section Across the ILAW Disposal Site.

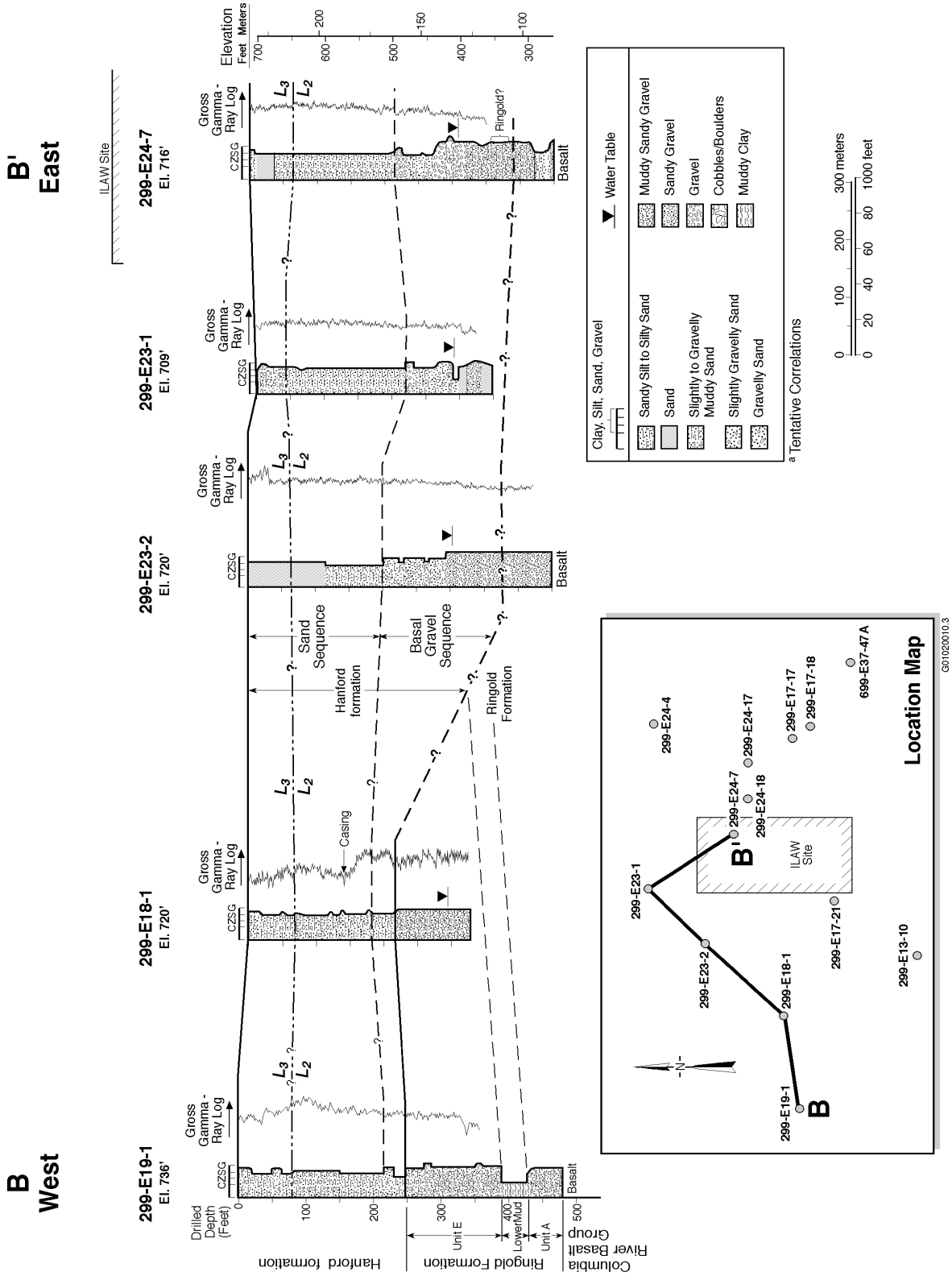

Figure 2-14. Alternate West to East Cross-Section Across the New ILAW Disposal Site.

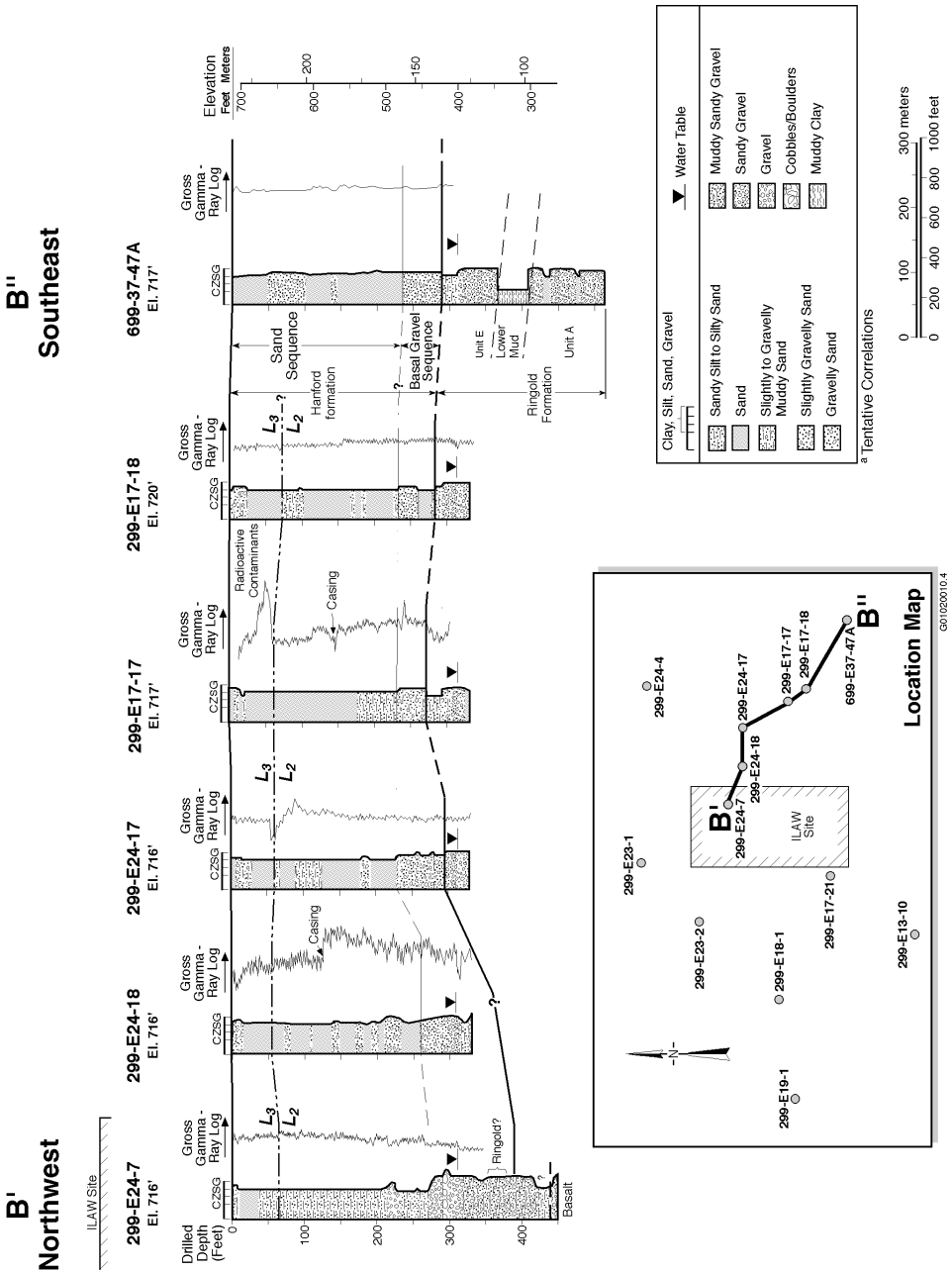

Figure 2-15. Southwest to Northeast Cross-Section Across the ILAW Disposal Site.

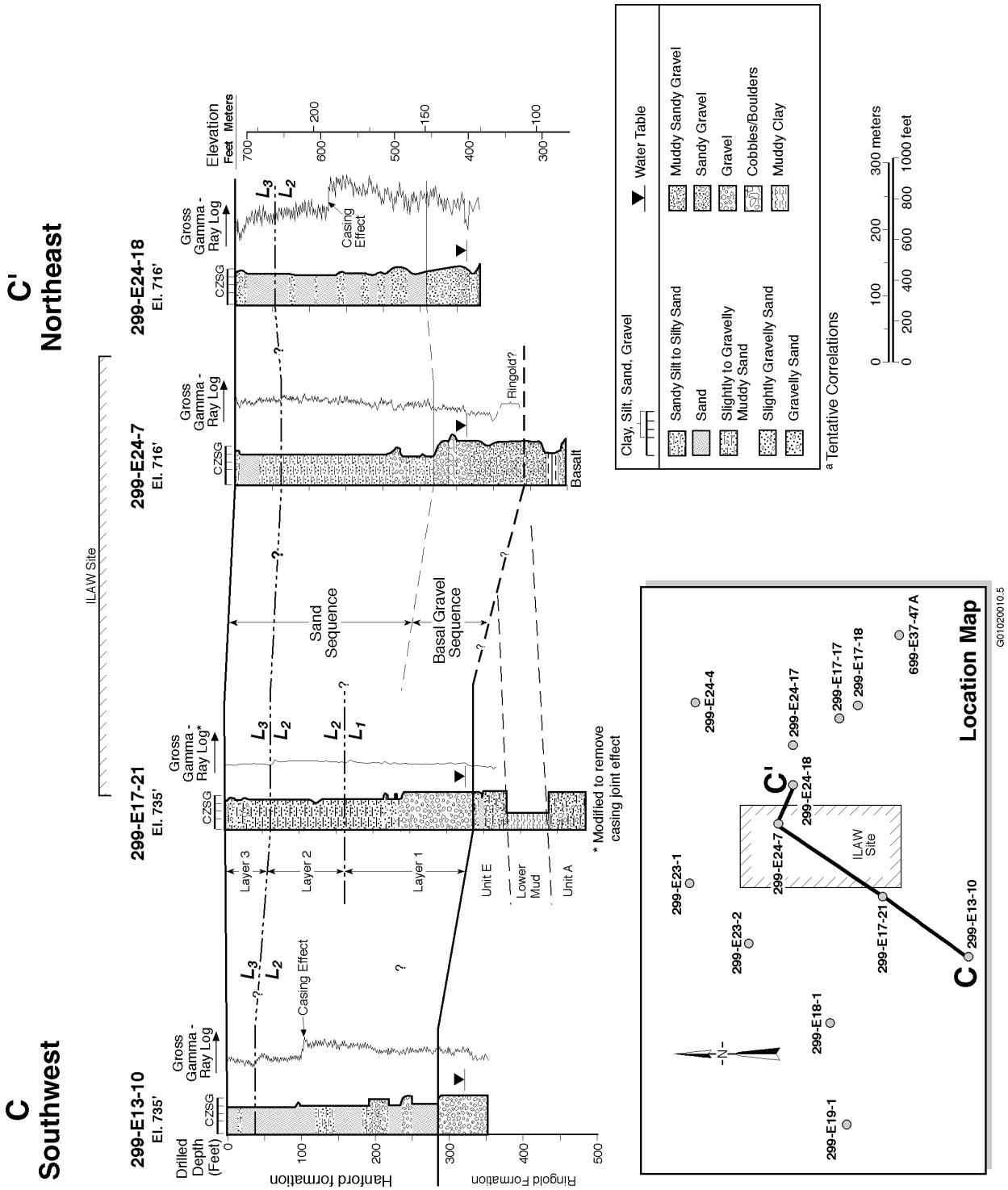

Figure 2-16. Alternate Southwest to Northeast Cross-Section Across the ILAW Disposal Site.

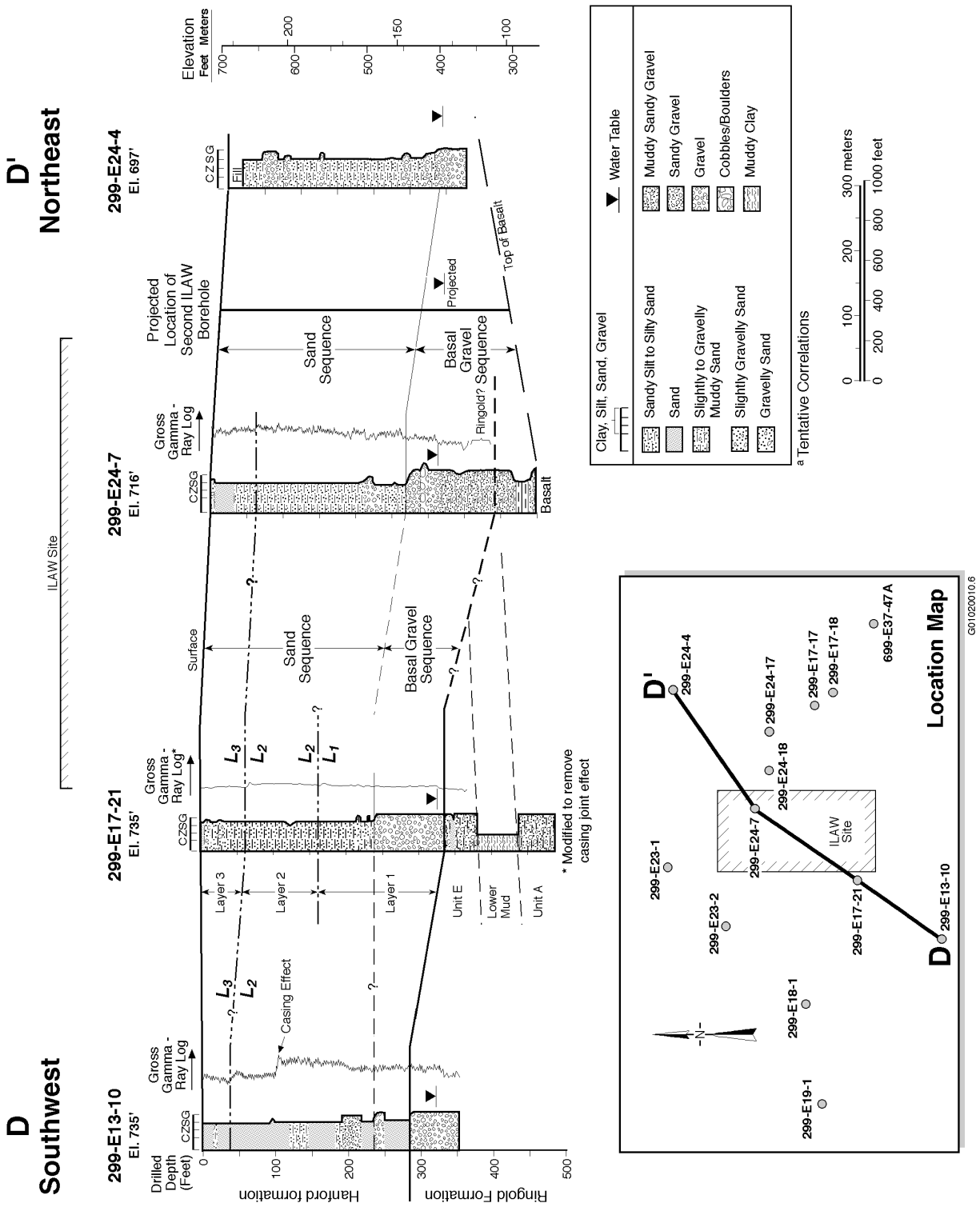

The stratigraphy of the new ILAW disposal site is divided from youngest to oldest into the following units:

Eolian deposits

Hanford formation, sandy unit (H2 of Lindsey 1994b)

- -Layer 3 (extends into upper gravelly unit)
- -Layer 2
- -Layer 1

Hanford formation, basal gravel units (H3 of Lindsey 1994b)

Ringold Formation

- -Unit E
- -Lower Mud
- -Unit A

Columbia River Basalt Group.

Sequences of sandy gravels to gravelly sands (G1, G2, G3, G4) and sand to silty sand units (S, S1, S2, S3) can be recognized in the Hanford formation layers (Table 2-1) but correlation across the area is tentative at this time because of the distance between boreholes, the poor quality of some data, and the local nature of thin units in the Hanford formation. Additional boreholes will be necessary to verify these correlations.

2.2.8.3 Columbia River Basalt Group. Previous studies (DOE 1988b; Reidel 1994a) have shown that the youngest lava flows of the Columbia River Basalt Group at the 200-East Area are those of the 10.5 million-year old Elephant Mountain Member. The Elephant Mountain Member is continuous beneath the new disposal site. No erosional windows are known or suspected to occur in the new ILAW disposal site area.

2.2.8.4 Ringold Formation. Because few boreholes penetrate much of the entire Ringold Formation at the new ILAW disposal site (Figure 2-17), data are limited. The Ringold Formation reaches a maximum thickness of 95 m (285 ft) on the west side of the new ILAW disposal site and thins eastward. It consists of three units of Lindsey's (1996) member of Wooded Island. The member of Taylor Flats has been identified in borehole 699-47-37A (Lindberg 1997) east of the site but this correlation was tentative. The deepest unit encountered is the lower gravel, Unit A. Lying above Unit A is the Lower Mud and overlying the Lower Mud is an upper gravel, Unit E. The upper Ringold (sand and silt of the member of Taylor Flat) is not present at the ILAW disposal site (Figure 2-10). Unit A and Unit E are equivalent to mapping unit P_L~~M~~cg (Table 2-1), Pliocene-Miocene continental conglomerates of Reidel (1994a, 1994b). The Lower Mud is equivalent to the mapping unit P_L~~M~~c, Pliocene-Miocene continental sand, silt, and clay beds of Reidel (1994a, 1994b).

Figure 2-17. Isopach Map of the Ringold Formation at the ILAW Disposal Site.

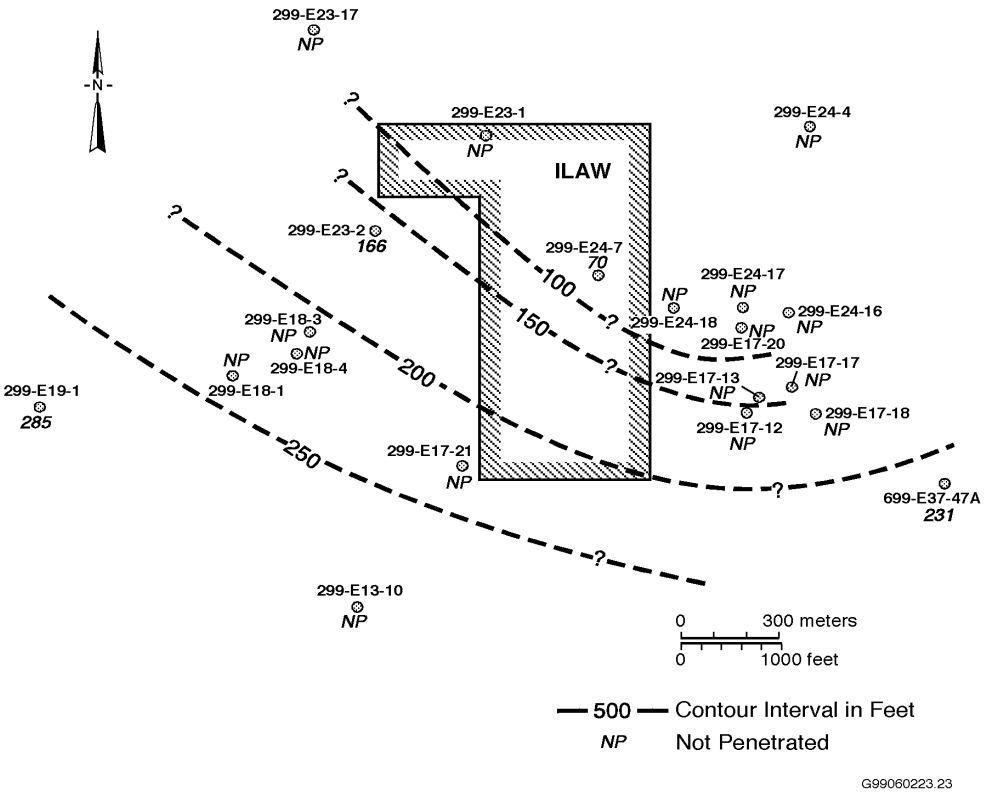

2.2.8.4.1 Unit A. Only three boreholes penetrated Unit A in the study area. Unit A is 61 ft (19 m) thick on the west side of the ILAW site but thins to the northeast (Figure 2-10). Unit A is described on borehole logs as a sandy gravel consisting of both felsic and basaltic rocks.

It is interpreted as Lindsey's (1996) fluvial gravel facies, which consists of conglomerates. There are sporadic yellow to white interbedded sands and silts with silt and clay lenses. Green-colored, reduced-iron stain is present on some grains and pebbles. Although the entire unit appears to be partially cemented, the zone produced abundant water in borehole 299-E17-21 (Reidel 1998b).

2.2.8.4.2 Lower Mud. Sixty-one feet (19 m) of the Lower Mud was encountered at the new ILAW site characterization borehole (299-E17-21). The upper most part (about 4 ft [1 m]) is described on borehole logs as a yellow sandy to silty mud and is interpreted as Lindsey's (1996) lacustrine facies, which consists of clays, silts, and silty sands. The silty clay grades downward into about 34 ft (10 m) of blue clay with beds of silt to slightly silty clay. The blue clay, in turn, grades down into 23 ft (7 m) of brown silty clay with organic rich zones and occasional wood fragments. The Lower Mud is absent in the center of the ILAW site (Figure 2-10; boreholes 299-E23-1 and 299-E24-7).

2.2.8.4.3 Unit E. Unit E is described on borehole logs as a sandy gravel to gravelly sand. It is interpreted to consist of as much as 50 ft (15 m) of conglomerate with scattered cobbles up to 10 in. (25 cm) in size. The conglomerate consists of both felsic and basaltic clasts which are well rounded with a sand matrix supporting the cobbles and pebbles. Cementation of this unit ranges between slight and moderate. The upper contact of Unit E is not easily identified at the new ILAW site. In the western part of the study area, unconsolidated gravels of the Hanford formation directly overly the Ringold Unit E gravels. The dominance of basalt in the Hanford formation and the absence of any cementation are the key criteria used for distinguishing them here (Reidel 1998b). In the central and northeastern part of the study area, Unit E is interpreted to have been eroded (e.g., boreholes 299-E24-7 and 299-E17-21, Figure 2-10). Unconsolidated gravels and sands typical of the Hanford formation replace them.

2.2.8.4.4 Upper Ringold (Member of Taylor Flat). The upper Ringold is not present at the new ILAW disposal site but has been tentatively identified in the southeast corner of 200 East Area in borehole 699-E37-47A (Lindberg 1997). These sediments do not appear to be present at the ILAW disposal site (Figure 2-10).

2.2.8.4.5 Unconformity at Top of Ringold Formation. The surface of the Ringold Formation is irregular in the ILAW disposal site area (Figure 2-18). A NW-SE trending erosional channel or trough is centered along the northeast portion of the site (Figures 2-10 and 2-18). The deepest portion of the trough occurs near borehole 299-E24-7 in the northern portion of the new ILAW disposal site. This trough is interpreted to be a smaller part of a much larger trough under the 200 East Area resulting from scouring by the Missoula floods or post-Ringold fluvial incision before the Missoula floods.

Figure 2-18. Structural Contour Map on the Surface of the Ringold Formation.

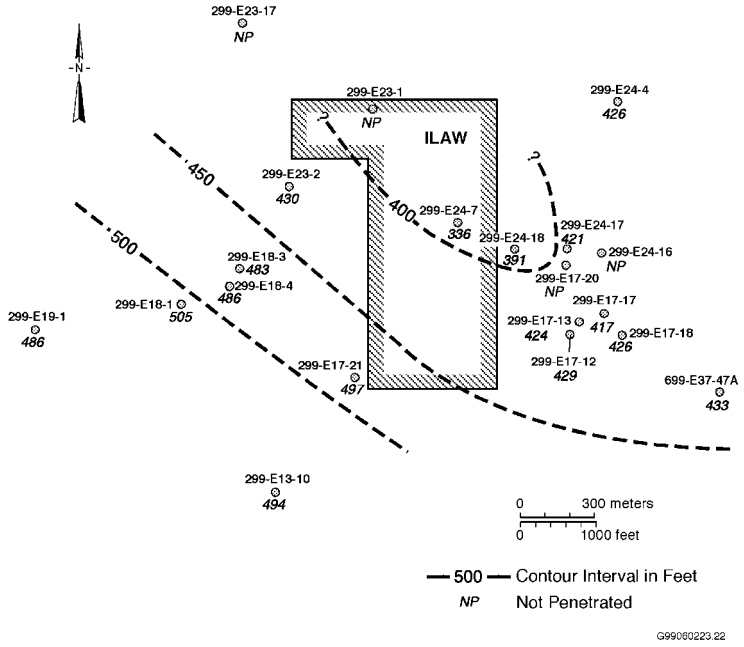

2.2.8.5 Hanford Formation. The Hanford formation is as much as 116 m, (380 ft) thick in and around the ILAW disposal site (Figures 2-10 and 2-19). It thickens in the erosional channel cut into the Ringold Formation and thins to the southwest along the margin of the trough. It may thin northeast of the trough but this is based on only one data point (Figure 2-19).

At the ILAW disposal site, the Hanford formation consists mainly of sand-dominated facies and lesser amounts of silt-dominated and gravel-dominated facies. It has been described on borehole logs as poorly sorted pebble to boulder gravel and fine- to coarse-grained sand, with lesser amounts of interstitial and interbedded silt and clay. In previous studies of the ILAW disposal site (Reidel 1998b), the Hanford formation was described as consisting of three units: an upper and lower gravel-dominated facies and a sand-dominated facies between the two gravel facies. The upper gravel-dominated facies appears to be thin or absent in the ILAW disposal area.

Figure 2-19. Isopach Map of the Hanford Formation at the New ILAW Disposal Site.

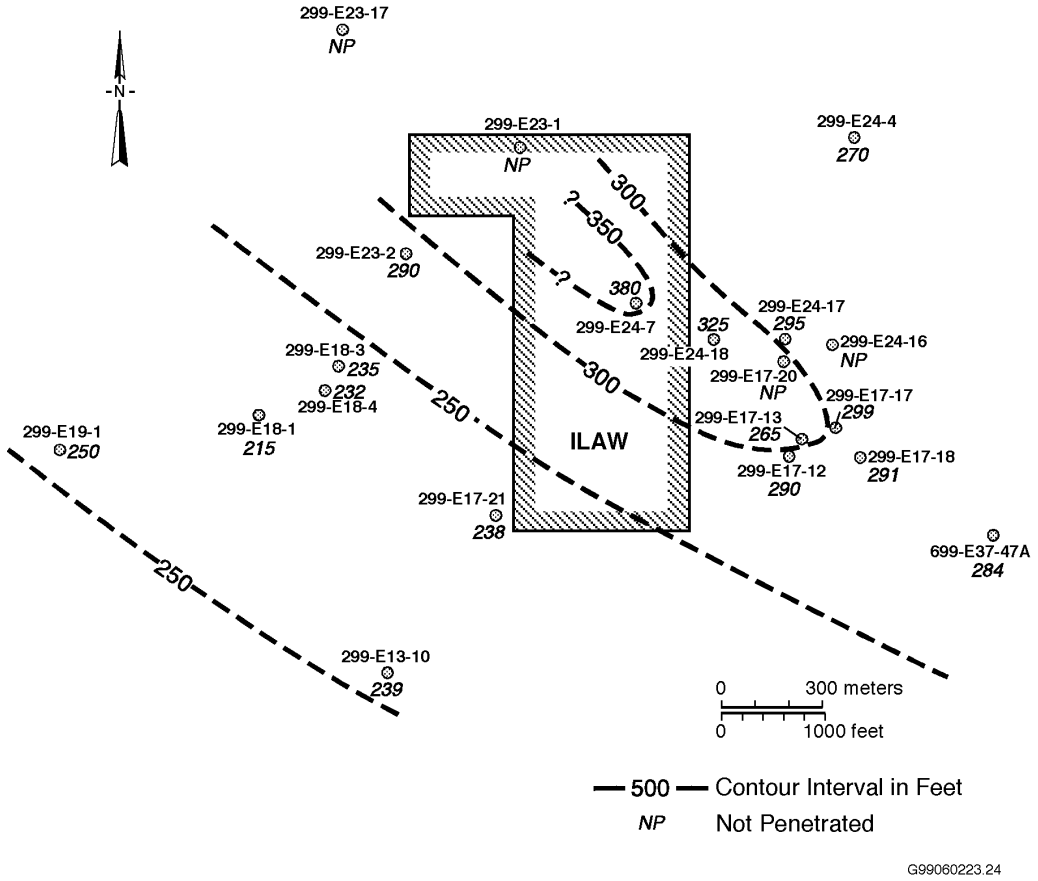

2.2.8.5.1 Basal Gravel Sequence. The lowermost 27 m (88 ft) of the Hanford formation encountered in borehole 299-E17-21 consists of gravel-dominated facies. Drill core and cuttings from this borehole indicate that the unit is clast-supported pebble to cobble gravel with minor amounts of sand in the matrix. Cobbles and pebbles are almost exclusively basalt with no cementation. In outcroppings these deposits display massive bedding, plane to low-angle bedding and large-scale planar forset cross-bedding, but such features typically cannot be observed in borehole core. This unit either pinches out west of the new ILAW disposal site or becomes more sand rich. It thickens to the northeast. The gravel is interpreted to be Missoula flood gravels deposited in the erosional channel carved into the underlying Ringold Formation (Figure 2-18).

This basal gravel sequence is equivalent to unit H3 of Lindsey (1994b) (Table 2-1), and is equivalent to mapping unit Qfg1, Missoula Outburst flood gravel deposits of Reidel (1994a, 1994b). The sand unit overlying this gravel has reversed polarity, indicating that these units are older than 780 thousand years old.

2.2.8.5.2 Sandy Sequence. The upper portion of the Hanford formation consists of at least 73 m (240 ft) of sand-dominated and silt-dominated facies. These deposits have been described as fine- to coarse-grained sand with minor amounts of silt and clay and some gravelly sands. This sequence is equivalent to unit H2 of Lindsey (1994a), and is equivalent to the following mapping units of Reidel (1994a, 1994b): Qfs1, Qfs2, and Qfs3, Missoula Outburst Flood Deposits consisting of sand, silt, and clay (Table 2-1).

Three paleosols (soils) were identified in core and drill cuttings from borehole 299-E17-21 (Reidel 1998b). Paleosol Horizon 1 occurs at 49 m (163 ft) drilled depth (Figure 2-10), paleosol Horizon 2 at 18 m (58 ft) drilled depth, and paleosol Horizon 3 at 1.5 m (5 ft). The paleosol horizons are as much as 15 cm (6 in.) thick with a sharp upper surface. The horizons have a light brown color compared to the darker sands below and some $CaCO_3$ cementation. The lack of well-defined bedding laminations rhythmics like the sands below suggests some bioturbation but no root casts were observed in the core. The paleosol grades downward into normal sands.

The three paleosol horizons represent time intervals when soil development took place and are interpreted to represent three time periods between Missoula flood deposition. Reidel (1998b) called the layers defined by the paleosols: Layer 1 as that part of the Hanford formation extending from the paleosol horizon at 49 m (163 ft) to the top of the basalt gravel at 75 m (247 ft). Layer 2 extends from the top of the second paleosol horizon 18 m (58 ft) to the top of the first paleosol at 49 m (163 ft). Layer 3 extends from the top of the third paleosol horizon at 1.5 m (5 ft) depth to the second paleosol horizon at 18 m (58 ft) drilled depth. The presence or exact depth of these layers is not known elsewhere at the ILAW disposal site and can only be inferred.

Layer 1. Layer 1 is 26 m (84 ft) thick in borehole 299-E17-21. It is a zone of sand and silt with a poorly developed caliche layer at the top. Only the upper several inches are cemented

but $CaCO_3$ extends to a depth of about 3.3 m (10 ft) below the top. $CaCO_3$ fragments or grain coatings were found to a depth of at least 66 m (218 ft).

The lower 6 m (20 ft) of Layer 1 consists of interbedded sands and gravels. The basal gravel sequence underlying Layer 1 appears to grade upward into a sequence of interbedded sands and gravels. At least three upward fining zones of gravels to sands were recognized in Layer 1. These zones are equivalent to unit H2A of Lindsey (1994a).

Planar-laminar sands with minor silt lenses dominate the upper 54 ft (16 m) of Layer 1. This sequence consists of fining upward sands, well-compacted, slightly $CaCO_3$-cemented sands, and well-laminated sands. $CaCO_3$ associated with development of the paleosol extends well down into this layer.

Layer 1 is part of unit H2 of Lindsey (1994a), and is equivalent to mapping unit Qfs1 of Reidel (1994a, 1994b) (Table 2-1). Mapping unit Qfs1 is a Missoula Outburst Flood Deposits consisting of sand, silt, and clay that is 780 thousand years old and has a reversed magnetic polarity. A Paleomagnetic study by the University of California, Santa Cruz, has shown that this layer has reversed magnetic polarity. Layer 1 has only been identified in borehole 299-E17-21. Data from surrounding boreholes is of too poor of quality to identify this layer.

Layer 2. The upper 27 m (90 ft) of Layer 2 is principally the sand- and silt-dominated facies. They have been described as fine- to medium-grained sand with minor amounts of interstitial silt. Throughout the sands are disseminated flakes of $CaCO_3$ and $CaCO_3$-cemented sand grains. Several fining upward zones were recognized as well as highly compacted zones of sand and silt with faint laminations. Layer 2 was correlated to other boreholes using geologists logs and archived chip samples. In addition, the paleosol that forms the top of this layer appears to responsible for zones of lateral spreading of contaminants under waste disposal sites immediately east of the ILAW disposal site.

Layer 2 is also part of unit H2 of Lindsey (1994a), and may be equivalent to mapping unit Qfs2 of Reidel (1994a, 1994b) (Table 2-1). The mapping unit is a Missoula Outburst Flood Deposits consisting of sand, silt and clay that is older than 13 thousand years and younger than 780 thousand years. Mapping unit Qfs2 has a normal magnetic polarity.

Layer 3. Layer 3 is 16 m (53 ft) thick in borehole 299-E17-21. The paleosol at the top of Layer 3 is a 3 cm (1.1 ft) thick, oxidized and leached zone of pebbly, fine-grained sand and silt with some pebbles with a 10-cm (4-in.) poorly developed caliche zone (sand and silt cemented by $CaCO_3$). Several distinct gravelly sands are present within several feet of the paleosol at the top of this layer. This forms the surface of much of the new ILAW disposal site north of the eolian deposits.

The lower 8 m to 10 m (25 to 30 ft) of Layer 3 consists principally of sand with interstitial silt and minor silt beds that are interpreted as lenses. Several minor silt beds are locally present. Gravelly sand, as described on geologists logs, marks a transition to finer grained sand with more silt at a drilled depth of approximately 8 m (25 ft).

Layer 3 is interpreted to consist of the upper gravelly sequence and the upper part of the sandy sequence defined in previous studies. It is part of unit H2 of Lindsey (1994) and is equivalent to mapping unit Qfs3 of Reidel (1994a, 1994b) - Outburst Flood Deposits consisting of sand, silt, and clay that is about 13 thousand years old. An ash from the 13 thousand year old eruption of Mt. St. Helens (Set S Ash) is typically found near the top of this unit in many places throughout the Pasco Basin. The ash was not recognized in any of the boreholes near the ILAW disposal site but has been identified in an excavation 100 m west of the site.

2.2.8.5.3 Eolian Unit. Eolian deposits cover the southern part of the ILAW disposal site. Borehole 299-E17-21 was sited on a stabilized sand dune. The eolian unit is composed of fine- to coarse-grained sands with abundant silt. Calcium-carbonate coating found on the bottom of pebbles and cobbles in drill core through this unit is typical of Holocene caliche development in the Columbia Basin. This unit is equivalent to mapping unit Qd, Holocene Dune Sand, of Reidel (1994a, 1994b) (Table 2-1).

2.2.8.5.4 Clastic Dikes at the ILAW Disposal Site. Clastic dikes have not been observed at the ILAW disposal site. Clastic dikes, however, have been observed in excavations surrounding the site (e.g., PUREX, U.S. Ecology, and Canister Storage excavation). At the new ILAW site, clastic dikes are probably not observed because they are covered by wind blown sediments and a cover of “old growth” sagebrush. The ubiquitous presence of clastic dikes in the 200 East Area suggests that they are probably present at the site.

2.2.9 Regional Hydrology

This section describes the concept of recharge rate for the surface and subsurface hydrology of the Hanford Site region and the disposal facility sites. The surface hydrology is important in determining possible surface pathways for dissolved or suspended contaminants, as well as for identifying sources of infiltration. The groundwater hydrology helps determine possible flow paths for contaminants released from a disposal facility and provides a basis for determining vadose zone thickness.

2.2.9.1 Surface Hydrology. The hydrology of the Pasco Basin (Figure 2-20) is characterized by a number of surface sources and aquifers. Surface drainage enters the Pasco Basin from several other basins, including the Yakima River Basin, the Horse Heaven Basin, the Walla Walla River Basin, the Palouse/Snake Basin, and the Big Bend Basin. Within the Pasco Basin, major tributaries, the Yakima, Snake, and Walla Walla Rivers, join the Columbia River. Two intermittent streams, Cold Creek and Dry Creek, cut through the Hanford Site. Water drains through these pathways during wetter winter and spring months. No perennial streams originate within the Pasco Basin.

Figure 2-20. Hydrologic Basins Designated for the Washington State Portion of the Columbia Plateau (DOE 1988b).

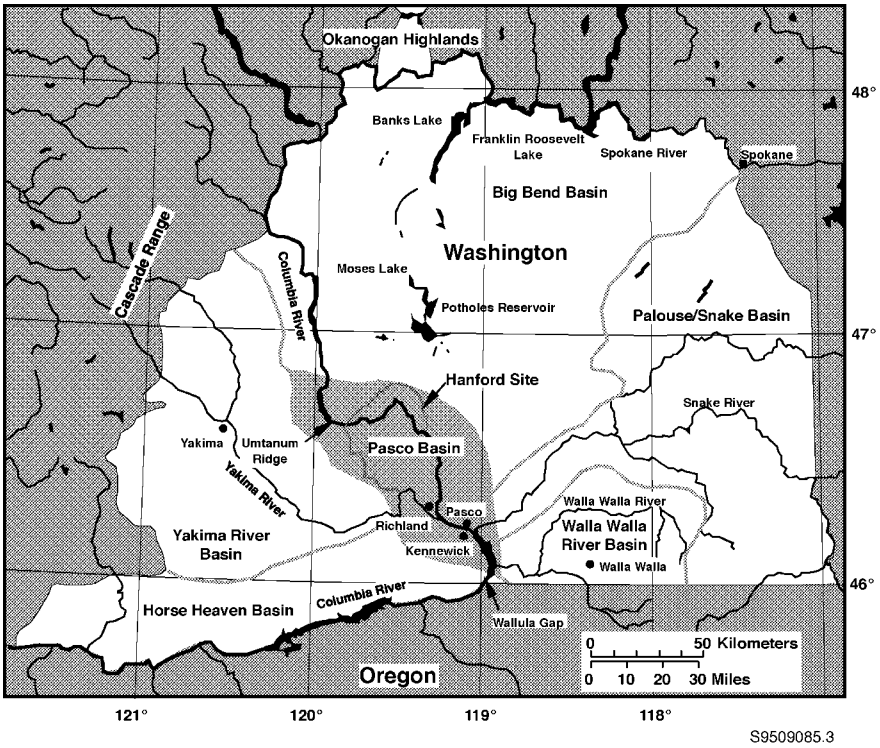

The total estimated precipitation over the basin averages 16.0 cm/y (6.3 in./y) (Section 2.2.5.2). Mean annual runoff from the basin is estimated to be less than 3.1 x 10^7 m^3/y (2.5 x 10^4 acre ft/y), or approximately 3 percent of the total precipitation. The remaining precipitation is assumed to be lost through evapotranspiration, with perhaps a few percent contributing to the recharging of the groundwater (DOE 1988b).

The Hanford Site has one pond, West Lake, and various water disposal ponds. West Lake, located 2.7 km (1.7 mi) north of the 200 East Area, is a shallow pond with an average depth of about 1 m (3 ft) and a surface area of 4 hectares (10 acres). While described as a natural lake, the source of recharge to the lake is groundwater that is locally mounded because of infiltration from 200 Area operations. The pond is a topographic depression that intersects the artificially elevated water table (DOE-RL 1993b-1). 200 Area disposal activities are scheduled to halt within a few decades. As this happens, the water table will drop and West Lake will become an intermittent seasonal pond (DOE-RL 1993c). Waste water ponds, cribs, and ditches associated with nuclear fuel processing and waste disposal activities, although present on the Hanford Site, will not be an important source of water in the future.

No surface streams are near the proposed disposal facilities, but current disposal ponds have an artificial influence on net contributions to the water table. These disposal ponds and related facilities are not expected to exist after current operations end, so their long-term influence is not considered in this performance assessment.

The surface drainage characteristics of the Hanford Site and regional area indicate that the Columbia River and its tributaries are the major surface drainage pathways. The Columbia River is the dominant pathway. The large volume of flow in the Columbia River (typically 1,000 to 3,000 m^3/s [Dirkes 1999-1]) through the Pasco Basin and downstream greatly dilutes any contaminants that reach the river.

DOE conducts routine water-quality monitoring of the Columbia River for both radiological and nonradiological parameters. The Pacific Northwest National Laboratory (PNNL) has been reporting the water quality data since 1973. Ecology has issued a Class A (excellent) quality designation for Columbia River water from Grand Coulee Dam, through the Pasco Basin, to McNary Dam (*Washington Administrative Code* [WAC] 173-201). This designation requires that all industrial uses of this water be compatible with other uses, including drinking, wildlife habitat, and recreation. The Columbia River water is characterized by a low suspended load, a low nutrient content, and an absence of microbial contaminants (Dirkes 1999-1).

2.2.9.2 Flooding. Neitzel (2000-5) describes flooding potentials at the Hanford Site. Except for catastrophic glacier flooding, which is not expected for tens of thousands of years, no floods are expected to affect the Hanford Central Plateau.

The flows for the three largest probable Columbia River flood scenarios range from 17,000 m^3/s to 600,000 m^3/s (600,000 to 21 million ft^3/s). The probable maximum flood on the Columbia River (DOE 1986b), based on natural conditions, has been calculated to be 40,000 m^3/s (1.4 million ft^3/s). This is greater than the 500-year flood. A landslide resulting in Columbia River blockage, followed by flooding could yield a maximum flow of 17,000 m^3/s (600,000 ft^3/s). The U.S. Army Corps of Engineers estimated that a 50 percent breach in the Grand Coulee Dam, the largest dam in the region, would yield flows of 600,000 m^3/s (21 million ft^3/s). None of these flow rates are large enough to cause the Columbia River waters to reach the Hanford Central Plateau.

A flood risk analysis of Cold Creek (west of the 200 West Area) was conducted to characterize a basaltic repository for high-level radioactive waste (Skaggs 1981). Based on this evaluation, the probable maximum flood would be 8 km (5 mi) to the west of the new disposal facility site and its closest approach would be about 6 km (3.6 mi) to the south. The distance would be even greater for the existing disposal facility site.

2.2.9.3 Groundwater Hydrology. The groundwater pathway is considered the most likely pathway for contaminants released from an immobilized low-activity tank waste disposal facility for the following reasons:

Low precipitation in the Pasco Basin

Lack of surface transport pathways near the disposal facilities

Subsurface location of the disposal facilities

Near-surface lysimeter measurements showing downward movement of water

Samples showing the existence of radioactive contaminant plumes in the groundwater because of past Hanford Site operations.

Evaluating this pathway will require information about the types of aquifers present, depths to the water table, regional flow paths, and the net recharge rate.

The hydrology of the Pasco Basin is characterized by a multiaquifer system. This system consists of four hydrologic units corresponding to the upper three formations of the Columbia River Basalt Group (Grande Ronde Basalt, Wanapum Basalt, and Saddle Mountains Basalt) and the overlying suprabasalt sediments (the Hanford formation and Ringold Formation). The basalt aquifers consist of the tholeitic flood basalts of the Columbia River Basalt Group and relatively minor amounts of intercalated sediments of the Ellensburg formation. Confined zones in the basalt aquifers are present in the sedimentary interbeds and/or interflow zones that occur between dense basalt flows. The main water-bearing portions of the interflow zones are networks of interconnecting vesicles and fractures in the flow tops and bottoms (DOE 1988b).

The uppermost aquifer system consists of fluvial, lacustrine, and glaciofluvial sediments. Within the Pasco Basin, this aquifer is regionally unconfined and is contained primarily within the Ringold Formation and the Hanford formation. The main body of the unconfined aquifer usually occurs within the Ringold Formation. The water table in the southwestern Pasco Basin is generally within Ringold fluvial gravels. In the northern and eastern Pasco Basin, the water table is generally within the Hanford formation. Hydraulic conductivities in the Hanford formation are usually greater than in the gravel facies of the Ringold Formation (Graham 1981). However, fine-grained deposits in the Ringold Formation form locally confining layers for Ringold fluvial gravels.

The base of the uppermost aquifer system is defined as the top of the uppermost basalt flow. This aquifer system is bounded laterally by anticlinal basalt ridges and is about 152 m (500 ft) thick near the center of the Pasco Basin. Within the Hanford Site, this uppermost aquifer system lies at depths ranging from less than 0.3 m (1 ft) below the ground surface near West Lake and the Columbia and Yakima Rivers, to more than 107 m (350 ft) in the central portion of the Cold Creek syncline.

Because the uppermost unconfined aquifer is considered the primary pathway for possible contaminant transport from an immobilized low-activity tank waste disposal facility, it is especially important in this performance assessment.

Before the liquid waste disposal systems, such as B Pond, began operating, and before the onset of large regional irrigation projects, the groundwater table for the Hanford Site could be represented by a 1944 water table map (Figure 2-21). This water map includes limited irrigation near the former towns of White Bluff and Hanford, but not the extensive irrigation now common in Cold and Dry Creeks. The 1944 water table contours suggest that groundwater flow is easterly toward the Columbia River with a relatively uniform hydraulic gradient (approximately 1.5 m/km [5 ft/mi]). Regional groundwater flow was generally toward the east-northeast, although flow north of Gable Mountain was more to the north.

Effluent disposal at the Hanford Site has altered hydraulic gradients and flow directions of the uppermost aquifer system, particularly near the 200 Areas. Figure 2-22 shows a recent water table map influenced by effluent disposal actions. Regional irrigation projects had a minor influence on the changes shown in Figure 2-22. Groundwater flow is still nominally easterly toward the Columbia River, but mounding occurs in the 200 East Area near B Pond. Groundwater flow north of Gable Mountain now trends in a more northeasterly direction as a result of mounding near reactors and northerly flow through Gable Gap between Gable Mountain and Gable Butte. South of Gable Mountain, flow is interrupted locally by the groundwater mounds in the 200 Areas. Some groundwater from the 200 Areas flows to the north between Gable Mountain and Gable Butte. For the time periods considered in this performance assessment, effluent disposal operations will have stopped.

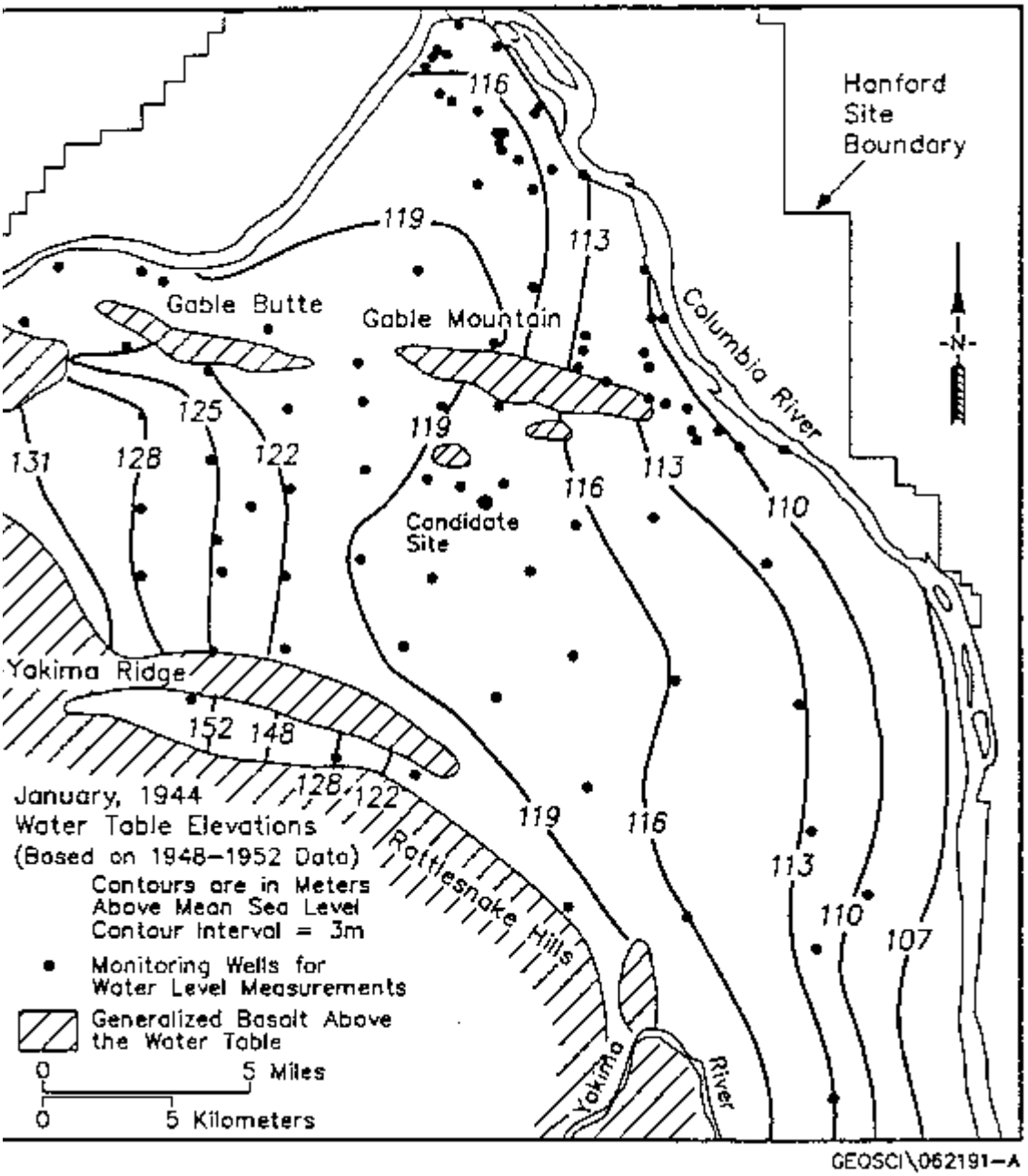

Figure 2-21. Hindcast Water Table Map of the Hanford Site, January 1944 (ERDA 1975).

Figure 2-22. Hanford Site Water Table Map, June 1989 (Smith 1990).

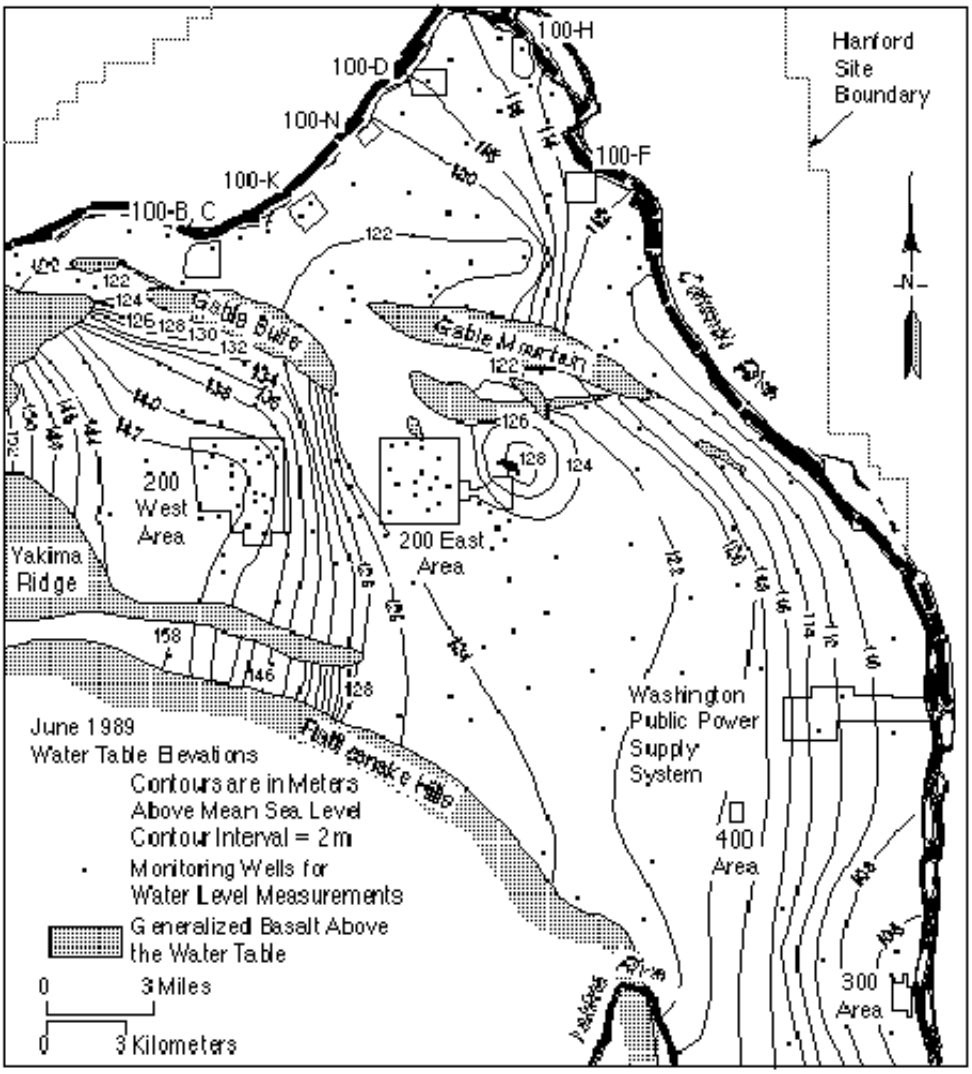

2.2.9.4 Natural Recharge Rates. The information in this section is based on *Recharge Data Package for the Immobilized Low-Activity Waste 2001 Performance* Assessment (Fayer 1999). Recharge is the amount of total precipitation that infiltrates into the unsaturated zone (vadose zone) after runoff, evaporation, and transpiration by plants have occurred. Recharge from rain and snow melt is a major hydrologic variable affecting contaminant transport from an immobilized low-activity tank waste disposal facility.

Studies conducted over the last 25 years at the Hanford Site are summarized in the following paragraphs. These studies indicate that long-term recharge can vary greatly depending on factors such as climate, vegetation, land use, and soil texture. As noted in Section 2.2.5, most of the very small amount of precipitation at the Hanford Site falls in the winter and spring. Because of the dry conditions at the Site, most of the precipitation is stored in near-surface soils until used by plants or evaporates during the hot summer months. Natural plants have adapted to use all the water in the near-surface zone. Because of the large storage capacity of the near surface soils, water rarely (on just a few days per decade) exits downwards from this near-surface zone. Such rare events typically occur following the rapid melting of a snow pack.

Most recharge rate data at the Hanford Site have been measured directly using a combination of drainage and weighing lysimeters (Rockhold 1995, Gee 1992). These lysimeters are vertical tubes as much as 5 m long in the ground filled with various type of soils and covered with various types of vegetation. At the bottom of the lysimeters, the water that passed through the tube of soil is collected and measured (by volume or weight). The measurements can be used to determine the rate at which moisture escapes the near-surface part of the vadose zone. Because no mechanisms are known to exist that trap the moisture, the measured rate from the lysimeters is considered a good approximation for the recharge rate of the conditions (soil, vegetation, and precipitation) simulated by the lysimeter.

The recharge rate depends on the seasonal distribution of precipitation, type of surface soil and vegetation, and climatic conditions. Maximum recharge events occur following the wettest winter periods. Under normal conditions, the recharge rate is highest in coarse-textured soils without vegetation and is at the measurement threshold in fine-textured soil with or without vegetation. Coarse soil surfaces that are either vegetated with shallow-rooted species or bare exhibit recharge on the order of 50 percent of the precipitation.

Fayer and Walters (Fayer 1995) estimated recharge rates based on measurements (lysimeters, tracers, and regional studies) and on numerical modeling. Estimates made using these methods were assigned to specific soil-vegetation combinations and distributed across the Hanford Site using a soil map and a vegetation-land use map. The long-term average rates varied from 2.6 mm/y (0.1 in./y) for several soil and vegetation combinations in the 200 Areas (including the immobilized low-activity tank waste disposal facility sites) to 127.0 mm/y (5.0 in./y) for basalt outcrop with no vegetation at the crest of Rattlesnake Mountain (Fayer 1995).

For the sites of interest to ILAW disposal, surface soils are dominated by Rupert Sands and Burbank Loamy Sand. Fayer (1999), summarized in Section 3.4.6 along with the human influences on recharge, estimates that the natural recharge rate through the two types of soils are

0.9 mm/y and 4.2 mm/y, respectively. It should be noted that the Burbank Loamy Sand soil type was not considered in the 1998 ILAW PA (Mann 1998a). See Section 3.4.6 for a fuller description of recharge rates and the choice of values used in this performance assessment.

2.2.10 Geochemistry

The information in this section is taken from *Mineralogy of Selected Sediment Samples from Borehole 299-E17-21*, (Mattigod 2000). This section discusses the mineralogy of the ILAW disposal site, based on recently obtained samples from the borehole located at the southwest edge of the ILAW disposal Site (Reidel 1998a). Information about Geochemical methods and parameters used in the performance assessment analysis is given in Section 3.4.3.3.

The dominant minerals in the sand fractions of all samples were quartz (about 66 to 82 percent by mass) and feldspars (about 15 to 31 percent) (Table 2-3). These minerals (quartz and anorthite and orthoclase feldspars) constituted approximately 92 to 99 percent of the total mass of the sediment samples. Trace quantities of muscovite mica, chamosite (a type of chlorite) and ferrotschermakite (an amphibole mineral) also were detected in sand fractions. The silt fractions of these samples also were dominated by quartz (about 61 to 76 percent) and feldspars (about 19 to 44 percent). Compared to sand fractions, the silt fractions contained higher amounts of muscovite and chamosite (about 1 to 5 percent), and ferrotschermakite (1 to 10 percent). Illitic mica was the dominant mineral at about 42 to 60 percent by mass in clay fractions of all the sediment samples (Table 5). About 14 to 17 percent chlorite and about 21 to 28 percent kaolinite also were found in clay fractions. Minor amounts (3 to 12 percent) of smectite (a mineral important for its geochemical reactivity) also were detected in clay fractions of all samples. Overall, quartz and feldspars dominated the sand fractions, whereas the clay fractions were dominated by illitic mica and chlorite. These size-dependent mineral distributions are typical of primary (quartz and feldspars) and secondary (illite, chlorite, kaolinite, and smectite) mineral occurrence in soils undergoing chemical weathering. The mineralogy of these sediments was typical of published mineralogy of other Hanford formation sediments (Schramke, 1988).

Layers of high $CaCO_3$ (calcite) are found in the 200 West Area. Calcite can affect the mobility of certain contaminants and tends to buffer pore moisture. However, Mattigod (2000) found less than 5% of calcite in any of the samples they analyzed from the ILAW disposal site. Moreover, such layers are readily visible in geologic logs and have not been seen in other boreholes near the ILAW disposal site.

Based on the semiquantitative mineralogy data and the mass distribution of particles in each size fraction (Table 2-3), the mineral distribution was computed on the bulk soil basis. As expected, in all samples (predominantly sandy in texture), the minerals that are dominant in sand and silt fractions, quartz and feldspars, also dominate the mineralogy of bulk soils at approximately 91 to 95 percent). All other minerals occur in minor to trace concentrations in these soils.

Although the mineralogy of these soils are dominated by quartz and feldspar minerals, other minerals such as illite, chlorite, smectite and kaolinite, which have characteristics such as

high surface areas, ionizable exchange sites, and specific adsorption interlayer sites significantly influence bulk soil chemical properties such as cation exchange capacity (CEC). Therefore, calculations were made to assess the contribution of each mineral to the overall CEC of whole soil. The results show that although the minerals mica, chlorite, smectite and kaolinite together constitute only about5 to 9 percent of the total soil mass, they account for about 40 – 60 percent of the total exchange capacity of the whole soils. Only trace amounts (less than 0.6 percent) of smectite were detected in these soils however, because of this mineral's very high surface area, it accounts from about 4 to 17 percent of the CEC of the whole soils. Also, it is well established that minerals such as illitic mica in Hanford formation sediments specifically adsorb radionuclides such as ^{137}Cs (Mattigod et al. 1994a, 1994b). Therefore, mica although constituting only about 3 to 5 percent of the soil mass would significantly affect the specific adsorption of alkali cations such as cesium and potassium by the whole soil.

Also, the calculated CEC of the whole soils agreed reasonably well with the measured CEC values except in the case of samples 24A, 31A, and 35A. The measured CEC values for these samples were about twice as high as the calculated values. Because the mineralogy of these samples were not significantly different from other core samples, the anomalously high measured CEC values were attributed to the presence of trace amounts of carbonates present in these sediments.

Table 2-3. Semiquantative Estimates (wt%) of Minerals in Selected Sediments from ILAW Borehole (from Mattigod 2000).

		Fraction	Quartz	Feldspar	Mica	Chlorite	Amphibole	Smectite	Kaolinite
7A	Sand	0.921	62	12	1	1	--	--	--
	Silt	0.055	12	5	1	1	--	--	--
	Clay	0.024	--	--	3	1	--	Tr	1
	All		74	17	5	2	--	Tr	1
10A	Sand	0.821	63	21	1	1	--	--	--
	Silt	0.146	8	3	Tr	1	--	--	--
	Clay	0.033	--	--	2	Tr	--	Tr	1
	All		71	23	3	2	--	Tr	1
14A	Sand	0.794	59	28	1	1	1	--	--
	Silt	0.136	3	2	Tr	Tr	Tr	--	--
	Clay	0.070	--	--	3	1	--	Tr	1
	All		62	30	2	2	1	Tr	1
16A	Sand	0.947	66	19	1	1	1	--	--
	Silt	0.038	6	3	Tr	Tr	Tr	--	--

Table 2-3. Semiquantative Estimates (wt%) of Minerals in Selected Sediments from ILAW Borehole (from Mattigod 2000).

		Fraction	Quartz	Feldspar	Mica	Chlorite	Amphibole	Smectite	Kaolinite
	Clay	0.014	--	--	2	Tr	--	Tr	1
	All		72	22	3	1	1	Tr	1
20A	Sand	0.090	65	18	1	1	1	--	--
	Silt	0.088	6	2	Tr	1	1	--	--
	Clay	0.012	--	--	2	1	--	Tr	1
	All		71	20	3	3	2	Tr	1
24A	Sand	0.913	59	28	1	1	--	--	--
	Silt	0.061	5	2	Tr	Tr	Tr	--	--
	Clay	0.026	--	--	2	1	--	Tr	1
	All		64	30	2	2	Tr	Tr	1
31A	Sand	0.884	53	16	1	1	1	--	--
	Silt	0.100	17	5	Tr	Tr	Tr	--	--
	Clay	0.015	--	--	2	1	--	Tr	2
	All		70	22	3	2	1	Tr	2
35A	Sand	0.983	68	25	1	1	1	--	--
	Silt	0.011	1	--	--	--	--	--	--
	Clay	0.006	--	--	1	1	--	Tr	1
	Allk		69	25	2	1	1	Tr	1

Tr: Trace quantity < 0.5%.

2.2.11 Natural Resources

The Central Plateau of the Hanford Site has no important natural resources. No major mining operations exist in the Hanford Site area. Oil and gas exploration have occurred; however, no economically viable accumulations were found. Some local gravel processing is being done in the area.

As noted in the hydrology section (Section 2.2.9), the unconfined aquifer is not a significant resource for water. Monitoring wells on the Hanford Site normally have screen lengths of 6.1 m (20 ft) (Evans 2000).

2.2.12 Regional Background Contamination and Hanford Site Monitoring

The Hanford Site has an extensive monitoring program. Studies have been directed at determining background levels of possible contaminants in the soil (DOE-RL 1994b and DOE-RL 1995b) and in the groundwater (Johnson 1993). Also, reports are issued annually covering general environmental conditions (Dirkes 1999) and groundwater monitoring (Hartman 2000).

2.2.12.1 Soil Background Levels. Low concentrations of ^{90}Sr, ^{137}Cs, and ^{239,240}Pu were measured in samples of soil and vegetation during 1998 (Dirkes 1999-2). The levels were similar to those measured in previous years. No discernible increase in concentration could be attributed to current Hanford Site operations. DOE-RL 1995b summarizes all the measurements taken to determine radionuclide background levels at the Hanford Site. Table 2-4 displays the average of the measurements.

Table 2-4. Activity of Radionuclides in Hanford Sitewide Background Data Set (DOE-RL 1995b).

Nuclide	Activity (pCi/g)	Nuclide	Activity (pCi/g)	Nuclide	Activity (pCi/g)
^{40}K	15.4	^{60}Co	0.00132	^{90}Sr	0.0806
^{137}Cs	0.417	^{154}Eu	0.0083	^{155}Eu	0.0234
^{226}Ra[a]	0.686	^{232}Th+D	0.687	^{235}U+D	0.0271
^{238}U+D	0.675	^{238}Pu	0.00158	$^{239/240}$Pu	0.00935

"+D" indicates that daughters are included

[a] ^{226}Ra is part of ^{238}U decay chain and is included in that entry.

2.2.12.2 Groundwater Background Levels. Sample results from environmental monitoring can vary depending on local operations, so a regional baseline study was conducted using these and other Sitewide monitoring results (Johnson 1993). Groundwater background values and trigger threshold levels are shown in Table 2-5.

Table 2-5. Background Values for Hanford Site Groundwater. [a]

Constituent (Concentration)	Groundwater Background Values [b]	Provisional Threshold Values
Aluminum (ppb)	<2	<200
Ammonium (ppb)	<50	<120
Arsenic (ppb)	3.9 ± 2.4	10
Barium (ppb)	42 ± 20	68.5
Beryllium (ppb)	<0.3	<5
Bismuth (ppb)	<0.02	<5
Boron (ppb)	<50	<100
Cadmium (ppb)	<0.2	<10
Calcium (ppb)	40,400 ± 10,300	63,600
Chloride (ppb)	10,300 ± 6,500	NC
Chromium (ppb)	4±2	<30
Copper (ppb)	<1	<30
Fluoride (ppb)	370 ± 100	1,340, 775[c]
Iron-mid (ppb)	NA	291
Lead (ppb)	<0.5	<5
Magnesium (ppb)	11,800 ± 3,400	16,480
Manganese (ppb)	7±5	NC
Mercury (ppb)	<0.1	<0.1
Nickel (ppb)	<4	<30
Nitrate (ppb)	NA	12,400
Phosphate (ppb)	<1,000	<1,000
Potassium (ppb)	4,950 ± 1,240	7,975
Selenium (ppb)	<2	<5
Silver (ppb)	<10	<10
Silicon (ppb)	NA	26,500
Sodium (ppb)	18,260 ± 10,150	33,500
Strontium (ppb)	236 ± 102	264.1
Sulfate (ppb)	34,300 ± 16,900	90,500
Uranium (pCi/L)	1.7 ± 0.8	3.43

Table 2-5. Background Values for Hanford Site Groundwater. [a]

Constituent (Concentration)	Groundwater Background Values [b]	Provisional Threshold Values
Vanadium (ppb)	17 ± 9	15
Zinc (ppb)	6 ± 2	NC
Field alkalinity(ppb)	NA	215,000
Laboratory alkalinity (ppb)	123,000 ± 21,000	210,000
Field pH	NA	(6.90, 8.24)
Laboratory pH	7.64 ± 0.16	(7.25, 8.25)
Total organic carbon (ppb)	586 ± 347	2,610, 1,610[c]
Field conductivity (μmho/cm)	NA	39
Laboratory conductivity (μmho/cm)	380 ± 82	530
TOX, LDL (ppb)	NA	60.8, 37.6[c]
Total carbon (ppb)	NA	50,100
Gross alpha (pCi/L)	2.5 ± 1.4	63, 5.79[c]
Gross beta (pCi/L)	19 ± 12	35.5, 12.62[c]
Radium (pCi/L)	<0.2	0.23

[a] From Tables 5-9 and 5-11 of DOE-RL 1992.
[b] Results shown are mean ± one standard deviation, unless only an upper limit is given.
[c] Potential outlier observation(s) were removed.

LDL = lower detectability limit
NA = not available
NC = not calculated
TOX = total organic halides

2.2.12.3 Radiation Background Levels. Various natural and human-produced sources contribute to radiation doses. These sources include natural terrestrial and cosmic background radiation, medical treatment and x-rays, natural internal body radioactivity, and inhalation of naturally occurring radon. Figure 2-23 shows the national average dose from each of these sources to an individual. Of the contributions shown in Figure 2-23, natural background contributes 300 mrem to the estimated per capita annual dose to individuals living near the Hanford Site. Human-produced sources contribute an additional 65 mrem. In contrast, annual Hanford Site environmental reports (e.g., Dirkes 1999-3) estimate that the maximum annual dose to an individual from Hanford Site operations in 1998 was about 0.02 mrem. This is similar to values seen over the last 4 years.

The public is exposed to radiation at or near the Hanford Site from industrial sources other than DOE operations. These sources include the low-level radioactive waste burial site operated by U.S. Ecology, the nuclear generating station operated by Energy Northwest, the nuclear fuel production plant operated by Siemans Nuclear Power Corporation, the low-level waste compacting facility operated by Allied Technology Corporation, and a decontamination facility operated by Pacific Nuclear Services. Based on information gathered from these companies, Dirkes (Dirkes 1999-3) conservatively determined that the total 1998 annual dose for the hypothetical maximally exposed individual from those activities also was 0.02 mrem.

Figure 2-23. Averages for Natural and Human-Produced Sources of Radiation (NCRP 1987).

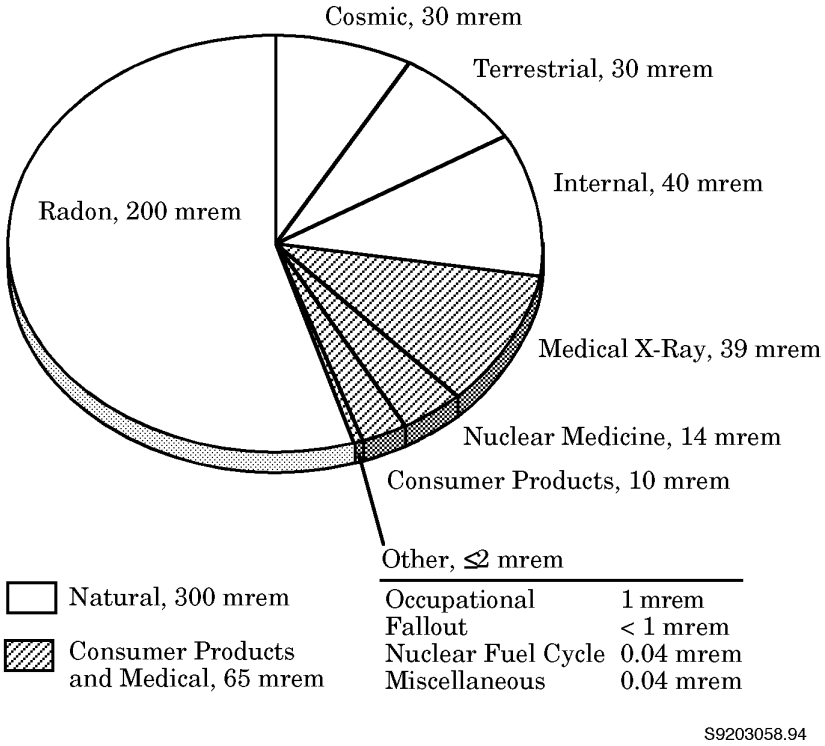

2.3 WASTE CHARACTERISTICS

2.3.1 Overview

The source of the waste material to be incorporated into a solidified waste form is the waste currently stored in the Hanford Site's single- and double-shell tanks. This section covers the activities from the current storage of special material production waste through the delivery of the treated waste at the disposal sites.

The TWRS record of decision (DOE 1997b) states that the waste will be retrieved from the tanks, then chemically separated to form the high- and low-activity radioactive waste fractions. The high-activity radioactive waste fraction will contain most of the radionuclides. This waste fraction will be vitrified, and the product stored until it can be transferred to a licensed high-level waste repository. The low-activity radioactive waste fraction contains the bulk of the nonradioactive chemicals and is predominantly the soluble components of the tank waste. This waste fraction will be solidified in a glass or other form that meets the DOE specifications.

It is proposed to dispose of the immobilized low-activity waste form on Site in a manner that allows the waste to be retrievable for at least 50 years, although this time period has not been adopted officially.

2.3.2 Underground Tank Storage

To store the liquid high-level radioactive waste generated by Hanford Site operations since 1944, 149 single-shell tanks and 28 double-shell underground tanks were built. The tanks are grouped into 18 tank farms containing over 204,000 m^3 (53.6 Mgal) [Hanlon 2000-1] of waste. The consistency of the tank waste ranges from dilute aqueous solutions to thick paste to hard solid.

Four basic chemical processing operations generated the radioactive waste solutions. These operations were the bismuth phosphate process, the REDOX process, the PUREX process, and the tributyl phosphate process. The first three processes recovered plutonium from irradiated reactor fuels. The last process recovered uranium waste generated in the bismuth phosphate process. Other specialized campaigns recovered ^{137}Cs, ^{90}Sr, and other special nuclear materials. The aqueous waste was made alkaline to control corrosion in the carbon-steel underground tanks. Anderson (1990) provides a history of the liquid waste generation and its subsequent handling and storage in the tank farms.

Most of the tank waste has undergone one or more treatment steps (for example, neutralization, precipitation, decantation, or evaporation). The neutralized waste contains sodium nitrate and nitrite, sodium hydroxide, sodium aluminate, sodium phosphate, various insoluble hydroxides and phosphates, usually small quantities of organic materials, and various

radionuclides (approximately 250 MCi). The main effect of the treatment steps other than neutralization was to reduce the water content of the waste.

2.3.3 Tank Waste Retrieval

According to the Tri-Party Agreement (Ecology 1998), as much waste as possible, given current technology, must be removed from the tanks for treatment and immobilization. Unless limited by waste retrieval technology, the single-shell tank waste residues must not exceed 360 ft^3 (approximately 10 m^3) in each 200-series tank, which can hold 208 m^3 (55,000 gal) of waste. For the 100-series tanks, which have volumes above 2,000 m^3 (500,000 gal), the limit is 30 ft^3 (approximately 1 m^3). On a tank-by-tank basis, the DOE can request that the EPA and Ecology approve a higher residue limit.

2.3.4 Separations

The purpose of the separations step [DOE 1997b] is to separate the retrieved tank waste into the following two radioactive waste fractions:

A low-activity fraction containing the bulk of the non-radioactive material and limited amounts of radionuclides. This waste will be immobilized and disposed in the 200 Areas on the Hanford Site.

A much smaller high-activity fraction containing most of the radionuclides. This waste will be immobilized, then stored until a licensed Federal high-level repository is ready to receive it.

In the Tank Waste Remediation System Operation and Utilization Plan (TWRSO&UP) the best-basis tank-by-tank inventories (BBI) were partitioned into water-soluble and water-insoluble phases using the most recent water wash data for each tank (Hendrickson 1999). Caustic wash data (Colton 1997) were applied to the HLW feed calculations (Kirkbride 1999). The tank inventory components were distributed between liquid and solid phases in the TWRSO&UP by applying tank-specific wash factors for every BBI analyte (Hendrickson 1999). Global caustic leach factors were applied to the water-insoluble phases to model the LAW generated as part of the HLW feed preparation.

This strategy is intended to achieve reasonable waste disposal costs in comparison with the costs of disposing of all of the tank waste at the proposed high-level repository, while providing adequate protection of the public and the environment. DOE plans to accomplish the treatment of tank waste in two phases. Phase 1 is planned to be a demonstration with waste treatment and immobilization. In this phase about 10% of the tank waste by volume (or about 25% by activity) would be treated. In Phase 2, contractors would provide waste treatment and immobilization services and retrieve waste from the remainder of the tanks. In both phases DOE would store and dispose of the immobilized product.

ORP plans to use the following three-step approach during Phase 1 (2002 through about 2018).

1. Separate the soluble components from the insoluble components by means of in-tank "sludge washing" followed by settle-decant of the supernant liquid.

2. Treat the soluble fraction to provide a feed to the low-activity waste immobilization facility that is in accordance with the NRC's "incidental waste" classification for Hanford Site waste (Paperiello 1997). The NRC requires that the waste meet the following criteria.

   - The waste has been processed (or will be processed further) to remove key radionuclides to the maximum technically and economically practical extent possible.

   - The waste will be incorporated into a solid physical form at a concentration level that does not exceed the applicable concentration limits for Class C low-level waste as set out in 10 CFR 61 (10 CFR 61-2).

   - The waste is to be managed, pursuant to the *Atomic Energy Act of 1954* (AEA 1954), so that safety requirements comparable to the performance objectives set out in 10 CFR 61 (10 CFR 61 - 3) are satisfied.

3. Wash the insoluble fraction in the tank, then use enhanced in-tank sludge washing (alkaline leaching) to remove more soluble nonradioactive material from the feed going to the high-level waste vitrification facility. Any additional separations required will be performed in the separations facility.

Performance details may differ during the second production period, but equivalent separations are expected.

The NRC staff (Paperiello 1997) has indicated that such a separations activity along with an assessment consistent with NRC standards (10 CFR 61) would allow the NRC to treat the low-activity waste as 'incidental waste,' which does not come under NRC licensing authority.

2.3.5 Immobilization of the Low-Activity Waste

After waste-type separation, the low-activity waste will be immobilized into glass. Current plans involve vitrification in a joule-heated ceramic DuraMelter. The DuraMelter vitrification system imposes certain operational and process requirements on the glass formulations that include:

- Viscosity limits of 1 to 15 Pa·s at 1100°C
- Electrical conductivity limits of 0.2 to 0.7 S/cm at 1100 to 1200°C
- Liquidus temperature below 950°C.

Other factors affecting melter operations that are also important include:

- Ability to retain sulfur in the glass matrix without the formation of molten salt phases during processing; these phases are more corrosive, electrically conductive, and fluid than the glass melt, and have lower melting points.
- Compatibility of the glass melts with the projected glass contact refractory (primarily Monofrax K-3) and the metallic components of the melter (e.g., electrodes, bubblers, thermowells, etc.).

In addition to these processing constraints, the DOE imposes additional product acceptance constraints. Detailed specifications regarding waste package size, compressive strength, crystallinity, etc. have been developed (DOE/ORP 2000c).

A large number of LAW glasses has been formulated by staff at the Vitreous State Laboratory (VSL) in Washington D.C. that meet these processing and product acceptance requirements while achieving waste loadings ranging from 6 to 31 mass%. Supplemental to the VSL work, a set of 77 glasses has been formulated and is currently being tested under a project funded by EM-50 (Vienna et al., 2000). The combined set of these glasses covers a very wide-ranging, multidimensional compositional space. While no single method could accurately depict the entire range in compositional variability that has been considered, it is possible to capture the bulk of the range in variability by separating the glass into univalent, divalent, trivalent, and tetravalent metal oxides that make up the majority (>95%) of the glass composition. Two ternary diagrams can then be constructed, as shown in Figure 2-24, which provide insight with respect to the composition space investigated to date. In general, the EM-50 series of glasses has been formulated with lower amounts of divalent metal oxides than are currently being considered by the VSL. Discussions with VSL staff have indicated a desire to increase the concentration of CaO, which has been shown to increase sulfur solubility in the glass, and ZnO, which apparently retards corrosion of the melter refractories. In contrast, the EM-50 glasses bound very well the range in total alkali contents that have been considered by VSL. The reader should also note the position of LAWABP1 and HLP-31 glasses in Figure 2-24, which are the two glasses that form the base and sensitivity cases with respect to compositional effects on the glass release rate in this performance assessment.

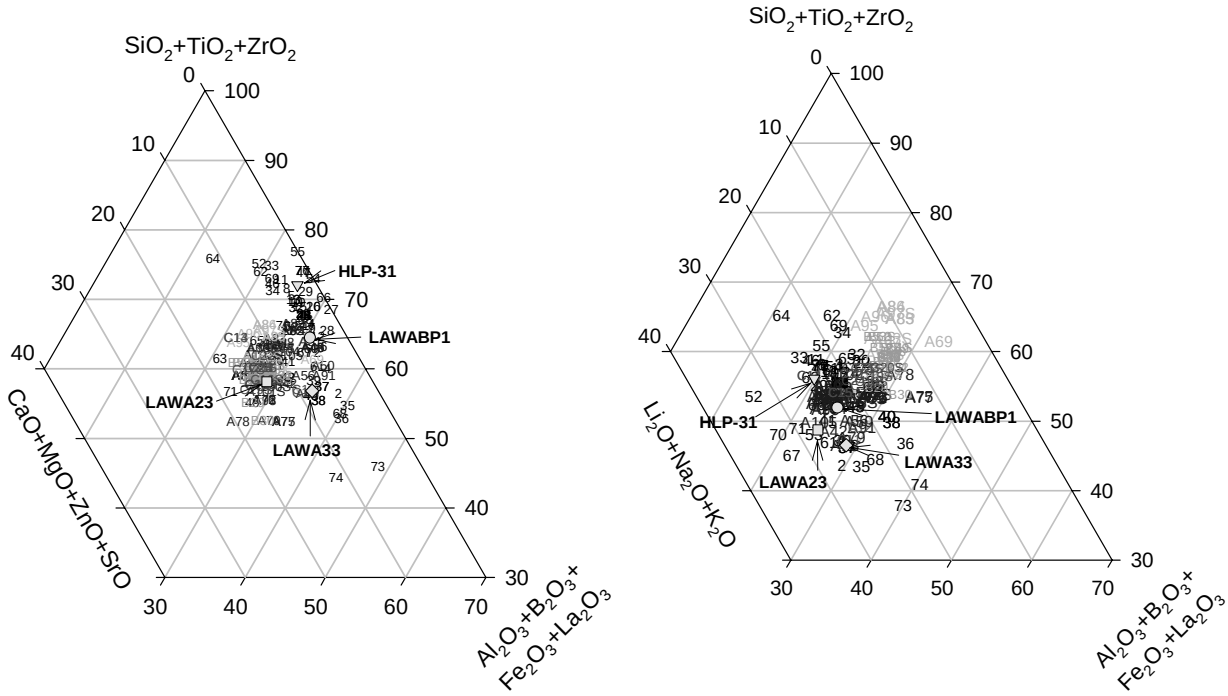

Figure 2-24. Ternary Diagrams Depicting Compositional Variability for ILAW Glasses. Symbols "A##" (Blue) are Envelope A glasses, low sulfur; "A##" (Cyan) are Envelope A glasses, high sulfur; "B##" (Green) are Envelope B glasses; "C##" (Red) symbols are Envelope C glasses; and (Black) symbols with numbers only are the EM-50 HLP series glasses. Reference ILAW glasses evaluated extensively for ILAW performance assessments are shown as diamonds (Yellow).

In addition to the processing and product acceptance requirements discussed previously, there are two acceptance specifications with respect to the chemical durability of the ILAW glass product of importance to this PA, which are as follows:

1. Product Consistency Test (PCT): The normalized mass loss of sodium, silicon, and boron shall be measured using a seven-day PCT run at 90°C as defined in ASTM C1285-98. The test shall be conducted with a glass to water ratio of 1 gram of glass (-100 +200 mesh) per 10 milliliters of water. The normalized mass loss shall be less than 2.0 grams/m^2. Qualification testing shall include glass samples subjected to representative waste form cooling curves. The PCT shall be conducted on waste form samples that are statistically representative of the production glass.

2. Vapor Hydration Test (VHT): The glass corrosion rate shall be measured using a seven day VHT run at 200°C as defined in the DOE concurred upon Product and Secondary Waste Plan. The measured glass alteration rate shall be less than 50 grams/(m^2-day). Qualification testing shall include glass samples subjected to representative waste form cooling curves. The VHT shall be conducted on waste form samples that are statistically representative of the production glass.

Figure 2-25 shows the available data with respect to VHT and PCT test results in comparison with the product durability specifications. The results show that most of the ILAW glasses that have been tested comply with the product specifications. The baseline glass formulation used in this PA (LAWABP1) plots in the middle range of product performance as measured by these two tests; however, HLP-31 glass (sensitivity case glass) violates both acceptance criteria. Although not the poorest performing glass that has been tested, HLP-31 does represent an extreme in terms of glass composition and durability with respect to the majority of the ILAW glasses tested to date. Figure 2-25 also shows that the short-term PCT-A test is a poor predictive test in terms of longer-term glass durability, which is better represented by the more aggressive VHT. For the majority of the ILAW glasses, PCT-A normalized release is between 0.2 and 0.6 g/m², a factor of 3 spread. However, these same glasses exhibit more than 4 orders of magnitude spread in their VHT corrosion rate. These data present a compelling argument for maintaining both PCT-A and VHT tests as combined product acceptance tests for ILAW.

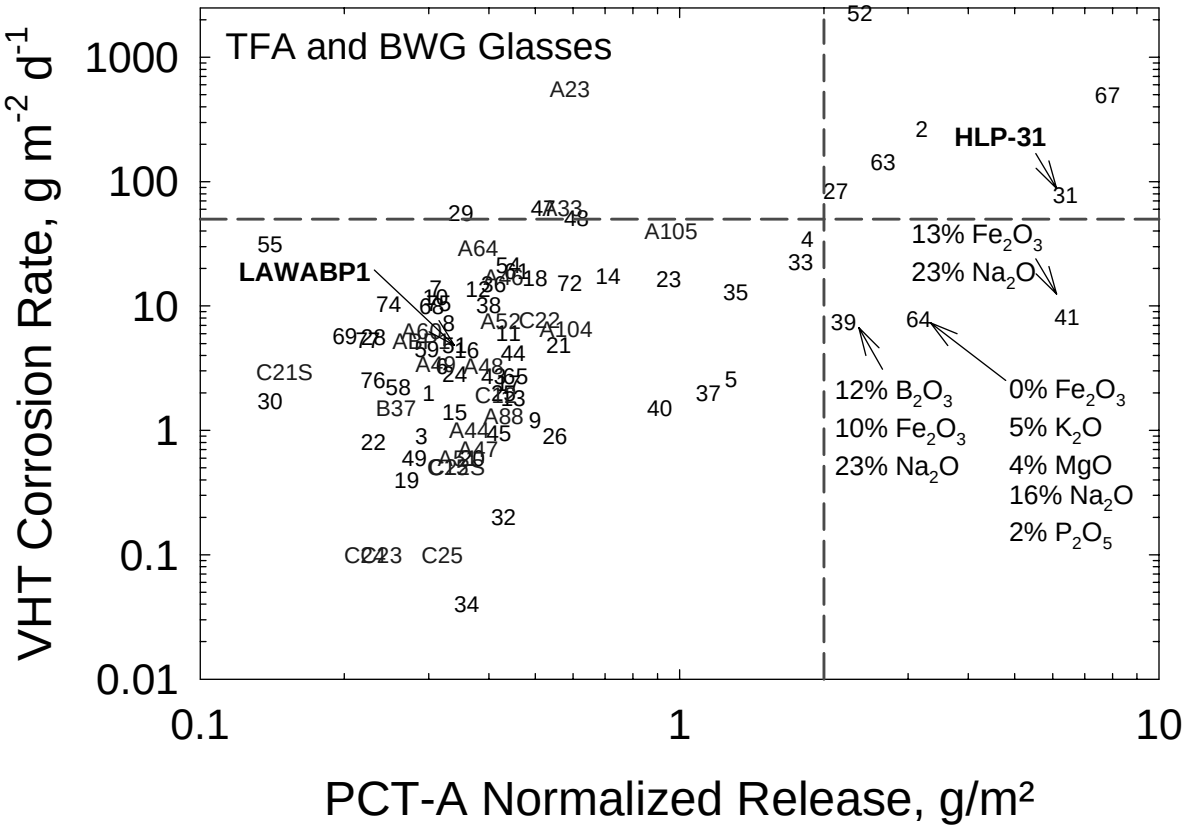

Figure 2-25. Comparison of VHT and PCT-A Test Performance of ILAW Glasses with Respect to DOE Product Acceptance Specifications

2.3.6 Packaging and Certification

The physical, chemical, and radiological properties of the waste at the time of disposal have not been completely determined. At the time of the start of this analysis, the waste form was expected to be contained in metal containers with external dimensions of 1.4 m by 1.4 m by 1.4 m (about 4.6 by 4.6 by 4.6 ft) (DOE-RL 1996). Modification 12 of the BNFL contract (see DOE/BNFL 1998) was issued on January 24, 2000, and required ILAW canisters in the form of right circular cylinders (1.22 m diameter by 2.29 m tall). This occurred after the data packages used in these analyses were issued and will not be explicitly addressed in this report. Future work will use the latest dimensions for the waste package and other facility information. However, a sensitivity case in this analysis shows that such a container size change is not significant to the conclusions of this performance assessment.

Based on Case 3 of the TWRSO&UP (Kirkbride 1999), Phase 1 produces a total of 117,605 MT of ILAW, which corresponds to approximately 19,295 ILAW packages. The Phase 1 contractor will deliver the ILAW product in 1.4 m cube-shaped packages. Each package contains 2.3 m^3, or 6095 kg, of glass. Phase 2 produces a total of 301,374 MT of ILAW, which corresponds to approximately 49,446 ILAW packages. Because no specific guidance is provided for Phase 2 ILAW packaging, the Phase 1 standard package was used for Phase 2. Table 2-6 summarizes the ILAW volume, mass, and number of packages for the reference case (Case 3 of the TWRSO&UP) (Kirkbride 1999).

Table 2-6. Summary of Phase 1 and Phase 2 ILAW Package Production.

	Total m^3 glass	Total MT glass	Total Packages
Phase 1	44379	117605	19295
Phase 2	113726	301374	49446
Total	158105	418979	68741

A product-acceptance strategy has been prepared (Westsik 1997) and is being revised to accommodate the latest waste form formulations. Implementing the strategy requires a product-acceptance process that consists of a series of steps over many years. The steps include developing and maintaining product specifications, conducting contractor qualification testing and evaluation before production, DOE verification testing before production, contractor certification testing and reporting during production, and DOE acceptance testing according to a not-yet-determined product acceptance procedure during ILAW production and operation of the disposal facilities.

2.3.7 Transportation and Waste Emplacement

After the DOE has approved a waste package for acceptance, DOE may choose to have the contractor store that package for up to 90 days. The details of this interim storage activity have not yet been defined. After the storage period has ended, DOE will transport the packages

to the disposal site. Current plans call for the packages to be transported by a special truck. For remotely handled waste (all the waste considered in this performance assessment), cranes will remove the waste package from the vehicle and place it directly into the disposal facility.

2.4 DISPOSAL TECHNOLOGY

The design process for the disposal facilities evolved since the last performance assessment. Conceptual designs were developed for the modification and use of the existing disposal vaults (Pickett 1998a) and the construction of new concrete disposal vaults (Pickett 1998b). In December 1999, the DOE identified the remoted-handed (RH) waste trench as the baseline concept for ILAW disposal at the Hanford Site. The RH waste trench complex would be constructed in the same location as the new ILAW disposal facility.

Future disposal designs may include alternative trench disposal concepts, reuse of processing canyon facilities, and reuse of the storage tanks. Once plans are developed, the analyses of any of these options will be performed in future performance assessments.

Since the last performance assessment was issued, a preliminary closure plan was issued (Burbank 2000) and approved (Boston 2000).

2.4.1 Current Remote-Handled Trench Planning

2.4.1.1 Preconceptual Design. The RH Waste trench complex would be constructed in the ILAW disposal site (see Figure 2-26 for the potential locations of trenches within the disposal site). The RH waste trench conceptual model is depicted in Figure 2-27. The RH waste trench internal dimensions are 260 m long by 80 m wide by 10 m deep. The trench sides have a 3:1 slope. Trench construction requires excavation of 1.9×10^5 m^3 of soil. The trench liner surface area is about 2.9×10^4 m^2.

The trench is provided with a primary and secondary liner as depicted in Figure 2-28. Beneath both the primary and secondary liner is an admix layer (bentonite clay/soil mixture) 0.5 m and 1 m thick, respectively. The operations layer consists of crushed concrete and soil. The thickness of this layer is assumed to be 0.9 m (3.0 ft). Because the liners have relatively short design lives (at most hundreds of years) compared to the waste form, the liners are not considered in the simulations.

The specific design shown in Figure 2-28 was taken from the remote-maintained Radioactive Mixed Waste (RMW) Land Disposal Facility (drawing H-2-131579 Rev. 3). The primary and secondary drainage gravel are for the two drainage (leachate) collection systems associated with RCRA-compliant disposal facilities. Both the primary and secondary drainage layers consist of a geocomposite drainage layer on top of high-density polyethylene (HDPE), as required by RCRA. The geocomposite cage consists of geonet bonded to geotextile. Geotextile is placed above each gravel layer. The specifications for

these materials as used in the RMW Land Disposal Facility trenches are given in the WHC Project W-025 specifications (WHC 1994).

Figure 2-26. Layout of ILAW Disposal Facility.

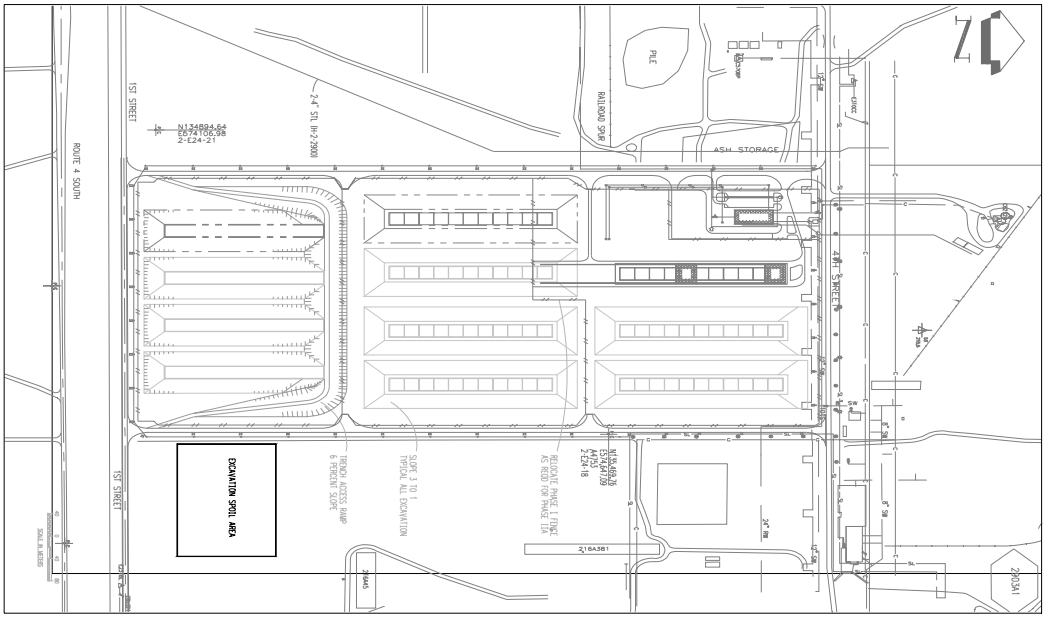

Because the trench walls have a fairly shallow slope (3 m run for every 1 m rise) each successive layer can be increased in both length and width. Whereas the first layer could be 14 packages wide by 132 packages long (14-by-132 matrix), the second layer could be a 22-by-140 matrix (assuming 1.5 m center-to-center packing of the ILAW packages). The uppermost (fourth) layer could be a 42-by-160 matrix. This means that, while a baseline new ILAW disposal facility trench capacity is 11,088 ILAW packages, the RH waste trench capacity theoretically could be 16,448 packages.

Packing the ILAW packages in such large, contiguous matrix (42 by 160 packages for the fourth lift [a single layer of ILAW packages and cover soil]) would, however, create operational impediments. About 100 ecology blocks (i.e. shielding blocks) would be required to create a shielding array between the leading face and operations area of the fourth lift. When it became necessary to advance the ecology blocks, movement of such a large number would be a significant undertaking, potentially requiring several shifts to complete. During this period the trench would be unavailable to receive ILAW packages.

Figure 2-27. RH Waste Trench Conceptual Model.

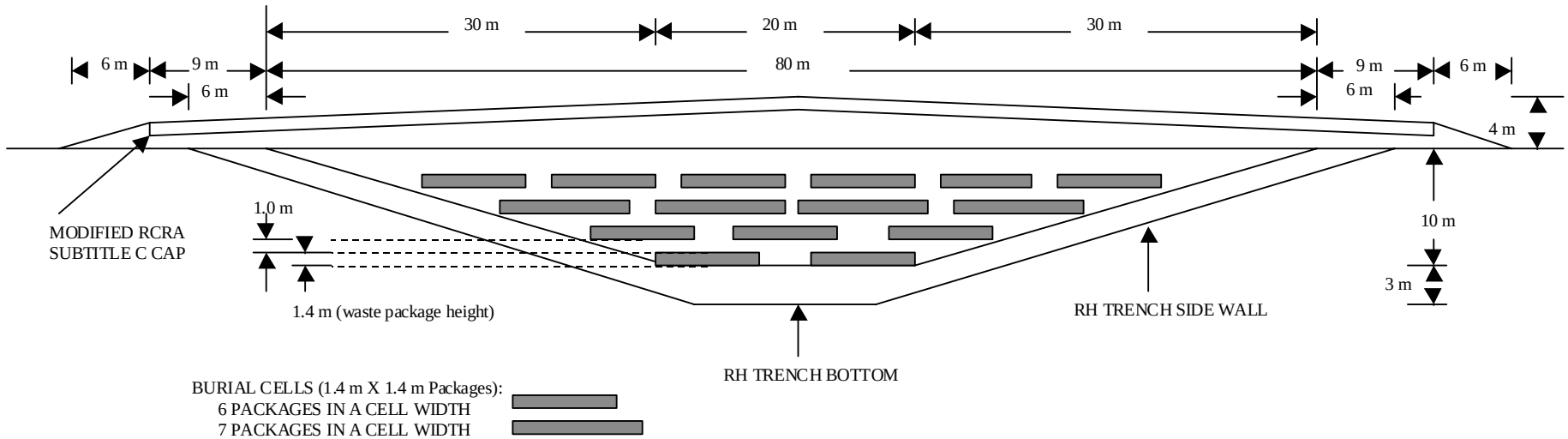

Figure 2-28. RH Waste Trench Liner Details.

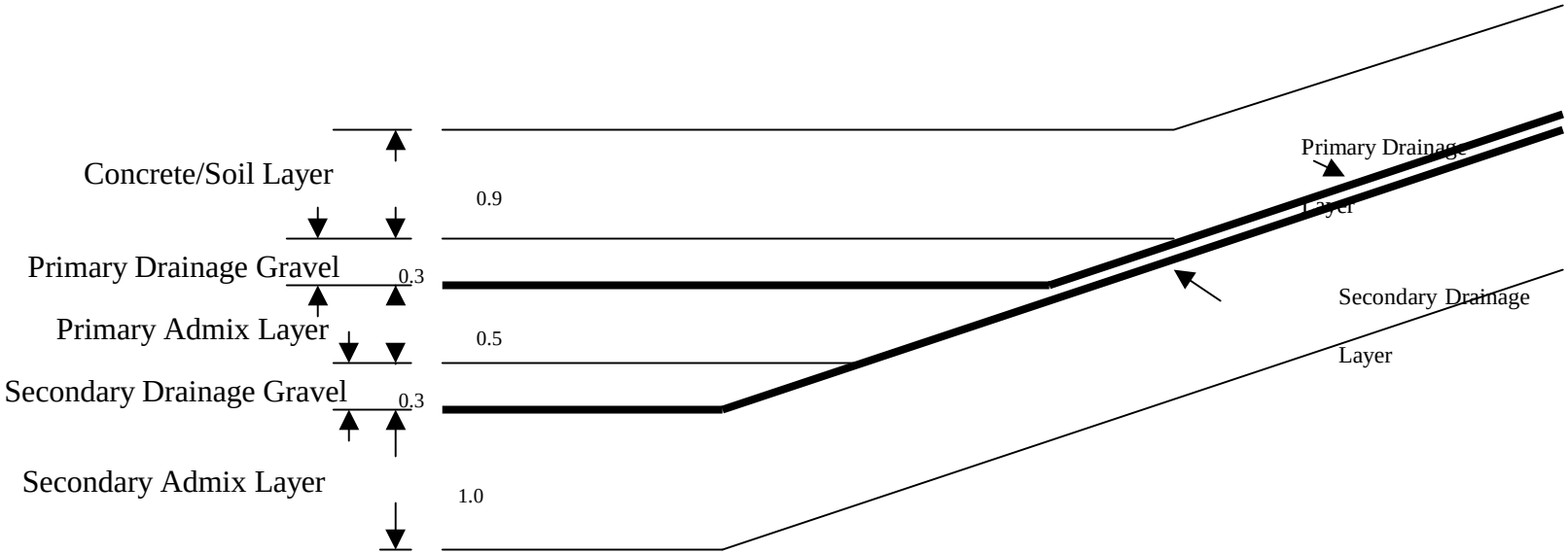

To facilitate continuous receiving operations, the matrix is limited to a smaller size than that which would contiguously cover the entire layer. These smaller matrices, called burial cells, provide the following benefits.

Corridors are created within the disposal matrix to facilitate access for operational activities such as the placement of cover soil.

The size of the exposed leading face is minimized.

The number of ecology blocks required to establish an effective radiation shield is reduced to a number that can be moved easily in a single shift.

A larger portion of the trench can be covered with a rain curtain, thereby reducing the quantity of collected leachate that must be dispositioned.

Figure 2-26 shows a conceptual layout of a trench with these burial cells. Specific details of the trench packing are presented in Table 2-7. Given this packing density, approximately 6 trenches are needed to accommodate the entire Phase 1 and Phase 2 ILAW production.

Table 2-7. Trench Packing Characteristics.

Layer	Cells per layer	Matrix size per cell	Packages per layer
1	2	6 x 132	1,584
2	3	6 x 140	2,520
3	4	7 x 150	4,200
4	6	6 x 160	5,760
Total packages per trench			14,064

2.4.1.2 Trench Fill Material. The RH waste trench preconceptual model includes backfilled soil around and on top of the waste containers in the facility. The soil was included in this concept for the following three reasons:

For structural support. The initial design from *Immobilized Low Level Waste disposal Options Configuration Study*, WHC-SD-WM-TI-686 (Mitchell 1995) had void space between the immobilized low-activity waste containers and between the containers and the ceiling. Filling this space with soil would help prevent significant subsidence of the physical barriers when the components of the disposal system (waste container, waste form, disposal facility structure) fail and collapse into the void space.

To wick moisture away from the waste containers.

To provide radiation shielding for the facility workers.

2.4.1.3 Disposal Unit Closure. All the concepts have a similar barrier philosophy. The uppermost barrier is the surface barrier designed to minimize intrusion and recharge. Beneath the surface barrier, a sand-gravel capillary break will divert any moisture that may come through the surface barrier away from the trench. These two barriers implement the goal of minimizing the amount of water that enters the trench. However, the extent of the barriers differs for the different concepts. The current preconceptual design has a modified RCRA-compliant subtitle C barrier (Puigh 1999) with a 2 percent slope (see Figure 2-27). More information can be found in *Preliminary Closure Plan for the Immobilized Low Activity Waste Disposal Facility* (Burbank 2000), which was approved by Boston 2000b.

2.4.1.4 Disposal Site Closure. Disposal site closure is presumed to consist of applying the surface barrier between the units and placing passive controls on the surface. The intent of the surface barrier is to use evaporation and plant transpiration to minimize the influx of precipitation into the disposal system. The surface barrier includes a sand and gravel layer to work as another capillary break to deter burrowing animals, plant root intrusion, and inadvertent intruders.

Passive controls are assumed to be used to deter inadvertent intrusion. However, the type of passive controls has not yet been selected. However, markers, riprap stone, fencing, and administrative controls are being considered.

2.4.2 ILAW Concrete Vault Design—Alternative Concept

An earlier conceptual design for the ILAW disposal facilities (Pickett 1998b) uses a long concrete vault concept divided into cells. Each vault will be an underground, open-topped, concrete vault approximately 23 m (76 ft) wide and 207.8 m (686 ft) long. The total vault height was increased to 11.0 m to accommodate the new waste package dimensions. The top of the vault walls will extend 1 m (3.3 ft) above grade. Each vault will be divided into 11 cells, separated by concrete partition walls. The concrete vault concept is analyzed in this performance assessment to provide a relative measure of its performance when compared to the RH waste trench concept and as a general sensitivity case for facility design. Also, the immobilized waste program is considering the use of the existing concrete vaults for other disposal needs.

Each vault will be built above a RCRA-compliant leak detection and collection system. The leak detection and collection system consists of a cast-in-place reinforced concrete basin approximately 209.5 m (687.3 ft) long and 24.7 m (81 ft) wide with walls 1.07 m (3.5 ft) high. The basin floor is 0.6 m (2 ft) thick and contains steel reinforcing bars within. The catch basin is lined with two flexible membrane liners, and on top of these lie a layer of gravel with perforated collection pipe routed to sumps, one at each end of a vault. Liquids entering the sump can be removed using a portable pump lowered down a riser pipe.

Interim closure for each filled cell in the new disposal facility will consist of using inert backfill material followed by a "controlled density fill," unreinforced concrete. A waterproof membrane will be placed above the "controlled density fill." After all cells in the vault have been filled and interim closed, a closure cap consisting of a capillary break followed by a modified RCRA C cap will be placed over the entire vault.

2.4.3 Possible Future Disposal Concepts

The disposal alternatives and generation analysis (Burbank 1997) investigated a series of possible disposal facilities including the following:

- A land-filled trench (without RCRA-compliant double containment)
- Existing large concrete buildings
- Existing underground tanks.

The existing tank waste contains listed hazardous waste and, hence, falls under the jurisdiction of RCRA. Unless such waste is treated to no longer be hazardous and is "delisted" (formally removed from regulation), the RCRA requirements (40 CFR 260 to 40 CFR 268) apply. In Washington State, Ecology administrates these federal regulations under WAC 173-303. An important requirement is that the waste be double contained and monitored. That is, the waste volume must be monitored and a second containment system must be in place to hold any leaked waste until it can be collected. The proposed RH waste trench and the conceptual design for the concrete disposal vaults (Pickett 1998b) have such systems. The production of the immobilized low-activity waste (ILAW) will destroy all significant quantities of listed hazardous waste and the ILAW will have properties making it an extremely stable waste form. Thus ILAW should be able to be delisted. However, if the ILAW is not delisted, a RCRA-compliant facility would be needed (see Figure 2-28). Such a facility is estimated to add about 3 to 4 million dollars in construction costs for each row over a base construction cost of about 25 million dollars.

Because of the significant variation in expected tank waste compositions, many of the disposal packages may have radiation levels low enough to permit contact handling. Burbank (1997) investigated the possibility of configuring some of the disposal rows as contact-handled waste disposal trenches. The construction costs for such facilities (4.6 million dollars for a mixed waste trench and 1.3 million dollars for a non-mixed waste trench) are significantly lower than for concrete structures. Lifetime operating costs for the trenches (approximately 11 million dollars per trench) also would be significantly lower than for the concrete facilities (approximately 21 million dollars per vault row). However, the number and production timing of such contact-handled packages cannot be determined until further information is available concerning individual tank inventories, the tank retrieval sequence, efficiencies of waste separation, and vendors' separation plans. The program is actively considering this option for waste later in the program.

The Hanford Site's plateau has a number of facilities that are or soon will be considered surplused. Burbank 1997 investigated the use of both the very large process canyon buildings and the underground tanks presently storing the waste. It is estimated that the building could hold only as little as 24 percent of the ILAW packages in their interior. The per-package life-cycle cost of this option is about a factor of 2.5 higher than for new concrete structures, primarily because these large radioactive facilities need extensive modifications and a large closure area. If waste packages were placed outside these facilities as well, the life-cycle cost per package would be comparable to the concrete facilities costs. In neither case, have avoidance costs of demolishing the canyon buildings been considered. Note that none of the canyon buildings will be available for many years. However, the program is considering this option for waste received after 2010.

The use of single-shell tanks as the disposal facility for waste packages also was investigated by Burbank (1997). The conclusion was that the capital costs for opening the domes of the tanks to allow access for the current package shape was prohibitively expensive (100 to 300 million dollars per equivalent vault row).

3.0 ANALYSIS OF PERFORMANCE

3.1 OVERVIEW

This chapter describes the models, computer codes, and input data used to analyze the long-term performance of the proposed disposal facilities. For the analyses, the information discussed in Chapter 2 is translated into a conceptual physical model, then into a numerical model. The chapter also provides justification for the translations.

The strategy for this assessment was to define and analyze both a base analysis case and sensitivity cases bracketing the base analysis case. The base analysis case was developed using best information for the environmental, waste form, and disposal facility parameters and how the parameters will change with time. These best estimates are defined and justified in separate published reports that have been combined in *Data Packages for the Hanford Immobilized Low-Activity Tank Waste Performance Assessment: 2001 Version* (Mann/Puigh 2000a). Sensitivity cases were developed based on the uncertainty information provided in the data packages. The base analysis case was defined in *Simulations for Hanford Immobilized Low-Activity Tank Waste Performance Assessment: 2001 Version* (Puigh 2001), which also contains a list of sensitivity cases.

This chapter shows how the physical systems presented in Chapter 2 are translated into the numerical models that produce the results presented in Chapters 4 and 5. The chapter covers the following topics:

Inventory Source (Section 3.2). Describes the radionuclide inventories.

Pathways and Scenarios (Section 3.3). Explains the pathways and scenarios that were analyzed.

Values and Assumptions (Section 3.4). Presents the assumptions use in the analyses, including the actual data.

Performance Assessment Methodology (Section 3.5). Presents methodology used in the analyses, including the actual data used, respectively.

3.2 INVENTORY SOURCE

Screening analyses reduced the number of relevant radionuclides to 31. A DQO process was used to reduce the number of chemicals to 46. This is the first Hanford Site PA that has addressed chemicals.

3.2.1 Relevant Contaminants of Concern

Both radionuclides and chemicals are treated in this performance assessment. For a fuller discussion of how the included chemicals were chosen, see Section 1.6.2.8.

3.2.1.1 Radioactive Contaminants. The anticipated tank waste inventories were prescreened (Schmittroth 1995a) to determine which radionuclides dominate human health impacts and hence are potential problems for the inadvertent intruder and groundwater pathway scenarios. This prescreening effort included the following activities:

- Calculating the quantities of all isotopes produced during materials production at the Hanford Site
- Calculating, using a simple one-dimensional steady-state model, the transport of such isotopes through the vadose zone beneath the Hanford Site (using both accepted Hanford Site geochemical retardation and unretarded contaminant transport)
- Converting groundwater concentrations to drinking water doses
- Calculating inadvertent intrusion using the homesteader scenario.

The study indicated that the following radionuclides are potentially most important for each scenario:

- Selenium-79, $^{93}Nb^{m}$ (from ^{93}Zr and ^{93}Mo), ^{99}Tc, ^{129}I, and uranium isotopes and their daughters for the groundwater scenario
- Uranium, plutonium, neptunium, and americium isotopes and their daughters for the groundwater scenario in which geochemical retardation effects are ignored
- Strontium-90, ^{99}Tc, ^{137}Cs, ^{126}Sn, ^{227}Ac, ^{239}Pu, and ^{241}Am for the inadvertent intruder scenario.

In the 1998 ILAW PA (Mann 1998a) the radionuclides analyzed were limited to the top 12 contributors from the groundwater scenario, the top 14 contributors from the unretarded groundwater scenario, and the top 10 contributors from the inadvertent intruder scenario. That analysis found that ^{99}Tc, ^{79}Se, and the uranium isotopes were the most important for the groundwater scenario and that ^{126}Sn was the most important one for the inadvertent intruder scenario. The *White Paper Updating the Conclusions of the 1998 ILAW Performance Assessment* (Mann/Puigh 2000b) found that ^{99}Tc, ^{129}I, and the uranium isotopes were most important for the groundwater scenario and that ^{126}Sn, ^{239}Pu, and ^{241}Am were most important for the inadvertent intruder scenario. The relative change in importance for ^{79}Se and ^{129}I were the result of recent geochemical work supporting this PA (see Kaplan 1999 and Section 3.4.3.3) in which laboratory measurements on Hanford Site soils show that Se is retarded, while iodine is not.

Previous Hanford Site performance assessments (Wood 1995a and Wood 1996) have shown that uranium, ^{129}I, and ^{99}Tc are the main radionuclides of concern. Because radionuclides in Hanford Site surface waters come from groundwater, radionuclides important for surface water protection are taken from the groundwater selection analysis.

For this 2001 ILAW PA analysis, the most important radionuclides screened by Schmittroth 1995a again were used. These 36 isotopes contribute over 99 percent of the dose for the scenarios.

3.2.1.2 Chemical Contaminants. A DQO process was performed (Wiemers 1998) to identify the important chemical contaminants. The organics included were those that had greater than 100 analytical detects in tank wastes or greater than 20 analytical detects in TWINS Solids/Liquid Hits. This is the first performance assessment at the Hanford Site to include chemicals.

3.2.2 Decay Data

Decay data (particularly half lives) are needed both for inventory estimates and for dosimetry calculations (see Section 3.4.7). The nuclear data used in this assessment are presented in *Dosimetry Data Package for the Hanford Immobilized Low-Activity Tank Waste Performance Assessment* (Rittmann 1999), and Appendix O of Mann/Puigh (2000a). Most half-lives are well known. As noted in the 1998 ILAW PA, however, the previously accepted half-lives of ^{79}Se and ^{126}Sn now are thought to be underestimates (Chunsheng 1997 and Zhang 1996). This underestimate for ^{126}Sn has been confirmed (Brodzinski 1998). Thus, the inventories for ^{79}Se and ^{126}Sn (as expressed in Ci) from Kirkbride 1999 have been reduced by factors of 0.08 and 0.4, respectively.

3.2.3 Inventory

> Inventory values are based on detailed reactor histories and a conservative analysis of separations processes.

The inventory for this study is from *Immobilized Low Activity Tank Waste Inventory Data* Package (Wootan 1999) except where noted. This study is based mostly on the best basis inventory program of the Hanford Tanks Program. These values are based on detailed simulations of reactor production histories, chemical separations, and waste processing simulations as verified and supplemented by actual measurements of constituents in various tanks. For the chemicals not listed in the tank inventories, concentration limits for land disposal (40 CFR 268) were used.

Forty-six radionuclides and 25 chemicals are explicitly treated in the best basis tank inventories. These materials were selected by the TWRS [Tank Waste Remediation System] Characterization Program (Kupfer 1999) as those important for safety, disposal, and processing requirements. This set includes all the radionuclides identified as significant in the 1998 ILAW PA (Mann 1998a), along with those identified in the screening studies for the ILAW PAs (Schmittroth 1995).

The nominal ILAW inventories for all the materials explicitly included are based on the *Tank Waste Remediation System Operation and Utilization Plan* (Kirkbride 1999). The best basis tank-by-tank inventories (BBI) as of October 1, 1998, were adjusted for waste transfers not accounted for in the BBI, and for non-BBI analytes that are in the waste treatment contract. The BBI inventories were adjusted to a common date (October 1, 1998). The BBI values are based on a tank-by-tank evaluation of measurements from a tank, as well as modeling results of transfers to and from the tank. The retrieval and feed delivery process was modeled by estimating liquid and solid partitioning (Hendrickson 1999) and following the April 1, 1999, DOE guidance (Taylor 1999b) on schedules and contract requirements. Vitrification losses (melters, stack emissions, secondary waste streams, etc.) were explicitly included in the model and are described in Kirkbride 1999. The total ILAW waste volume is estimated to be 1.581×10^5 m^3. The required number of waste packages needed to contain the projected ILAW

inventory is estimated as 68,741. Kirkbride 1999 represents the ILAW project's official estimate until the next waste treatment plant contractor's flow sheets become available.

Table 3-1 provides the total inventory in the tanks and in the ILAW packages, as well as the expected average and maximum concentration in the ILAW packages for each radionuclide and chemical affecting the performance objectives and goals given in Tables 1-3 and 1-4. The upper bound ILAW inventory given in Table 3-1 represents the estimated upper bound for these inventories in ILAW. The upper bound estimates are based on either contract limits (for strontium, technetium, cesium, neptunium, plutonium, americium, and curium) or are taken to be the BBI tank inventories without separation. The average package concentration is calculated by dividing the total inventory for each contaminant by the number of waste packages estimated to be produced (68,471 packages). The maximum batch concentration is estimated from the comparison of the batch-to-batch variation in Kirkbride's (1999) flow process calculations to the average inventories in a waste package. These estimates reflect the tank-to-tank variation in inventory. For most components, the upper bound limit on total ILAW inventory was taken as the BBI tank inventory, ignoring any processing and separation losses. For radionuclides limited by the contract specifications (^{99}Tc, ^{137}Cs, ^{90}Sr, and transuranic), the contract limits (DOE/BNFL 1998) were used as upper bounds. Ignoring the processing losses between the tank inventory and the ILAW inventory provides a very conservative bounding value, but was used to compensate for the lack of information about the uncertainty of the separations factors (wash and leach effectiveness, off-gas treatment, solids retention).

Table 3-1. ILAW Inventories and Concentrations for Important Constituents.

(Curies, decayed to October, 1994, for radionuclide and kg for chemical and Ci/m^3 for radionuclide and kg/m^3 for chemical)

Material	Tank Inventory	ILAW Inventory	Upper Bound ILAW Inventory	Average Package Concentration	Maximum Batch Concentration
3-H	2.46E+04	0.00E+00	2.46E+04	0.00E+00	0.00E+00
14-C	4.38E+03	0.00E+00	4.38E+03	0.00E+00	0.00E+00
59-Ni	8.58E+02	1.67E+02	8.58E+02	1.06E-03	4.02E-03
60-Co	1.99E+04	4.18E+03	1.99E+04	2.64E-02	3.07E-01
63-Ni	8.45E+04	1.62E+04	8.45E+04	1.02E-01	3.91E-01
79-Se	5.74E+01	4.80E+01	7.45E+01	3.03E-04	5.45E-03
90-Sr [a]	5.99E+07	4.50E+06	5.85E+06	2.85E+01	5.43E+01
93-Zr	4.12E+03	1.25E+03	4.12E+03	7.94E-03	3.37E-02
93m-Nb	2.53E+03	8.36E+02	2.53E+03	5.29E-03	4.47E-02

Table 3-1. ILAW Inventories and Concentrations for Important Constituents.

(Curies, decayed to October, 1994, for radionuclide and kg for chemical and Ci/m^3 for radionuclide and kg/m^3 for chemical)

Material	Tank Inventory	ILAW Inventory	Upper Bound ILAW Inventory	Average Package Concentration	Maximum Batch Concentration
99-Tc	2.89E+04	5.79E+03	6.65E+03	3.66E-02	9.96E-02
106-Ru	1.27E+05	8.94E+02	1.27E+05	5.65E-03	2.59E-01
113m-Cd	1.67E+04	7.97E+03	1.67E+04	5.04E-02	2.14E-01
125-Sb	2.47E+05	5.20E+04	2.47E+05	3.29E-01	6.50E+00
126-Sn	4.64E+02	1.69E+02	4.64E+02	1.07E-03	4.17E-03
129-I	1.01E+02	2.20E+01	1.01E+02	1.39E-04	1.81E-03
134-Cs	8.71E+04	3.76E+02	4.89E+02	3.73E-01	1.35E+01
137-Cs[b]	6.37E+07	9.11E+05	1.18E+06	5.76E+00	7.80E+00
151-Sm	2.61E+06	7.80E+05	2.61E+06	4.93E+00	2.42E+01
152-Eu	1.45E+03	3.07E+02	1.45E+03	1.94E-03	4.21E-02
154-Eu	1.83E+05	3.77E+04	1.83E+05	2.38E-01	6.13E+00
155-Eu	1.76E+05	3.15E+04	1.76E+05	1.99E-01	7.36E+00
226-Ra[c]	6.31E-02	5.70E-02	1.14E+03	3.61E-07	1.56E-05
227-Ac[c]	8.76E+01	6.06E-02	8.75E+01	3.83E-07	1.76E-06
228-Ra[c]	7.71E+01	3.30E+01	7.75E+01	2.09E-04	1.06E-03
229-Th[c]	1.81E+00	3.40E-01	1.81E+00	2.15E-06	1.14E-05
231-Pa[c]	1.56E+02	3.44E-01	1.53E+02	2.17E-06	1.05E-05
232-Th	4.40E+00	1.28E+00	4.40E+00	8.09E-06	5.97E-05
232-U	1.49E+02	3.46E+01	1.49E+02	2.19E-04	1.64E-03
233-U	5.72E+02	1.31E+02	5.72E+02	8.26E-04	6.22E-03
234-U	3.42E+02	4.41E+01	3.42E+02	2.79E-04	1.95E-03

Table 3-1. ILAW Inventories and Concentrations for Important Constituents.

(Curies, decayed to October, 1994, for radionuclide and kg for chemical and Ci/m^3 for radionuclide and kg/m^3 for chemical)

Material	Tank Inventory	ILAW Inventory	Upper Bound ILAW Inventory	Average Package Concentration	Maximum Batch Concentration
235-U	1.46E+01	1.79E+00	1.46E+01	1.13E-05	7.97E-05
236-U	1.24E+01	1.43E+00	1.24E+01	9.03E-06	3.68E-05
237-Np	1.85E+02	8.10E+01	3.00E+02	5.13E-04	1.78E-03
238-Pu	2.70E+03	1.06E+02	3.94E+02	6.72E-04	2.69E-03
238-U	3.28E+02	4.83E+01	3.28E+02	3.06E-04	2.02E-03
239-Pu	5.55E+04	3.05E+03	1.13E+04	1.93E-02	9.50E-02
240-Pu	1.13E+04	5.25E+02	1.95E+03	3.32E-03	1.34E-02
241-Am	1.07E+05	1.08E+04	4.01E+04	6.85E-02	1.69E+00
241-Pu	1.66E+05	7.17E+03	1.66E+05	4.53E-02	1.98E-01
242-Cm	1.72E+02	5.76E+01	1.72E+02	3.64E-04	1.16E-02
242-Pu	1.07E+00	4.49E-02	1.66E-01	2.84E-07	1.69E-06
243-Am	1.76E+01	6.89E-01	2.55E+00	4.36E-06	9.01E-05
243-Cm	3.47E+01	6.73E+00	2.49E+01	4.26E-05	5.18E-04
244-Cm	7.84E+02	1.01E+02	3.73E+02	6.36E-04	6.77E-03
Ag^+ (silver)	1.51E+03	1.08E+02	3.03E+03	6.83E-04	5.68E-03
As^{5+} (arsenic)	2.08E+01	1.76E+01	4.15E+01	1.12E-04	7.42E-03
Ba^{2+} (barium)	1.70E+03	1.86E+01	3.39E+03	1.17E-04	7.24E-03
Be^{2+} (beryllium)	1.09E+02	6.14E-01	2.18E+02	3.89E-06	5.48E-04
Cd^{2+} (cadmium)	4.18E+02	6.30E+01	8.36E+02	3.98E-04	5.13E-03
Cl^- (chlorine)	9.37E+05	9.31E+05	9.37E+05	5.89E+00	1.55E+01
CN^- (cyanide)	1.09E+05	0.00E+00	1.09E+05	0.00E+00	0.00E+00

Table 3-1. ILAW Inventories and Concentrations for Important Constituents.

(Curies, decayed to October, 1994, for radionuclide and kg for chemical and Ci/m^3 for radionuclide and kg/m^3 for chemical)

Material	Tank Inventory	ILAW Inventory	Upper Bound ILAW Inventory	Average Package Concentration	Maximum Batch Concentration
Cr (TOTAL)(chromium)	6.72E+05	2.74E+05	6.72E+05	1.73E+00	1.27E+01
Cu^{2+} (copper)	3.15E+02	7.33E-01	6.31E+02	4.63E-06	2.54E-05
F^- (fluoride)	1.20E+06	9.94E+05	1.20E+06	6.28E+00	2.75E+01
Fe^{3+} (iron)	1.40E+06	4.48E+04	1.40E+06	2.83E-01	2.86E+00
Hg^{2+} (mercury)	2.10E+03	1.92E+02	2.10E+03	1.22E-03	3.38E-02
Mn^{4+} (manganese)	1.96E+05	1.38E+04	1.96E+05	8.71E-02	4.20E-01
NH_3 (ammonia)	5.01E+05	0.00E+00	5.01E+05	2.53E+00	4.24E+01
Ni^{2+} (nickel)	1.80E+05	3.05E+04	1.80E+05	1.93E-01	2.96E+00
NO_2^- (nitrite)	1.26E+07	0.00E+00	1.26E+07	0.00E+00	0.00E+00
NO_3^- (nitrate)	5.25E+07	0.00E+00	5.25E+07	0.00E+00	0.00E+00
Pb^{2+} (lead)	8.40E+04	7.83E+03	8.40E+04	4.95E-02	2.73E-01
Se^{6+} (selenium)	6.11E-01	5.33E-01	1.22E+00	3.37E-06	2.96E-05
SO_4^{2-} (sulfate)	3.91E+06	3.39E+06	3.91E+06	2.15E+01	9.12E+01
Tl^{3+} (thallium)	2.54E+04	NA	5.08E+04	0.00E+00	0.00E+00
Zn^{2+} (zinc)	2.89E+03	1.98E+03	5.79E+03	1.25E-02	1.19E-01
U (TOTAL) (uranium)[d]	7.61E+04	1.73E+04	7.61E+04	1.11E-01	2.16E+00
1,1,1-trichlorethane[e]	NA	0.00E+00	9.17E+02	0.00E+00	0.00E+00
1,1,2-trichloroethane[e]	NA	0.00E+00	9.17E+02	0.00E+00	0.00E+00
benzene[e]	NA	0.00E+00	1.53E+03	0.00E+00	0.00E+00
carbon tetrachloride[e]	NA	0.00E+00	9.17e+02	0.00E+00	0.00E+00
chloroform[e]	NA	0.00E+00	9.17E+02	0.00E+00	0.00E+00

Table 3-1. ILAW Inventories and Concentrations for Important Constituents.

(Curies, decayed to October, 1994, for radionuclide and kg for chemical and Ci/m^3 for radionuclide and kg/m^3 for chemical)

Material	Tank Inventory	ILAW Inventory	Upper Bound ILAW Inventory	Average Package Concentration	Maximum Batch Concentration
ethyl benzene[e]	NA	0.00E+00	1.53E+03	0.00E+00	0.00E+00
methylene chloride[e]	NA	0.00E+00	4.59E+03	0.00E+00	0.00E+00
n-butyl alcohol[e]	NA	0.00E+00	3.98e+02	0.00E+00	0.00E+00
toluene[e]	NA	0.00E+00	1.53E+03	0.00E+00	0.00E+00
trichloroethylene (1,1,2-trichloroehylene)[e]	NA	0.00E+00	9.17E+02	0.00E+00	0.00E+00
xylenes-mixed isomers (sum of m-, o-, and p-xylene)[e]	NA	0.00E+00	4.59E+03	0.00E+00	0.00E+00
1,4-dichlorobenzene[e]	NA	0.00E+00	9.17E+02	0.00E+00	0.00E+00

[a]The ^{90}Sr will have ^{90}Y daughter in equilibrium
[b]The ^{137}Cs will have ^{137m}Ba daughter in equilibrium
[c]These values have been adjusted based on the Kufper (1999) estimate for tank inventory. Inventories for radionuclides are as of 10/1/98.
[d]Total uranium is expressed as kg/m^3 (i.e. as a chemical).
[e]Tank inventories of specific organic compounds are not available; organic compounds are not expected to survive the vitrification process. "NA" indicates components for which inventory information is not available.

The ILAW packages must meet the land disposal restriction (LDR) treatment standards for compliance with RCRA and the "Washington State Dangerous Waste Regulations" contained in WAC 173-303. The LDR regulations are found in 40 CFR 268 and WAC 173-303-140. The privatization regulatory DQO (Wiemers 1998) identified a set of regulatory constituents that plausibly could be in the tank waste and might be considered during permitting activities supporting the treatment facility. The TWRS-P Project Dangerous Waste Permit Application (BNFL 1999) compared these constituents to the "Universal Treatment Standards" (40 CFR 268.48) and provided a list of components and LDR treatment standards. These LDR treatment standards provide an upper bound concentration for acceptability of the ILAW product. These maximum concentrations were multiplied by the total glass mass, along with a safety factor of 1.3 (assumed) to allow for uncertainty in the total glass mass, to provide bounding inventories of trace hazardous organic chemicals in the ILAW product.

The key materials are as follows:

^{3}H No tritium is expected to survive the vitrification process to end up in ILAW packages (Kirkbride 1999).

^{14}C No ^{14}C is expected to survive the vitrification process and end up in the ILAW packages (Kirkbride 1999).

^{79}Se Results are based on models, but are considered conservative, because the model ignores previous removals such as disposals to cribs.

^{90}Sr Values are constrained by the contract (DOE/ORP 2000c) based on Class C limit and assumption that this constraint applies to all ILAW waste.

^{99}Tc Values based on BBI (reference inventory) and phase 1 contract requirement (DOE/ORP 2000c) to remove 80 percent of the tank inventory from ILAW. Calculation assumes this requirement extends to Phase 2 ILAW production. The tank inventory estimate is felt to be conservative because any losses associated with the offsite shipments are not factored into the BBI inventory for ^{99}Tc. Based on the results on this performance assessment, studies are proceeding to study the benefits of eliminating the 80 percent removal requirement from the contract.

^{126}Sn Values are based on BBI estimate with a separations factor of 36 percent of the BBI (Kirkbride 1999). Few tank measurements for ^{126}Sn exist. The BBI estimates for ^{126}Sn in tanks 241-AZ-101 and 241-AZ-102 are higher than the measurements.

^{129}I Values are based on BBI and estimate for 0.22 captured and recycled into ILAW (Kirkbride 1999).

^{137}Cs Values are constrained by the contract (DOE/ORP 2000c) based on the Class C limit.

U Many of the values are based on total uranium analysis of samples.

Ra These are daughter products of uranium and thorium that were not treated correctly in the Hanford Defined Waste (HDW) model because uranium, thorium, and plutonium were decayed before separations (Kupfer 1999). The values in Table 3-1 have been adjusted based on the Kufper (1999) estimate for tank inventory.

^{227}Ac This is a daughter product of uranium and thorium that was not treated correctly in the HDW model because uranium, thorium, and plutonium were decayed before separations (Kupfer 1999). The values in Table 3-1 have been adjusted based on the Kufper (1999) tank inventory estimate.

^{229}Th This is a daughter product of uranium and thorium that was not treated correctly in the HDW model because uranium, thorium, and plutonium were decayed before separations (Kupfer 1999). The values in Table 3-1 have been adjusted based on the Kupfer (1999) tank inventory estimate.

^{241}Am The values are equal to approximately 10 percent of the total BBI tank inventory estimate (separations estimate from Kirkbride [1999]) and are felt to be conservative.

^{231}Pa This is a daughter product of uranium and thorium that was not treated correctly in the HDW model because uranium, thorium, and plutonium were decayed before separations

(Kupfer 1999). The values in Table 3-1 have been adjusted based on the Kufper (1999) tank inventory estimate.

^{237}Np The values are based on the BBI and the large separations factor (44 percent of BBI) from Kirkbride (1999). The BBI estimate is felt to be conservative because the inventory estimate is 30 percent higher than the global estimate for all ^{237}Np produced by the reactors. Tanks 241-AN-103 and 241-AN-105 are thought to have 30 percent of the ^{237}Np, but only bounding value estimates are provided for these two tanks.

Pu Plutonium values are based primarily on weapons production accountability records and samples. Significant separation factors (5 percent of BBI) are taken from Kirkbride (1999).

Table 3-2 summarizes the changes that have occurred to the inventory estimates since the last ILAW performance assessment released in 1998 (Mann 1998a). The changes are given for the radionuclides found to be most important in this performance assessment. These changes can be grouped into the following categories: changes in the estimated tank inventories, changes in the half-life estimates, and changes to the estimated separation factors associated with the separation and processing of the tank waste stream into high-level and low-activity fractions.

Table 3-2. Inventory Estimate Changes from 1998 ILAW PA.

	ILAW Inventory Estimate (Ci)*		Sources of Changes			
Radionuclide	1998 PA	2001 PA	Tank Inventory*	Half-life	Separation Factor	Total
^{3}H	8.04E+04	0.00E+00	0.31	1.00	0.00	0.00
^{14}C	7.73E+00	0.00E+00	1.10	1.00	0.00	0.00
^{79}Se	1.03E+03	4.80E+01	0.70	0.08	0.84	0.05
^{90}Sr	1.61E+06	4.50E+06	1.12	1.00	2.49	2.80
^{99}Tc	2.23E+04	5.79E+03	1.06	1.00	0.24	0.26
^{126}Sn	1.58E+03	1.69E+02	0.73	0.40	0.36	0.11
^{129}I	6.62E+00	2.20E+01	1.53	1.00	2.18	3.32
^{137}Cs	4.51E+05	9.11E+05	1.41	1.00	1.43	2.02
^{231}Pa	1.45E+02	3.44E-01	1.08	1.00	0.00	0.00
^{233}U	2.58E+01	1.31E+02	1.33	1.00	3.82	5.08
^{234}U	1.80E+01	4.41E+01	1.14	1.00	2.15	2.45

^{238}U	1.78E+01	4.83E+01	1.10	1.00	2.46	2.71
^{237}Np	3.74E+00	8.10E+01	2.47	1.00	8.76	21.66
^{240}Pu	4.31E+02	5.25E+02	1.58	1.00	0.77	1.23
^{241}Am	4.25E+03	1.08E+04	2.02	1.00	1.26	2.54

* Tank and ILAW Inventories not adjusted for differences in decay dates for 1998 PA (01/01/10) and 2001 PA (10/01/94)

In Table 3-2 the tank inventory change is the ratio of the 2001 ILAW PA inventory estimate (Wootan 1999) to the 1998 ILAW PA inventory estimate (Mann 1998a). (The estimates were not corrected for the difference in inventory reference date, January 1, 2010 for the 1998 ILAW PA and October 1, 1994 for the 2001 ILAW PA). The tank inventory changes are due to the evolution in our understanding from the earlier estimates, based primarily on reactor production calculations and estimates for processing campaigns that initially generated the waste in the tanks, to more mature models for these processes and specific composition measurements conducted on waste samples from the tanks. From Table 3-2 the following radionuclide inventory estimates changed by more than 40%: ^{3}H, ^{14}C, ^{129}I, ^{137}Cs, ^{237}Np, ^{240}Pu and ^{231}Am.

In Table 3-2 the change in inventory estimate due to a change in the half-life estimate impacted the inventory, expressed in Ci, for ^{79}Se and ^{126}Sn.

The change in estimated separation factors between the 2001 ILAW PA and the 1998 ILAW PA are represented by the change in separation factor given in Table 3-2. The change in separation is estimated by dividing the ratio of ILAW inventory to tank inventory for the 2001 ILAW inventory (estimates given in Table 3-1) by the ratio of the ILAW inventory to the tank inventory for the 1998 ILAW inventory (estimates given in Table 3-1 in Mann 1998a). A separation factor value of one would correspond to the case where the same separation factors were assumed for both the 1998 and 2001 ILAW inventory estimates. The value of approximately zero indicates that those isotopes that were estimated to be important in the 1998 ILAW PA are essentially removed for the ILAW inventory estimates for the 2001 ILAW PA. Specifically, ^{3}H, ^{14}C, and ^{231}Pa are no longer important due to their separation from the ILAW waste form. Similarly, ^{237}Np separation factor is larger; and therefore, a larger fraction of the tank inventory is estimated to be in the ILAW waste form when compared to the 1998 ILAW PA.

Finally, the total source of changes given in Table 3-2 is the product of the tank inventory, half-life, and separation factor changes given in the table. This total represents the difference in the ILAW inventory estimates between the 2001 ILAW PA and the 1998 ILAW PA that are also given in Table 3-2. From an examination of these results the major sources of the differences in the ILAW inventory are indicated. Specifically, the relatively low inventories on ^{3}H, ^{14}C, and ^{231}Pa are attributed primarily to increased separation factors estimated for this performance assessment. The lower ^{79}Se inventory is associated with the change in the half-life estimate for this radionuclide. The lower ^{126}Sn inventory is attributed to lower estimate for the tank inventory, the longer half-life estimate, and increased separations when compared to the

1998 ILAW estimates. The lower ^{99}Tc inventory is due to the increased separations factor. The higher ^{129}I, U, ^{237}Np, and ^{241}Am inventories are due to higher estimates for the tank inventory and larger separation factors during processing.

3.2.4 Release Rate from Waste Form

The radionuclide source term used in the transport calculations is based not only on the inventory, but also on the release rate of the radionuclides from the ILAW packages. The release rate is a function of the waste form composition and the disposal facility design, which affects water transport and the resulting chemical environment in the disposal facility.

For an accurate determination of the source term, the chemical and physical processes controlling contaminant release from the waste form must be explicitly modeled. This assessment uses computer simulations for waste form corrosion and contaminant release. These simulations are described in Section 3.3.3. The release rates of radionuclides from the waste form actually used in the calculations are described in Section 3.4.4.3.

3.3 PATHWAYS AND SCENARIOS

This section covers the selection criteria, the pathways chosen and not chosen, and the exposure pathways chosen and not chosen. Special emphasis is given to justifying the choices. In this discussion, "pathways" refers to the environmental paths (e.g., groundwater) by which contaminants move from the waste form to the human environment. Scenarios are the environmental and human-caused events (e.g., human intrusion or irrigation) that influence how contaminants move or affect humans.

3.3.1 Selection Criteria

Relevant pathways and scenarios for these analyses were selected mainly based on pathways and scenarios used in earlier Hanford Site long-term environmental analysis documents (see Section 1.5). As noted in Section 1.5.1, five Hanford Site performance assessments for the disposal of low-level waste have already been done (Kincaid 1995, Mann 1998a, Wood 1995a, Wood 1995b, and Wood 1996). The most important environmental impact statements (EIS) have been the Hanford Defense Waste EIS (DOE 1987), the Tank Waste Remediation System EIS (DOE 1996b), and the *Final Hanford Comprehensive Land-Use Plan Environmental Impact Statement* (DOE 1999h) and its associated record of decision (DOE 1999i). These documents have been fairly consistent in their choice of pathways and scenarios.

After reviewing the relevant documents, reviews, and guidance, pathways and scenarios were selected for the current performance assessment (Mann 1999b). Selection was based on the relevance of the pathway or scenarios to the current disposal action and performance objectives.

3.3.2 Pathways

The most important pathways are through the use of contaminated groundwater and inadvertent intrusion. The pathways remain unchanged from the 1998 ILAW PA.

The selection of pathways for this performance assessment is covered more fully in *Scenarios of the TWRS Low-Level Waste Disposal Program* (Mann 1999b). Possible scenarios were suggested by analyzing the performance objectives introduced in Chapter 1 and determining which pathways could lead to a level of exposure that could equal or exceed the specified performance objective. Postulated land use also was studied to determine possible additional pathways. Finally, likely natural events were identified (such as catastrophic glacial age flooding).

3.3.2.1 Release Mechanism. In previous Hanford Site performance assessments and environmental impact statements, the dominant pathway was through groundwater. Infiltration of moisture from precipitation entered the engineered system, where the moisture could cause the contaminants (for example in a glass-water interaction) to be released or could simply carry away already-released contaminants. The moisture and released contaminants travel downward through the vadose zone until the contaminants reach the unconfined aquifer where humans can encounter the radioisotopes through recovery of the groundwater resource for use in residential and agricultural settings. From previous analyses (Rawlins 1994, Mann 1995b, Mann 1998a, Mann/Puigh 2000a) supporting the Hanford Low-Level Tank Waste Program, this pathway again is expected to be dominant.

3.3.2.2 Future Land Use. In 1992 the HFSUWG was charged to determine potential future uses of the various parts of the Hanford Site. This group consisted of local, state, and federal officials, representatives of affected Indian tribes and agricultural and labor organizations, as well as members of environmental and other special interest groups. The efforts of the HFSUWG form the basis of the Hanford Site Comprehensive Land Use plan (DOE 1999h). The HFSUWG summary report (HFSUWG 1992a-2) states

> *"In general, the Working Group desires that the overall cleanup criteria for the Central Plateau should enable general usage of the land and groundwater for other than waste management activities in the horizon of 100 years from the decommissioning of waste management facilities and closure of the disposal areas."*

The following four general land uses can be envisioned for the Central Plateau over the time of interest to a performance assessment.

- Industrial or commercial
- Dry-land farming
- Irrigated farming
- Natural.

The present land use is heavy industrial. If this use is maintained, records of past activities, particularly those for the disposal of nuclear materials, are likely to be kept. In addition, in an industrial area, liquid discharges to the ground would be highly regulated and kept small.

Like the Central Plateau, the Horse Heaven Hills, south of the Hanford Site, are near the Columbia River, but are at a significantly higher elevation. Although the amount of irrigation is increasing at certain locations, comparatively little irrigation occurs in the Horse Heaven Hills because of the relatively high energy (hence economic) cost of bringing water to the surface. Dry-land farming continues to be the main use for the land of the Horse Heaven Hills.

East of the Central Plateau, across the Columbia River, irrigated farming is extremely common. The water, however, does not come from the nearby stretches of the Columbia River. The water comes from the Columbia Basin Project, which uses water stored behind the Grand Coulee Dam, over 322 km (200 mi) upstream of the Hanford Site. The water is gravity-fed to

the farms. The regional geography makes such a water delivery system unlikely for the Central Plateau.

Finally, west of the Central Plateau is the Fitzner/ Eberhardt Arid Lands Ecology Reserve, a nature preserve area. This area now is part of the Hanford Reach National Monument (Clinton 2000).

For the base analysis case, the land use assumption was that knowledge of the disposal activities has been retained and that water discharges to the ground are minimized. These assumptions are consistent with the assumptions of the HFSUWG, the DOE (DOE 1999h), and the local planning authorities, all of which are using a 50- to 100- year planning horizon.

3.3.2.3 Land-Use-Driven Scenarios. The pathways described here assume that some controls remain in place to prevent public intrusion into the disposal site. That is, the barriers and markers that are to be left will effectively prevent open use of the land over the disposal site. The land surrounding the marked area, however, could be farmed and could contain wells.

Based on previous analyses at the Hanford Site, the main exposure pathway is expected to be the contamination of the underground aquifer leading to various exposure scenarios. Other pathways include the upward diffusion through the engineered system into the air.

3.3.2.3.1 Unconfined Aquifer Contamination. Contamination of the unconfined aquifer is caused by water (natural or human-introduced) penetrating through the ground surface layer, interacting with the engineered structure (including the waste), then transporting contaminants down through the unsaturated sediments to the unconfined aquifer.

The main effects of land use on the analyses presented in this performance assessment are as follows:

- The amount of water penetrating through the ground surface layer above the disposal facility
- The direction and magnitude of flow of the unconfined aquifer from regional irrigation
- The amount of well water pumped to the surface.

Because the site of the disposal facility is assumed to be known to the surrounding population, it was assumed that the surface immediately above the disposal facility will not be used. Thus the only source of water would be natural rain or snowfall. The infiltration rate, the rate at which water actually penetrates through the surface layer and enters the sand-gravel capillary barrier, is described in Section 3.4.6 and is expected to be small (less than 5 mm/year).

The second major consequence of land use is on the flow of groundwater in the unconfined aquifer. Analysis (ERDA 1975) of groundwater flow before the start of Hanford Site operations shows a predominantly west-to-east flow (Figure 2-12). Current calculations for post-operation conditions (Bergeron 2000) predict a similar flow (Figure 3-1). These groundwater calculations form an important part in this analysis.

Figure 3-1. Predicted Groundwater Flowlines for Post Hanford Conditions.

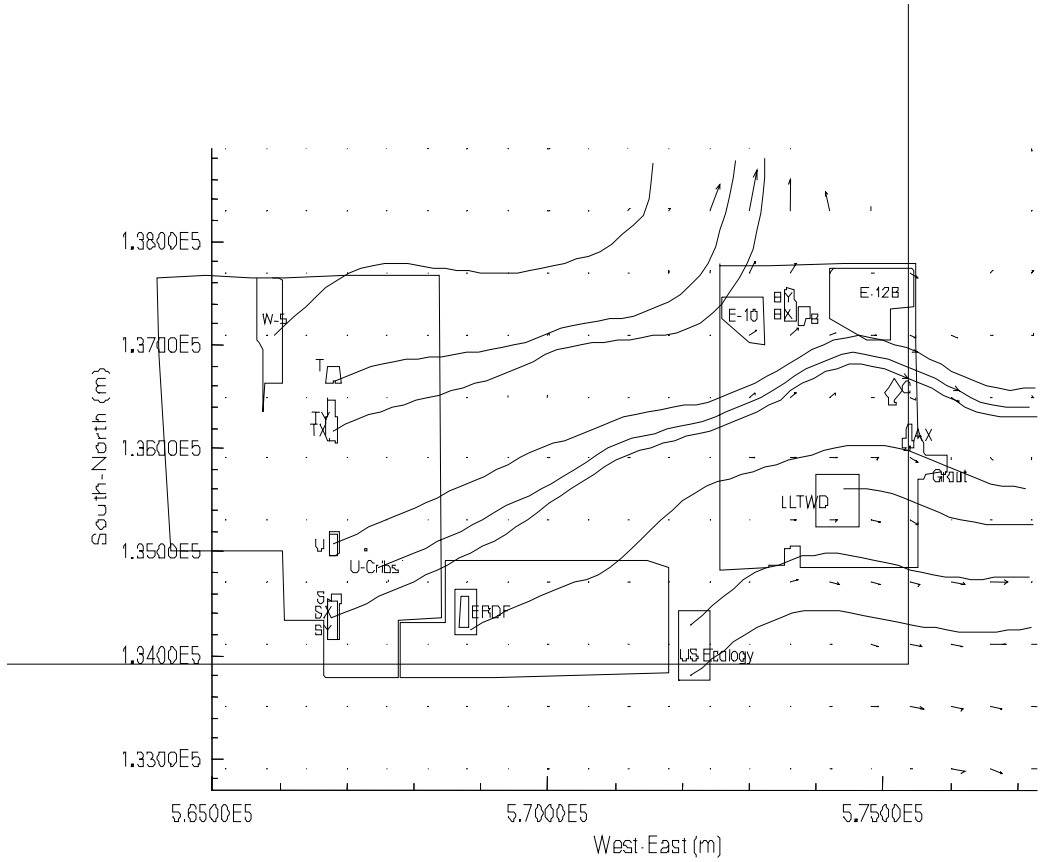

The creation of ponds and the large amount of water discharged to the ground have altered the natural flow of groundwater (Dirkes 1997) (Figure 2-13). Possible irrigation on the Central Plateau that also would affect groundwater must be considered. No irrigation was assumed for the base analysis case because the energy requirements for irrigation in the Central Plateau are significantly higher than for other nearby regions and no known irrigation rights exist. However, irrigation on the plateau was considered in sensitivity cases to determine the effects of selected irrigation on the regional flow of the groundwater in the unconfined aquifer. Irrigation on the 200 Areas was considered unlikely because this area will be dedicated to waste disposal and irrigation would be considered an inadvertent intrusion.

The main impact of irrigation would be to change the water table and potentially the flow direction. Sensitivity cases chosen to investigate this effect were set up to change the regional recharge by a factor of three.

The last major effect is the amount of water being taken from a well. At the locations of the proposed disposal facilities, the unconfined aquifer contains only a limited amount of water. Because the amount of water is so limited, either only a small amount would be pumped from the unconfined aquifer or the well would extend much deeper and tap the confined aquifer instead of

the unconfined aquifer. Thus, minimum distortion of the groundwater flow field in the unconfined aquifer was assumed for the base analysis case. Sensitivity cases were considered, however, to determine the effect of the amount of pumping on the groundwater flow field and the calculated doses.

3.3.2.3.2 Surface Water. The major surface water source in the region is the Columbia River. Here the main impact of land use is possible irrigation of land near the river. The Columbia River is a more likely source of water than the unconfined aquifer for irrigating farmland near the river because of the land's low elevation and nearness to the river. The current plan (DOE 1999i) is a preservation land use along the river. This is reinforced by the recent establishment of the Hanford Reach National Monument, which contains much of Hanford Site land near the Columbia River. For the base analysis case, the assumption was that no irrigation would occur downgradient from the plateau.

3.3.2.3.3 Air Resources. Gases and vapors could travel upward from the facility through the soil to the ground surface. This pathway is maximized with minimum downward water movement. No water flow is considered in the calculations for the protection of air resources.

3.3.2.4 Natural Event Scenarios. The main natural events to be expected are as follows:

- Wind erosion of the surface above the disposal facility
- Earthquakes
- Flooding caused by post-glacial events.

Wind erosion and earthquakes are considered drivers for changes in the engineered structure as a function of time. They are described in Section 3.4.5.7. Massive regional flooding has occurred many times during the past 50,000 years (see Section 2.2.7.2). The flood in the scenario, which is caused by the release of water during glacial retreat from a receding ice dam removes 30 m or more of ground, including the disposal units. In this scenario, the waste is assumed to be uniformly redeposited over an area equivalent to the Hanford Site. Seasonal flooding or flooding caused by collapsed dams would not affect the disposal site (see Section 2.2.9.2).

3.3.3 Contaminant Release Scenario

> Contaminant release from a glass waste form is a complex chemical, physical process that is becoming better understood.

The actual waste form that will contain the contaminants is not yet known. Glass formulations are evolving but borosilicate glasses having a relatively low silica content (~40%) and high sodium content (~20%) have received the most study. In the previous ILAW PA (Mann 1998a), glasses with higher silica contents were analyzed. Section 3.3.3.1 gives a general description of the contaminant release scenario. Section 3.3.3.2 focuses on what occurs during the water-waste form interaction for silicate glasses. The contaminant release rate used in the base analysis case calculations is described in Section 3.4.4.3.

3.3.3.1 General Description. The contaminant release scenario is based on a water-waste form interaction. Initially, the disposal facility design (Section 2.4) delays new moisture from entering the trenches. Eventually, water enters the trenches and moves downward to the waste packages. When it reaches a waste package, the water first interacts with the container, aiding its corrosion. Once the container is breached, water is assumed to reach the waste form. The water starts interacting with and breaking down the waste form. The waste form then releases the contaminants into the available water. The release rate will depend on the material, temperature, and the local chemical environment. The available water transports the contaminant from the waste package and through the disposal facility. If the trench contains a getter material that sorbs the contaminant, the effective contaminant release rate will be affected. Finally, the moisture and contaminants migrate to the vadose zone through cracks at the bottom of the disposal facility.

3.3.3.2 Contaminant Release Based on Glass Corrosion. Studies have shown (Cunnane 1994) that silicate glasses corrode over three stages.

> Silicate glasses corrode over three stages. During the second stage, the corrosion rate becomes very low. Unless the third stage occurs (resulting in corrosion rates approaching the “forward rate”), glass corrosion can stay small indefinitely.

The first stage occurs under dilute-solution conditions. Under these conditions, the water surrounding the waste does not contain significant concentrations of many elements released from the glass. The glass reacts at a characteristic initial rate (the “forward rate”) that depends only on glass composition, temperature, and solution pH. During this time, the glass matrix dissolves and releases contaminants into the water.

The second stage occurs as the concentration of elements released from the glass in the contacting water increases. The rate of glass corrosion continually slows as the concentration of glass components in the solution increases. The reaction may reach a point where the glass corrosion rate cannot be distinguished from zero. This rate has been called the saturation rate where apparent saturation occurs with respect to the glass phase. The solution is not saturated in a thermodynamic sense because glass is metastable. The solution is saturated in a kinetic sense in that the corrosion rate approaches a very low constant value. Recent work by McGrail (2000) indicates that the rate of Na^+-H^+ ion exchange is the rate controlling process in this stage.

The third stage of glass corrosion *could* occur as secondary mineral phases begin to precipitate from the "saturated" fluid in contact with the glass. Precipitation of many of these mineral phases will cause the solution to become undersaturated with respect to the glass. This undersaturation may affect the glass corrosion rate. Mass transfer between the solution and the secondary mineral phases will maintain undersaturation. The resulting glass corrosion rate will depend on the specific chemistry of the secondary mineral phases that are formed and the kinetics of the precipitation. Glass corrosion could remain near the low rate attained during the second stage or could accelerate back to a rate near the forward rate. Both cases have been observed in the laboratory and in the field with natural glasses.

The glass corrosion process releases contaminants into the moisture in contact with the glass. However, the contaminant release rate is not necessarily proportional to the glass corrosion rate. Rather, each contaminant is subject to chemical reactions that can significantly alter the concentration of the contaminants in the moisture that eventually exits the disposal trench. These reactions include oxidation-reduction, dissolution-precipitation, and adsorption. Experiments and numerical analysis are proceeding to better understand the actual contaminant release process. Testing on reference low-activity waste glasses has been completed. Testing has begun on waste forms proposed by the RPP contractors.

3.3.4 Contaminant Transport

Outside the disposal trench, contaminant transport is treated as an extension of moisture movement using the K_d model.

Previous analyses (Kincaid 1995, Mann 1995b, Mann 1998a, Mann/Puigh 2000b,Wood 1995a, Wood 1995b, and Wood 1996) have shown that contaminants are transported mainly by their movement in the aqueous phase. Contaminant transport can occur as contaminants move with the water and diffuse through water. Other transport mechanisms involve vapor-phase transport of the gaseous contaminations and massive movements caused by catastrophic events such as glacial-age flooding. Sections 3.3.4.1 through 3.3.4.4 describe how the contaminant transport mechanisms were modeled. Appendix D contains the equations actually used in the models.

3.3.4.1 Moisture Movement. Two distinct moisture-content regimes are present during contaminant transport: the unconfined aquifer and the vadose zone. In the unconfined aquifer, all the pore space of the porous sediment matrix is filled with water; the matrix is water saturated. In the vadose zone, the pore space is only partially filled with water; the vadose zone is unsaturated.

Water flow through a saturated porous medium, such as the unconfined aquifer, is governed by the empirical relationship described by Darcy's Law (Freeze 1979) and by the conservation of mass. Darcy's law defines the discharge of water through a cross section of a porous medium. However, in contaminant transport, the average velocity of water flowing through the pores of the medium is needed. The average velocity of the pore water is determined by dividing the discharge, or Darcy velocity of the water by the water-filled porosity of the medium. Total porosity is defined as the ratio of void space to total volume.

In an unsaturated medium, the pores are not completely filled with water. For such a medium, moisture content is defined as the ratio of water-filled void space to the total volume and the average velocity of the pore water is determined by dividing the Darcy velocity by the moisture content. Additional effects (capillary forces, the dependence of hydraulic conductivity

on moisture content, etc.) must be considered when analyzing an unsaturated medium. The Richards equation (Richards 1931) becomes the governing equation.

The important parameters in these equations are the following:

- Matric potential (or pressure head) as a function of moisture content (water retention function)
- Hydraulic conductivity as a function of moisture content (relative permeability function)
- The source or sink of moisture.

Under extremely dry conditions, water vapor diffusion may be important. Water vapor diffuses through porous media along vapor pressure gradients. The presence of water-soluble components (in the waste form, for example) depresses the water vapor potential and causes the water vapor to diffuse from the surrounding soils. This water then could condense at the location of the water-soluble material and leach contaminants from that surface. Important factors in this process are the level to which the water vapor pressure is depressed and the effective diffusion coefficient of water vapor.

3.3.4.2 Advective, Dispersive, and Diffusive Transport. The equation for the advective, dispersive, and diffusive transport of contaminants can be viewed as a mass balance on a differential volume.

The parameters important in this equation are as follows:

- The pore water velocity
- The dispersion coefficient
- The effective porosity of the soil layer
- The retardation factor that depends on the soil's density and wetted porosity and chemical distribution coefficient
- The effective diffusion coefficient.

An increase in the retardation factor increases the time for the contaminant to reach the aquifer. In the absence of an advective component, the diffusion process could bring water-soluble contaminants to the land surface via diffusion in a continuous liquid pathway.

Because of the very dry conditions present in Hanford Site soils and expected in the disposal facility, diffusive transport may be more important than advective movement in some cases. Because of the large storage capacity of the surface soils, the effect of large transient storms is confined to the top few feet of soil.

3.3.4.3 Vapor Transport. Some contaminants may move upward from the disposal facility to the surface in the vapor phase. In this document, gaseous contaminants are analyzed. Fick's law governs such movement.

3.3.4.4 Solid Transport. If another glacial-age catastrophic flood (such as the Missoula floods) occurs, the contaminants will be widely dispersed. For this case, the entire inventory is assumed to be mixed with soil to a depth of 20 m (66 ft) (the depth of the disposal facility) over the Hanford Site south of the Columbia River (an area of 906 km^2 [350 mi^2]). Glacial-age catastrophic floods have deposited soils over a far greater area (to the extent of carrying most of the soil all the way to the Pacific Ocean) and mixed the soil to greater depths than assumed here. The all-pathways scenario described in Section 3.3.5 is used to estimate the dose.

3.3.5 Exposure Scenarios

The two major exposure scenarios are drinking contaminated water and living on a small farm.

Two major exposure scenarios considered are drinking contaminated water and exposures via all-pathways while living on a small farm (the all-pathways dose). The details of these scenarios and the justification for all the parameters used in them are found in Rittmann (1999). The expected characteristics of potential future agricultural activities at the Hanford Site are given in *Evaluation of the Potential for Agricultural Development at the Hanford Site*, (Evans 2000). Values for the parameters used in these scenarios are discussed in Section 3.4.7 and are given in Appendix B.

3.4 VALUES AND ASSUMPTIONS

This section describes and justifies the conceptual models and data for those models that were used in the analyses. It covers the selection criteria and key assumptions for the conceptual models; describes the models and their associated data, the waste form, release rate, disposal facility, and moisture and moisture infiltration rate. It also covers the dosimetry parameters. The models actually used in the computer simulations were derived from these conceptual models and are described in Section 3.5. Sensitivity cases are gathered together in Section 3.5.5 and illustrate both uncertainty and bounding conditions.

3.4.1 Selection Criteria

The following criteria are used to select between the alternatives:

- The ability to justify the choice
- The availability of experimental evidence
- The use of best calculational methods.

The overriding criteria were the ability to justify the data and the calculational methods selected. The justification process requires that all data, assumptions, and processes be questioned for applicability. *Does each selection realistically portray probable situations?* This

process quickly identifies errors, misunderstandings, and false assumptions that can be corrected. It also provides insight into the true requirements for methods and the true need for data.

Whenever possible, direct experimental evidence is the basis for selecting data or approaches for the conceptual models. However, in most cases, collecting direct experimental evidence is not possible. Sometimes collecting all the evidence could take too long (e.g., observing the behavior of glass for 10,000 years). Sometimes the amount of data is too large to obtain (e.g., determining hydrologic parameters for the entire vadose zone).

When direct experimental evidence is limited, the available data are used to support analytical simplifications. This approach has two major facets. The first is extrapolating laboratory-measured data to field conditions, as in the case of hydrologic parameters. The second is measuring various effects of the total process to form a complete picture, as was done to determine the infiltration rate. The infiltration rate was determined by combining short-term lysimetry with mid- and long-term tracer measurements and moisture movement simulation studies.

Much experimental and analytical effort has been spent collecting information and producing the understanding needed for this analysis. This effort has been documented in a series of data packages. These have been consolidated in Mann/Puigh 2000a:

> The large amount of experimental and analytical data used in this performance assessment have been documented in a series of data packages that have been reviewed.

- *Disposal Facility Data for the Hanford Immobilized Low-Activity Tank Waste* (Puigh 1999)
- *Evaluation of the Potential for Agricultural Development at the Hanford Site* (Evans 2000)
- *Exposure Scenarios And Unit Dose Factors For The Hanford Immobilized Low-Activity Tank Waste Performance Assessment* (Rittman 1999)
- *Far-Field Hydrology Data Package For The Immobilized Low-Activity Waste Performance Assessment* (Khaleel 1999)
- *Geochemical Data Package For The Immobilized Low-Activity Waste Performance Assessment* (Kaplan 1999)
- *Geologic Data Packages for 2001 Immobilized Low-Activity Waste Performance Assessment* (Reidel 1999)
- *Immobilized Low Activity Tank Waste Inventory Data Package* (Wootan 1999)
- *Near Field Hydrology Data Package for the Immobilized Low-Activity Waste 2001 Performance Assessment* (Meyer 1999)
- *Recharge Data Package for the Immobilized Low-Activity Waste 2001 Performance Assessment* (Fayer 1999)
- *Waste Form Release Data Package for the 2001 Immobilized Low-Activity Waste Performance Assessment* (McGrail 1999, McGrail 2001).

Each data package has undergone a hierarchy of reviews.

In addition, significant amounts of experimental effort are planned to support future performance assessments (see Section 6.4). The statements of work (Puigh 2000) outline the experiments that will be performed to determine geology, hydrology, glass performance, other material performance, and infiltration rate.

Analytical and calculational studies are a major part of the effort to provide data for processes, such as glass corrosion, that will be evolving over thousands of years. Analytical and computational tools were selected with the intention of using them to provide the most insight and accurate simulations of these processes.

3.4.2 Key Assumptions

Even though much of the Site-, facility-, and waste form-specific data needed for a performance assessment have been obtained, some additional assumptions must be made. The key assumptions are as follows.

- The location and layout of the disposal facilities, which dictates geology, stratigraphy, infiltration rate, and associated parameters, will not change.
- The waste form composition, which influences the release rate of contaminants, will be similar to that currently being proposed.
- Our knowledge of tank inventory and the separation and treatment processes used to produce the ILAW packages is adequate.
- The disposal facility design will not change significantly.

As noted in Section 2.2.2, the location for the new disposal facility has been decided. However, the layout of the facility on the reserved land may change as design activities accelerate. Sensitivity cases will be run to determine the impact of different layouts and trench positions at the disposal site.

As noted in Section 2.3.5, the waste form has not been determined. The composition may be varied to best treat the various compositions of tank waste. However, a strong connection continues to exist among the performance assessment team, those developing the glass compositions, and the basic research community. The main glass composition used in this analysis (LAWABP1) is expected to be typical of the glass actually produced. Sensitivity cases will be run for different compositions and for the uncertainties in the glass dissolution process.

The actual composition of the waste form (both radioactive and nonradioactive) is not known. This composition is based on what contaminants are presently in the tanks, the retrieval methods used, the separation processes used, and the glass production system. Although much is known about the composition in each of the 177 tanks presently containing the waste, the system is complex. Each tank has multiple layers containing different elements and compounds. Moreover, the method and timing of retrieval will affect the mixing of waste types in the tanks and, hence, the waste composition. Moreover, final design of the separations, vitrification, and recycling systems for producing ILAW has not begun and is subject to change. For these analyses, only the mean composition based on the estimated total radionuclide inventory was

used. As retrieval scenarios and treatment designs are better defined and individual tank contents become better known, composition variations in the waste form will be determined. Possible variations are investigated through sensitivity cases in these analyses.

Finally, only conceptual ideas exist for the facility design (See Section 2.4). Important features have been identified and preliminary investigations have been done (Puigh 1999). Thus, certain design features can be included with some confidence. Much more work remains as the conceptual design ideas are translated into preliminary, then final, designs. An important part of such work will be experimental and analytical studies of how the design features behave over time.

3.4.3 Site

This section translates the geology, hydrogeology, and geochemistry described in Mann/Puigh (2000a) into a conceptual model and values that can be used in the analyses supporting this performance assessment. The location and stratigraphy of the disposal site are discussed first. Next, the hydrologic and geochemical properties of the vadose zone are addressed. Finally, the properties and structural features of the unconfined aquifer are examined.

3.4.3.1 Location and Stratigraphy. As noted in Section 2.2.2 of this report, the location of the disposal facility was determined (Rutherford 1997) to be in the south-central part of the 200 East Area. The main strata at this location are the Hanford formation and the Ringold Formation.

The proposed disposal site is in the 200 East Area of the Hanford Site.
The geology has been established by a series of boreholes.

The geology of the ILAW disposal site is given in *Geologic Data Package for the 2001 ILAW PA* (Reidel 1999), which is attached as Appendix G to Mann/Puigh (2000a). The Hanford Site lies in the Pasco Basin of the Columbia Plateau. The Columbia Plateau consists of a sequence of thick basalt flows laid down 4 to 15 million years ago. Overlying the basalt flows are sediments of the late Miocene, Pliocene, and Pleistocene ages, known as the Ringold Formation and, nearer the surface, the Hanford formation. The Hanford formation arises from deposits from a series of post-glacier flooding from approximately 1,000,000 to 13,000 years ago, and consists mainly of unconsolidated sand and sandy gravel layers. The unconfined aquifer is near the interface between the Hanford formation and Ringold Formation throughout the Hanford Site. At the ILAW disposal site, the interface is about 103 m (338 ft) below the surface. Clastic dikes have been observed at the Hanford Site and are assumed to exist at the new ILAW site.

The stratigraphy at the ILAW disposal site has the top of the Columbia River Basalt Group at an elevation of approximately 84 m (275 ft) above sea level. The top of the Ringold Formation ranges between 91 m and 122 m (300 and 400 ft) (north to south). The Hanford formation gravel sequence is approximately 27 m to 46m (88 to 150 ft) thick (south to north); and the Hanford formation sand sequence varies from 64 m to 76 m (210 to 250 ft) (north to south). Within the sandy sequence, three paleosols were identified from borehole 299-E17-21 (Reidel 1998). Paleosol Horizon 1 occurs at 49 m (163 ft) drilled depth, paleosol Horizon 2 occurs at 18 m (58 ft) drilled depth, and paleosol Horizon 3 occurs at 1.5 m (5 ft) drilled depth. These paleosol horizons are as much as 15 cm (6 in.) thick with a sharp upper surface interface.

Finally, Eolian deposits cover the southern part of the new ILAW disposal site and range in thickness between 3 m and 15 m (10 to 50 ft) (south to north). The current water table is in the Hanford formation gravel sequence below most of the new disposal site. See Figure 2-12 for a representative stratigraphy for the ILAW disposal site.

The large discharge of water from Hanford Site operations has significantly affected the level and flow of the unconfined aquifer. However, DOE has agreed to severely limit such discharges; at the time of this analysis no discharges are expected. Based on calculations using the Hanford Sitewide groundwater model (Cole 1997), the present location of the aquifer at the disposal site is 98 m (321 ft) below the surface level or 122 m (400 ft) above mean sea level. This model is in good agreement with measurements of changing water table levels over the past two decades. Computer simulations were used to define the level of the unconfined aquifer after Hanford Site operations cease. Current estimates of the post-Hanford Site-operations water table (Bergeron 2000) suggest this level will be 102 m (334 ft) below the surface level or 118 m (387 ft) above mean sea level. This level was used for the base analysis case. The post-Hanford unconfined aquifer is expected to be in the Hanford formation at the disposal site, because of the presence of the ancestral Columbia River channel.

To determine the sensitivity of hydrologic parameters in each layer, sensitivity cases were run that replaced the sandy layer with the gravelly sand and vice versa. In addition, a sensitivity case was run that included clastic dikes; another was run extending the vadose zone by 3 m. Similarly, for groundwater calculations, a sensitivity run was made changing the Hanford formation to the Ringold Formation.

3.4.3.2 Vadose Zone Hydrologic Parameters. Hydrologic processes describe how moisture moves through the subsurface. Because distinct regions are associated with subsurface flow and transport at the ILAW disposal site, the system has been divided into two parts: near-field and far-field.

> The vadose zone hydrologic parameters have been derived from laboratory measurements on local field samples. Gravel, upscaling, and other corrections have been applied for use in these analyses.

Near- and far-field hydrologic parameters (volumetric moisture content and hydraulic conductivity) for these analyses come from laboratory analyses of samples from construction materials and from strata found near the disposal site. Field samples were taken from locations near the disposal site. Corrections were made for the gravel content and for primary drainage. This resulted in moisture-retention data. A detailed discussion of the data and methods used to derive them can be found in the work of Khaleel (1999). The following paragraphs summarize the methods and data.

The moisture retention data can be described in an empirical relationship following the methods of van Genuchten 1980. The moisture retention function is

$$\theta(\psi) = \theta_r + [\theta_s - \theta_r] * \{1 + [\alpha\psi]^n\}^{-m} \qquad (3.1)$$

where

$\theta(\psi)$ = the volumetric moisture content [dimensionless]
ψ = the matric potential or pressure head [m]
θ_r = the residual moisture content [dimensionless]

θ_s = the saturated moisture content [dimensionless]
α = a fitting parameter (m^{-1})
n = a fitting parameter [dimensionless]
m = 1 - 1/n.

Using the Mualam 1976 model and this form for moisture retention, the hydraulic conductivity is

$$K(S_e) = K_s * S_e^{\,n} * \{1 - [1- S_e^{\,1/m}]^{\,m}\}^2 \qquad (3.2)$$

where

$K(S_e)$ = the unsaturated hydraulic conductivity [m/t]
K_s = the saturated hydraulic conductivity [m/t]
S_e = effective saturation = $(\theta - \theta_r) / (\theta_s - \theta_r)$
n = the pore-connectivity parameter [dimensionless], estimated by Mualam to be about 0.5 for many soils. In this work, n is taken to be 0.5.

The RETC code (van Genuchten 1991) was used to determine values for θ_r, θ_s, α, and n. Values for K_s were determined by fitting laboratory data to a lognormal distribution.

3.4.3.2.1 Near-Field Hydrology Data. The processes and data important for moisture flow in the zone between the surface and the bottom of the engineered disposal facility are described in *Near-Field Hydrology Data Package for the Immobilized Low-Activity Waste 2001 Performance Assessment* (Meyer 1999), which is Appendix L in Mann/Puigh (2000a). Physical and hydraulic properties (particle size distribution, particle density, bulk density, porosity, water retention, and hydraulic conductivity as a function of moisture content) and associated transport parameters (dispersivity and effective diffusion coefficient) are given for the surface cover materials, the vault structure, diversion layers, the water conditioning layer, and the backfill materials. Table 3-3 presents best-estimate parameter values for near-field materials. Best estimate values for transport parameters (which are relatively unimportant in this analysis) can be found in Meyer (1999) (Chapter 5).

Table 3-3. Best-Estimate Hydraulic Parameter Values For Near-Field Materials.

Material	ρ_p (g/cm^3)	ρ_b (g/cm^3)	θ_s	θ_r	α (cm^{-1})	n	K_s (cm/s)
Surface Barrier							
Silt loam-gravel admixture	2.72	1.48	0.456	0.0045	0.0163	1.37	8.4×10^{-5}
Compacted silt loam	2.72	1.76	0.353	0.0035	0.0121	1.37	1.8×10^{-6}
Sand filter	2.755	1.88	0.318	0.030	0.538	1.68	8.58×10^{-5}
Gravel filter	2.725	1.935	0.290	0.026	8.1	1.78	1.39×10^{-2}

Table 3-3. Best-Estimate Hydraulic Parameter Values For Near-Field Materials.

Material	ρ_p (g/cm^3)	ρ_b (g/cm^3)	θ_s	θ_r	α (cm^{-1})	n	K_s (cm/s)
Gravel drainage	2.725	1.935	0.290	0.006	17.8	4.84	2.0
Asphaltic concrete	2.63	2.52	0.04	0.000	1.0×10^{-7}	2.0	1×10^{-11}
Capillary Break							
Diversion layer sand	2.8	1.65	0.371	0.045	0.0683	2.08	3.00×10^{-2}
Diversion layer gravel	2.8	1.38	0.518	0.014	3.54	2.66	1.85
Trench/Vault							
Filler material	2.63	1.59	0.397	0.005	0.106	4.26	3.79×10^{-2}
Glass waste	2.68	2.63	0.02	0.00	0.2	3	0.01
Vault concrete	2.63	2.46	0.067	0.00	3.87×10^{-5}	1.29	1.33×10^{-9}
Backfill	2.76	1.89	0.316	0.049	0.035	1.72	1.91×10^{-3}

ρ_p = particle density ρ_b = dry bulk density

θ_s = saturated water content θ_r = residual water content

α,n = van Genuchten fitting parameters K_s = saturated hydraulic conductivity

3.4.3.2.2 Far-Field Hydrology. The processes and data important for moisture flow in the zone between the bottom of the engineered disposal facility and the water table are described in *Far-Field Hydrology Data Package for the Immobilized Low-Activity Waste Performance Assessment* (Khaleel 1999), which is Appendix M in Mann/Puigh (2000a). Two units of the Hanford formation make up this zone: the sandy unit and the Lower Hanford gravel unit.

Khaleel (1999) summarizes the hydraulic parameter estimates based on data from the ILAW borehole and data on gravelly samples from the 100 Area boreholes. Statistical fits (normal or log-normal) were made for each parameter, with Table 3-4 proving the best estimate (or mean) values affecting moisture flow. The document also describes the processes for upscaling such small-scale laboratory measurements to field-scale applications, and provides recommendations for determining which parameters to use at that scale. Best estimate values for transport parameters associated with the base-case effective transport parameters (bulk density, diffusivity, and dispersivity) also are described in Khaleel (1999).

Table 3-4. Best-Estimate Hydraulic Parameter Values For Far-Field Layers.

Formation	θ_s	θ_r	α (1/cm)	n	ℓ	K_s (cm/s)
Sandy	0.375	0.041	0.057	1.768	0.5	2.88×10^{-3}
Gravelly	0.138	0.010	0.021	1.374	0.5	5.60×10^{-4}

θ_s = saturated water content θ_r = residual water content

α,n = van Genuchten fitting parameters ℓ = pore size distribution factor

K_s = saturated hydraulic conductivity

Overall, compared to the sandy sequence, the gravelly sequence is characterized by a much smaller saturated water content, higher bulk density, higher log-conductivity variance, smaller log-unsaturated conductivity variance, a much smaller macroscopic anisotropy and smaller dispersivities (Khaleel 1999). An anisotropy ratio (ratio of horizontal to vertical hydraulic conductivity) in excess of one results in an enhanced lateral migration. To model restricted lateral migration (i.e., a conservative assumption), an isotropic model was used for both strata.

Longitudinal dispersivities of 200 cm and 30 cm were used for the sandy and gravelly sequences, respectively (Khaleel 1999). Lateral dispersivities were estimated to be $1/10^{th}$ of the longitudinal estimates. The effective, large-scale diffusion coefficients for both sandy and gravel-dominated sequences are assumed to be a function of volumetric moisture content, θ. VAM3DF uses the Millington-Quirk 1961 empirical relation:

$$D_e(\theta) = D_0 \frac{\theta^{10/3}}{\theta_s^2} \tag{3.3}$$

where

$D_e(\theta)$ is the effective diffusion coefficient of an ionic species
D_0 is the effective diffusion coefficient for the same species in free water.

The molecular diffusion coefficient for all species in pore water is assumed to be 2.5×10^{-5} cm^2/s (Kincaid 1995).

Sensitivity cases were run to test the sensitivity to different hydraulic properties (including diffusion).

3.4.3.3 Geochemical Retardation Factors.

Chemical interactions with the facility, near-field materials, and the soil in the vadose zone can greatly slow the transport of contaminants. Geochemical effects are based on the discussion

Geochemical parameters are based on laboratory measurements of field samples using a variety of fluids. Parameters are given for 5 zones and include corrections for gravel content and the surrounding chemical environment.

and values presented in *Geochemical Data Package for the Hanford Immobilized Low-Activity Tank Waste Performance Assessment* (Kaplan 1999), also provided in Appendix N of Mann/Puigh (2000a).

The geochemistry is described using two parameters: the distribution coefficient (K_d value) and the solubility product of a specified solid. The distribution coefficient is a thermodynamic construct. It is the ratio of the concentration of a species reversibly adsorbed or exchanged to a geomedia's surface site divided by the concentration of the species in solution. Parameters are given for the following five zones:

- **Near-Field**. Inside the disposal facility (K_d and solubility values)
- **Degraded Concrete Vault**. (K_d and solubility values)
- **Chemically Impacted Far-Field in Sand Sequence**. (K_d values only)
- **Chemically Impacted Far-Field in Gravelly Sequence**. (K_d values only)
- **Far Field in Gravel Sequence**. Unconfined aquifer (K_d values only).

The amount of slowing is described by a multiplicative factor known as the geochemical retardation factor, which involves the distribution coefficient. Geochemical retardation in unsaturated conditions is predicted to be

$$R_f = 1 + \rho K_d / \theta \tag{3.4}$$

where

R_f is the geochemical retardation factor (dimensionless)
ρ is the bulk density of the material (g/cm^3)
K_d is the chemical distribution coefficient (liter/g)
θ is the volumetric moisture content (dimensionless).

A derivation of the general contaminant transport equation is given in the 1998 ILAW PA report (Mann 1998a, Appendix D, Section D.2.3). The chemical distribution coefficient (K_d) is measured in the laboratory by comparing the amount of material trapped in or on the soil matrix to the amount of material in the water phase.

Tables 3-5 and 3-6 provide estimates for K_d from recent measurements and for the K_ds used in the analyses in this report. Unless otherwise stated, the K_ds are provided for the chemically impacted far-field sandy sequence beneath the disposal facility (Table 3-5) and the near-field materials (Table 3-6). The "Probable K_d" is the best estimate for the K_d. Finally, the "K_d value used" refers to the value of K_d used in the analyses provided in this report.

For convenience in modeling, a subset of K_d values was used in these analyses. The computer code VAM3DF (See Section 3.5.3) treats the chemical distribution coefficients as point-estimate values, not as probability functions. Therefore, the actual K_d values used were reduced to one of eight value sets for the near and far fields (see Tables 3-5 and 3-6). This K_d value was conservatively chosen to be one of the following six values:

0 corresponding to technetium

0.6 mL/g corresponding to uranium

4.0 mL/g corresponding to selenium

10 mL/g corresponding to strontium

80 mL/g corresponding to tin and cesium

150 mL/g corresponding to plutonium.

These values are less than or equal to the probable K_d value provided in these tables. The elements selected were shown to be the most important in the 1998 ILAW PA. The values in parentheses provided in Table 3-5 are for the unperturbed (near neutral pH, ionic strengths between 0 and 0.01, and only trace contaminant concentrations) far-field sand sequence.

Because radionuclides spend significantly less time in the unconfined aquifer than in the vadose zone, no credit was taken in this analysis for increased travel time in the unconfined aquifer because of geochemical retardation.

Values are based on site-specific samples for the most part, but in a few cases depend on literature values or chemical similarity. Table 3-5 provides the best estimate K_d values for the chemically impacted far-field sand sequence. The gravel-corrected best estimate K_d values for the chemically impacted far-field gravel sequence are a factor of 10 smaller than the values given in Table 3-5. The values in parentheses in the table are for the unperturbed far-field sand sequence. The aqueous phase is assumed to be untainted Hanford formation groundwater except for trace levels of radionuclide and the solid phase is assumed to be natural Hanford formation sand-dominated sequence sediment. The literature values on which these values were based had an aqueous phase near neutral pH, ionic strength between 0 and 0.01, and trace radionuclide concentrations.

Table 3-5. Best-Estimate K_d Values For The Far-Field Sand Sequence.

Radionuclide	Probable K_d[a,b] (mL/g)	Value Used[a,c] (mL/g)
Ac	350.	150.
Am	350.	150.
C [(d)]	20. (5.)	4.
Ce	350.	150.
Cl	0.	0.
Cm	350.	150.
Co	300.	150.

Table 3-5. Best-Estimate K_d Values For The Far-Field Sand Sequence.

Radionuclide	Probable K_d[a,b] (mL/g)	Value Used[a,c] (mL/g)
Cs	80.	80.
Eu	350.	150.
^3H	0.	0.
I	0.	0.
Nb	80.	80.
Ni	80.	80.
Np	0.8	0.6
Pa	0.8	0.6
Pb	100.	80.
Pu	200.	150.
Ra	10.	10.
Ru	1.	0.6
Se	4.	4.
Sn	80.	80.
Sr	10.	10.
Tc	0.	0.
Th	300.	150.
U [(d)]	10. (0.6)	0.6
Zr	300.	150.

Table 3-5. Best-Estimate K_d Values For The Far-Field Sand Sequence.

Radionuclide	Probable K_d[a,b] (mL/g)	Value Used[a,c] (mL/g)

[a]The values in the table are for the chemically impacted far-field sand sequence. The aqueous phase is moderately altered from the cement and glass leachate emanating from the near field; pH is between 8 (background) and 11, and the ionic strength is between 0.01 (background) and 0.1. The solid phase is in the sand-dominated sequence and is slightly altered because of contact with the caustic aqueous phase.

[b]Probable K_d is the best estimate for K_d

[c]Value Used is the K_d value used in the analyses provided in this report

[d]The values in parentheses in the table are for the unperturbed far-field sand sequence. The aqueous phase is assumed to be untainted Hanford formation groundwater, except for trace levels of radionuclide and the solid phase is assumed to be natural Hanford formation sand-dominated sequence sediment. The literature values on which the values were based had an aqueous phase near neutral pH, ionic strength between 0 and 0.01, and trace radionuclide concentrations.

Other important geochemical data (e.g., near-field field values for important radionuclides) are displayed in Table 3-6. For the analyses in this PA, the K_ds for the unconfined aquifer were set equal to zero. Note that the K_d values in concrete used for uranium and iodine have been set equal to zero, which is conservative.

Because the vadose zone calculations are run in terms of K_d bins, rather than actual materials, it is possible to calculate the effect of changing K_d values after the vadose zone calculations are complete. Thus, sensitivities to K_d values will be given for the most important materials. In addition, a sensitivity case is run to determine the importance of a getter material just beneath the disposal facility.

Table 3-6. Other Important Geochemical Values.

Element	Probable Value[a,b]	Value Used[a,c]	Zone and Geochemical Value
Tc	1	0	Zone 1: Near-Field K_d (mL/g)
U	20	0.6	Zone 1: Near-Field K_d (mL/g)
U	1×10^{-7}	1×10^{-7}	Zone 1: Near Field Solubility (M)
I	2	0	Zone 2: Degraded Aged Concrete K_d (mL/g)
U	100	0	Zone 2: Degraded Aged Concrete K_d (mL/g)
U	1×10^{-7}	1×10^{-7}	Zone 2: Degraded Aged Concrete Solubility (M)

[a] The values in the table are for the chemically impacted far-field sand sequence. The aqueous phase is moderately altered from the cement and glass leachate emanating from the near field; pH is between 8 (background) and 11, and the ionic strength is between 0.01 (background) and 0.1. The solid phase is in the sand-dominated sequence and is slightly altered because of contact with the caustic aqueous phase.

[b] "Probable K_d" is the best estimate for K_d

[c] "Value Used" is the K_d value used in the analyses provided in this report

3.4.3.4 Unconfined Aquifer Properties and Boundaries. Groundwater flow and contaminant transport were calculated with the current version of the Hanford Sitewide Groundwater model. This three-dimensional model, currently being used by the Hanford Groundwater Project and recommended as the proposed Sitewide groundwater model in the Hanford Site groundwater model consolidation process, is based on the Coupled Fluid, Energy, and Solute Transport (CFEST-96) Code (Gupta 1987). The specific implementation of this model is more fully described in Wurstner 1995 and Cole 1997. This specific model was most recently used in the Hanford Site Composite Analysis (Cole 1997; Kincaid 1998), which is a companion analysis to the 1998 performance assessment analyses of the ILAW disposal (Mann 1998a) and the solid waste burial grounds in the 200 East and 200 West Areas (Wood 1996 and 1995a). The composite analysis also is a companion document to the Remedial Investigation/Feasibility Study (RI/FS) (DOE/RL 1994a) done to support the Environmental Restoration Disposal Facility.

3.4.3.4.1 Hydrogeologic Framework. The conceptual model of groundwater flow is based on nine major hydrogeologic units in the left hand column shown in Figure 3-2. The basis for identifying these major hydrogeologic units in the aquifer system is more fully described in Thorne (1992, 1993, and 1994). Although nine hydrogeologic units were defined, only seven are found below the water table during post-Hanford Site operations conditions. Odd-numbered Ringold model units (5, 7, and 9) are predominantly coarse-grained sediments. Even-numbered Ringold model units (4, 6, and 8) are predominantly fine-grained sediments with low permeability. The Hanford formation combined with the pre-Missoula gravel deposits were designated model unit 1. Model units 2 and 3 correspond to the Plio-Pleistocene deposits. These units lie above the current water table. The predominantly mud facies of the upper Ringold unit identified by Lindsey (1995) was designated model unit 4. However, a difference in the definition of model units is that the lower, predominantly sand, portion of the upper Ringold unit described in Lindsey (1995) was grouped with model unit 5, which also includes Ringold gravel/sand units E and C. This was done because the predominantly sand portion of the upper Ringold is expected to have hydraulic properties similar to units E and C. The lower mud unit identified by Lindsey (1995) was designated units 6 and 8. Where they exist, the gravel and sand units B and D, which are found within the lower Ringold, were designated model unit 7. Gravels of Ringold unit A were designated unit 9 for the model, and the underlying basalt was designated model unit 10. However, the basalt was assigned a very low hydraulic conductivity and was essentially impermeable in the model.

The lateral extent and thickness distribution of each hydrogeologic unit were defined based on information from well drillers' logs, geophysical logs, and an understanding of the geologic environment. These interpreted areal distributions and thicknesses were then integrated into EarthVision (Dynamic Graphics, Inc., Alameda, California), a three-dimensional, visualization software package that was used to construct a database of the three-dimensional hydrogeologic framework.

Figure 3-2. Comparison of Generalized Geology and Hydrostratigraphic Columns.

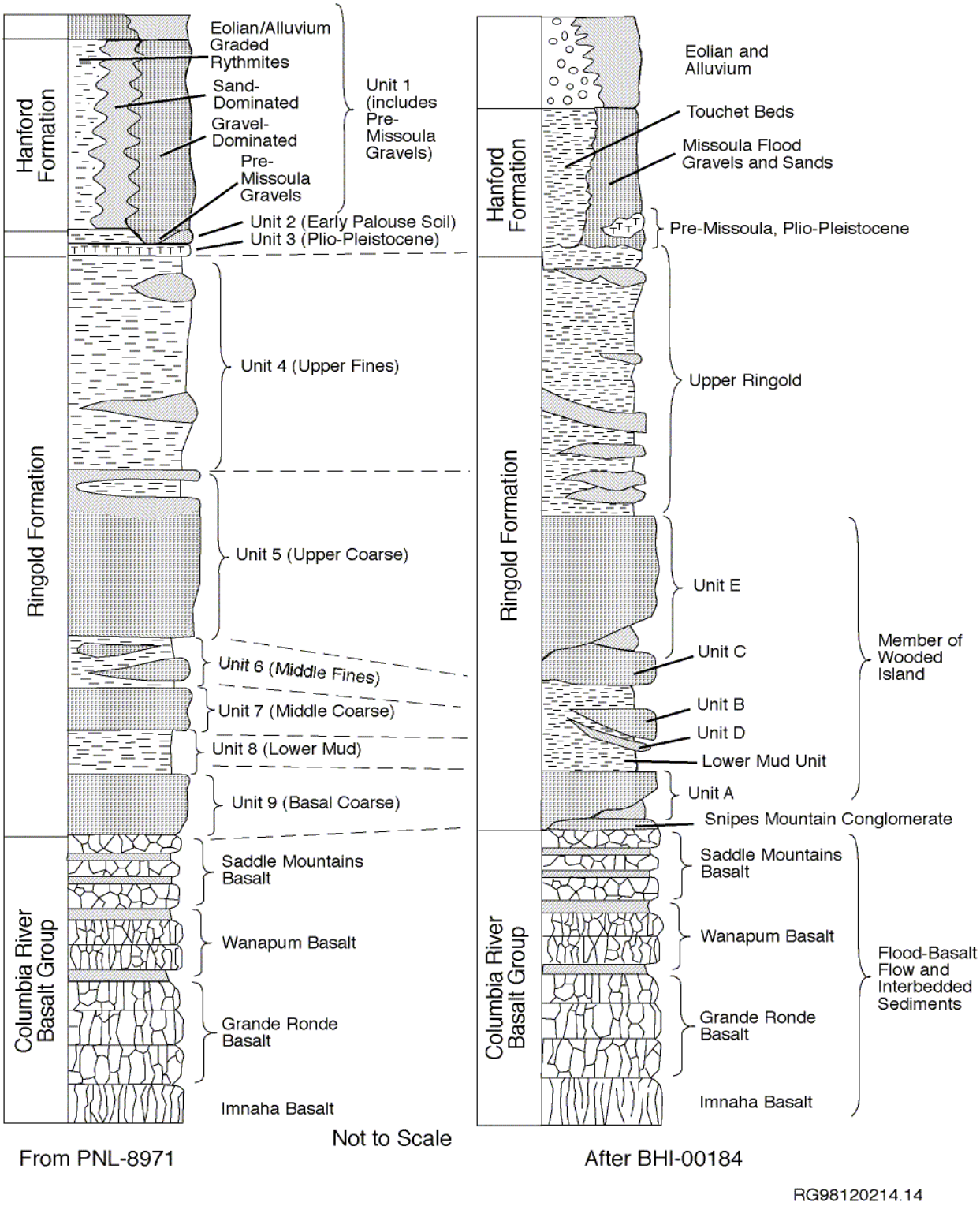

3.4.3.4.2 Recharge and Aquifer Boundaries. Both natural and artificial recharges to the aquifer were incorporated in the model. Natural recharge to the unconfined aquifer system occurs from infiltration of 1) runoff from elevated regions along the western boundary of the Hanford Site; 2) spring discharges originating from the basalt-confined aquifer system, also along the western boundary; and 3) precipitation falling across the site. Some recharge also occurs along the Yakima River in the southern portion of the site. Natural recharge from runoff and irrigation in the Cold Creek and Dry Creek Valleys, up-gradient of the site, also provides a source of groundwater inflow. Areal recharge from precipitation on the site is highly variable, both spatially and temporally, and depends on local climate, soil type, and vegetation. A recharge distribution based on Fayer 1995 for 1979 was applied in the model.

The other source of recharge to the unconfined aquifer is wastewater disposal. A large volume of artificial recharge from wastewater discharged to disposal facilities on the Hanford Site over the past 50 years has significantly impacted groundwater flow and contaminant transport in the unconfined aquifer system. However, the volume of artificial recharge has decreased significantly in the recent past and the water table is expected to return to more natural conditions after site closure.

The flow system is bounded by the Columbia River on the north and east and by the Yakima River and basalt ridges on the south and west. The Columbia River represents a line of regional discharge for the unconfined aquifer system. The amount of groundwater discharging to the river is a function of local hydraulic gradient between the groundwater elevation adjacent to the river and the river-stage elevation. This hydraulic gradient is highly variable because the river stage is affected by releases from upstream dams. To approximate the long-term effect of the Columbia River on the unconfined aquifer system in the three-dimensional model, the CHARIMA river-simulation model (Walters et al. 1994) was used to generate the long-term, average river-stage elevations for the Columbia River. The river itself is represented as a constant-head boundary in the uppermost nodes of the model at the approximate locations of the river's left bank and channel midpoint. Nodes representing the thickness of the aquifer below the nodes representing mid-point of the river channel were treated as no-flow boundaries. This boundary condition is used to approximate the location of the groundwater divide that exists beneath the Columbia River where groundwater from the Hanford Site and the other side of the river discharge into the Columbia. The Yakima River was also represented as a specified-head boundary at surface nodes approximating its location. Like the Columbia River, nodes representing the thickness of the aquifer below the Yakima River channel were treated as no-flow boundaries.

At Cold Creek and Dry Creek Valleys, the unconfined aquifer system extends westward beyond the boundary of the model. To approximate the groundwater flux entering the modeled area from these valleys, both constant-head and constant-flux boundary conditions were defined. A constant-head boundary condition was specified for Cold Creek Valley for the steady-state model calibration runs. Once calibrated, the steady-state model was used to calculate the flux condition that was then used in the post-Hanford steady state flow simulation. The constant-flux boundary was used because it better represents the response of the boundary to a declining water table than a constant-head boundary. Discharges from Dry Creek Valley in the model area, resulting from infiltration of precipitation and spring discharges, are approximated with a prescribed-flux boundary condition.

The basalt underlying the unconfined aquifer sediments represents a lower boundary to the unconfined aquifer system. The potential for interflow (recharge and discharge) between the basalt-confined aquifer system and the unconfined aquifer system is postulated to be small relative to the other flow components estimated for the unconfined aquifer system. Therefore, interflow with underlying basalt units was not included in the current three-dimensional model. The basalt was defined in the model as an essentially impermeable unit underlying the sediments.

3.4.3.4.3 Flow and Transport Properties. To model groundwater flow, the distribution of hydraulic properties, including both horizontal and vertical hydraulic conductivity and porosity were needed for each hydrogeologic unit defined in the model. In addition, to simulate movement of contaminant plumes, transport properties were needed, including contaminant-specific distribution coefficients, bulk density, effective porosity, and longitudinal and transverse dispersivities.

In the original model calibration procedure described in Wurstner 1995, measured values of aquifer transmissivity were used in a two-dimensional model with an inverse model-calibration procedure to determine the transmissivity distribution. Hydraulic head conditions for 1979 were used in the inverse calibration because measured hydraulic heads were relatively stable at that time. Details concerning the updated calibration of the two-dimensional model are provided in Cole 1997.

Hydraulic conductivities were assigned to the three-dimensional model units so that the total aquifer transmissivity from inverse calibration was preserved at every location. The vertical distribution of hydraulic conductivity at each spatial location was determined based on the transmissivity value and other information, including facies descriptions and hydraulic property values measured for similar facies. A complete description of the seven-step process used to vertically distribute the transmissivity among the model hydrogeologic units is described in Cole 1997. The hydraulic conductivity distribution resulting from this redistribution of aquifer transmissivity in the upper part of the aquifer is provided in Figure 3-3.

Estimates of model parameters were developed to account for contaminant dispersion in all transport simulations. Specific model parameters examined included longitudinal and transverse dispersion coefficients (D_l and D_t) as well as estimates of effective bulk density and porosity of the aquifer materials. This section briefly summarizes estimated transport properties.

In general, the horizontal dispersivity for aquifer transport is typically set at 10% of the travel length in the direction of flow and the transverse dispersivity is set at 10% of the longitudinal value. For predictions at 100 m (328 ft) downgradient of the facility, this would mean a longitudinal dispersivity of at least 10 m (32.8 ft) would be required. For this analysis, a lower longitudinal dispersivity of 5 m (16.4 ft) was selected to be within the range of recommended grid peclet numbers (P_e <4) for acceptable solutions. The 10-m (32.8-ft) estimate is about one-quarter of the grid spacing in the finest part of the local-scale model grid in the 200-Area plateau where the smallest grid spacing is on the order of 20 m by 20 m (65.6 ft by 65.6 ft).

Figure 3-3. Hydraulic Conductivity Distribution Obtained for the Uppermost Unconfined Aquifer from Inverse Calibration for 1979 Conditions.

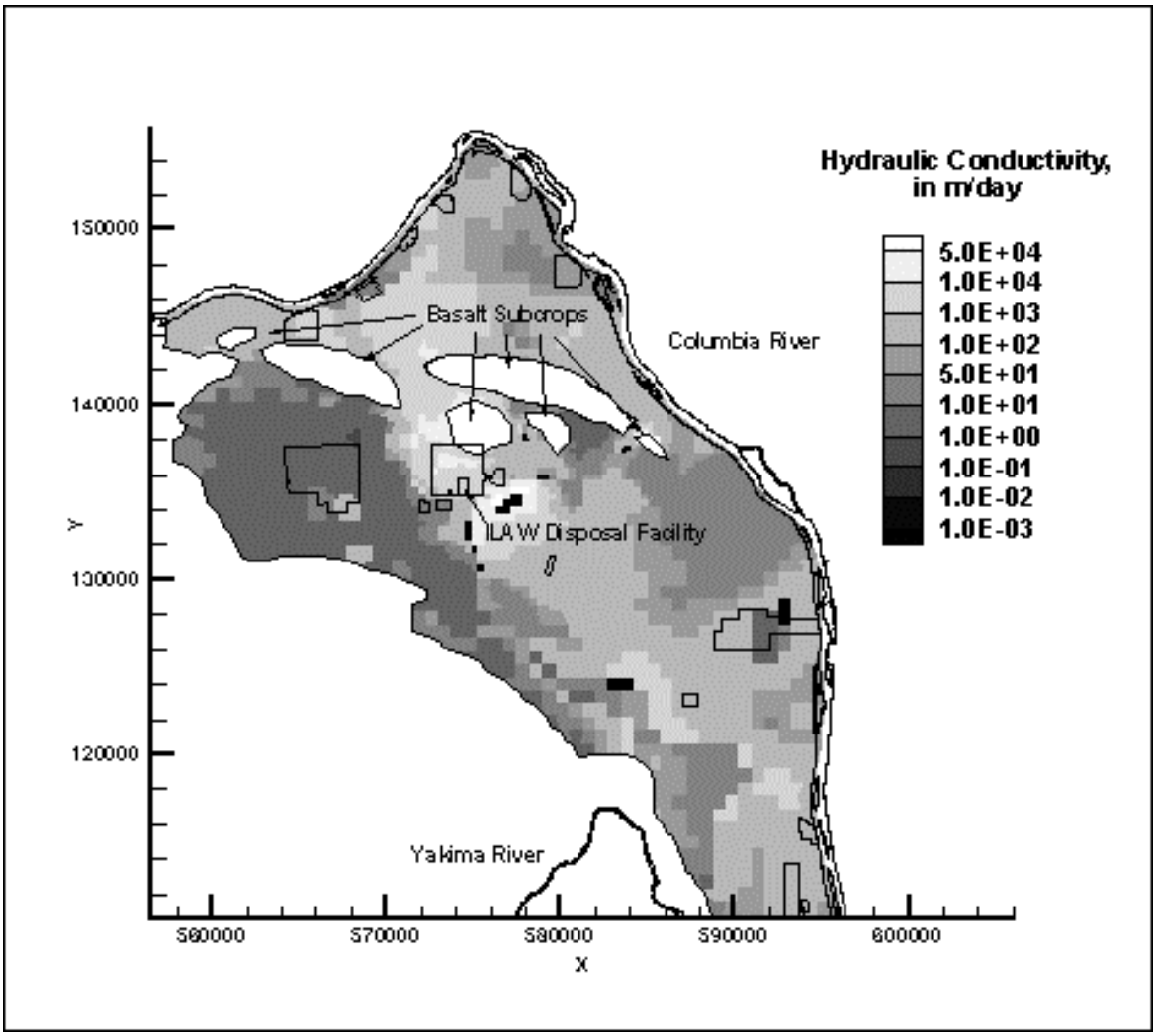

The effective transverse dispersivity was assumed to be one-tenth of the longitudinal dispersivity. Therefore, 0.5 m (1.6 ft) was used in all simulations.

For purposes of this analysis, no adsorption was assumed in the groundwater transport modeling. All simulations were based the transport of a non-sorbed, long-lived radionuclide. Iodine-129 was used as the surrogate radionuclide in all calculations.

For purposes of these calculations, a bulk density of 1.9 g/cm^3 was used for all simulations. The effective porosity was estimated from limited measurement of porosity and specific yields obtained from multiple-well aquifer tests. The effective porosity values range from 0.01 to 0.37. Laboratory measurements of porosity, which range from 0.19 to 0.41, were available for samples from a few Hanford Site wells and were also considered. The few tracer tests conducted indicate effective porosities ranging from 0.1 to 0.25. Based on the ranges of values considered, a best estimate of an effective porosity value for all simulations was assumed to be 0.25.

Information on transport properties used in past modeling studies at the Hanford Site is provided in Wurstner 1995. Estimates of model parameters were developed to account for contaminant transport and dispersion in all transport simulations. Specific model parameters estimated included longitudinal and transverse dispersivity (D_l and D_t) and aquifer porosity. This section briefly summarizes estimated transport properties.

For the regional scale analysis, a longitudinal dispersivity of 95 m was selected to be within the range of recommended grid Peclet numbers ($P_e < 4$) for acceptable solutions. The 95 m estimate is about one-quarter of the grid spacing in the finest part of the model grid in the 200 Area plateau where the smallest grid spacing is on the order of about 375 m by 375 m. The effective transverse dispersivity was assumed to be 10 percent of the longitudinal dispersivity. Therefore, 9.5 m was used in all simulations.

3.4.3.4.4 Groundwater Sensitivity Cases. Groundwater sensitivity cases are run to determine the effect of different placement and orientation of the disposal facility, different pumping rates, different hydraulic properties of the aquifer, as well as different regional conditions.

3.4.4 Waste Package

The waste package geometry is still evolving as design of the treatment plant and disposal facility continues.

3.4.4.1 Waste Package Geometry. The DOE intends to process approximately 10% of the waste from the Hanford tanks in an initial phase (Phase 1). (The plans in early 2000 identify a minimum of 6,000 packages [having cubic geometry with a side length of 1.4 m] and Kirkbride 1999 estimates that approximately 70,000 ILAW packages will be generated for all the ILAW in Phase 1 and Phase 2). The product description and specifications defined in this section are based on the DOE contract (DOE/BNFL 1998). The definition of the product form and specification for the remaining 91% of the Hanford tank waste are not defined at this time. For the purposes of this assessment activity, all the ILAW waste products are assumed equivalent to the DOE specifications for the Phase 1 contract and current plans.

The ILAW product consists of a silicate glass monolith sealed in a stainless steel (304L) package. The headspace above the silicate glass in the package is filled with silicate sand (BNFL 1998). The steel package has external dimensions of 1.4 m x 1.4 m x 1.4 m (-0 m/+0.05 m tolerances). The stainless steel side-wall thickness of the package is 6 mm. The package top is 12 mm plate and the bottom is 8 mm plate. Each ILAW package is planned to be filled to within 85% capacity (by volume) by ILAW and the void space would be filled with silicate sand such that the remaining free fill space is less than 5% (by volume). The top lid will be welded using the tungsten-inert gas (TIG) process.

Modification 12 of the BNFL contract (see DOE/BNFL 1998), which was issued on January 24, 2000, and the current contract with Bechtel Washington (DOE 2000c) require ILAW canisters in the form of right circular cylinders (1.22 m diameter by 2.29 m tall). This contract modification occurred after the data packages used in these analyses were issued and will hence are not part of the base analysis case. Sensitivity cases for the new dimensions were run, however. Future work will use the latest dimensions for the waste package and other facility information. However, a sensitivity case in this analysis shows that such a container size change is not significant to the conclusions of this performance assessment.

For the waste form calculations discussed in Section 3.5.3, the glass waste material was assumed to be fractured. Also, the surface area was assumed to be 10 times greater than that of an unfractured 1.4 m cube (Farnsworth 1985, Peters 1981). Hence,

$$A_{glass}^{S} = \frac{A_{glass}}{V_{glass}} = \frac{6(1.4)^2}{(1.4)^3} \times 10 = 42.8 \text{ m}^2\text{m}^{-3} \tag{3.5}$$

where

A_{glass}^{S} = the specific surface area of the glass,

A_{glass} = the surface area of the glass, and

V_{glass} = the volume of the glass.

The surface area of the steel waste package was determined by assuming that both the inner and outer surfaces of the steel container were available to react.

$$A_{steel}^{S} = \frac{A_{steel}}{V_{steel}} = \frac{12(1.4)^2}{\left[0.012 + 0.008 + 4(0.006)\right](1.4)^2} = 272.73 \text{ m}^2\text{m}^{-3} \tag{3.6}$$

where

A_{steel}^{S} = the specific surface area of the steel container,

A_{steel} = the surface area of the steel container, and

V_{steel} = the volume of the steel container.

> The waste form release rate is calculated as a function of the time- and spatial dependent chemical environment surrounding the glass forms. The parameters are based on a large series of experiments using different methods.

3.4.4.2 Waste Form Release Rate. The 1998 ILAW PA (Mann 1998a) showed that the release rate from the waste form was one of the key parameters in the performance assessment. This rate is a major determinant of the impact of disposal as well as setting the temporal structure of that impact. The data for determining the waste form release rate are given in *Waste Form Release Data Package for the 2001 Immobilized Low-Activity Waste Performance Assessment* (McGrail 2001) and appendix K of Mann/Puigh 2001.

Dissolution of the glass waste form is the required first step to release a specific radionuclide. Because glass dissolution rate depends on a variety of parameters (amount of moisture, amount of silicic acid [the main by-product of dissolved glass] in solution, pH, amount and type of secondary phases) that will vary with time and location in the disposal system, the dissolution rate must be calculated. However, in order for the calculations to be technically defensible, they must be based on an accepted paradigm and an extensive database.

Over the last few decades, a general rate equation has been fashioned to described the dissolution of glass (and more ordered materials) into aqueous solution:

$$k = \vec{k}\alpha_{H^+}^{-\eta} e^{\frac{-E_a}{RT}} \left[1 - \left(\frac{Q}{K} \right)^{\sigma} \right] \prod_j \alpha_j^{\eta_j} \tag{3.7}$$

where:

k	= dissolution rate, g/m²/d
$\vec{k}$	= intrinsic rate constant, g/m²/d
a_{H^+}	= hydrogen ion activity
a_j	= activity of the jth aqueous species that acts as an inhibitor or as a catalyst of dissolution
E_a	= activation energy, kJ/mol
R	= gas constant, kJ/(mol·K)
T	= temperature, K
Q	= ion activity product
K	= pseudoequilibrium constant
η	= pH power law coefficient
σ	= Temkin coefficient.

Equation (3.7) is an approximation for glass because glass is metastable, and the reaction proceeds one way (i.e. glass dissolves). Equation (3.7) also just describes the net chemical reaction of glass matrix dissolution. There are a number of secondary chemical reactions that also need to be considered. One important reaction is the exchange of alkali ions in the glass for H^+ in water (McGrail 2000). The waste form contains high concentrations of sodium (up to 25 weight percent). At the temperatures of interest, the exchange of sodium in the glass with H^+ in the water is important because the reaction effectively increases the pH of the solution. Finally, dissolution/precipitation reactions are important because they can strip chemicals from the aqueous solution, affecting the glass corrosion rate or trapping important contaminants.

The parameters in these equations are established by a set of various experiments, performed at various temperatures and pHs:

- single-pass flow-through test
- product consistency test
- vapor hydration test
- pressurized unsaturated flow-through test.

The exact glass composition for ILAW has not been determined. The ILAW PA activity has worked with BNFL, Inc. and the DOE Tank Focus Area (Vienna 2000) to investigate a set of glasses in the BNFL, Inc. processing space. For the 2001 ILAW PA, the base analysis case uses LAWABP1 as the reference glass and HLP-31 glass as a sensitivity case. The LAWABP1 glass has the most extensive database of any glass in its processing space and its composition is based on the composition of preliminary BNFL, Inc. glasses. The corrosion reaction for LAWABP1 glass used in the waste form release calculations is:

$$
\begin{aligned}
&\mathrm{LAWABP1} + 4.42\times10^{-1}\ H^{+} + 1.89\times10^{-1}\ H_2O \rightarrow 1.36\times10^{-1}\ AlO_2^{-} \\
&\quad + 1.84\times10^{-1}\ B(OH)_3(aq) + 1.13\times10^{-2}\ Cl^{-} + 1.82\times10^{-4}\ CrO_4^{2-} \\
&\quad + 1.46\times10^{-3}\ F^{-} + 2.16\times10^{-2}\ Fe(OH)_3(aq) + 1.54\times10^{-7}\ IO_3^{-} \\
&\quad + 3.23\times10^{-2}\ K^{+} + 8.48\times10^{-3}\ La^{3+} + 1.71\times10^{-2}\ Mg^{2+} + 4.46\times10^{-1}\ Na^{+} \\
&\quad + 7.79\times10^{-4}\ HPO_4^{2-} + 3.52\times10^{-8}\ PuO_2(CO_3)_3^{4-} + 8.63\times10^{-4}\ SO_4^{2-} \\
&\quad + 1.77\times10^{-8}\ SeO_4^{2-} + 4.82\times10^{-1}\ SiO_2(aq) + 6.59\times10^{-7}\ TcO_4^{-} \\
&\quad + 2.15\times10^{-2}\ Ti(OH)_4(aq) + 9.81\times10^{-7}\ UO_2(OH)_2(aq) \\
&\quad + 2.20\times10^{-2}\ Zn^{2+} + 2.94\times10^{-2}\ Zr(OH)_4(aq)
\end{aligned}
\tag{3.8}
$$

The stoichiometric coefficients for I, Pu, Se, Tc, and U are based on the average package concentration from the *Immobilized Low Activity Tank Waste Inventory Data Package* (Wootan 1999).

3.4.4.3 Waste Form Data Used in this PA. The *Waste Form Release Data Package for the 2001 Immobilized Low-Activity Waste Performance Assessment* (McGrail 2001) should be referred to for a detailed discussion of the derivation of parameters used in this analysis. However, a few figures from that report are included here to provide the reader a feeling for the amount of data available and key findings from the experiments. Table 3-7 provides a summary of the best-estimate values for parameters important in calculating contaminant release from the LAWABP1 (and HLP-31) glass waste forms.

Table 3-7. Summary of Best Estimate Rate Law Parameters for LAWABP1 and HLP-31 Glasses at 15°C.

Parameter	Meaning	LAWABP1	HLP-31	Comments
$\vec{k}$	forward rate constant ($g\ m^{-2}\ d^{-1}$)	3.4×10^{6}	1.0×10^{7}	HLP-31 based on 26°C data only
K_g	apparent equilibrium constant for glass based on activity product $a[SiO_2(aq)]$	4.9×10^{-4}	ND	Not Defined. The HLP-31 glass dissolution rate did not change as function of $a[SiO_2(aq)]$
η	pH power law coefficient	0.35	0.35	HLP-31 value assumed same as LAWABP1
E_a	activation energy of glass dissolution reaction (kJ/mol)	68	68	HLP-31 value assumed same as LAWABP1
σ	Temkin coefficient	1	1	Assigned constant
r_x	Na ion-exchange rate ($mol\ m^{-2}\ s^{-1}$)	3.4×10^{-11}	0	No detectable ion exchange rate for HLP-31

Secondary Mineral Phase Reaction	Log K (15°C)
$Al(OH)_3(am)\ \Phi\ AlO_2^- + H^+ + H_2O$	-13.10
Analcime $\Phi\ 0.96AlO_2^- + 0.96Na^+ + 2.04SiO_2(aq)$	-9.86
Anatase $+ 2H_2O\ \Phi\ Ti(OH)_4(aq)$	-6.64
Baddeleyite $+ 2H_2O\ \Phi\ Zr(OH)_4(aq)$	-9.29
Goethite $+ H_2O\ \Phi\ Fe(OH)_3(aq)$	-11.09
Herschelite $\Phi\ 1.62Na^+ (aq) + 0.50K^+ (aq) + 2.26AlO_2^- + 4SiO_2(aq) + 0.14H^+ + 5.93H_2O$	-40.94
$La(OH)_3(am) + 3H^+\ \Phi\ 3H_2O + La^{3+}$	22.55
Nontronite-Na $+ 2H_2O\ \Phi\ 0.330AlO_2^- + 2Fe(OH)_3(aq) + 0.330Na^+ + 3.67SiO_2(aq)$	-43.33
$PuO_2 + HCO_3^- + 0.5O_2(aq)\ \Phi\ PuO_2(CO_3)_3^{4-} + H_2O + H^+$	-15.92

Secondary Mineral Phase Reaction	Log K (15°C)
Sepiolite + $8H^+$ Φ $4Mg^{2+}$ + $6SiO_2(aq)$ + $11H_2O$	31.29
$SiO_2(am)$ Φ $SiO_2(aq)$	-2.85
Weeksite + $2H^+$ Φ $2K^+$ + 2 $UO_2(OH)_2(aq)$ + $6SiO_2(aq)$ + $3H_2O$	-5.25
Soddyite Φ $2UO_2(OH)_2(aq)$ + $SiO_2(aq)$	-20.24
Theophrastite + $2H^+$ Φ Ni^{2+} + $2H_2O$	13.33
$Zn(OH)_2(am)$ + $2H^+$ Φ $2H_2O$ + Zn^{2+}	14.44

Figure 3-4 displays the forward reaction rate (or intrinsic rate constant) as measured by the single-pass flow-through test for a number of glasses. Previous experience has shown that borosilicate glasses all have a similar forward reaction rate dependence on pH and temperature. The data in Figure 3-4 confirm this expectation. The glasses represented in Figure 3-4 represent both high and low-temperature melting LAW glass, and even a lanthanide borosilicate (LABS) that has no alkali content at all. We conclude that there is a high degree of confidence in being able to predict the forward rate of reaction as a function of pH and temperature for virtually any realistic ILAW glass composition. These data are also important in that they set the physical upper bound on the release rate from ILAW glasses, assuming the temperature and pH in the disposal system are known or can be calculated. However, an exception to this conclusion is HLP-31 glass. The forward reaction rate of HLP-31 glass is much higher than any other silicate-based glass we have studied. McGrail et al. (2001) found that HLP-31 was phase separated and attribute the high forward reaction rate to the formation of borate rich regions that leave portions of the glass susceptible to hydrolysis reactions. Clearly, glass homogeneity is an important consideration that impacts durability.

Figure 3-4. Forward Reaction Rate as a Function of Temperature and Solution pH for Several Borosilicate Glasses.

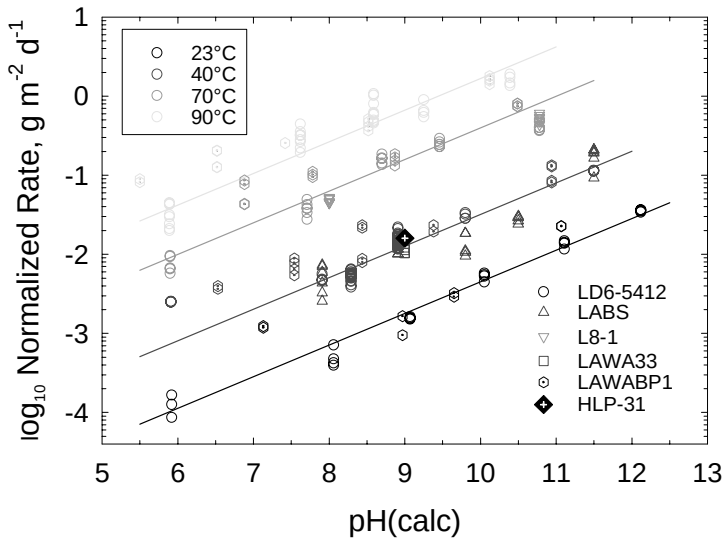

Figure 3-5 shows the effect of increasing the concentration of aluminum (as aluminate, AlO_2^-) and silicic acid on the dissolution rate of LAWABP1 glass. As the concentration of these species increases, the glass dissolution rate initially drops but then becomes invariant at higher concentrations. McGrail et al. (2001) discuss how alkali ion exchange controls the rate of glass dissolution in solutions with high concentrations of Si (and Al). The measured rate of Na ion exchange for LAWABP1 glass as a function of temperature is given in Figure 3-6.

Figure 3-5. Plot of Dissolution Rate at 90ºC Versus Mixed Al-Si Activity Product. The exponents 0.136 and 0.482 are the mol fractions of Al and Si in LAWABP1 glass.

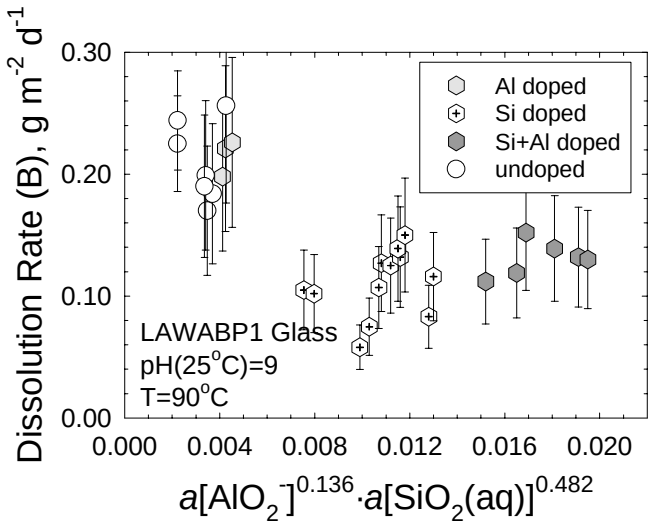

Longer-term dissolution behavior is determined by the other tests. Figure 3-6 shows the normalized release rates as measured from the PUF test. Differential rates of release are

observed for the major glass components, which reflects their solubility behavior in water. Zinc, Zr, and Ti all form very insoluble hydroxides, which controls their release rate. In contrast, B and Na are highly soluble, and so have the highest elemental release rates. Bulk dissolution behavior is typically indexed by the rate of B release, as no solid phases are expected to form that would affect its solution concentration. Also note that the data from both the PUF and SPFT experiments is internally consistent. The high solid-to-liquid ratio in the PUF test establishes high concentrations of dissolved glass components. The average dissolution rate of LAWABP1 glass in the PUF test (≈0.1 g m^{-2} d^{-1}) is essentially identical to the dissolution rate measured in SPFT experiments (0.12 g m^{-2} d^{-1}, Figure 3-5) in solutions near saturation with respect to amorphous silica. This is an important validation of the glass dissolution model.

Figure 3-6. Excess Sodium Release via Ion Exchange as a Function of Temperature for LAWABP1 Glass at pH(25°C)=9.

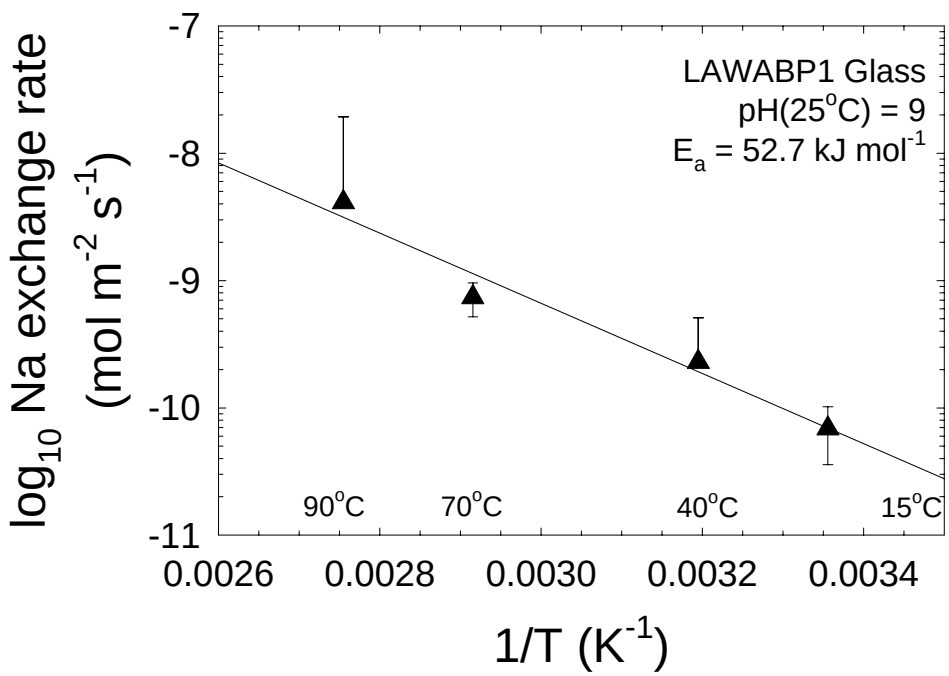

Another important validation of the underlying model is that the correct concentration of elements in solution released during long-term static tests can be predicted, as evidenced in Figure 3-8. In this case, the evolution of the solution composition in PCTs with LAWABP1 glass was predicted with the EQ3/6 geochemical code, along with a predicted paragenetic sequence of secondary phases shown in Figure 3-9. Secondary phases identified from these calculations along with phases directly observed from PUF and VHT experiments are listed in Table 3-7 and were included in the waste form release simulations with STORM.

The above discussion focuses on LAWABP1 glass, since it has been the most studied low-level waste glass. It is recognized that the actual glass produced will likely be (somewhat) different from LAWABP1. In Section 6.5, we show that the performance of LAWABP1 is in the middle of the performance space of the large number of ILAW glasses tested and so is representative of average performance that might be expected from actual ILAW glasses.

Figure 3-7. Normalized Release Rates in PUF Test with LAWABP1 Glass.

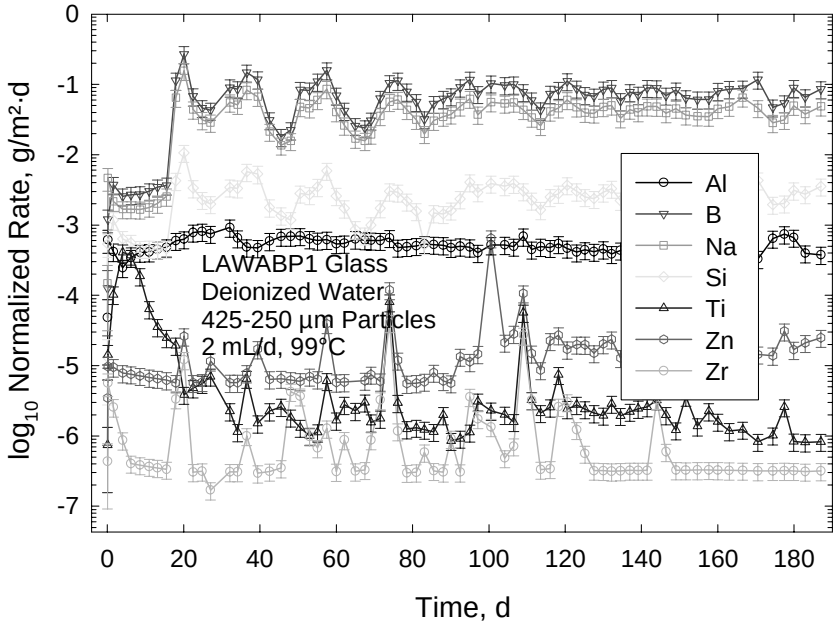

Figure 3-8. Comparison of PCT Solution Concentration Data with the Solution Composition Calculated with the EQ3/6 Code.

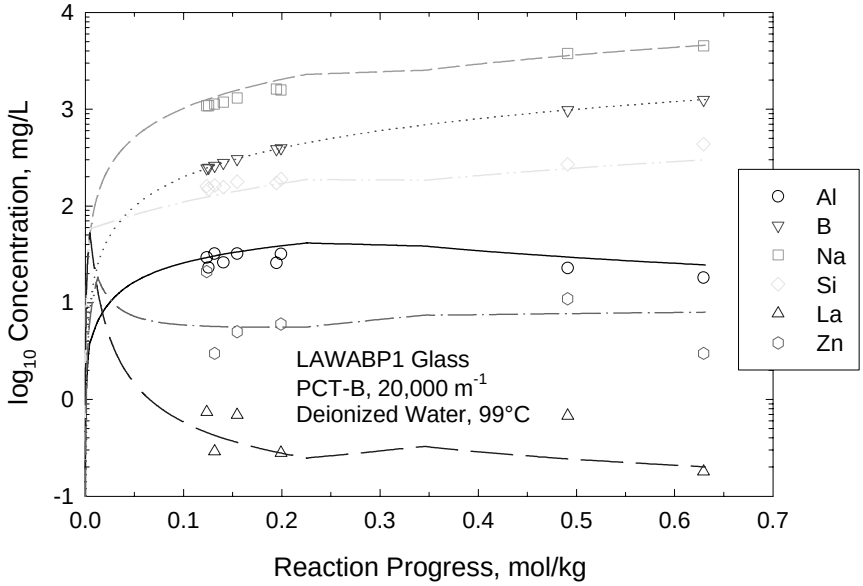

Figure 3-9. Predicted Paragenetic Sequence of Alteration Phases Formed During the Reaction of LAWABP1 Glass in Deionized Water. PuO_2 and soddyite were also predicted to form. However, they are not shown because of the very small mol fractions associated with these phases.

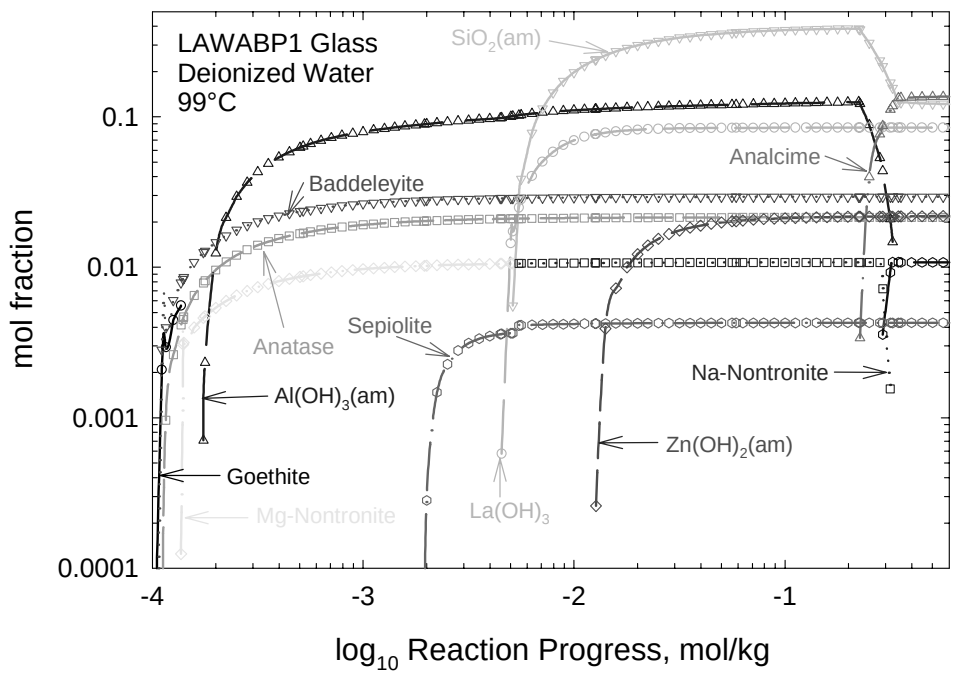

3.4.4.4 Sensitivity Cases. Because of the importance of waste form release to this performance assessment, a number of sensitivity cases are run. A large number of runs investigate the dependence of release on the amount of moisture entering the disposal facility (the rates being varied from 0.1 mm/y to 50. mm/y). Sensitivity cases are run to determine the importance of various glass dissolution mechanisms (e.g., pore water environment, Na-H ion exchange, secondary phases). Sensitivity cases were also run to determine the effect of surrounding materials (iron, concrete) and for how the packages are placed in the facility. A different glass composition is simulated, and laboratory results mimicking long term performance is given for a variety of glass compositions. Results from a two-dimensional calculation were also run to determine the sensitivity to the dimensionality of modeling. Finally, the model is extended to groundwater to estimate pH changes that might appear deeper in the vadose zone.

3.4.5 Disposal Facility

The disposal facility is modeled using the present conceptual designs for the facility discussed in Section 2.2. Unlike the 1998 ILAW PA, the disposal facility is proposed to be a series of large trenches.

The RH trench and concrete vault concepts summarized in Section 2.2 are used for the calculations. The RH trench has been chosen as the reference design for the base analysis case. The dimensions for the RH trench model are taken from Figure 2-25. The dimensions for the concrete vault model were taken from the description provided in Section 2.2.2.

The key components of the disposal system are the surface barrier, the sand-gravel capillary break, the trench (or vault) and the filler material. The surface barrier is assumed to be a modified RCRA-compliant subtitle C cap as described in Puigh 1999 (Section 4.0). Note that the cap is shaped like an inverted "v" and placed with its apex along the length dimension (north-south) and centered over each trench or vault. The slope of the cap is 2%. The cap extends 9 m beyond the inside edge of the RH trench (see Figure 2-25). (The surface cap extends 6 m beyond the long dimension edge of each new waste trench). This cap includes an asphalt layer and has a design life of 500 years. Beneath the surface cap is a sand-gravel capillary break. The sand

layer is assumed to be 1 meter thick. A gravel layer is built up 3 meters at the apex and with a 2% slope to support the surface cap. This height assures that the waste packages are greater than 5 meters below the surface (per 10 CFR 61 requirements).

The trench and vault dimensions are as defined in Section 2.2. The leachate collection systems are ignored in the moisture and transport modeling. The leachate collection systems can be ignored because of the relatively short design life for these material (less than 500 years for concrete and 100 years for HDPE) compared to the travel time through the vadose zone (1,000-2,000 years). The 1998 ILAW PA (Mann 1998a) examined the potential impact of the concrete vault trapping water and then failing ("bathtub effect") and a similar case (see Section 3.5.5.6) is done in this document for the use of trenches. The analysis showed little effect on the estimated impacts at the time of compliance. The material between the packages in the trench (or vault) is assumed to be backfill material as defined in Meyer 1999. Additional details on the numerical model calculations for the facility can be found in Sections 3.5.2, 3.5.3, and 3.5.4.

A series of cases is performed to investigate the sensitivity to disposal facility design. The importance of surface barrier performance is investigated by varying the infiltration rate exiting the barrier. The best estimate case estimates the usefulness of the subsurface sand-gravel capillary barrier. Other cases look at the effect of shortening the surface barrier, the use of vertical barriers, and the consequences of a break in the capillary barrier. Finally, a set of calculations looks at the concrete vault design.

3.4.6 Infiltration Rate

The recharge rate is based on long-term lysimeter and tracer measurements combined with computer simulations.

The term recharge is used to denote the rate at which moisture flows past the root zone (that is, very near surface) into a region where moisture flow follows simpler models. Recommendations for recharge rates are taken from *Recharge Data Package for the Immobilized Low-Activity Waste 2001 Performance Assessment* (Fayer 1999), and are also provided in Appendix J of Mann/Puigh (2000a). Long-term estimates of moisture flux through a fully functional surface cover, the cover side slope, and the immediate surrounding terrain, as well as for degraded cover conditions are needed. These estimates were derived from lysimeter and tracer measurements collected by the ILAW PA activity and by other projects combined with a modeling analysis.

Values for the recharge are given in Table 3-8. Values are given for two separate surface soils, Rupert sands and Burbank loamy sands. The Rupert sands are located at the site of the existing grout vaults and at the southernmost 60% of the new ILAW disposal site. The Burbank loamy sand is located at the northernmost 40% of the new ILAW disposal site. Impacts from degradation of the surface barrier, vegetation change, climate change, and irrigation were considered in establishing the best estimate and bounding values.

For the base analysis case we have assumed the conservative position that the surface barrier has failed shortly after it was installed and used the recharge rate for Burbank loamy sand for just below the modified RCRA-compliant subtitle C surface cap.

Because of its importance to waste form release and to travel time, a number of infiltration rate sensitivity cases are run. Values range from 0.1 mm/yr to 50. mm/yr. Cases are run where the infiltration rate is time dependent and where it is spatially dependent.

Table 3-8. Recharge Rate Estimates (mm/year).[a]

Surface feature	Pre-Hanford	Construction	Cover and Post Cover Design Life
Surface cover	na	na	0.1 (0.01, 4.0)
Cover side slope	na	na	50 (4.2, 86.4)
Rupert sand	0.9 (0.16, 4.0)	0.9 (0.16, 4.0)	0.9 (0.16, 4.0)
Burbank loamy sand	4.2 (2.8, 5.5)	4.2 (2.8, 5.5)	4.2 (2.8, 5.5)
Construction	na	55.4 (50, 86.4)	na

[a]Best estimate case given, with values for reasonable bounding cases given in parentheses; na = not applicable

3.4.7 Exposure Parameters

Exposure parameters follow Hanford Site practices.

Dosimetry scenarios and parameter values are based on the discussion and values presented in *Dosimetry Data Package for the Hanford Immobilized Low-Activity Tank Waste Performance Assessment* (Rittmann 1999), and also appendix O of Mann/Puigh (2000a). The scenarios for human exposure to the hazardous materials associated with the ILAW glass are defined in appendix B (Mann, 1999b). Table 3-9 provides the unit dose factors (mrem per Ci exhumed) for the intrusion scenario where a post-intrusion resident lives near the exhumed waste associated with a well drilled through the disposal site. Table 3-10 provides the total unit dose factors for five exposure scenarios where the exposure includes contamination of the groundwater. These scenarios are for industrial, residential, agricultural, and population exposures as defined in the Hanford Site Risk Assessment Methodology (HSRAM) (DOE/RL 1991). The Native American subsistence resident exposure is discussed in DOE/RL 1997.

In the *Evaluation of the Potential for Agricultural Development at the Hanford Site* (Evans 2000), well screen heights in the local tri-county area were surveyed. The continued use of the 4.6-meter (15 foot) well screen height is justified, given that most screen heights are larger than this value.

Sensitivity cases are run to determine the difference caused by various dosimetry sets as well as different scenarios.

Table 3-9. Annual Unit Dose Factors for Post-Intrusion Resident (mrem per Ci exhumed).

Radionuclide	External	Internal	Radionuclide	External	Internal
H-3	0.0	$1.46x10^{2}$	U-234	$9.04x10^{-1}$	$2.68x10^{3}$
Se-79	$4.24x10^{-2}$	$1.24x10^{2}$	U-235+D	$1.66x10^{3}$	$2.51x10^{3}$
Sr-90+D	$5.15x10^{1}$	$2.00x10^{4}$	U-236	$4.81x10^{-1}$	$2.54x10^{3}$
Tc-99	$1.69x10^{-1}$	$7.93x10^{2}$	U-238+D	$2.61x10^{2}$	$2.45Ex10^{3}$
Sn-126+D	$2.41x10^{4}$	$1.05x10^{2}$	Np-237+D	$2.30x10^{3}$	$2.39x10^{4}$
I-129	$2.58x10^{1}$	$6.70x10^{3}$	Pu-239	$6.48x10^{-1}$	$1.18x10^{4}$
Cs-137+D	$6.80x10^{3}$	$1.23x10^{3}$	Pu-240	$3.34x10^{-1}$	$1.18x10^{4}$
Pa-231	$4.78x10^{2}$	$3.81x10^{4}$	Am-241	$9.98x10^{1}$	$1.23x10^{4}$
U-233	3.21	$2.74x10^{3}$			

Table 3-10. Total Annual Unit Dose Factors for Low-Water Infiltration Cases (mrem per pCi/L in the groundwater).

Nuclide	HSRAM Industrial [(a)]	HSRAM Residential [(a)]	All Pathways Farmer [(a)]	Native American Sustenance Resident [(a)]	Columbia River Population [(b)]
H-3	1.62×10^{-5}	4.92×10^{-5}	4.58×10^{-5}	1.03×10^{-4}	2.29×10^{-1}
Se-79	2.18×10^{-3}	7.26×10^{-3}	1.15×10^{-2}	3.10×10^{-2}	5.03×10^{1}
Sr-90+D	3.83×10^{-2}	1.30×10^{-1}	1.19E-01	3.38×10^{-1}	5.53×10^{2}
Tc-99	3.65×10^{-4}	1.31×10^{-3}	3.54×10^{-3}	1.23×10^{-2}	1.46×10^{1}
Sn-126+D	5.28×10^{-3}	4.07×10^{-2}	5.63×10^{-2}	1.20×10^{-1}	2.36×10^{2}
I-129	6.90×10^{-2}	2.31×10^{-1}	3.77×10^{-1}	1.21	1.64×10^{3}
Cs-137+D	1.25×10^{-2}	4.84×10^{-2}	7.53×10^{-2}	2.14×10^{-1}	3.25×10^{2}
Pa-231	2.68	8.87	7.08	1.84E+01	3.40×10^{4}
U-233	7.51×10^{-2}	2.45×10^{-1}	2.19^{-1}	5.77×10^{-1}	1.04×10^{3}
U-234	7.35×10^{-2}	2.40×10^{-1}	2.14×10^{-1}	5.65×10^{-1}	1.02×10^{3}
U-235+D	6.93×10^{-2}	2.28×10^{-1}	2.03×10^{-1}	5.34×10^{-1}	9.62×10^{2}
U-236	6.99×10^{-2}	2.28×10^{-1}	2.04×10^{-1}	5.37×10^{-1}	9.65×10^{2}
U-238+D	6.95×10^{-2}	2.27×10^{-1}	2.03×10^{-1}	5.34×10^{-1}	9.60×10^{2}
Np-237+D	1.12	3.72	2.97	7.73	1.42×10^{4}
Pu-239	8.94×10^{-1}	2.96	2.36	6.14	1.13×10^{4}
Pu-240	8.94×10^{-1}	2.96	2.36	6.14	1.13×10^{4}
Am-241	9.19×10^{-1}	3.05	2.43	6.32	1.17×10^{4}

[(a)] Annual dose in mrem for a groundwater concentration of 1 pCi/L

[(b)] Annual dose in person-rem per Columbia River concentration of 1 pCi/L

3.5 PERFORMANCE ASSESSMENT METHODOLOGY

This section describes how the performance of the system was determined. That is, this section explains how the data and conceptual models presented in Sections 3.2 through 3.4 are translated into a numerical model suitable for computer simulation. First, the strategy of the computer simulation is introduced. Then the computer code selection criteria are summarized. The codes used are then described and their selection justified. Next the process of translating the disposal facility concepts and the natural system into computer models is described. Finally, the parameters used in the computer simulations are given.

Calculations of relatively simple equations (for example, gaseous diffusion or glacial-age catastrophic flood consequences) were done by hand. These equations will be treated in Chapter 4, where the results are discussed.

3.5.1 Integration

3.5.1.1 Strategy. Previous long-term environmental assessments at the Hanford Site have consistently shown that the groundwater pathway is the most important. This pathway also requires the most calculations. The conceptual model used for this and earlier Hanford Site performance assessments take the following eight steps:

1. The water leaves the very-near-surface soil region at the infiltration rate, which is a function of time due to facility degradation.

2. The water moves toward the waste form, but most of it is diverted by any intact capillary barrier.

3. The water that is not diverted is chemically modified by the local environment, interacts with the waste form, accumulates contaminants, and again is chemically modified by the local environment.

4. The water (possibly a reduced amount) leaves the disposal facility carrying contaminants with it. Some contaminants may interact with the material in the disposal facility, slowing the release of the contaminants to the surrounding natural environment.

5. The water moves through the undisturbed, unsaturated zone (vadose zone) below the disposal facility down to the unconfined aquifer. The contaminants also are transported through the vadose zone, again possibly undergoing some geochemical sorption.

6. The water and contaminants move and mix with the water in the unconfined aquifer until they are extracted from the aquifer and brought to the surface or until they reach the Columbia River.

7. Contaminants are normally extracted by being carried to the surface with groundwater being pumped through a well.

8. The radionuclide contaminants then result in human exposure through a variety of pathways (ingestion, inhalation, and external radiation).

Figure 3-10 shows these eight steps as a flow chart.

Figure 3-10. Eight Sequential Steps for the Groundwater Pathway.

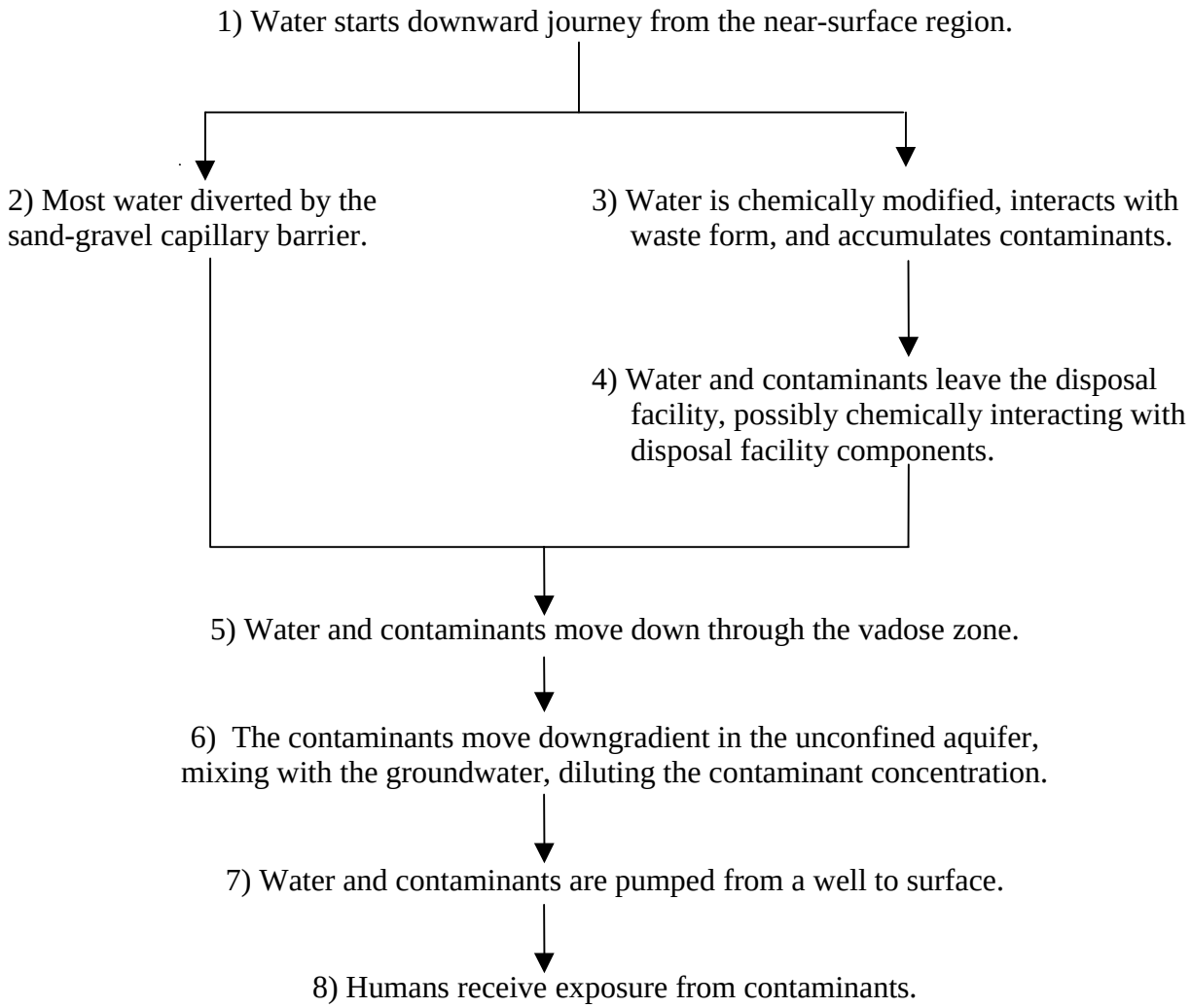

These groundwater analyses start at the time of disposal site closure. However, given the relatively short duration of disposal operations (2007 through 2028) compared to the travel time of the contaminants (thousands of years) or the release time of the waste form (hundreds of thousands of years), the exact definition of this start time is unimportant.

The results for each step are computed separately and used in the next step so that computations can be made more easily. Such an approach is taken to maximize computational efficiency. Some of the computer simulations take 100 hours of computer time; some take a few minutes. Each is a highly specialized calculation. However, the overall model is always considered at each step and consistent data are used throughout.

The strategy for the current computations is to define a base analysis case, then develop sensitivity cases derived from that base analysis case. In some instances the sensitivity cases are built on an alternative case, such as the one describing the concrete vault concept. The results for the base analysis case and the sensitivity cases are presented in Chapter 4. Chapter 6 combines the results of the computer simulations, the simpler calculations, and the other analyses to integrate and interpret how the contaminants will affect the environment in the long term.

3.5.1.2 Base Analysis Case. The base analysis case provides the "best" information on how the system may evolve given the information available. The base analysis case is not necessarily the way the system will behave. As more information concerning the waste form, the disposal facility design, and disposal site location is gathered, the definition of the base analysis case is expected to evolve. The approach used in the base analysis case is conservative, but reasonable. It should be noted that the base analysis case does not include the sand-gravel capillary barrier that is presently part of the conceptual design. As will be seen when the results of the best estimate case are given in Sections 4.3.7 through 4.3.11 and in the corresponding sensitivity cases, the impacts resulting from such a barrier depend on its detailed parameters that have not yet been established through a detailed design process. Thus, the inclusion of the capillary barrier is treated as a case separate from the base analysis case.

The details of the models and related data for the base analysis case are presented in Sections 3.5.3 and 3.5.4, respectively. The major features of the base analysis case are as follows:

- The location of the facility is that selected for the new disposal facility (Rutherford 1997)
- The future land use of the 200 Areas is as a protected area, without artificial recharge (for example, no irrigated farming occurs)
- The design of the disposal facility is based on a pre-conceptual design based on the Hanford Radioactive Mixed Waste Burial Trench and is documented in Puigh 1999 (Section 3.4.5)
- The long-term contaminant release rate from the waste form is calculated based on the scenarios described in Section 3.3.2
- The data for the natural system are those collected and interpreted for this performance assessment (Section 3.4.3).

The 1998 ILAW PA showed that the key variable in the analysis is the waste form release rate, which must be calculated over thousands of years. To conduct this calculation, we have pursued a methodology where the waste form release rate is evaluated by modeling the basic physical and chemical processes that are known to control dissolution behavior instead of using empirical extrapolations from laboratory "leaching" experiments commonly used in other performance assessments. We adopted this methodology for the following reasons:

- The dissolution rate, and hence radionuclide release rate from silicate glasses is not a state function, i.e. a constant that can be derived independent of other variables in the system. Glass dissolution rate is a function of three variables (neglecting glass composition itself): temperature, pH, and composition of the fluid contacting the glass. The temperature of the ILAW disposal system is a known constant. However, both pH and composition of the fluid contacting the glass are variables that are affected by flow rate, reactions with other engineered materials, gas-water equilibria, secondary phase precipitation, alkali ion exchange, and by dissolution of the glass itself (a classic feedback mechanism). Consequently, glass dissolution rates will vary both in time and as a function of position in the disposal system. There is no physical constant such as a "leach rate" or radionuclide release rate parameter that can be assigned to a glass waste form in such a dynamic system.

- One of the principal purposes of the ILAW PA is to provide feedback to engineers regarding the impacts of design options on disposal system performance. A model based on empirical release behavior of the waste form could not provide this information. For example, we have found little effect on waste form performance regardless of whether stainless or cast steel is used for the waste form pour canister. However, significant impacts have been observed when large amounts of concrete are used in constructing vaults for ILAW. The concrete raises the pH of the pore water entering the waste packages and so increases glass corrosion.

Unfortunately, the robust methodology we have employed does not come without some penalties. The principal penalty is the increased amount of information that is needed about the reaction mechanisms controlling the dissolution behavior of the waste form. Significantly more laboratory experiments are required to parameterize the models used for our simulations. Second, the model itself is markedly more complex. Execution times with today's fastest workstations can take weeks for one- and two-dimensional simulations and three-dimensional simulations can only be attempted on today's most sophisticated massively parallel computers. Still, we believe the benefits, particularly with regards to the technical defensibility of the methodology and results, far outweigh the penalties.

3.5.1.3 Best Estimate Case. The base analysis case assumes that there is no subsurface sand-gravel capillary barrier even though the current planning includes one. This is done because the exact properties of this subsurface barrier are not well known and such uncertainty could lead to misleading results. Thus, a separate case is performed with the subsurface sand-gravel capillary as part of the simulation.

3.5.1.4 Sensitivity Cases. The purpose of the sensitivity cases is to determine the uncertainty from the use of various parameters and the sensitivity of various assumptions. The data packages on which this assessment is based provide uncertainty estimates for the parameters used. The results of the sensitivity cases can provide the effects of these data uncertainties. Larger uncertainties, however, arise from choices not yet finalized on waste form composition as well as disposal facility design, layout, and location. Most of the sensitivity cases investigate the effect of such choices.

3.5.2 Computer Codes

This section discusses the computer codes used for this performance assessment and justifies their technical adequacy. The general selection criteria used to select the major computer codes are first summarized. Sections 3.5.2.2 through 3.5.2.5 describe each major computer code used and the reason for its selection.

Computer codes will be used for four purposes:

- to calculate contaminant release rates from the waste packages and from the disposal facility,

- to calculate moisture flow and contaminant transport in the vadose zone (including moisture flow into the disposal facility),

- to calculate moisture flow and contaminant transport in groundwater, and

- to normalize and merge the results of the preceding codes.

Figure 3-11 illustrates also the overall computational strategy for the ILAW PA.

The near-field environment is defined as the domain through the trench or vault to some distance below the floor of the disposal facility. A coupled unsaturated flow, chemical reactions, and contaminant transport simulator (STORM) was used within the near-field (Bacon 2000). The plume exiting the region near the vault is expected to be of high ionic strength and pH, and will migrate down into the near-field vadose zone for some distance. However, at some distance from the disposal vaults, geochemical conditions will approach those more typical of the Hanford vadose zone and for which simplifying assumptions (such as linear sorption, negligible precipitation/dissolution, no changes in hydraulic properties, and no fluid density gradient effects) can be used. This region is defined as the far-field environment and can be simulated using standard, non-reactive (chemical reactions not specifically included in calculations) flow and transport codes. For the ILAW PA, computations in the far-field domain were done using VAM3DF (Huyakorn 1995), a variably saturated flow and transport code.

Figure 3-11. Modeling Strategy for Assessing ILAW Disposal System.

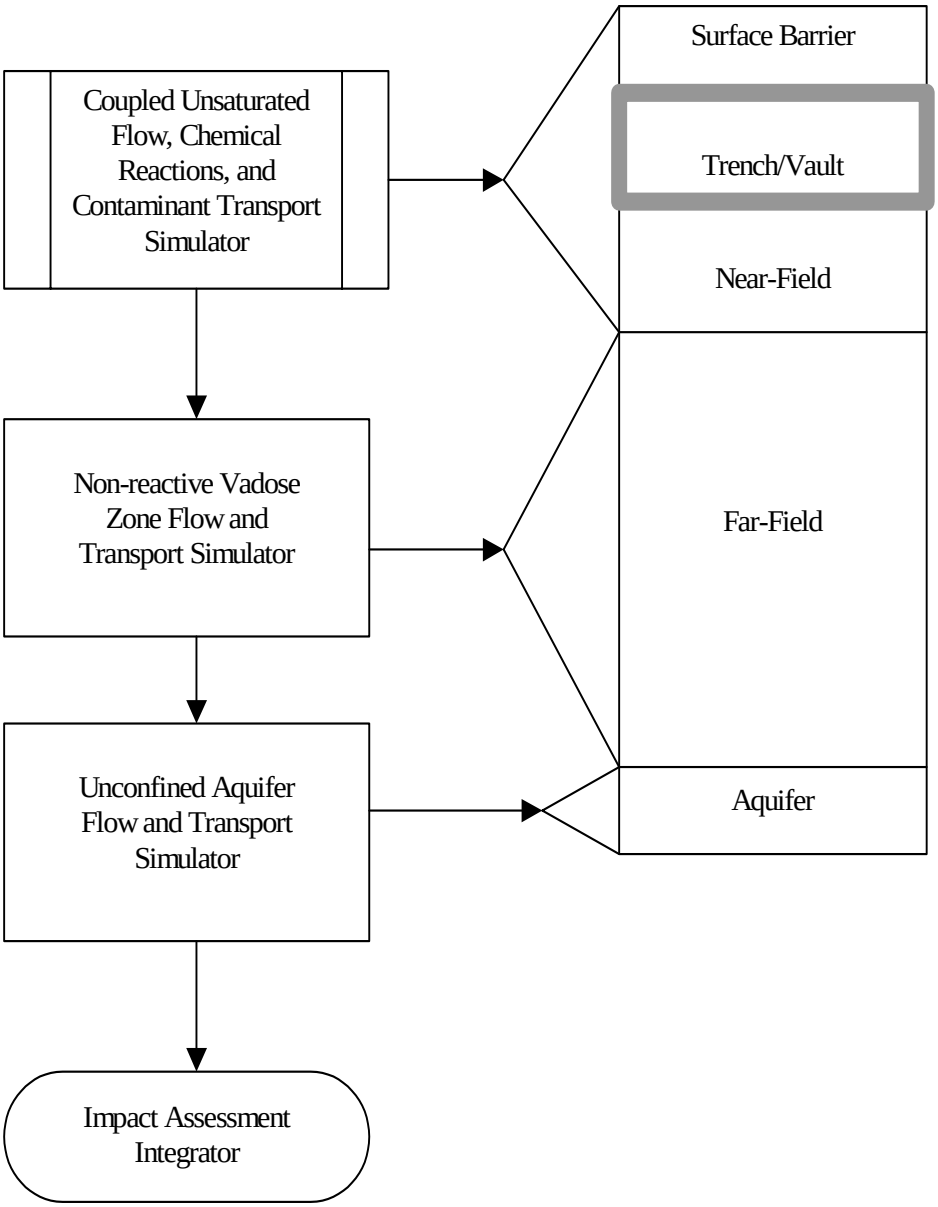

The primary reason for switching from the near-field simulator to VAM3DF is to apply a less complicated code for the far-field, and therefore a faster turnaround for the numerical simulations. The radionuclide flux exiting the far-field domain to the unconfined aquifer will be provided by VAM3DF and will be used as a boundary condition for the unconfined aquifer flow and transport simulator. Sorption to soils is treated by VAM3DF by the use of the effective chemical distribution coefficient (K_d) rather than by a set of chemical reaction equations. Calculations in the groundwater aquifer are performed using the Hanford Site model and associated code, CFEST-96, (Gupta 1987). The Hanford Site Groundwater Program has recommended this code for performing saturated flow and transport simulations for the Hanford Site. Finally, the results of each of the sequential calculations are combined to estimate the impacts from the disposal system using the INTEG program (Mann 1996b). This program combines the results from the far field calculations, the groundwater calculations, and the dosimetry data to estimate impacts related to the performance objectives.

3.5.2.1 General Selection Criteria for Computer Codes. The major computer codes used for this assessment were selected based on meeting general code selection criteria and functional criteria related to the simulation being done. Large computer codes were needed for computing in the following three functional areas:

- Calculation of the contaminant release rate from glass
- Calculation of water flow and contaminant transport in the vadose zone
- Calculation of water flow and contaminant transport in the unconfined aquifer.

The codes considered had to first meet the general code selection criteria.

The general code selection criteria were based on government code selection documents and the experience of others. The waste management code selection criteria of the DOE (Case 1988) and the NRC (Kozak 1989) were used to develop these selection criteria. The criteria were also shaped by the experience gained from other DOE performance assessments (WSRC 1992, Kincaid 1995, Mann 1998a) and codes selected for earlier Hanford Site risk assessments (DOE/RL 1991a). The general required selection criteria included the following:

- Having the appropriate scientific framework
- Having documentation covering the underlying theory, use, and verification
- Being under configuration control.

General desirable criteria included the following:

- Suitable hardware requirements
- Suitable complexity
- Flexible interfaces with other codes
- A bias against proprietary codes
- Familiarity of the users with the code.

Mann 1995c details the development of the general selection criteria and the complete criteria. A slight modification of these criteria were adopted by the major projects of the Hanford Groundwater / Vadose Zone

The actual codes selected also had to meet criteria related to the function being simulated. Sections 3.5.2.2 through 3.2.2.5 summarize the codes chosen and the reasons for their selection. References to specific functional criteria will be given in their sections or related appendices.

STORM was chosen as the code to estimate containment release rates from the waste form and subsequent transport in the disposal facility.

3.5.2.2 Calculation of the Contaminant Release Rate from Glass. The *Subsurface Transport Over Reactive Multiphases* (STORM) code (Bacon 2000) is the source-term code used for estimating the time-dependent flux of radionuclides released from the waste form and the subsequent transport of contaminants in the disposal facility. STORM contains two important factors that allow the code to simulate the processes in the disposal facility. First, the code is based on basic principles of physics, chemistry, and thermodynamics that provide the best estimate of contaminant release over the spatial and long time periods of interest. Second, the model for the disposal facility can be coupled with a model for radionuclide release, thus providing the ability to couple the effects of facility design with waste form performance.

Using chemical reaction rates (including the glass corrosion rates) and moisture values in the trench (or vault) fromVAM3DF (Section 3.5.2.3), STORM provides the source term for the vadose zone calculations. STORM calculates the following:

- The flow of moisture in the disposal facility
- The degradation of the waste form with corresponding release of radionuclides
- The chemical reactions that depend on time and space (including the formation of secondary mineral phases and the consumption of water)
- The transport of the water and contaminants through the disposal facility.

3.5.2.2.1 Selection. STORM was selected (McGrail 1998a) because it best met the criteria and requirements for the disposal system release model (McGrail 1994) and the general code requirements (Mann 1995c). The needed capabilities were identified from an analysis of the important physical and chemical processes expected to affect LAW glass corrosion and the mobility of radionuclides. The available computer codes with suitable capabilities were ranked in terms of the feature sets implemented in the code that match a set of physical, chemical, numerical, and functional capabilities needed to assess release rates from the engineered system. The highest ranked computer code was found to be the STORM code.

3.5.2.2.2 Code Description. STORM calculates the total mass flux of radionuclides leaving the disposal facility by solving a coupled set of equations. The set describes the radionuclide release from the waste form and the mass transport of the radionuclides from the waste form through the disposal facility, constrained by chemical reactions. This coupled set of equations is commonly known as the reaction-transport equation. The value for radionuclide release from the waste form is taken from either an assumed constant release rate or a simulation using a mechanistic glass corrosion model. More detailed documentation of the design and models used in the STORM code is found in the STORM User's Guide (Bacon 2000).

3.5.2.2.3 Code History. The STORM code was developed at PNNL for the U.S. Department of Energy for evaluation of arid land disposal sites. It is a merged version of the AREST-CT code (Engel 1995a and Engel 1995b) and the STOMP code (White 1996). AREST-CT was originally developed at PNNL to support the engineered-system performance analyses for the proposed high-level waste repository at Yucca Mountain, Nevada. It was used in the 1998 ILAW PA to estimate contaminant releases for some sensitivity cases. STOMP, also developed at PNNL, is a general, coupled non-isothermal multiphase flow and transport simulator. It has been used for a variety of Hanford Site analyses including the Hanford Site Composite Analysis (Kincaid 1998).

3.5.2.2.4 Verification. The verification studies for STORM are documented in Chapter 8 of *Subsurface Transport Over Reactive Multiphases (STORM): A General, Coupled Nonisothermal Multiphase Flow, Reactive Transport, and Porous Medium Alteration Simulator, Version 2, User's Guide* (Bacon 2000), which is included as Appendix D in Mann/Puigh (2000a).

3.5.2.3 Calculation of Water Flow and Contaminant Transport in the Vadose Zone. The VAM3DF code is used to estimate the moisture flow into the disposal facility and the moisture flow and contaminant transport from the disposal facility into groundwater.

VAM3DF calculates moisture flow and contaminant transport in the vadose zone.

3.5.2.3.1 Selection. Mandatory and desirable criteria for a vadose zone moisture flow and contaminant code were published (Mann 1998b). These criteria were based on the needs identified in the creation of the 1998 ILAW PA. They are also consistent with vadose zone code selection criteria recently published by other Hanford Site projects (Mann 1999c). The developers of the three codes, which have been historically, used the most for Hanford Site vadose zone calculations (PORFLOW, STOMP, and VAM3D-CG) submitted responses to the criteria. All three codes meet the mandatory criteria, but three independent evaluators (Voogd 1998) selected VAM3D-CG as the code best meeting the desirable criteria. A later version of VAM3D (labeled VAM3DF) is actually used in these calculations.

3.5.2.3.2 Code Description. VAM3DF (Huyakorn 1999) calculates saturated-unsaturated groundwater flow and solute transport with variable water table positions and highly non-linear soil moisture conditions. The code can simulate transient or steady-state problems in one, two, or three dimensions using a finite element model. Special grid elements (in the shape of hexahedrals) are used to define discrete volumes with irregular geometry. The size of these elements can vary. Many "fine" elements can be used in places where the geometry varies quickly. Such finer elements allow a better description of regions in which the values of parameters and variables are changing rapidly. An orthogonal curvilinear grid can also be used to represent flow domains.

3.5.2.3.3 Code History. VAM3DF is the latest in a series of variably saturated analysis model codes from HydroGeoLogic, Inc. to model moisture and contaminant movement for the vadose zone and groundwater. VAM codes have been used in many Hanford Site analyses. VAM3D-CG was used in the solid waste burial ground performance assessments (Wood 1995a and Wood 1996) and as the groundwater code in the 1998 ILAW PA (Mann 1998a). Relative to VAM3D-CG, VAM3DF includes decay chain nuclide analyses, data fusion (not used in this PA), as well as other improvements.

3.5.2.3.4 Verification. VAM3DF has been verified and validated by HydroGeoLogic, Inc. (Huyakorn 1999). A separate validation package was done for this performance assessment (Finfrock 2000a) and is included in the data packages for this PA.

3.5.2.4 Calculation of Water Flow and Contaminant Transport in the Unconfined Aquifer. The Richland Field Manager (Wagoner 1996) directed the Hanford Groundwater Program to establish a single groundwater model for the Hanford Site. The Hanford Groundwater Program has selected CFEST as the interim code. Documentation of code formulation, user's guides, and verification are given in Gupta 1987. Documentation of the specific application of the CFEST

CFEST is the groundwater modeling code.

code to the site-wide groundwater flow and transport model at Hanford is provided in Wurstner 1997, Cole 1997, and Kincaid 1998. Documentation of code selection is provided in DOE/RL 2000.

3.5.2.5 Integration of Results. INTEG (Mann 1996b) calculates a specific impact (whether dose rate or concentration level) based on the inventory, vadose zone transport, aquifer transport, and dosimetry factors. The dose rate calculated depends on the type of dosimetry factor (i.e., all-pathways, drinking water). The program solves the following equation for each year under consideration.

$$\textit{Response} = \sum_i I_i(t)\, \Gamma_i(t)\, w_i\, D_i / (r\, A) \qquad (3.9)$$

where

I_i = the amount (or inventory) of radionuclide i (Ci). The time-dependent value is calculated by INTEG based on the initial inventory and on decay and the ingrowth from other radionuclides.

Γ_i = the flux of contaminants at the bottom of the vadose zone normalized to an unit source inventory for radionuclide i ([Ci/y]/Ci). The time-dependent value is calculated by VAM3DF.

w_i = the ratio of the concentration of radionuclide i at the well location relative to the contaminant concentration at the bottom of the vadose zone (dimensionless). This quantity was called the well intercept factor in earlier Hanford performance assessments. The peak value as calculated by CFEST is used.

D_i = the dose rate factor (mrem/y per Ci/m^3). The values are taken from the tables in Appendix B. D_i is unity when the response that is calculated is a concentration.

r = the recharge rate (m/y). The value at 10,000 years is used at all analysis times.

A = the area over which the contaminant flux enters the aquifer (m^2). The value used is the area of the disposal facility being modeled.

The program is modeled after GRTPA (Rittmann 1993), which served a similar function in earlier work (Rawlins 1994 and Mann 1995b). INTEG allows greater freedom in specifying data used in the integration. The code has been benchmarked against the results of GRTPA (Mann 1996b). An auxiliary code was written to translate the output of VAM3DF into a readable format for INTEG.

3.5.2.6 Spreadsheets. Commercial spreadsheets were used in determining inadvertent intrusion doses. The Excel spreadsheet was used for developing the spreadsheet cells and the calculations. The spreadsheet calculations were compared with hand calculations documented in Rittmann 1999 and verified as part of the review by the Hanford Environmental Dose Oversight Panel (HEDOP).

3.5.3 Computer Models

This section describes the numerical models used in this performance assessment: waste form release (STORM), disposal facility barrier and vadose zone (VAM3DF), and groundwater (CFEST). The actual data used is discussed in the next section.

3.5.3.1 Waste Form Release. Contaminant releases were calculated for both the trench and concrete vault designs, each having a different model. However, the model that applies to both types of disposal facility types is given first. More information can be found in *2001 ILAW PA Waste Form Release Rate Sensitivity Analysis* (Bacon 2001).

3.5.1.1.1 Waste Form Release Model. The waste package containers were assumed to consist of 304 stainless steel. The corrosion reaction for 304 stainless steel is given by Cloke 1997:

$$\begin{aligned}
&\text{Steel} + 2.9262\times10^{-2}\ H^+ + 1.7618\ H_2O + 3.4169\times10^{-1}\ O_2(aq) \rightarrow \\
&\quad 3.4667\times10^{-3}\ HCO_3^- + 3.4701\times10^{-1}\ CrO_4^{2-} + 1.1828\ Fe(OH)_3(aq) \\
&\quad + 3.5167\times10^{-2}\ Mn^{2+} + 9.9093\times10^{-3}\ NO_3^- + 1.8583\times10^{-1}\ Ni^{2+} \\
&\quad + 8.8004\times10^{-4}\ HPO_4^{2-} + 5.2008\times10^{-4}\ SO_4^{2-} + 1.7325\times10^{-2}\ SiO_2(aq)
\end{aligned} \tag{3.10}$$

The 304L stainless steel corrosion rate was conservatively assumed to be a constant $6.87\text{x}10^{-14}$ mol cm^{-2} s^{-1} (Cloke 1997), taking into account changes in the steel corrosion rate due to changes in pH or water chemistry.

Other materials in the simulations, including vault concrete, backfill, Hanford Sand, and vault filler, contain additional solid phases. The backfill material was assumed to consist of 40% albite, 40% quartz, 10% K-feldspar and 10% illite (Mann 1998a). Degraded vault concrete was assumed to consist of backfill with 15% Portlandite added. The vault filler and Hanford Sand were assumed to have the same mineral composition as the backfill material. The dissolution reactions and equilibrium constants associated with each of these minerals are detailed in the *Waste Form Release Data Package for the 2001 Immobilized Low-Activity Waste Performance Assessment* (McGrail 2001).

Model grids were 5 cm in vertical resolution; this is slightly larger than the 3.66 cm grid spacing used in the 1998 ILAW PA. The time steps used in these calculations were calculated automatically by the code given a convergence criterion of $1\text{x}10^{-6}$. This ensures that predicted values of aqueous species concentrations and mineral volumes are accurate to 0.0001 percent between iterations for a given time step. If this cannot be achieved within a certain number of iterations, the time steps are automatically reduced. Numerous simulations were conducted to ensure that the grid spacing and convergence criteria chosen for the simulations were small enough to ensure accuracy, yet large enough to allow the simulations to finish in a reasonable

amount of time. For comparison, the base case remote handled trench simulation was rerun with a grid spacing of 2.5 cm, and also with a convergence criterion of 5×10^{-7}. Results for these simulations were not significantly different than reported herein.

The flow simulations used the following boundary conditions: constant specified flux at the upper boundary and free drainage at the lower boundary. The reactive transport simulations used the following boundary conditions: specified aqueous species concentrations at the upper boundary and no diffusion across the lower boundary. The flux of the contaminant across the lower boundary is therefore limited to advection

$$f = c\rho_w v \tag{3.11}$$

where

c = concentration of the contaminant (mol kg^{-1})

ρ_w = density of water (mol m^{-3})

v = specific discharge (m s^{-1}).

The normalized contaminant flux to the vadose zone is calculated by summing all the fluxes across the bottom boundary of the model, and normalizing the total flux according to the amount of Tc in all the waste packages at the start of the simulation. The normalized flux of the contaminant across the lower boundary, F, in units of ppm/y, was calculated using

$$F = \frac{\sum_{i=1}^{N} f_i \Delta x_i \Delta y_i}{I} (3.1558 \times 10^7 \text{ s yr}^{-1})(1 \times 10^6 \text{ ppm}) \tag{3.12}$$

where

f_i = contaminant flux across the bottom of an individual grid block (μmoles m^{-2} s^{-1})

$\Delta x_i \Delta y_i$ = cross-sectional area of an individual grid block (m^2)

I = inventory of the contaminant in the waste packages (μmol), where

$$I = V_{wp}(1-\theta_T)V_G \rho_G \gamma_{Tc} \tag{3.13}$$

where

V_{wp} = volume of the waste packages (m^3)

θ_T = total porosity of the material representing the waste packages (0.02)

V_G = fraction of each waste package that is glass (0.85)

ρ_G = molar density of LAWABP1 glass (38776.1450 moles m^{-3})

γ_{Tc} = mole fraction of the contaminant in LAWABP1 glass (e.g., 6.59×10^{-1} μmoles Tc $mole^{-1}$ glass)

The volume of the waste packages, V_{wp}, was 5.6 m^3 for the RH Trench simulations and 8.4 m^3 for the new ILAW concrete vault simulations. For 1-D simulations the cross-sectional area of the grid block was 1 m^2. For the 2-D sensitivity case, the cross sectional area applies per meter of trench.

3.5.3.1.2 Waste Form Release Model for Trenches. The remote handled trench simulations encompass a 1-D vertical profile near the center of a single trench (Figure 3-12). It is assumed that the material representing the waste packages is 85% glass, 2% stainless steel and 13% filler by volume. The steel container was assumed to not provide a water barrier at the start of the simulation.

Figure 3-12. Material Zones for Remote Handled Trench Waste Form Release Simulations.

3.5.3.1.3 Waste Form Release Model for Concrete Vaults. The new ILAW vault simulations encompass a 1-D vertical profile at the center of a single vault (Figure 3-13). It is assumed that the material representing the waste packages is 85% glass, 2% stainless steel and 13% filler by volume. The steel container was assumed to not provide a water barrier at the start of the simulation.

Figure 3-13. Material Zones for New ILAW Vault Waste Form Release Simulations.

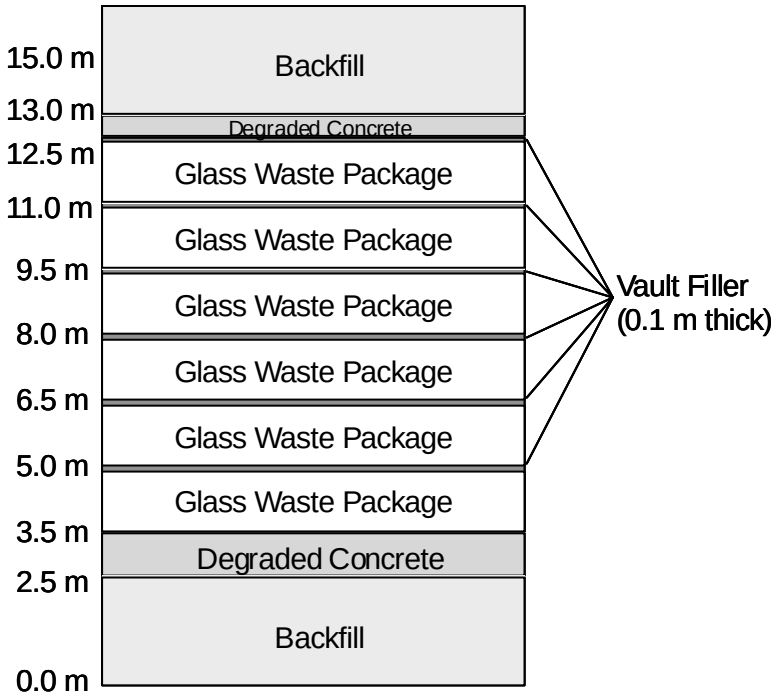

3.5.3.2 Disposal Facility Barrier and Vadose Zone. Because VAM3DF is used to both estimate the moisture flux into the disposal facility as well as the moisture flow and the contaminant transport from the disposal facility to the groundwater (the far-field problem) two types of model were used. More information can be found in *Near Field, Far Field and Estimated Impact Calculations for the Hanford Immobilized Low-Activity Tank Waste Performance Assessment: 2001 Version* (Finfrock 2000b).

3.5.3.2.1 Disposal Facility Barrier Model.

Model Description. The top of the near-field model corresponds to the bottom of the modified RCRA-compliant subtitle C' surface cap (which is not modeled), and is bounded below by an arbitrary contact immediately below the engineered facility. The lower boundary is located at –15 meters below the pre-disposal site surface grade. The upper two meters of the near-field model represents a capillary barrier with a one-meter thick sand layer over a 1-meter thick gravel layer. The capillary barrier peaks at the center of the facility (the left side of the model) and slopes down at a 2% grade to where the cap ends. Beyond the end of the barrier, the model represents a 'side slope', consisting of backfill material, out to the right hand side of the model. The near-field region is modeled as a two dimensional, half cell that is symmetrical about the centerline.

The trench extends from the pre-facility surface grade down to –10 m depth. The floor of the trench extends horizontally from 0 to 10 m, then slopes upward at a 3:1 incline for 30 m. Sediments inside of the trench are classified as backfill while the sediments outside of the trench are Hanford sands. The capillary barrier over the trench peaks at 3.0 m above the pre-facility surface grade (at the centerline) and extends out 49 m to the end of the cap. Beyond this point, the downward slope continues with backfill material out to the right hand edge of the model (60 m).

For the concrete vault conceptual model the vault top is set 1 m above the pre-facility surface grade and extends down 8 m. The vault forms a box structure that extends 11.5 m out from the centerline. The vault is set in a trench that extends out 17.5 m from the centerline and then slopes up at a 1.5:1 incline for 13.5 m. Again, the material inside the vault, and the material surrounding the vault in the trench, is backfill and the material outside of the trench is Hanford sands. The vault walls are 1 m thick and are modeled as degraded concrete. The capillary barrier over the vault, peaks at 4.0 m above the pre-facility surface grade (at the centerline) and extends out 17.5 m to the end of the cap. Beyond this point, the downward slope continues with backfill material out to the right hand edge of the model (37 m).

Boundary Conditions. Boundary conditions include flux in at the top of the model and a constant hydraulic head condition at the model base of –15.1 m. The side boundaries are implicitly defined as no-flow by the numerical code.

Flux applied to the top of the model ranged from 1.0×10^{-4} m/y to 5.0×10^{-2} m/y, depending upon assumed surface recharge conditions. In the base analysis case recharge is assumed to be the natural recharge rate (4.2×10^{-3} m/y) over the region where the barrier is present and 5.0×10^{-2} m/y beyond the barrier. This case assumes that the barrier is no longer functional and recharge to the waste packages is at a steady-rate of 4.2×10^{-3} m/y from above. The near-field calculations are only performed on fluid flow so there is no contaminant flux included in the models.

Grid. The near-field model is simulated as a two dimensional, vertical slice through the ILAW site. Lateral girding is represented by the X coordinate and vertical girding is represented by the Y coordinate.

The near-field trench model consists of 121 x 58 quadrilateral grid blocks in the X and Y directions, respectively, for a total of 7018 nodes in an X-Y plane. A third dimension is required for definition of the model elements. The Z coordinates are 0 and 1, representative of unit depth. A minimum of two Z-planes is required to define the model elements. Therefore, the total number of nodes for the model is 14036, which encompass 6840 elements. Grid spacing in the X direction is uniformly 0.5. Grid spacing in the Y direction ranges from 0.5 m down to 0.01 meters where material interfaces exist.

The near-field vault model consists of 75 x 76 quadrilateral grid blocks in the X and Y directions, respectively, for a total of 5700 nodes in an X-Y plane. There are 11,400 total nodes for both required planes, which represent 5550 model elements. As with the trench, the X node spacing is 0.5 m and the Y node spacing is variable, ranging from 0.5 down to 0.01 meters at material interfaces.

3.5.3.2.2 Far-Field Model. The far field extends from the bottom of the waste disposal facilities to ground water. The material beneath the waste facilities is Hanford sand, which is projected to extend to a depth of 65 meters below surface level. Beneath the Hanford sand is the Hanford gravel that extends to the projected post-Hanford water table at 103 meters below land surface. Each material is represented as a homogeneous medium for the respective sediment types. The porous media is assumed to be isotropic, which means there is no spatial distortion caused by sedimentary layering or lateral pressure gradients in the system. Hydraulic and chemical parameters used in the model are derived from the data package of Khaleel (1999) and Kaplan (1999).

The far field is simulated as a two-dimensional domain, horizontally layered system for each of two waste disposal facility designs. The far field model is designed to correspond to the one half trench and one half vault lateral dimensions. Consequently, the RH trench model domain extends 50 meters from left to right and the new ILAW vault model domain is 21.5 meters across. The upper boundary of the model domain in the far field corresponds to the lower boundary used for the waste form calculations at 15 meters below land surface. The lower boundary is located at the water table at 103 meters below land surface.

The contaminant flux along the upper boundary for the far field calculation is given by the one-dimensional contaminant flux times the quantity of waste at a given distance from the model axis (y-axis in figures). For the concrete vault the quantity of waste is constant out to the edge of the stacked packages (10 m). For the RH trench the average waste package stack is 4 high over the first 9 m from the model axis and then decreases to three then two then one-package heights at the edge of the trench. For the RH trench we have assumed that the one-dimensional results are applicable to a waste package stacking of two or even one package since the pH and the LAWABP1 dissolution rates are comparable in each of the four waste package layers (see Section 4.2).

3.5.3.3 Groundwater Model. The model used for groundwater calculations is that one established by the Hanford Site Groundwater Program, a program separately managed by the DOE's Richland Field Office, not by the Office of River Protection. The base-case groundwater flow and transport of contaminants from the ILAW facility was calculated with the current version of the Hanford site-wide groundwater model. This three-dimensional model, currently being used by the Hanford Groundwater Project and recommended as the proposed site-wide groundwater model in the Hanford Site groundwater model consolidation process, is based on the Coupled Fluid, Energy, and Solute Transport (CFEST-96) Code (Gupta et al. 1987, and Gupta 1997). The Hanford Site groundwater model has been recently independently reviewed (Gorelick et al. 1999).

This model is described in Wurstner et al. (1995) and Cole et al. (1997), and was most recently used in the Hanford Site Composite Analysis (Cole et al. 1997; Kincaid et al. 1998), which is a companion analysis to the existing preliminary PA analyses of the ILAW disposal facility (Mann et al. 1997) and the solid waste burial grounds in the 200-East and 200-West areas (Wood et al. 1996, 1995). The Composite Analysis is also a companion document to the Remedial Investigation/Feasibility Study (RI/FS) (DOE 1994) that supports the Environmental Restoration Disposal Facility.

3.5.3.3.1 Simulation of Site-Wide Steady-State Flow Conditions. Past projections of post-Hanford water-table conditions have estimated the impact of Hanford operations ceasing and the resulting changes in artificial discharges that have been used extensively as a part of site waste-management practices. Simulated results of future transient behavior in the Hanford unconfined aquifer by Cole et al. (1997) showed an overall decline in the hydraulic head and hydraulic gradient across the entire water table over the entire Hanford Site. The results of these simulations indicate that the water table would reach steady state in 100–350 years in different areas over the Hanford Site.

Given the expected long delay of contaminants reaching the water from the disposal facility, the hydrologic framework of all groundwater transport calculations was based on a postulated post-Hanford steady-state water table as estimated with the three dimensional model. The predicted water table for post-Hanford conditions for these assumed steady-state conditions across the site and in the area between the ILAW new disposal facility and the Columbia River are illustrated in Figures 3-14 and 3-15. The overall flow attributes of this water table surface are consistent with the previously simulated flow patterns described in Wurstner et al. (1995), Cole et al. (1997) and Law et al. (1996). From the ILAW new disposal facility, groundwater moves southeasterly near the site and then in an easterly and northeasterly direction before discharging into the Columbia River north of the old Hanford town site.

3.5.3.3.2 Contaminant Transport Between Disposal Facilities and Columbia River. Flow conditions established with the site-wide model provide the basis for the transport simulations of contaminants released from disposal facilities toward the Columbia River. Constant mass releases equivalent to those used in the local-scale model were introduced into the site-wide at the approximate location of the ILAW disposal facilities. Concentration levels were evaluated in groundwater in close proximity to the Columbia River as well as several intermediate points between the disposal areas and the river. To establish consistency of the site-wide scale calculations with those made in the local scale models, concentrations levels were evaluated and compared at approximately 1-km down gradient of the source areas in both the local-scale and site-wide models. Predicted concentrations levels at 1 km in the site-wide and local-scale models are expected to be somewhat consistent with each other but will not be the same because of inherent differences in the grid resolution used in each model. Predicted concentration levels in the site-wide model close to the source areas will in general be expected to be somewhat lower than are predicted in the local-scale models.

Figure 3-14. Predicted Water Table for Post-Hanford Conditions for Assumed Steady-State Conditions (as Simulated after 350 Years).

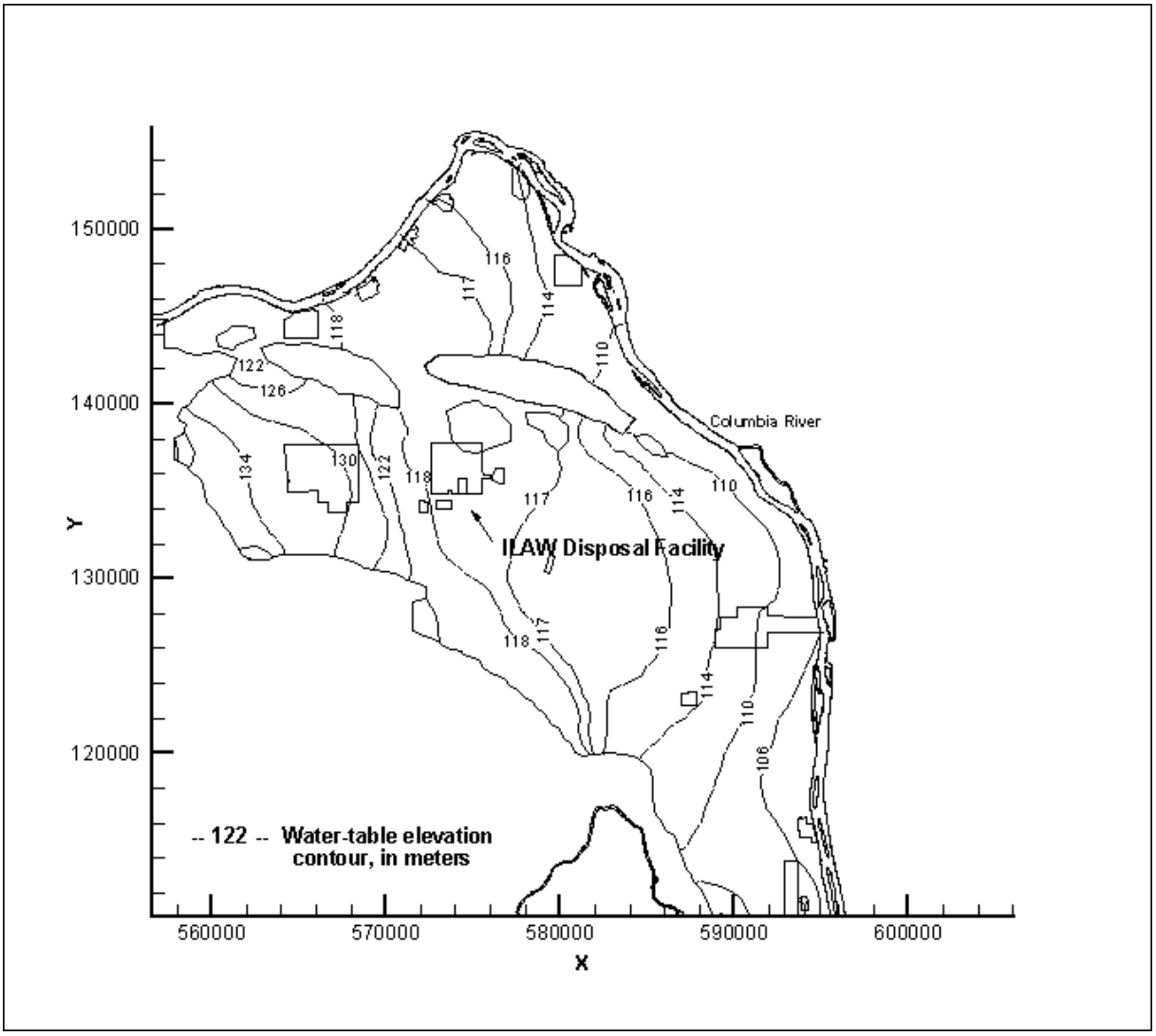

Figure 3-15 Predicted Water Table for Post-Hanford Conditions for Assumed Steady-State Conditions between ILAW Disposal Facility and Columbia River (as Simulated after 350 Years).

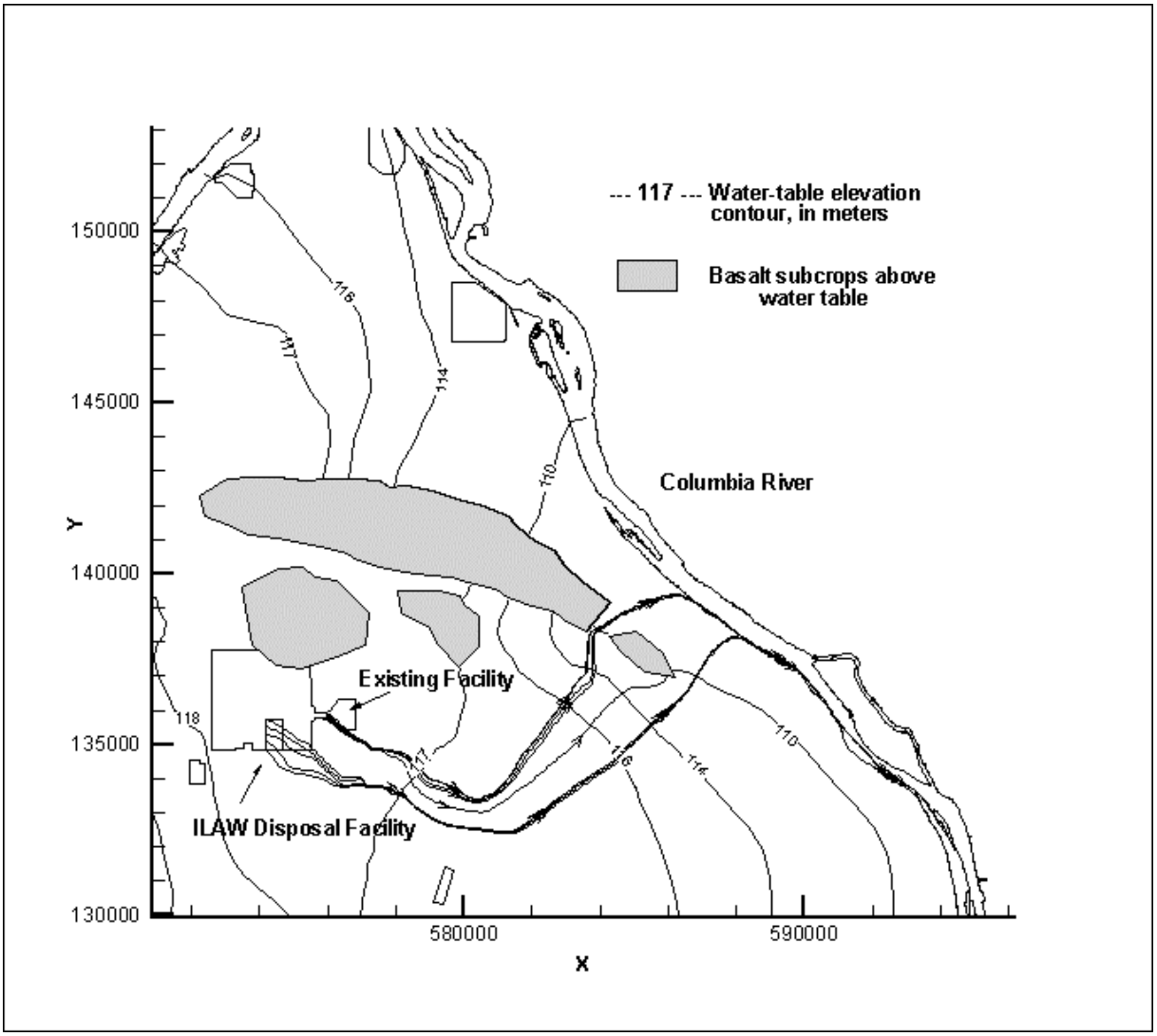

3.5.3.3.3 Local-scale Model Development and Description. The base analysis case for the groundwater flow and transport calculations included evaluated current disposal concepts at the new ILAW disposal facility that will be located in south-central 200 East Area. The approach used in this analysis was to construct a local-scale model to represent flow and transport conditions near these facilities to a hypothetical well 100-m downgradient. The boundary conditions for this local model were based on flow conditions calculated in the site-wide model.

Because the travel time in the aquifer (tens of years) is so short compared to the travel time in the vadose zone (thousands of years), the concentrations in the aquifer quickly adjust to the small changes in the contaminant flux entering the aquifer from the vadose zone. To be

conservative, the footprint of the contaminant flux entering the aquifer was taken to be the same as the trench layouts.

3.5.3.3.4 Grid Design. The grid used in the local-scale model required refinement both areally as well as vertically. The discretized grid for the local-scale model telescopes in from the grid used in regional scale calculations. The grid extends over an area of about 4100 meters in the west to east direction and 4100 m in the north-south direction (See Figure 3-16). It progressively varies in size from the outmost subdivided coarse triangular grids made on the regional scale 375 m by 375 m grid spaces to the finest grid spacing of 20 by 20 m in vicinity of the ILAW disposal area. The total number of surface elements in the three-dimensional model is 9157 elements. The three-dimensional model, based on this surface grid, comprises a total of 31604 elements (9157 surface and 22,447 subsurface elements) and 32618 nodes.

The vertical grid spacing for the transport (as well as the flow) model consisted of multiple transport layers that subdivided the major hydro-stratigraphic units. The basic approach for this subdivision is the same was used in Kincaid (1998) to support groundwater transport calculations used in the Composite Analysis. The basic thickness of each of these transport layers was 8 m. The transport layers were defined from the water table surface to the basalt to account for the overall saturated thickness and to adequately represent contaminant concentrations in the three-dimensional model. At every model node each of the major hydro-stratigraphic units below the water table was represented by at least one transport model layer. Nonconductive (e.g., mud units) below the water table were always represented by at least 2 transport model layers regardless of their saturated thickness in order to assure the vertical flow and transport through these units was appropriately represented. For units whose saturated thickness was <12 m thick, the layer thickness was set to the actual saturated thickness of the unit. Nonconductive and conductive units whose saturated thickness was >12 m were divided into multiple transport model layers in the same manner. For all units with thickness >12 m, the transport layering algorithm is as follows: create as many uniform 8-m transport layers as possible until the remaining unaccounted for saturated thickness is >12 m but <=16 m, then create two additional transport layers set to half of the remaining saturated thickness of the hydrostratigraphic unit being layered.

At the local-scale, a total of six hydrogeologic units were found to be present: 1) the Hanford formation (unit 1) and several units belonging to the Ringold Formation, including Unit 5, 6, 7, 8, and 9). The three-dimensional distribution of these units in the local-scale model is depicted in Figure 3-17. A better description of the model design features and the hydraulic properties used to support groundwater calculations in this report can be found in Bergeron and Wurstner (2000).

Figure 3-16. Finite Element Grid Used in Local –Scale Model.

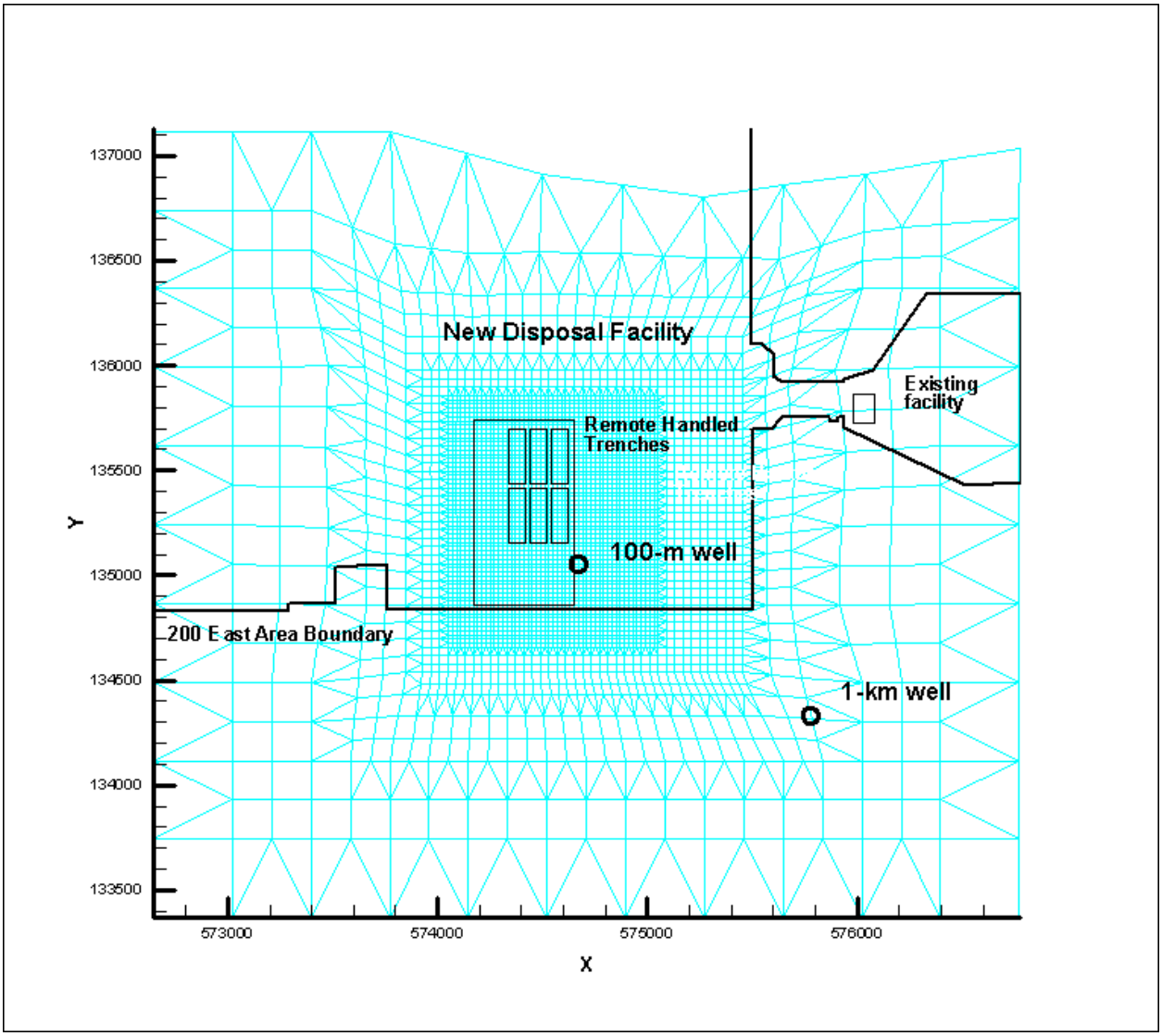
New Disposal Facility
Remote Handled Trenches
Existing facility
100-m well
200 East Area Boundary
1-km well
137000
136500
136000
135500
135000
134500
134000
133500
Y
573000
574000
575000
576000
X

Figure 3-17. Three-Dimensional Distribution of Major Hydrogeologic Units in the Local-Scale Model.

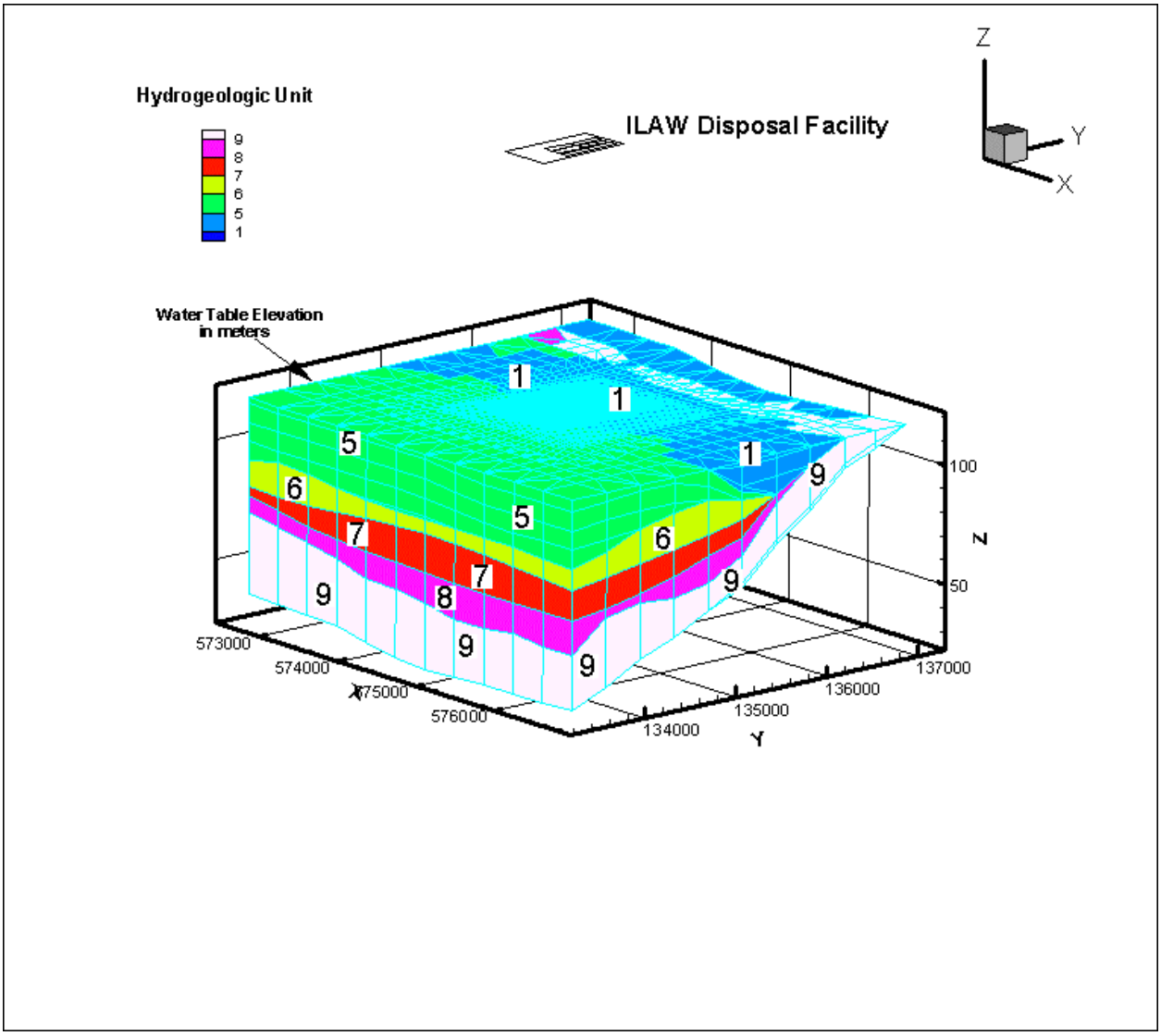

Table 3.10 summarizes the input data.

3.5.4 Input Data

This section specifies the data actually used in the computer models for the base analysis case. The intent is to follow the data given in Sections 3.2, 3.3, and 3.4 as closely as possible. Data used in the sensitivity cases are given in Section 3.5.5.

3.5.4.1 Contaminant Release Data. The data for the calculation of contaminant release rate from the waste package and subsequent transport inside the disposal facility are those given in Sections 3.4.3, 3.4.4, and 3.4.5. Table 3-7 summarizes the important values used.

3.5.4.2 Vadose Zone Data. The input data used for the base analysis case are those given in Section 3.4.3 and are summarized in Table 3-11.

3.5.4.3 Aquifer Modeling. This section describes the hydraulic, transport, and other parameters of the Hanford Site groundwater model.

3.5.4.3.1 Hydraulic Properties. The hydraulic conductivity and porosity estimates used in the local-scale model were developed based on the following assumption: regional scale estimates of hydraulic properties in the site-wide model can be interpolated using local-scale model grid coordinates to represent local-scale properties in vicinity of the ILAW disposal facility area. The resulting two-dimensional distributions of these properties for each model unit is provided in Figure 3-18. The estimated values are, in general, indicative of the regional high trends in hydraulic properties found in the central part of the Hanford Site. Specifically, the ancestral Columbia River deposited very coarse alluvial deposits in a deep channel extending to the south of the ILAW site and to the north between Gable Butte and Gable Mountain. Estimated hydraulic conductivities directly below the disposal range from several thousand to tens of thousands m/day in the Hanford formation and several hundred m/day in the permeable parts of the Ringold Formation (Units 5, 7, and 9). Relatively low hydraulic conductivities are estimated for low permeability units within the Ringold Formation (Units 6 and 8).

The best estimate of an effective porosity of 0.25 used in the site-wide model were also used in all transport simulation made with the local-scale model.

Table 3-11. Base Analysis Case Input Data for the Disposal Facility.

Parameter	Value	Section with Justification for Using Value
Soil Layering (two dimensional model used)		
Hanford formation Upper Gravel Sequence Sand Sequence Lower Gravel Sequence	 6 m (20 ft) (on surface) 60 m (197 ft) 35 m (98 ft) (bottom)	Section 3.4.3.1
Ringold Formation Unit E	 30 m (98 ft), below Hanford formation	Section 3.4.3.1
Hydrologic Parameters		
Vadose Zone Soil Layer	Calculated based on curve-fitting parameters and saturated hydraulic conductivity. See reference section.	Section 3.4.3.2 (Values given in Table 3-4)
Construction Material	Calculated based on curve-fitting parameters and saturated hydraulic conductivity. See reference section.	Section 3.4.3.2 (Values given in Table 3-3)

Table 3-11. Base Analysis Case Input Data for the Disposal Facility.

Parameter	Value	Section with Justification for Using Value
Infiltration Rate		
At the Disposal Facility Side slope Everywhere else	 50.0 mm/y 4.2 mm/y	Section 3.4.6
Geochemical Parameters		
Chemical Distribution Coefficients (K_d) Tc, I, Chemicals, Others U, Np, Pa, Ru C Sr, Ra Cs, Nb, Ni, Pb, Sn Ac, Am, Ce, Cm, Co, Eu, Pu, Th, Zr	 0.0 mL/g 0.6 mL/g 4.0 mL/g 10.0 mL/g 80.0 mL/g 150.0 mL/g	Section 3.4.3.3
Contaminant Release Rate		
Relative Radionuclide Release Rate	Calculated release based on initial release rate and time-dependent surface area. See reference section .	Section 3.4.4.3 (Values given in Table 3-7)
Disposal Facility Degradation		
Concrete	degraded at 500 years	Section 3.4.5.7

Table 3-11. Base Analysis Case Input Data for the Disposal Facility.

Parameter	Value	Section with Justification for Using Value
Natural materials	properties do not degrade, but system performance changes because of materials rearrangement	Section 3.4.6.7

3.5.4.3.2 Transport Properties. Estimates of model parameters were developed to account for contaminant dispersion in all transport simulations. Specific model parameters examined included longitudinal and transverse dispersion coefficients (D_l and D_t) as well as estimates of effective bulk density and porosity of the aquifer materials. This section briefly summarizes estimated transport properties.

In general, the horizontal dispersivity for aquifer transport is typically set at 10 percent of the travel length in the direction of flow and the transverse dispersivity is set at 10 percent of the longitudinal value. For predictions at 100 m downgradient of the facility, this would mean a longitudinal dispersivity of at least 10 m would be required. For this analysis, a lower longitudinal dispersivity of 5 m was selected to be within the range of recommended grid peclet numbers ($P_e < 4$) for acceptable solutions. The 5 m estimate is about one-quarter of the grid spacing in the finest part of the local-scale model grid in the 200-Area plateau where the smallest grid spacing is on the order of 20 m by 20 m. The effective transverse dispersivity was assumed to be one-tenth of the longitudinal dispersivity. Therefore, 0.5 m was used in all simulations.

3.5.4.3.3 Base Case: Areal Sources Representing New Facility Disposal Concept.

The remote-handled trench disposal concept was evaluated in the initial base case calculations. For this concept, the new ILAW disposal facility will consist of a set of seven remote-handled waste trenches in the configuration illustrated in Figure 2-24. Each waste trench will be an underground, open-topped, trench approximately 80 m wide, 260 m long and 10 m deep with 3:1 side slopes.

The primary objective of the groundwater flow and transport calculations were to determine the well-intercept factor. The well intercept factor (WIF) is defined as the ratio of the concentration at a well location in the aquifer to the concentration entering the aquifer. For purposes for these calculations, the bulk concentration of source entering was assumed to be 1 Ci/m^3. The rate of mass flux associated with this concentration is a function of the infiltration rate assumed for the disposal facility covered by the modified RCRA-compliant subtitle C cap. With an assumed rate of 4.2 mm/y assumed for the disposal facility, the resulting solute flux, which is a product of the contaminant concentration in the infiltrating water and the infiltration rate, entering the aquifer from each of the disposal concepts is 4.2×10^{-3} $Ci/y/m^2$.

In all model simulations performed, the WIF was calculated at a hypothetical well located approximately 100 meters downgradient from the boundary of the disposal along the centerline of the simulated plume. A pumping rate of 10 liters per day was used at the hypothetical downgradient well location. This pumping rate would provide sufficient drinking water for a family of five at an assumed intake of 2 liters per person per day.

3.5.4.4 Integration of Results. In addition to data already discussed, the input data for INTEG were taken from the output of the vadose zone and the aquifer models. Inventories were taken from Section 3.2.2. Dose conversion factors were taken from Section 3.3.5.

Figure 3-18. Distribution and Hydraulic Conductivities of Major Hydrostratigraphic Units in Local-scale Model.

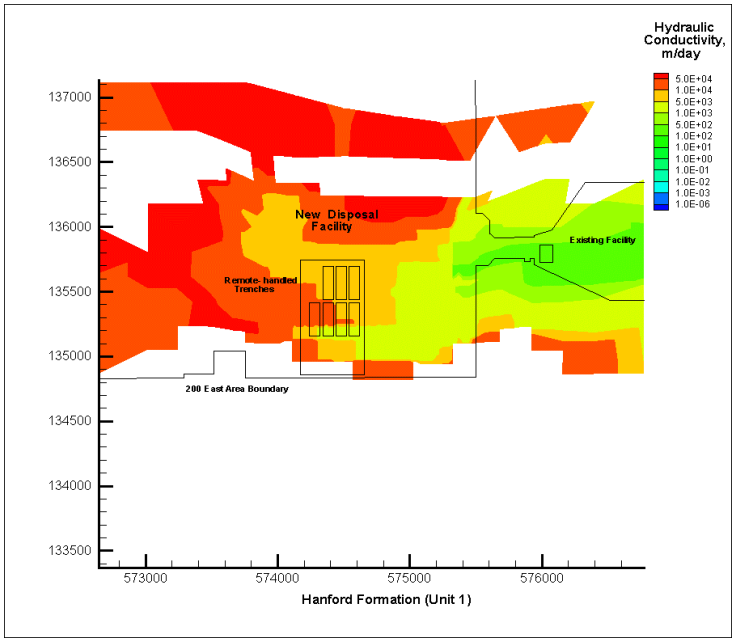
Hydraulic Conductivity, m/day
5.0E+04
1.0E+04
5.0E+03
1.0E+03
5.0E+02
1.0E+02
1.0E+01
1.0E+00
1.0E-01
1.0E-02
1.0E-03
1.0E-06
137000
136500
136000
135500
135000
134500
134000
133500
573000
574000
575000
576000
New Disposal Facility
Existing Facility
Remote- handled Trenches
200 East Area Boundary
Hanford Formation (Unit 1)

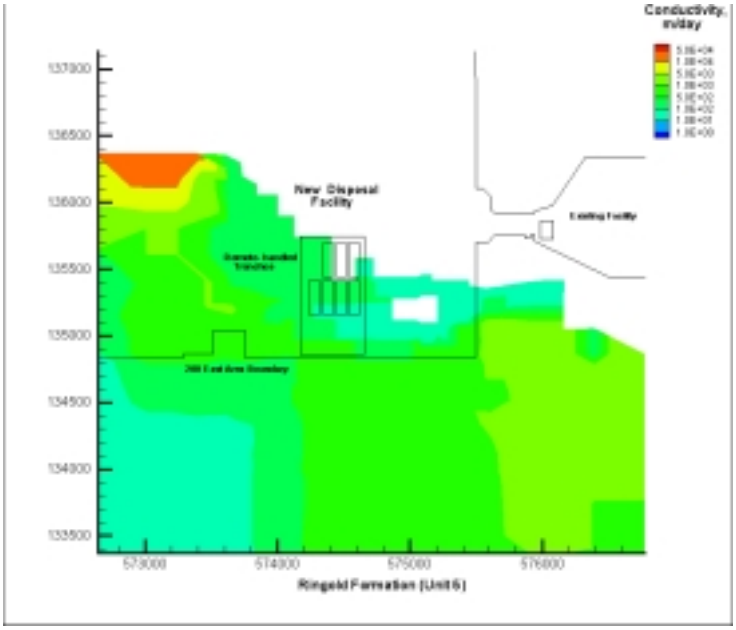
Conductivity, m/day
New Disposal Facility
Existing Facility
Ringold Formation (Unit 6)

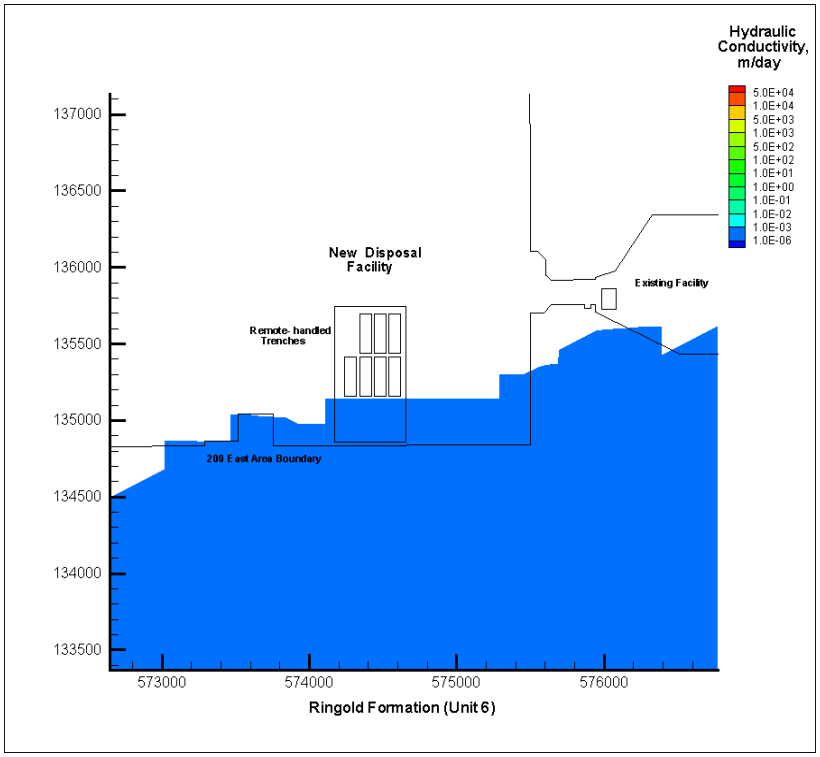
Hydraulic Conductivity, m/day
5.0E+04
1.0E+04
5.0E+03
1.0E+03
5.0E+02
1.0E+02
1.0E+01
1.0E+00
1.0E-01
1.0E-02
1.0E-03
1.0E-06
137000
136500
136000
135500
135000
134500
134000
133500
New Disposal Facility
Remote- handled Trenches
Existing Facility
200 East Area Boundary
573000
574000
575000
576000
Ringold Formation (Unit 6)

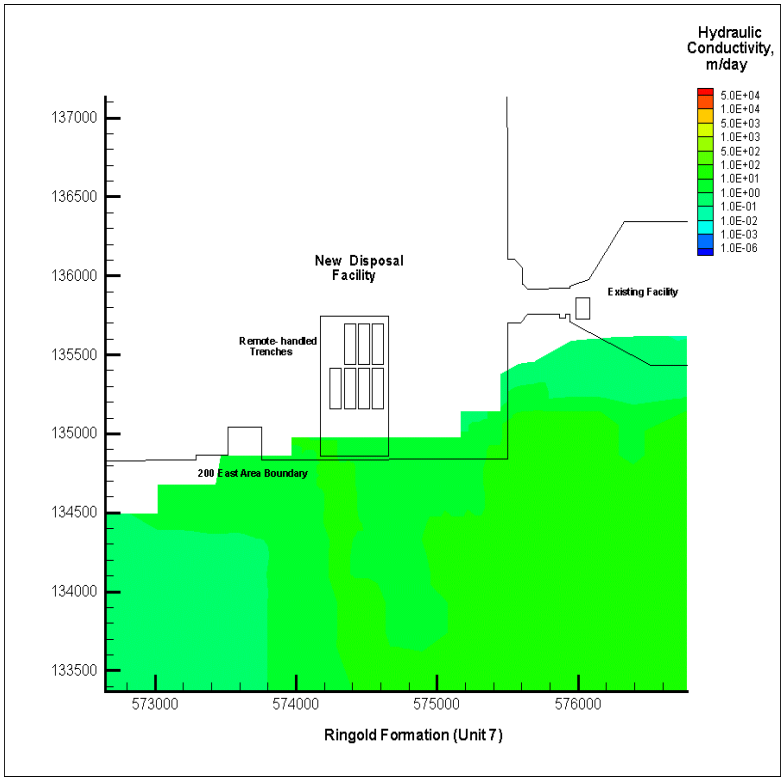
Hydraulic Conductivity, m/day
5.0E+04
1.0E+04
5.0E+03
1.0E+03
5.0E+02
1.0E+02
1.0E+01
1.0E+00
1.0E-01
1.0E-02
1.0E-03
1.0E-06
137000
136500
136000
135500
135000
134500
134000
133500
New Disposal Facility
Remote- handled Trenches
Existing Facility
200 East Area Boundary
573000
574000
575000
576000
Ringold Formation (Unit 7)

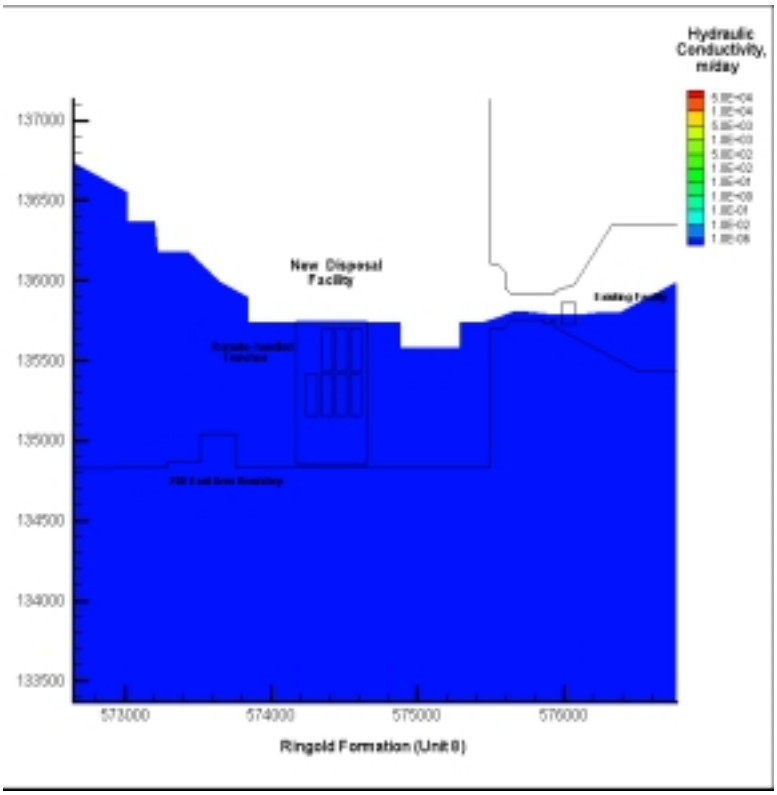
Hydraulic Conductivity, m/day
New Disposal Facility
137000
136500
136000
135500
135000
134500
134000
133500
573000
574000
575000
576000
Ringold Formation (Unit 8)

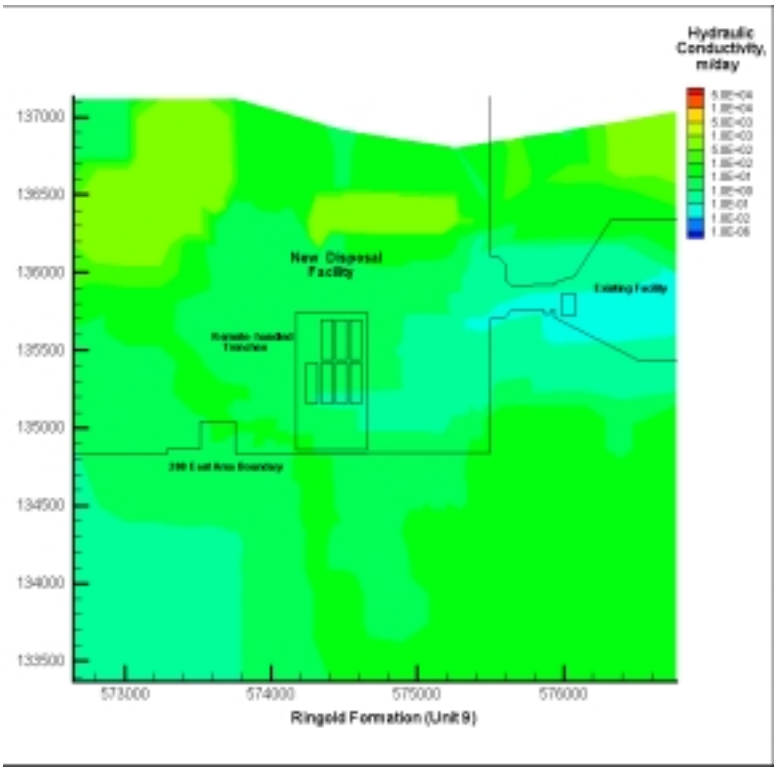
Hydraulic Conductivity, m/day
5.0E+04
1.0E+04
5.0E+03
1.0E+03
5.0E+02
1.0E+02
1.0E+01
1.0E+00
1.0E-01
1.0E-02
1.0E-03
137000
136500
136000
135500
135000
134500
134000
133500
573000
574000
575000
576000
New Disposal Facility
Existing Facility
Ringold Formation (Unit 9)

3.5.5 Sensitivity Cases.

> Sensitivity cases are used to determine the robustness of the results obtained from the base analysis case.

Sensitivity cases were run to determine the effect of various assumptions and data values. For most sensitivity cases, only one parameter or one set of parameters differs from the base analysis case or another sensitivity case. Thus, the change, if any, in the final answer will indicate the effect of that parameter on the overall answer. Table 3-13 (at the end of this section) summarizes the sensitivity cases. Sections 3.5.5.1 through 3.5.5.12 discuss the sensitivity cases and explain why each case was run.

3.5.5.1 Scenario-Dependent Sensitivity Cases. The scenario-dependent sensitivity cases are selected analyses to determine the extent to which results related to a scenario depend on selected values or assumptions. Several scenario-dependent cases were developed. Land-use, drinking water, and catastrophic natural scenarios were considered (Section 3.3).

Because inadvertent intrusion is an artificial case, its parameters are quite uncertain. Some parameters (such as the inventory of key contaminants) will vary because of near-term decisions on waste treatment, while others will vary depending on the actions of the hypothetical inadvertent intruder. Such actions will include the drilling method used (which affects the size of the hole drilled and the size of the glass chunks unearthed) and the area over which the waste is spread. Sensitivity cases are run for each of these uncertainties to provide a feeling for the effect of such variations.

Predicting land use at the Hanford Site for the next 10,000 years is impossible. Natural conditions were assumed for the base analysis case (Section 3.3.2.2). For land-use sensitivity cases, the effects of various land uses were calculated. The following uses were examined:

- Irrigated farming on top of the disposal facility with an infiltration rate of 50 mm/y (1.85 in./y). Such irrigation is considered as an inadvertent intrusion. However, in this analysis such irrigation is calculated as part of the groundwater scenario, instead of part of the inadvertent intruder scenario.

- Irrigated farming in other parts of the Hanford Site Central Plateau with recharge three times the current values. This case could also mimic a change in climate resulting in more precipitation. Such increased recharge will distort the groundwater flow and change the water table height.

- Industrial use of the 200 Area, which is assumed to decrease the infiltration rate over the entire 200 Area by a factor of 3.

The point of compliance follows current requirements of the DOE order on radioactive waste management (DOE 1999g). However, because of the complexity of the Hanford Site, other points of compliance (for example, at the edge of the central site's buffer zone) could be chosen. Thus, impacts at a series of locations are estimated. In the base analysis case, the well is assumed to be 100 m (328 ft) downgradient from the disposal facility. To determine the effect of the well position, the well was located at various other distances (including the 200 Area fence line) along flow lines down to the Columbia River.

The drinking water scenario is based on the pumping rate and the location of the well. Minimal pumping (0.01 m^3/day = 10 liters/day [2.6 gallons/day], corresponding to a family of five using the well only to obtain drinking water) is assumed for the base analysis case. As pumping is increased, water is taken from a wider area, resulting eventually in drawing in water that is uncontaminated. Pumping rates of 10 to 1,000 m^3/day (2,640 to 2,640,000 gallons/day) were used to determine the effect of the pumping rate on the drinking water dose.

Finally, the effects of catastrophic natural events were evaluated. The base analysis case does not evaluate a catastrophic natural event. Neither seasonal flooding nor even the collapse of the region's largest dam would cause water to reach the disposal facility. However, a catastrophic ice-age flood similar to those that occurred over 10,000 years ago, would affect the disposal facility and is analyzed. However, such a flood is not expected to occur during the next 50,000 years.

3.5.5.2 Inventory-Dependent Sensitivity Cases. The inventory of radionuclides that will be in the waste form is uncertain. The inventory in the waste form depends on the amount and type of waste presently stored in the Hanford Site tanks, the process used to separate tank waste into low-activity and high-level waste streams, and the method of immobilization. At present, the separation process that will be used is unknown, as are the details of the immobilization method. These sensitivity cases are designed to evaluate the effect of different amounts of key radioisotopes.

Currently, the plan is to have a separate separations process to allow no more than 20 percent of the technetium in the tank waste to go into the ILAW package. To determine the impact of removing this process step (which is currently being studied by DOE/ORP), a sensitivity case having all of the technetium go into ILAW was analyzed.

The inventory data package (Wootan 1999) estimated the uncertainties in the inventory as well as bounding cases. These uncertainties and bounding values were used for the key contaminants (^{99}Tc, U, and ^{129}I for the groundwater pathway and ^{126}Sn, ^{239}Pu, and ^{241}Am for the inadvertent intruder case).

In the supporting document (WHC 1996) for the DOE petition to the NRC for the separated waste to be considered as non-high-level waste, various uncertainty bands are given. The amount of cesium separation may be different from what is assumed in the base analysis case. A sensitivity case increasing the amount of ^{137}Cs to 9.0 MCi was performed, a increase by a factor of 10 from the base analysis case.

3.5.5.3 Infiltration-Dependent Sensitivity Cases. Infiltration is important because it is a main driver for the waste form release and because moisture carries the released contaminants to the groundwater. The base analysis case uses an infiltration rate into the surface barrier of 4.2 mm/year, which corresponds to the natural recharge of the Burbank loamy sand soils of the site. However, the southern region of the site contains Rupert sands, which have a lower natural recharge rate of 0.9 mm/year. Moreover, the surface barrier is expected to have a quite low infiltration rate (<0.1 mm/year) and last at least 500 years. Finally, there is always the possibility that the surface is grossly disturbed or that large amounts of water are placed on the site. Each of these cases (0.1, 0.9, 4.2, and 50 mm/year) was investigated assuming that infiltration was time-independent. Finally, a sensitivity case was simulated that treats the barrier in a degraded form (i.e., the infiltration rate is 0.1 mm/yr for the 500 years of its design life, then immediately increases to the natural rate of the Burbank loamy sand soil – 4.2 mm/year).

3.5.5.4 Geology-Dependent Sensitivity Cases. Because the geology of the subsurface can only be inferred from a relatively few measurements, its exact three-dimensional nature remains uncertain. Because the 1998 ILAW performance assessment showed relatively little sensitivity to the geologic parameters, only a few cases were run in this assessment. The base analysis case treats the subsurface as a two-dimensional structure consisting of Hanford formation sands in the upper layer and Hanford gravels in the lower. Sensitivity cases were run that assumed the entire formation was Hanford sands and the entire formation were Hanford gravels. In addition, a case was run assuming that clastic dikes were present. Finally, the effect of increasing the depth of the vadose zone by 3 meters was performed as the equilibrium level of the water table has not yet been reached due to the conditioning effect of past Hanford operations.

3.5.5.5 Facility-Dependent Sensitivity Cases. The disposal facility is still undergoing design. Thus, many of the details of its structure can be impacted by this assessment. Two major design features are the surface barrier and the sand-gravel capillary barrier. Additionally, the effect of the material used to fill in between the ILAW packages was investigated. Although the base design is the trench concept, the project still has control over the 4 existing concrete vaults originally constructed for grout disposal.

Two important features of the surface barrier are its extension past the disposal facility and its transition from its elevated positions to natural ground level. A sensitivity case was run shortening the distance that the surface barrier extends past the disposal facility. In addition, the current design has a side slope that allows the change in elevation from the natural ground slope to the elevated level of the cap. A sensitivity case was run to investigate the effect if the infiltration rate of this side slope changed from its presumed value (50 mm/y) to the same as the natural condition (4.2 mm/y) of flat surfaces.

Previous calculations had shown that a sand-gravel capillary barrier would divert significant amounts of moisture from the disposal facility. The base analysis case assumed no such barrier (for ease of calculation). Thus, a sensitivity case was run with such a barrier over the facility. In addition, a sensitivity case was run with a vertical gravel barrier to the side of the disposal facility to see the effect of such a capillary barrier. The degradation of the sand-gravel capillary barrier was also simulated and is described in the next section.

Another sensitivity case replaces the backfilled material placed between the ILAW packages with sand to examine the effect of hydraulic parameters of the filler material. The hydraulic materials determine the amount of moisture surrounding the waste form and hence influence the contaminant release rate.

As noted the current design is a trench concept. However, because the project still has the four concrete vaults left from the grout disposal effort and because concrete vaults are the basis of the current waste disposal authorization statement, the effects of using concrete vaults was investigated. Fewer sensitivity cases were run than for the trench concept, as the concrete vault is no longer the baseline design.

3.5.5.6 Facility Degradation-Dependent Sensitivity Cases. Although the design of the trench concept is simple and uses mainly natural materials, it is recognized that the components of the disposal facility will not last forever. The main features of interest are the surface barrier, the sand-gravel capillary barrier, and the bottom surface. The design life of the surface barrier is estimated to be 500 years. As noted in Section 3.5.5.3, the base analysis case assumes that the surface barrier fails immediately, and that sensitivity runs assume the barrier lasts 500 years or for an infinite time. The failure of the sand-gravel capillary barrier is assumed to be a subsidence event that causes a meter-long length to drop 0.3 meter the entire long length of the barrier. Finally, there is the possibility that the bottom of the disposal facility will retain water (and hence contaminants) for an extended time causing a bathtub effect. The consequences of such a bathtub effect were stimulated assuming that the disposal facility was intact for up to 2,000 years. Since the time of compliance is 1,000 years, these results are only useful for determining peak values at much later times.

3.5.5.7 Hydraulic Parameter-Dependent Sensitivity Cases. Moisture flow is important to the performance assessment. Hydraulic parameters were varied to determine the effect on contaminant transport. The base analysis case treats the moisture flow to be anistropic as has been measured for the soil conditions of the Hanford Site. However, as this reduces vertical flow, a case assuming isotropic flow conditions was also run. The effect of different hydraulic parameters was treated by assuming different properties in the disposal facility (backfilled soils versus sand) and in the vadose zone (presumed geometry versus all sand or all gravels).

3.5.5.8 Waste Form-Dependent Sensitivity Cases. Because of the importance of waste form release to this performance assessment, a wide variety of cases were run. These included sensitivity to the

- Chemical reaction matrix used,
- Moisture infiltration used,
- Surrounding materials present, and
- Other effects.

The base analysis case uses a kinetic rate law involving SiO_2(aq) to control the glass dissolution rate. Thus, as the glass dissolves, more silicon goes into solution, slowing the glass dissolution until there is enough silicon in solution to form secondary reaction products, which then control the total aqueous silicon concentration. It should be noted that the calculations do NOT simulate the incorporation of contaminants into secondary products as there is insufficient information about the mechanism of any such incorporation and whether the radionuclides would remain sequestered over the long time periods involved in this analysis.

Three sensitivity cases were run to investigate the impact of the chosen chemical reaction network. The first assumes that the amount of silicon in the solution has no effect on the glass dissolution rate. That is, the forward reaction rate of the glass is the reaction rate at all times. Since the forward reaction rate of glass depends on pH, and since the pH increases as more sodium is released from the glass, the actual glass dissolution rate increases as a function of time. The second sensitivity case assumes that the alkali ion exchange reaction that substitutes hydrogen in the water with sodium in the glass does not take place. Laboratory measurements show that such a reaction is important at the low temperatures expected in the disposal facility. Finally, a sensitivity case is run assuming that no secondary products are formed and hence the amount of silicon in solution is affected only by the rate of glass dissolution balanced by the rate of mass transfer out of the disposal facility.

Moisture is important in the waste form release calculations. It is the solvent; it forms the medium in which dissolved glass components interact; and it transports the contaminants through the disposal facility to the vadose zone. Infiltration rates from 0.1 to 50 mm/y (0.1, 0.5, 0.9, 4.2, 10, and 50 mm/y) were investigated. Infiltration rates must drop below 0.005 mm/y before there is not enough water to dissolve the glass.

As glass dissolution is a chemical reaction, surrounding materials can affect the reaction rate. Also surrounding materials can affect the moisture flow. Therefore, the presence or absence of the following materials were investigated: sand versus backfilled soil as a filler material between the ILAW packages, stainless steel containers for the ILAW packages, a conditioning layer above the ILAW packages, and a concrete vault.

Finally, other calculations were run to investigate a variety of effects. The most important is probably waste form composition. However, final glass compositions have not yet been determined. Therefore as a sensitivity case, LAWABP1 glass was replaced with HLP31 glass. This glass has a slightly higher waste loading (23% versus 20%), a higher silicon content (55.8% versus 48.2%), but a lower aluminum content (5.1% versus 13.6%). Table 3-12 lists the composition for the two glasses by oxide mass fraction.

The base analysis case used Tc as the contaminant transported in the disposal facility. To investigate the effect of retardation in the disposal facility, a case was run using uranium as the contaminant. Most of the waste form simulations used a one-dimensional model. A sensitivity case was run using a two-dimensional model to determine the sensitivity to dimension. Finally a case was run that included the vadose zone in the model so that it could be determined how far into the vadose zone chemical effects actually extended.

Table 3-12. Elemental Compositions of LAWABP1 and HLP31 (by mole fraction).

	LAWABP1	HLP31			LAWABP1	HLP31
Al	1.36E-01	5.06E-02		Mg	1.71E-02	1.47E-02
B	1.84E-01	2.22E-01		Na	4.46E-01	4.79E-01
Ca	-	1.15E-04		P	7.79E-04	5.45E-04
Cl	1.13E-02	5.82E-03		S	8.63E-04	6.44E-04
Cr	1.82E-04	7.64E-04		Si	4.82E-01	5.58E-01
F	1.46E-03	3.39E-04		Ti	2.15E-02	1.48E-02
Fe	2.16E-02	2.71E-02		Zn	2.21E-02	7.29E-03
K	3.23E-02	6.44E-03		Zr	2.94E-02	4.82E-03
La	8.48E-03	-		O	1.873	1.875

3.5.5.9 Geochemical-Dependent Sensitivity Cases. Although the calculations in the disposal facility use a chemical network approach, the calculations in the vadose zone use a simple K_d model. As noted just above, the chemical network approach was used in a sensitivity case to determine the adequacy of the K_d approach. Also, K_d values for key contaminants (Tc, U, I, and Se) were changed to determine sensitivity and, in addition, K_d values for all contaminants were set to zero to determine an extreme case. Finally, the K_d value for iodine and uranium was increased at the bottom of the disposal facility to model the high absorption of iodine and uranium in concrete.

3.5.5.10 Exposure Parameter-Dependent Cases. The manual for the new DOE order on radioactive waste management specify that EPA dose conversion factors be used in the performance assessment. A few cases were run using dose conversion factors from DOE and from previous Hanford studies. In addition, a variety of exposure scenarios (corresponding to the standard Hanford set) were investigated (see Appendix B). These range from industrial to Native American scenarios.

3.5.5.11 Location/Layout of the Facility. The current plan is to use east-west trenches in the south central part of the 200 East Area. However, final design has not yet been performed. Thus, the layout of the trenches as well as the location of the trenches on the site has not been determined. The effect of various choices was investigated. Also, it is possible that existing concrete vaults (about a kilometer east of the disposal site) could be used. The effect of this location was also investigated.

Table 3-13. List of Sensitivity Cases.

Except for intrusion scenarios, the performance measures calculated were the drinking water dose and the all-pathways dose. For the intrusion scenarios, the acute and continuous doses were calculated.

Discussion Section	Sensitivity Case (Unless noted all cases treat groundwater scenario)	Results Presented in Section
Scenario		
3.5.5.1	Intrusion scenario (time of intrusion, amount of waste retrieved, stability of waste form, area of garden)	5.4.2
	Investigate regional change in recharge from irrigation or vegetation changes	4.7.5
	Investigate effects of different well locations	4.3.5
	Investigate effects of different pumping rates at well	4.7.3
	Treat natural events, such as glacier flooding	4.14
Inventory		
3.5.5.2	Investigate assumption that all tank waste Tc in ILAW	4.8.2
	Investigate inventory uncertainty of key contaminants	4.8.2
	Investigate increasing the inventory in the inadvertent intruder cases	5.4.3

Table 3-13. List of Sensitivity Cases.

Except for intrusion scenarios, the performance measures calculated were the drinking water dose and the all-pathways dose. For the intrusion scenarios, the acute and continuous doses were calculated.

Discussion Section	Sensitivity Case (Unless noted all cases treat groundwater scenario)	Results Presented in Section
Recharge		
3.5.5.3	Use natural recharge of Rupert sands – 0.9 mm/y (base analysis case uses 4.2 mm/y)	4.6.2
	Use high recharge rate – 50 mm/y	4.6.2
	Use low recharge rate – 0.1 mm/y	4.6.2
	Use low recharge for 500 years, then use 4.2 mm/y	4.6.2
Geology		
3.5.5.4	Investigate effect if entire Hanford formation is sandy	4.6.3
	Investigate effect if entire Hanford formation is gravelly	4.6.3
	Investigate effect of having clastic dikes at disposal site	4.6.3
	Investigate effect of increasing depth of vadose zone by 3 meters	4.6.3

Table 3-13. List of Sensitivity Cases.

Except for intrusion scenarios, the performance measures calculated were the drinking water dose and the all-pathways dose. For the intrusion scenarios, the acute and continuous doses were calculated.

Discussion Section	Sensitivity Case (Unless noted all cases treat groundwater scenario)	Results Presented in Section
	Facility	
3.5.5.5	Use capillary break – best estimate case (base analysis case assumes no capillary break)	4.4
	Investigate effect of side slope – 4.2 mm/y (base analysis case assumes 50 mm/y)	4.4
	Investigate effect of adding vertical gravel break (base analysis case assumes no vertical break)	4.4
	Investigate short surface barrier	4.4
	Investigate the type of material to fill in between ILAW packages	4.4
	Investigate use of concrete vaults	4.4

Table 3-13. List of Sensitivity Cases.

Except for intrusion scenarios, the performance measures calculated were the drinking water dose and the all-pathways dose. For the intrusion scenarios, the acute and continuous doses were calculated.

Discussion Section	Sensitivity Case (Unless noted all cases treat groundwater scenario)	Results Presented in Section
Degradation		
3.5.5.6	Failure of surface barrier	4.4
	Investigate failed capillary break	4.4
	Investigate bath tub effect	4.4
Hydrologic Parameters		
3.5.5.7	Investigate effect of having hydraulic conductivity same vertically as horizontal (base analysis case assumes anisotropy)	4.4
	Investigate changing facility filler material to sand	4.5.5
	Investigate changing Hanford sand hydrologic properties to Hanford gravel hydraulic properties	4.6.3
	Investigate changing Hanford gravel hydrologic properties to Hanford sand hydraulic properties	4.6.3

Table 3-13. List of Sensitivity Cases.

Except for intrusion scenarios, the performance measures calculated were the drinking water dose and the all-pathways dose. For the intrusion scenarios, the acute and continuous doses were calculated.

Discussion Section	Sensitivity Case (Unless noted all cases treat groundwater scenario)	Results Presented in Section
Waste Form		
3.5.5.8	Use forward rate of reaction (base analysis and best-estimate cases use full reaction network)	4.5.2
	Investigate simplifications to full reaction network (no ion exchange reaction, no secondary product production)	4.5.3
	Investigate waste form release as a function of the infiltration rate (0.1, 0.5, 0.9, 4.2, 10., and 50. mm/y). The base case uses 4.2 mm/y.	4.5.4
	Investigate effect of using sand as filler material (base analysis case using backfill)	4.5.5.1
	Investigate effect of having stainless steel containers (base analysis case ignores effect)	4.5.5.2
	Investigate effect of having a chemical conditioning layer (base analysis case assumes no such feature)	4.5.5.3
	Investigate the use of concrete vaults (base analysis and best-estimate cases use trench)	4.5.6
	Investigate different waste loading/glass composition – HLP31 (base analysis case uses LAWABP1)	4.5.7
	Investigate other effects (diffusion parameter, contaminant = U, 2d calculation, extend calculation to groundwater)	4.5.8

Table 3-13. List of Sensitivity Cases.

Except for intrusion scenarios, the performance measures calculated were the drinking water dose and the all-pathways dose. For the intrusion scenarios, the acute and continuous doses were calculated.

Discussion Section	Sensitivity Case (Unless noted all cases treat groundwater scenario)	Results Presented in Section
Geochemical		
3.5.5.9	Investigate effect of chemical trapping of I and U in base of disposal facility	4.6.3
	Investigate the effect of changing U K_d to 0	4.6.3
	Investigate the effect of changing I K_d to 0.6 mL/g	4.6.3
	Investigate the effect of all K_ds to 0	4.6.3
Exposure		
3.5.5.10	Investigate the use of different dose factor sets (base analysis case uses EPA)	4.8.4
	Investigate different ingestion, inhalation, and time of exposure	4.8.4

Table 3-13. List of Sensitivity Cases.

Except for intrusion scenarios, the performance measures calculated were the drinking water dose and the all-pathways dose. For the intrusion scenarios, the acute and continuous doses were calculated.

Discussion Section	Sensitivity Case (Unless noted all cases treat groundwater scenario)	Results Presented in Section
Location/Layout of Facility		
3.5.5.11	Investigate various layout of trenches on disposal site	4.7.2
	Investigate use of existing concrete vaults	4.5.6

4.0 RESULTS OF ANALYSES

4.1 INTRODUCTION

This chapter presents the results of the analyses described in Chapter 3. It also discusses the data and methods affecting those results. This chapter emphasizes understanding the suite of analyses rather than the computational results as such. The detailed results and additional information on the calculational results can be obtained from the following documents that are combined in Puigh 2001:

- *Waste Form Release Calculations for the 2001 Immobilized Low-Activity Waste Performance Assessment* (Bacon 2001)
- *Near-Field, Far-Field, and Estimated Impact Calculations for the Hanford Immobilized Low-Activity Tank Waste Performance Assessment: 2001 Version* (Finfrock 2000b)
- *Groundwater Flow and Transport Calculations Supporting the Immobilized Low-Activity Waste Disposal Facility Performance Assessment* (Bergeron 2000)

This chapter is divided into four parts, organized by scenario:

- General Comments (Section 4.2)
- The results from the groundwater scenarios, including the impact on surface water (Sections 4.3 - 4.11)
- The results from the releases to air (Section 4.12)
- The results from biotic pathways (Section 4.13)
- The results of catastrophic events (Section 4.14)
- The ALARA analysis (Section 4.15).

For each scenario, the contaminant concentrations in drinking water and the all-pathway dose are calculated. Chapter 7 provides comparisons with performance objectives.

4.2 COMMENTS ON CALCULATIONS

4.2.1 Presentation of Results

This subsection describes how the results will be presented for each major subset of calculations:

- Moisture flow into the disposal facility
- Contaminant release from the waste form and into the vadose zone
- Moisture flow and contamination transport in the vadose zone
- Moisture flow and contaminant transport in the groundwater
- Integration of calculations.

Because of the long times considered in this analysis, moisture flux into the disposal facility was considered time independent. Calculations in the previous ILAW performance Assessment (Mann 1998a) show that moisture content reaches equilibrium conditions relatively rapidly and transient moisture effects (during construction, for example) have relatively little impact on the results. Also, most of the cases considered have a spatially independent moisture influx into the system. Thus, moisture flow into the disposal facility is presented as a single number (i.e., the result is time and space independent). For the other cases, calculated moisture flows are displayed graphically.

Because the waste form calculations treat moisture flow, chemical reactions, waste form degradation, and contaminant release, as well as contaminant transport, the calculations were quite time consuming. Thus, most results come from one-dimensional calculations. In general, results are displayed as a contaminant flux leaving the disposal facility as a function of time, generally showing a relatively fast build up to a nearly constant value.

Because of the disposal facility's size along the "long" dimension, vadose zone calculations can be reduced to two dimensions. However, because of the vadose zone's thickness and the dispersion of contaminants as they travel to the groundwater, the contaminant flux entering the groundwater does not significantly vary spatially. Thus, most results of contaminant flux entering the groundwater will not be displayed as a function of distance from the disposal facility's centerline.

In most vadose zone calculations for other disposal sites, the time during which release occurs is short relative to the travel time in the vadose zone. This results (see Section 4.9.2) in peaked contaminant releases to the groundwater. That is, the rate at which contaminants enter the groundwater rises, reaches a peak then declines somewhat more slowly than the initial rise. However, because of the slow rate that the glass waste form degrades, the results of most of these simulations show a different temporal behavior. In these simulations, the time dependence is determined by the rate of waste form degradation rather than vadose zone travel time. Thus, the rate at which contaminants enter the groundwater looks more like a step function. The time of the step is determined by the travel time in the vadose zone and by the time needed for moisture to start attacking the waste packages, which in this analysis is assumed to be zero. The shape of the

rise is determined mostly by vadose zone properties, but is relatively unimportant when addressing performance objectives, since such objectives address peak values. The height of the step is determined by the contaminant release rate from the disposal system because the vadose zone does not store mobile or near-mobile contaminants; it only delays their reaching the groundwater.

Given that the contaminants enter the groundwater at a fairly constant rate (after a delay, due to travel in the vadose zone) and that the travel times in the groundwater are small compared to those in the vadose zone, the groundwater calculations use a time-independent source to calculate groundwater effects. Although some plume maps are provided, most groundwater results are presented as well intercept factors which are defined as the ratio of the contaminant concentration at the point of calculation (expressed as Ci/m^3) to the contaminant concentration entering the groundwater (expressed as Ci/m^3). The key parameters driving the well intercept factor are the groundwater flow velocities and the distance from the disposal facility. Groundwater flow velocities are themselves determined by geology, hydraulic conductivities, and differences in hydraulic "pressure" (including pumping speed at the well location).

The integration of calculations includes the adding of inventory and dosimetry information. The temporal shape of the results is dominated by the waste form release calculations. Thus, although time- and space-dependent information is displayed, for most of the sensitivity cases, the calculated impacts are tabulated only at 1,000 years, 10,000 years, and the time of maximum value.

All positions on the Hanford Site depicted in these sections are described using the Hanford coordinate system. One unit in this system equals 1 meter. Thus, distances are easily inferred.

4.2.2 Calculational Accuracy and Stability

All of the calculations were very stable and did not suffer significant mass loss. This is in contrast with the 1998 ILW PA where fractional mass balance errors of 3.5 percent occur after 50,000 years.

4.3 RESULTS OF GROUNDWATER SCENARIOS, BASE ANALYSIS AND BEST ESTIMATE CASES

The groundwater scenario is covered in many sections, so various key points can be emphasized in context.

4.3.1 Overview

This section presents the results of the analyses for the base analysis and best-estimate groundwater contamination cases. Sections 4.3.2 through 4.3.6 provide the results for the base analysis case and Sections 4.3.7 through 4.3.11 provide the results for the best-estimate case. The following sections provide the sensitivity analyses:

- Section 4.4 (moisture flow into the disposal facility)
- Section 4.5 (waste form release)

- Section 4.6 (vadose zone moisture flow and contaminant transport)
- Section 4.7 (groundwater flow and contaminant transport)
- Section 4.8 (other factors)
- Section 4.9 (extreme cases).

Section 4.10 describes the effect of other Hanford Site activities on the groundwater affected by this disposal action. Section 4.11 puts into context the information given in Sections 4.3 through 4.10.

4.3.2 Base Analysis Case: Moisture Flow Into Disposal Facility

> The surface barrier is assumed to have degraded to natural conditions; the side slope barrier remains in place; and no capillary barrier is present. Thus, the infiltration rate is 4.2 mm/year, except directly under the side slope where it increases to 50 mm/year.

The base analysis case assumes that the surface barrier has degraded to natural conditions and that no capillary barrier is present under the surface barrier. The side slope barrier connecting the surface barrier and the undisturbed soil remains, yielding a high recharge rate of 50 mm/year. Elsewhere a recharge rate of 4.2 mm/year (corresponding to Burbank loamy sands) is used. Because of the large size of the disposal facility, the small size of the side slope, and the strong vertical flow in such conditions, the moisture flow recharge rate into the facility is basically 4.2 mm/year everywhere. The recharge rate for the Burbank sandy loams is used, because it is higher than the natural recharge rate for the Rupert sands (0.9 mm/year), the other type of soil on the disposal site.

This simple case was chosen for the base analysis case not only to speed calculations, but because we recognize that the sand-gravel capillary barrier used in the best estimate case (Section 4.3.7) has not yet been designed. Because the sand-gravel capillary barrier results in much lower impacts, the base analysis case is conservative relative to the best estimate case.

4.3.3 Base Analysis Case: Waste Form Release

> The release rate from the disposal facility is based on deterministic simulation of the degradation of LAWABP1 glass and the resulting contaminant transport. The result is a small release that builds over long times, reaching 0.71 ppm/year at 10,000 years.

Time-dependent, one-dimensional calculations of waste form release and resulting contaminant transport were performed using LAWABP1 glass as the waste form. These calculations model the changing chemical environment as the waste form degrades and the various chemical reactions proceed. Figure 4-1 displays the volumetric water content (i.e., the fraction of the available pore volume occupied water) for the base case as a function of vertical position in the disposal facility. Because of the high sodium content of the glass, the pH inside the facility is a strong function of time and space. Figure 4-2 shows the variation of pH with vertical position for various times. Glass dissolution is a strong function of the pH in the surrounding fluid (see Section 3.4.4). Sensitivity cases are described in Section 4.5. The two-dimensional simulation is described in Section 4.5.8.

Figure 4-1. Moisture Content Inside the Disposal Facility for Various Recharge Rates. The base analysis case uses 4.2 mm/year.

The top of the disposal facility (below cap) is at 15 meters with the bottom at 4.5 m.

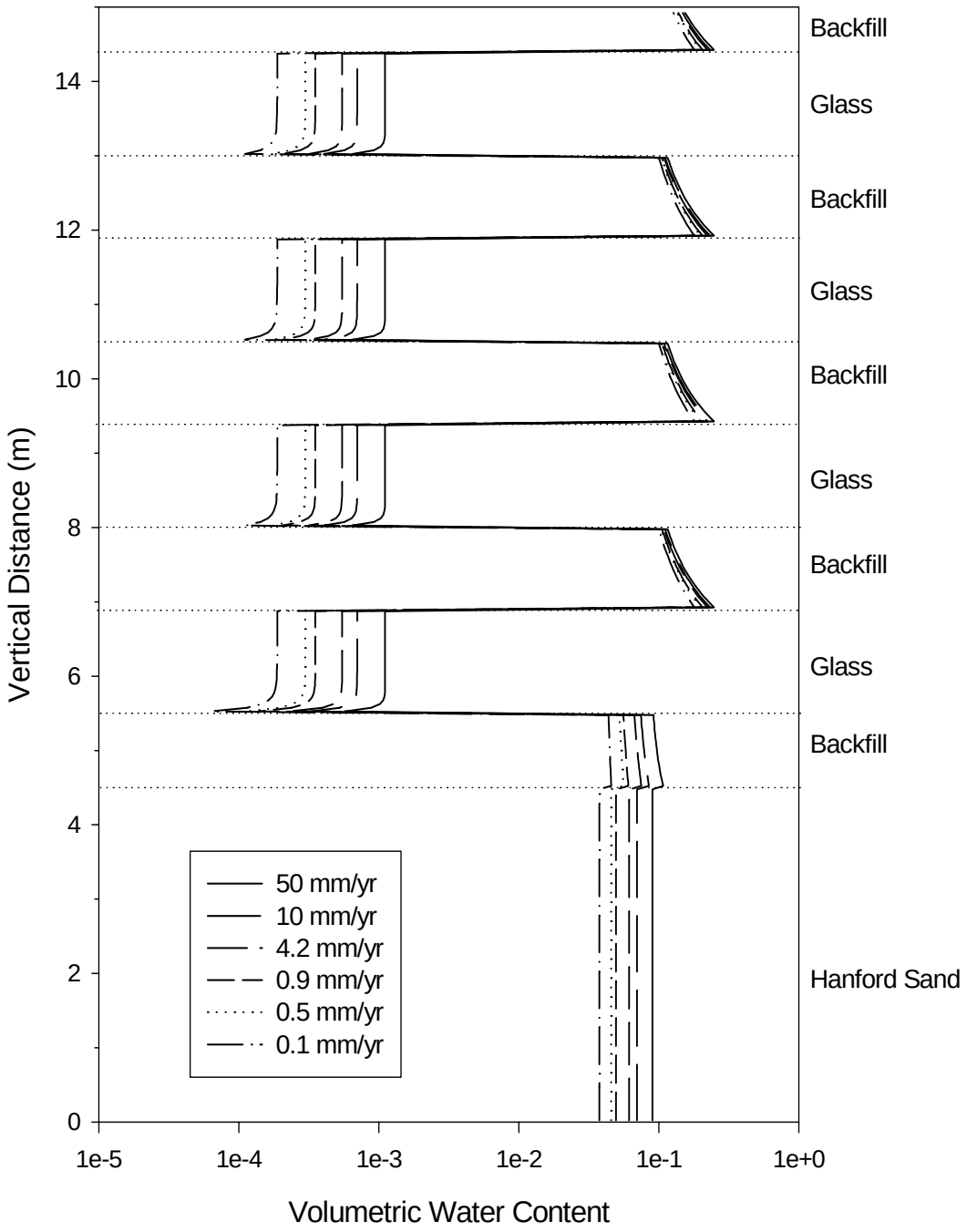

Figure 4-2. pH inside the Disposal Facility for Base Analysis Case.

The top of the disposal facility (below cap) is at 15 meters with the bottom at 4.5 m.

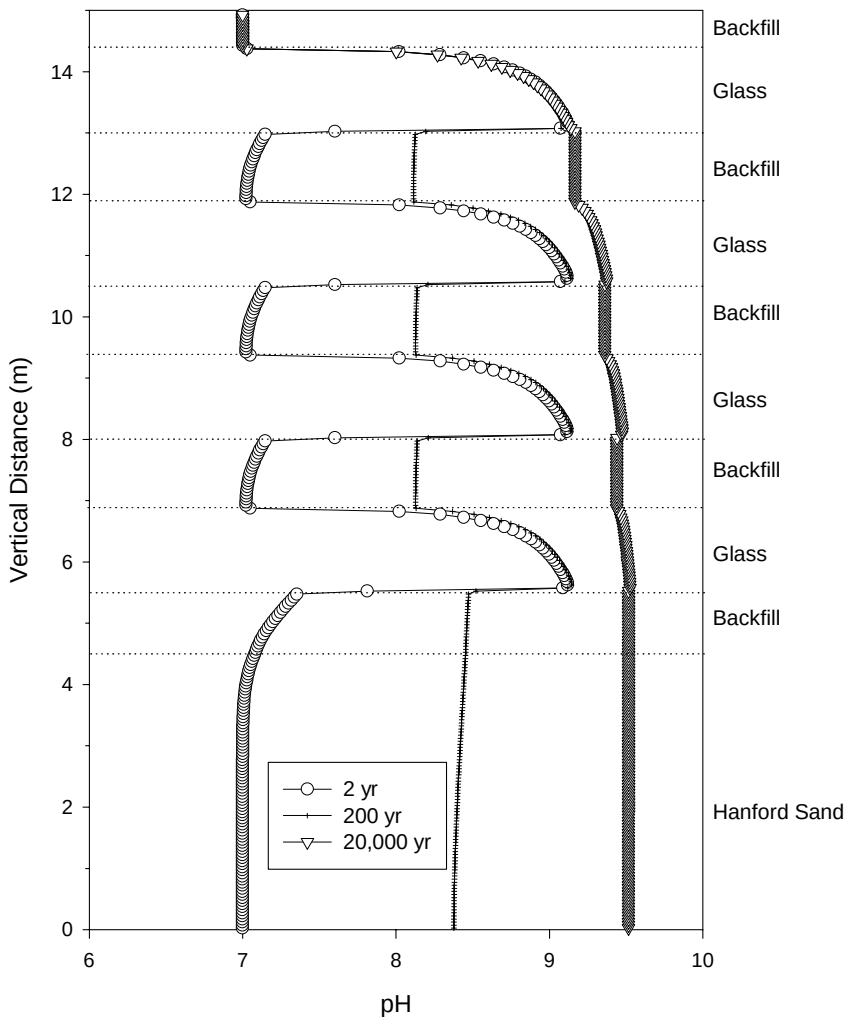

Figure 4-3 displays the results of the one-dimensional simulation of the waste form release as a function of time and space the disposal facility. Figure 4-4 displays the contaminant flux to the vadose zone from the disposal facility (assuming unit concentration initially for each contaminant) for the base case as well as for other recharge rates (ranging from 0.1 to 50 mm/year). (Section 4.5.4 discusses the effect of varying the amount of moisture flow.) Table 4-1 presents the inventory-normalized contaminant flux released to the vadose zone for various times for the base analysis case.

Figure 4-3. Waste Form Dissolution as a Function of Time and Space Inside the Disposal Facility.

The top of the disposal facility (below cap) is at 15 meters with the bottom at 4.5 m.

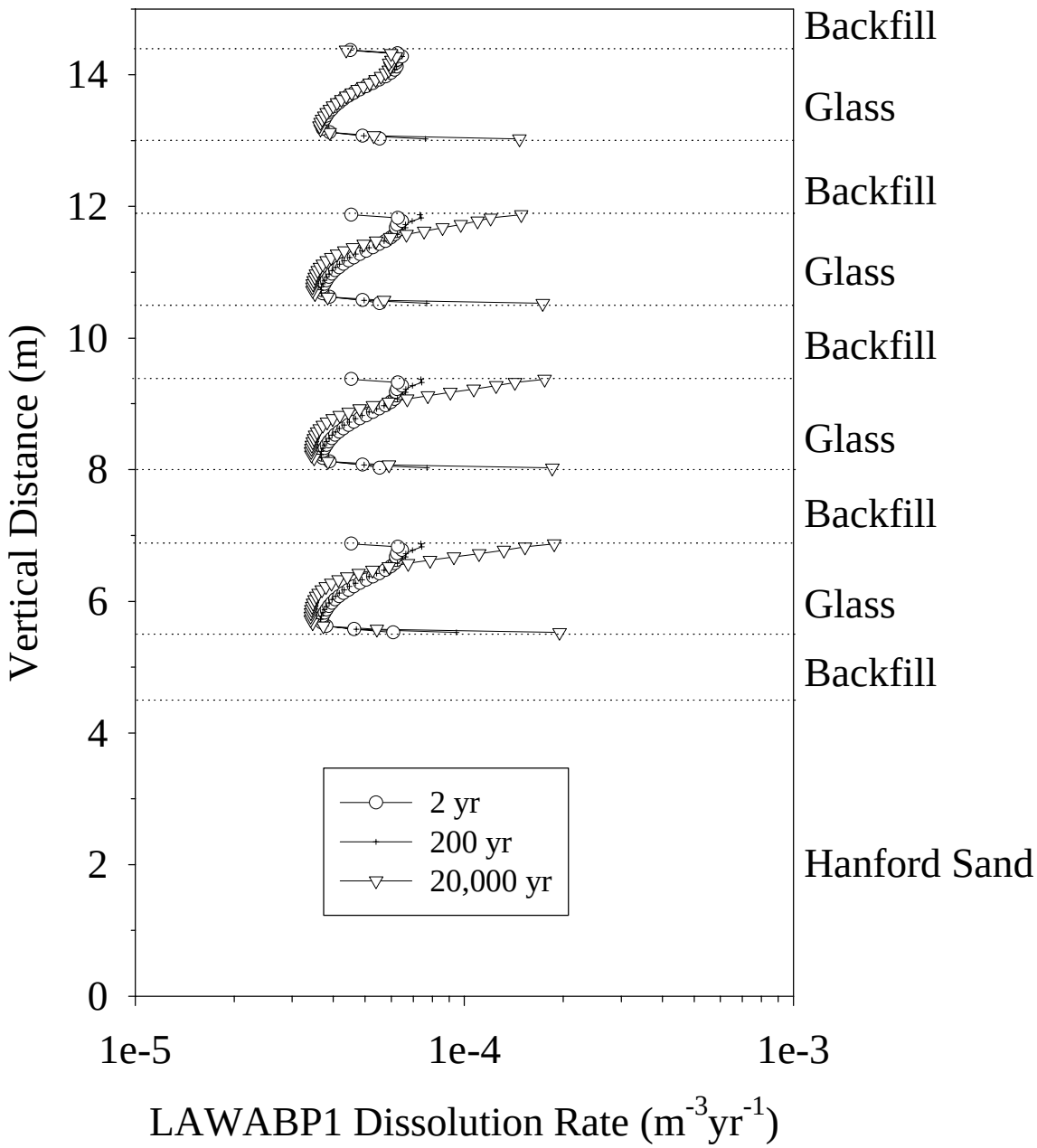

Figure 4-4. Relative Contaminant Flux to the Vadose Zone from the Disposal Facility (Assuming Unit Concentration Initially) for the Base Analysis Case and Other Infiltration Rates.

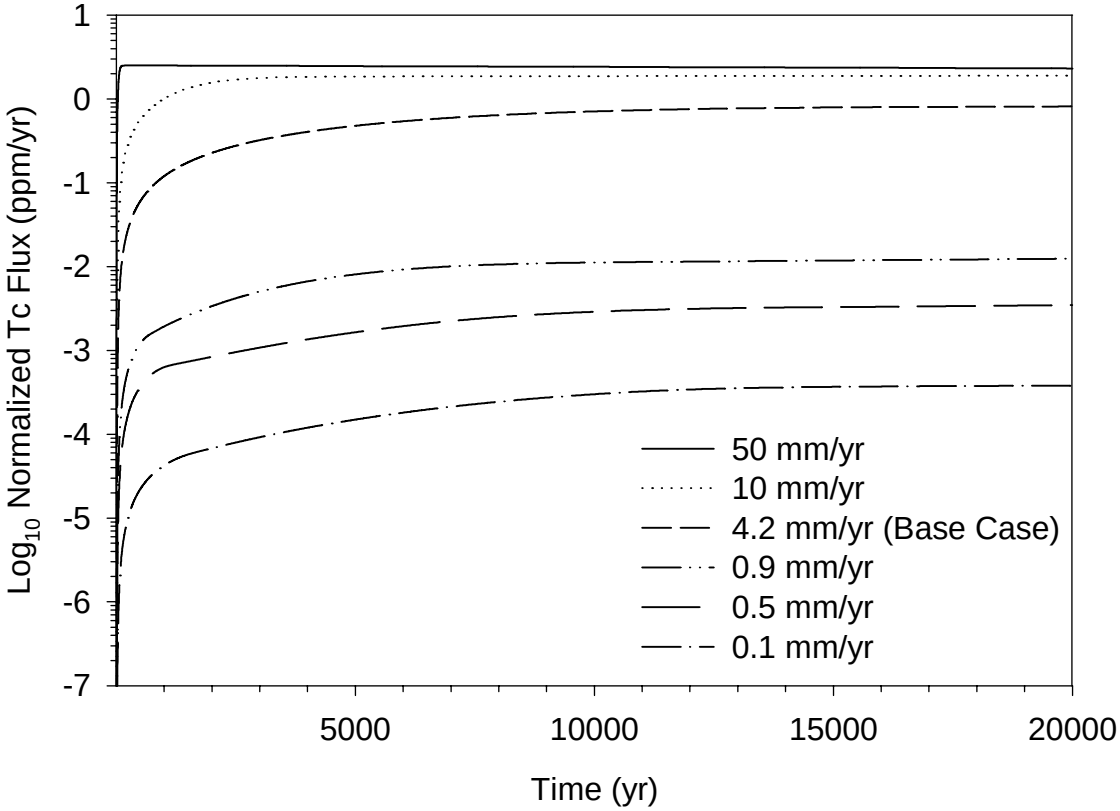

Table 4-1. Inventory-Normalized Contaminant Release to the Vadose Zone for Various Times for the Base Analysis Case.

Time (years)	Inventory-Normalized Contaminant Flux to the Vadose Zone (ppm/year)
500	0.06
1,000	0.12
2,000	0.23
5,000	0.48
10,000	0.71
20,000	0.81
50,000	0.87
100,000	0.93

The technetium flux released to the vadose zone is proportional to the TcO_4^- concentration at the lower boundary and the water flux rate. At early times, the TcO_4^- concentrations increase sharply in the glass surface layers. Glass dissolution and low water contents in the glass surface layers (Figure 4-1), coupled with a low water flux rate, causes TcO_4^- concentrations to increase rapidly in these layers. In contrast, mass transport from the glass layers is required to buildup technetium concentrations in the backfill layers. Therefore, concentrations in the backfill layers increase slowly as products of glass dissolution move from the glass layers into the backfill layers. Dilution also occurs in the backfill layers because of their much higher water content than the glass layers. Predicted glass dissolution rates (Figure 4-3) increase with time in each glass layer, but are relatively similar for each layer.

The glass dissolution rate for these simulations is highest on the edges of the glass layers. This is where the pH of the pore water is highest (Figure 4-2) and the SiO_2 (aq) concentrations are lowest. Because the glass dissolution rate is relatively low, the surface area of the glass does not decrease significantly by 20,000 years. The pH and TcO_4^- concentrations increase more rapidly in the glass layers early in the simulation, although by 20,000 years, concentrations throughout the profile are relatively similar. This indicates that at early times, the TcO_4^- flux across the lower boundary is limited by the movement rate of TcO_4^- from the glass layers.

4.3.4 Base Analysis Case: Moisture Flow And Contaminant Transport in the Vadose Zone

For the base analysis case, a time-independent surface recharge rate of 4.2 mm/year was assumed across the surface barrier, then 50 mm/year was assumed for the side slope and natural conditions (that is, for distances greater than 50 m from the trench center). The estimated moisture content for the far-field zone is shown for the base analysis case in Figure 4-5. The volumetric water content varies from 11 percent (directly beneath the disposal facility) to 15 percent (directly beneath the side slope area with a 50 mm/year recharge rate) for the Hanford formation sandy sequence, upper part of Figure 4-5. In the Hanford formation gravels, the volumetric water content is less and varies less (6 percent to 7.4 percent), lower part of Figure 4-5.

Figure 4-5. The Estimated Moisture Content for the Far-Field Zone for the Base Analysis Case.

The bottom of the disposal facility is at –10.5 m, i.e. just above the top of the figure. Distance is measured along the short dimension of the trench (See Figure 2-24).

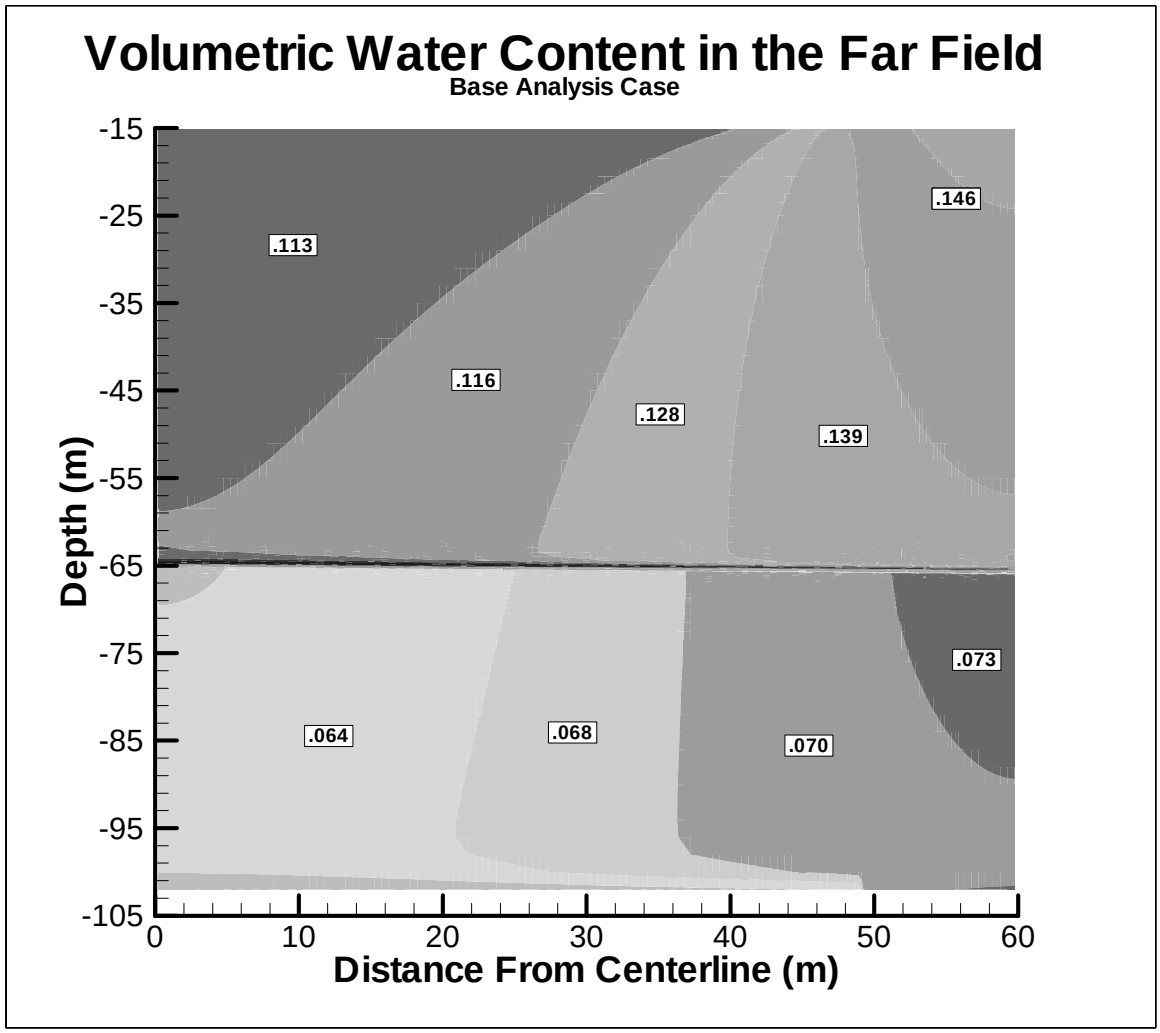

To calculate contaminant transport, the contaminant flux leaving the disposal facility and entering the vadose zone are needed along with the moisture field. To translate the waste form results from Section 4.3.3, the moisture flux (or Darcy flow) was calculated. As seen in Figure 4-6, for the base analysis case, the moisture flux is quite constant as a function of distance from the center of the trench to the edge, where the higher recharge rates exist. Also, as seen in Figure 4-6, the capillary break (best estimate case), the capillary break significantly reduces the moisture flow through the region containing the waste packages (x dimension is less than 32m, y dimension is between -1 and -10 m). A local 1-m subsidence in the failed capillary break leads to moisture flows approaching 2 mm/year below the subsidence. Finally, a shortened capillary break (short surface barrier) leads to higher Darcy velocities in the waste package region when compared to the best analysis case. See Section 4.4 for a discussion of these sensitivity cases.

Figure 4-6. Darcy Velocity at the Top of the Far Field (Bottom of the Disposal Facility).

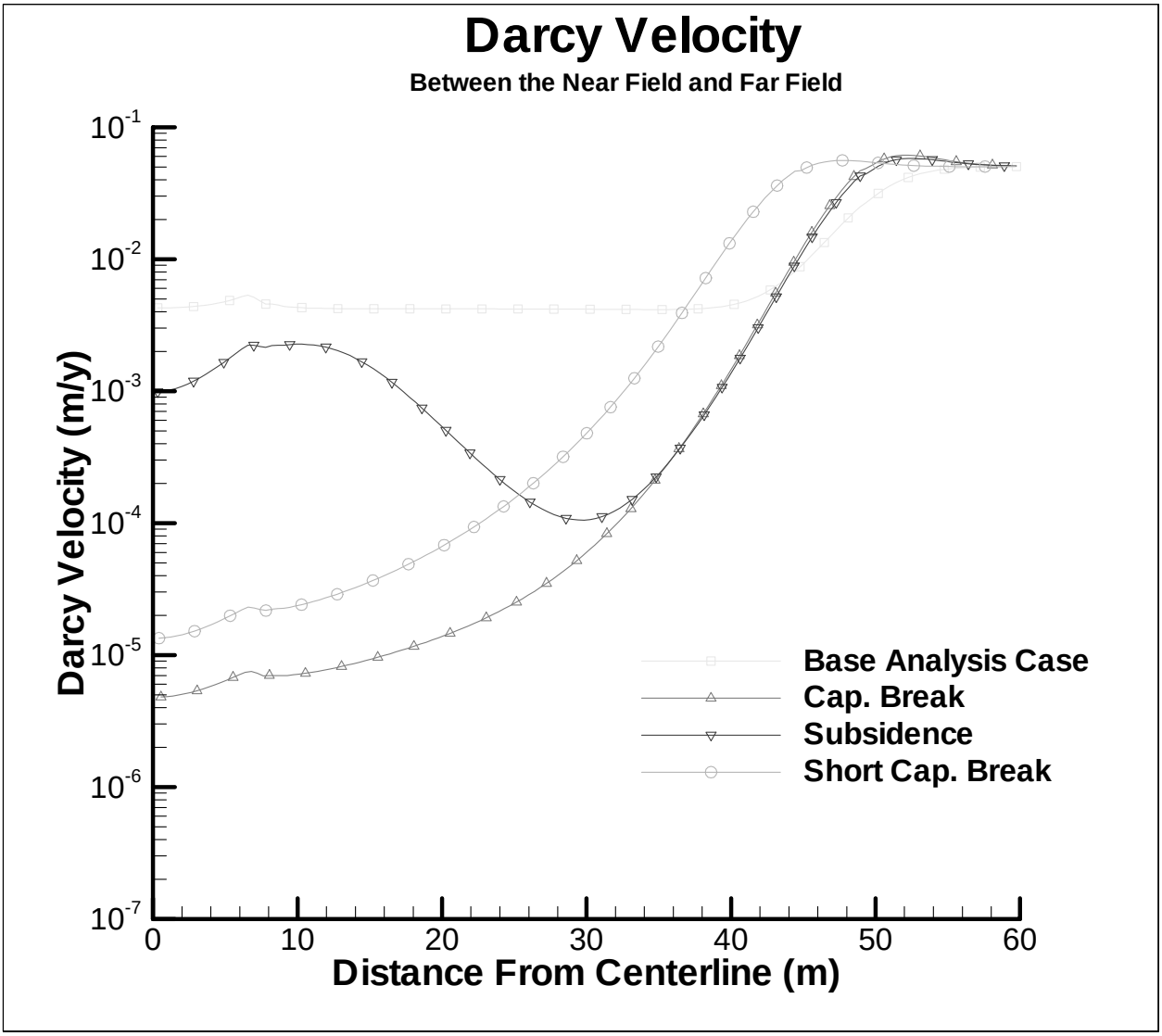

Figure 4-7 shows the result of combining the waste form release results and the moisture flow calculations. It also shows the inventory-normalized contaminant flux to the vadose zone (i.e., the flux leaving the disposal facility) at 1,000 years for the mobile contaminants for the base analysis case, the best estimate case, the shortened capillary break, and the capillary break subsidence case. The step-wise decrease in contaminant flux for the base analysis case is caused directly by the arrangement of four layers of waste packages in the disposal facility. Near the edge of the facility, fewer layers are present, so less inventory is available for release to the environment. The contaminant concentrations for the two cases where the capillary break is functioning are significantly lower than the base analysis case at 1,000 years. (For these two cases, we have assumed that the waste form release rate was equal to the waste form release rate calculated for a recharge rate of 0.1 mm/year. This assumption is conservative when calculating the contaminant transport to the aquifer. However, this assumption leads to a higher

Figure 4-7. Inventory-Normalized Mobile Contaminant Concentration at the Bottom of the Disposal Facility (i.e., Entering the Vadose Zone) at 1,000 years.

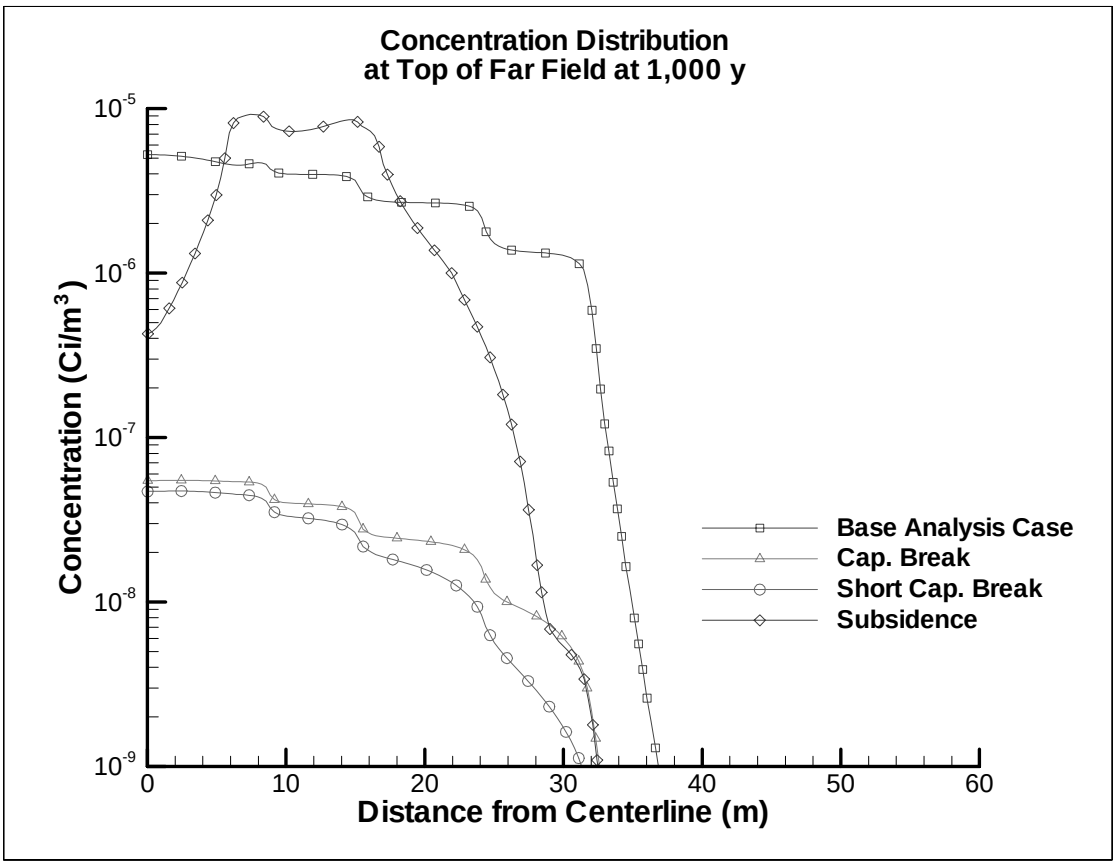

concentration at the bottom of the disposal facility for the best estimate case when compared to the shortened barrier because the contaminant release rate is the same and the shortened capillary break has a higher Darcy flux.) Finally, the case where subsidence is assumed to occur in the capillary break leads to contaminant concentrations higher than those associated with the base analysis case for a portion of the area directly beneath the discontinuity. For these sensitivity cases, the contaminant fluxes are nearer the centerline of the disposal facility than for the base analysis case because of the increased moisture flux

The contaminant flux then is calculated as a function of its position in the vadose zone, time, and K_d bin. Figure 4-8 displays the mobile contaminant concentration entering the groundwater at 10,000 years as a function of distance horizontally from the trench center. By the time the contaminants reach the groundwater, the sharp step features have dissolved. As seen in Figure 4-9, the total inventory-normalized contaminant flux entering the groundwater is similar to that leaving the disposal facility, except for the time delay.

Figure 4-8. Mobile Contaminant Concentration Just Prior to Entering the Groundwater at 10,000 Years.

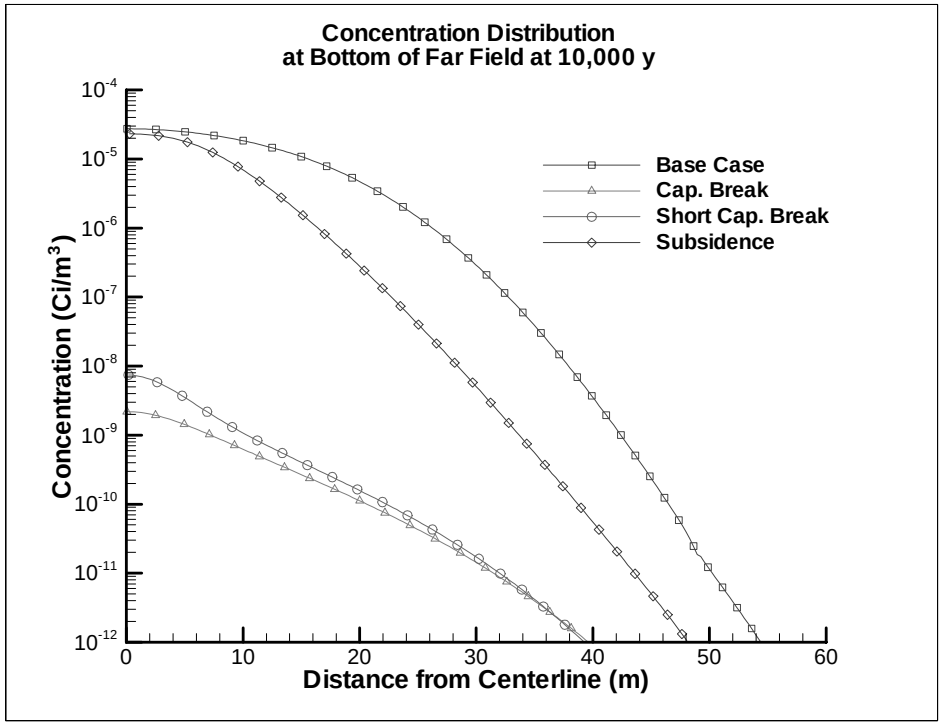

Figure 4-9. Inventory-Normalized Contaminant Flux Summed Over Horizontal Distance as a Function of Time and K_d Bin (Linear Scale).

"Facility Release" refers to values just below the disposal facility.

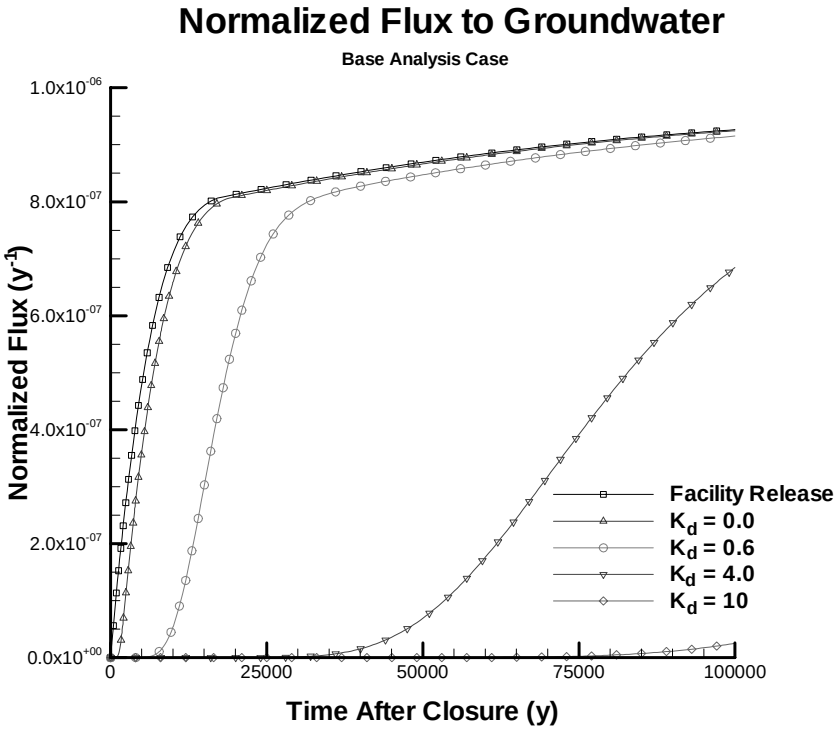

Figure 4-10 shows the contaminant flux summed over horizontal distance as a function of time and K_d bin. Only the mobile contaminants reach the groundwater during the time of compliance (the first 1,000 years). At 10,000 years, the slightly retarded contaminants (K_d = 0.6 mL/g) also are beginning to reach the groundwater, but their inventory-normalized contribution is still approximately 1 order of magnitude less than the mobile contribution. Higher K_d contaminants ($K_d \geq 4$ mL/g) do not contribute to the estimated doses at 10,000 years and are even less important.

Figure 4-10. Inventory-Normalized Contaminant Flux Summed Over Horizontal Distance as a Function of Time and K_d Bin (Logarithmic Scale).

"Facility Release" refers to values just below the disposal facility.

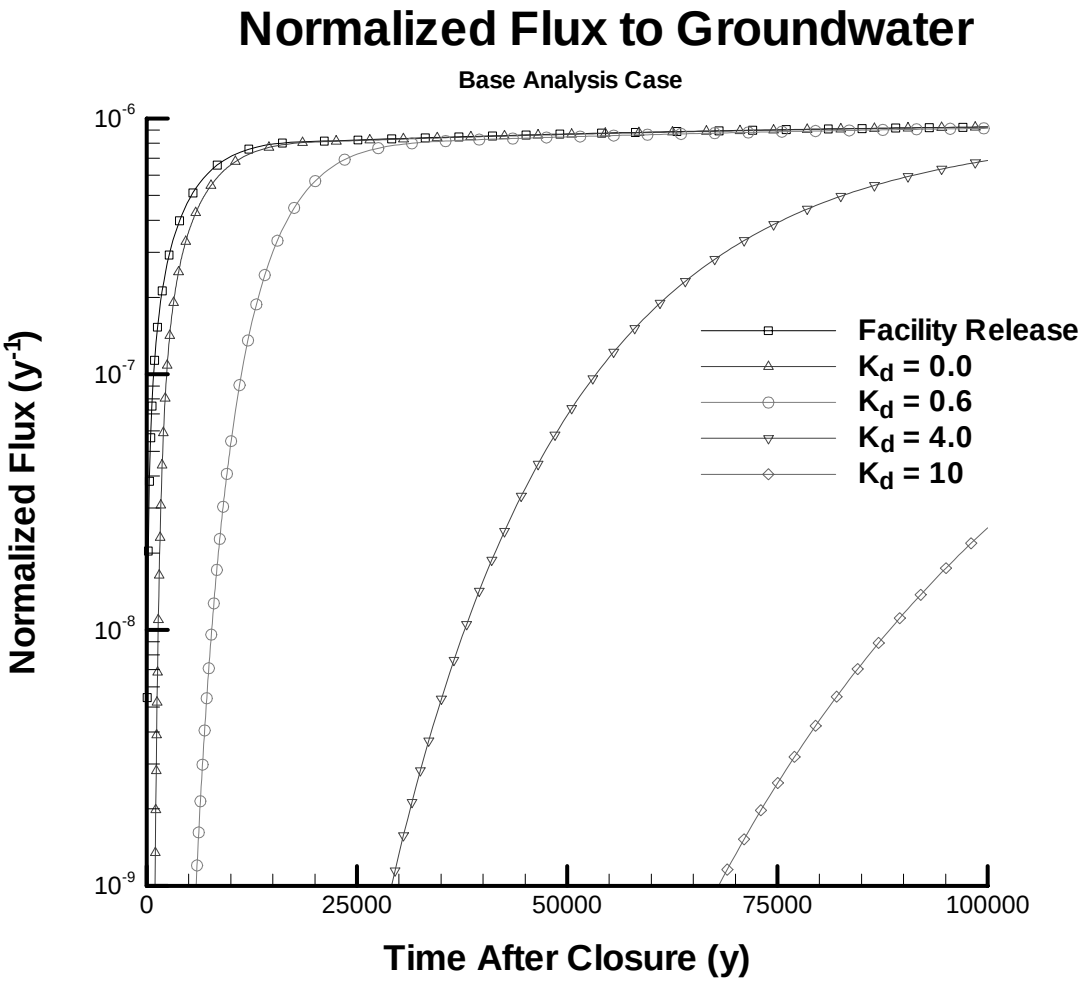

4.3.5 Base Analysis Case: Moisture Flow And Contaminant Transport in Groundwater

As noted in Section 2.8, the disposal site lies on top of the ancient channel of the Columbia River. This channel has high hydraulic conductivity and hence is a conduit for groundwater flow. Much greater dilution is estimated in this PA than in the 1998 PA (Mann 1998a).

The contaminant travel time in the vadose zone for even the most mobile contaminants will be about a thousand years. Thus, by the time the contaminants reach the groundwater, the unconfined aquifer will not be influenced by Hanford Site operations. The full Hanford Site groundwater model was used to establish boundary conditions for the local model. Figure 4-11 displays the water table elevation predicted by the local groundwater model for such future conditions.

Figure 4-11. Water Table Elevation Predicted by the Hanford Site Groundwater Model for Steady-State Conditions After Hanford Site Operations.

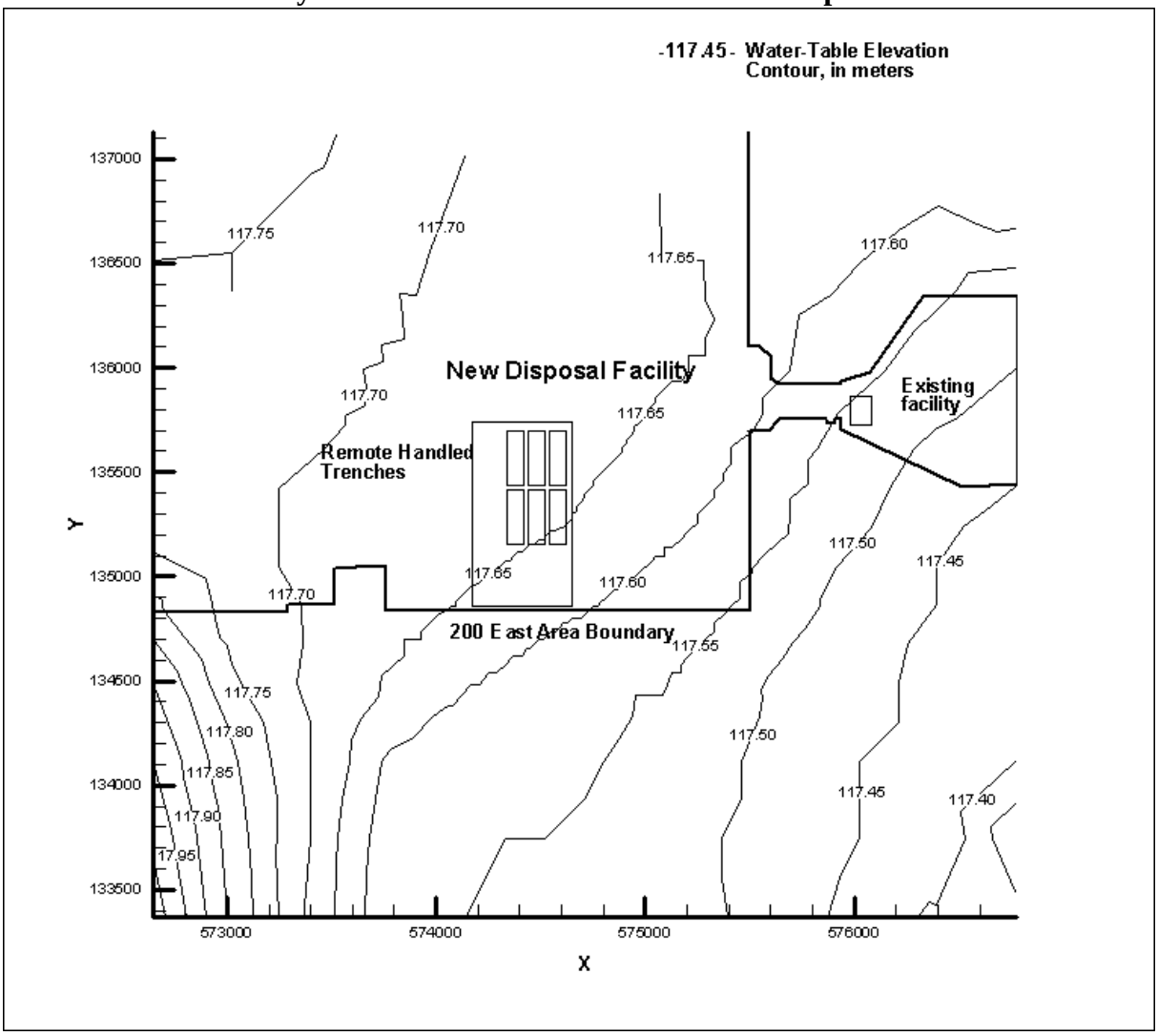

Using this flow field, contaminant groundwater concentrations were calculated assuming a unit contaminant flux entering the groundwater directly beneath the disposal facility. Figure 4-12 displays the resulting contaminant plume in the horizontal dimensions, while Figure 4-13 displays the vertical distribution along the line A-A' (defined in Figure 4-12), which is near the centerline of the plume.

Figure 4-12. Base Analysis Case Contaminant Groundwater Plume at the Water Table, Showing the Contaminant Concentration Values.

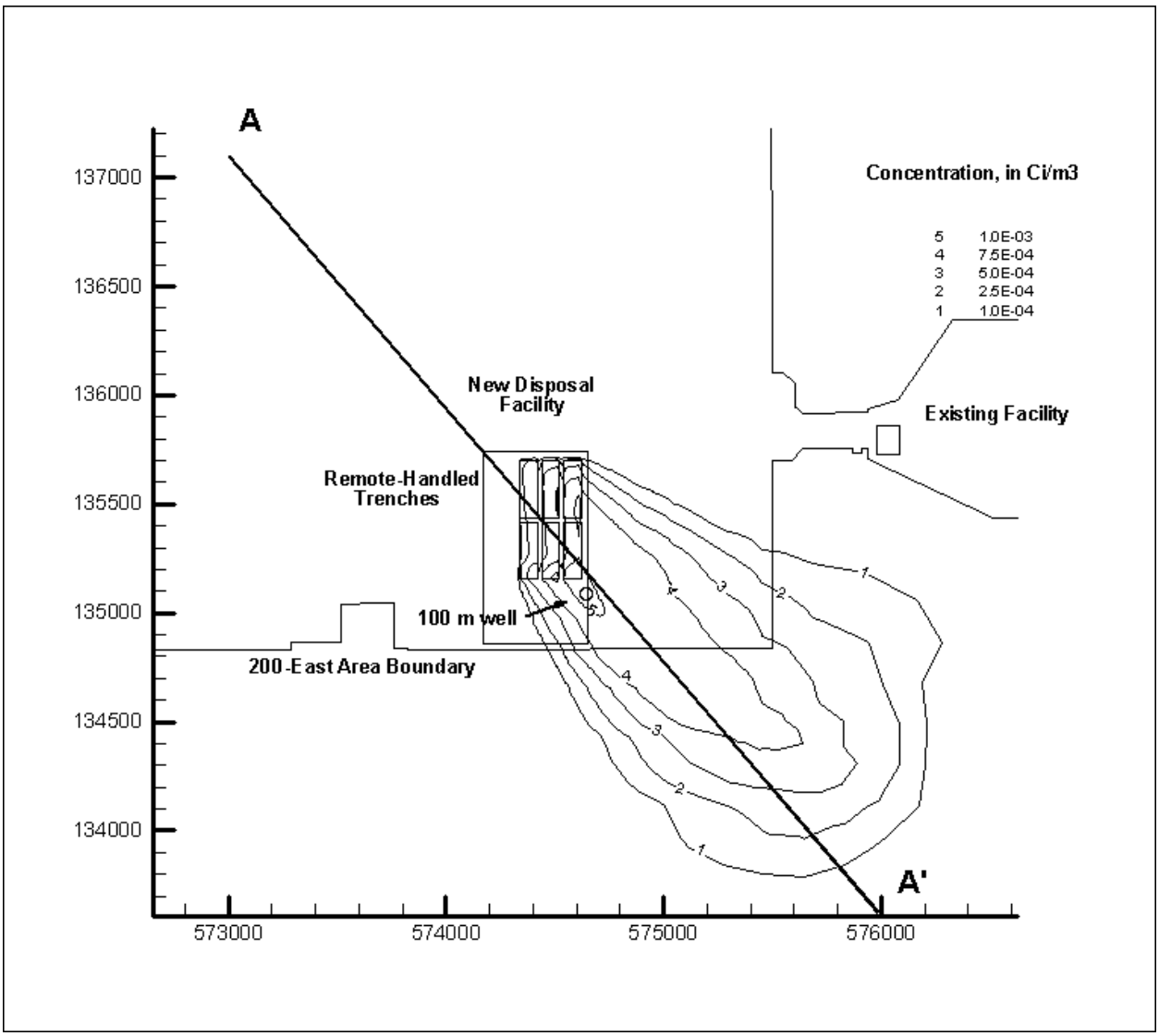

Figure 4-13. Vertical Distribution of the Groundwater Plume Along the Line A-A', Which Is Near the Centerline of the Plume.

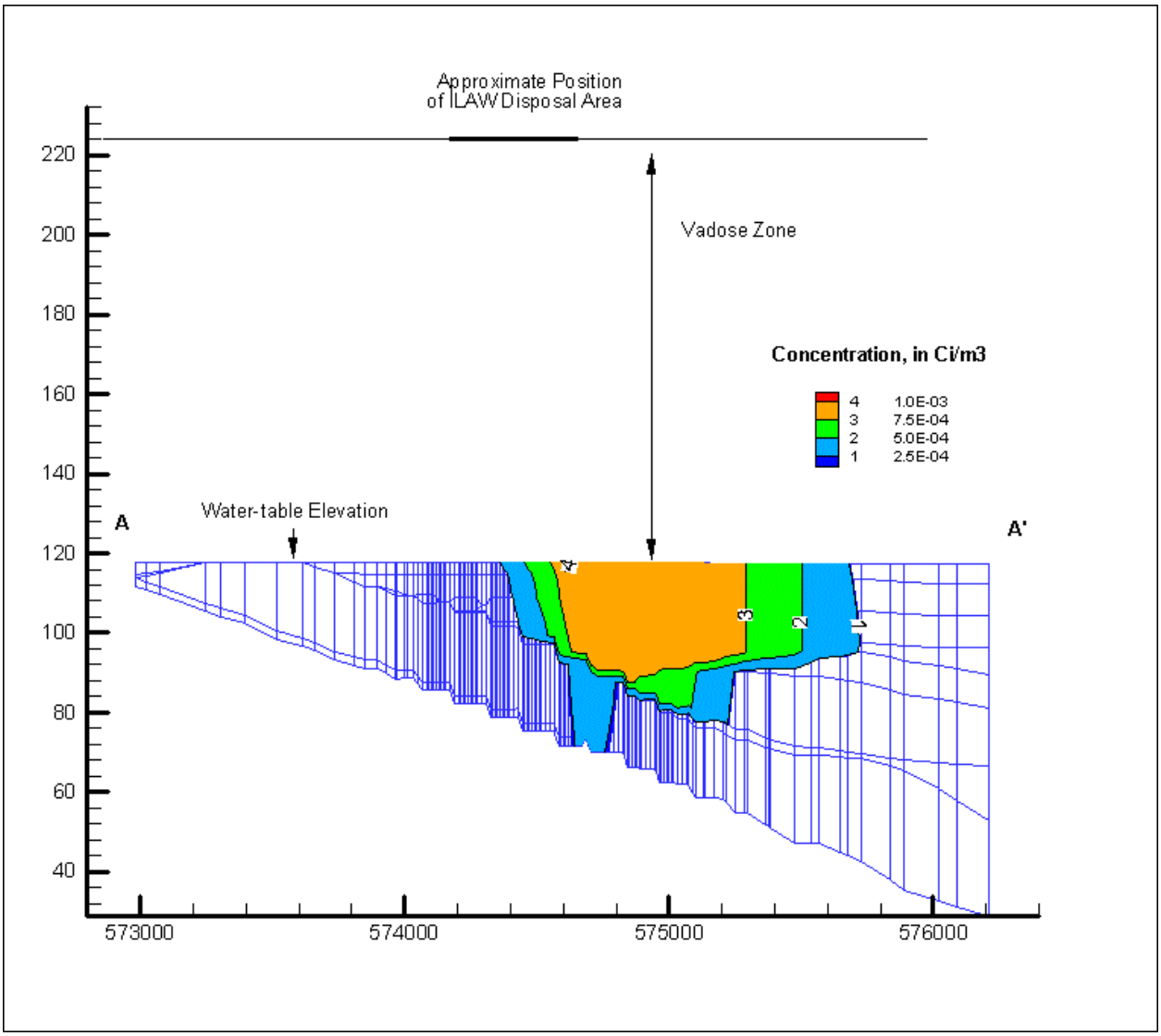

From these results, the well intercept factor (WIF) can be calculated. The well intercept factors for wells at 100 m and 1,000 m as a function of time are displayed in Figure 4-14. The well intercept factor quickly reaches asymptotic values of 1.05×10^{-3} and 0.78×10^{-3} (respectively for the 100 m and 1,000 m wells) for trenches located in the northern part of the ILAW disposal site. That the groundwater concentration quickly reaches the asymptotic value is not unexpected given the high conductivity in the ancestral Columbia River channel and the nearness of the observation points.

The small decrease in the WIF between 100 and 1000 m is expected given the relatively short distance of transport within the underlying high permeabilities of the Hanford gravels. The effect of the high permeabilities is quite evident in Figure 4-12 and will become more evident when a different location is discussed in Section 4.7.2.

Figure 4-14. Well Intercept Factor for Wells at 100 m and 1,000 m as a Function of Time for the Base Analysis Case.

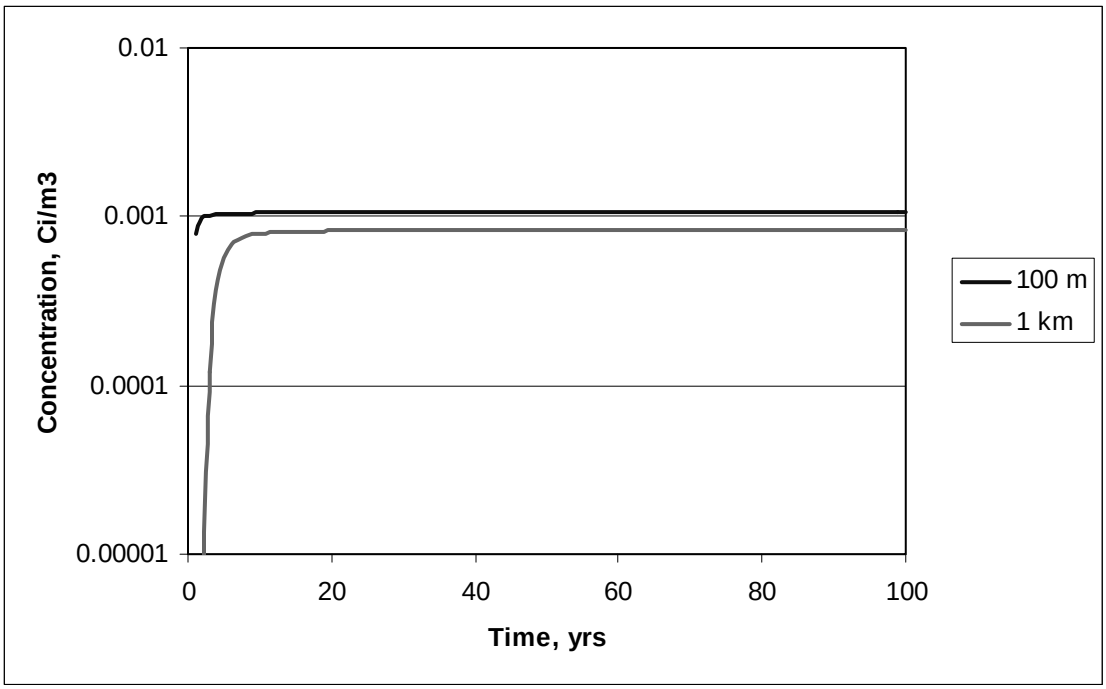

To calculate groundwater concentrations at greater distances from the disposal facility, the full-scale Hanford Site groundwater model was used. Figure 4-15 displays the asymptotic areal distribution of the contaminant plume for greater distances, while Table 4-2 shows the values. Because the full-scale model uses different grid sizes than the local scale model and because the effect of the ancestral Columbia River channel is better represented in the local scale model, the calculated groundwater concentrations differ at 1000m (5.4×10^{-4} versus 7.8×10^{-4}). Figure 4-16 provides the time history of the groundwater concentrations at the greater distances. Again the travel times (as compared to the vadose zone travel times or the waste form degradation times) are quite short. The travel time to the Columbia River is on the order of 200 to 300 years.

Figure 4-15. Asymptotic Areal Distribution of the Contaminant Groundwater Plume for Large Distances.

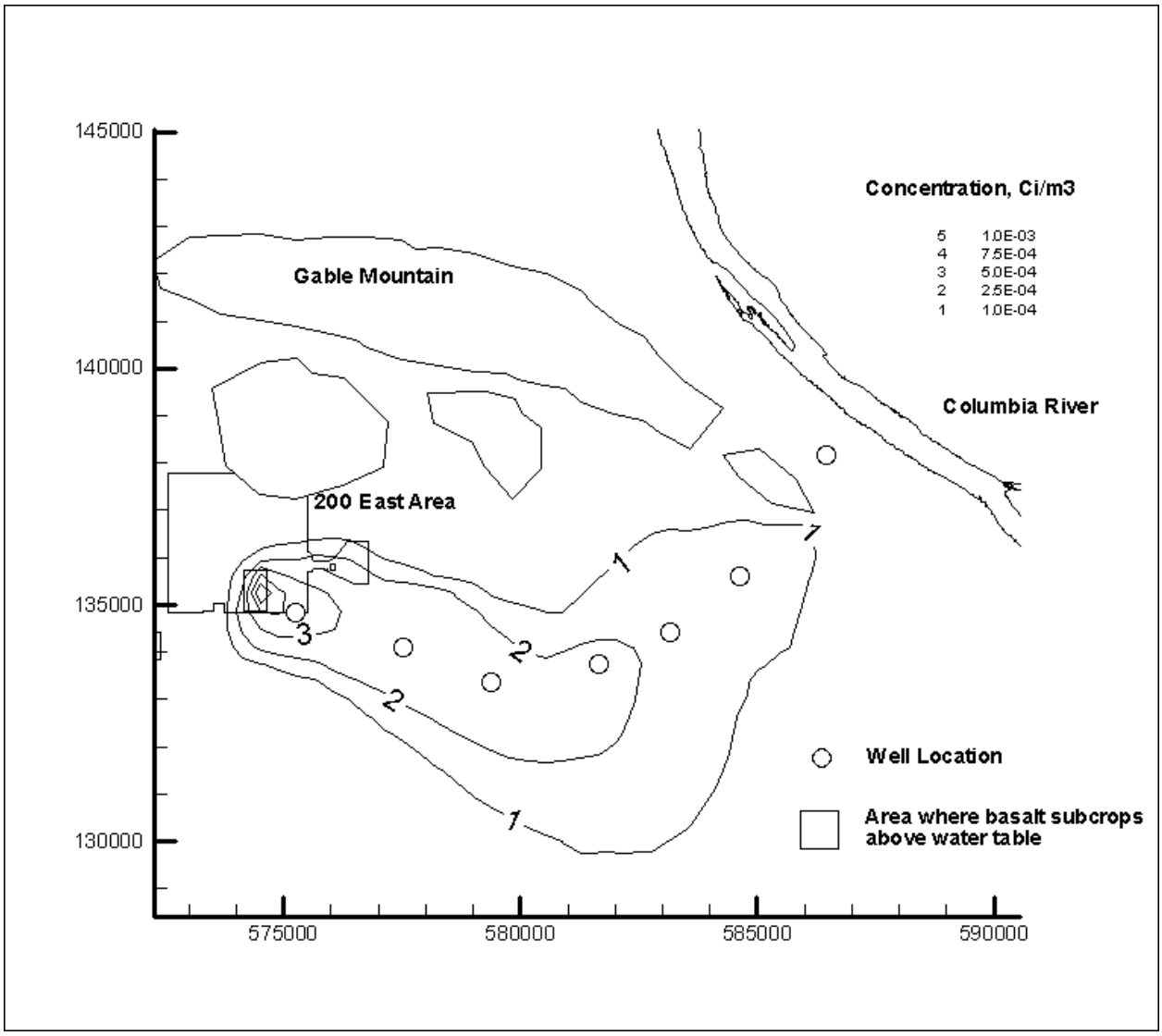

Table 4-2. Well Intercept Factors.

Distance* (km)	Local Model	Hanford Site Model
0.1	1.05E-03	
1.0	7.8E-04	5.4E-04
3.1		3.8E-04
5		3.3E-04
7.6		2.8E-04
9.3		2.4E-04
11.1		1.9E-04
14.8 (river well)		9.8E-05

*Approximate downgradient distances from disposal facilities for well locations shown in Figure 4-15.

Figure 4-16. Time History of Groundwater Concentrations At The Greater Distances.

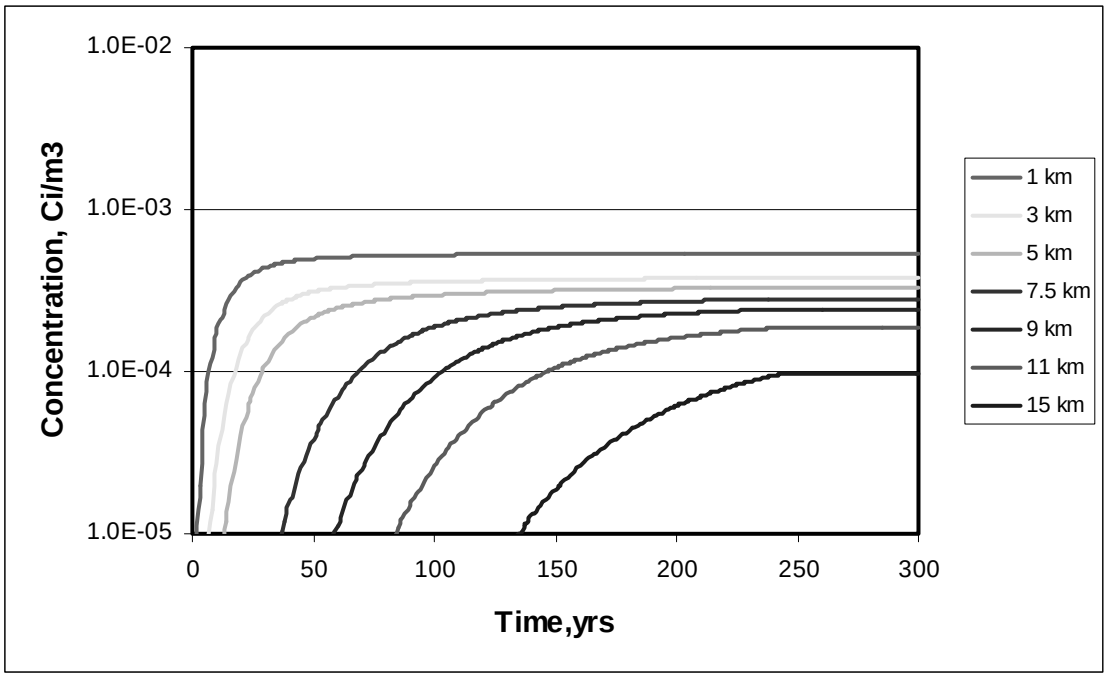

4.3.6 Base Analysis Case: Conversion into Dose

Once the contaminant concentrations are calculated, it is relatively simple to convert the results into dose using the dosimetry parameters from Section 3.4.7. Table 4-3 displays the estimated impact from the base analysis case for a well 100 m downgradient from the disposal facility. As can be seen, all the calculated levels are quite low.

In the 1998 ILAW performance assessment (Mann 1998a), the most restrictive impact was caused by the drinking water dose from beta- and photon-emitting radionuclides. At 10,000 years, this dose was calculated to be 2.0 mrem in a year resulting mainly from ^{99}Tc (75 percent) and ^{79}Se (20 percent). This performance assessment shows much lower numbers at 10,000 years (0.010 mrem/y). The highest value calculated for the beta/photon drinking water dose is 0.013 mrem/year at about 76,500 years. Table 4-4 shows the major contributions at 1,000 years and 10,000 years to the estimated beta and photon drinking water dose at a well 100 m downgradient from the disposal facility. Figure 4-17 shows the time dependence. In this assessment, ^{99}Tc is still the most important radionuclide, contributing approximately 58 percent of the dose at 1,000 and 10,000 years. However, the next most important radionuclide is ^{129}I, which contributes approximately 42 percent at 1,000 and 10,000 years. The switch of selenium and iodine is a direct result of site-specific data increasing selenium's K_d from 0. to 4.0 mL/g and decreasing iodine's K_d from 3.0 to 0 mL/g (see Section 3.4.3.3).

The all-pathways dose, like the drinking water dose, is small. Table 4-5 shows the major contributions at 1,000 years and 10,000 years to the estimated all-pathways dose at a well 100 m downgradient from the disposal facility. Figure 4-18 shows the time dependence. The major contaminants of concern at short times are ^{99}Tc and ^{129}I, with the uranium isotopes and ^{237}Np

becoming more important at approximately 10,000 years. The maximum all-pathways dose was calculated at about 100,000 years, having a value of 0.6 mrem/year.

As in the 1998 ILAW performance assessment, the concentration of alpha emitters is small because they are not mobile in the Hanford formation soils. Table 4-6 shows the major contributions at 10,000 years to the estimated concentration of alpha emitters at a well 100 m downgradient from the disposal facility. Figure 4-19 shows the time dependence. Again the concentration of alpha emitters is small. No significant concentration of alpha-emitting radionuclides occurs before 3,000 years. The uranium isotopes and ^{237}Np are the major drivers.

As one progresses from the disposal site, the impacts of alpha emitters become less. Table 4-7 displays the impacts at 100 m and 1000 m from the disposal facility, as well as at a well just before the groundwater mixes with the Columbia River. As noted in the groundwater section (Section 4.3.5), the impacts do not drop quickly for distances close to the disposal facility because of the presence of the ancestral Columbia River channel. At the Columbia River, the impacts are reduced by a factor of 9 because of radionuclide dispersion in the groundwater.

The impact from chemicals in the waste form is very small. Table 4-8 displays the estimated impacts at 1,000 and 10,000 years to the groundwater. Because all chemicals are treated as mobile, they have a similar time dependence as the ^{99}Tc curve shown in Figure 4-18. Similarly, Table 4-9 displays the estimated impacts to the surface water calculated at a well just before entering the Columbia River. Again, the estimated impacts to both the groundwater and surface waters are at least a factor of 1,000 lower than the performance goals.

Table 4-3. Estimated Impacts from the Base Analysis Case for a Well 100 m Downgradient from the Disposal Facility.

Type of Impact	Value at		Performance Objective
	1000 years*	10,000 years	
Dose (mrem in a year) from beta- and photon-emitting radionuclides in drinking water	0.000021	0.0102	4.0
All-pathways dose (mrem in a year)	0.000078	0.070	25.0
Concentration (pCi/L) of alpha-emitting radionuclides	1.0×10^{-16}	0.034	15.0
Radium concentration (pCi/L)	0.0	0.0	3.0
Uranium concentration (pCi/L)	0.0	0.025	----

*Time of compliance is 1,000 years.

Table 4-4. Major Radionuclide Contributors at 1,000 Years and 10,000 Years to the Estimated Beta/Photon Drinking Water Dose at a Well 100 m Downgradient from the Disposal Facility.

Radionuclide	1,000 years*		10,000 years	
	Dose (mrem/yr)	Fraction	Dose (mrem/yr)	Fraction
^{99}Tc	0.0000123	0.58	0.00584	0.57
^{129}I	0.0000088	0.41	0.00434	0.43
Others	0.0000002	0.01	0.00002	0
Total	0.0000213	----	0.0102	-----

*Time of compliance is 1,000 years.

Figure 4-17. Time Dependence of the Estimated Beta/Photon Drinking Water Dose at a Well 100 m Downgradient from the Disposal Facility.

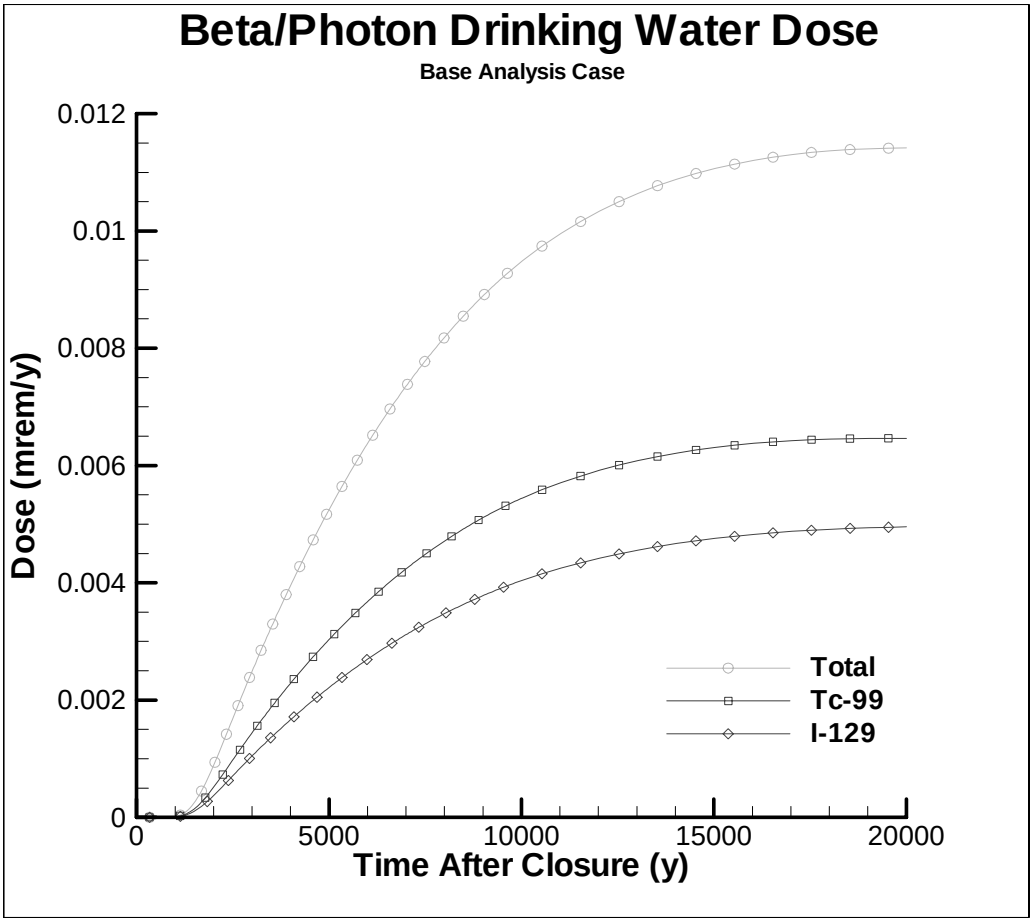

Table 4-5. Major Radionuclide Contributors at 1,000 Years and 10,000 Years to the Estimated All-Pathways Dose at a Well 100 m Downgradient from the Disposal Facility.

Radionuclide	1,000 years*		10,000 years	
	Dose (mrem/yr)	Fraction	Dose (mrem/yr)	Fraction
^{99}Tc	0.0000552	0.71	0.0262	0.37
^{129}I	0.0000224	0.29	0.0110	0.16
^{231}Pa	0.0	0.0	0.00048	0.01
^{233}U	0.0	0.0	0.00310	0.04
^{234}U	0.0	0.0	0.00104	0.01
^{238}U	0.0	0.0	0.00108	0.02
^{237}Np	0.0	0.0	0.0270	0.39
Other	0.0000002	0.0	0.0001	0.0
Total	0.0000778	----	0.0700	-----

*Time of compliance is 1,000 years.

Figure 4-18. Time Dependence of the Estimated All-Pathways Dose at a Well 100 m Downgradient from the Disposal Facility.

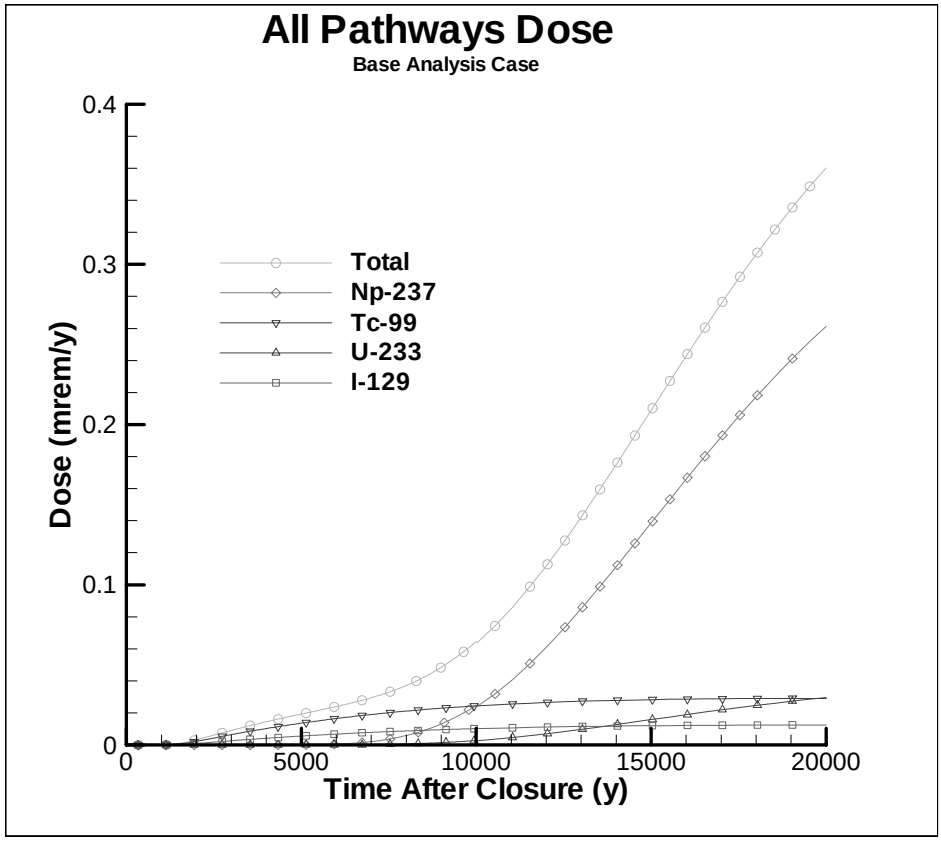

Table 4-6. Major Radionuclide Contributors at 10,000 Years to the Estimated Concentration of Alpha Emitters at a Well 100 m Downgradient from the Disposal Facility. No Significant Concentration Occurs Before 3,000 Years.

Radionuclide	10,000 years	
	Concentration (pCi/L)	Fraction
^{231}Pa	0.0000684	0.00
^{233}U	0.0142	0.42
^{234}U	0.00486	0.14
^{235}U	0.000199	0.01
^{236}U	0.000167	0.0
^{238}U	0.00530	0.16
^{237}Np	0.00910	0.27
Other	0.0000055	0.00
Total	0.0339	-----

Figure 4-19. Time Dependence of the Concentration of Alpha Emitters Dose at a Well 100 m Downgradient from the Disposal Facility.

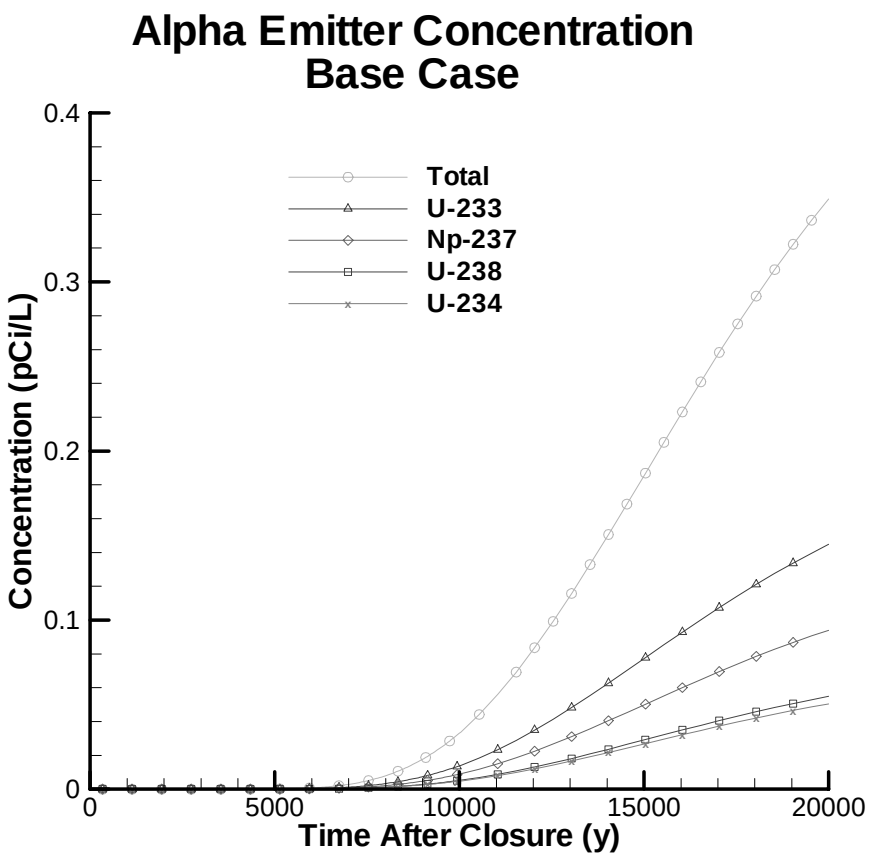

Table 4-7. Estimated Impacts at 1,000 Years from the Base Analysis Case for a Well at Various Locations Downgradient from the Disposal Facility.

Type of Impact	Estimated Impact at 1,000 year* at Well Location		
	100 m	1,000 m	Just Before Entering the Columbia River
Dose (mrem in a year) from beta/photon radionuclides in drinking water	2.13×10^{-5}	1.58×10^{-5}	1.98×10^{-6}
All-pathways dose (mrem in a year)	7.78×10^{-5}	5.78×10^{-5}	7.26×10^{-6}
Concentration (pCi/L) of alpha-emitting radionuclides	1.02×10^{-16}	7.58×10^{-17}	9.99×10^{-18}
Radium concentration (pCi/L)	0.0	0.0	0.0
Uranium concentration (pCi/L)	0.0	0.0	0.0

*Time of compliance is 1,000 years

Table 4.8. Impacts from Chemicals at 1,000 Years and 10,000 Years at a Well 100 m Downgradient from the Disposal Facility.

Chemical	Performance Goal (mg/L) [1]	Estimated Impact (mg/L) @ 1,000 y [2] Nominal Inventory	Estimated Impact (mg/L) @10,000 y	
			Nominal Inventory[4]	Upper Bound Inventory[4]
Ammonia (NH_3)	NA	0.00E+00	0.00E+00	6.63E-04
Antimony (Sb)	0.006	0.00E+00[3]	0.00E+00[3]	0.00E+00[3]
Arsenic (As)	0.00005	4.75E-11	2.33E-08	5.49E-08
Barium (Ba)	1	5.02E-11	2.46E-08	4.48E-06
Beryllium (Be)	0.004	1.66E-12	8.12E-10	2.88E-07
Cadmium (Cd)	0.005	1.70E-10	8.33E-08	1.11E-06
Chlorine (Cl)	250	2.51E-06	1.23E-03	1.24E-03
Chromium (Cr)	0.05	7.40E-07	3.62E-04	8.89E-04
Copper (Cu)	1	1.98E-12	9.70E-10	8.35E-07
Cyanide (CN)	0.2	0.00E+00	0.00E+00	1.44E-04
Fluorine (Fl)	4	2.68E-06	1.31E-03	1.59E-03
Iron (Fe)	0.3	1.21E-07	5.93E-05	1.85E-03
Lead (Pb)	0.05	2.11E-08	1.04E-05	1.11E-04
Manganese (Mn)	0.05	3.73E-08	1.83E-05	2.59E-04
Mercury (Hg)	0.002	5.19E-10	2.54E-07	2.78E-06
Nickel (Ni)	NA	8.24E-08	4.03E-05	2.38E-04
Nitrate (NO_3)	10	0.00E+00	0.00E+00	6.94E-02
Nitrite (NO_2)	1	0.00E+00	0.00E+00	1.67E-02
Nitrite plus Nitrate	10	0.00E+00	0.00E+00	8.61E-02
Selenium (Se)	0.01	1.44E-12	7.05E-10	1.61E-09
Silver (Ag)	0.05	2.92E-10	1.43E-07	4.01E-06

Table 4.8. Impacts from Chemicals at 1,000 Years and 10,000 Years at a Well 100 m Downgradient from the Disposal Facility.

Chemical	Performance Goal (mg/L) [1]	Estimated Impact (mg/L) @ 1,000 y [2] Nominal Inventory	Estimated Impact (mg/L) @10,000 y	
			Nominal Inventory[4]	Upper Bound Inventory[4]
Sulphate (SO_4)	250	9.16E-06	4.48E-03	5.17E-03
Thallium (Tl)	0.002	0.00E+00	0.00E+00	6.72E-05
Uranium (U-total)	NA	4.67E-08	2.29E-05	1.01E-04
Zinc (Zn)	5	5.35E-09	2.62E-06	7.66E-06
1,1,1-Trichlorethane	0.003	0.00E+00	0.00E+00	1.21E-06
1,1,2,2,-Tetrachloroethane	0.005	0.00E+00	0.00E+00	0.00E+00
1,1,2-Trichlorethylene	0.005	0.00E+00	0.00E+00	1.21E-06
1,1,2-Trichloroethane	0.005	0.00E+00	0.00E+00	1.21E-06
1,4-Dichlorobenzene	0.004	0.00E+00	0.00E+00	1.21E-06
Benzene	0.001	0.00E+00	0.00E+00	2.02E-06
Carbon tetrachloride	0.0003	0.00E+00	0.00E+00	1.21E-06
Chloroform	0.007	0.00E+00	0.00E+00	1.21E-06
Dichloromethane (Methylene chloride)	0.005	0.00E+00	0.00E+00	6.07E-06
Ethyl benzene	0.1	0.00E+00	0.00E+00	2.02E-06
N-butyl alcohol	NA	0.00E+00	0.00E+00	5.26E-07
o-Xylene	0.7	0.00E+00	0.00E+00	6.07E-06
Toluene	1	0.00E+00	0.00E+00	2.02E-06

[1]Groundwater performance goal (see Table 1.4).
[2]1,000 years is the time of compliance.
[3]Antimony inventory assumed equal to zero.
[4] Nominal and upper bound inventory are defined in Section 3.2.3.
NA Not Applicable

Table 4-9. Impacts from Chemicals at 1,000 Years and 10,000 Years at a Well Just Before Entering the Columbia River.

Chemical	Performance Goal (mg/L)[1]	Estimated Impact (mg/L) @ 1,000 y [2] Nominal Inventory	Estimated Impact (mg/L) @10,000 y	
			Nominal Inventory[4]	Upper Bound Inventory[4]
Ammonia (NH_3)	4	0.00E+00	0.00E+00	6.94E-05
Antimony (Sb)	0.006	0.00E+00[3]	0.00E+00[3]	0.00E+00[3]
Arsenic (As)	0.05	4.98E-12	2.44E-09	5.75E-09
Barium (Ba)	2	5.26E-12	2.58E-09	4.70E-07
Beryllium (Be)	0.004	1.74E-13	8.51E-11	3.02E-08

Table 4-9. Impacts from Chemicals at 1,000 Years and 10,000 Years at a Well Just Before Entering the Columbia River.

Chemical	Performance Goal (mg/L)[1]	Estimated Impact (mg/L) @ 1,000 y [2] Nominal Inventory	Estimated Impact (mg/L) @10,000 y	
			Nominal Inventory[4]	Upper Bound Inventory[4]
Cadmium (Cd)	0.00077	1.78E-11	8.73E-09	1.16E-07
Chlorine (Cl)	230	2.63E-07	1.29E-04	1.30E-04
Chromium (Cr)	0.011	7.75E-08	3.80E-05	9.31E-05
Copper (Cu)	0.0078	2.07E-13	1.02E-10	8.74E-08
Cyanide (CN)	0.0052	0.00E+00	0.00E+00	1.51E-05
Fluorine (F)	4	2.81E-07	1.38E-04	1.66E-04
Iron (Fe)	NA	1.27E-08	6.21E-06	1.94E-04
Lead (Pb)	0.0015	2.22E-09	1.09E-06	1.16E-05
Manganese (Mn)	NA	3.90E-09	1.91E-06	2.72E-05
Mercury (Hg)	0.000012	5.43E-11	2.66E-08	2.91E-07
Nickel (Ni)	0.115	8.63E-09	4.23E-06	2.49E-05
Nitrate (NO_3)	10	0.00E+00	0.00E+00	7.28E-03
Nitrite (NO_2)	1	0.00E+00	0.00E+00	1.75E-03
Nitrite plus Nitrate	10	0.00E+00	0.00E+00	9.02E-03
Selenium (Se)	0.005	1.51E-13	7.39E-11	1.69E-10
Silver (Ag)	NA	3.06E-11	1.50E-08	4.20E-07
Sulphate (SO_4)	NA	9.59E-07	4.70E-04	5.42E-04
Thallium (Tl)	NA	0.00E+00	0.00E+00	7.04E-06
Uranium (U-total)	NA	4.89E-09	2.40E-06	1.05E-05
Zinc (Zn)	0.072	5.60E-10	2.74E-07	8.02E-07
1,1,1-Trichlorethane	0.2	0.00E+00	0.00E+00	1.27E-07
1,1,2,2,-Tetrachloroethane	0.005	0.00E+00	0.00E+00	0.00E+00
1,1,2-Trichlorethylene	0.005	0.00E+00	0.00E+00	1.27E-07
1,1,2-Trichloroethane	0.005	0.00E+00	0.00E+00	1.27E-07
1,4-Dichlorobenzene	0.075	0.00E+00	0.00E+00	1.27E-07
Benzene	0.005	0.00E+00	0.00E+00	2.12E-07
Carbon tetrachloride	0.005	0.00E+00	0.00E+00	1.27E-07
Chloroform	NA	0.00E+00	0.00E+00	1.27E-07
Dichloromethane (Methylene chloride)	0.005	0.00E+00	0.00E+00	6.36E-07
Ethyl benzene	0.1	0.00E+00	0.00E+00	2.12E-07
N-butyl alcohol	NA	0.00E+00	0.00E+00	5.52E-08
o-Xylene	0.7	0.00E+00	0.00E+00	6.36E-07
Toluene	1	0.00E+00	0.00E+00	2.12E-07

Table 4-9. Impacts from Chemicals at 1,000 Years and 10,000 Years at a Well Just Before Entering the Columbia River.

Chemical	Performance Goal (mg/L)[1]	Estimated Impact (mg/L) @ 1,000 y [2] Nominal Inventory	Estimated Impact (mg/L) @10,000 y	
			Nominal Inventory[4]	Upper Bound Inventory[4]

[1]Surface water performance goal (see Table 1.4)
[2]1,000 years is the time of compliance.
[3]Antimony inventory assumed equal to zero.
[4] Nominal and upper bound inventory are defined in Section 3.2.3.
NA Not applicable

4.3.7 Best Estimate Case: Moisture Flow Into Disposal Facility

The difference between the base analysis case and the best estimate case is the presence of the sand-gravel capillary barrier in the best estimate case. In the base analysis case, this volume was assumed to be sand. This subsurface barrier would divert moisture away from the top of the disposal facility. If the barrier works as well in practice as it does in theory, the results are impressive (see Figure 4-7 where the moisture influx rates for the base analysis case and the best estimate case are shown). Inclusion of the barrier would reduce the influx rate from about 4.2 mm/y to less than 0.01 mm/y.

As seen from Figure 4-6, the moisture flux (or Darcy velocity) greatly decreases with a capillary barrier in place. Directly underneath the barrier, the drop in moisture velocity is over 4 orders of magnitude, resulting in a Darcy velocity of less than 0.003 mm/year. Even at 32 m from the center of the trench (outer edge of waste package region), the Darcy velocity is down by over two orders of magnitude. As expected, at the edge of the cap, the velocity increases to approximately 60 mm/year. This decreased moisture flux within the waste package region results in a much lower contaminant concentrations as seen in Figure 4-7, where the best estimate case is labeled “Cap. Break” for capillary break. For the best estimate case, the moisture velocities inside the disposal are quire small (being less than 0.1 mm/y). Therefore, to reduce computational time the contaminant release rate associated with a recharge rate of 0.1 mm/year was used in these calculations. This assumption leads to conservative estimates for the contaminant flux leaving the disposal facility. It should be noted that, because these calculations do not include water consumption by the glass dissolution reaction, the release rates shown are even lower than presented here.

Figure 4-20 shows the volumetric moisture content in the far field when the capillary barrier is in place. The moistest area (15 percent) remains unchanged as the 50 mm/year recharge at the edge of the facility remains unchanged. However, directly beneath the disposal facility the volumetric moisture drops from 11 percent (base analysis case) to 6 percent.

Figure 4-20. Volumetric Moisture Content With The Sand-Gravel Capillary Barrier Atop The Disposal Facility.

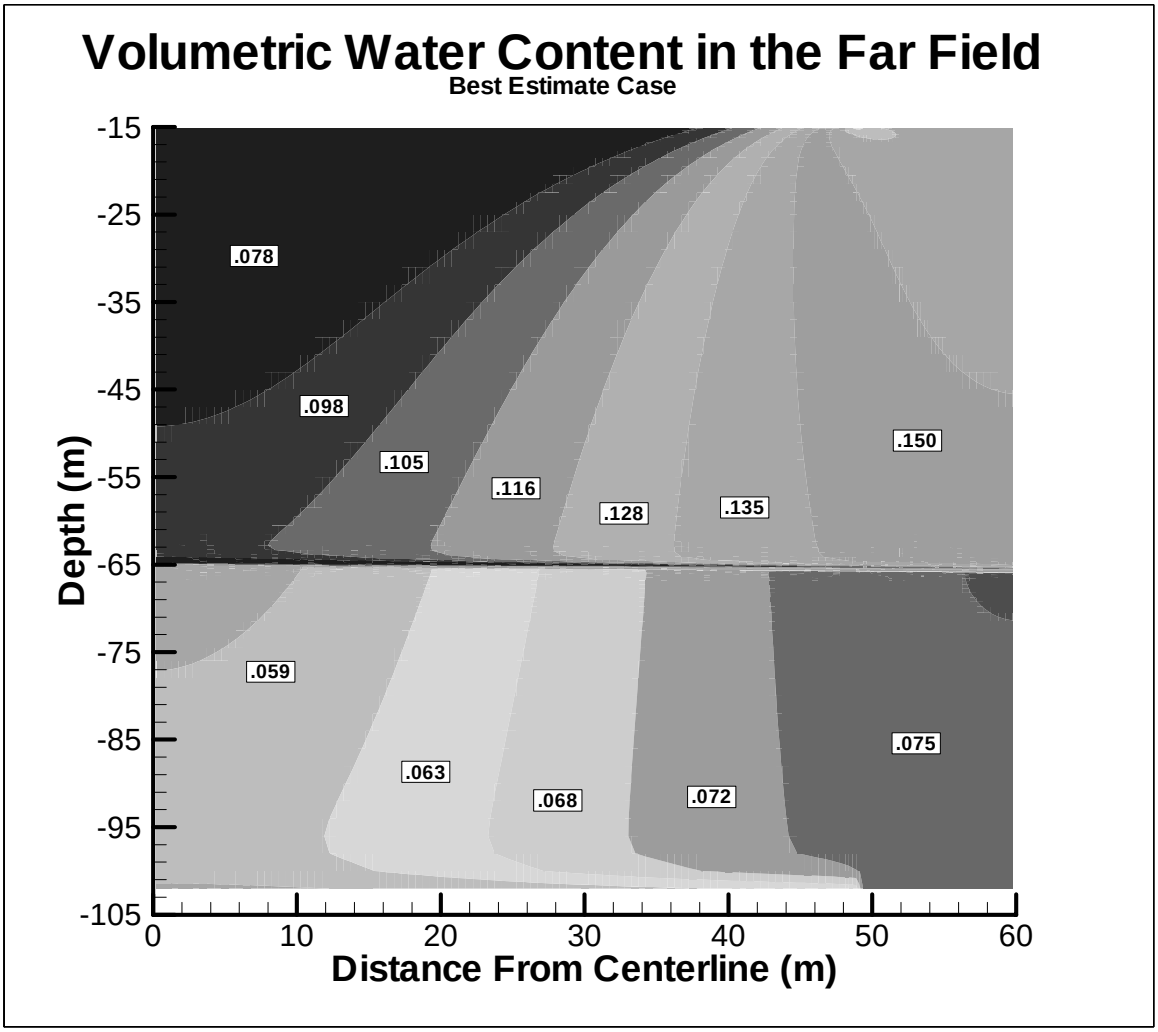

4.3.8 Best Estimate Case: Waste Form Release

Waste form release is calculated for a series of infiltration rates, so that a space-dependent release rate from the disposal facility can be estimated.

As discussed in Section 4.3.3, calculations of the waste form release rate and of the contaminant fluxes out of the disposal facility were performed using a one-dimensional model for various recharge rates. Based on the space-dependent moisture flows calculated in Section 4.3.7, these contaminant fluxes then were translated into a space-dependent contaminant flux out of the disposal facility.

Figure 4-7 (curve labeled "Cap. Break") displays the resulting calculated contaminant concentration out of the disposal facility at 1,000 years for the best estimate case. As can be seen, the stair-step effect caused by the layers of waste packages remains, but the contaminant flux leaving the disposal facility is lower by two orders of magnitude when compared to the base analysis case.

4.3.9 Best Estimate Case: Moisture Flow And Contaminant Transport in the Vadose Zone

This large decrease in contaminant flux continues as the material moves through the vadose zone. As seen from Figure 4-8 (curve labeled "Cap. Break"), the contaminant flux at 10,000 years at its spatial peak is over four orders of magnitude less with a capillary barrier than without one.

As would be expected, the total inventory-normalized contaminant flux entering the groundwater for the best estimate case (Figure 4-21) is much lower than the base analysis case. At 10,000 years, the best estimate case has values over 4 orders of magnitude less. This large difference is because of the lower contaminant flux leaving the disposal facility, as well as the longer travel time in the vadose zone caused by the lower moisture flow. Figure 4-22 compares the contaminant flux leaving the disposal facility (entering the vadose zone) with the contaminant flux entering the groundwater (leaving the vadose zone). Unlike the base analysis case where the vadose travel time is about a thousand years, for the best estimate case, the vadose zone travel time is on the order of a few tens of thousands of years. Also, the contribution of the less mobile contaminants is less when compared to the base analysis case because the contaminant flux for these radionuclides (K_d = 0.6 mL/g) is more than two orders of magnitude less than the mobile contaminants (K_d = 0 mL/g) at 10,000 years (see Figure 4-22).

Figure 4-21. Total Inventory-Normalized, Mobile (K_d = 0 mL/g), Contaminant Flux to the Groundwater for the Base Analysis and Best Estimate Cases as a Function of Time.

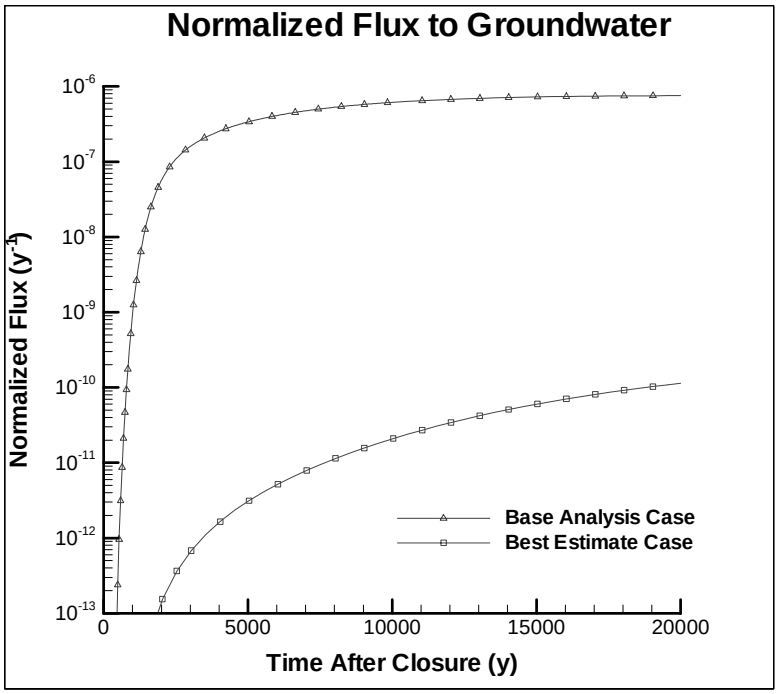

Figure 4-22. Comparison of Total Inventory-Normalized Contaminant Flux Leaving the Disposal Facility and Entering into the Groundwater for the Best Estimate Case for K_d = 0 and 0.6 mL/g as a Function of Time.

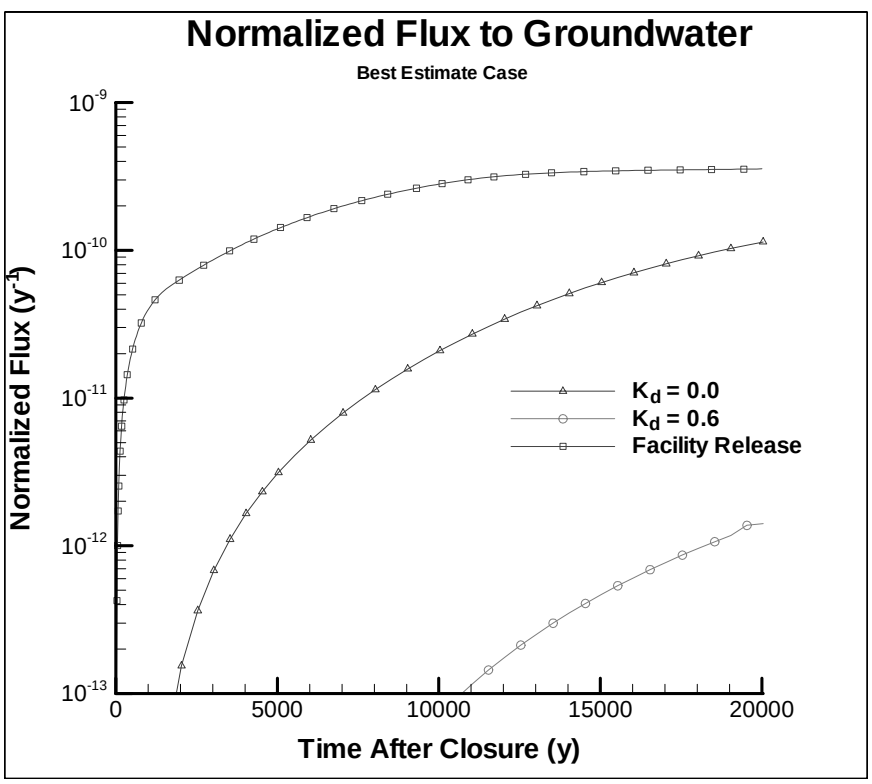

4.3.10 Best Estimate Case: Moisture Flow And Contaminant Transport in Groundwater

The presence of a sand-gravel capillary barrier does not affect groundwater flow as the amount of recharge with or without the capillary barrier is insignificant at the disposal location compared to the regional moisture influx that actually controls the magnitude of groundwater flow. Therefore the results from Section 4.3.5 are used without any changes.

4.3.11 Best Estimate Case: Conversion into Dose

The presence of the subsurface sand-gravel capillary barrier greatly reduces moisture flow into the disposal facility, which greatly reduces contaminant release from the waste form and greatly increases travel time to the groundwater. Table 4-10 presents the impacts from this best-estimate case.

Table 4-10. Estimated Impacts From The Best Estimate Case For A Well 100 Meters Downgradient From The Disposal Facility.

Type of Impact	Value at		Performance Objective
	1000 years*	10,000 years	
Dose (mrem in a year) from beta/photon radionuclides in drinking water	4.7×10^{-11}	3.5×10^{-7}	4.0
All-pathways dose (mrem in a year)	1.7×10^{-10}	1.3×10^{-6}	25.0
Concentration (pCi/L) of alpha-emitting radionuclides	2.2×10^{-22}	5.0×10^{-8}	15.0
Radium concentration (pCi/L)	0.0	0.0	3.0
Uranium concentration (pCi/L)	0.0	3.7×10^{-8}	----

*Time of Compliance is 1,000 years.

4.4 SENSITIVITY CASES: MOISTURE FLOW INTO DISPOSAL FACILITY

Table 4-11 shows the large number of two-dimensional simulations that were run. These simulations varied recharge rates, barrier design, and the type of disposal facility (trench versus vault). The resulting Darcy rates for key cases are shown in Figure 4-6.

The effect of recharge rates is as expected. The greater the rate, the more moist the soil and the greater the moisture flux. Without a subsurface capillary barrier, there is little difference in the moisture velocity fluxes. The large differences in all-pathways dose result from the strong dependence of contaminant release from the waste form on moisture content.

As shown in Section 4.3.7, the presence of the sand-gravel capillary barrier is significant. It reduces the amount of moisture entering the disposal facility by about four orders of magnitude in the driest areas. Even at the edge of the disposal facility, the moisture flux is still reduced by two orders of magnitude. The moisture flux does increase outside the facility, rising to approximately 60 mm/year outside the barrier. However, this high velocity region is away from the waste and has minimal effect on the waste form release.

If the surface barrier and the capillary barrier are shortened by 5 m so it extends only 12 m past the last waste package, the velocity past that package increases by about a factor of 5 compared to the full barrier case. The estimated impacts for both the beta-photon drinking water and all-pathways doses are approximately a factor of 20 larger for the shortened capillary break analysis when compared to the best estimate case. At 10,000 years, the estimated beta-photon drinking water and all-pathways doses for the shortened capillary break are approximately a factor of three greater than the doses estimated for the best estimate case (see Table 4-10).

To investigate the importance of subsidence, a local failure of the capillary barrier is postulated. A 1-meter subsidence in the capillary barrier refers to a trough created in the capillary break 10 meters from the trench centerline. The trough is created by displacing the surface barrier downward 0.3 m over a 1-meter distance (the third dimension being ignored in this two-dimensional calculation). The selection of a 0.3 m downward displacement corresponds to a complete collapse of the free volume (5%) in the stack height of four waste packages. In this subsidence case, the local recharge increases to 11.2 mm/year over a relatively small region. Moisture is diverted into the region just underneath the failure. The higher moisture increases the contaminant release from the waste form, leading to larger estimated impacts. The total effect on the all-pathways dose of having 1 m of the subsurface sand-capillary barrier fail is to increase the estimated impact from 1.7×10^{-10} mrem/year to 2.0×10^{-8} mrem/year at 1,000 years and from 1.3×10^{-6} mrem/year to 1.5×10^{-2} mrem/year at 10,000 years when compared to the best estimate case.

Table 4-11. Summary of Near-Field Hydraulic Sensitivity Calculations.

Description	Basic Model	Velocity Range [a] (mm/y)	All-Pathways Dose (mrem/y)[b]	
			1,000 years [c]	10,000 years
Base analysis case	Trench	4.1 - 4.3	7.8×10^{-5}	7.0×10^{-2}
Rupert sand (0.9 mm/year)	Trench	0.87 - 0.95	1.38×10^{-8}	5.22×10^{-4}
Low recharge rate (0.1 mm/year)	Trench	0.098 - 0.11	2.54×10^{-11}	2.64×10^{-6}
High recharge (50 mm/year)	Trench	49. - 51.	3.99×10^{-1}	1.61
Full barrier (best estimate case)[d]	Trench	1.2×10^{-4} - 8.5×10^{-3}	1.71×10^{-10}	1.31×10^{-6}
Full barrier –High recharge rate (50 mm/year)	Trench	1.0×10^{-3} - 1.0×10^{-1}	7.3×10^{-9}	3.76×10^{-6}
Base case – sand backfill	Trench	4.1 - 4.2	1.64×10^{-3}	2.35×10^{-1}
No side slope effect	Trench	4.2 - 4.2	4.01×10^{-6}	4.48×10^{-2}
Vertical hydraulic barrier	Trench	1.2×10^{-4} - 8.3×10^{-3}	0.00	7.51×10^{-7}
Capillary barrier failure[e]	Trench	0.0094 - 11.1	1.95×10^{-8}	1.45×10^{-2}
Shorter capillary barrier[f]	Trench	1.2×10^{-4} - 1.5×10^{-2}	3.12×10^{-9}	4.41×10^{-6}
Burbank sand (4.2 mm/year)	Vault	4.1 - 4.8	2.21×10^{-2}	7.38×10^{-1}

[a] Over region of waste packages
[b] Performance objective is 25 mrem/year
[c] Time of compliance is 1,000 years
[d] Labeled as "Cap. Break" in Figure 4-6
[e] Labeled as "Subsidence" in Figure 4-6
[f] Labeled as "Short. Cap. Break" in Figure 4-6

4.5 SENSITIVITY CASES: WASTE FORM RELEASE

4.5.1 Overview

The 1998 ILAW performance assessment (Mann 1998a) showed that the estimated impacts strongly depended on the rate of waste form release. Therefore, a large number of sensitivity runs were made to determine the sensitivity of the results to various inputs and assumptions. Table 4-12 provides a summary of the results. It should be noted that relative changes in the waste form release rate translate directly into changes in impacts (with a time delay corresponding to the vadose zone travel time), because the waste form release rates dominate the time structure of the problem. All of these sensitivity cases, but one, were simulated in one-dimension.

4.5.2 Forward Rate of Reaction

Forcing glass dissolution to be at the maximum rate increases the estimated release rate from the disposal facility by a factor of 9.

As glass dissolves, silicon is released into the surrounding fluid. As the SiO_2(aq) concentration in the fluid increases, the rate of glass dissolution decreases. However, the exact description of how this rate slows is still a matter of research. To obtain a bounding case, the glass dissolution model was run assuming that the glass dissolution is always at the maximum rate consistent with temperature (which is unvarying) and pH, the so-called forward rate of reaction. Figure 4-23 compares the inventory-normalized contaminant flux to the vadose zone when the forward rate is used.

As expected, the release rate to the vadose zone greatly increases (by a factor of ~9) over the base case if the forward rate is used. This is because of a combined higher intrinsic rate of glass dissolution and a higher pH in the disposal facility.

It should be noted that the *White Paper Updating the Conclusions of the 1998 ILAW Performance Assessment* (Mann/Puigh 2000b) only used forward rate calculations, which explains why the estimated impacts in that document are higher than those in this PA.

Table 4-12. Summary of Waste Form Sensitivity Calculations. The flux ratio translates into the impact ratio (except for a time delay corresponding to the vadose zone travel time).

Section	Description	Basic Model	Flux Ratio @ 1,000 years	Flux Ratio @ 10,000 years	Reason Higher or Lower than Base Case
4.3.3	Base case - 4.2 mm/year recharge	Trench	Base case	Base case	
4.5.2	Forward rate, 4.2 mm/year recharge	Trench	9.93	8.71	Forward rate
4.5.3	Assume no ion exchange	Trench	0.79	0.83	Lower pH
4.5.3	Assume no secondary phase formation	Trench	0.52	0.53	Higher Si concentration
4.5.3	Increase ion exchange rate by 5 times while also using forward rate	Trench	12.17	9.51	Forward rate, higher pH
4.5.4	0.1 mm/year recharge	Trench	0.0004	0.0004	Lower recharge
4.5.4	0.5 mm/year recharge rate	Trench	0.0052	0.0041	Lower recharge
4.5.4	0.9 mm/year recharge rate	Trench	0.016	0.016	Lower recharge
4.5.4	10 mm/year recharge rate	Trench	8.44	2.64	Higher recharge
4.5.4	50 mm/year recharge rate	Trench	20.9	3.40	Higher recharge
4.5.5.1	Change filler material in trench to sand	Trench	9.13	1.62	Water content/diffusion higher in sand
4.5.5.2	Include steel in waste packages	Trench	1.03	1.02	Steel corrosion increases pH
4.5.5.3	Add conditioning layer at top	Trench	0.99	0.92	Higher Si concentration
4.5.6	4.2 mm/year recharge	Vault	8.55	2.67	Vault, glass packed closer, higher pH
4.5.6	Replace concrete everywhere with backfill material	Vault	9.11	2.48	Vault, glass packed closer, higher pH
4.5.6	0.9 mm/year recharge rate	Vault	0.75	0.20	Vault, lower recharge
4.5.6	0.1 mm/year recharge	Vault	0.055	ran to 1800 years	Vault, lower recharge
4.5.7	Increase Waste Loading / Alternate Glass Formulation	Trench	164	76	Higher release rate, no dependence on Si
4.5.8	Increase diffusion for all aqueous species by a factor of 10	Trench	0.06	0.011	Lower pH
4.5.8	Replace Tc with U	Trench	1.03	1.00	Slight soddyite precipitation
4.5.8	Full two-dimensional simulation	Trench	2.65	ran to 2,000 years	Lower water flux through glass
4.5.8	Extend contaminant release model to groundwater	Trench	0.93	1.09	Position of lower boundary has small affect on release rate

Figure 4-23. Inventory-Normalized Contaminant Flux to the Vadose Zone for Different Glass Dissolution Models.

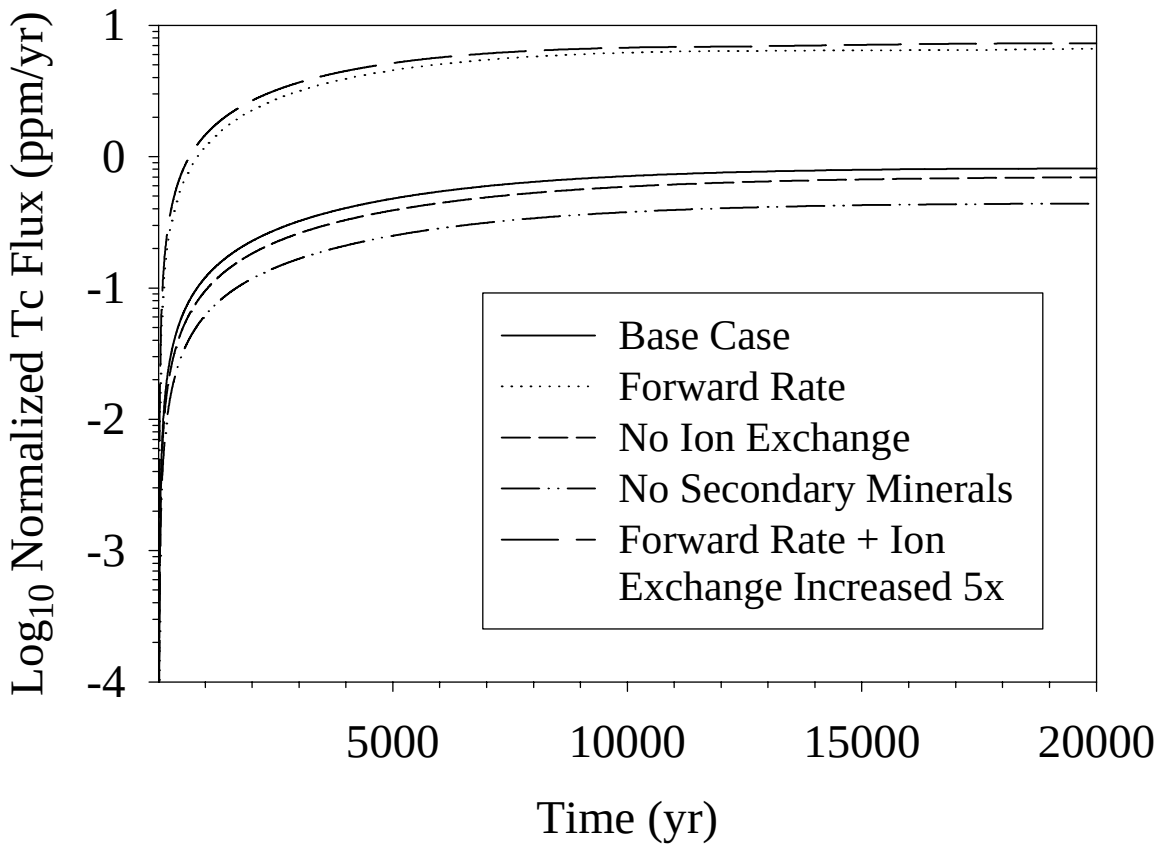

4.5.3 Glass Dissolution Rate

Neglecting the sodium ion exchange or the creation of secondary minerals slightly reduces the estimated release rate.

The main reaction that causes glass to dissolve in water is breaking the bridging oxygen bonds that hold the glass matrix together. However, other reactions also go into the waste form release calculations. The two most important are the sodium ion exchange reaction and the formation of secondary minerals that affect the silicon concentration.

In the sodium ion exchange reaction, hydrogen ions in the water replace the sodium in the glass. This reaction thus increases the amount of sodium in the water and the pH. Because of the high sodium content of the glass and because this reaction has a lower activation energy than the matrix destruction reaction, it can be significant under ILAW disposal conditions. The effect of neglecting the sodium ion exchange reaction is shown in Figure 4-23. If no ion exchange reaction is present, the glass dissolution is reduced, but not significantly. If the ion exchange rate

for the forward rate simulation is increased five times, the result is a slight increase in the overall glass dissolution rate.

As the amount of silicon builds up in the fluid, it can precipitate out as a secondary mineral, thus reducing the concentration. This causes the glass to dissolve more quickly. As seen in Figure 4-23, the effect is real and if the precipitation rate is rapid enough to reduce the silica in solution to very low values, glass dissolution rates can accelerate back up to the forward rate of reaction.

Secondary minerals also can trap important contaminants. Research for the ILAW PA program has shown that 80 percent of the technetium can be trapped in such materials. However, although the experiments are continuing (see section 7.8.2 for a more complete discussion of future work on waste forms), we do not know yet whether such trapping is a short-term effect or will last the hundreds and thousands of years necessary to affect these calculations. Therefore, this performance assessment assumes that none of the important contaminants are trapped in secondary phases over the long term. Once better data are obtained for the secondary minerals, the effects will be incorporated in future performance assessments.

4.5.4 Effect of Infiltration Rate

> The waste release rate from the disposal facility increases as the infiltration rate increases. However, the release rate saturates for infiltration rates of about 50 mm/year.

Moisture plays an important role in glass dissolution because it carries the reaction products away from the dissolving glass and into the vadose zone. Two effects are important: one is the transport of the contaminants once they are released and the other is the effect on the local chemistry.

Figure 4-4 shows the estimated contaminant flux from the disposal facility into the vadose zone. Higher recharge rates flushes dilute water through the system, lowering the silicon concentration in the fluid surrounding the glass and increasing the glass dissolution rate. However, the higher recharge rates have a point of diminishing returns. The diluting effect of higher recharge also restricts increases in pH. Such increases in pH would increase the glass dissolution rate. As seen from Figure 4-4, above 10 mm/y, the release rates from the disposal facility increase little with increased recharge rate.

These calculations neglect the fact that water is needed to dissolve the glass (see equation 3.8 in Section 3.4.4.2). However, at the 0.1 mm/year recharge rate (the lowest rate calculated), the glass dissolution rate would be limited to 0.015g/(m^2 day), which still is 7 times the forward rate at 15°C and pH=9 for LAWABP1 glass. Thus ignoring water consumption is a valid strategy.

4.5.5 Effect of Materials Surrounding ILAW Packages

> The material surrounding the waste form can have a significant effect for times less than 5,000 years. However, neither the waste container nor the preconditioning layer has much affect.

Many design decisions still need to be made concerning the disposal facility. Some of these will affect the glass dissolution rate. This

section investigates the effect of the following:

- Different filler material between the ILAW packages
- Steel containers
- Conditioner layering above the disposal facility.

4.5.5.1 Effect of Filler Material on Glass Dissolution. The ILAW packages will be separated by filler material. For the base analysis case, the hydraulic properties of backfill material (i.e., excavated material) were used. Figure 4-24 shows the effect of replacing such material with sand. Although over long periods the dissolution rates approach each other, at short times (less than 5,000 years), they are significantly different. The difference is caused by the sands having a lower moisture content, and thus a higher linear pore velocity at a recharge rate of 4.2 mm/y. The higher pore velocity in the intervening sand layers allows Tc to be transported downward to the bottom of the facility more rapidly. The moisture content within the glass layers is very similar whether the filler material is backfill or sand, and thus the long-term dissolution rates are very similar for these two cases.

Figure 4-24. Contaminant Flux to the Vadose Zone Assuming Different Surrounding Materials.

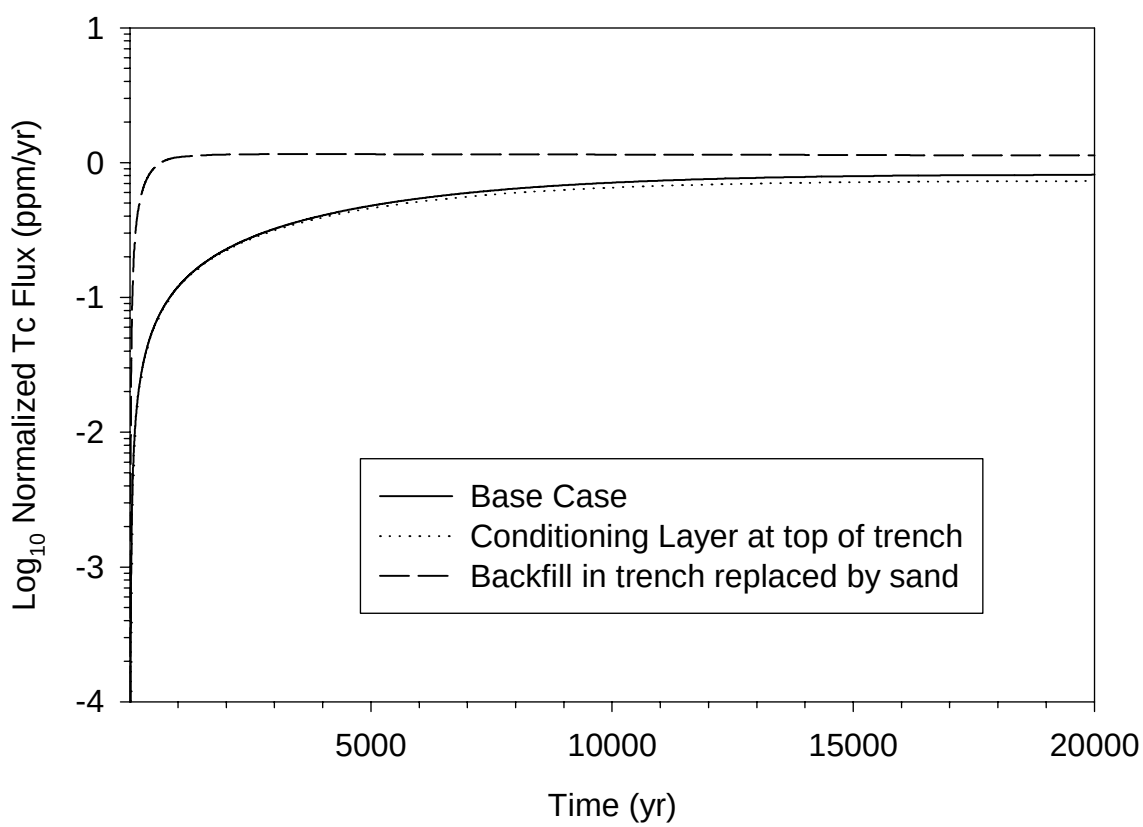

4.5.5.2 Steel Containers. The base analysis case and subsequent calculations have ignored that the ILAW waste package is actually glass surrounded by a stainless steel container. Including the stainless steel in the reaction network increases the pH slightly, because the corrosion reaction consumes H^+. However, as shown in Figure 4-25, the effect is small when the steel containers are modeled correctly as layers separate from the glass waste. If the steel is completely mixed with the glass in one material zone, it raises the local pH and enhances the precipitation of the iron-bearing clay nontronite, which lowers the silicon concentration and significantly increases the glass dissolution rate. This underscores the importance of using at least a one-dimensional model to simulate the layered waste form, as opposed to a "zero-dimensional" reaction kinetics code, such as EQ3/6, where all materials in the waste form would be mixed together.

Figure 4-25. Contaminant Flux to the Vadose Zone Assuming Different Surrounding Materials.

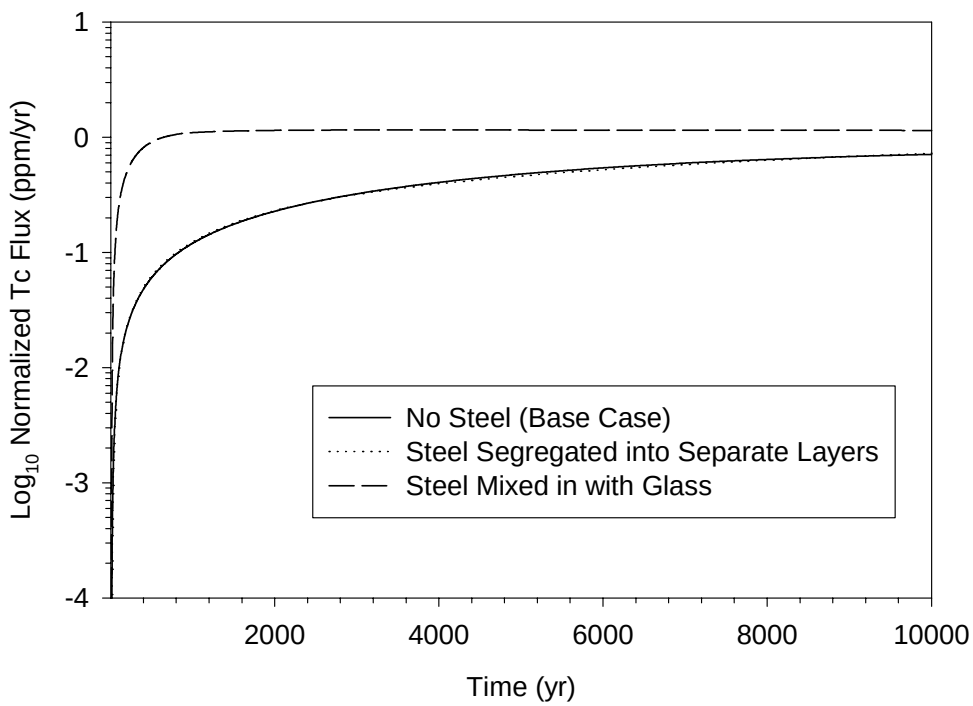

Presently, the plan is to have the ILAW in 304L stainless steel packages. Because this large amount of steel could add potential contaminants to the groundwater, a separate simulation was run to model the release of chromium and nickel to the vadose zone. Based on limited knowledge of steel corrosion rates gained in the Yucca Mountain Project (Cloke et al. 1997), a constant rate of steel corrosion of 6.9×10^{-14} mol cm^{-2} s^{-1} was assumed. By assuming this rate, the stainless steel corrodes away (i.e. is oxidized) entirely within about 1,100 years. Corrosion and oxidation of the 304L is also assumed to release Cr directly to the aqueous phase as Cr(VI), i.e. the important intermediate step of oxidizing Cr(III) to Cr(VI) was assumed to occur faster than the rate of Cr(III) release from steel corrosion. Because Cr(VI) is present almost entirely as the

soluble and mobile CrO_4^{2-} ion, the approximately 10^7 kg of chromium in the stainless steel would also be released in about 1,100 years. In contrast, the solution concentrations of Ni are constrained by precipitation of theophrastite [$Ni(OH)_2$], resulting in negligibly small Ni release to the vadose zone.

4.5.5.3 Conditioning Layer. The amount of silicon in the fluid surrounding the glass is important. Some preconceptual designs for the closure cover had a layer of silica-bearing material just above the disposal facility to precondition the water. Using crushed soda bottles was considered, but because of cost and because its higher surface area than the waste glass would make the crushed glass dissolve too quickly, their use was not considered further. However, these calculations considered the use of 1 m- thick silica sand just above the glass region. However, as seen from Figure 4-24, the effect is quite small.

4.5.6 Effect of Type of Disposal Facility

> The release rate from the concrete vault is higher (about 3 or more for times less than 5,000 years) than the release rate from the trench.

The 1998 ILAW performance assessment (Mann 1998a) assumed that the ILAW packages would be disposed in underground concrete vaults. Although such concrete vaults are not now part of the baseline, the project is responsible for four unused concrete vaults (the unused grout vaults). Therefore, calculations were performed using these vaults not only to provide a bridge from the 1998 ILAW PA results, but to allow their future use if needed.

The results of the concrete vault simulations are shown in Figure 4-26. For the 4.2 mm/year recharge rate case, the vault has a higher concentration flux to the vadose zone than the trench, particularly at early times. Note that if the concrete is replaced with backfill, the vault values are unchanged. This suggests that the vault performs more poorly than the trench because of the dense waste configuration in the vault rather than because of chemical effects as suggested in Mann/Puigh (2000b).

As in the trench simulations, assuming lower recharge rates results in significantly lower contaminant fluxes to the vadose zone. The 0.1-mm/year recharge rate simulation was unable to progress past 1,800 years because of high concentrations in the vault, which were close to the maximum allowable concentrations of 2.1 mol/kg. For these lower recharge rate simulations, the trench design again performs better, being over an order of magnitude better at 1,000 years.

Figure 4-26. Contaminant Flux to the Vadose Zone for Vault Simulations.

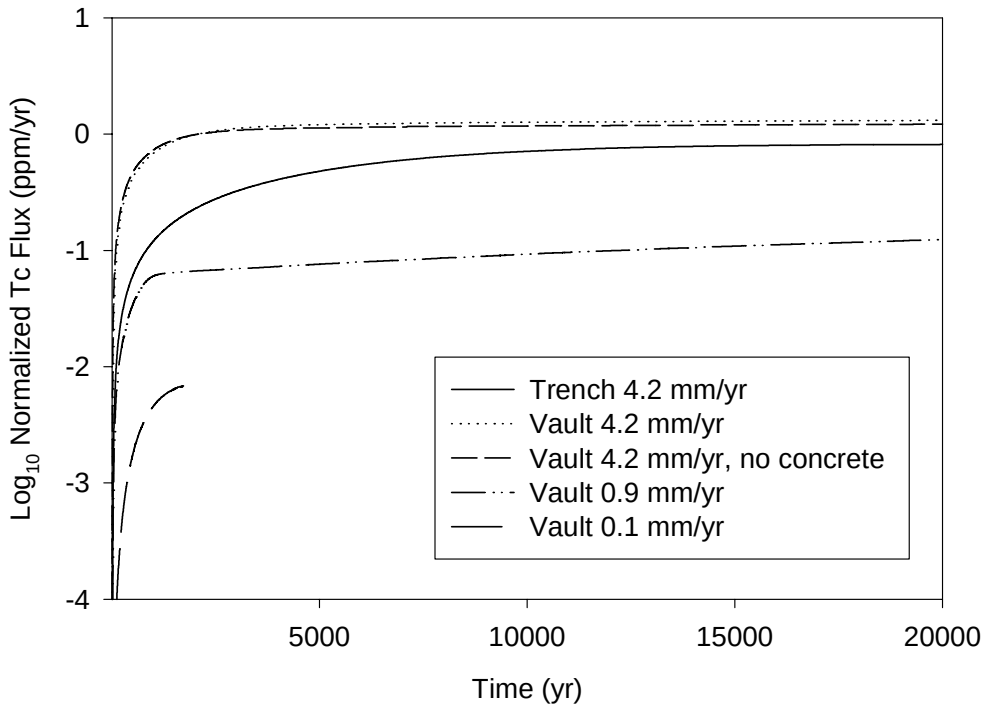

4.5.7 Effect of Waste Loading and Other Glass Compositions

The base analysis case uses a sodium waste loading of 20 weight percent. Increasing the Na_2O loading in LAW glasses has several impacts that can affect the long-term dissolution rate of the product. First, sodium is a glass "network breaker." Adding sodium to silicate glasses depolymerizes the glass, making its structure less interconnected and, so, generally less durable when contacted by water. Second, increased sodium content may make the glass more susceptible to alkali ion exchange reactions. The net affect of ion exchange is to raise the pH of water percolating through the disposal system, thereby increasing the glass dissolution rate. Lastly, increasing the Na_2O content tends to expand the stability field and rate of zeolitic alteration phase formation as the glass reacts with water. The formation of zeolite (a class of hydrous aluminum silicate minerals) can decrease the amount of dissolved silica, thus causing dissolution rate excursions, sometimes all the way back to the forward rate of reaction. Thus, higher sodium loading will likely shrink the composition region from which acceptable LAW glasses can be formulated.

There is only a limited experimental base for LAW glasses at other than 20 weight percent Na_2O loading. From the limited data in Figure 4-27, a simple linear regression gives a slope of $10^{0.2x}$, where x is the mass percent Na_2O. Consequently, a 5 percent increase in Na_2O loading would increase the glass corrosion rate by approximately ten times. However, to conduct a more detailed analysis, laboratory experiments with HLP-31 glass (see Vienna 2000),

which has a Na_2O loading of 23 weight percent, were performed to establish the necessary input parameters for STORM simulations. The results (see Figure 4-28) show a very unusual glass corrosion behavior in that the dissolution rate is apparently unaffected by an increasing concentration of silicon in the aqueous phase, up to near saturation with respect to amorphous silica. Also, the congruent release of Na and B indicates that little or no Na ion exchange is occurring, despite the higher waste loading. Finally, the forward rate of reaction for this glass is about ten times larger than for LAWABP1 glass at the same temperature and pH. The reasons for this unusual behavior may be related to microscale phase separation as a result of the heat treatment used to simulate canister cooling. In any event, to model the performance of this glass in the disposal system, the glass dissolution rate was not allowed to decrease as the Si concentration in the disposal system pore water increased. No experimental data were available on the pH-dependence of the dissolution rate so it was assumed that the reaction rate increased according to $10^{0.4*pH}$, identical to the power law determined for LAWABP1 glass.

Figure 4-27. VHT Corrosion Rate as a Function of Waste Loading (from Vienna [2000]).

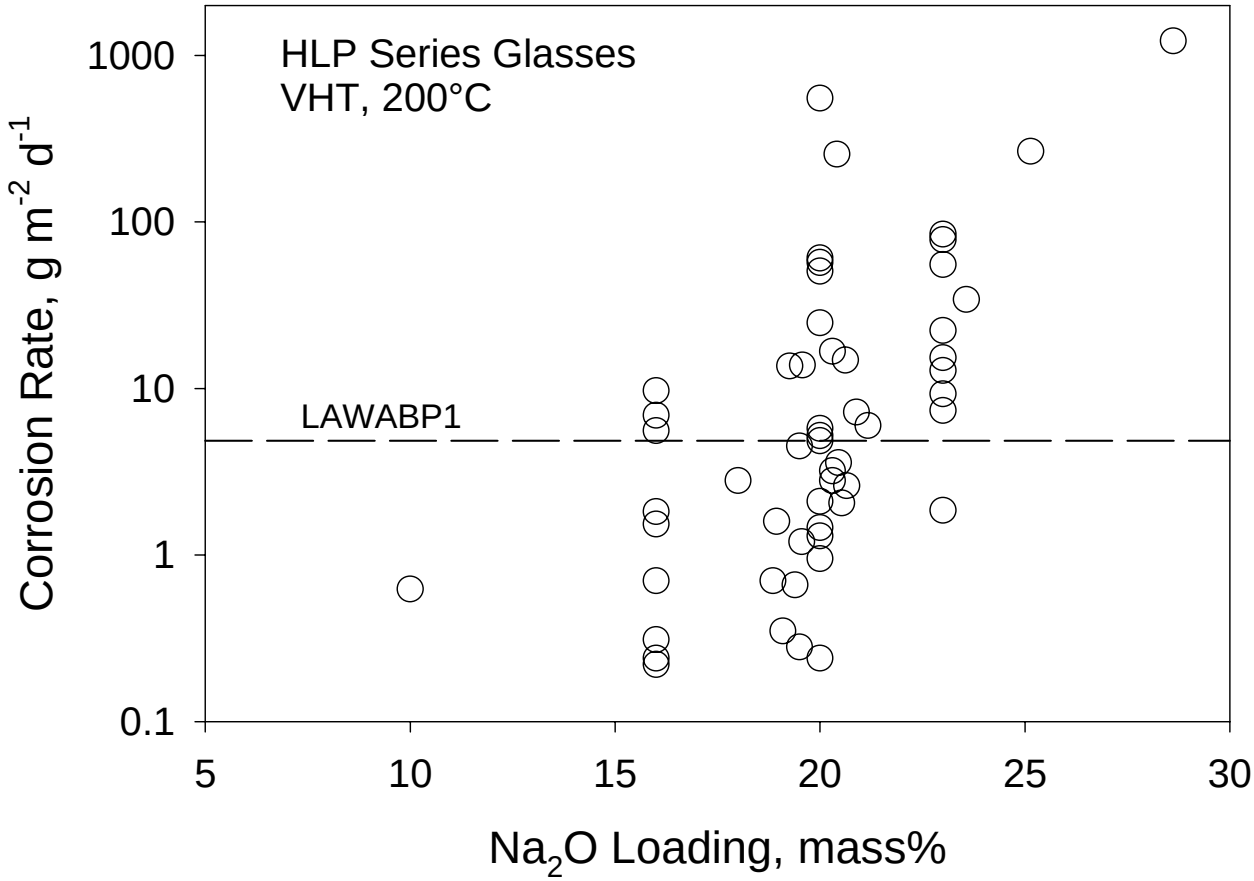

Figure 4-28. Dependence of HLP-31 Glass Dissolution Rate on Concentration of Silicic Acid.

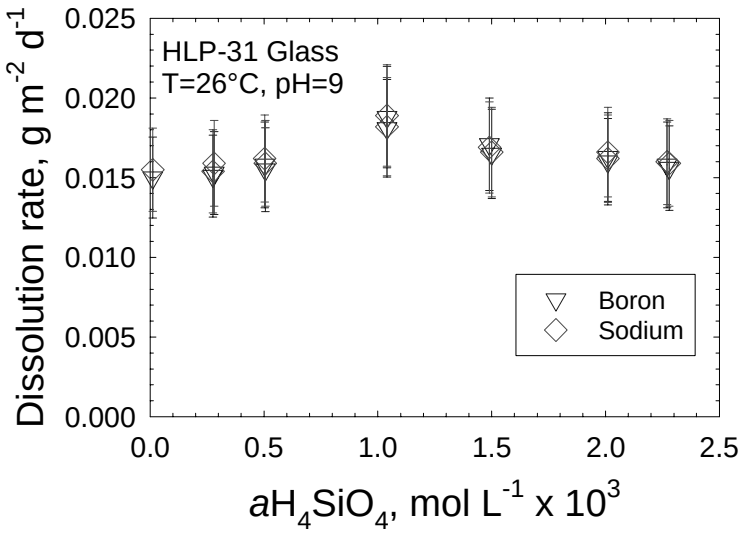

The calculated inventory-normalized contaminant flux to the vadose zone for HLP-31 glass is 75 to 164 times larger (Table 4.12) than that for the base case simulation with LAWABP1 glass, as shown in Figure 4-29. The higher forward reaction rate of HLP-31 glass generates a higher calculated pH in the glass layers as compared with LAWABP1 glass. The combined effect of these factors, and the fact that the rate does not diminish with increasing Si concentration, increases the total release rate much more than the forward rate difference between the glasses alone would indicate. The decline in release rate after 5,000 years occurs because of the decreasing surface area of HLP-31 glass, which changed very little for the slower dissolving LAWABP1 glass over the same time period.

The STORM simulations show the strong sensitivity of release rates to the durability of the glass. Available testing data indicate that Na_2O loadings of 20 to 25 weight percent might be achieved and still produce glasses that will have acceptable long-term performance. VHT testing shows several glasses at 23 weight percent Na_2O loading with a corrosion rate that is nearly as good as LAWABP1 glass (Vienna 2000). Only very limited data at waste loadings above 25 weight percent Na_2O are available. Although it may be possible to formulate acceptable glasses at this waste loading, the acceptable glass composition region will be much smaller than is observed at waste loadings of 20 weight percent Na_2O and lower. Additional studies are needed if waste loadings approaching 25 weight percent Na_2O are desired. Major increases in waste loading on the order of 50 to 100 percent (30 to 40 weight percent Na_2O) are probably not possible with silicate-based glasses. A different glass-forming system, such as the phosphate system, would need to be considered. However, changing to a different glass forming system would also require a different melter design, flow sheet, etc. Also, non-silicate waste glasses have received almost no attention since the early 1980's. Consequently, a significant research and development effort would be required to evaluate long-term performance issues with these glasses.

Figure 4-29. Inventory-Normalized Contaminant Flux to the Vadose Zone for Different Glass Formulations.

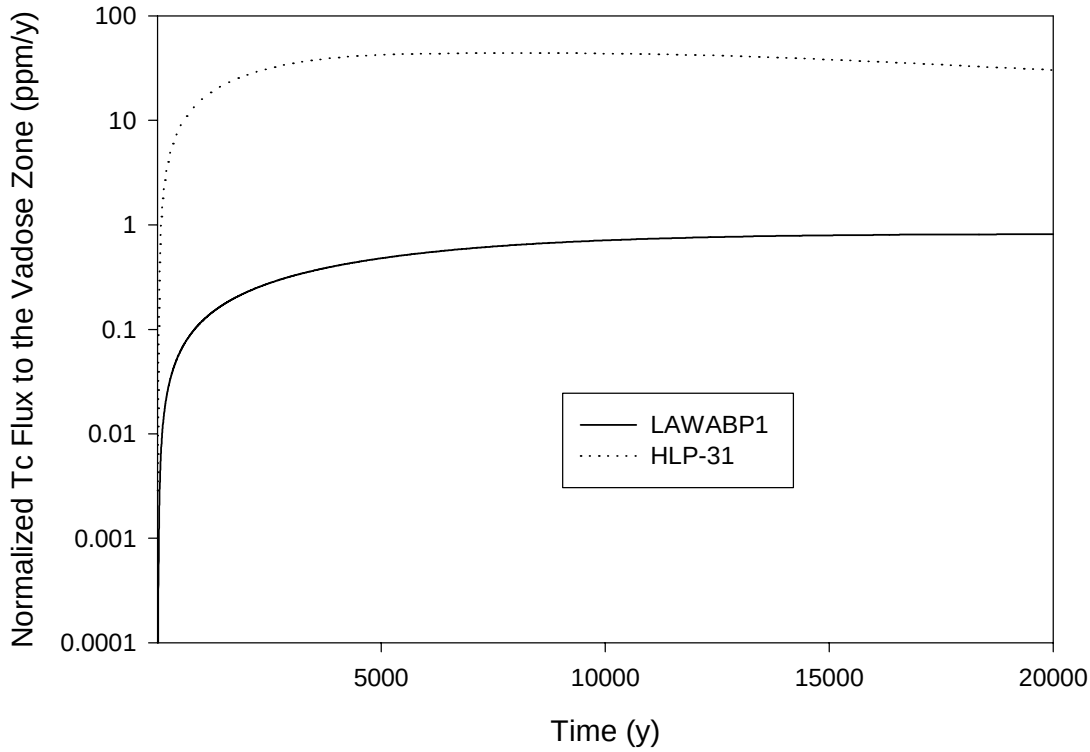

4.5.8 Effect of Waste Package Design

The waste form release sensitivity cases thus far have been based upon a cubic waste package with edge dimension of 1.4 m (Puigh 1999). Recent planning for ILAW disposal (DOE/ORP 2000c) has identified a right-circular cylindrical geometry with 1.2 m outside diameter and 2.3 m height as the preferred container configuration. Assuming 85% of the container's available volume is filled with the glass waste form, the height of glass within one container would be approximately 2 m. Current planning (DOE/ORP 2000a) would have three layers of waste packages stacked within an RH trench with dimensions similar to those discussed in Section 2.4. This would result in a maximum glass stack height of 5.9 m.

The vault sensitivity case used a waste stacking height of 7.2 m. Because the principal effect of waste stacking height is to increase the pH of the fluid exiting the bottom of stack (from reaction with the glass), the 7.2 m height of the vault sensitivity case should provide an upper bound of ^{99}Tc release for the 5.9 m stacking height associated with the new container design. The base analysis case was calculated for a waste stacking height of 4.8 m of glass. Therefore, the release from the RH trench using the new canister design is anticipated to lie between the release rates for the base case and the vault case for a given infiltration rate. From Tables 4-1 and 4-12, the anticipated release rate from the RH trench using the new canister design for an infiltration rate of 4.2 mm/y is assumed to be between 0.012 and 1.0 ppm/y at 1,000 years after

facility closure and between 0.71 and 1.9 ppm/y at 10,000 years after facility closure. These estimates neglect the additional dilution that will occur because of the slightly lower volume of glass per package (2.2 m^3 versus 2.3 m^3 for the cubic container) and the larger volume of backfill per cubic meter of glass, which results from less efficient container packing.

4.5.9 Other Calculations

Some other calculations were performed to determine the sensitivity to parameter and model choices. These included the following:

- Increasing the value of the diffusion coefficient
- Modeling the contaminant as uranium
- Extending the reactive transport calculations through the vadose zone to groundwater
- Performing a two-dimensional calculation inside the disposal facility
- Performing a simulation of the "bathtub effect," where the lower boundary of the trench becomes impermeable to water flow, causing the trench to become saturated with water.

Because the moisture content within the disposal facility is so low, advective transport also is low. Under these conditions, diffusion of the contaminants is important. Increasing the aqueous diffusion coefficient for all species from 5×10^{-9} m^2/second (base analysis case) to 5×10^{-8} m^2/second significantly increases the transport of species, increasing the mixing of the aqueous products of glass dissolution. This results in a significantly lower pH in the glass layers and hence a dissolution between 10 and 100 times lower than the base case, depending on the time.

The base analysis case modeled technetium as the main contaminant and did not consider secondary phases. A sensitivity case was run treating uranium as the main contaminant and explicitly treating the secondary phases known to trap uranium. Three uranium aqueous species were considered: $UO_2(CO_3)_2^{2-}$, $UO_2(CO_3)_3^{4-}$, and $UO_2(OH)_2(aq)$. Two secondary minerals were considered: weeksite, $K_2(UO_2)_2Si_6O_{15}{:}4H_2O$, and soddyite, $(UO_2)_2(SiO_4){:}2HO_2$. Only soddyite precipitated, and it did so in miniscule amounts for a very short period. Because of the slow release rate from the glass, steady rate of mass transport through the system, and strong carbonate complexes associated with U(vi), the pore fluid remained undersaturated with respect to weeksite and soddyite and the uranium remained dissolved in the aqueous phase. Hence, the inventory-normalized fluxes for total uranium are identical to those predicted for technetium.

A sensitivity case was run that is identical to the base case, except that the Hanford sand layer was assumed to extend 88 m to the water table. Thus, the total depth of this extended source-term model was 103 m for the extended grid, as opposed to 15 m for the base case simulation. This simulation covered 5,000 years. Simulated pH (Figure 4-30) and TcO_4^- (Figure 4-31) concentrations for the upper 15 m of the extended simulation are very similar to those of

the base case until after 10,000 years, when the effect of the lower water table boundary begins to propagate up the profile. Even so, the technetium release rate is very similar for the base case and the extended simulation, the flux from the extended simulation being 7 percent lower at 1,000 years and 9 percent higher at 10,000 years than the base case. Longitudinal diffusion causes a decrease in the concentrations of aqueous species across the depth of the Hanford sand. pH decreases slightly from the top of the Hanford sand to the water table (Figure 4-30). TcO_4^- decreases from the top of the Hanford Sand to the water table by a factor of 3 at 2,000 years. By 20,000 years, the profile is closer to steady state, and the decrease in technetium is only 9 percent from the top of the Hanford sand to the water table.

A sensitivity case was run that considers the consequences of the trench liner being impermeable to flow, thus causing the trench to become saturated with water. The trench was initially considered to be saturated with water, with no flow across the bottom boundary. Simulated TcO_4^- (Figure 4-32) and total water mass (Figure 4-33) concentrations are similar to those predicted by the base case. However, because the amount of water in the profile is so much higher than in the base case, the amount of technetium released is much higher.

Figure 4-30. pH for RH Trench Simulation Extended to Water Table. (See Figure 3-13 for Location of Boundaries Between Material Zones and Material Names.)

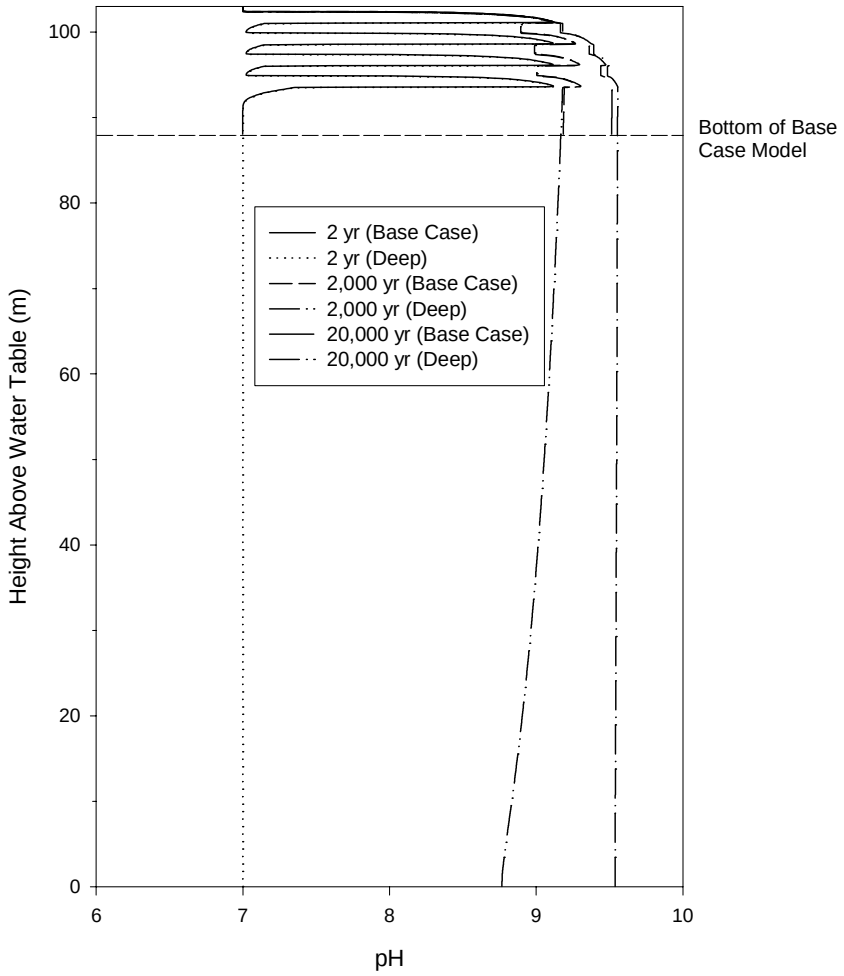

Figure 4-31. TcO_4^- **for RH Trench Simulation Extended to Water Table. (See Figure 3-13 for Location of Boundaries Between Material Zones and Material Names.)**

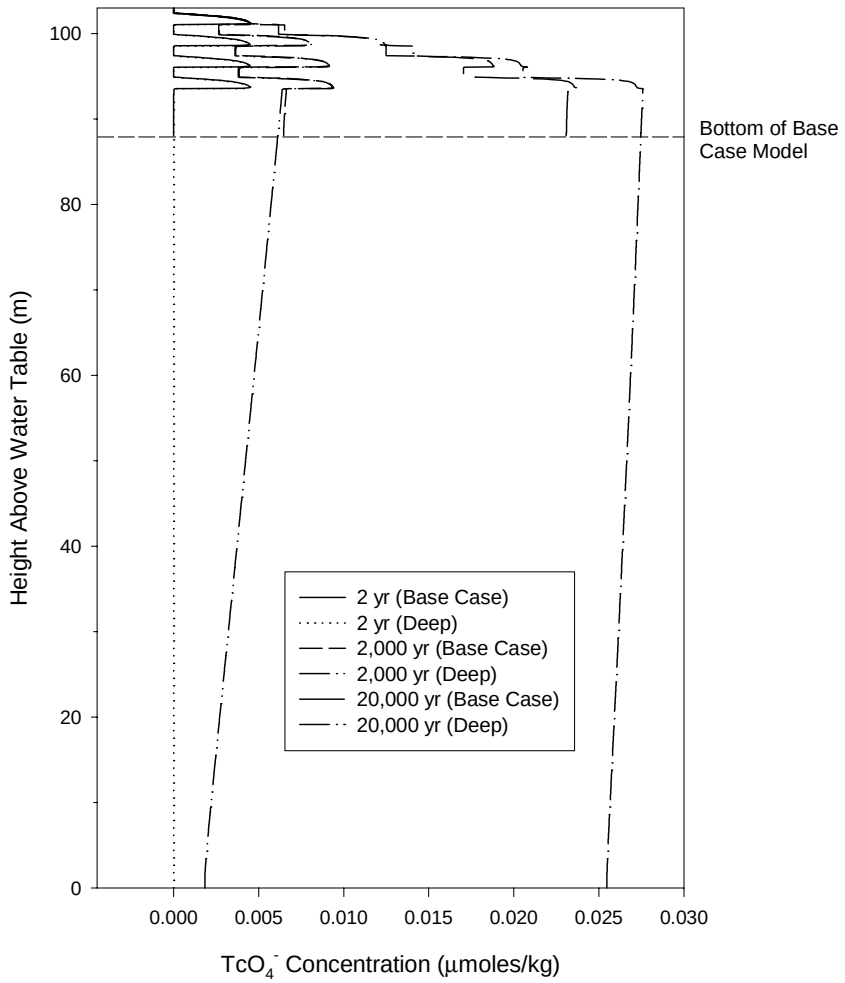

Figure 4-32. TcO_4^- **For Fully-Saturated RH Trench Simulation With No Flow ("Bathtub Effect").**

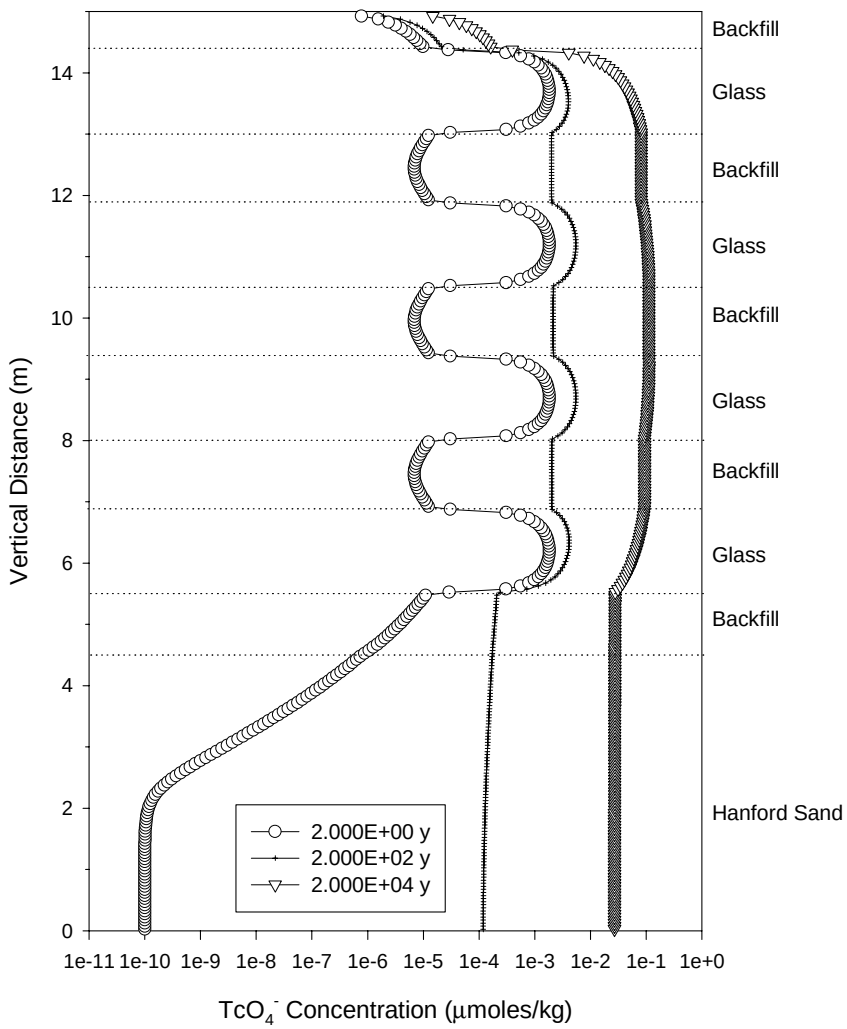

Figure 4-33. Total Water Mass Per Node. (Each Node Has A Volume Of 0.05 m^3.) For Fully-Saturated RH Trench Simulation With No Flow ("Bathtub Effect").

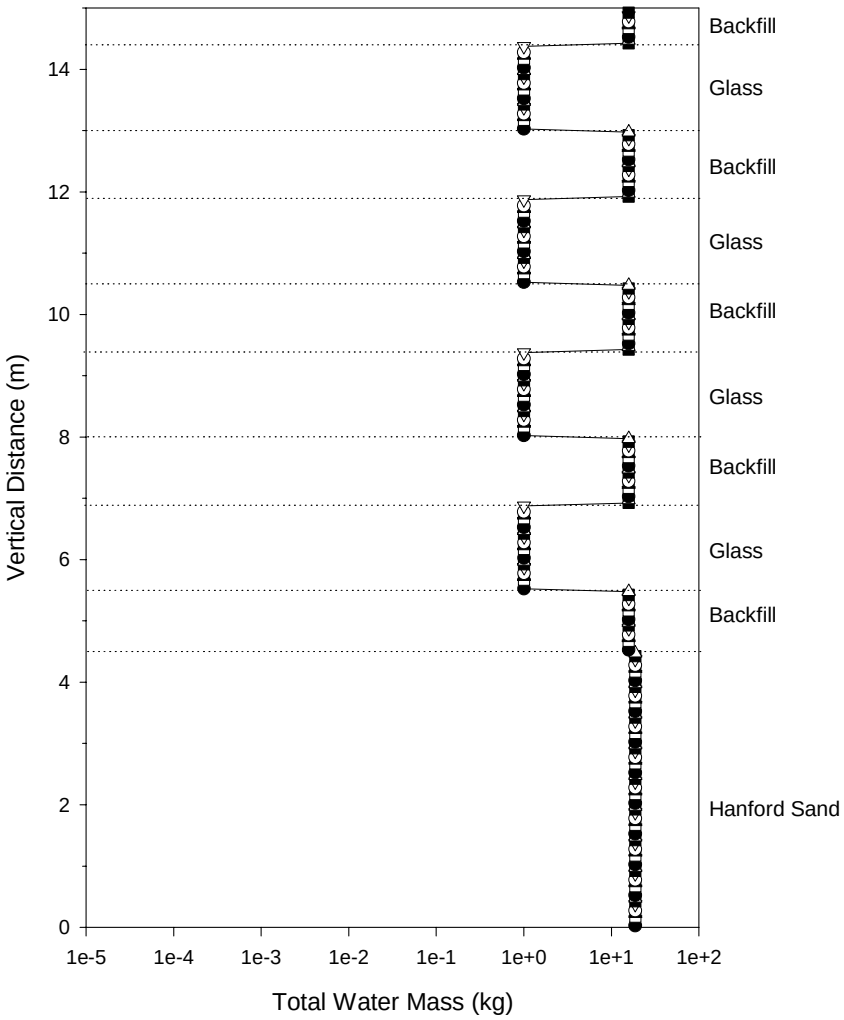

A full two-dimensional simulation of the trench scenario was developed for comparison to the one-dimensional simulation used as the base case. The two-dimensional simulation reaches steady state earlier and shows a lower maximum (or steady state) technetium release rate than the one-dimensional simulation (Figure 4-34). In the two-dimensional simulations, water flows around the glass waste packages. This lowers the water content in, and water flux through the waste packages, and increases the technetium concentrations in the waste packages. The glass dissolution rate for these simulations is highest on the edges of the glass layers. This is where the pH of the pore water is highest and the SiO_2(aq) concentrations are lowest.

This two-dimensional simulation required over a month of computation to reach a simulation time of 2,000 years, while the one-dimensional simulation required only 5.3 days to reach a simulation time of 100,000 years. The results of this comparison support the contention that the predictions of one-dimensional simulations are conservative with respect to, and not dramatically different from, those of the two-dimensional simulations.

Figure 4-34. Inventory-Normalized Contaminant Flux to the Vadose Zone for One-Dimensional (1D) and Two-Dimensional (2D) Simulations. Note that the 2D simulations only go to 2,000 years.

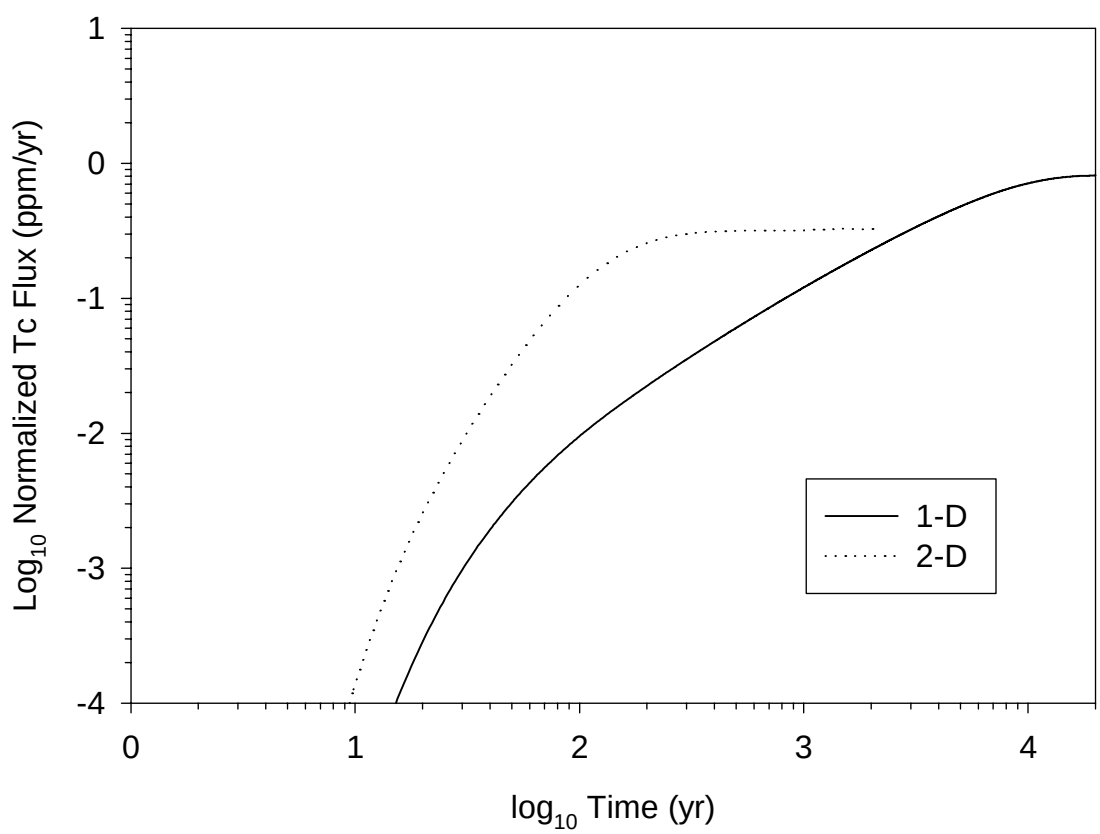

4.6 SENSITIVITY CASES: VADOSE ZONE MOISTURE FLOW AND CONTAMINANT TRANSPORT

4.6.1 Overview

This section discusses the calculations of the moisture flow and contaminant transport in the far-field vadose zone. The major items that will be covered are as follows:

- Recharge
- Vadose zone properties
- Waste form release time dependence.

Table 4-13 summaries the results of the simulations by providing the travel times through the vadose zone. Travel time is defined as the time at which the contaminant flux to the aquifer for the mobile contaminants (K_d = 0 mL/g) is 50 percent of its maximum value, which may be at the maximum time for which calculations were performed (i.e. 20,000 years).

4.6.2 Recharge

As can be seen from the results of the base analysis (Section 4. 3.4) and the best estimate (Section 4.3.9), the recharge rate is important in determining when the contaminant flux enters the groundwater. Figure 4-35 shows the total contaminant flux entering the groundwater normalized to a unit inventory in the waste form for four different recharge rates, assuming no capillary barrier is placed over the disposal facility. Because these calculations used the corresponding waste form release rates, the results reach different asymptotic values. Table 4-13 shows the estimated impacts to the all-pathways doses for different recharge rates. The estimated impacts of recharge rates on the other performance objectives are provided in Appendix D, Table D-1.

The recharge rate of 50 mm/year is consistent with an estimated recharge rate for irrigation farming above the disposal site. The corresponding beta / gamma drinking water dose and alpha concentrations associated with a well 100 meters downgradient from the disposal site would increase to 0.037 mrem/year and 1.52 pCi/L at 10,000 years after facility closure. The alpha concentration and the all-pathway dose are more impacted than the beta/photon drinking water dose because the contaminants with K_d= 0.6 mL/g are transported more rapidly through the vadose zone when compared to the base analysis case. These estimated impacts for irrigation directly above the disposal site are far below the performance objectives at 1,000 and 10,000 years after facility closure. Moreover, if irrigation were to occur in the region surrounding the ILAW disposal site, then the directional flow of the groundwater would change and the resulting impacts would be lower than the case described above due to additional dilution in the groundwater (see section 4.7.5).

Table 4-13. Travel Times and All-Pathways Doses for the Various Vadose Zone Sensitivity Cases.

Description	Travel Time (y)	All-Pathways Dose (mrem/y)[a]	
		1,000 years[b]	10,000 years
Base case - 4.2 mm/year	5,400	7.78×10^{-5}	7.00×10^{-2}
0.1 mm/year	13,500	2.54×10^{-11}	2.64×10^{-6}
0.9 mm/year	7,300	1.38×10^{-8}	5.22×10^{-4}
50. mm/year	<200	3.99×10^{-1}	1.61
0.1 mm/year for 500 years, then 4.2 mm/year[c]	5,900	6.65×10^{-8}	6.06×10^{-2}
Isotropic flow field	5,300	4.83×10^{-5}	4.96×10^{-2}
10x increase in diffusion	5,300	1.16×10^{-4}	8.05×10^{-2}
2 times increase in dispersion	5,300	1.37×10^{-4}	8.73×10^{-2}
Vadose zone is all sand	5,700	1.96×10^{-5}	3.91×10^{-2}
Vadose zone in all gravel	5,000	3.80×10^{-4}	3.87×10^{-1}
Clastic dike	5,400	6.96×10^{-5}	6.42×10^{-2}
Vadose zone 3 m thicker	5,500	6.51×10^{-5}	6.86×10^{-2}
U $K_d = 0$	5,400	2.09×10^{-4}	1.29×10^{-1}
$K_d = 0$ for all radionuclides	5,400	3.68×10^{-2}	8.69
Facility K_d's (concrete)	5,400	5.79×10^{-5}	3.72×10^{-2}
Capillary barrier (4.2 mm/year) Best Estimate Case	>13,000	1.71×10^{-10}	1.31×10^{-6}
Capillary barrier (50 mm/year)	9,300	$7.33 \mathrm{X} 10^{-9}$	$3.76 \mathrm{X} 10^{-6}$
Vertical hydraulic barrier	>13,000	0.00	7.51×10^{-7}
Shorter capillary barrier	>13,000	3.12×10^{-9}	4.41×10^{-6}
Capillary barrier failure	6,800	1.95×10^{-8}	1.45×10^{-2}
Sand backfill	1,800	1.64×10^{-3}	2.35x10-1
No side-slope effect	5,600	4.01×10^{-6}	4.48×10^{-2}
Forward rate	4,600	7.59×10^{-4}	6.54×10^{-1}
No ion exchange	5,500	6.13×10^{-5}	5.71×10^{-2}
No secondary phase formation	5,600	3.86×10^{-5}	3.57×10^{-2}
Include steel in waste packages	6,900	7.95×10^{-5}	6.98×10^{-2}
Top conditioning layer	5,000	7.72×10^{-5}	6.66×10^{-2}
Waste form aqueous diffusion (x10)	1,700	5.66×10^{-10}	1.61×10^{-3}
Alternative glass formulation (HLP31)	3,000	9.41×10^{-3}	6.23
Forward Rate + Ion Exchange Increased 5X	4,350	7.97×10^{-4}	7.46×10^{-1}

[a] Performance objective is 25 mrem/year
[b] Time of compliance is 1,000 years
[c] Estimated from base analysis case

Figure 4-35. Total Inventory-Normalized Contaminant Flux to the Groundwater as a Function of Recharge Rate (No Capillary Barrier).

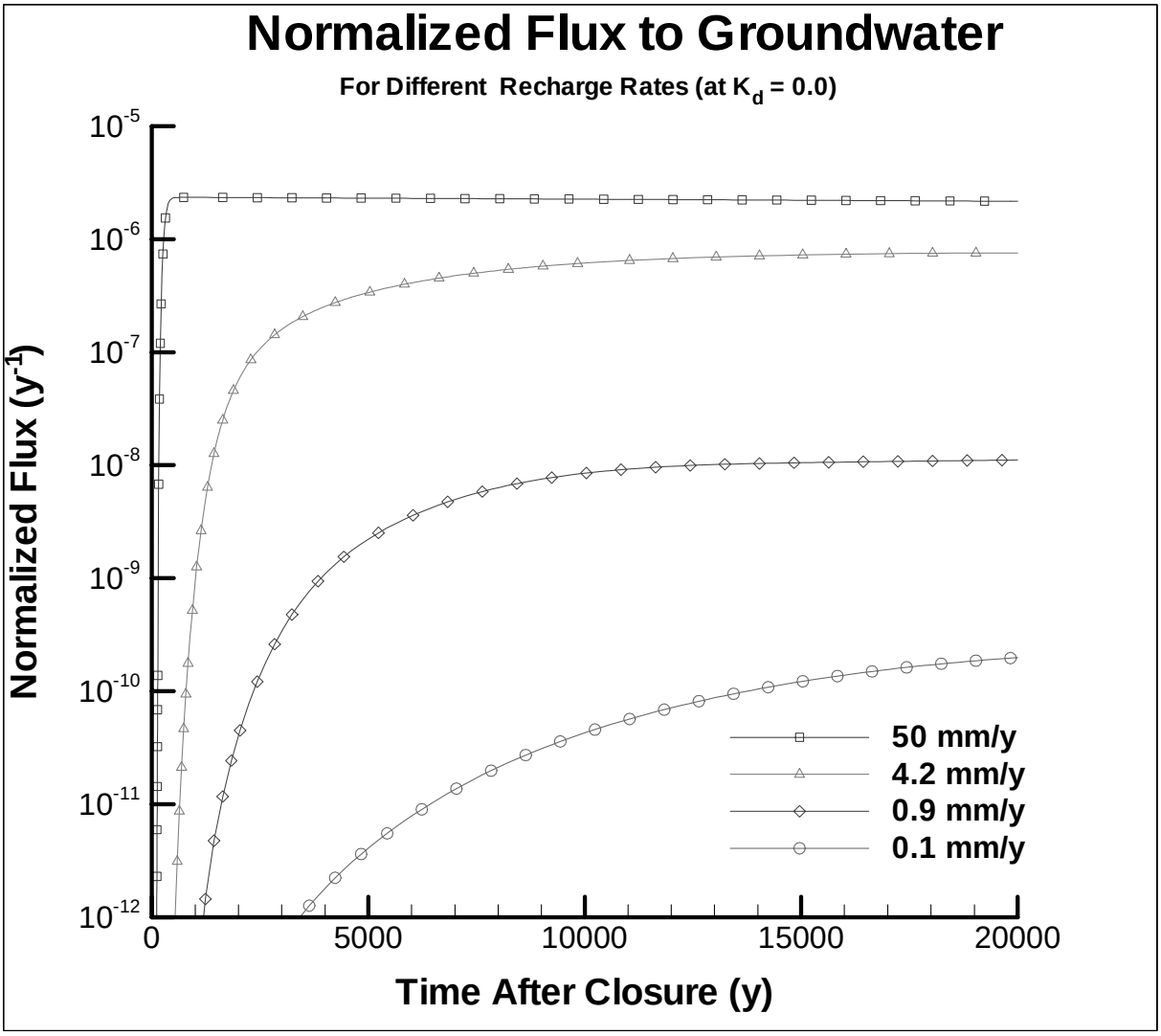

4.6.3 Vadose Zone Properties

The major vadose zone properties are the hydrology and geology parameters and the geochemical properties. The hydrology and geology parameters affecting the contaminant transport in the vadose zone are the hydraulic properties of the media, dispersivity and diffusivity. To explore the sensitivity to hydraulic properties, two sensitivity cases were run using the following assumptions: Assumed the vadose zone was all Hanford sand, and assumed the vadose zone was all Hanford gravels. Sensitivity cases were run exploring the sensitivity of the estimated impacts to the media's dispersivity and to diffusion of the contaminants: Increased the dispersivity by a factor of two and an isotropic calculation. Finally, a sensitivity case was run with the inclusion of a clastic dike.

Figure 4-36 shows the impact of assuming the entire vadose zone has hydraulic properties of either all sand or all gravel. Little impact occurs to the mobile contaminant flux to the aquifer as a function of time. However, the impact to less mobile contaminants is significant. This is caused by the gravel correction that is applied to the K_d's. Because of the limited surface area of gravels compared to sands or silts, the K_d for gravels is reduced. For the all-gravel case, the contaminants with K_d = 0.6 mL/g are significantly more mobile than in the base analysis case because the effective K_d for gravel is 0.06 mL/g for the entire vadose zone. Therefore, the travel time is faster. On the other hand, the all-sand case has a K_d = 0.6 mL/g assigned to the entire vadose zone and the corresponding travel times for these contaminants are significantly slower. The result is that at 10,000 years the alpha concentration is 2.54 x 10^{-3} pCi/L for the all-sand case, 3.39 x 10^{-2} pCi/L for the base analysis case, and 3.60 x 10^{-1}pCi/L for the all-gravel case. The corresponding all-pathways dose at 10,000 years is estimated to be 3.91 x 10^{-2} mrem/year for the all-sand case, 7.00 x 10^{-2} mrem/year for the base analysis case, and 3.87 x 10^{-1} mrem/year for the all-gravel case.

Figure 4-36. Total Inventory-Normalized Contaminant Flux to the Groundwater Assuming the Vadose Zone is All Sand or All Gravel (No Capillary Barrier - Recharge = 4.2 mm/year).

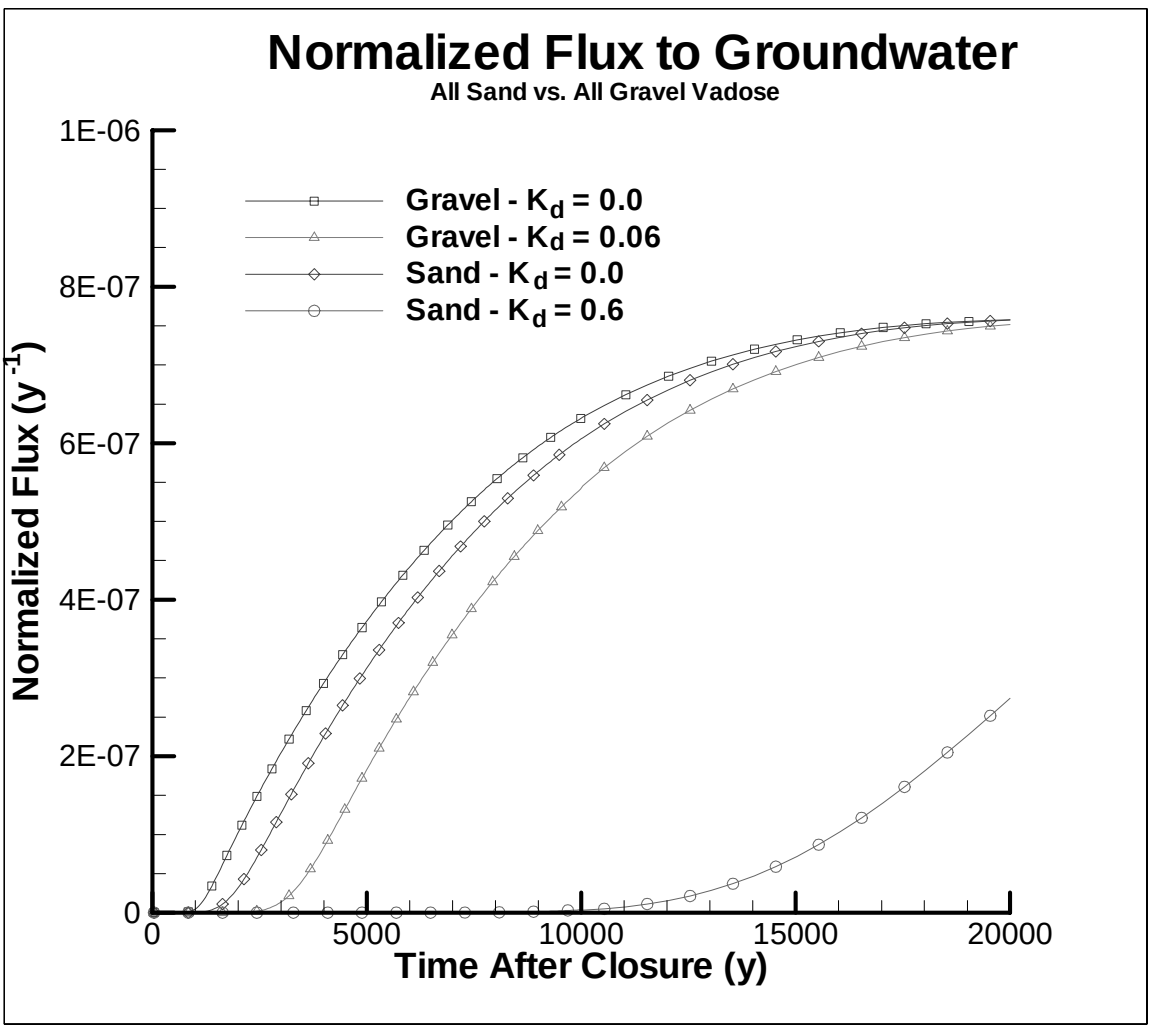

Changing the degree of dispersion and diffusion in the vadose zone affects the estimated impacts slightly. The travel times for the mobile contaminants are affected only slightly and the corresponding estimated beta-photon drinking water doses are not affected at all (see Appendix D, Table D-1). The less mobile contaminants are affected more significantly and the resulting all-pathways doses reflect these impacts. Specifically, an isotropic flow field in the vadose zone leads to lower estimated impacts for the all-pathways dose (see Table 4-13). Increased diffusion is anticipated to decrease transport. Dispersion tends to spread the contaminant plume laterally. For the base case, this moves the plume into the higher flow field associated with the side slope (recharge = 50 mm/year). Therefore, the estimated impacts should be higher with an increase in dispersion.

The geochemical properties affect the travel time for the contaminants through the vadose zone. Sensitivity cases were run that included the geochemical properties of a potential concrete layer beneath the remote handled waste disposal facility along with the geochemical properties of the vadose zone. The sensitivity case for the concrete layer assumed that the 1 m-thick concrete mixture layer had the chemical properties of degraded concrete (see Table 3-6 for probable values). The iodine and uranium contaminant transport is retarded in this region. The resulting estimated impacts to the all-pathway dose at 1,000 years after facility closure was 5.9×10^{-5} mrem/year (base case estimated impact is 7.8×10^{-5} mrem/year). The reduction in the estimated dose at 1,000 years was caused by a decrease in the contribution from ^{129}I. The resulting estimated impacts to the all-pathway dose at 10,000 years after facility closure was 0.037 mrem/year (base case estimated impact is 0.070 mrem/year). The reduction in the estimated dose at 10,000 years was primarily caused by a decrease in the uranium flux to the aquifer when compared to the base analysis case.

Changing geochemical parameters in the vadose zone does not change the travel time for mobile contaminants, but such a change determines which contaminants are mobile. The most important slightly retarded isotopes are the uranium isotopes. Changing the K_d value of uranium from 0.6 to 0 mL/g, increases the concentration of alpha emitters by approximately13 orders of magnitude to 0.00061 pCi/L at 1,000 years after facility closure (still far below the performance objective of 15. pCi/L). Decreasing the uranium K_d to 0 mL/g also increases the all-pathways dose by a factor of 3 at 1,000 years and by less than 2 at 10,000 years compared to the base analysis case.

If the retardation factors for all radioisotopes are set to zero, the estimated impacts increase even more. The estimated impacts are compared to the base analysis case in Table 4-14. At 1,000 years the estimated all-pathways dose is 3.68×10^{-2} mrem/year compared to the base analysis case estimate of 7.78×10^{-5} mrem/year. At 10,000 years the estimated all-pathways dose is 8.69 compared to 6.86×10^{-2} mrem/year for the base analysis case. Assigning $K_d = 0$ mL/g to the radium radionuclides leads to a estimated radium concentration of 5.95×10^{-3} pCi/L at 10,000 years compared to an estimate of 0 pCi/L for the base analysis case.

Table 4-14. Estimated Impacts from Sensitivity Case Where All Radionuclides are Assumed Mobile (K_d = 0 mL/g) Compared to the Base Analysis Case for a Well 100 m Downgradient from the Disposal Facility.

Type of Impact	Estimated Impacts (all K_d = 0 mL/g)		Estimated Impacts Base Analysis Case	
	1000 years*	10,000 years	1000 years*	10,000 years
Dose (mrem in a year) from beta-photon radionuclides in drinking water	0.000031	0.015	0.000021	0.0102
All-pathways dose (mrem in a year)	0.037	8.7	0.000078	0.070
Concentration (pCi/L) of alpha-emitting radionuclides	0.016	4.34	1.0×10^{-16}	0.034
Radium concentration (pCi/L)	0.0000038	0.0060	0.0	0.0
Uranium concentration (pCi/L)	0.00061	0.30	0.0	0.025

*Time of compliance is 1,000 years.

The final sensitivity case considered for the vadose zone is that of a clastic dike located beneath the disposal facility. The specific calculation assumes that a vertical clastic dike, 1 m wide, extends from a depth of -16 m to -99 m beneath each trench at a location 15 m from the trench centerline (see Finfrock [2000b] for details.) The remaining parameters are similar to the base analysis case. This presumed preferential flow path does not affect the contaminants reaching the aquifer. The reason for the relatively small effect for this preferred path is associated with the clastic dike acting as a capillary break with respect to the relatively high recharge from the side slope region (recharge = 50 mm/year). In comparing the results of the clastic dike estimated impacts to the case where the side slope recharge is 4.2 mm/year, the capillary break estimated impacts are higher as anticipated. These impacts are summarized in Table 4-15 and Appendix D, Table D-1.

Table 4-15. Estimated Impacts from Clastic Dike Simulation Compared to the Base Analysis Case for a Well 100 m Downgradient from the Disposal Facility.

Type of Impact	Estimated Impacts Clastic Dike		Estimated Impacts Base Analysis Case	
	1000 years*	10,000 years	1000 years*	10,000 years
Dose (mrem in a year) from beta-photon radionuclides in drinking water	0.000019	0.0101	0.000021	0.0102
All-pathways dose (mrem in a year)	0.000070	0.0642	0.000078	0.070
Concentration (pCi/L) of alpha-emitting radionuclides	9.16×10^{-17}	0.0281	1.0×10^{-16}	0.034

*Time of compliance is 1,000 years.

4.6.4 Waste Form Release or Disposal Facility Time Dependence

For most vadose zone calculations, the time dependence of the source release has no or at most a minor impact on the results of the vadose zone calculations. For these calculations the time dependence of the source is critical as seen from Figures 4-9 and 4-10, where the flux entering the groundwater has the same temporal shape as the flux leaving the disposal facility. Therefore, for each different waste form release or disposal facility case, a vadose zone calculation was run. These calculations show that the vadose zone's main influence is to delay the contaminants from reaching the groundwater. Thus, the details of the calculations are not presented here. Explicit cases were run for the following:

- Forward rate of waste form release
- No ion exchange in waste release
- Alternative glass composition
- Uranium release in near field
- Capillary barrier (best estimate case)
- Shorter barrier
- Barrier subsidence
- Vault as the disposal facility.

The results from these analyses are summarized in Appendix D, Table D-1.

4.7 SENSITIVITY CASES: GROUNDWATER FLOW AND CONTAMINANT TRANSPORT

4.7.1 Overview

Because of the short travel time in the groundwater compared to the waste form release rates and the vadose zone travel times, the groundwater calculations were separated from the other calculations. The results of the groundwater calculations are given in terms of the well intercept factor, which is the ratio of the inventory-normalized contaminant groundwater concentration at the point of interest (e.g. at the well head 100 meters downgradient from the disposal facility – expressed as Ci/m^3) to the total inventory-normalized contaminant concentration entering the groundwater (expressed as Ci/m^3).

Calculations were performed for the following variables:

- Disposal facility layouts and location
- Pumping rates at the well retrieving the contaminated water
- Hydraulic conductivities beneath the waste disposal site
- Regional influences.

Table 4-16 displays the ratios of the well intercept factors for the various groundwater sensitivity cases to the WIF of the base analysis case at two locations. Because the amount of water entering through the vadose zone directly under the disposal facility is insignificant compared to the total groundwater flow, impacts are proportional to the well intercept factor.

Table 4-16. Ratio of Well Intercept Factors for the Various Groundwater Sensitivity Cases.

Section	Description	WIF/(Base Case WIF)	
		Ratio at 100 m	Ratio at 1,000 m
4.3.5	Base case	--	--
4.7.2	Trenches at south end of site	1.50	1.16
4.7.2	90° rotation	1.91	1.36
4.7.2	Smaller layout	0.27	0.27
4.72	Larger layout	1.20	1.18
4.72	Existing vault site	0.43	0.07
4.7.3	30 L/day pumping	1.00	1.00
4.7.3	100 L/day pumping	1.00	1.00
4.7.3	300 L/day pumping	1.00	1.00
4.7.3	1000 L/day pumping	1.00	1.00
4.7.4	Reduced hydraulic conductivity by a factor of 3	11.98	4.86
4.7.5	Regional increase in recharge by a factor of 3	0.92	0.41
4.7.5	Regional decrease in recharge by a factor of 3	0.68	0.65
4.7.5	Decrease in regional upgradient boundaries by a factor of 2	0.84	0.82

4.7.2 Disposal Facility Layouts and Location

The layout of the disposal units at the disposal site has not been determined. In addition, the existing concrete vaults at the eastern edge of the 200 Area still might be used. The current planning is for the units to be placed in the north end of the site (the base analysis case). A series of different sensitivity cases were used to examine the effect of different assumptions on facility location and layout.

One sensitivity study examined the effect of locating the six disposal-facility trenches evaluated in the base case at the south end of the ILAW disposal-facility area. One of the key factors in the calculated WIF for the base-case analysis was the assumed hydrogeologic unit and corresponding hydraulic conductivity found at the water table directly below the facility. With the disposal trenches located in the northern part of the ILAW disposal facility area, the disposal facility is largely underlain by relatively high permeability sediments associated with the Hanford formation. Moving the disposal trenches to the south end of the facility area will position the disposal facility closer to the water-table contact between the Hanford formation and the lower permeability sediments associated with the Ringold Formation. The change in postulated hydraulic properties at the water table will result in a different velocity distribution beneath the facility that could affect calculated WIFs.

The direction of plume movement in this case is very similar to the base case, but calculated WIFs are 50 percent higher than for the base case at 100 m and about 16 percent higher at 1 km. This result is consistent with the postulation that, with a thinner distribution of Hanford formation sediments in the south end of the facility, the overall distribution of groundwater velocities would be lower and the resulting WIF would be higher than for the base case.

Another sensitivity case examined the effect on the WIF of rotating the orientation of the six remote handled trenches evaluated in the base case by 90 degrees. Conceptually, flow across the facility is predominantly in a northwest to southeast direction. The change in orientation would put the longest dimension of the individual remote handled trenches in an orientation closer to parallel to the dominant direction of flow. This would conceivably decrease the effective width of the disposal facility relative to groundwater flow and increase the magnitude of the WIF.

While changing the trench configuration did have some effect on the calculated WIFs, the resulting WIF at the 100 m (328-ft) well was 90 percent higher than the 100 m (328-ft) well WIFs calculated for the base case. The calculated WIF at 1 km (0.62 mi) was increased by about 36 percent over the 1 km (0.62 mi) WIF in the base case.

As seen in Figure 4-8, the contaminant flux does not have a significant horizontal component except in cases of very low recharge and vadose zone moisture content. The concrete vaults have a smaller footprint (36,750 m^2) than the trenches (124,800 m^2). Therefore, a case was run assuming the footprint of the concrete trenches. Differences between the WIFs calculated for this case and the remote-handled trench case are directly attributable to assumptions used for source release areas in both cases. The ratio of the WIFs between this case and the base case at 100 m are on the order of 0.27, which is reflective, though slightly lower, than the ratio of the release areas (0.29).

Other sensitivity cases examined the effect of increasing the effective surface area of release at the water table beyond the basic footprint of the base case. After transport through the vadose zone, contaminants originating from the individual disposal units would disperse in a pattern likely to be larger than the original footprint of the individual trench configuration. In this sensitivity case, two subcases were evaluated. One case evaluated a source-release area for the remote-handled trench concept reflective not only of the individual remote-handled trench areas, but of the intervening inter-trench areas. Another evaluated a source-release area for the concrete-vault concept reflective not only of the individual concrete vault areas, but of the intervening inter-trench areas.

Calculations for this case showed that the assumed 20 percent increase in the source-release area resulted in about a 20-percent increase in the WIFs over the base-case values at both the 100-m and 1-km wells. This result is consistent with the additional contaminant mass introduced at the water table for this case. This result, combined with previous results for remote-handled trench base case and the concrete vault releases, suggests a linear relationship between the source-release area and calculated WIFs over the range of the assumed release area.

Groundwater flow and transport also were calculated for the site located at the existing grout facility containing the four existing empty concrete vaults. The large differences between the WIFs calculated for this case and those calculated for the remote-handled trench case are attributable to assumptions used for source release areas and the lower estimated values for hydraulic properties used for hydrogeologic units in the existing grout facility model. The remote-handled trench calculations were based on an assumed release area of 124,800 m^2, reflecting the footprint of the assumed six-trench configuration. The concrete vault calculations were based on the assumed 2,560 m^2 release area, reflecting the footprint of the smaller four-concrete-vault configuration. The ratio of the WIFs between the two cases at 100 meters are on the order of 0.43, which is much higher than expected given that the ratio of the release area is on the order of 0.02. The higher than expected WIF in this case is caused by the lower hydraulic conductivities used in this local scale model. Hydraulic conductivities used for the Hanford formation beneath the existing grout facilities, which are on the order of 200 m/day to 300 m/day, are about 25 to 50 times lower than those beneath the new ILAW disposal facility area, which vary from about 6,500 m/day to 14,500 m/day). In general, the lower hydraulic conductivities used in the existing grout facility model contribute to lower pore water velocities and lower horizontal flow beneath the existing grout facility, and create an overall increase in the calculated WIF. The general increase in the WIF for this case reflects differences in the release area and the estimated hydraulic properties.

4.7.3 Pumping Rates at the Well Retrieving the Contaminated Water

Results of these sensitivity cases showed that pumping in the ranges of rates investigated would have little effect on the calculated WIFs. The effect of these relatively low pumping rates is consistent with the fact that water pumped at the 100 m (328-ft) well location is largely pulled from the Hanford formation soils. Given the magnitude of the estimated permeabilities of the Hanford formation at the location of the 100 m (328 ft) well (about 4,400 m/day), the hydraulic effect of the pumping would be minimal and would not significantly alter the local flow field and the overall plume movement. Calculated WIFs for these cases are virtually identical as those calculated at the 100 m (328 ft) well and at 1 km (0.62 mi) in the base case.

4.7.4 Hydraulic Conductivities Beneath the Site

The estimated hydraulic properties and interpretations of the distribution of major hydrogeologic units used in the Sitewide model and local-scale models are based on interpretations of limited measurements and well log information. Uncertainties in estimates of hydraulic properties and boundaries of the major units are associated with these interpretations. This sensitivity study investigates the effect of the position and the associated hydraulic-property differences between the Hanford formation and the underlying Ringold Formation (Unit 5). Directly beneath the disposal-facility area, the estimated hydraulic conductivities of the Hanford formation range from 2500 m/day to 30,000 m/day (27,340 to 32,808 yd/day). In contrast, the hydraulic conductivity of the Ringold Formation (Unit 5) ranges from 40 m/day to 350 m/day (44 to 383 yd/day). For this sensitivity study, the permeability of the Hanford formation where it exists beneath the disposal facility was lowered to the hydraulic-conductivity levels of the underlying Ringold Formation. Conceptually, this change effectively reduces simulated

velocities and flow rates in the hydrogeologic unit at the water table and would result in an increase in the calculated WIFs.

The reduction in hydraulic conductivities changed the primary direction of groundwater flow beneath the facility to a more easterly direction (Bergeron 2000). WIFs calculated at the 100-m (328-ft) well and at 1 km (0.62 mi) indicate that a reduction in the hydraulic conductivity of the underlying Hanford formation to those in the Ringold Formation (Unit 5) below the Hanford formation would increase calculated WIFs by about an order of magnitude (a factor of 12 higher) at the 100- m (328-ft) well. The resulting WIF for the 4.2 mm/year recharge rate at 1 km (0.62 mi) was calculated to be a factor of about 5 higher than at the same location in the base case.

4.7.5 Regional Influences

Results of earlier work by Lu (1996) and the results of this study have shown that the characteristics of the hydrogeologic unit and the estimated water table are an important consideration and will influence the calculated WIFs downgradient of the ILAW facility. The actual position of the water table in the far future is indeed uncertain, and a series of sensitivity studies were done to examine the effect of factors that could affect the position of the water table beneath the ILAW facility. The two main factors that could influence the water table position include the estimated levels of regional natural recharge and inflow onto the Hanford Site from upgradient offsite sources.

One sensitivity case examined the effect of increasing regional natural recharge on the regional and local water-table conditions. In this case, the recharge was increased by a factor of three in the Sitewide model, and the resulting predicted water table was used to evaluate the effect of these changes in the local-scale flow and transport model.

According to Bergeron (2000), the simulated change in natural recharge in the Sitewide model raised the regional water table and significantly changed the overall predicted regional flow path for the ILAW facility from southeast and east toward the Columbia River to a predominant flow path north through the gap between Gable Butte and Gable Mountain to the Columbia River. The discharge area to the Columbia River for these conditions is eventually in the vicinity of the 100 N Area.

Locally, the water table was raised by about 3 m (16 ft) in the vicinity of the new disposal facility, resulting in an increased saturation of the Hanford formation beneath the ILAW facility. Results for this case, summarized in Table 4-16, indicate about a 8-percent reduction in the calculated WIF over the base case WIF at the 100-m (328 ft) well location. At the 1-km (0.62 mi) location, the resultant WIF was 18 to 57 percent lower than the WIF at the 100-m well location in the base case for the same assumed recharge rate. The decrease in the WIF at both locations suggests an increased amount of dilution resulting from this case.

Another sensitivity case examined the effect of reducing regional natural recharge on the regional and local water table conditions. In this case, the recharge was reduced by a factor of three. Results of this simulated change in natural recharge in the Sitewide model lowered the regional water table, but did not significantly change the overall predicted regional flow path for

the ILAW facility from southeast and east toward the Columbia River. The discharge area into the Columbia River for these conditions is, as in the base case, in the vicinity of the old Hanford town site.

Locally, water-table conditions were changed slightly from the base conditions and the water table was lowered by about 1.2 m (4 ft) near the new disposal facility, resulting in a slight decrease in saturation of the Hanford formation beneath the ILAW facility. Although the water table dropped for this case, the overall simulated hydraulic gradient in the vicinity of the disposal facility was a factor of 1.9 higher than was calculated in the base case (1.25×10^{-4} m/m [meter/meter] versus 6.6×10^{-5} m/m). So although this case resulted in a decrease in the water table, the amount of water beneath the facility increased slightly resulting in an increase in dilution and an overall reduction in the calculated WIF for this case. Results for these simulated conditions indicate a 32-percent reduction in the calculated WIF over the base case at the 100- m (328-ft) well location (7.1×10^{-4} versus 1.05×10^{-3}) for the 4.2 mm/y recharge rate case. At the 1 km (0.62 mi) location, the resultant WIF (5.4×10^{-4}) was 35 percent lower than the WIF at the same location in the base case (7.8×10^{-4}) for the same assumed recharge rate.

A final sensitivity case examined the effect of reducing regional boundary fluxes on the regional and local water table conditions at the Cold Creek and Dry Creek entrances to the Hanford Site as well as recharge to the unconfined aquifer from springs emanating along the base of Rattlesnake Hills. In this case, the simulated boundary fluxes were reduced by a factor of two.

Results of the simulated change in natural recharge in the Sitewide model lowered the regional water table, but did not significantly change the overall predicted regional flow path for the ILAW facility from southeast and east toward the Columbia River. The discharge area into the Columbia River for these conditions is, as in the base case, in the vicinity of the old Hanford town site.

Locally, water-table conditions were changed slightly from the base conditions and the water table elevation was lowered by about 0.5 m (1.6 ft) near the new disposal facility resulting in a slight decrease in saturation of the Hanford formation and slight changes to flow conditions beneath the ILAW facility. As in the previous case, the water table dropped and the overall hydraulic gradient in the vicinity of the disposal facility was a factor of 1.5 higher than was calculated using the base case (1.0×10^{-4} m/m versus 6.6×10^{-5} m/m). As in Case 8, this case resulted in a decrease in the water table and the amount of water beneath the facility increased slightly, resulting in more dilution and an overall reduction in the calculated WIF for this case. Results for these simulated conditions indicate about a 16-percent reduction in the calculated WIF over the base case WIF at the 100 m (328-ft) well location (8.8×10^{-4} versus 1.05×10^{-3}) for the 4.2 mm/y recharge rate case. At the 1 km (0.62-mi) location, the resultant WIF (6.8×10^{-4}) was 18 percent lower than the WIF at the same location in the base case (7.8×10^{-4}) for the same assumed recharge rate.

4.8 SENSITIVITY CASES: OTHER FACTORS

The groundwater pathway results are very sensitive to ^{99}Tc inventory and well screen depth. Other modeling parameter choices have only minor effects.

4.8.1 Overview

This section describes the sensitivity to the amount of radionuclides in the waste (the inventory), the land use assumed, the library of dosimetry parameters chosen, the location of the facility, and calculational assumptions.

4.8.2 Inventory

As only a few radionuclides dominate the impacts, only a few sensitivity cases related to inventory are given. Table 4-17 displays the sensitivity of variables to key radioisotopes. Performing no technetium separation increases the beta-gamma drinking water and all-pathways dose by a factor of 3 (depending on the impact and the time period looked at). Reducing the amount of technetium to zero decreases the beta-gamma drinking water and all-pathways dose by a factor of between 2 and 3. Changing the amount of uranium has a major effect on the concentration of alpha emitters and a minor effect on the all-pathways dose at 10,000 years. Doubling the amount of iodine increases the beta-gamma drinking water dose by about 50% and the all-pathways dose by about 25%. Even if all the radioisotopes are at their bounding values, the estimated impacts only increase by a factor of 2.5 for the beta-photon drinking water and all-pathways doses, and by a factor of 5 for the alpha concentration (when compared to the base analysis case), still well below performance objectives.

Finally, the impacts were estimated assuming the upper bound estimates for all radionuclides and assuming technetium separations did not occur. These sets of calculations represent an extreme estimate for the total inventory in the waste. The results from these calculations increased the base analysis case estimated impacts by a factor of 5, still well below the performance objectives.

Chemicals from the ILAW contribute so little that even using the bounding inventory in the glass waste form makes little difference in the importance of the results (See Tables 4-8 and 4-9). Chemicals from the ILAW contribute so little that even using the bounding inventory makes little difference in the importance of the results (See Tables 4-8 and 4-9). A possible exception is the chromium in the 304L stainless steel container. Not only is there more chromium in the containers (~9×10^6 kg) than in the immobilized waste form (2.7×10^5 kg), but the assumed steel corrosion rate results in the release of its constituents faster than the glass waste form. Using the chromium release rates from Section 4.5.5.2 and assuming that all of the chromium is mobile, the estimated concentration in groundwater 100 meters down gradient at 1,000 years after disposal is 0.023 mg/L, peaking at 2,850 years at 1.13 mg/L, and falling to 0.070 at 10,000 years. The performance goal for chromium is only 0.05 mg/L. These calculations should be bounding as there are probably kinetic constraints on the rate of oxidation

Table 4-17. Sensitivity of Variables to Key Radioisotope Inventories.[a]

Case	Drinking Water				All-Pathways Dose (mrem/year)	
	βγ Dose (mrem/year)		α concentration (pCi/L)			
	1,000 y	10,000 y	1,000 y	10,000 y	1,000 y	10,000 y
Base analysis case	0.000021	0.0102	1.0×10^{-16}	0.034	0.000078	0.070
Increase Tc inventory to 5 times original amount (i.e., No Tc separation)	0.000070 (3.3)	0.034 (3.3)	1.0×10^{-16} (1.00)	0.034 (1.00)	0.00030 (3.9)	0.175 (2.5)
Reduce Tc to zero	0.000009 (0.43)	0.0043 (0.43)	1.0×10^{-16} (1.00)	0.034 (1.00)	0.000023 (0.30)	0.044 (0.63)
Double inventory of I	0.000030 (1.4)	0.015 (1.5)	1.0×10^{-16} (1.0)	0.034 (1.0)	0.00010 (1.3)	0.081 (1.2)
Double inventory of U	0.000021 (1.0)	0.0102 (1.0)	1.0×10^{-16} (1.0)	0.058 (1.7)	0.000078 (1.0)	0.076 (1.1)
All inventory at bounding values with Tc separation occurring	0.000055 (2.6)	0.027 (2.7)	4.8×10^{-16} (4.8)	0.19 (5.5)	0.00017 (2.2)	0.31 (4.4)
All inventory at bounding values and Tc inventory at maximum value	0.00010 (4.8)	0.049 (4.9)	4.8×10^{-15} (4.8)	0.19 (5.5)	0.00038 (4.9)	0.41 (5.9)

[a] The relative change compared to the base analysis case is given in parenthesis.

of Cr(III) to Cr(VI). In the present STORM simulations, global equilibrium with atmospheric levels of O_2(g) was assumed, which results in the dominant oxidation state of Cr as +6 (Pourbaix, 1977). However, future simulations should consider kinetics in constraining the oxidation rate of Cr. Because Cr(III) is less soluble and less mobile than Cr(VI), the effect would be to dramatically lower projected Cr releases to the vadose zone.

4.8.3 Land Use

Land use could affect the disposal facility by changing the regional amount of water entering the aquifer or by the exposure pathways. The concept of changing the regional recharge rate is discussed in Section 4.7.5 and is relatively small. Changes in exposure pathways are discussed in Section 4.8.4.

4.8.4 Dosimetry Parameters

The base analysis case assumes that all knowledge of the disposal facility is lost and a residential farmer is exposed. Table 4-18 displays all-pathways doses for three other exposure scenarios (industrial, residential, and agricultural) for land located near the disposal facility. The industrial scenario represents potential doses to workers primarily caused by drinking well water. The resident scenario represents an individual living near the disposal site and being exposed to well water and produce grown in a garden irrigated with well water. The agricultural scenario represents an individual living on a farm and includes exposure to meat and dairy products from animals exposed to pastures irrigated with well water. As seen in Table 4.18, the estimated impact to the all-pathway dose at 1,000 years after facility closure range from 9.9×10^{-6} to 1.3×10^{-4} mrem/year with the industrial scenario estimated to have the lowest estimated dose and the agricultural scenario having the highest estimated dose. Similarly, at 10,000 years after facility closure, the all-pathway estimated doses range from 0.053 to 0.10 mrem/year, with the industrial scenario estimated to have the lowest estimated dose and the agricultural scenario having the highest estimated dose.

Table 4-18. All-Pathways Doses for Three Other Exposure Pathways for Points Located Near the Disposal Facility.

Case	All-Pathways Dose (mrem/y)	
	1,000 years*	10,000 years
Base analysis case (resident farmer)	0.000078	0.070
Industrial	0.0000099	0.053
Residential	0.000034	0.055
Agricultural	0.000126	0.100

* Time of Compliance is 1,000 years

A Native American scenario was investigated for locations near the Columbia River. Because the Native American scenario requires large amounts of water, such a scenario is likely only near the river. Use of this scenario increases the all-pathways dose from 7.3×10^{-6} to 2.8×10^{-5} mrem/year at 1,000 years after facility closure (neglecting travel time in the aquifer) when compared to the base analysis case. Similarly, the impact to the all-pathway dose at 10,000 years after facility closure is estimated to increase from 0.0065 to 0.022 mrem/year when compared to the base analysis case.

Finally, the sensitivity of the estimated impacts to a different set of dosimetry factors was estimated. Specifically, calculations were performed for the all-pathway farmer scenario using the DOE dose factors (see Rittmann 1999 and Appendix B). The resulting estimated impacts for the all-pathway dose at 1,000 and 10,000 years after facility closure were approximately 10 percent lower using the DOE dose factors.

4.8.5 Facility Location

The sensitivity to the location of the disposal facility is investigated in Section 4.7.2.

4.8.6 Ignored Processes and Conditions

The major processes involved in contaminant transport have been modeled. However, the following processes also should be discussed:

- Upward diffusion of contaminants
- Upward migration by capillary action
- Consumption of water in the glass dissolution process.

Upward diffusion and upward migration only become important with extremely low recharge rates. Both processes produce a characteristic time, T, which depends on the soil diffusivity, D, and on the length to be traversed, L,

$$T = L^2 / D. \tag{4.1}$$

For the case of upward diffusion, the equation can be derived from Fick's law (see Section 4.9). For the case of capillary rise, the equation can be derived by ignoring the gravity term in the flow equation. Using a length of 6 m (the total thickness of materials above the waste) and a soil diffusivity of 1.25×0^{-7} cm^2/second (from Section 3.4.3.2), the characteristic time is almost 100,000 years.

Moreover, as noted in Section 3.4.4.3, water must be present to dissolve the glass. Because the aquifer is so far below the disposal facility, capillary action could not bring water up to the waste. The only mechanism for providing the quantity of water needed to dissolve a significant amount of the waste form is recharge. Therefore, under extremely dry conditions, no contaminants would be mobile.

The current waste form calculations do not take into account water consumed by the corrosion process. From section 3.5.5.8 a recharge rate of 0.005 mm/year is estimated to be totally consumed by glass corrosion. This recharge rate is much smaller than the recharge rate for the base analysis case and the other sensitivity studies investigated in this performance assessment where the capillary break is ignored. However, the estimated recharge rates for the best estimate case are the order of 8.5×10^{-3} mm/year in the waste package region (see Table 4-11). Therefore, the estimated impacts for the sensitivity cases with a functioning capillary break are overestimated.

4.9 SENSITIVITY CASES: EXTREME CASES

4.9.1 Overview

In the review of the *Hanford Low-Level Tank Waste Interim Performance Assessment* (Mann 1996a), a visible stakeholder noted (Appendix F.1 of Mann 1998a) that the public is concerned about not only what is expected, but also how bad the situation could be if some assumption in the analysis is wrong. Such comments have carried important weight with the program. This chapter discusses extreme cases, which are considered to be impossible, at least for most of the waste, but provide insights into extreme bounds of system performance.

4.9.2 Instantaneous Waste Form Release

Sections 4.3.4 (base case) and 4.5 (sensitivity cases) describe the deterministic calculations used to estimate the contaminant release from the glass blocks. Such release is expected to be extremely small, taking hundreds of thousands of years to complete. An extreme case is that all of the waste is released at one time (or at least during a period that is much shorter than the vadose zone travel time). Although physically and chemically impossible, such a case demonstrates the importance of understanding the waste form release mechanism. This case also allows us to determine the impact of any potential contamination on the outside of the ILAW packages. Such contamination would be expected to release very quickly.

Figure 4-37 displays the contaminant flux entering the groundwater assuming that all contaminants release from the waste form at a constant rate over 1 year. The shape of such a flux follows a classic vadose zone transport curve. Table 4-19 displays the estimated impacts, assuming all contaminants are release over this short time period.

Figure 4-37. Inventory-Normalized Contaminant Flux Entering the Groundwater Assuming All Contaminants Release from the Waste Form at Once.

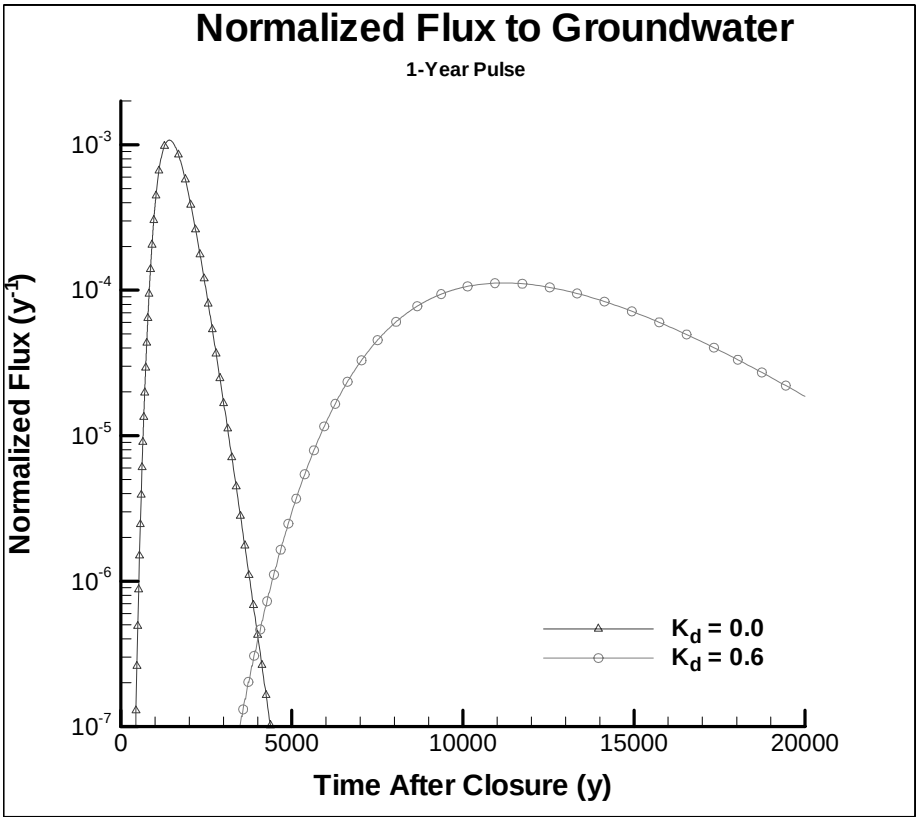

Table 4-19. Effect on Estimated Impacts Assuming All Contaminants Release at Once.

Impact	Base Analysis Case		Instantaneous Release		
	1,000 years	10,000 years	1,000 years	10,000 years	Maximum (Time of Peak)
βγ drinking water dose (mrem/y)	0.000021	0.0102	7.41	0.0	16.9 (1,385 y)
α concentration in water (pCi/L)	1.0×10^{-16}	0.034	3.6×10^{-11}	66.4	69.3 (11,150 y)
All-Pathways (mrem/year)	0.000078	0.070	27.1	62.9	67.2 (11,150 y)

There is about a five-order-of-magnitude increase for the impacts at 1,000 years. This reflects the importance of the slow release from glass. For the beta-gamma emitters, all of which are mobile, the contaminants travel through the vadose zone and the groundwater to the 100 m-

downgradient point-of-compliance well within 10,000 years. The peak impact for the beta-gamma drinking water dose is seen at 1,350 years. The alpha-emitters are retarded and are still rising at 10,000 years, reaching a peak at about 11,000 years. At 10,000 years, the all-pathways dose and the concentration of alpha emitters in the groundwater for the instantaneous release case is about two to three orders larger than the base analysis case. The beta/photon dose is insignificant at 10,000 years because the most important radioisotopes (i.e., those having $K_d = 0$) have already flowed past the point of compliance (see Figure 4-37).

However, for all impacts, even if there were an instantaneous release of the entire ILAW inventory, the impacts would be within a factor of five of performance objectives. Such low impacts from instantaneous release can be explained by the dispersion in the vadose zone and the dilution in the groundwater. By the time the contaminants reach the groundwater, travel in the vadose zone has increased the temporal spread to 980 years (the full width at the height that corresponds to half the maximum value). Such a spread is consistent with previous calculations for the ILAW site, as well as with other Hanford Site calculations for this travel time. The dilution in the groundwater is the same for this case as for the base analysis case.

The major contributors to the estimated impact to the beta-photon drinking water dose, the all-pathway dose, and the alpha concentration are summarized in Tables 4-20, 4-21, and 4-22, respectively.

Table 4-20. Major Radionuclide Contributors at 1,000 Years and 10,000 Years to the Estimated Beta-Photon Drinking Water Dose at a Well 100 m Downgradient from the Disposal Facility for Instantaneous Release.

Radionuclide	1,000 years*		10,000 years		Peak Exposure**	
	Dose (mrem/y)	Fraction	Dose (mrem/y)	Fraction	Dose (mrem/y)	Fraction
^{99}Tc	4.27	0.58	0.0	---	9.80	0.58
^{129}I	3.08	0.41	0.0	---	7.07	0.42
Other	0.05	0.01	0.0	---	0.03	----
Total	7.41	---	0.0	---	16.9	---

* Time of compliance is 1,000 years.
** See Table 4-19 for time of peak exposure.

Table 4-21. Major Radionuclide Contributors at 1,000 Years and 10,000 Years to the Estimated All-Pathways Dose at a Well 100 m Downgradient from the Disposal Facility for Instantaneous Release.

Radionuclide	1,000 years*		10,000 years		Peak Exposure**	
	Dose (mrem/y)	Fraction	Dose (mrem/y)	Fraction	Dose (mrem/y)	Fraction
^{99}Tc	19.2	0.71	0.0	0	0.0	0
^{129}I	7.8	0.29	0.0	0	0.0	0
^{231}Pa	---	---	0.93	0.02	1.05	0.02
^{233}U	---	---	5.95	0.09	6.34	0.09
^{234}U	---	---	1.99	0.03	2.13	0.03
^{238}U	---	---	2.06	0.03	2.20	0.03
^{237}Np	---	---	51.9	0.83	55.4	0.83
Other	0.1	0	0.07	0	0.08	0
Total	27.1	---	62.9	---	67.2	---

* Time of compliance is 1,000 years.
** For time of peak exposure, see Table 4-19.

Table 4-22. Major Radionuclide Contributors at 10,000 Years to the Estimated Concentration of Alpha Emitters at a Well 100 m Downgradient from the Disposal Facility for Instantaneous Release.

Radio-nuclide	1,000 years		10,000 years		Peak Exposure**	
	Concentration (pCi/L)	Fraction	Concentration (pCi/L)	Fraction	Concentration (pCi/L)	Fraction
^{231}Pa	0.0	---	0.13	0	0.15	0
^{233}U	0.0	---	27.16	0.42	28.95	0.42
^{234}U	0.0	---	9.32	0.14	9.95	0.14
^{238}U	0.0	---	10.17	0.16	10.85	0.16
^{235}U	0.0	---	0.38	0.01	0.41	0.01
^{236}U	0.0	---	0.32	0	0.34	0
^{237}Np	0.0	---	17.46	0.27	18.64	0.27
Other	0.0	---	0.01	0	0.01	0
Total	0.0	---	64.95	---	69.3	---

* Time of compliance is 1,000 years.
** For time of peak exposure, see Table 4-19.

4.9.3 Instantaneous Vadose Zone Travel

Sections 4.3.5 (base case) and 4.6 (sensitivity cases) describe the deterministic calculations of contaminant transport in the vadose zone. These calculations show that travel times are thousands of years for mobile contaminants to hundreds of thousands of years for more retarded species. An extreme case is to assume that the travel time is zero. Although contrary to our basic knowledge of moisture flow and contaminant movement, such a case shows the importance of the vadose zone for the performance assessment.

Table 4-23 displays the estimated impacts assuming that travel through the vadose zone is instantaneous. Release of waste glass contaminants directly to the groundwater has the following effects on the estimated doses when compared to the base analysis case. First, the beta-photon drinking water doses are significantly higher at 1,000 years after facility closure when compared to the base case. At 10,000 years after closure, the estimated impacts of an instantaneous transport through the vadose zone are comparable to the base case. This is because the waste glass release of contaminants is relatively constant after an initial transient period. Note that the peak beta-photon dose (0.80 mrem/year) occurs approximately 70 years after plant closure. The major contributors to this dose are ^{90}Sr (0.74 mrem/year) and ^{137}Cs (0.055 mrem/year). This highlights the important effect of the vadose zone to delay transport of radionuclides and allow those isotopes with relatively short half-lives to decay before reaching the aquifer. As shown in Table 4-23, the alpha concentration in the groundwater is much higher than the base case at both 1,000 and 10,000 years after facility closure. This result is caused by the additional retardation of contaminant flow for the alpha emitters in the base analysis case (see Figure 4-9).

For this sensitivity case, both the beta-photon drinking water and all-pathway dose performance objectives are met. The alpha concentration performance objectives also are met at 1,000 and 10,000 years after facility closure. For this extreme case, the radium radionuclides would reach the groundwater. At 1,000 years after facility closure, the radium concentration in the groundwater would be 3.5×10^{-4} pCi/L. At 10,000 years after facility closure, the radium concentration in the groundwater would be 5.8×10^{-3} pCi/L. Both these estimated impacts are well below the performance objective of 5 pCi/L. The total alpha concentration at 10,000 years after facility closure is 4.6 pCi/L, well below the performance objective of 15 pCi/L.

Table 4-24 compares the effect on the all-pathways dose when instantaneous transport through the vadose zone occurs for the most important radioisotopes. For the all-pathways dose, ^{239}Pu and ^{241}Am contribute over 89 percent of the estimated dose at 1,000 years after facility closure. At 10,000 years, ^{209}Po (2 percent), ^{229}Th (3 percent), ^{237}Np (4 percent), ^{239}Pu (82 percent), and ^{240}Pu (7 percent) contribute over 98 percent of the estimated dose. Except for ^{237}Np, all these radionuclides have assigned K_d = 150 mL/g and would not be expected to reach the aquifer in 10,000 years, even if the recharge rate were as high as 50 mm/year if the vadose zone was present.

Table 4-23. Estimated Impacts Assuming Instantaneous Vadose Zone Travel.

Impact	Base Analysis Case		Instantaneous Vadose Zone Travel		
	1,000 years	10,000 years	1,000 years	10,000 years	Maximum (Time of Peak)
$\beta\gamma$ drinking water dose (mrem/y)	0.000021	0.0101	0.0029	0.016	0.80 (70 y)
α concentration in water (pCi/L)	1.0×10^{-16}	0.032	1.48	4.58	4.8 (13,100 y)
All-Pathways (mrem/y)	0.000078	0.069	3.39	9.36	9.4 (11,100 y)

Table 4-24. Effect On The All-Pathways Dose When Instantaneous Vadose Zone Travel Occurs For The Most Important Radioisotopes.

Radioisotope	Base Analysis Case		Instantaneous Vadose Zone Travel	
	1,000 years	10,000 years	1,000 years	10,000 years
^{99}Tc	0.0000552	0.0262	0.0051	0.028
^{129}I	0.0000224	0.0110	0.0021	0.012
^{231}Pa	0.0	0.000463	0.0007	0.006
^{233}U	0.0	0.00296	0.0071	0.040
^{234}U	0.0	0.000994	0.0024	0.014
^{238}U	0.0	0.00103	0.0024	0.014
^{237}Np	0.0	0.0258	0.0612	0.351
^{209}Po	----	----	0.0051	0.206
^{229}Th	----	----	0.0090	0.310
^{239}Pu	----	----	1.744	7.681
^{240}Pu	----	----	0.276	0.612
^{241}Am	----	----	1.268	0.000005
Other	0.0000002	0.0002	0.008	0.086
Total	0.0000778	0.0686	3.39	9.36

4.9.4 Bathtub Effect

The effect of trapping water within the trench for a period of time, then having a sudden release of the trapped water was investigated in Finfrock (2000b). A simplified calculation was performed assuming all free space within the trench was filled with water. A waste form calculation was performed to determine the amount of contaminant released from the waste form as a function of time (see Figure 4-32 and Bacon 2001). The released contaminant concentration then was assumed to instantly enter the groundwater. The peak all-pathway dose for this bounding calculation was estimated to be 2.3 mrem/year if the release occurred after 100 years and 8.1 mrem/year if the release occurred after 1,000 years. The major contributors to the all-pathway dose for the 100-year release case are ^{241}Am (41 percent), ^{239}Pu (14 percent), ^{90}Sr (36 percent), ^{137}Cs (6 percent), and ^{240}Pu (2 percent). The major contributors to the all-pathway dose for the 1,000-year release case are ^{241}Am (37 percent), ^{239}Pu (52 percent), ^{237}Np (2 percent), and ^{240}Pu (8 percent). If chemical adsorption is considered (i.e., if only those radionuclides with

K_d less than 4 mL/g are assumed to reach the groundwater with concentrations equivalent to the estimated concentrations in the trench before the release), then the peak all-pathway dose was estimated to be 0.015 mrem/year if the release occurred after 100 years and 0.19 mrem/year if the release occurred after 1,000 years. The major contributors to the all-pathway dose for the 100-year release case are ^{237}Np (73 percent), ^{99}Tc (6 percent), ^{129}I (3 percent), ^{233}U (9 percent), ^{238}U (3 percent), and ^{234}U (3 percent). The major contributors to the all-pathway dose for the 1,000-year release case are ^{237}Np (75 percent), ^{99}Tc (6 percent), ^{129}I (3 percent), ^{233}U (9 percent), ^{238}U (3 percent), and ^{234}U (3 percent). These are upper bound estimates because any spreading in the plume as it is transported through the vadose zone has not been included in the estimate. (Note that for the pulse case (i.e., the instantaneous release rate case discussed in Section 4.9.2), the peak concentration is reduced by a factor of 1,000 as the contaminants are transported through the vadose zone. The reduction is anticipated to be less than the pulse case.) Calculations performed in the 1998 ILAW PA (Mann 1998a) estimated this effect to impact the estimated dose by less than 3 percent if the effect were to last for 2000 years.

4.10 CUMULATIVE IMPACTS FROM HANFORD SITE ACTIVITIES

Other actions at the Hanford Site will have a minimal effect on this disposal action. This disposal action will have minimal effect on other Hanford Site actions.

4.10.1 Introduction

The Defense Nuclear Facilities Safety Board recommended (DNFSB 1994) that, when evaluating of the impact of the disposal of radioactive waste, DOE consider not just the impact from the disposal action under consideration but all other government actions that might affect those impacts. This recommendation has been inserted into DOE O 435.1 (DOE 1999b). The Richland Operations Office has submitted a composite analysis (Kincaid 1998) that addressed all the Hanford Site's disposal and closure actions on the Hanford Site's central plateau for which inventories had been established. The DOE has conditionally approved this composite analysis (DOE 1999d). The analysis presented here will focus on the results of the composite analysis and the results of the 1998 ILAW PA (Mann 1998a).

4.10.2 Hanford Site Composite Analysis

A Composite Analysis (Kincaid 1998) was submitted to DOE-Headquarters supporting the active and planned low-level waste disposal on the 200 Area Plateau. DOE (DOE 1999d) conditionally approved this composite analysis. It is a companion analysis to PAs for active and planned disposal, and remedial investigations and feasibility studies for remediation sites. With some limitations primarily based on available inventory data, this was a first iteration analysis to discover the potential long-term impacts to an offsite individual from all waste forms to reside at the Hanford Site at the time of Site closure. For the Composite Analysis, the offsite individual resided outside the exclusive waste management area and buffer zone as defined by the Hanford Future Site Uses Working Group (HFSUWG 1992). The analysis considered a 1,000 year regulatory period following Site closure and reached the following conclusions:

- Significant releases from the liquid discharge sites, tank leaks, losses from tanks during tank waste recovery operations, and pre-1988 solid waste burial grounds that occurred or began before Site closure were separated in time significantly from any discharges from the active or planned disposal.

- Peak all-pathways dose to the maximally exposed individual outside the buffer zone after Site closure (assumed in 2050) was less than 6 mrem in a year. This was the result of the agricultural scenario. Lesser doses resulted from the residential, industrial, and recreational scenarios. Despite high uncertainty in the inventories of past liquid discharges, tank leaks, tank losses, and pre-1988 burial grounds, this analyses indicated dose outside the buffer zone would not exceed the dose constraint of 30 mrem in a year.

- Maximum contaminant concentrations are highest now and will decline with time. Releases from liquid discharge sites, tank leaks, future tank losses, and pre-1988 burial grounds continue to enter the aquifer over the next few decades, but, in general, the rate of nuclide mass releasing to the aquifer will decline from now until Site closure and then continue to decline.

- No releases from the TWRS immobilized low-activity waste disposal facilities, the Environmental Restoration Disposal Facility trench and the graphite cores of the production reactors are seen during the regulatory period of 1,000 years or the full 1,500 years analyzed.

Future iterations of the Composite Analysis will be based on a more fully consistent inventory for all post-closure waste sites, including canyon buildings and associated facilities, which include permanent filters, and the PUREX tunnels.

4.10.3 Results from 1998 ILAW PA

Because the 1998 Hanford Site Composite Analysis (Kincaid 1998) performed simulations only out to 1,500 years and because this analysis goes out 10,000 years, this section provides an extended discussion of overlapping plumes. This section repeats the discussion that appeared in the 1998 ILAW PA (Mann 1998a).

One of the important differences in the current and past ILAW performance assessments relates to the groundwater models used in both assessments. Although no detailed comparisons between the current model and the model described in Lu (1996) have been made, some general observations about the two models and their past predictions were made in Cole (1997). In general, the results of past regional transport analyses of tritium, ^{129}I, ^{99}Tc, and uranium with the three-dimensional models described in Cole (1997) agreed with past Sitewide modeling results obtained by Chiaramonte (1996) in support of the Environmental Restoration Program. However, because of basic differences in assumptions made about the hydrogeologic framework and the horizontal and vertical discretization used in each model, discrepancies between model predictions on subregional and local-scales should be expected. A direct comparison of a calculated WIF for the Concept 1 source analyzed by Lu (1996) by Bergeron (2000) using the current model produced a WIF that was a factor of 10 lower than the WIF calculated by Lu

(1996) in the previous PA. The hydraulic conductivities used by the current model and the model used by Lu (1996) for the Ringold Formation are on the same order of magnitude, between 40 m/day and 300 m/day in the current model and between 70 m/day and 245 m/day in model used by Lu (1996). However, the current model contains areas of the Hanford formation beneath the facility and, as a result, has areas of very high permeability (between 2,200 m/day and 30,000 m/day) in the area of the source release.

The main pathway affected in an integrated analysis is the groundwater pathway. Inadvertent intruder scenarios and releases to the air are controlled at the source point. As will be seen in Section 4.14, the impacts of catastrophic events on waste that has been disposed are not significant.

Assuming that the disposal facility is placed just southwest of the PUREX facility, the previous Hanford Site actions that would affect groundwater downgradient of the disposal facility are those activities upgradient of the facility. From Figure 3-1 of the 1998 ILAW PA or from Figure 3-1 of this PA, those actions are the operations at the S, SX, SY, and U tank farms and the disposal of waste at the Environmental Remediation Disposal Facility and the commercial low-level waste disposal site operated by a commercial firm (U.S. Ecology).

Using the aquifer model described in Section 3.5.3.3 of the 1998 ILAW PA, mixing effects were calculated (appendix of Lu 1996) for the transport of contaminants from these potential sources to a well 100 m downgradient of the disposal facility. The mixing factors are displayed in Table 4-25. Because of the distance from the sources, the mixing factors are significantly less than from the low-level tank waste disposal site.

Table 4-25. Mixing Factors* from Other Sources for a Well 100 m Downgradient of the Low-Level Tank Waste Disposal Site.

	Upstream Sources				
	Low-Level Tank Waste Site	ERDF Site	S, SX, SY Tank Farm	U Tank Farm	Commercial LLW Disposal Site
Mixing Factor*	1.77×10^{-3}	3.01×10^{-4}	2.08×10^{-4}	1.25×10^{-4}	8.91×10^{-5}
Fraction of Base Analysis Case	1.00	0.17	0.12	0.07	0.05

*Mixing factor is the contaminant concentration in well water divided by the contamination concentration at the bottom of the vadose zone.

Both the DOE (DOE 1999b) and the NRC (10 CFR 61-4) mandate that a member of the general public can receive an exposure of no more than 25 mrem in a year at the edge of a disposal facility. Assuming that the other sources have their maximum impact and ignoring any time factors that might reduce the effect of the overlap, the other sources could add no more than 10.3 mrem in a year. Adding this to the amount estimated in Section 4.3.6 (all-pathway dose = 0.070 mrem/year) yields a total dose of less than 10.4 mrem in a year for the first 10,000 years. Moving the point of compliance to the 200 East Area fence will reduce the estimated compliance dose by less than 25 percent.

4.11 SUMMARY OF GROUNDWATER PATHWAY CASES

Estimated impacts to the groundwater resource have been calculated for the base analysis case. These estimated impacts are significantly lower than the performance objectives that have been established for this disposal action (see Section 1.6). A best estimate calculation has been performed for the proposed disposal action that indicates additional margin when compared to the base analysis case. Finally, a series of sensitivity calculations have been performed to provide the reader with an understanding of the relative sensitivity of these results to both hypothetical and extremely unlikely situations. The results taken in total provide a convincing argument that the proposed disposal of ILAW waste in a remote handled trench facility concept will not violate the performance objectives for protecting the groundwater resources.

The results from the base analysis case calculations are summarized in Tables 4-3 through 4-9. The base analysis case is based on site-specific data and includes conservative assumptions when needed to ease calculations. At 1,000 years after facility closure, the estimated impacts are more than 5 orders of magnitude less than the performance objectives for the radionuclides (Table 4-3). At 10,000 years after facility closure, the estimated impacts remain more than a factor of 400 less than the performance objectives. The estimated impacts for the chemicals associated with the glass waste are more than a factor of 1,000 less than the performance objectives (Table 4-8).

The results from the best estimate case calculations are summarized in Table 4-10. The best estimate case is based on a functioning capillary break located above the facility and on site-specific data, and includes conservative assumptions when needed to ease calculational resource demands. The lower moisture flux into the facility caused by the capillary break results in estimated impacts that are more than three orders of magnitude less than the estimated impacts for the base analysis case.

Sensitivity cases were calculated to investigate the sensitivity of the base analysis case to key parameters and assumptions. These key parameters and assumptions included moisture flow into the facility (Section 4.4), different facility concepts (Section 4.4), waste form performance (Section 4.5), vadose zone properties (Section 4.6), groundwater moisture flow assumptions (Section 4.7), inventory (Section 4.8.2), and dosimetry parameters (Section 4.8.4). In all cases the performance objectives for protecting the groundwater were met.

Extreme cases also were calculated to demonstrate worst case performance for the disposal action. The specific cases investigated included an instantaneous release of all contaminants from the waste form in 1 year, and the instantaneous transport of the contaminants through the vadose zone. Although these cases were highly incredible, the resulting impacts did not exceed the performance goals for protecting the groundwater by more than a factor of 10.

The calculations show that the peak values of impacts to groundwater are most sensitive to those parameters determining the inventory of ^{99}Tc, the rate of waste form release, and the amount of dilution in the groundwater. Recharge and geochemical parameters are important in establishing the time of arrival.

4.12 EFFECTS OF RELEASES TO AIR

This section describes the migration of nuclides from the glass waste, through the facility to the ground surface, and into the atmosphere. The primary transport mechanism is gaseous diffusion. Other mechanisms were considered and found to be insignificant. The initial inventory combined with the small glass dissolution rate and the delay associated with diffusion reduces the surface release rate to levels that are well below the performance objectives for the ILAW.

4.12.1 Upward Diffusion of Radionuclides

The principal mechanism by which nuclides migrate from the waste to the ground surface is gaseous diffusion. The diffusion of radioactive gases such as tritium (as water vapor), ^{14}C (as carbon dioxide), and ^{222}Rn (an inert gas) can be represented using Fick's law of diffusion with a loss term for radioactive decay (Jury 1991). The amount available for diffusion, i.e., the source concentration, is changing with time due to the corrosion of the glass and radioactive decay. Two cases must be considered because the ^{222}Rn is being produced by a decay chain that includes ^{238}U, ^{234}U, ^{230}Th, and ^{226}Ra.

For ^{3}H and ^{14}C the source concentration increases with time after closure due to corrosion of the glass and decreases with time due to radioactive decay. If we first assume that all of the ^{3}H and ^{14}C released during the year diffuses away from the trench, then the source concentration for these two radionuclides is shown below. This assumption will be tested by comparing the predicted total airborne emission rate with the estimated total corrosion rate of the glass. The two release rates should be comparable in a system near steady-state. The total amount entering the air each year after diffusion through the cover should not be greater than the total amount that is released from the glass each year.

$$C_0(t) = f \; C_G(0) \, e^{-\lambda t} \tag{4.2}$$

where

$C_0(t)$ = diffusion source concentration in the waste trench, i.e., the average concentration of gas that is free to diffuse through the cover soil, Ci/m^3

$C_G(0)$ = average gas concentration in the waste trench at closure (t=0), Ci/m^3. This is computed as the total inventory in the waste trench divided by the trench volume.

f = bounding annual waste dissolution fraction, 9.3×10^{-7} per y (Table 4-1). It is the fraction of the total that is released by corrosion of the glass.

t = elapsed time since closure, y

λ = radioactive decay constant for the nuclide under consideration, per y. It is computed as the natural logarithm of 2 divided by the half life in years.

The source concentration is largest initially. The calculation of the maximum source concentration is shown in Table 4-26.

Table 4-26. Calculation Summary for ^{3}H and ^{14}C

	^{3}H	^{14}C
Nuclide Half Life	12.33 y	5,730 y
Decay Constant, λ	0.05622 y^{-1}	1.210E-04 y^{-1}
Bounding Waste Inventory at Closure, A_G (from Table 3-1)	3,251 Ci	4,361 Ci
Average Trench Concentration at Closure, $C_G(0)$	4.59E-03 Ci/m^3	6.16E-03 Ci/m^3
Total Waste Release Rate at Closure, f A_G	3.02E-03 Ci/y	4.06E-03 Ci/y
Maximum Source Concentration, $C_0(0)$	4.27E-09 Ci/m^3	5.73E-09 Ci/m^3
Diffusion Flux into the Air, $J(z_0)$	2.68E-08 Ci/m^2 per y	3.62E-08 Ci/m^2 per y
Activity Airborne Annually	3.34E-03 Ci/y	4.51E-03 Ci/y
CAP88-PC Dose Factor	0.0237 mrem/Ci	1.32 mrem/Ci
Air Pathway Dose	7.91E-05 mrem/y	5.96E-03 mrem/y

Numbers for the radionuclide half life are from ENDF/B-VI.

Decay constants are the natural logarithm of 2 divided by the half life (1 y = 365.25 d).

The bounding inventories for ^{3}H and ^{14}C have been decayed 36 years corresponding to the difference between the inventory date (1994) and plant closure (2030).

The average concentration initially in the trenches is calculated as the bounding waste inventory at closure divided by the volume of the six waste disposal trenches, 708,000 m^3.

The total glass release rate is the initial inventory at closure times the bounding annual dissolution fraction, 9.3×10^{-7}.

The maximum source concentration is calculated from the trench concentration at closure, the bounding annual dissolution fraction, and the decay time since closure.

The diffusion flux into the air is calculated from the diffusion model described in the text.

The annual airborne emission from the disposal facility is calculated as the product of the bounding diffusion flux, the facility footprint area (124,800 m^2), and the release duration (1 y).

Unit release dose factors are from *Exposure Scenarios and Unit Dose Factors for the Hanford Immobilized Low-Activity Tank Waste Performance Assessment* (Rittmann 1999).

For calculating diffusion in the presence of radioactive decay the source concentration is assumed to be constant because it changes very slowly with time. This assumption tends to exaggerate the diffusion flux at the surface. The steady-state diffusion equation is shown below. It also assumes the diffusion characteristics of the waste cover are uniform with depth.

$$D\frac{\partial^2 C}{\partial z^2} = \lambda C \tag{4.3}$$

The solution to the above equation has an exponential dependence in elevation as shown below. The boundary conditions that the soil concentration is C_0 at the waste (z=0) and zero at the surface ($z=z_0$) have been included. The solution is only valid from z=0 to $z=z_0$.

$$C = C_0\left[\frac{e^{-z\sqrt{\lambda/D}} - e^{-(2z_0 - z)\sqrt{\lambda/D}}}{1 - e^{-2z_0\sqrt{\lambda/D}}}\right] \tag{4.4}$$

$$J(z) = -D\frac{\partial C}{\partial z} \quad \text{thus} \quad J(z_0) = \frac{2\sqrt{\lambda D}\, C_0\, e^{-z_0\sqrt{\lambda/D}}}{1 - e^{-2z_0\sqrt{\lambda/D}}} \tag{4.5}$$

where

C = gas concentration at elevation z in the soil, Ci/m^3. At the bottom of the soil cover, the soil concentration matches the gas concentration in the waste, i.e., $C=C_0$. At the top of the cover the gas concentration is zero.

D = diffusion coefficient for low atomic number gases moving through soil, 0.01 cm^2/s = 31.56 m^2/y

J = upward diffusion flux, Ci/m^2 per y

z = vertical position in the soil, m. The bottom of the soil column is z=0, while the ground surface is $z=z_o$=5 m.

λ = radioactive decay constant for the nuclide, per y.

Previous calculations did not use the boundary condition that the surface concentration is zero. In effect, an infinite medium was assumed. This underestimates the surface diffusion flux (J) by at least a factor of two. Longer half-life nuclides show a larger difference.

The diffusion flux at the surface is shown in Table 4-26. The small values for diffusion flux are largely due to the slow release rate from the glass. The values shown are bounding numbers for the following reasons.

- The estimated glass dissolution rate is 9.3×10^{-7} per year after 10,000 years. It is the peak glass dissolution rate for the base analysis case (see Section 4.3.3).

- Only ^{222}Rn is an inert gas that will faithfully follow the diffusion model. The ^{3}H and ^{14}C will undergo chemical reactions and be part of compounds that are likely to exist in the soil or the glass corrosion products. For ^{3}H these compounds include water and hydroxides. For ^{14}C these compounds include carbonates and carbides. The effect of these chemical reactions is to slow the migration to the surface and the resulting release rate from the ground surface. This effect has not been included in the diffusion calculations to maximize estimated consequences.

- The predicted airborne emission rate from the surface of the facility exceeds the estimated waste release rate. For ^{14}C, the total initial waste release rate due to corrosion is 0.00406 Ci/y while the predicted emission rate from the facility surface is 0.00451 Ci/y. The fact that the airborne emission rate is larger than the glass release rate suggests that the maximum source concentration should be smaller.

The source concentration of ^{222}Rn is based on the amount of ^{226}Ra that has dissolved. The ^{226}Ra produces ^{222}Rn by radioactive decay. The amount of ^{226}Ra slowly increases for two reasons. First, an increasing fraction of the glass matrix has dissolved. Second, ^{226}Ra is being produced by the radioactive decay of ^{238}U and ^{234}U. The peak ^{222}Rn flux occurs after all the glass has dissolved, and the ^{226}Ra has reached radioactive equilibrium with the ^{238}U. This equilibrium occurs after times greater than 1×10^{6} years after closure.

The initial inventory of ^{238}U in the disposal facility is 328 Ci. After a few million years, the glass matrix has released the uranium and the ^{230}Th, ^{226}Ra, and ^{222}Rn are all in radioactive equilibrium with the ^{238}U. Thus the ^{222}Rn inventory in the trench is 328 Ci, and the average concentration in the waste trench is 4.63×10^{-4} Ci/m^{3}. It has been assumed that no migration of the uranium out of the trench has taken place during this time.

The calculation of the diffusion flux for ^{222}Rn is carried out using the formula given previously. The diffusion flux at the ground surface is 3.03×10^{-5} Ci/m^{2} per year, or 0.96 pCi/m^{2} per second.

4.12.2 Mechanisms Affecting the Diffusion Flux

There are four environmental factors that can affect the rate of gas transport through the soil. These are barometric pressure, temperature, wind, and rain (Jury 1991). Each of these will be discussed in terms of its effect on the gaseous diffusion rate from the ground surface calculated above.

4.12.2.1 Atmospheric Pressure. An increase in atmospheric pressure will compress the air above the soil and drive air into the soil. The motion of air into the soil is impeded by the tortuosity of the flow channels and the small diameter of the surface openings between soil grains. When the atmospheric pressure decreases gases in the soil expand and the gas near the surface is released into the atmosphere. The effect on gases diffusing from underground is to slow the release rate while the atmospheric pressure increases, and increase the release rate when the atmospheric pressure decreases.

However, atmospheric pressure variation represents a very small change in the average pressure. The annual standard deviation of barometric pressure variations was at most 0.72% during the years 1988 through 1991 (Crippen 1993). The annual extremes for these years were at most 3.1% from the average. Such small variation suggests the influence of atmospheric pressure changes is small. This suspicion is born out in literature cited in *Soil Physics* (Jury 1991). A soil permeable column 3 m deep was affected by typical barometric pressure variations to a depth of at most 0.56 cm. Thus, barometric pressure changes will have little influence on the average diffusion flux from the surface.

4.12.2.2 Atmospheric Temperature. The air temperature at the ground surface varies sinusoidally during the day as well as during the year. The daily variation does not penetrate as deeply as the seasonal variation. The seasonal temperature change at a depth of 5 m in sandy soil is about 10% of the seasonal temperature change at the surface (Jury 1991). The variation in temperature decreases exponentially with distance below the surface. In addition, there is a phase shift that increases with depth. The cyclic variation in soil temperature will cause air movement due to the expansion and contraction of the air as the temperature increases and decreases. This air movement can be expected to increase the average diffusion flux at the surface.

However, the influx of air is limited to a shallow layer near the surface, just as with barometric pressure changes. The monthly average air temperature at Hanford typically ranges from -12° C to 30° C with an average around 12° C (Hoitink 1994). Thus the near-surface soil layer experiences a seasonal temperature variation no more than 10% on the absolute temperature scale. While this variation is an order of magnitude greater than the barometric pressure change, it is confined to a relatively shallow layer near the surface. Thus, temperature changes will have little effect on the average diffusion flux from the surface. If the 10% variation is assumed to accelerate gas transport in the top 10% of the soil cover, then the soil cover thickness is effectively reduced by 0.5 m. With a cover thickness of 4.5 m, the ^{222}Rn diffusion flux increases from 0.96 pCi/m^2 per second to 1.98 pCi/m^2 per second.

4.12.2.3 Wind. The motion of air over the ground surface will create areas with higher pressure and areas with lower pressure. This varying surface pressure is similar in effect to the

barometric pressure variation, but on a much shorter time scale. Experience with temperature changes suggests that the rapid variation will not penetrate as deeply into the soil. Thus the enhanced gaseous release rate will affect gas migration to a depth less than the 0.5 cm predicted for barometric pressure variation. It is concluded that wind effects will have little effect on the average diffusion flux from the surface.

4.12.2.4 Rainfall. As the water infiltrates the soil, it displaces some air from the soil pore space. As the water moves deeper, the pore space is refilled with air from the nearby pore space. This air motion will increase the mixing between adjacent layers and should increase the average diffusion flux as well.

However, as the water moves deeper in the soil, the water and air coexist in the pore space so that the motion of water has no effect on the diffusion of gases. Thus the rainfall effect is limited to a shallow surface layer. The overall effect on the average diffusion flux is very small. The largest recorded 24-h rainfall at the Hanford Meteorological Station is 4.85 cm (1.91 in), which occurred on October 1 and 2, 1957. Using a soil porosity of 35% means the water would saturate the soil to a depth of 14.0 cm (5.5 in). Thus the normal rainfall at Hanford affects gas motion in the soil to a depth considerably less than the normal temperature variation.

4.12.3 Consequences and Comparison with Performance Objectives

The only performance objective for diffusion flux applies to ^{222}Rn, and is 20 pCi/m^2 per second. The calculated bounding value for ^{222}Rn flux is 0.96 pCi/m^2 per second which is well below this objective.

The performance objectives for ^{3}H and ^{14}C are that the dose downwind be less than 10 mrem/y. The air pathway dose downwind was estimated using the formula shown below.

$$\text{Air Pathway Dose} = J\ A\ T\ DF \tag{4.6}$$

where

J = flux of the radionuclide from the soil surface, Ci/m^2 per y. Values are given in Table 4-26.

A = cross-sectional area of the disposal facility trenches when viewed from above, (6)(80 m)(260 m) = 124,800 m^2

T = duration of the release, 1 y

DF = air pathway dose factor from CAP88-PC for an annual release, mrem

The air transport factor and air pathway dose factors developed in Section 3.2.1 of *Exposure Scenarios and Unit Dose Factors for the Hanford Immobilized Low-Activity Tank*

Waste Performance Assessment (Rittmann 1999). The air transport factor is a bounding value that applies to annual emission near the border of a large area source. The dose factors were obtained using the CAP88-PC software from EPA (Parks 1992). The air pathway dose calculation is summarized in Table 4-26. The total dose from these air emissions (0.006 mrem/y) is well below the performance objective of 10 mrem/y. Note that the best estimate ILAW inventory in the waste form does not include either ^{3}H or ^{14}C.

4.13 EFFECTS FROM BIOTIC PATHWAYS

Because of the nature of the waste form (containerized glass logs) and the depth of placement of the waste placement (more than 5 m), biotic pathways are not credible. That is, the ability for plant and animal life to transport the contaminants is extremely unlikely. Neither plants nor animals have a direct means of access to waste over the time of compliance (1,000 years). Moreover, given the low moisture content inside the disposal facility (see Sections 4.3.2 and 4.3.7), plant roots would not survive.

4.14 EFFECTS OF CATASTROPHIC EVENTS

Based on the discussion presented in Section 3.3.2.4, the only scenario considered is that of an ice-age flood that scrapes away all material down to 20 m (the depth of the disposal facility), then redeposits the material over the area of the Hanford Site. As noted in Section 2.2.5.4, the next such event might be expected in about 50,000 years.

From the 1998 ILAW PA (Mann 1998a), using the farm scenario as the exposure scenario, and assuming that all the waste is in a form that can be inhaled or ingested, the predicted dose is estimated to be 0.76 mrem (EDE) in a year. Practically all the predicted dose (more than 98 percent) comes from the external exposure of ^{126}Sn and its daughters. If the glacier flood occurs as early as 10,000 years, the predicted dose increases to 1.01 mrem (EDE) in a year. If the flood occurs at 100,000 years, the predicted dose is 0.53 mrem (EDE) in a year. These values are much less than the 25 mrem (EDE) in a year maximum established for the first 10,000 years for the all-exposure pathways. If the flood only redistributes the waste over an area equivalent to the 200 Areas (78 km^2), the predicted dose at 50,000 years [14 mrem (EDE) in a year] is still less than the all-pathways limit. Because the current inventory estimates (Wootan 1999) are comparable to those used in the 1998 ILAW PA (with the ^{126}Sn inventory reduced by a factor of approximately 10), these estimated impacts are conservative.

4.15 ALARA ANALYSIS

> The Immobilized Waste Program is incorporating ALARA principles by the close cooperation of the performance assessment and design activities. When operations begin, they too will be integrated.

To keep exposures as low as reasonably achievable (ALARA) design, operations, and analysis projects must cooperate closely. The RPP Immobilized Waste Program is committed to such integration and already has had some success. The design of the waste treatment facility and disposal facility are expected to be optimized using the results of these studies.

4.15.1 Past ALARA Activities

Much of the early emphasis of the Immobilized Waste Program's performance assessment activity was to investigate the impact of various facility design options on long-term performance. These reports (Rawlins 1994 and Mann 1995d) helped guide early program thinking. The interim performance assessments (Mann 1996a and Mann 1997a) were used by the engineering staff in their alternatives generation analyses (for example, Burbank 1997) to investigate various disposal options, including the use of trenches and existing facilities as was discussed in Section 2.4.2.

The performance assessment activity was actively involved in selecting the new disposal site. Although many factors were considered (Shord 1995), the input from the performance assessment activity played a significant role.

The initial plans had ILAW disposal taking place in underground concrete vaults similar to those constructed for the grout disposal program. However, Burbank (1999) analyzed various options and found that the trench design had superior financial and scheduling qualities. At the time, the environmental impacts were thought similar. As documented in a preliminary analysis (Mann/Puigh 2000b) and confirmed by analyses in the document (Sections 4.4 and 4.5.6), in fact, ILAW disposal in a trench design has lower environmental impacts than the similar disposal in a concrete vault. The principles underlying this conclusion are that the chemical interactions between the disposal facility structures and the waste form are more important than the structural integrity of the disposal facility over the long times considered in this analysis. The life cycle cost savings are 272 million dollars (of 560 million dollars).

The specifications for waste form performance also have changed. In the initial request for proposals for waste treatment (DOE/RL 1996), the specifications were limits on fractional release rates for ^{99}Tc (2.8 x 10^{-14} second^{-1}) and for ^{79}Se, ^{129}I, ^{237}Np, and uranium isotopes (1.4x10^{-13} second^{-1}) based on a 7-day PCT (Product Consistency Test) measurement at 20 ^{o}C. Based on testing performed by the ILAW PA activity (McGrail 2001) and by EM-50 (Vienna 2000), it became obvious that this specification was incomplete. The present specification (DOE/ORP 2000c), which is heavily based on PA activities, states

"2.2.2.17 <u>Waste Form Testing</u>:

2.2.2.17.1 <u>Leachability Index</u>: The waste form shall have a sodium leachability index greater than 6.0 when tested for 90-days in deionized water using the ANSI/ANS-16.1 procedure.

2.2.2.17.2 <u>Product Consistency Test</u>: The normalized mass loss of sodium, silicon, and boron shall be measured using a seven-day product consistency test run at 90°C as defined in ASTM C1285-98. The test shall be conducted with a glass to water ratio of 1 gram of glass (-100 +200 mesh) per 10 milliliters of water. The normalized mass loss shall be less than 2.0 grams/m^2. Qualification testing shall include glass samples subjected to representative waste form cooling curves. The product consistency test shall be conducted on waste form samples that are statistically representative of the production glass.

2.2.2.17.3 Vapor Hydration Test: The glass corrosion rate shall be measured using a seven day vapor hydration test run at 200°C as defined in the DOE concurred upon Product and Secondary Waste Plan. The measured glass alteration rate shall be less than 50 grams/(m^2-day). Qualification testing shall include glass samples subjected to representative waste form cooling curves. The vapor hydration test shall be conducted on waste form samples that are statistically representative of the production glass."

4.15.2 Future ALARA Activities

The designs of both the waste treatment facility and the disposal facility have not been completed. Therefore, the sensitivity cases presented in this report may be used to aid the designers of these facilities in making choices that would minimize long-term impacts at a reasonable cost. The Office of River Protection and the River Protection Project are committed to using the results of this assessment to optimize designs.

Important information was gained in developing this performance assessment that can impact future ALARA analyses. The major information areas include the estimated impacts that inventory modifications, minimization of moisture movement through the disposal facility, contaminant release rates from the ILAW packages, chemical conditioning and trapping within the disposal facility and facility layout have on the environmental performance of the ILAW disposal system.

The inventory of key contaminants will depend not only on the amount of such contaminants presently stored in underground tanks, but also on the separation of such waste into low-activity and high-level waste streams. The design of the separations process can be optimized to minimize impacts from ILAW disposal while having minimal impacts on operational concerns and on the storage and disposal of the IHLW. Section 4.8.2 discusses the effect of varying the amount of technetium, iodine, and uranium in the ILAW packages and the resulting impact on groundwater impacts. Particularly in the case of technetium separation, this analysis provides useful information on the impact of including further technetium separation or even removing this separation process. Section 5.4.3.1 shows the impact on the intruder dose on changing key inventories. It should be noted that reduction of ^{137}Cs will have important near-term consequences; a fact that is driving the waste treatment contractor to remove as much ^{137}Cs as possible in order to meet their own ALARA concerns and drive down maintenance costs.

As shown in Section 4.5.4, reducing moisture flow through the disposal facility significantly reduces the impact on the contaminant release rate from the ILAW packages. In addition, Section 4.6.2 shows that the reduction of the moisture flow through the vadose zone greatly increases the travel time and hence reduces the impacts at the time of compliance. Thus, these sections show the potential value of various design features (surface covers [including the impact of varying dimensions], moisture diverters, vertical moisture barriers) that could such modify moisture flow as documented in Section 4.4. The potential inclusions of such features and their resulting cost benefit will be studied during the detailed design process.

The contaminant release rate from the ILAW packages is a major driver on the long-term estimated impacts. Extensive research programs are being performed by the waste treatment

contractor, by the Department of Energy's Environmental Management Science Program, as well as by the performance assessment activity. All of this information is being shared among these research programs. This combined knowledge will aid the waste treatment contractor in choosing the waste form composition that best balances the requirements of long-term performance, processibility, and costs. Already the long-term performance of the waste treatment contractor's glass has been improved by well over an order of magnitude. In addition, the results from Section 4.5, which show minimal impact from the composition of the container material, allow more freedom in the selection of container materials.

Special features can be placed in the facility to chemically change the environment. The disposal facility designers can use in the information from Section 4.5.5 to optimize the selection of backfill material and whether the presence of a layer, which would chemically condition the chemical properties of the incoming moisture, are cost effective. The results from Section 4.6.3 can be used to determine the effectiveness of a potential concrete layer to chemically trap iodine and uranium. The estimated impacts on the all-pathways dose from a 1 meter-thick concrete mixture at the bottom of the disposal trench are a 25% reduction at 1,000 years and a 50% reduction at 10,000 years.

The information in Section 4.7.2 can be used in the detail design of the layout of the disposal facility within the footprint of the disposal site. Placing the trenches at the southern end of the side would slightly increase all groundwater estimated impacts (by a factor of 50% at 100 meters and by 16% at 1,000 m) when compared to the groundwater estimated impacts if the trenches were at the northern end. Rotating the orientation of the trenches by 90 degrees would also increase the estimated groundwater pathway impacts.

The information presented above, along with other design data, will be used in the designs of both the waste treatment plant and the disposal facility. Studies have already begun on the appropriateness of technetium separation and the amount of waste loading in the ILAW packages. Similarly modifications to the conceptual design are being considered based on the results of this work. The results of such decisions will be documented in future performance assessments.

5.0 RESULTS FOR AN INADVERTENT INTRUDER SCENARIO

5.1 OVERVIEW

The DOE intends to control the disposal sites for as long as the waste may be dangerous to an intruder. However, DOE recognizes that an inadvertent intruder may happen onto the site and not be discovered until after exposure has occurred.

As noted in Section 1.6, the time of compliance is 500 years after closure. However, results will be presented for the period of 100 years to 1,000 years after closure. The performance objective for the driller scenario is 500 mrem (EDE) for a one-time exposure, while the performance objective for the homesteader scenario is 100 mrem (EDE) per year for a continuous exposure. The time of closure is taken to be 2030. All the analyses presented in this section assume that the surface barrier is in place (Section 2.4.1). All calculations were performed using a spreadsheet to calculate decay and to convert inventory concentrations into doses.

5.2 INADVERTENT INTRUDER SCENARIOS

The pathways described here assume that no memory of the disposal facility remains. The following two principal cases of intruders were considered:

- The disposal facility is compromised by irrigation for commercial farming. A large amount of water enters the disposal facility, causing increased contaminant release and increased transport of the contaminants to the unconfined aquifer.

- An inadvertent intruder digs or drills into the disposal site and brings some of the waste to the surface, receiving an acute dose. Another intruder (the homesteader) tills the waste into the soil and grows vegetables, receiving a continuous dose while engaged in various activities.

The scenario of irrigated farming on the disposal site is basically the same as the sensitivity case for the groundwater scenario where the infiltration rate is 50 mm/year. However, instead of a small amount of water naturally infiltrating the disposal facility, a much larger amount of water enters the disposal facility (see Section 4.6.2). The larger amount of water increases the contaminant release rate from the engineered facility. The increased amount of water certainly speeds the transport of the contaminants through the vadose zone into the unconfined aquifer. The estimated impacts are higher than for the base analysis case, but are still significantly lower than the performance objectives. If regional irrigation occurs, the well intercept factor from Section 4.7.2 is reduced by a factor of 0.92, indicating additional dilution. This scenario will not be addressed further in this section.

The following three intruder scenarios that involve bringing waste from the disposal facility to the surface usually are considered in a performance assessment.

- Excavating for a basement or building foundation

- Drilling for groundwater or minerals
- Living where waste has been exhumed and scattered over the surface.

Scenario 1 is not considered credible because the top of the waste is 5 m (16.4 ft) or more below the surface. Neither basements for home residences nor foundations for commercial structures are likely to extend this far below the surface. This scenario was not evaluated in these analyses.

Scenario 2, the construction of small water wells, is possible. The driller scenario begins with the assumption that some time after disposal operations have ended, a well is drilled through the waste. Drilling at the disposal site is unintentional, and the waste is not recognized as a potential hazard, even though it is assumed to be in the form of glass chunks. The waste, along with uncontaminated soil taken from the well, is spread over a work area near the well. The dose to the worker is the sum of the contributions from inhalation of resuspended dust, ingestion of trace amounts of soil, and external exposure at the center of a slab of contaminated soil.

Scenario 3 considers a family planting a garden using the material taken from the well. Each individual of concern receives dose by direct exposure to the radiation field in the garden, by inhaling resuspended dust, by ingesting trace amounts of soil, and by consuming garden produce. Given than a well is constructed (scenario 2), it is possible, if not probable, that some sort of homesteading will occur.

5.3 FACILITY DESCRIPTION AND ASSUMPTIONS FOR THE INADVERTENT INTRUDER ANALYSIS

Selecting values for parameters important in inadvertent intruder scenarios is difficult. Because such intrusion is postulated to be in the future, the nature of the intrusion is ill defined. Moreover, uncertainty abounds about the proper values to be used in a given scenario. DOE O 435.1 provides no specific guidance on the intruder scenario analysis. For this report the specific exposure scenario is defined in Rittmann (1999) and is based on intruder scenarios analyzed in earlier Hanford Site PAs (Wood 1995a, Wood 1996, and Mann 1998a).

For the inadvertent intruder scenarios, the most important variables are the amount of waste exhumed, the size of the area over which the waste is spread, and the physical integrity of the waste. Additional parameters, such as exposure time and inhalation rates, also are important but are not typically treated as variables.

The amount of waste material taken from the disposal site is assumed to be the maximum average waste distribution times the area of the borehole for the well. The maximum average waste distribution for the trench design is calculated for the central region for the trench (200 m x 20 m) and is defined as the waste volume divided by the area of this central region. For this performance assessment, the diameter of the well is assumed to be 0.3 m (1 ft). Although consistent with the diameters used in earlier Hanford Site performance assessments, this value is larger than the range of well diameters commonly found in local communities (10.2 cm to 25.4

cm [4 to 10 in.]). Table 5-1 provides the facility parameters used for the remote-handled waste trench and the alternative concept, the concrete vault.

The area over which the driller spreads the waste is assumed to be 100 m^2 (about 1,100 ft^2). This value has been historically used in Hanford Site performance assessments. The homesteader is assumed to spread the waste over a garden, which is taken to be 200 m^2. In earlier Hanford Site performance assessments, the garden area has been as large as 2,500 m^2 (0.62 acre). The 200 m^2 garden was chosen for this performance assessment because the size represents an area large enough to supply a significant portion of a person's vegetable and fruit diet and because the smaller size produces a higher dose, making it the conservative scenario. Household gardens in the vicinity of the Hanford Site range in size from 10 m^2 to 1,000 m^2 (107 ft^2 to 0.25 acre) (Napier 1984). In both scenarios the soil mixing depth is assumed to be 15 cm (5.9 in.). This value has been used in other onsite performance assessments and is the typical rooting depth for garden vegetables.

The integrity of the waste form becomes important in determining the amount of radionuclides available for inhalation or uptake by plants and animals. For the base case, 99 percent of the radionuclides exhumed are assumed to stay within the waste form (i.e., only 1 percent is available for ingestion and inhalation). This is slightly less than in previous studies, which considered only corrosion of the waste form, and accounts for some mechanical erosion of the waste form during drilling. The importance of this assumption was investigated by sensitivity cases.

The worker at the well drilling site is assumed to be exposed 8 hours a day for 5 days. The dose to the worker is the sum of the contributions from inhaling resuspended dust (0.12 mg/hour), ingesting trace amounts of soil (100 mg/day), and external exposure at the center of a slab of contaminated soil for 40 hours. The dose factors for this scenario can be found in Rittmann (1999) and are summarized in Appendix B, Table B-3. The homesteader is assumed to be exposed for 1 year. The soil inhalation rate for the homesteader is 573 mg/year. The incidental ingestion rate is the same as for the driller, 100 mg/day. The resulting dose factors are given in Rittmann (1999) and summarized in Appendix B, Table B-4.

Table 5-1. Facility Dimensions and Waste Volume Exhumed.

	Remote-Handled Waste Trench[1]	Concrete Vault
Waste package dimensions (m)[2]	1.4 x 1.4 x 1.2	1.4 x 1.4 x 1.2
Facility dimensions (m)	200.0 x 20.0	18.3 x 21.0
Layers of waste packages	4	6
Packages per layer[3]	1584	168
Surface area (m^2)	4000	384
Waste volume (m^3)	14900	2380
Average areal distribution of waste (m^3/m^2)	3.73	6.20
Volume waste exhumed (m^3)	0.272	0.453

[1]Only the central portion of the trench is considered. If the fringe regions were averaged in, the areal distribution and volume exhumed would be lower.
[2]The waste package is 1.4 m high but is filled only 85 percent full, so it is treated here as being 1.2 m high.
[3] The number of packages in the bottom layer in the trench is used as an approximation for the number of packages above the central region in the upper layers.

5.4 INADVERTENT INTRUDER ANALYSIS RESULTS

5.4.1 Driller Scenario

The results for the driller scenario are presented in Table 5-2 and displayed in Figure 5-1. The estimated acute exposure dose at 100 years after facility closure is 44 mrem. The major contributor to the acute dose is ^{137}Cs, which contributes approximately 95 percent of the exposure dose. ^{90}Sr and ^{126}Sn contribute 2.9 and 1.4 percent, respectively.

The estimated acute exposure dose at 500 years after facility closure (time of compliance) is 0.8 mrem. The major contributor to the acute dose is ^{126}Sn, which contributes approximately 82 percent of the dose. ^{241}Am and ^{237}Np contribute 10 and 4 percent, respectively. As discussed in Section 3.2, approximately 36 percent of the ^{126}Sn, 44 percent of the ^{237}Np, and 10 percent of the ^{241}Am of the initial tank inventories remain in the waste after processing (Kirkbride 1999). These numbers may change when specific flowsheet information is obtained.

Figure 5-1. Inadvertent Intruder Results for the Driller Scenario - Base Intruder Case.

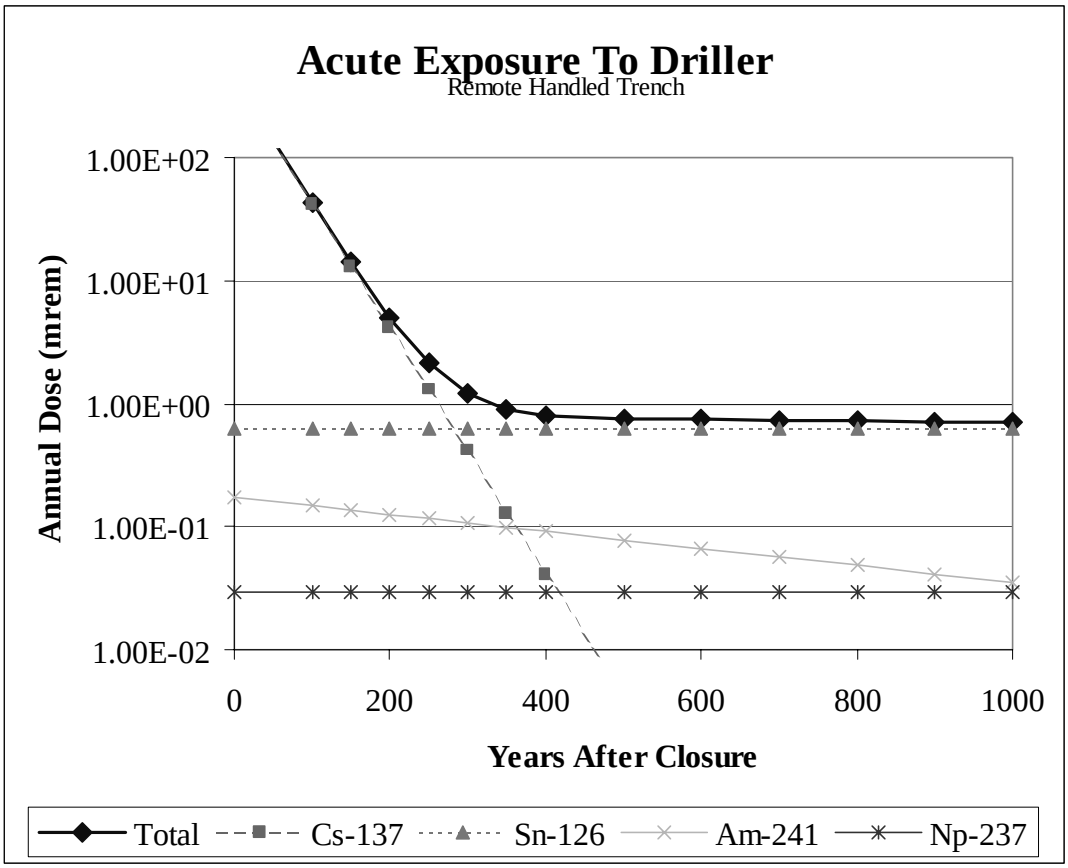

These estimates are sensitive to the parameters assumed for the scenario. A number of sensitivity studies were performed to quantify the dependance on these parameters. The results of these studies are discussed in Section 5.4.3. None of the sensitivity cases changes the conclusion that the driller scenario meets the performance objective.

5.4.2 Homesteader Scenario

The results for the homesteader scenario are presented in Table 5-3 and displayed in Figure 5-2.

The estimated chronic exposure dose at 100 years after facility closure is 541 mrem. The dose remains above 100 mrem per year out to approximately 150 years. The major contributor to the acute dose is ^{137}Cs, which contributes approximately 85 percent of the dose. ^{90}Sr and ^{126}Sn contribute 13 and 1.3 percent, respectively. The estimated chronic exposure dose at 500 years after facility closure (time of compliance) is 10.2 mrem. The major contributor to the homesteader dose is ^{126}Sn, which contributes approximately 69 percent of the dose. ^{241}Am and ^{239}Pu contribute 17 and 6 percent, respectively. As discussed in Section 3.2, approximately 36 percent of the ^{126}Sn, 5.5 percent of the ^{239}Pu, and 10 percent of the ^{241}Am of the initial tank inventories remain in the waste after processing (Kirkbride 1999). These numbers may change when specific flowsheet information is obtained.

These estimates are sensitive to the parameters assumed for the scenario. A number of sensitivity studies were performed to quantify the dependance of the estimated intruder impacts on these parameters. The results of these studies are discussed in Section 5.4.3. The only sensitivity case where the estimated impact exceeds the performance objective is the case that investigates having all the waste packages in the stack to have the maximum batch concentration of the key radionuclides (^{126}Sn and ^{241}Am). The remaining sensitivity cases do not change the conclusion that the homesteader scenario meets the performance objective.

Figure 5-2. Inadvertent Intruder Results for the Homesteader Scenario - Base Intruder Case.

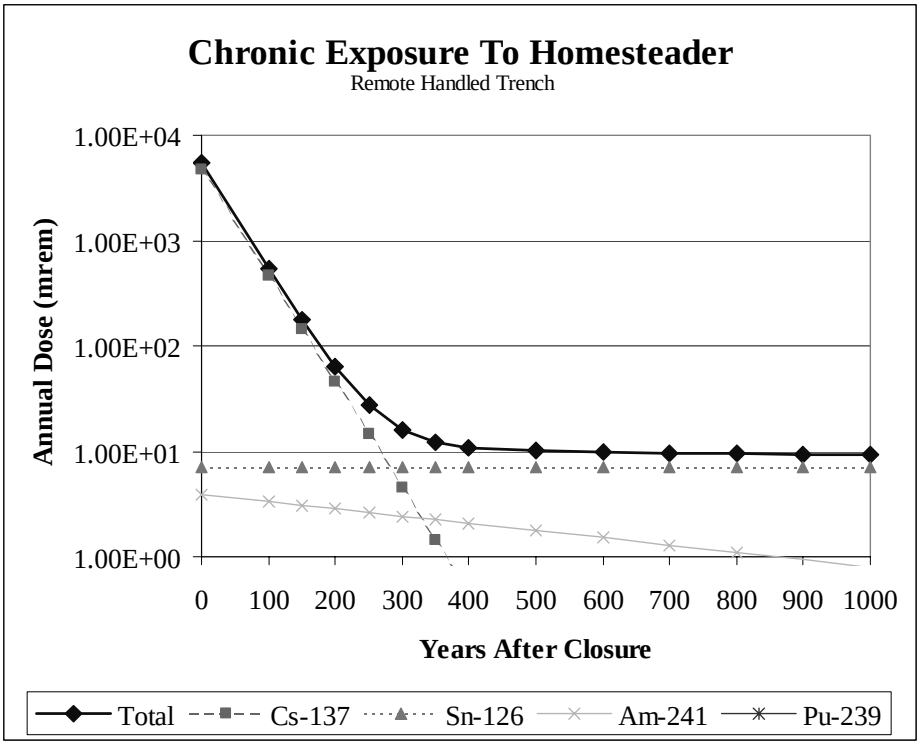

5.4.3 Uncertainties

5.4.3.1 Waste Loading. To estimate the uncertainty in the inadvertent intruder estimated dose contributed by uncertainties in the inventory, the maximum batch concentrations listed in Table 3-1 were used. The maximum batch concentration reflects the tank-to-tank variation in inventory for each radionuclide. For example, the ratio of the maximum batch concentration to the average batch concentration for ^{126}Sn, ^{239}Pu, and ^{241}Am are 3.9, 4.9, and 25, respectively.

If just one of the waste packages affected by the driller had the maximum batch concentration and the remaining 3 packages (assuming a 4-layer stack) had average batch concentrations, the estimated acute exposure would be approximately a factor of 1.1 higher than

the base case at 100 years and a factor 2.3 higher at 500 years. This would result in a dose that is still well below the performance objectives. For the homesteader scenario, the ratios would be 1.2 at 100 years and 2.7 at 500 years. This also would meet performance objectives.

If all of the packages in the facility (or all of the packages affected by the drilling) were maximum batch packages, the dose to the driller would be a factor of 1.5 higher than the base case at 100 years, and a factor of 6.1 higher than the base case at 500 years. This would result in a dose that is still well below the performance objectives. For the homesteader, the ratios would be 1.6 at 100 years and 7.6 at 500 years. In this case, the dose would still be below the performance objectives.

These estimated impacts can be mitigated through operational controls based on projected container inventories. Such operational controls will be better defined as the project matures.

5.4.3.2 Stability of Waste Form. It is assumed that the waste form will not completely shatter into fine grains. Rather, most of the radionuclides would remain in the waste form, making them unavailable for ingestion or inhalation. The base case for this analysis assumed 1 percent of the waste was available for ingestion or inhalation. For this case, the exposure is dominated by external radiation rather than by ingestion or inhalation. Previous ILAW performance assessments have assumed smaller numbers for the availability of material for ingestion or inhalation based only on corrosion (ignoring mechanical processes). Sensitivity studies were performed to assess the impact of assuming that 10 or 100 percent of the radionuclides are available for ingestion or inhalation. Increasing the availability of materials for ingestion or inhalation from 1 to 10 percent increased the dose to the driller by approximately 10 percent. The same change increased the dose to the homesteader by a factor of approximately 2. Increasing the availability from 1 percent to 100% increased the dose to driller by a factor of about 2, compared to a factor of 15 for the homesteader. The results of these analyses are shown in Figures 5-3 and 5-4.

Figure 5-3. Predicted Driller Doses for Different Availability of Radionuclides for Ingestion and Inhalation.

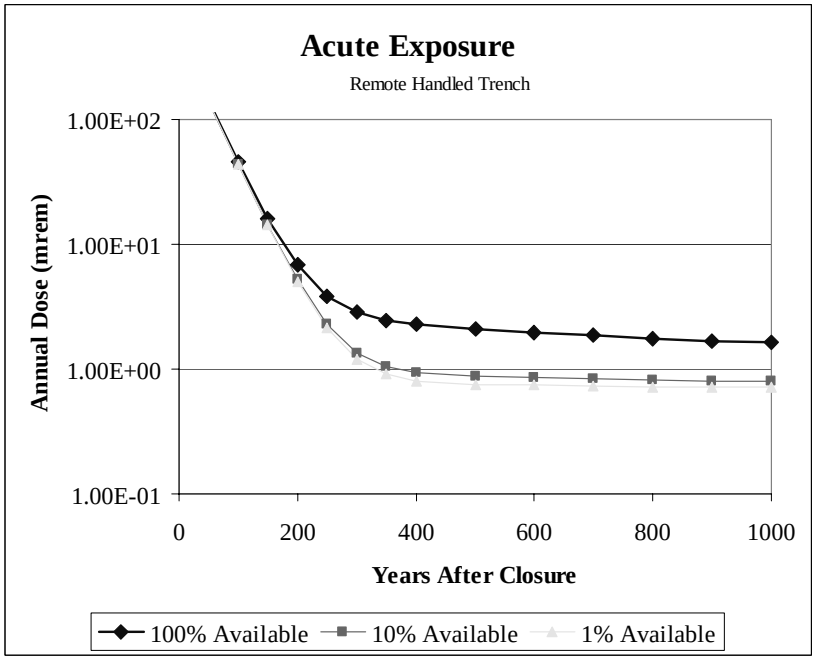

Figure 5-4. Predicted Homesteader Doses for Different Availability of Radionuclides for Ingestion and Inhalation.

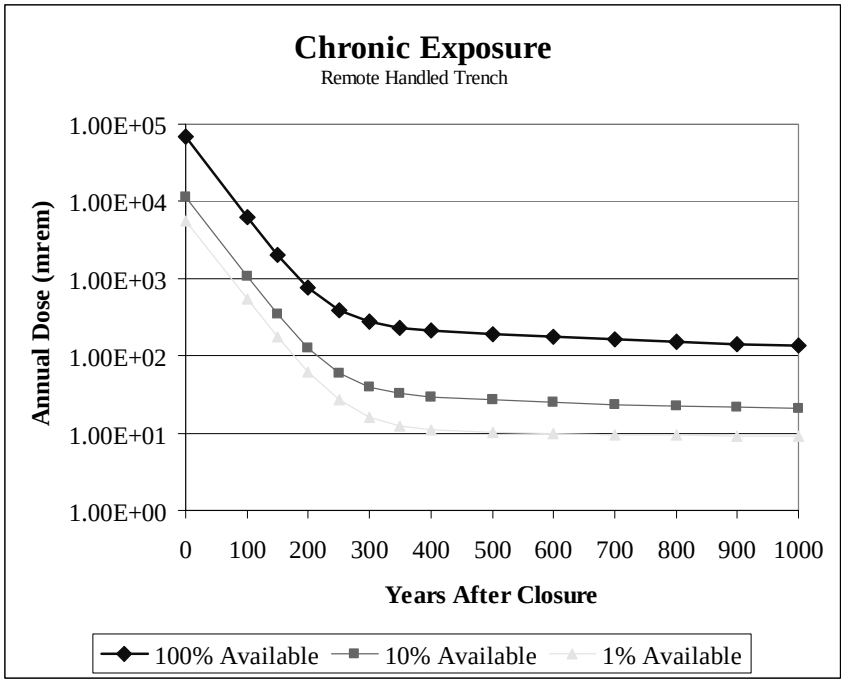

5.4.3.3 Area of Homesteader Garden. The predicted dose depends on the area of the homesteader garden and the amount of time the homesteader spends in the garden. The homesteader receives dose from external radiation when working in the garden or dose from internal exposure when eating produce from the garden. The radionuclide concentration in the soil, and consequently the dose rate, is inversely proportional to the size of the garden, which implies that a smaller garden will produce a larger dose. This is partially offset by the assumption that the homesteader will spend more time in a larger garden (the exposure time will be proportional to the garden size).

The base intruder case assumes a much smaller area (200 m^2) than assumed in previous Hanford Site performance assessments (up to 2,500 m^2). The change in garden size causes the internal dose estimates to increase by a factor that is the inverse of the ratio of the garden sizes (up to 12.5). However, the external doses from the larger garden are only 10 to 25 percent less than the external dose from the smaller garden because of the shorter time spent in the smaller garden. Therefore, where direct doses dominate, the smaller garden area produces only a moderate increase in total dose. For radionuclides where ingestion is the main exposure pathway (^{90}Sr, ^{99}Tc, plutonium isotopes, ^{241}Am), the ratio of the predicted dose is inversely proportional to the ratio of the garden areas.

5.4.3.4 Size of the Hole Drilled. The predicted dose is proportional to the amount of waste brought up from the disposal facility. For the base intruder case, the hole was conservatively estimated as 0.3 m (12 in.). However, a more likely maximum diameter is 0.2 m (8 in). Such a smaller diameter hole would bring up only 42 percent of the waste that would come from the 0.3-m (12-in.) hole. This reduces the predicted dose by a factor of 0.42.

5.4.3.5 Average Areal Distribution of the Waste. Because the predicted dose depends linearly on the amount of waste material brought to the surface, the predicted dose depends on the waste concentration. The waste is assumed to be averaged over both the container and the filler material. However, because the hole is assumed to go through the entire height of the disposal facility, the vertical dimension becomes unimportant. This makes the average areal distribution (the volume of waste beneath each square meter of facility surface area [see Table 5-1]), rather than the normal density, important.

The average areal distribution of the disposal facility could differ from the base intruder case for any of the following:

- A different design of the disposal facility (for example, using dirt spacers between vault rows)
- Different ratios of waste material to filler material in a vault
- Different assumptions of the total height of waste
- Different waste loading (because of sodium content or other reasons).

The new contract (DOE/ORP 2000c) has altered the waste package designs to have a height of 2.3 m. These packages would be stacked 3 high. This would result in a stacking height of 6.9 m. This stacking height would increase doses by a factor of 1.44 compared to the base analysis case (assuming the package footprint, spacing, and waste loading remained constant).

The alternative (concrete vault) concept results in 0.453 m^3 of waste exhumed versus 0.272 m^3 (see Table 5-1). This corresponds to increasing the dose by a factor of 1.67.

5.4.3.6 Other Factors. The remaining factors are less important in determining the predicted dose. Such factors include the use of dose conversion factors and estimates of the amount of secondary radionuclides (i.e., those that don't dominate the dose) present.

The dose conversion factors important to the homesteader scenario are the external dose conversion factors as this exposure pathway dominates over ingestion or inhalation. The factors used in the base intruder case are the ones from the EPA (EPA 1993). For ^{126}Sn, the DOE external dose conversion factor (DOE 1988c) is a factor of 4.45 larger than the EPA factor. The DOE value is larger because it assumes all the radionuclides are on the surface of the soil and no shielding of the photon radiation occurs. The EPA factor, on the other hand, is based on the more realistic assumption of mixing over a 15 cm layer. Earlier Hanford Site PAs have used dose factors based on GENII (Napier 1988), which uses models similar to the EPA model. For ^{126}Sn, the external dose conversion factor from GENII is 20 percent higher than the EPA value. For ^{137}Cs, the ratios of the external dose conversion factors are similar to those for ^{126}Sn. For ^{90}Sr, ^{239}Pu, and ^{241}Am, the ratios of the GENII external dose conversion factors to the EPA values are 1.69, 1.11, and 0.66.

Because ^{126}Sn and ^{137}Cs dominate the intruder dose results, changes in the amount of other radionuclides is relatively unimportant. Using different processing strategies, the amount of ^{90}Sr might be as much as twice the amount assumed in the base intruder case (9.0 MCi versus 4.5 MCi). Even using the maximum amount of ^{90}Sr would increase the total predicted dose at 100 years by less than 15 percent because ^{90}Sr does not significantly contribute to the estimated dose unless it is ingested. Changes in the amount of other isotopes are predicted to be less significant to the intruder dose.

5.5 SUMMARY OF THE INADVERTENT INTRUDER SCENARIO

The estimated dose for the driller scenario is 44 mrem at 100 years and 0.8 mrem at 500 years. This meets the performance objective by more than two orders of magnitude. At the time of compliance the dose originates primarily from ^{126}Sn.

The estimated dose for the homesteader scenario is 541 mrem at 100 years and 10.2 mrem at 500 years. This easily meets the performance objective of 100 mrem at 500 years. At the time of compliance the dose originates primarily from ^{126}Sn.

Table 5-2. Driller Intruder Dose (mrem) at Various Intrusion Times (years after closure).

Nuclide	100 y	200 y	300 y	400 y	500 y	600 y	800 y	1000 y
Co-60	3.38E-07	6.57E-13	1.28E-18	2.49E-24	4.85E-30	9.44E-36	3.58E-47	1.36E-58
Ni-59	8.11E-10	8.1E-10	8.09E-10	8.09E-10	8.08E-10	8.07E-10	8.06E-10	8.04E-10
Ni-63	7.15E-08	3.58E-08	1.79E-08	8.96E-09	4.48E-09	2.24E-09	5.62E-10	1.41E-10
Se-79	3.13E-07	3.13E-07	3.13E-07	3.13E-07	3.13E-07	3.13E-07	3.13E-07	3.13E-07
Sr-90+D	1.274391	0.108614	0.009257	0.000789	6.72E-05	5.73E-06	4.16E-08	3.02E-10
Zr-93	4.71E-05	4.72E-05	4.72E-05	4.72E-05	4.72E-05	4.72E-05	4.72E-05	4.72E-05
Nb-93m	8.83E-08	1.2E-09	1.63E-11	2.22E-13	3.03E-15	4.12E-17	7.62E-21	1.41E-24
Tc-99	0.000253	0.000253	0.000253	0.000253	0.000253	0.000253	0.000252	0.000252
Ru-106+D	2.05E-41	5.29E-71	1.4E-100	3.5E-130	9E-160	2.3E-189	1.5E-248	1E-307
Cd-113m	2.27E-06	1.67E-08	1.22E-10	8.95E-13	6.56E-15	4.81E-17	2.58E-21	1.39E-25
Sn-126+D	0.623751	0.623575	0.623399	0.623224	0.623048	0.622873	0.622522	0.622171
Sb-125	4.04E-14	3.8E-25	3.57E-36	3.35E-47	3.15E-58	2.96E-69	2.61E-91	2.3E-113
I-129	9.94E-05	9.94E-05	9.94E-05	9.94E-05	9.94E-05	9.94E-05	9.94E-05	9.94E-05
Cs-134	2.4E-18	6.03E-33	1.52E-47	3.81E-62	9.59E-77	2.41E-91	1.5E-120	9.6E-150
Cs-137+D	41.40264	4.107346	0.407469	0.040423	0.00401	0.000398	3.92E-06	3.85E-08
Sm-151	0.000124	5.74E-05	2.66E-05	1.23E-05	5.7E-06	2.64E-06	5.65E-07	1.21E-07
Eu-152	0.000546	3.01E-06	1.66E-08	9.17E-11	5.06E-13	2.8E-15	9.51E-18	9.43E-18
Eu-154	0.001486	4.66E-07	1.46E-10	4.58E-14	1.44E-17	4.51E-21	4.43E-28	4.36E-35
Eu-155	3.57E-09	1.32E-15	4.88E-22	1.81E-28	6.67E-35	2.47E-41	3.37E-54	4.6E-67
Ra-226+D	0.000177	0.00017	0.000162	0.000156	0.000149	0.000143	0.000131	0.00012
Ra-228+D	1.54E-08	8.94E-14	5.2E-19	3.02E-24	1.76E-29	1.02E-34	3.45E-45	1.17E-55
Ac-227+D	5.47E-07	2.26E-08	9.38E-10	3.88E-11	1.61E-12	6.66E-14	1.14E-16	1.96E-19
Th-229+D	0.000175	0.000173	0.000171	0.00017	0.000168	0.000167	0.000164	0.00016
Th-232	0.006012	0.006012	0.006012	0.006012	0.006012	0.006012	0.006012	0.006012
Pa-231	0.000255	0.000257	0.000257	0.000256	0.000256	0.000255	0.000254	0.000253

Table 5-2. Driller Intruder Dose (mrem) at Various Intrusion Times (years after closure).

Nuclide	100 y	200 y	300 y	400 y	500 y	600 y	800 y	1000 y
U-232	0.026695	0.009889	0.003663	0.001357	0.000503	0.000186	2.56E-05	3.51E-06
U-233	0.000994	0.001624	0.002248	0.002866	0.003478	0.004084	0.005277	0.006448
U-234	3.29E-05	4.32E-05	5.88E-05	7.94E-05	0.000105	0.000135	0.000207	0.000296
U-235+D	0.000464	0.000467	0.000469	0.000472	0.000475	0.000478	0.000483	0.000489
U-236	7.61E-07	7.61E-07	7.61E-07	7.61E-07	7.61E-07	7.61E-07	7.61E-07	7.61E-07
U-238+D	0.001975	0.001975	0.001975	0.001975	0.001975	0.001975	0.001975	0.001975
Np-237+D	0.029629	0.029628	0.029628	0.029627	0.029626	0.029625	0.029623	0.029621
Pu-238	5.41E-05	2.46E-05	1.12E-05	5.07E-06	2.31E-06	1.06E-06	2.37E-07	6.76E-08
Pu-239	0.005087	0.005072	0.005058	0.005043	0.005029	0.005014	0.004986	0.004957
Pu-240	0.000841	0.000832	0.000824	0.000815	0.000806	0.000798	0.000781	0.000765
Pu-241+D	0.003338	0.002851	0.002432	0.002074	0.00177	0.00151	0.001101	0.000804
Pu-242	6.97E-08	6.97E-08	6.97E-08	6.97E-08	6.97E-08	6.97E-08	6.96E-08	6.96E-08
Am-241	0.147413	0.125711	0.107222	0.09147	0.078049	0.066614	0.048573	0.035477
Am-243+D	0.000208	0.000206	0.000204	0.000202	0.0002	0.000199	0.000195	0.000191
Cm-242	1.5E-07	6.8E-08	3.09E-08	1.4E-08	6.41E-09	2.94E-09	6.57E-10	1.87E-10
Cm-243	4.88E-05	4.32E-06	4.08E-07	6.47E-08	3.43E-08	3.14E-08	3.08E-08	3.04E-08
Cm-244	9.68E-07	4.52E-07	4.37E-07	4.32E-07	4.27E-07	4.23E-07	4.14E-07	4.05E-07
Total	43.52674	5.024938	1.200949	0.807429	0.756135	0.740875	0.722715	0.710143

Note: Nuclides with “+D” added to their name include the contributions from short-lived progeny, which are assumed to be in equilibrium at all times

Table 5-3. Homesteader Intruder Dose (mrem/year) at Various Intrusion Times (years after closure).

Nuclide	100 y	200 y	300 y	400 y	500 y	600 y	800 y	1000 y
Co-60	3.55E-06	6.91E-12	1.35E-17	2.62E-23	5.1E-29	9.92E-35	3.76E-46	1.42E-57
Ni-59	1.35E-05	1.35E-05	1.35E-05	1.34E-05	1.34E-05	1.34E-05	1.34E-05	1.34E-05
Ni-63	0.001387	0.000694	0.000347	0.000174	8.69E-05	4.35E-05	1.09E-05	2.73E-06
Se-79	0.000105	0.000105	0.000105	0.000105	0.000105	0.000105	0.000105	0.000105
Sr-90+D	68.36017	5.82622	0.496559	0.042321	0.003607	0.000307	2.23E-06	1.62E-08
Zr-93	0.000729	0.00073	0.00073	0.00073	0.00073	0.00073	0.00073	0.00073
Nb-93m	1.08E-06	1.47E-08	1.99E-10	2.71E-12	3.69E-14	5.02E-16	9.29E-20	1.72E-23
Tc-99	0.080603	0.080576	0.08055	0.080524	0.080497	0.080471	0.080418	0.080365
Ru-106+D	1.67E-40	4.31E-70	1.1E-99	2.9E-129	7.3E-159	1.9E-188	1.3E-247	8.3E-307
Cd-113m	0.002179	1.6E-05	1.17E-07	8.58E-10	6.29E-12	4.61E-14	2.48E-18	1.33E-22
Sn-126+D	7.008526	7.006551	7.004577	7.002604	7.000631	6.998659	6.994716	6.990775
Sb-125	4E-13	3.76E-24	3.53E-35	3.32E-46	3.12E-57	2.93E-68	2.59E-90	2.3E-112
I-129	0.003508	0.003508	0.003508	0.003508	0.003508	0.003508	0.003508	0.003508
Cs-134	2.29E-17	5.77E-32	1.45E-46	3.64E-61	9.16E-76	2.3E-90	1.5E-119	9.2E-149
Cs-137+D	460.9885	45.73233	4.536872	0.45008	0.04465	0.00443	4.36E-05	4.29E-07
Sm-151	0.009765	0.00452	0.002093	0.000969	0.000448	0.000208	4.45E-05	9.53E-06
Eu-152	0.005985	3.3E-05	1.82E-07	1.01E-09	5.55E-12	3.13E-14	6.74E-16	6.73E-16
Eu-154	0.016049	5.03E-06	1.58E-09	4.95E-13	1.55E-16	4.87E-20	4.79E-27	4.71E-34
Eu-155	3.74E-08	1.38E-14	5.1E-21	1.89E-27	6.97E-34	2.58E-40	3.52E-53	4.81E-66
Ra-226+D	0.002021	0.001936	0.001854	0.001775	0.0017	0.001628	0.001493	0.001369
Ra-228+D	1.63E-07	9.5E-13	5.52E-18	3.21E-23	1.87E-28	1.09E-33	3.67E-44	1.24E-54
Ac-227+D	7.38E-06	3.06E-07	1.27E-08	5.24E-10	2.17E-11	8.99E-13	1.54E-15	2.65E-18
Th-229+D	0.002137	0.002117	0.002097	0.002077	0.002058	0.002038	0.002	0.001963
Th-232	0.068329	0.068329	0.068329	0.068329	0.068329	0.068329	0.068329	0.068329

Table 5-3. Homesteader Intruder Dose (mrem/year) at Various Intrusion Times (years after closure).

Nuclide	100 y	200 y	300 y	400 y	500 y	600 y	800 y	1000 y
Pa-231	0.003634	0.003666	0.00366	0.003652	0.003645	0.003637	0.003621	0.003606
U-232	0.300969	0.111491	0.041301	0.0153	0.005668	0.0021	0.000288	3.95E-05
U-233	0.017478	0.025185	0.032816	0.040371	0.047852	0.05526	0.069856	0.084166
U-234	0.002165	0.002286	0.002466	0.002704	0.002995	0.003339	0.004172	0.005188
U-235+D	0.005238	0.005278	0.005319	0.005359	0.005399	0.005439	0.005519	0.005599
U-236	6.36E-05	6.36E-05	6.36E-05	6.36E-05	6.35E-05	6.35E-05	6.35E-05	6.35E-05
U-238+D	0.023784	0.023784	0.023784	0.023784	0.023784	0.023784	0.023784	0.023784
Np-237+D	0.354485	0.354473	0.354462	0.35445	0.354439	0.354427	0.354404	0.354381
Pu-238	0.006677	0.00303	0.001376	0.000625	0.000285	0.00013	2.82E-05	7.24E-06
Pu-239	0.619496	0.617718	0.615945	0.614176	0.612413	0.610655	0.607154	0.603673
Pu-240	0.105175	0.10407	0.102977	0.101895	0.100825	0.099765	0.09768	0.095638
Pu-241+D	0.075626	0.064539	0.055018	0.046905	0.039993	0.034104	0.024813	0.018069
Pu-242	8.7E-06	8.7E-06	8.69E-06	8.69E-06	8.69E-06	8.69E-06	8.69E-06	8.68E-06
Am-241	3.338169	2.845473	2.425705	2.068071	1.763374	1.503777	1.094172	0.796851
Am-243+D	0.002472	0.002449	0.002427	0.002405	0.002382	0.002361	0.002317	0.002275
Cm-242	1.85E-05	8.39E-06	3.81E-06	1.73E-06	7.87E-07	3.59E-07	7.72E-08	1.91E-08
Cm-243	0.000576	5.23E-05	6.26E-06	2.21E-06	1.85E-06	1.81E-06	1.8E-06	1.78E-06
Cm-244	0.000119	5.65E-05	5.46E-05	5.4E-05	5.34E-05	5.29E-05	5.17E-05	5.07E-05
Total	**541.4061**	**62.89131**	**15.86502**	**10.93303**	**10.16954**	**9.859373**	**9.439349**	**9.140571**

Note: Nuclides with “"+D” added to their name include the contributions from short-lived progeny, which are assumed to be in equilibrium at all times

6.0 INTERPRETATION OF RESULTS

6.1 OVERVIEW

This chapter integrates the results presented in Chapters 4 and 5. The many different results presented in those chapters are reviewed and consolidated to provide a reasoned basis for evaluating the performance of the disposal facility. This interpretation provides a rational basis to conclude that the performance of the disposal facility has been completely addressed, the analysis is logically interpreted, the results are correct representations of the facility performance, and the results are sufficiently rigorous. This chapter also provides information for establishing waste acceptance criteria.

6.2 INTEGRATION OF RESULTS

Section 7.1 compares the results to the performance objectives in detail. However, based on the results from Chapters 4 and 5, a few general principles stand out:

- All performance objectives associated with release and migration of radionuclide to the point of compliance are met with a wide margin (ratio of predicted value to performance objectives). The intruder dose performance objective is met with a smaller margin (which is expected to increase based on recent knowledge of the separation of Sn-126 in the Waste Treatment Plant (WTP). The performance goals associated with release and migration of hazardous chemicals to the point of compliance is met with an even wider margin than met by radionuclides.
- A few key radionuclides are important (^{99}Tc, ^{129}I, ^{237}Np, and uranium isotopes for the groundwater pathway and ^{126}Sn, ^{239}Pu, and ^{241}Am for the inadvertent intruder scenario)
- The waste form release rate determines the temporal shape and is a major driver in determining the magnitude of the groundwater and human health impacts
- Infiltration rates are important because they affect waste form release rates and travel times
- The disposal system design can affect infiltration rates into the disposal facility
- The placement of the disposal facility over the ancient Columbia River bed increases the amount of dilution relative to other locations
- The performance objectives are by and large satisfied even if extreme assumptions are used.

As in all previous Hanford Site assessments, the mobile, long-lived radionuclides are most important for the groundwater pathway. Although the relative importance depends on the performance measure being used (beta-photon dose from drinking water, alpha concentration in drinking water, all-pathways), it is clear that ^{99}Tc, ^{129}I, uranium isotopes, and ^{237}Np are the most

important isotopes. Table 6-1 provides the information for the all-pathways dose. Section 4.3.6 provides more information.

Table 6-1. Important Radioisotopes in Groundwater Pathway.

	Groundwater All-pathways Dose (mrem/year)		
	1,000* Years	10,000 years	100,000 years
^{99}Tc	0.0000552 (71%)	0.0262 (37%)	0.0273 (4%)
^{129}I	0.0000224 (29%)	0.0110 (16%)	0.0153 (3%)
^{231}Pa	0.0	0.00048 (1%)	0.0219 (4%)
^{233}U	0.0	0.0031 (4%)	0.0456 (8%)
^{234}U	0.0	0.00104 (1%)	0.0177 (3%)
^{238}U	0.0	0.00108 (2%)	0.0180 (3%)
^{237}Np	0.0	0.0270 (39%)	0.4388 (75%)
Other	0.0000002	0.0001 (0%)	0.0014 (0%)
Total	0.0000778	0.0700	0.588

*Time of compliance (percentage contribution is given in parenthesis)

For the inadvertent intruder scenario, a different set of radioisotopes is important. As shown in Table 6-2, the isotopes that are important vary with time (also see Figure 5-2). At short times, the important radioisotopes are ^{90}Sr and ^{137}Cs, which have half lives around 30 years. However, by the time of compliance (500 years), these two isotopes have decayed and the long-lived isotopes are important (^{126}Sn, ^{239}Pu, and ^{241}Am) with ^{126}Sn contributing over two-thirds of the total dose. A fuller discussion is given in Section 5.4.

Table 6-2. Important Radioisotopes in Homesteader Inadvertent Intruder Scenario.

	Dose to Inadvertent Homesteader (mrem/year)		
	100 Years	500 years *	1,000 years
^{90}Sr	68.4 (13%)	0.00 (0%)	0.00
^{126}Sn	7.0 (1%)	7.00 (70%)	6.99 (76%)
^{137}Cs	461. (85%)	0.04 (0%)	0.00
^{237}Np	0.4	0.35 (3%)	0.35 (4%)
^{239}Pu	0.6	0.61 (6%)	0.60 (7%)
^{240}Pu	0.1	0.10 (1%)	0.10 (1%)
^{241}Am	3.3 (1%)	1.76 (17%)	0.80 (9%)
Others	0.6	0.31 (3%)	0.30 (3%)
Total	541.4	10.17	9.14

*Time of compliance (percentage contribution is given in parenthesis)

As found in the 1998 ILAW performance assessment (Mann 1998a), the time structure of the waste form release drives the time dependence of the main impacts from the groundwater pathway. This is not difficult to understand because the travel times in the vadose zone and in the groundwater are so much shorter than the release times associated with the waste form. Basically, the disposal facility provides a steady source to the vadose zone (and subsequently to the groundwater) with these latter two zones just diluting and delaying the arrival of the contaminants at the point of observation in the groundwater. Thus, waste form release continues to be a major driver in the groundwater pathway. For more information, see Section 4.3.3 on the waste form release results for the base analysis case and Section 4.3.6 on the integration of results for the base analysis case.

Infiltration rates are important as they affect waste form release rates and travel times. Figure 4-4 shows a four order of magnitude increase in the waste form release rate as the infiltration rates increases from 0.1 to 10 mm/year. Figure 4-35 shows that the travel time through the vadose zone to the groundwater decreases as the infiltration increases. At 10,000 years, the difference in contaminant flux to the groundwater is about 5 orders of magnitude for infiltration rates varying between 0.1 and 50 mm/year. The difference at shorter times is even larger. For example at 1,000 years (the time of compliance), the contaminant flux from 50 mm/year infiltration is about 300 times the flux corresponding to infiltration of 4.2 mm/year and well over 5 orders of magnitude larger than the contaminant flux corresponding to 0.9 mm/year.

Disposal design can affect infiltration rates into the disposal facility. This is most easily seen by comparing the results from the base analysis case, which assumes a natural recharge of 4.2 mm/year, and the best estimate case, which assumes a sand-gravel capillary barrier. Such a barrier greatly reduces infiltration and hence release rate. When comparing the normalized flux to the groundwater for the base analysis and best estimate cases in Figure 4-21, the presence of the sand gravel capillary barrier could reduce the contaminant flux to groundwater by over four orders of magnitude.

The relationship of disposal facility placement to the ancient Columbia River bed affects the amount of dilution. The 1998 ILAW performance assessment ignored the presence of the ancient Columbia River Bed. The higher flow through this region and the difference in the facility footprints between the 1998 ILAW PA and this analysis has led to well intercept factors that are approximately a factor of 10 lower for this assessment. Also this geological structure tends to minimize the spreading of the contaminant plume laterally. Therefore, the WIFs at 100 m and 1,000 m are similar (see Table 4-2).

Estimated impacts from two extreme cases demonstrated that even using extreme assumptions do not lead to levels greatly higher than performance objectives. The first case assumed that the waste form released all contaminants over the period of 1 year. This is an increase in the release rate of the waste form by a factor of approximately 1,000,000. The resulting peak estimated impacts (see Table 4-19) were approximately a factor of 1,000 higher than the estimated impacts at 10,000 years for the base analysis case. However, the peak estimated impacts are only a factor of four above the groundwater performance objectives. The second case assumed the disposal facility was located just above the unconfined aquifer (i.e., there was no vadose zone). The waste form was assumed to release its contaminants as

estimated for the base analysis case. The resulting estimated impacts for the groundwater scenario were approximately a factor of 100 higher than the estimated impacts at 10,000 years for the base analysis case. The estimated impacts remained below the groundwater performance objectives. The major radionuclide contributors for this case assuming no vadose zone are anticipated to be chemically retarded in their transport through the vadose zone. Specifically ^{90}Sr and ^{137}Cs are the major contributors to the beta-photon drinking water dose, with the peak occurring at 70 years after facility closure, and have measured K_d = 10 and 80 mL/g, respectively. Similarly, the major contributor to the all-pathway dose at 10,000 years after facility closure is ^{239}Pu which has a measured K_d = 200 mL/g.

6.3 VERIFICATION OF PERFORMANCE ASSESSMENT RESULTS

This section discusses the basis to conclude that the performance of the ILAW disposal action has been completely addressed, the analysis is logically interpreted, the results are representative of the facility performance, and the results are sufficiently rigorous.

The completeness of the ILAW performance assessment activity can be judged on the effort to determine not only the best estimate case but also other cases that might affect the impacts of waste disposal. An important comment (See Section 1.6.4) is that the public not only wants to know what is expected to happen, but also how bad the consequences could be if these expectations are wrong. Thus, in the creation of the data packages and simulations for this performance assessment (Mann/Puigh 2000a and Puigh 2001) investigations were included to determine basic processes and whether the parameters being measured and the associated models are appropriate. The best example of this is the strategy for glass analysis (See Appendix E). In this document, numerous sensitivity studies (see Section 3.5.5) were conducted to determine how possible alternative choices could affect the results. Other examples are placement of the disposal facility (Section 4.7.2), design of the disposal facility (Sections 4.37 through 4.3.11, Section 4.5.5, 4.5.6), alternative glass formulation (Section 4.5.7), and different inventories (Section 4.8.3). Other cases were run to determine the dependence of the results based on model choices. Examples are waste release models (Section 4.5.2 and 4.5.3) and the presence of clastic dikes in the vadose zone (Section 4.6.3). Still other cases were run to determine the sensitivity of the results to uncertainties in parameters. Examples are infiltration rates (Sections 4.5.4 and 4.6.2), vadose zone parameters (Section 4.6.3), and groundwater flow (Sections 4.7.4 and 4.7.5).

That this analysis is logically interpreted can be judged by reviewing the simple overall approach presented in Section 3.3. Calculations involving the air pathway and the inadvertent intruder scenarios are straightforward. In concept, the groundwater pathway is straightforward (water enters the disposal facility, waste degrades because of water contact, the water carries the released contaminants to groundwater which carries the contaminants to the point of compliance). Despite the straightforwardness of the concept, the models used in each step are fairly complicated. However, for each step, simple models (no barrier case, forward rate for glass degradation, mobile contaminant transport, and simple groundwater dilution) are provided to show that the complicated models provide appropriate results.

These results are not the exact representations of the facility performance because the disposal facility has not been designed and the waste form has not been finally specified.

However, through the use of conservative as well as best estimate cases, this performance shows how likely candidate designs and waste forms will perform. In addition, sensitivity cases were run to determine the effect of various choices. The models and codes used are well established (Section 3.5) and the data establishing the values for the parameters in the models and codes are based on extensive sets of measurements and have been thoroughly documented (Mann/Puigh 2000a). For important features like glass degradation and groundwater flow, calculations have been compared to laboratory and field measurements.

This PA uses state-of-the art data, methods, and codes, which cause the results to be sufficiently rigorous. Moreover, as stated earlier, by comparing these results to those for simpler cases and to bounding cases, any limitations of the methods or codes would have an insignificant consequence to the overall interpretation.

6.4 BASIS FOR WASTE ACCEPTANCE LIMITS

Because waste acceptance limits are determined based on a comparison to performance objectives, the discussion of actual waste acceptance limits is postponed to Section 7.6.1. These limits will be determined by comparing the results of the base analysis case to the performance objectives for each radioisotope or chemical material.

7.0 PERFORMANCE EVALUATION

7.1 OVERVIEW

This chapter compares the estimated impacts found in Chapters 4 and 5 with the performance objectives established in Chapter 1 (Section 7.2) as well as the sensitivity of the results to key parameters (Section 7.3). Section 7.4 discusses the conservatisms and caveats associated with the analysis. This chapter also defines those requirements (Section 7.6), both on the waste form and on the disposal facility design, that are derived from long-term performance and shows that meeting these requirements does not require heroic effort and so the requirements are likely to be achieved. Section 7.7 describes the reasons why the results from this assessment differ from the assessment document in the 1998 ILAW PA (Mann 1998a). The chapter concludes by describing the work planned to update the information contained in this PA.

7.2 COMPARISON OF ESTIMATED IMPACTS TO PERFORMANCE

This section compares the estimated impacts to the performance objectives for each area of protection cited in Section 1.3:

- Protection of the general public
- Protection of the inadvertent intruder
- Protection of groundwater resources
- Protection of surface water resources
- Protection of air resources.

The inadvertent intruder estimated impacts depend on inventory and facility design, and can be mitigated to some extent operationally. The estimated impacts for the other performance objectives (except for air resources) depend on inventory, waste form release rate, facility design, and groundwater flow rate.

7.2.1 Protection of General Public

Table 7-1 compares the performance objectives for protecting the general public with the results from the base analysis and best estimate cases. The estimated all-pathways doses are significantly lower than the performance objectives during the first 10,000 years. The DOE time of compliance is 1,000 years.

Table 7-1. Comparison of Estimated Impacts with Performance Objectives for Protecting the Public. The DOE time of compliance is 1,000 years.

Performance Measure	Performance Objective	Estimated Impact at 1,000 years	Estimated Impact at 10,000 years	
			1998 ILAW PA	Present Results
All-pathways [mrem in a year]	25.0			
Base analysis case		0.000078	6.4	0.070
Best estimate case		1.7×10^{-10}	nc*	1.3×10^{-6}

* nc = "not calculated" in the 1998 ILAW PA

7.2.2 Protection of Inadvertent Intruders

Table 7-2 compares the estimated impacts to the performance objectives for protecting the inadvertent intruder. The time of compliance starts at 500 years after closure. The acute exposure performance objective is met by a factor greater than 500. ^{126}Sn is the most important radionuclide. The continuous exposure performance objective is met by a factor of approximately four for the base analysis case. ^{126}Sn, ^{241}Am, and ^{239}Pu are the major contributors. These results are similar in magnitude to those found in the ILAW PA (Mann 1998a).

Table 7-2. Comparison of Estimated Impacts with Performance Objectives for Protecting the Inadvertent Intruder. The time of compliance starts at 500 years.

Performance Measure	Performance Objective	Estimated Impact at 500 years	
		1998 ILAW PA	Present Results
Acute exposure [mrem]	500.0	5.5	0.76
Continuous exposure [mrem in a year]	100.0	27.5	10.2

The estimated impacts for the inadvertent intruder can be mitigated through operational controls based on projected container inventories. Such operational controls will be better defined as the project matures.

7.2.3 Protection of Groundwater Resources

Table 7-3 compares the estimated impacts to the performance objectives for protecting the groundwater resources. At the DOE time of compliance (1,000 years) and the point of compliance (at a well 100 m downgradient of the disposal facility), the groundwater impacts are not significant. At 10,000 years the estimated impact is approximately a factor of 400 less than the performance objectives for beta-photon emitters and the alpha-emitting radionuclides for the base analysis case.

The concentration of radium is insignificant. The most important drivers are the inventories of technetium, iodine, neptunium, and uranium, the release rate from the waste form, and the amount of mixing in the aquifer. Retardation of uranium isotopes as they migrate through the natural vadose zone is important in achieving the alpha-emitting radionuclides performance objective. The anticipated retardation of the uranium isotopes through any concrete associated with the engineered facility has not been included in these estimates. (See Section 4.6.5 for a description of this case and its results.)

Table 7-3. Comparison of Estimated Impacts with Performance Objectives for Protecting Groundwater Resources. The DOE time of compliance is 1,000 years. The point of compliance is a well 100 m downgradient of the facility.

Performance Measure	Performance Objective	Estimated Impact at 1,000 years	Estimated Impact at 10,000 years	
			1998 ILAW PA	Present Results
Emitters [mrem/year]	4.0			
Base analysis case		2.1×10^{-5}	2.0	0.0102
Best estimate case		4.7×10^{-11}	nc*	3.5×10^{-7}
Alpha-emitters [pCi/L]	15.0			
Base analysis case		1.0×10^{-16}	1.7	0.034
Best estimate case		2.3×10^{-22}	nc*	4.8×10^{-8}
Ra [pCi/L]	5.0			
Either case		0.0	<0.001	<0.001

* nc = "not calculated" in the 1998 ILAW PA

7.2.4 Protection of Surface Water Resources

Table 7-4 compares the estimated impacts to the performance objectives for protecting the surface water resources. The DOE time of compliance is 1,000 years and the point of compliance is at a well intercepting the groundwater just before it mixes with the Columbia River. The estimated impacts are approximately three orders of magnitude lower than the performance objectives for the base analysis case. The estimated impacts at a well just before the river are conservative with respect to the quality of the river water.

Table 7-4. Comparison of Estimated Impacts with Performance Objectives for Protecting Surface Water Resources (Base Analysis Case). The DOE time of compliance is 1,000 years. The point of compliance is a well intercepting the groundwater before entering the Columbia River.

Performance Measure	Performance Objective	Estimated Impact at 1,000 years	Estimated Impact at 10,000 years	
			1998 ILAW PA	Present Results
All-Pathways [mrem/y]	25.0	7.3×10^{-6}	0.22	0.0065
Emitters [mrem/y]	1.0	2.0×10^{-6}	0.070	0.00095
Alpha Emitters [pCi/L]	15.0	1.0×10^{-17}	0.058	0.0032
Ra [pCi/L]	3.0	0.0	<0.001	<0.001

7.2.5 Protection of Air Resources

Table 7-5 compares the estimated impacts to the performance objectives for protecting air resources. The DOE time of compliance is 1,000 years and the point of compliance is just above the disposal facility. The estimated impacts are over three orders of magnitude lower than the performance objectives.

Table 7-5. Comparison of Estimated Impacts with Performance Objectives for Protecting Air Resources. The DOE time of compliance is 1,000 years. The point of compliance is just above the disposal facility.

Performance Measure	Performance Objective	Estimated Impact at 1,000 years	
		1998 ILAW PA	Present Results
Radon [pCi m^{-2} $second^{-1}$]	20.0	<0.001	<0.96
Other radionuclides (^{3}H and ^{14}C) [mrem in a y]	10.0	$<10^{-8}$	$<6 \times 10^{-3}$

7.2.6 Summary

All of the estimated impacts easily meet the performance objectives set out in Section 1.3 for the remote-handled waste trench base analysis case. The estimated all-pathways dose, beta-photon drinking water dose, and concentration of alpha-emitting radionuclides in groundwater for the base analysis case are more than a factor of 300 lower than the corresponding performance objective at 10,000 years after facility closure (2030). This margin increases by well over an order of magnitude if the time of compliance of 1,000 years is used. Using the results of the best estimate case (where a subsurface sand-gravel capillary barrier is in place), the margin increases by orders of magnitude more. The

inadvertent intruder continuous exposure doses are estimated to be a factor of approximately four below the performance objective.

7.3 PERFORMANCE SENSITIVITY TO KEY PARAMETER UNCERTAINTIES

The key uncertainties of this analysis are as follows:

- Disposal facility design and layout
- Waste form performance
- Groundwater flow
- Inventory.

7.3.1 Disposal Facility Design And Layout

Disposal facility design and layout affect impacts in two ways. They modify the amount of moisture available to degrade the waste form and that is available to carry the released contaminants to the groundwater. Facility layout also affects the amount of groundwater available for diluting the contaminants reaching groundwater.

Infiltration into the disposal facility has a major effect on the results of the analysis. Most human-made features are expected to degrade relatively quickly compared to the waste form. Nonetheless, through the use of natural materials, certain features, such as the subsurface sand-gravel capillary barrier or vertical barriers, might be expected to last a long time. In particular, the capillary barrier has a major impact on the amount of moisture entering the actual disposal facility and hence on the effect of that moisture. By comparing the results of the base analysis case and the best estimate case, the sand-gravel capillary barrier is estimated to reduce the impacts by many orders of magnitude. (See Sections 4.3.7, 4.5.4, and 4.6.2.)

The presence of the ancestral Columbia River channel has a significant effect of focusing the groundwater flow beneath the disposal facility. Because relatively few boreholes define this channel, its exact shape is uncertain. However, even if the channel is replaced by the Ringold Formation (the relatively tight geologic unit through which the ancestral Columbia River cuts), the impacts increase by only about an order of magnitude at a well 100 m down gradient and by even less farther out. The effects of small changes in the channel shape are minor, as shown in the relatively small change (50 percent) in impacts if the disposal facility is moved to the south end of the disposal site. Section 4.7 has a fuller description.

7.3.2 Waste Form Performance

The degradation of the waste form sets the time structure of system performance and, so has a major effect on the estimated impacts of the disposal action. A wide variety of sensitivity and uncertainty cases were run. Even if the glass degrades at the fastest rate possible (the “forward rate”), the impacts increase by only an order of magnitude from the

base analysis case. Increasing the moisture that the glass contacts does have an impact (a factor 8 increase in the glass dissolution rate for a factor of 2.5 increase in infiltration rate at 1,000 years, but only a factor of 2.6 at 10,000 years). However, the base analysis case uses an infiltration rate (4.2 mm/year) corresponding to the wetter of the two natural conditions found on the disposal site.

These analyses are based on the very extensive database of the LAWABP1 glass. If a different glass is used, the results may change. Some glasses have been tested that would perform much more poorly than LAWABP1; however, many glass compositions are available that perform better than LAWABP1. (See Section 7.5, Figure 7-2, for a fuller discussion of the uncertainty in glass performance.)

7.3.3 Groundwater Flow

Because the amount of water entering the aquifer with the contaminants is so small compared to the groundwater flow, the estimated impacts from this disposal action are inversely proportional to the groundwater flow.

The groundwater flow beneath the Hanford Site is presently changing. During the Site's early history, large amounts of water (including radioactive and hazardous waste) were discharged directly to the ground. This caused the groundwater table to form mounds that are now gradually dissipating. Thus, present groundwater flow measurements are not indicative of future groundwater flow.

The estimates of groundwater flow used here are based on the Hanford Site groundwater model. This model was used in the Hanford Site Composite Analysis (Kincaid 1998). The sensitivity of the estimated impacts to this model was investigated by a large number of sensitivity studies (Section 4.7). In general, sensitivity is relatively low except for the case where the ancestral Columbia River channel is replaced by the Ringold Formation. In this case the impacts locally increase by an order of magnitude. However, small changes in the exact shape of this channel should not greatly affect the estimated impacts.

7.3.4 Inventory

Only a few contaminants (^{99}Tc, ^{126}Sn, ^{129}I, ^{137}Cs, uranium isotopes, ^{237}Np, ^{239}Pu, and ^{241}Am) drive the results. The inventory in the ILAW packages results from a separation process on waste from the Hanford Site tanks. For the purposes of this performance assessment, Hanford Site tank waste is reasonably well characterized. The separation step, separating the tank waste into low-activity waste and high-level waste, still is being designed.

^{99}Tc drives the groundwater results, while ^{137}Cs drives the inadvertent intruder dose at times of less than 200 years. Both of these isotopes have separation steps in the tank waste treatment process. This assessment uses the requirements of the tank treatment contract (DOE/BNFL 1998) and the separations information provided in Wootan (1999). However, other cases are examined and the changes are relatively small.

The amount of ^{126}Sn and ^{129}I is relatively uncertain. Whether tin will be in the low-activity waste stream or the high-level waste stream is unclear. To be conservative, tin was assumed to be in the low-activity waste stream for this analysis. The amount of iodine in the waste tanks also is poorly known. Most of the iodine is believed to have escaped through the air pathway during the initial chemical treatment of the fuel many decades ago. To be conservative, all the iodine was assumed to go to the low-activity stream. However, because of its high volatility, 90 percent of the iodine does not go into the glass during the treatment process but instead will be trapped on air filters that will be disposed in the onsite solid waste disposal sites.

The amount and chemistry of other key materials (uranium isotopes, ^{237}Np, ^{239}Pu, and ^{241}Am) are quite well known because these materials were the main products of the Hanford Site's original mission. Small changes do not have significant effects.

7.3.5 Other Factors

A variety of other factors could affect the estimated results. However, such factors are investigated in the sensitivity cases. The biggest changes not yet considered in this section are retardation factors. The present values are based on extensive site-specific experiments. Significant changes are not expected from this data set.

7.4 CONSERVATISMS AND CAVEATS

7.4.1 Conservatisms

The intent of this assessment was to be as realistic and rigorous as possible. However, the presence of some still-unmade decisions (disposal facility design, waste form composition, pretreatment separations) has created the need for some conservatism.

The present disposal facility conceptual design has a subsurface sand-capillary barrier. The exact specifications for this disposal facility feature have not been determined. Thus, the base analysis case assumes no capillary barrier, resulting in a significant conservatism. Moreover, the base analysis case assumes a natural recharge equivalent to the wetter of the two soil types, thus causing more moisture flux into the disposal facility. Because estimated performance depends greatly on this infiltration, actual results should be less. However, the actual performance will depend on the performance of the degraded surface barrier, which could be composed entirely of Burbank sandy loam, the wetter of the two soil types.

All but one of the waste form calculations were one dimensional. This has the effect of driving all moisture through the disposal facility's glass-containing regions. In actuality, water will be diverted around the glass waste form because the filler material has much higher hydraulic conductivity than the waste form. Also, all glass was assumed to be LAWABP1 with 20-weight percent waste loading. However, based on current plans, little if any of the glass is likely to have such a high contaminant loading and the average loading is likely to be less. As will be seen in Section 7.5, which discusses glass performance, lower

waste loading means better waste form performance because of lower pH conditions in the trench.

The separation step in the treatment process has not yet been determined. To be conservative, the maximum likely amount of ILAW inventory was assumed to be in the ILAW packages.

7.4.2 Caveats

This effort, as is true for the rest of the ILAW PA effort, is being performed before all decisions concerning ILAW have been made. The treatment plant designer still must decide on the waste form composition that will be used. Although the flow sheet is becoming finalized, its details still must be transmitted to the ILAW PA activity. Similarly, the detail design for the disposal facility does not yet exist. Finally, although the amount of disposal site-specific information has increased, more data are still needed.

This analysis is based on a waste form composition in the composition space that BNFL Inc. (the original treatment plant designer) has chosen. However, the treatment plant designer will not select its glass waste form composition for some months. Similarly, the treatment flow sheets used here are those developed by the Hanford Site contractor. Although the effects of these flow sheet decisions are expected to be small, they still must be investigated to determine the size of the change in the environmental impacts. In particular, once the waste form composition and process range are known, significant waste form testing (similar to that performed for LAWABP1) will be conducted.

The present design for the disposal facility is based on conceptual designs based on the existing mixed-waste trench at the Hanford Site. As detailed design occurs, the dimensions are expected to change and the materials will be more closely specified. Again, the impacts of these changes are expected to be small.

Finally, more geotechnical data (both from the ILAW disposal site and for the Hanford Site as part of the Hanford Site Groundwater/Vadose Zone Integration Project) will be obtained. These data will be incorporated to better define conceptual models and the parameters used to implement those models. Based on the 1998 ILAW PA, the effect of the new data will be a better understanding of the flow and transport, but relatively little change in values is expected.

The impacts from the decisions discussed above will be addressed in the performance assessment annual summaries and performance assessment revisions. Both of these sets of documents are required by the *Maintenance Plan for the Hanford Immobilized Low-Activity Tank Waste Performance Assessment* (DOE/ORP 2000a) as well as the DOE order on radioactive waste management (DOE 1999b).

7.5 UNCERTAINTIES REGARDING GLASS PERFORMANCE

The calculations and long-term performance results discussed in earlier sections of this document are based on a detailed analysis of the release behavior of LAWABP1 glass. However, it is a virtual certainty that the produced ILAW glasses will not have this specific composition. Consequently, it is important to assess the likelihood that the glass waste forms that will be produced will have long-term durability characteristics approximating those of LAWABP1 glass. Unfortunately, doing so is impossible quantitatively for the following reasons. Specific glass formulations for ILAW disposal have not been selected for production. Insufficient experimental data are available to perform STORM simulations with the glasses, even if the compositions themselves were available.

As an intermediate step, the relative performance of BNFL Inc.-type glass compositions can be compared in highly accelerated laboratory tests designed to elucidate the long-term behavior of the materials on a practicable time scale (McGrail, et al. 1998b). Two experimental methods are principally used for this purpose (McGrail et al. 1998b), the vapor hydration test (VHT) and the pressurized unsaturated flow (PUF) test. Briefly, in the VHT, monolithic samples are exposed to saturated water vapor at temperatures typically of 100°C to 300°C in a sealed vessel. This environment greatly accelerates the progression of glass corrosion by water and can result in the formation of alteration phases. The principal uses of the test are as follows:

- As a screening tool to quickly determine if a glass is likely to corrode at an extreme rate
- As a convenient means of generating alteration phases for analysis within a short period
- For a measure of the alteration rate at elevated temperatures.

In contrast, the patented[1] PUF test is an open-system test where water flows through a bed of coarsely ground glass under conditions of partial hydraulic saturation (McGrail et al. 1997). A computer control system stores test data to disk from several thermocouples, pressure sensors, inline sensors for effluent pH and conductivity, and column weight from an electronic strain gauge to accurately track water mass balance and saturation level. Experience in running PUF tests with a number of different ILAW glass compositions has proven the method to be highly effective in accelerating the progression of the glass corrosion process into the so-called “Stage 3” regime representative of longer-term corrosion behavior, and detecting glasses that are unstable with respect to secondary phases that form as a result of the glass-water reaction processes during the test.

A matrix of 56 glass compositions was subjected to VHTs at 200°C for sufficiently long periods to obtain a statistically meaningful measure of the glass corrosion rate (Vienna 2000). The glasses varied the concentrations of SiO_2, Al_2O_3, B_2O_3, Fe_2O_3, TiO_2, ZnO, ZrO_2,

[1] Patent #5974859, “Method and Apparatus for Measuring Coupled Flow and Reaction Processes,” 1999.

MgO, and Na_2O across a wide composition range that covers, with high probability, the expected processing composition range of the ILAW producer. The test matrix was designed in collaboration with staff at the Catholic University of America who are principally responsible for ILAW waste form development to ensure that the selected components and ranges were relevant to glasses under current development. For details on the specific glass compositions involved, please see Vienna (2000). In Figure 7-1, we plot the logarithm of the measured VHT corrosion rate for 50 glass compositions. (Note that results for six of the test glasses were not yet available.) Immediately obvious from the plot is that a large fraction of the test glasses have corrosion rates less than 10 g/(m²·d). This result was quite unexpected because the aggressive, high-temperature conditions of the VHT were anticipated to produce high corrosion rates for a significantly larger fraction of the test glasses.

Figure 7-1. Radial Distribution Plot of 200°C VHT Corrosion Rates for HLP Series of ILAW Glasses. Radial coordinates are $\log_{10}$ corrosion rate, g/(m²·d).

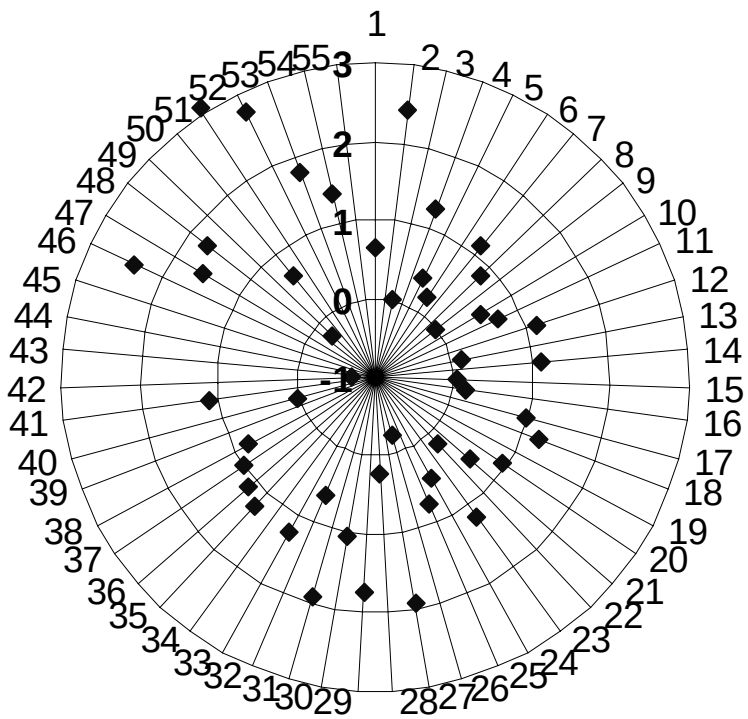

To more quantitatively analyze the results, the VHT corrosion rate data have been replotted in the form of a cumulative distribution function, as shown in Figure 7-2 for glasses studied under the Tank Focus Area (TFA). The measured 200°C VHT corrosion rate for LAWABP1 glass is 4.4 g/(m²·d) and the corresponding data point is highlighted in Figure 7-2. This glass is near the midpoint of the distribution (half of the data set have higher rate and half lower) of 7.2 g/(m²·d). A full 80 percent of the tested glasses have 200°C VHT

corrosion rates less than 30 g/(m²·d). This is about eight times faster than the VHT rate for LAWABP1 glass. However, a glass reacting eight times faster than LAWABP1 still would fall well within the margin of safety available to meet groundwater pathway performance objectives, based on the data in Table 7-9.

Figure 7-2. Cumulative Distribution Plot of 200°C VHT Corrosion Rates for HLP Series of ILAW Glasses.

The data were fit to a three-parameter logistic function of the form $y = a/[1+(x/x_o)^b]$.

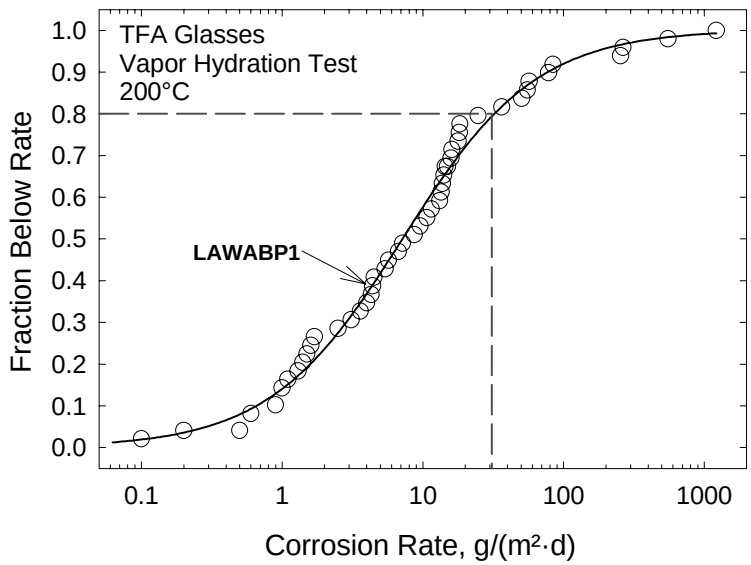

Because of the much greater complexity of the hardware and support equipment, fewer experimental data exist in terms of compositions tested via the PUF system. The latest available data relevant to BNFL Inc. compositions are shown in Figure 7-3. The lines in the figure were computed using a 4-point moving average for the HAN28, LAWA23, and LAWA33 glasses and a 10-point moving average for the HLP-10, HLP-31, and LAWABP1 glasses. A comparison of the peak dissolution rate observed in PUF tests versus the dissolution rate estimated in VHTs at 200°C is plotted in Figure 7-4. The peak dissolution rate was used from the PUF tests because, for the glasses with high dissolution rates, the apparent corrosion decreases with time as the total unreacted glass surface area decreases. This is not taken into account in the corrosion rate calculation.

The results suggest a good correlation between the VHT and PUF test results ($R^2 = 0.91$). Similar secondary phases formed in both types of tests, which is probably why a correlation exists between the results. The available data obviously still are very limited. However, the VHT appears to be a good indicator of glass performance in the PUF test, and both accelerated tests are providing a consistent picture of long-term performance of ILAW glasses as a function of glass composition. These results should be confirmed as additional PUF test data are developed on more ILAW glasses. Meanwhile, it appears virtually certain that glasses can be formulated and manufactured that will meet performance objectives for disposal of low-activity tank waste.

Figure 7-3. Comparison of Glass Corrosion Rate in PUF Tests at 99°C and 2 mL/d.

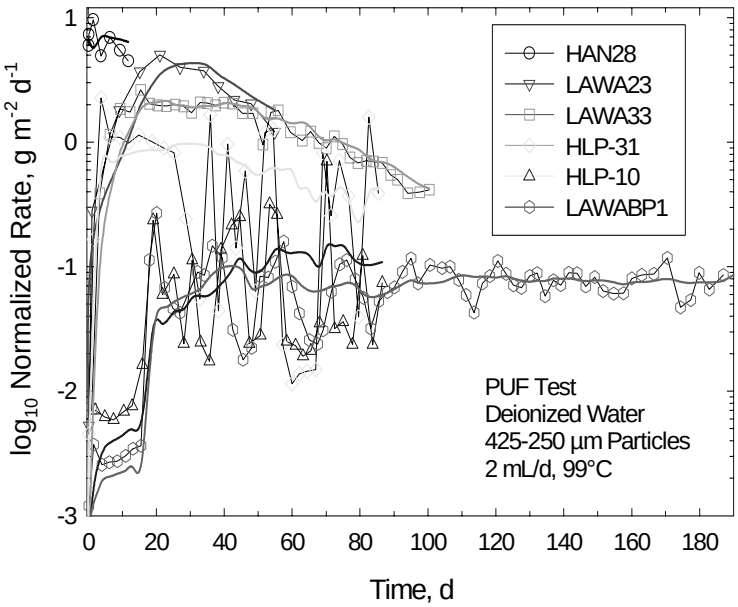

Figure 7-4. Comparison of Glass Corrosion Rate in PUF Tests at 99°C and VHT Tests at 200°C.

Solid line is the regressed fit and the dashed lines are the 95 percent confidence interval**.**

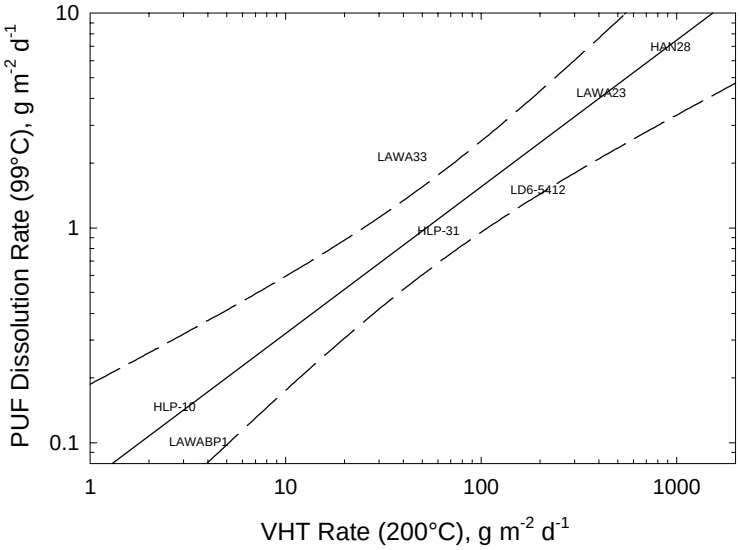

7.6 REQUIREMENTS SET BY PERFORMANCE ASSESSMENT

7.6.1 Introduction

The analysis presented so far was designed to establish an understanding of how the engineered and natural systems behave. Based on this understanding, this section derives the waste form and disposal facility requirements based on long-term human health and safety and environmental performance objectives. Section 7.6.2 and 7.6.3 derive the equations and restrictions based on protecting the inadvertent intruder and groundwater. Sections 7.6.4 and 7.6.5 describe how the derived restrictions apply to the waste form and disposal facilities. Section 7.6.6 describes why the requirements set in the preceding sections are likely to be met.

Data and methods used to establish requirements on the waste form and disposal facilities come mainly from the data and methods used in the base analysis case (Chapter 3) and the base intruder cases (Section 5.3). However, the performance goals for groundwater protection are selected to be more conservative than the performance objectives described in Section 1.6. This will provide an additional margin of safety early in the design process so that engineering tradeoffs, if needed, can more easily be made in a complex, non-linear system.

Only the homesteader inadvertent intruder and groundwater scenarios were used to establish requirements for the waste form and the disposal facilities. Doses from the driller inadvertent intruder, the surface water, and the air release scenarios when compared to their performance objectives are much less restrictive than those from the groundwater and homesteader scenarios. The performance goals are given in Table 7-6.

Table 7-6. Performance Goals for Requirement Cases.

Performance Measure	Requirement Point	Performance Objective	Performance Goal
Continuous inadvertent intruder dose	Disposal Facility	100 mrem/year @ 500 years	100 mrem/year @ 500 years
All-pathways dose	Well 100 m downgradient	25 mrem/year @ 1,000 years	5 mrem/year @ 10,000 years
Beta-gamma drinking water dose	Well 100 m downgradient	4 mrem/year @ 1,000 years	1 mrem/year @ 10,000 years
Alpha-emitter concentration	Well 100 m downgradient	15 pCi/L @ 1,000 years	5 pCi/L @ 10,000 years

From these performance goals, requirements can be derived for parameters more under the control of designers (waste treatment plant specifications and disposal facility specifications) and of operators (waste treatment plant and disposal facility). Such types of requirements are shown in Table 7-7.

Table 7-7. Types of Operation Parameters to be Restricted by PA.

Type of Requirement	Source
Limits on product of inventory and contaminant release rate	Present analysis: Table 7-9
Limits on inventory concentration times effective height	Present analysis: Table 7-8
Limits on inventory concentration	Class C limits [10 CFR 61] Contract (DOE/ORP 2001)
Limits on smearable inventory	Present analysis: Table 7-10 Contract (DOE/ORP 2001)

7.6.2 Requirement Development Based on Inadvertent Intruder Protection.

For the protection of the homesteader, the dose to the inadvertent intruder depends on the amount of each contaminant retrieved (A_i) multiplied by the effective dosimetry parameter (d_i^h), summed over all the contaminants i. Thus, the intruder dose (D^h) must be less than the performance goal established in Table 7-6 (D^h_{max}),

$$D^h = \sum_i k_1 A_i d_i^h \le D^h_{\max} \tag{7.1}$$

where

D^h = the dose to the inadvertent intruder (mrem/year)

k_1 = a constant that includes the effect of diluting the waste in the garden soil ($1/m^3$)

A_i = amount of contaminant i retrieved (Ci)

d_i^h = the dosimetry factor relating response to concentration of contaminant i in the inadvertent homesteader scenario [(mrem/year)/(Ci/m^3)], and

D^h_{max} = the maximum dose allowable in the homesteader scenario (mrem/year).

The amount of each contaminant retrieved depends on the volume of the waste retrieved times the concentration of the waste. Noting that the waste is homogeneous in each of the ILAW packages, the amount of each contaminant retrieved is

$$A_i = k_2 \sum_j \left[\frac{I_{i,j}}{V_j} \right] H_j \tag{7.2}$$

where the sum of j is the sum over packages in a vertical column,

k_2 = area of the hole going through the waste (m^2)

$I_{i,j}$ = the inventory of contaminant i in container j (Ci)

V_j = the volume of waste in container j (m^3), and

H_j = the height of waste within container j (m).

Combining equations 7.1 and 7.2 yields

$$\sum_{i,j}\left[\frac{I_{i,j}}{V_j}\right]d_i^h k^h H_j < D_{\max}^h \tag{7.3}$$

or

$$\sum_{i,j}\left[\frac{I_{i,j}}{V_j}\right]H_j / X_i < 1 \tag{7.4}$$

where

k^h = $k_1 * k_2$, i.e., the factor that accounts for the fraction of waste exhumed during drilling, the mixing of the waste in the soil, and transport to point of exposure (1/m), and

X_i = limiting value of [I/V]*H for contaminant i (Ci/m^2) = $D^h_{max}/(d_i^h k^h)$.

Recognizing that average values were used in the analyses presented in Chapter 5, the values of X_i can be calculated easily from data already presented in this PA.

$$\left[\left(\frac{I_i}{V}\right)H\right]_{\max} = X_i = \frac{D_{\max}^h}{k^d d_{Sn}^h}\left(\frac{I_i}{I_{Sn}}\right)\left(\frac{D_{Sn}^h}{D_i^h}\right) \tag{7.5}$$

where

I_i = the average inventory of contaminant in each container, each container having a volume V and a height H

D^h_i = the intruder dose for contaminant i, and

$$k^h d_{Sn}^h = \frac{D_{Sn}^h}{\sum_j [I_{Sn}/V]H} \tag{7.6}$$

The values for I are obtained from the column labeled “ILAW Package” in Table 3-1 that contains the average inventory in an ILAW package. Intruder dose values (D) are taken from Table 5-2 for the acute (driller) scenario and from Table 5-3 for the continuous (homesteader) scenario. The waste volume assumed in Chapter 5 is a cube 1.4 m on each side filled to 85 percent capacity, which corresponds to a waste height of 1.2 m.

The values for the dimensions of the ILAW package have changed over the past few years along with the number of packages in a vertical column. Therefore, restrictions are placed assuming that the dimensions and number of packages vary.

Table 7-8 displays the restrictions due to protection of the inadvertent intruder.

Table 7-8. Restrictions Based on Protecting Inadvertent Intruder.

$\Sigma[I_{ij} / V_j] H_j / X_i < 1.0$. All waste disposed must meet the NRC Class C limits, which also are treated as a sum of fractions rule. All waste produced during Phase 1 must have a lower average concentration than is shown in the last column.

Isotope	X_i or Max $[\Sigma I_{ij}/V_j]H_j$ (Ci/m^2)	Max $[I_{ij} / V_j]$ (Ci / m^3)		Avg $[I_{ij} / V_j]$
		$X_i / \Sigma H_j$ (1)	NRC Class C	Phase 1 Contract
^{59}Ni	3.80E+04	6.11E+03	-	-
^{60}Co	2.48E+29	4.00E+28	-	-
^{63}Ni	5.63E+05	9.07E+04	-	-
^{79}Se	1.39E+03	2.23E+02	-	-
^{90}Sr	3.79E+06	6.11E+05	7,000.	20.
^{93}Zr	5.22E+03	8.41E+02	-	-
$^{93}Nb^m$	6.88E+13	1.11E+13	-	-
^{99}Tc	2.18E+02	3.51E+01	3.	0.1
^{106}Ru	3.72E+158	5.98E+157	-	-
$^{113}Cd^m$	3.85E+12	6.19E+11	-	-
^{125}Sb	5.06E+58	8.15E+57	-	-
^{126}Sn	7.34E-02	1.18E-02	-	-
^{129}I	1.90E+01	3.06E+00	0.08	0.08
^{134}Cs	1.95E+77	3.15E+76	-	-
^{137}Cs	6.19E+04	9.97E+03	4,600.	3.
^{151}Sm	5.28E+06	8.51E+05	-	-
^{152}Eu	1.68E+11	2.70E+10	-	-
^{154}Eu	7.37E+17	1.19E+17	-	-
^{155}Eu	1.37E+35	2.21E+34		
^{226}Ra	1.02E-01	1.64E-02	0.027 (2)	0.027 (2)
^{227}Ac	8.47E+06	1.36E+06	0.027 (2)	0.027 (2)
^{228}Ra	5.36E+26	8.64E+25	0.027 (2)	0.027 (2)
^{229}Th	5.01E-01	8.08E-02	0.027 (2)	0.027 (2)

Table 7-8. Restrictions Based on Protecting Inadvertent Intruder.

$\Sigma[I_{ij} / V_j] H_j / X_i < 1.0$. All waste disposed must meet the NRC Class C limits, which also are treated as a sum of fractions rule. All waste produced during Phase 1 must have a lower average concentration than is shown in the last column.

Isotope	X_i or Max $[\Sigma I_{ij}/V_j]H_j$ (Ci/m^2)	Max $[I_{ij} / V_j]$ (Ci / m^3)		Avg $[I_{ij} / V_j]$
		$X_i / \Sigma H_j$ (1)	NRC Class C	Phase 1 Contract
^{231}Pa	2.86E-01	4.60E-02	0.027 (2)	0.027 (2)
^{232}Th	5.68E-02	9.15E-03	0.027 (2)	0.027 (2)
^{232}U	1.85E+01	2.99E+00	0.027 (2)	0.027 (2)
^{233}U	8.29E+00	1.33E+00	0.027 (2)	0.027 (2)
^{234}U	4.47E+01	7.20E+00	0.027 (2)	0.027 (2)
^{235}U	1.00E+00	1.62E-01	0.027 (2)	0.027 (2)
^{236}U	6.83E+01	1.10E+01	0.027 (2)	0.027 (2)
^{237}Np	6.95E-01	1.12E-01	0.027 (2)	0.027 (2)
^{238}Pu	1.13E+03	1.82E+02	0.027 (2)	0.027 (2)
^{238}U	6.18E+00	9.94E-01	0.027 (2)	0.027 (2)
^{239}Pu	1.51E+01	2.44E+00	0.027 (2)	0.027 (2)
^{240}Pu	1.58E+01	2.55E+00	0.027 (2)	0.027 (2)
^{241}Am	1.86E+01	3.00E+00	0.027 (2)	0.027 (2)
^{241}Pu	5.44E+02	8.76E+01		
^{242}Cm	2.22E+05	3.58E+04	0.027 (2)	0.027 (2)
^{242}Pu	1.57E+01	2.53E+00	0.027 (2)	0.027 (2)
^{243}Am	8.79E-01	1.41E-01	0.027 (2)	0.027 (2)
^{243}Cm	1.11E+04	1.78E+03	0.027 (2)	0.027 (2)
^{244}Cm	5.72E+03	9.21E+02	0.027 (2)	0.027 (2)

[1]A stacking height of 6.2 m (3 packages * 2.3 m each * 90 percent full) is used.
[2]NRC requirements are expressed in curies per gram. A density of 2.7 g/cm^3 was used for the waste form.

7.6.3 Requirement Development Based on Groundwater Protection

There are three performance measures that need to be used when using the groundwater scenario (all-pathways dose, beta/photon drinking water doses, and concentration of alpha emitters). Moreover, contamination of the groundwater could occur due to 1) the waste initially inside the ILAW packages reaching the groundwater, or 2) smearable contamination on the outside of the ILAW packages reaching the ground water.

7.6.3.1 Waste Inside ILAW Package. The long times, the Impact (D^{gw}) from the groundwater scenario (as discussed in Section 4.11) can be simply expressed and this impact must be less than the performance goal (D^{gw}_{max})

$$D^{gw} = \sum_i (I_i R) d_i^{gw} k^{gw} < D^{gw}_{\max} \tag{7.7}$$

or

$$\sum_i {I_i R}/{Y_i} < 1 \tag{7.8}$$

where the sum is over all contaminants i and where

I_i = the inventory of contaminant i (Ci)

R_i = the fractional release rate of contaminant i from the waste form (1/y)

d_i^{gw} = the dosimetry factor relating response to concentration of contaminant i in the groundwater scenario [(mrem/year)/(Ci/m^3) or 1 in the case of concentration]

k_i^{gw} = the factor that accounts for vadose zone and aquifer transport (years/m^3 or y/L)

D_{max}^{gw} = the maximum impact (drinking water dose, all-pathways dose, or concentration of alpha emitters) allowable in the groundwater scenario (see Table 7-6) (mrem/year or Ci/L)

Y_i = limiting value for (IR) [Ci/year].

The values of Y_i easily can be calculated from information already presented in this PA.

$$[I_i R]_{\max} = Y_i = \frac{D_{\max}^{gw}}{k_i^{gw} d_{ref}^{gw}} \left(\frac{I_i}{I_{ref}} \right) \left(\frac{D_{ref}^{gw}}{D_i^{gw}} \right) \tag{7.9}$$

where

D^{gw}_i = groundwater impact for contaminant i, and

$$k_i^{gw} d_{ref}^{gw} = \frac{D_{ref}^{gw}}{I_{ref} R_{\max}} \tag{7.10}$$

where ref = Tc for mobile (K_d = 0) contaminants and ref = ^{237}Np for retarded contaminants. The values for I are obtained from the Table 3-1 column labeled "ILAW Inventory." That column contains the total ILAW inventory. The impact values (D) are taken from Tables 4-4, 4-5, and 4-6 for the beta-photon drinking water dose, the all-pathways dose, and the concentration of alpha emitters, respectively, for the important radionuclide contributors. The maximum release rate (R_{max}) is 8×10^{-7}/year, which is taken from Table 4-1. (The maximum release rate is the value after about 20,000 years).

Because the details of the separations or treatment process that creates ILAW the waste form have not been determined, neither the ILAW inventory nor the release rate is known. Therefore, the Immobilized Waste Program will place restrictions on the product of the inventory (I_i) and on the release rate (R_i).

In the 1998 ILAW PA (Mann 1998a), an additional term was included in equations 7.7 and 7.8. This term, appearing as a divisor, accounted for different groundwater dilution as the length of the disposal facility perpendicular to the groundwater flow became larger. However, because the groundwater flow in this PA flows in the ancestral Columbia River channel, the disposal facility length is not especially significant. The width of the channel is more responsible for establishing the dilution factor, rather than the dimensions of the disposal facility.

Using these equations and associated values, restrictions on the release rate were calculated and are displayed in Table 7-9.

For groundwater protection, the most restrictive limit based on the beta-photon drinking water dose, alpha concentration, and all-pathways was used. Because the waste form performance is so important, the product of the total inventory times the release rate is important rather than the total inventory for a radionuclide.

As noted in Section 4.8.2, there is a potential for chromium from the ILAW container to be a problem. However, until more is known about the conversion of metallic chromium to Cr(VI) under disposal facility conditions, it is premature to set restrictions on the amount of chromium in the ILAW containers.

Table 7-9. Restrictions Based on Protecting Groundwater - ILAW Package.
$\Sigma[I_{ij} R] / Y_i < 1.0$.

Isotope	Y_i Max IR ($Ci\ y^{-1}$)	Limiting Quantity
^{99}Tc	7.93E-01	Drinking water dose
^{129}I	4.06E-03	Drinking water dose
^{231}Pa	2.87E-03	All pathways dose
^{233}U	3.69E-02	Alpha concentration [1]
^{234}U	3.60E-02	Alpha concentration [1]
^{238}U	3.65E-02	Alpha concentration [1]
^{237}Np	1.20E-02	All pathways dose

[1]Although uranium is not covered under the Federal Drinking Water regulations for alpha emitter concentration, it is included here.

7.6.3.2 Smearable Contamination. Although smearable contamination is not expected on the outside of the ILAW packages, some, even if not a measurable amount, is likely to be present. In this case, the restriction can be interpreted as

$$\sum_i I_i^{smear} d_i^{gw} k^{smear} < D_{\max}^{smear} \tag{7.11}$$

or

$$\sum_i {I_i^{smear}}/{Z_i} < 1 \tag{7.12}$$

where the sum is over all contaminants i and where

I_i^{smear} = the inventory of smearable contaminant i (Ci)

d_i^{gw} = the dosimetry factor relating response to concentration of contaminant i in the groundwater scenario [(mrem/year)/(Ci/m^3) or 1 in the case of concentration]

k_i^{smear} = the factor that accounts for vadose zone and aquifer transport (m^{-3} or 1/L)

D^{smear}_{max}= the maximum impact (drinking water dose, all-pathways dose, or concentration of alpha emitters) allowable in the groundwater scenario (taken as values in Table 7-6)(mrem/year or Ci/L)

Z_i = limiting value for I^{smear} (Ci).

The values of Z_i can be calculated easily from information already presented in this PA.

$$\left[I_i^{smear}\right]_{\max} = X_i = \frac{D_{\max}^{gw}}{k^{smear} d_{ref}^{gw}} \left(\frac{I_i}{I_{ref}} \right) \left(\frac{D_{ref}^{gw}}{D_i^{gw}} \right) \tag{7.13}$$

where

D^{gw}_i = groundwater impact for contaminant i, and

$$k^{smear} d_{ref}^{gw} = \frac{D_{ref}}{I_{ref}} \tag{7.14}$$

where ref = ^{99}Tc for mobile (K_d = 0) contaminants and ref =^{237}Np for retarded contaminants. The values for I are obtained from the column labeled "ILAW Inventory" in Table 3-1 that contains the total ILAW inventory. The impact values (D) are taken from Tables 4-20, 4-21, and 4-22 for the beta-photon drinking dose, the all-pathways dose, and the concentration of alpha emitters, respectively. The values for D^{gw}_{max} are the same as for the groundwater scenario.

Using these equations and associated values, restrictions on the amount of smearable contamination were calculated and are displayed in Table 7-10.

Table 7-10. Restrictions Based on Protecting Groundwater - Smearable Contamination.
[$\Sigma I_i / Z_i < 1.0$].

Isotope	Limiting Quantity	Z_i Max I^{smear} (Ci)	Max I^{smear} (pCi/m^2) [2]
^{99}Tc	Drinking water dose	5.91E+02	1.28E+09
^{129}I	Drinking water dose	3.11E+00	6.71E+06
^{231}Pa	All pathways dose	1.64E+00	3.53E+06
^{233}U	Alpha concentration [1]	2.26E+01	4.88E+07
^{234}U	Alpha concentration [1]	2.22E+01	4.78E+07
^{238}U	Alpha concentration [1]	2.23E+01	4.80E+07
^{237}Np	All pathways dose	7.31E+00	1.58E+07

[1]Because uranium is not covered under the Federal Drinking Water guidelines, the all-pathways dose is used as limiting quantity.
[2]Total area of waste packages taken as 463,500 square meters.

7.6.4 Waste Form Restrictions

Using the information generated in Sections 7.6.2 and 7.6.3, restrictions based on long-term performance can be placed on the ILAW glass and package. These fall into three categories, restriction on the waste concentration, waste release rate, and smearable contaminants on the surface of the ILAW package.

7.6.4.1 Concentration. The restrictions on waste concentration due to long-term performance are displayed in Table 7-8 (second column) and depend upon not only the waste concentration, but also the ILAW package height and the number of layers used in the disposal facility. However, using the current plans for package height and disposal facility operation [containers being 1.22 m in diameter by 2.3 m high, filled with 90 percent glass (DOE/ORP 2000c) and being stacked three containers high], concentration limits were derived and are displayed in the third column of Table 7-8. These limits are compared to the NRC class limits (fourth column of Table 7-8) and the average concentration presently in the contract (fifth column).

In general, the NRC Class C requirements are the most restrictive. For those radioisotopes having Class C restrictions, the limits from this analysis are more restrictive for ^{137}Cs, ^{231}Pa, ^{232}Th, and ^{235}U. For the non Class C radioisotopes, the most important restriction is for ^{126}Sn. However, for ^{90}Sr, ^{99}Tc, and ^{129}I, the Phase 1 contract is much more restrictive than either the limitations calculated here or NRC Class C limits.

7.6.4.2 Release Rate. For most risk analyses, the release time is short compared to travel time, and hence the release rate is unimportant. In these cases, the total inventory is restricted by the risk analysis. For ILAW disposal, however, the release time is much longer than the travel time. Thus, it is the product of the inventory and the release rate that is important. The restrictions on the product of inventory and release rate are shown in Table 7-9. Although it is the product that is important, using the current inventory, the contaminant release rate from the waste form should be less than 137 ppm/year.

7.6.4.3 Smearable Contamination.

The limits for smearable contamination are quite high and are displayed in Table 7-10. Less than 0.1 percent of the inventory of the key contaminants can appear on exposed surfaces as smearable contamination.

7.6.5 Disposal Facility Requirements

Most of the requirements imposed by the performance assessment analysis are on the waste form. However, a few are imposed on the disposal facilities. The major facility requirements deal with subsidence, recharge rate, layout, interactions with the waste form, and intruder protection.

The performance assessment assumes that subsidence is small based on the slow degradation of the waste form and the use of filler materials to minimize voids in the disposal

facility. This means that the facility must be constructed without significant void space. In addition, after waste is placed inside the facility, the spaces between the waste containers must be filled with a dry material. The estimated impacts of a 1 -m wide subsidence of 0.3 m depth in the remote-handled waste trench facility located 10 m from the RCRA-compliant cap apex and extending the long length of the trench are factors of 500 and 1,000 times larger for the alpha concentration and beta-photon drinking water dose, respectively, than the estimated impacts for the best estimate case at 10,000 years after facility closure. Facility performance enhancements associated with the RCRA-compliant cap and the capillary break can be effectively lost if massive subsidence occurs. For the subsidence case analyzed , the estimated impacts still are less than the estimated impacts for the base analysis case.

Because the waste form releases contaminants at a slow, approximately steady rate, the time dependence curve for exposure is shaped more like a plateau than a peak. Therefore, a major effect of the recharge rate is to affect the arrival of contaminants to the groundwater. If the second group of contaminants (i.e., those having K_d = 0.6 mL/g, such as uranium) arrived in significant quantities before 10,000 years, the all-pathways dose would greatly increase and restrictions may have to be placed on the recharge rate. The base analysis case shows that achieving the natural recharge rate (4.2 mm/year) is sufficient to meet performance objectives. If a subsurface sand-gravel capillary barrier is used, the infiltration rate could be far lower.

The requirement for groundwater protection [$\Sigma(I_i R_i) / Y_i < 1$] actually is on the disposal system. The designers of the disposal structures must ensure that materials are not used that would accelerate waste form degradation. Alternatively, the designers can add components (for example, hydraulic diverters, getters) to minimize the requirements on the waste form.

Designers of the engineered system may wish to add components to provide greater defense in depth. The major components would be an improved surface barrier to reduce the recharge rate, a hydraulic barrier to divert moisture from the waste, concrete pads to trap uranium, and other getter materials to trap important radionuclides such as technetium. The recharge rate is the main driving function for the system. Having a surface barrier that could reduce this rate would lengthen the time the contaminants take to reach the groundwater. Diverting water from the waste would likely reduce the contaminant release rate from the waste form and create a greater moisture shadow under the disposal system that also would delay contaminant travel. Concrete is known to highly retard movement of uranium isotopes, thus reducing their impact during the time of compliance. If an inexpensive getter could be found for technetium, such a material could also have important impacts.

7.6.6 Likelihood of Meeting Requirements

The likelihood of meeting the requirements for the waste form and the disposal facility is determined by establishing a case using the best available information.

Because the base analysis case met the performance objectives and the sensitivity cases showed the robustness of the assumptions and data, this system can reasonably be expected to meet the

requirements imposed in Sections 7.6.3 and 7.6.4. This section demonstrates that compliance.

7.6.6.1 Inadvertent Intruder Compliance Case. Current plans have a different container size and number of containers per stack than the configuration analyzed in Chapter 5. However, these plans are reflected in the requirements given in Table 7-8.

Table 7-11 compares the average inventory concentration and the bounding concentration in an ILAW package to the inadvertent intruder protection limits from Table 7-8. As expected from the results described in Chapter 5, in most cases the expected and bounding inventories are much less than allowed. The exceptions are some actinides (^{239}Pu, ^{241}Am, and ^{241}Pu), where the inventory must be reduced to meet Class C limits as required by the contract to produce ILAW (DOE/ORP 2000c).

Table 7-11. Comparison of ILAW Inventory Concentrations to Allowed Limits. (NRC Class C Limits Have Not Been Applied.)

Nuclide	Ratio of Averaged Inventory/ Allowed Inventory*	Ratio of Bounding Inventory /Allowed Inventory*
90-Sr	0.004	0.008
99-Tc	0.012	0.033
126-Sn	0.091	0.880
232-Th	0.001	0.007
232-U	0.008	0.061
233-U	0.031	0.230
234-U	0.010	0.072
237-Np	0.019	0.066
238-Pu	0.025	0.100
238-U	0.011	0.075
239-Pu	0.715	3.519
240-Pu	0.123	0.496
241-Am	2.537	62.393
241-Pu	1.678	7.333
242-Cm	0.013	0.430
243-Cm	0.002	0.019
244-Cm	0.024	0.251

*Allowed inventory is not corrected for decay

7.6.6.2 Groundwater Protection Compliance Case. For groundwater, the results do not change between the base analysis case and the compliance case. Thus the comparisons given in Section 7.2 are still valid. That is, a large margin exists between the requirements and the expected performance.

7.6.6.3 Smearable Contamination Compliance Case. The limits for smearable contamination (Table 7-10) are high. The contract specifications are that no more than 367 Bq/m^2 (or 1.22×10^4 pCi/m^2) of alpha contamination and no more than 3670 Bq/m^2 (or 1.22×10^5 pCi/m^2) of beta-gamma contamination should be present on the surface. Comparing the requirements of Table 7-10 to these numbers shows that this performance assessment is much less restrictive than the contract, especially with the safety margin built into this analysis.

7.7 SUMMARY OF THE IMPACT OF DIFFERENCES BETWEEN THE 1998 ILAW PA AND THIS DOCUMENT

Of the three types of scenarios (groundwater, air, and inadvertent intruder) studied in the 1998 ILAW PA (Mann 1998a) and this document, only the results for the groundwater scenario are significantly different. Five major differences occur in inputs between the 1998 ILAW PA and this document that affect the peak values of impact parameters for scenarios that contaminate groundwater:

- Time of compliance
- Inventory of mobile constituents
- Disposal facility design
- Waste form performance
- Groundwater dilution.

Other new data (such as recharge rates, geochemistry, and hydrology) affect the time that the peak occurs or the impact parameters through one of the last four inputs cited.

The 1998 ILAW PA used 10,000 years as the time of compliance. Because of new DOE guidance, the present time of regulatory compliance is 1,000 years. However, because of the slow travel time in the vadose zone, even the mobile constituents do not reach the groundwater in any significant quantity in only 1,000 years. To make comparisons with the 1998 ILAW PA easier, Table 7-12 summarizes the differences in impact parameters at 10,000 years.

The facility design effect is associated with areal distribution of the waste. For the remote-handled waste trench disposal concept, the areal footprint for the facility is 124,800 m^2. For the 1998 ILAW PA, the Concept 1 disposal facility had an areal footprint of 51,000 m^2. The larger areal distribution of the waste leads to a reduction factor of 0.41 associated with the contaminant concentration entering the aquifer over a larger area.

Table 7-12. Effect of Updated Model Inputs on the Estimated Beta/Gamma Drinking Water Dose at 10,000 Years. (1998 ILAW PA estimated this dose as 2.0 mrem/year.)

Updated Model Input	Beta-Gamma Drinking Water Dose
	Ratio 2001 ILAW PA to 1998 ILAW PA
Facility design	0.41
Technetium inventory	0.26
Ratio of other mobile contaminants to Tc[1]	1.32
Technetium dose factor	0.83
Waste form release rate/ vadose zone transport	0.30
Groundwater dilution	0.14
All inputs	0.0049

[1]based on updated K_d values for selenium, iodine, and neptunium.

The estimated impact at 10,000 years of changing the inventory of the mobile constituents is to reduce the present estimated groundwater impacts by a factor of 0.34 (0.26 * 1.32) when compared to the results from the 1998 ILAW PA (Mann 1998a). The lower estimated impact of inventory in the present analysis arises from two changes: the change in the inventories of ^{99}Tc, the most important radionuclide in either analysis, and of other mobile radionuclides. The 1998 ILAW PA assumed that 80 percent of the technetium in the tanks would end up in ILAW, while this document assumes, based on the contract between the treatment vendor and DOE, that only 20 percent of the technetium in the tanks will go into ILAW. The remaining slight difference in the technetium inventory results from a small change in tank inventory.

Based on disposal site-specific geochemical measurements, the determination of which contaminants are mobile has changed somewhat. Technetium-99 still is the most important mobile contaminant. In the 1998 ILAW PA, ^{79}Se was assumed to be mobile because no Hanford Site-specific data were available that indicated otherwise. Since then, we have learned that the half-life of ^{79}Se is longer than was believed. Also, disposal-site specific information has shown that selenium transport in the vadose zone is chemically retarded. However, iodine and neptunium, which were treated as relatively immobile in the 1998 ILAW PA, now are known through disposal-site specific information to be more mobile. Thus, where ^{99}Tc was 75 percent of the drinking water dose in the 1998 ILAW PA, it is only 57 percent in this document. Therefore, the relative contribution from other mobile contaminants has increased to 1.32 (0.75/0.57).

The new DOE O 435.1 requires the use of the EPA dose factors; the dose factor for ^{99}Tc was 0.83 of the dose factor used in the 1998 ILAW PA. In the 1998 ILAW PA, the release from the vaults was assumed to be that given in the request for proposal for treatment services (4.0×10^{-6}/year) (DOE/RL 1996). At 10,000 years after facility closure, the contaminant flux to the aquifer was 2.0×10^{-6}/year. In this document, the release from the

remote-handled waste trench is calculated by simulating the waste form release (rate = 0.8×10^{-6}/year at 10,000 years after facility closure) from LAWABP1 glass and performing the transport of contaminants through the vadose zone resulting in a contaminant flux of 0.7×10^{-6}/year at 10,000 years after facility closure. This results in a 30 percent decrease in the contaminant flux to the aquifer when compared to the 1998 ILAW PA values.

We now realize that the disposal site is situated over the old channel of the Columbia River. Also, the base analysis case used a recharge rate of 3 mm/year in the 1998 ILAW PA and a rate of 4.2 mm/year in this analysis. The hydraulic conductivity of the unconfined aquifer is higher, resulting in greater dilution, by about a factor of 7.

Combining these factors (inventory of mobile constituents, disposal facility design, waste form performance, and groundwater dilution), the overall effect is a reduction by a factor of about 200 from the 1998 ILAW PA for the estimated impacts to the groundwater.

7.8 FURTHER WORK

The ILAW performance assessment team is collecting information for the next version of this document. Plans for data collection and documentation for the program's life have been issued.

The Immobilized Waste Program is committed to providing information to the DOE and the public on the long-range human health and safety and the environmental impacts from the disposal of immobilized low-activity waste. The program realizes that this effort is just the beginning. The program realizes that although the analysis presented in this performance assessment is robust, it relies on data that may not reflect the actual facility design or the composition of the waste being disposed. The maintenance of the ILAW performance assessment is documented in the *Maintenance Plan for the ILAW Performance Assessment* (DOE/ORP 2000), which was approved by the DOE/ORP field manager and sent to DOE/LFRG as required (French 2000b).

The Program will provide additional analyses based on new data and methods as they become available so that the decision makers can make the appropriate decisions. To support these assessments, an extensive data collection and interfacing effort is planned (Puigh 2000). The type and amount of new data will be guided by the uncertainty of current data and the importance of such data to the results of future analyses. The major components of this data collection effort are as follows:

- Waste form data collection and model development
- Interactions with disposal facility designers
- Geotechnical data collection and model development
- ILAW inventory
- Other data collection (dosimetry, scenario development, performance objective selection).

7.8.1 Future Performance Assessments

As noted in Section 1.4 and presented in Table 1-2, a number of PAs will be produced that incorporate the latest data and information and that present the long-range impacts from disposal. These future PAs are expected to reaffirm the conclusions reached in this document. The next PA is planned to be submitted in 2005 to support the start-up of disposal operations. After that, PAs are scheduled on 5-year cycles. These later performance assessments would support new designs, the startup of new facilities, and the closure of filled facilities.

As with the 1998 ILAW PA and this document, a set of data packages will be published that will contain all data to be used in the 2005 ILAWPA. Each data package will contain the best estimate of the information needed for the analysis (and its uncertainties), along with reasonably bounding information so that the analysis can state what will not happen. Each data package will be reviewed; in the more important cases, the review will be performed by outside experts. If new data not contained in the data packages are used in the PA, they will be carefully documented and justified in the PA itself. The performance assessment will carefully follow the guidance provided by the DOE and information from the technical reviews of other PA documents and Hanford Site-relevant environmental analyses.

7.8.2 Waste Form Data Collection and Model Development

This analysis has shown that waste form behavior is the key parameter to the disposal of immobilized low-activity tank waste. Because of the projected slow release, the engineered system rather than the natural system will mainly determine the peak exposures.

In support of the 1998 ILAW PA, a significant effort was spent characterizing the low-level waste glass LD6-5412. Based on that experience, a plan was developed for estimating waste form performance thousands of years from now. Since then, a tremendous amount of work has been performed on a variety of potential low-level waste glasses, particularly LAWABP1. Based on this experience and on the review of that plan (SRC 2001), the plan remains basically unchanged and is presented in Appendix E. The plan still forms the core of the performance assessment waste form task.

Estimating long-term waste form performance will be based on simulating the environment and waste form as a function of time and position in the disposal facility. To be successful, such a strategy depends on an understanding of the processes involved, on a powerful computer code that incorporates those processes, and on well-tested and -understood parameters for those processes.

As noted in Section 3.3.3.2, scientists believe they understand the major processes of glass dissolution and contaminant release. The release of contaminants from a glass waste form in a dry environment over thousands of years is complex. Improvements on codes such as STORM are expected. The improvements will allow the code to better incorporate not only the chemical effects of waste form release, but also the hydraulic principles that govern the contaminant transport in the facility.

Four major types of experiments (SPFT, VHT, PCT, and PUF) will be used. The samples in the tests will be produced using the proposed formulations of the ILAW producers and radioactive waste from Hanford Site tanks. These tests not only will provide parameters for the computer code analyses, but will serve to validate the codes. Initially, tests will be performed with nonradioactive simulants of tank waste. Later tests on glasses made with actual waste will be performed.

The single pass flow-through (SPFT) tests determine how the glass dissolves under constant environmental conditions (temperature, pH, ion concentration). These tests pass a water solution of known ionic concentration at known temperatures through the glass. Because the dissolved glass never forms a significant fraction of the fluid, parameters such as the pH power law coefficient, the activation energy, and the rate law order can be determined. Also by investigating the entire data set, possible deviations from the model can be investigated and understood.

The vapor hydration tests (VHT) allow the determination of the formation of phases from the dissolved glass materials. Such phases could accelerate glass dissolution or could trap contaminants in a stable medium. These measurements normally are done at temperatures higher than 100 ^{o}C, which greatly accelerates glass dissolution and formation of the phases. By performing the tests at different temperatures, scientists can investigate the temperature effects and extrapolate the measurements to temperatures typical of ILAW disposal. VHT also can supplement the results of the product consistency test (PCT), which is run at lower temperatures.

PCT is a well-established test to determine how glass will dissolve in a static environment. In this test, the environmental conditions are established at the beginning of the test, then measured as the test proceeds. Because the ILAW waste contains so much sodium, the environmental conditions (particularly pH) change significantly. PCT tests are run at a variety of temperatures and surface-to-volume ratios. Such measurements allow the pseudo-equilibrium constant to be determined. These tests not only provide an integral check on the SPFT results, but also can provide information on the importance of reactions such as the sodium ion exchange reaction.

The pressurized unsaturated flow (PUF) test is unique among the tests because it is the only test performed in an unsaturated-moisture environment. In this test, water is forced to flow through a porous medium of glass at a slow rate. Because the disposal facility is expected to be extremely dry, the PUF tests will be used to determine whether (or how) any of the parameters or processes change under such dry conditions. PUF test results already have been used to determine the change in hydraulic conductivity as the glass dissolves, as well as determining other physical properties. The PUF tests, particularly those carried out over long periods, are expected to severely test the models and our understanding of them.

All this test information is being used to formulate, test, and calibrate the computer models, which are being modified to make them more robust and accurate. More chemical processes are being modeled. Our intent is to have a computer model that simulates the influx of water to the disposal facility, the corrosion of the glass, the release of the

contaminants from the original glass waste form and its secondary mineral phases, and the transport of those contaminants out of the engineered disposal system.

7.8.3 Interactions with Disposal Facility Designers

Disposal facility construction costs will be significant. The performance assessment team has been and will continue to work with the disposal facility designers to identify key components of the facility design so that cost-effective, safety-enhancing decisions can be made. A prime example of this was the decision to use a disposal facility design based on trenches instead of concrete vaults. Not only is the trench design more cost effective, but also contaminants will be released at a slower rate from it, causing less environmental impact. The performance assessment team will continue to work closely with the design team to determine the components that must be included in the models for future performance assessments.

To model the disposal facility, we need not only the design, but also the hydraulic and transport properties of the waste form and near-field environment materials. Movement of moisture through cracks in the waste form and the hydraulic and geochemical properties of the original and degraded materials will be investigated. Efforts to support design of surface and sand-gravel capillary moisture barriers, getter materials, and water conditioning layers are part of the multi-year plan.

7.8.4 Geotechnical Data Collection and Model Development

Geotechnical data describe the vadose zone and the unconfined aquifer. The vadose zone and the unconfined aquifer play an important role in the performance assessment because the vadose zone delays the arrival of contaminants and the aquifer supplies additional water with which the contaminants can mix. An integrated program covering all aspects of the Hanford Site's vadose zone and unconfined aquifer has just begun. The program should result in more efficient data collection and a more thorough method review.

In each of the next 2 years, a borehole will be drilled at the disposal site. These boreholes will provide samples for determining other geotechnical information. They also will allow access to the vadose zone for in situ moisture experiments and to the unconfined aquifer for groundwater testing. The samples from the boreholes, along with samples from other locations, will be used to determine the geologic strata underlying the disposal facilities and the hydraulic and geochemical properties of those strata. In addition, the samples will be used to determine chlorine content as a function of depth, which will provide the recharge rate over the last 13,000 years).

Other analyses will support the determination of geotechnical data needed and use those data once they are gathered. For example, the computer simulations of moisture flow in Hanford Site surface sediments will combine the long-term time-varying infiltration rates determined by chlorine measurements (both total Cl and ^{36}Cl) with short-term (a few decades) determination of the infiltration rate and climate, soil, and vegetation studies. Enhanced contaminant transport through colloidal movement or in clastic dikes also will be

studied. Studies of the spatial variability of soil hydraulics data and alternative conceptual models will be important for completing future performance assessments.

Because of the thickness of the vadose zone and the size of the disposal facilities complex geotechnical computer codes and models are needed to forecast future moisture flow and contaminant transport. These codes and models will be improved as new data and methods are developed.

7.8.5 ILAW Inventory

The inventory in each ILAW package will depend on the radionuclide inventories of the 177 individual tanks, the order and method of retrieval from those tanks, the blending on the retrieved contents, and the separations and the immobilization processes used by the ILAW producers.

The PA team will continue its close interface with the RPP Standard Inventory effort. The team also will closely interact with the RPP Retrieval Group to incorporate their plans into the ILAW estimates. Finally, contacts with the ILAW producers will occur to determine their separations and immobilization plans to better estimate the fraction of the waste they receive that will end up in low-activity tank waste product. The Program also will use such estimates for safety studies.

Once the ILAW packages are produced, the PA team will rely on product manifests. Thus, as ILAW packages are produced and product manifests become available, the complexity and uncertainty of the inventory estimate is expected to decrease.

7.8.6 Other Data Collection

Other information must be obtained for a successful PA. Dosimetry data must be collected. Scenarios must be developed and reviewed. Performance objectives must be selected and reviewed.

The Hanford Site has a DOE-chartered group (the Hanford Environmental Dose Oversight Panel) to standardize dosimetry data and methods and to review the results of calculations. The PA team will work closely with this group to ensure that its data and methods comply with Site standards.

The public has strong views concerning scenarios and performance objectives. The PA team will review existing guidance, Hanford Site activities (especially the environmental impact statement activities), and other Hanford Site project efforts, such as the Hanford Groundwater / Vadose Zone Integration Project’s regulatory path forward effort, to determine the scenarios and performance objectives to be used in future PAs.

7.9 CONCLUSION

This performance assessment analyzed the long-term environmental and human health impact of disposing of immobilized low-activity waste from Hanford Site tanks. This analysis confirms the conclusions of the 1998 ILAW PA that an understanding of ILAW contaminant transport exists and that the proposed disposal action can meet the performance objectives. Based on this expectation, requirements for waste acceptance and disposal facility performance were established. The final analysis of this performance assessment shows a "reasonable expectation" that these requirements will be met. Finally, this chapter concludes by explaining the additional effort that is under way to confirm the data used in this assessment and to document the effects of new information and understanding on the long-term impact of the disposal of this waste.

8.0 PREPARERS AND MAJOR REVIEWERS

CAROL A. BABEL, Physical Scientist, U. S. Department of Energy Office of River Protection (ORP).

B. S.	Medical Technology, University of Tulsa	1974
B. S.	Geology, University of Oklahoma	1985
M. S.	Hydrology, University of Arizona	1994

Ms. Babel is the ORP program manager for the Immobilized Low-Activity Waste Performance Assessment (ILAW PA) and served as the ORP review team lead for this document. She has managed this project for the past 2 years and reviewed this document as part of her responsibility for monitoring PA activities.

DIANA H. BACON, Senior Research Scientist, Hydrology Group, Pacific Northwest National Laboratory.

B.S.	Geology, George Mason University	1983
M.S.	Hydrology, New Mexico Institute of Mining & Technology	1986
Ph.D.	Geology, Washington State University	1997

Dr. Bacon has over 15 years of experience in vadose zone hydrology and geochemistry and numerical simulations of subsurface flow and transport. As a part of her doctoral studies, Dr. Bacon developed an inverse multiphase reactive transport code to simulate the effect of heterogeneous soil properties and transient changes in transport parameters on fractionation between CO_2 and the source of CO_2 in the vadose zone. In support of the Hanford Tank Low-Activity Waste Glass Performance Assessment Project and the Yucca Mountain Project, Dr. Bacon currently is developing the coupled nonisothermal, multiphase flow and transport code, STORM. She performed the waste form release calculations.

MARCEL P. BERGERON, Program Manager, Hydrology Group, Pacific Northwest National Laboratory.

B.A.	Geology, University of Vermont	1975
M.A.	Geology, Indiana University	1979

Mr. Bergeron joined Battelle, Pacific Northwest Laboratory, in May 1985 as a research hydrogeologist and has 21 years of experience in a wide variety of groundwater investigations and studies at hazardous waste and contaminated groundwater sites. Since joining Pacific Northwest Laboratory, Mr. Bergeron has devoted his attention to a variety of roles in hydrologic studies and investigations including technical contributions, project and task management, and line management roles. Technically, he has specialized in the area of hydrogeologic investigations with specific emphasis on applying groundwater flow and transport modeling. He performed the regional- and local-scale groundwater flow and transport modeling used to support this assessment. He led and oversaw the groundwater calculations.

NEIL R. BROWN, Project Manager, U.S. Department of Energy, Office of River Protection

B.S.	Material Science and Engineering, Rice University	1988
Ph.D.	Material Science and Engineering, Northwestern University	1992

Before joining DOE, Dr. Brown was a postdoctoral fellow at the Argonne National Laboratory where he studied corrosion characteristics of waste glass and soil remediation. At DOE, he has overseen technology development for the Low-Level Waste Program, as well as the development of TWRS privatization specifications. Currently Dr. Brown is the DOE Contract Officer for the treatment and vitrification effort as well as the DOE manager for the storage and disposal of the immobilized waste. He reviewed this document.

KENNETH C. BURGARD, Technical Lead For Storage And Disposal, Immobilized Waste Office, CH2M Hill Hanford Group, Inc.

B.S. Mining Engineering, University Of Missouri

Mr. Burgard has more than 30 years of experience in engineering, construction, and operations for various mining, processing, and nuclear projects as well as high-level and low-level storage and disposal projects. Relevant PA experience includes program management of the grout PA, project management of the LLW Grout Vault facility construction, program manager for the LLW Technology Group, manager of the ILAW glass testing program, and manager of the IHLW and ILAW conceptual designs to support privatization. Mr. Burgard also was responsible for the construction of numerous coal processing and shipping facilities throughout the United States. He managed this effort and reviewed the document.

MARY P. CURRY, Technical Writer/Editor, Lockheed Martin Services, Incorporated.

B.S.	Agriculture, Arizona State University	1977

Ms. Curry has written and edited technical material for the aerospace and nuclear industry since 1982 and worked at the Hanford Site since 1991. She edited the ILAW interim PA, the 1998 ILAW PA, and this document.

SCOTT H. FINFROCK, Nuclear Engineer, Nuclear and Environmental Initiatives, Flour Federal Services.

B.S.	Engineering, University of Washington	1983
M.S.	Nuclear Engineering, University of Washington	1987
M.S.	Computer Science, Washington State University	1993

Scott Finfrock has over 15 years of experience in numerical simulations of transport of radiation and radioactive materials. He was a key contributor to the Hanford Site solid waste PAs, particularly in the area of modeling transport through the vadose zone and groundwater. For this PA he was primarily responsible for integrating the results of the various calculations to determine the total impact from the disposal system.

EUGENE J. FREEMAN, Hydrogeologist, Hydrology Group, Pacific Northwest National Laboratory.

B.S.	Geology, Montana State University	1986
M.S.	Hydrology, University of Idaho	1995

Mr. Freeman has 10 years of experience in the field of hydrogeology. He has experience as a field hydrogeologist and numerical modeler. Mr. Freeman has performed work for both saturated and unsaturated systems and has spent the past 8 years analyzing and modeling moisture and contaminant distribution within the unsaturated sediments beneath the Hanford Site. He performed the vadose zone modeling outside of the waste package area.

RAZIUDDIN KHALEEL, Consulting Engineer, Nuclear and Environmental Initiatives, Flour Federal Services.

B.S.	Civil Engineering, Bangladesh University of Engineering and Technology	1966
M.S.	Water Science and Engineering, Asian University of Technology	1970
Ph.D.	Soil and Water Engineering, Texas A&M University	1977

Dr. Khaleel has over 25 years of experience in groundwater hydrology and numerical simulations of subsurface flow and transport. He was a key contributor to the Hanford Site solid waste PAs and the immobilized low-activity waste PA, particularly in the area of conceptual model development, direction of modeling, and in writing the document. For this document, he reviewed the approach, models, and results.

CHARLES T. KINCAID, Staff Scientist, Hydrology Group, Pacific Northwest National Laboratory.

B.S.	Civil Engineering, Humboldt State College	1970
Ph.D.	Engineering (Hydraulics), Utah State University	1979

Dr. Kincaid was the technical manager and key contributor to the *Performance Assessment of the Grouted Double-Shell Tank Waste Disposal at Hanford* and the *Composite Analysis for the Low-Level Waste Disposal in the 200 Area Plateau of the Hanford Site*. He has been the technical group leader of the Soil Physics Group and the Subsurface Transport Group. He was a key contributor in the development of contaminant transport codes and has contributed to various PAs. Dr. Kincaid reviewed this document.

PHILIP E. LaMONT, General Engineer, U.S. Department of Energy Office of River Protection.

B.S.	Chemical Engineering, Washington State University	1965
M.S.	Chemical Engineering, University of Idaho	1975

Mr. LaMont is a project director in the Hanford Site Tank Waste Remediation System Office. He has more than 20 years of experience in nuclear waste management. Mr. LaMont reviewed this document as part of his responsibility for managing projects for storage and disposal of the immobilized waste products from the planned treatment of Hanford Site tank waste.

FREDERICK M. MANN, Scientist, CH2M Hill Hanford Group

B.S.	Physics, Stanford University	1970
Ph.D.	Physics, California Institute of Technology	1975

Dr. Mann is the team leader for the ILAW Performance Assessment activity, which is charged with preparing this document. He was the main author of the 1998 version of the Hanford *Immobilized Low-Activity Tank Waste Performance Assessment*. He has worked for over 25 years in the field of nuclear data and the application of those data to large energy facilities. He has advised the DOE and the International Atomic Energy Agency. He is one of the main authors of this document.

B. PETER MCGRAIL, Staff Scientist V, Applied Geology and Geochemistry Department, Environmental Technology Division, Pacific Northwest National Laboratory.

B.S.	Nuclear Engineering, University of Missouri	1981
M.S.	Nuclear Engineering, University of Missouri	1983
Ph.D.	Environmental Engineering, Columbia Southern University (Magna Cum Laude)	1996

Dr. McGrail has been a staff member at Pacific Northwest National Laboratory for over 17 years and is the principal investigator and manager of a diverse range of projects including the DOE's Fissile Materials Disposition Program, Yucca Mountain Project, Hanford Low-Activity Tank Waste Disposal Project, a basic science (EMSP) project exploring ion-exchange processes in glasses, and a laboratory-directed research and development program exploring carbon sequestration processes in deep geologic formations. He is internationally known for his research on PAs of waste disposal systems, coupled diffusion-advection-reaction transport modeling, and corrosion of silicate glasses, with one patent and more than 150 publications and presentations on these topics. He has performed hundreds of experiments to evaluate the dissolution kinetics of waste forms and other geologic materials using batch and flow-through techniques, and has invented test equipment for conducting these measurements that operates under both water-saturated and unsaturated conditions. He recently completed development of an inverse reactive transport simulator (INVERTS), which is being used to model elution profiles of solutes and colloids from unsaturated flow experiments, including equilibrium and nonlinear kinetic adsorption processes. He also manages the Pacific Northwest National Laboratory's new X-ray Microtomography Laboratory and has been exploring application of high-resolution x-ray microtomography to develop a better understanding of multiphase flow and mass transport processes in porous media. Dr. McGrail directed the collection and analysis of the laboratory data used in the waste form release calculations discussed in this document.

RAYMOND J. PUIGH II, Manager, Nuclear and Environmental Initiatives, Fluor Federal Services.

B.S.	Physics, Louisiana State University	1970
Ph.D.	Physics, Florida State University	1976

Dr. Puigh has over 20 years of experience in nuclear fields ranging from nuclear data and testing to the impact of nuclear radiation on material properties. Relevant performance assessment experience includes metallurgy, tank waste inventory support, safety assessment support for selected tank farm operation projects, and management of environmental modeling staff responsible for the Hanford Solid Waste and ILAW performance assessments. He is one of the main authors of this document.

MARCUS I. WOOD, Principal Scientist, Waste Management, Fluor Hanford, Inc.

B.S.	Geology, University of North Carolina	1973
Ph.D.	Geology, Brown University	1980

Dr. Wood currently is responsible for developing the PA analyses for the disposal of solid low-level waste at the Hanford Site. He is the coordinating author of the Hanford Site solid waste performance assessments and has been largely responsible for the integration and the interpretation of the analytical results in those documents. He has coordinated similar analyses for the Environmental Restoration Disposal Facility (ERDF), at which wastes generated in the remediation of Hanford Site waste sites regulated under the *Comprehensive Environmental Resource Conservation and Recovery Act of 1981* and the 200 West Area low-level burial grounds are disposed. He has directed numerous projects to quantify the geochemical properties of radionuclides in the Hanford Site geohydrologic environment. He also was responsible for developing a multifunctional waste package backfill material for isolating spent fuel and high-level waste. He reviewed this document.

SIGNE K. WURSTNER, Senior Research Scientist, Hydrology Group, Pacific Northwest National Laboratory.

B.S.	Geology, Indiana University	1986
M.S.	Geology, Indiana University	1989

Ms. Wurstner joined Battelle as a full-time scientist October 1989. Her primary interests include numerical modeling of groundwater flow and transport processes and geographic information systems (GIS). Ms. Wurstner has been primarily involved in modeling groundwater flow and contaminant transport at the Hanford Site in both two and three dimensions, and was a major contributor to the development of an interface between the CFEST groundwater modeling software library and the commercial GIS package, ARC/INFO. She assisted in the regional- and local-scale groundwater flow and transport modeling used to support this assessment.

9.0 REFERENCES

(Does not Include Appendix E)

10 CFR 61, "Licensing Requirements for the Land Disposal of Radioactive Waste," *Code of Federal Regulations*, Volume 10, Part 61, Section 55, U.S. Nuclear Regulatory Commission, Washington, D.C., December 27, 1982 as amended May 25, 1989.

[1. Section 61.52(a)(2) mandates the protection for inadvertent intrusion for Class C wastes.]

[2. Section 61.55 describes waste classification. (May 1989)]

[3. Subpart C, sections 61.40 through 61.44 stated the performance objectives.]

[4. Section 61.41 mandates the protection for the general public.]

10 CFR 830.120, "Quality Assurance Requirements", Code of Federal Regulations, Volume 10 (Department of Energy), Section 830 (Nuclear Safety Management), Washington, D.C.

40 CFR 61H, Subpart H, "National Emission Standards for Emissions of Radionuclides Other than Radon from Department of Energy Facilities," *Code of Federal Regulations*, Volume 40, Part 61, Subpart H, Section 92, U.S. Environmental Protection Agency, Washington, D.C., December 15, 1989.

40 CFR 61Q, Subpart Q, "National Emission Standards for Radon Emissions from Department of Energy Facilities," *Code of Federal Regulations*, Volume 40, Part 61, Subpart Q, Section 192, U.S. Environmental Protection Agency, Washington, D.C., December 15, 1989.

40 CFR 141, "National Primary Drinking Water Regulations," *Code of Federal Regulations*, Volume 40, Part 141, Sections 15 and 16, U.S. Environmental Protection Agency, Washington, D.C., December 24, 1975.

40 CFR 193, "Radiation Site Cleanup Regulation," proposed *Code of Federal Regulations* by the U.S. Environmental Protection Agency.

40 CFR 196, "Environmental Radiation Standards for Management and Disposal of Low-Level Waste," proposed *Code of Federal Regulations* by the U.S. Environmental Protection Agency.

40 CFR 268, "Land Disposal Restrictions" (40 CFR 268), *Code of Federal Regulations*, Volume 40, Parts 268, U.S. Environmental Protection Agency, May 19, 1980 and as amended.

AEA1954, *Atomic Energy Act of 1954*, 42 USC 2011 or 2014 et seq.

Alm 1997, A. L. Alm (Assistant Secretary for Environmental Management) "Critical Assumptions for Department of Energy Low-Level Waste Disposal Facility Assessments", attachment to letter dated March 7, 1997 to John T. Conway (Chairman, Defense Nuclear Facilities Safety Board), U.S. Department of Energy, Washington, D.C.

Anderson 1990, J. D. Anderson, *A History of the 200 Area Tank Farms*, WHC-MR-0132, Westinghouse Hanford Company, Richland, Washington, June 1990.

ANSI/ASME 1989, *Quality Assurance Standard Requirements for Nuclear Facilities*, ANSI/ASME NQA-1, American National Standards Institute/American Society of Mechanical Engineers, New York City, New York, 1989.

Bacon 2000, D. H. Bacon, M. D. White, and B. P. McGrail, *Subsurface Transport Over Reactive Multiphases (STORM): A General, Coupled, Nonisothermal Multiphase Flow, Reactive, Transport, and Porous Medium Alteration Simulator, Version 2; User's Guide*, PNNL-13108, Pacific Northwest National Laboratory, Richland, Washington, February 2000. Also Appendix D of Mann/Puigh 2000a.

Bacon 2001, Bacon, D. H., and B. P. McGrail, *Waste Form Release Calculations for the 2001 Immobilized Low-Activity Waste Performance Assessment*, PNNL-13369, Pacific Northwest National Laboratory, Richland, Washington, February 2001. This document forms part of Puigh 2001.

Baker 1992¸V. R. Baker, B. N. Bjornstad, A. J. Busacca, K. R. Fecht, E. G. Kiver, U. L. Moody, J. G. Rigby, D. F. Stradling, and A. M. Tallman, "Quaternary geology of the Columbia Plateau," in RB Morrison (ed.), *Quaternary geology of the conterminous United States*. Geological Society of America, Boulder, Colorado, v. K-2, p. 215-238.

Berger 1991, A. Berger, H. Gallee, and J. L. Melice, "The Earth's Future Climate at the Astronomical Timescale," in *Future Climate Change and Radioactive Waste Disposal: Proceedings of International Workshop*, G. M. Goodess and J. P. Palutikof, eds, NSS/R257, U.K. Nirex Radioactive Waste Disposal, Ltd., Harwell, OX11 ORH, United Kingdom, pp. 148-165.

Bergeron 2000, M. P. Bergeron and S. K. Wurstner, *Groundwater Transport Calculations Supporting the Immobilized Low-Activity Waste Disposal Facility Performance Assessment*, PNNL-13400. Pacific Northwest National Laboratory, Richland, Washington, December 2000. This document forms part of Puigh 2001.

Bjornstad 1987, B. N. Bjornstad, K. R. Fecht, and A. M. Tallman, *Quaternary Stratigraphy of the Pasco Basin Area South-Central Washington*, RHO-BW-SA-563A, Rockwell Hanford Operations, Richland, Washington.

BNFL, 1999, *TWRS-P Project Dangerous Waste Permit Application*, BNFL-5193-RCRA-01, Rev. 0A, Richland, Washington.

Boston 2000a, H. L. Boston, (acting manager), memorandum to Carolyn L. Huntoon (Assistant Secretary), "U.S. Department of Energy (DOE), Office of River Protection (ORP) Approval and Implementation of the Hanford Site Remote-Handled Immobilized Low-Activity Waste (ILAW) Disposal Facility Preoperational Monitoring Plan," 00-PRD-071, U.S. Department of Energy, Office of River Protection, Richland, Washington, November 1, 2000.

Boston 2000b, H. L. Boston (acting manager), memorandum to Carolyn L. Huntoon (Assistant Secretary), "U.S. Department of Energy (DOE), Office of River Protection (ORP) Approval of the Hanford Site Transmittal of the Immobilized Low-Activity Waste (ILAW) Disposal Facility Preliminary Closure Plan," 00-PRD-63, U.S. Department of Energy, Office of River Protection, Richland, Washington, September 22, 2000.

Brodzinski 1998; R. L. Brodzinski, e-mail to F. M. Mann, October 19, 1998.

Burbank 1996, D. A. Burbank, Jr., *Alternatives Generation and Analysis for Immobilized Low-Level Waste Interim Storage Architecture*, WHC-SD-W465-AGA-001, Rev. 0, Westinghouse Hanford Company, September 1996.

Burbank 1997, D. A. Burbank and M. J. Klem, *Analysis of Alternatives for Immobilized Low-Activity Waste Disposal*, HNF-SD-TWR-AGA-004, Rev. 0, SGN Eurisys Services Corporation, Richland, Washington, October 1997. also published as HNF-4003, Lockheed Martin Hanford Company, Richland, Washington, March 1997.

Burbank 2000, D. A. Burbank, R. K. Biyani, and L. F. Janin, *Preliminary Closure Plan for the Immobilized Low Activity Waste Disposal Facility*, RPP-6911, Rev. 0, CH2M Hill Hanford Group, Inc., Richland, Washington, August 2000. This plan was approved by Boston 2000b.

Case 1988, M. J. Case and M. D. Otis, *Guidelines for Radiological Performance Assessments of DOE Low-Level Radioactive Waste Sites*, DOE-LLW-62T (Section 4.5.2.5), U.S. Department of Energy, Idaho Operations Office, Idaho Falls, Idaho, July 1988.

CERCLA, *Comprehensive Environmental Response, Compensation, and Liability Act of 1980*, 42 U.S. C. 9601, et seq.

Chatters 1991, J. C. Chatters, "Long-Term Climate Change Effects," *Hanford Site Protective Barrier Development Program: Fiscal Year 1990 Highlights*, L. L. Cadwell, ed., PNL-7831, Pacific Northwest Laboratory, Richland, Washington, pp. 2.23-3.1, September 1991.

Chatters 1992, J. C. Chatters and K. A. Hoover, "Response of the Columbia River Fluvial System to Holocene Climatic Change," *Quaternary Research*, Vol. 37, pp. 42-59.

CHG 2000 *Quality Assurance Program Description for the Tank Farms Contractor*, RPP-MP-600, revision 0, CH2M Hill Hanford Group Inc., Richland, Washington, 2000.

Chunsheng 1997, Li Chunsheng, Guo Jingru, and Li Daming, "A Procedure for the Separation of ^{79}Se from the Fission Products and Application to the Determination of the ^{79}Se Half-life", *Journal of Radioanalytical and Nuclear Chemistry*, 220 (1997) 69.

Clinton 2000, W. J. Clinton, "Establishment of the Hanford Reach National Monument", *Federal Register*, Volume 65, Number 114, pages 37253-37257, June 13, 2000.

Cloke 1997, P. L. Cloke, D. M. Jolley, and D. H. Lester, *Waste Package Development Design Analysis*, BBA000000-01717-0200-0050 Rev. 00, CRWMS/M&O, Las Vegas, Nevada, 1997.

Codell 1982, R.B. Codell, K.T. Key, and G. Whelan, *A Collection of Mathematical Models for Dispersion in Surface Water and Groundwater*, NUREG-0868, Nuclear Reactor Regulation, Nuclear Regulatory Commission, Washington, D.C., June 1982.

Cole 1997, C. R. Cole, S. K. Wurstner, M. P. Bergeron, M. D. Williams, P. D. Thorne. *Three-dimensional Analysis of Future Groundwater Flow Conditions and Contaminant Plume Transport in the Hanford Site Unconfined Aquifer System: FY 1997 Status Report*. PNNL-11801, Pacific Northwest Laboratory, Richland, Washington, December 1997.

Colton 1997, N. G. Colton, *Status Report: Pretreatment Chemistry Evaluation FY1997—Wash and Leach Factors for the Single-Shell Tank Waste Inventory*, PNNL-11646, Pacific Northwest National Laboratory, Richland, Washington.

Cowan 1996, S. P. Cowan, "Conditional Acceptance of the Hanford 200 West Area Burial Ground Performance Assessment," memorandum to Charles Hansen, U.S. Department of Energy, Washington, D.C., June 27, 1996.

Cropper 1986, J. P. Cropper and H. C. Fritts, 1986, *A 360 Year Temperature and Precipitation Record for the Pasco Basin Derived from Tree Rings*, DOE/RL-01830-T46, U.S. Department of Energy, Richland, Washington.

Cunnane 1994, J. C. Cunnane, J. K. Bates, W. L. Ebert, X. Feng, J. J. Mazer, D. J. Wronkiewicz, J. Sproul, W. L. Bourcier, B. P. McGrail, and M. K. Altenhofen, *High-Level Waste Nuclear Waste Glass: A Compendium of Characteristics*, DOE EM-0177, U.S. Department of Energy, Washington, D.C., 1994.

Delaney 1991, C. N. Delaney, K. A. Lindsey, and S. P. Reidel, *Geology and Hydrology of the Hanford Site: A Standardized Text for Use in WHC Documents and Reports*, WHC-SD-ER-TI-003, Revision 0, Westinghouse Hanford Company, Richland, Washington, 1991.

Dirkes 1999, R. L. Dirkes, R. W. Hanf, and T. M. Poston, *Hanford Site Environmental Report for Calendar Year 1998*, PNNL-12088, Pacific Northwest National Laboratory, Richland, Washington, September 1999.

1. Section 4.2.1 describes Columbia River flows.
2. Section 4.6 discusses surveillance of soil and vegetation.
3. Section 5 discusses potential radiological doses from Hanford Site operations.

DNFSB 1994, Defense Nuclear Facility Safety Board Recommendation 94-2, "Conformance with Safety Standards at DOE Low-Level Nuclear Waste and Disposal Sites," 59 *Federal Register* 47309 (1994).

DOC 1991, *1990 U.S. Census of Population and Housing, State and County Profiles, Washington* (Summary Tape 1A for Washington State), Office of Financial Management, U.S. Department of Commerce, Washington, D.C., 1991.

Dodge 1991, R. L. Dodge, W. R. Hansen, W. E. Kennedy, Jr., D. W. Layton, D. W. Lee, S. T. Maheras, S. M. Neuder, E. L. Wilhite, R. U. Curl, K. F. Grant, B. A. Heath, and K. H. Turner, *Performance Assessment Review Guide for Low-Level Radioactive Waste Disposal Facilities*, DOE/LLW-93, Radioactive Waste Technical Support Program, Idaho National Engineering Laboratory, Idaho Falls, Idaho, October 1991.

DOE 1987, *Final Environmental Impact Statement: Disposal of Hanford Defense High-Level Transuranic and Tank Wastes*, DOE/EIS-0113, U.S. Department of Energy, Washington, D.C., December 1987.

1. Section 4.2 and Appendix O describe the Hanford Site geology.]

DOE 1988a, *Radioactive Waste Management*, DOE Order 5820.2A, U.S. Department of Energy, Washington, D.C., September 26, 1988.

[1. Chapter III, Section 3 describes the requirement and content of a performance assessment.]

DOE 1988b, *Consultation Draft Site Characterization Plan*. DOE/RW-0164, Vols. 1-9, Office of Civilian Radioactive Waste Management, U.S. Department of Energy, Washington, D.C., 1988.

DOE 1991, "Quality Assurance", DOE Order 5700.6c, U.S. Department of Energy, Washington, D.C., August 21, 1991.

DOE 1993, *Radiation Protection of the Public and the Environment*, DOE Order 5400.5, U.S. Department of Energy, Washington, D.C., January 7, 1993.

[1. Chapter 1, Section 3 provides the DOE primary standard of 100 mrem effective dose equivalent to members of the public in a year.]

DOE 1997, *Waste Management Programmatic Environmental Impact Statement For Managing Treatment, Storage, and Disposal of Radioactive and Hazardous Waste*, DOE/EIS-0200-F, U.S. Department of Energy, Washington, D.C., May 1997.

[Pages 50 to 59 of the summary provide information of the low-level waste in the DOE complex, while pages 70 through 77 discusses high-level waste. Note that this EIS does not separate the Hanford Site tank waste into low- and high-level components.]

DOE 1996a, *Implementation Plan, Defense Nuclear Facilities Safety Board Recommendation 94-2, Compliance with Safety Standards at Department of Energy Low-Level Nuclear Waste and Disposal Sites*, Draft Revision 1, U.S. Department of Energy, Washington, D.C., March 11, 1996.

[The beginning of Section VII, "Radiological Assessment," discusses the use of DOE Order 5400.5 as the basis of the composite approach.]

DOE 1996b, *Environmental Impact Statement for the Tank Waste Remediation System*, DOE/EIS-0189, U.S. Department of Energy and the Washington State Department of Ecology, Washington, D.C., August 1996.

DOE 1996c, *Draft Hanford Remediation Action Environmental Impact Statement and Comprehensive Land Use Plan*, DOE/EIS-0222-D, U.S. Department of Energy, Washington, D.C., August 1996.

DOE 1997b, "Record of Decision for the Tank Waste Remediation System, Hanford Site, Richland, Washington," *Federal Register*, Volume 62, page 8693, February 26, 1997.

DOE 1999a, "Disposal Authorization Statement for the Hanford Site Low-Level Waste Disposal Facilities," memorandum from J. J. Fiore and M. W. Frei, U.S. Department of Energy, Headquarters, to R. T. French, U.S. Department of Energy, Office of River Protection, and K. A. Kline, U.S. Department of Energy, Richland Operations Office, Washington, D.C., October 25, 1999.

DOE 1999b, "Radioactive Waste Management", DOE O 435.1, U.S. Department of Energy, Washington, D.C., July 9, 1999.

DOE 1999c, *Low-Level Waste Disposal Facility Federal Review Group Manual*, Rev. 1, U.S. Department of Energy, Washington, D.C., November 1999.

DOE 1999d, Conditional Acceptance of the Immobilized Low-Activity Tank Waste Disposal Facility Performance Assessment and the Hanford Site 200 Plateau Composite Analysis, Memorandum from James J. Fiore and Mark W. Frei to Richard French and Keith A. Klein, U.S. Department of Energy, Washington, D.C., October 20, 1999.

DOE 1999e, *Format and Content Guide for U.S. Department of Energy Low-Level Waste Disposal Facility Performance Assessments and Composite Analyses*, U.S. Department of Energy, Washington, D.C., December 7, 1999.

DOE 1999f, *Maintenance Guide for U.S. Department of Energy Low-Level Waste Disposal Facility Performance Assessments and Composite Analyses*, U.S. Department of Energy, Washington, D.C., November 10, 1999.

DOE 1999g, *Manual for DOE O 435.1*, DOE M 435.1, U.S. Department of Energy, Washington, D.C., July 9, 1999.

1. Performance assessment requirements are presented in Chapter IV (Low-Level Waste), section P (disposal).

DOE 1999h, *Final Hanford Comprehensive Land-Use Plan Environmental Impact Statement*, DOE/EIS-0222-F, U.S. Department of Energy, Richland, Washington, September 1999. The Record of Decision was published in the *Federal Register* on November 12, 1999 (Vol. 64, pages 61615-61625) (see DOE 1999i).

DOE 1999i, "Record of Decision: Hanford Comprehensive Land-Use Plan Environmental Impact Statement," *Federal Register 64*, page 61615, November 12, 1999.

DOE 2000, "Immobilized Low-Activity Tank Waste Disposal Facility Performance Assessment Condition in the Disposal Authorization Statement," memorandum from Jay E. Roderick and William E. Murphie, co-chairs of the Low-Level Waste Disposal Facility Federal Review Group, U.S. Department of Energy, Washington, D.C., June 2, 2000.

DOE/BNFL 1998, *TWRS Privatization Contract No. DE-AC06-96RL13308, Contract with British Nuclear Fuels, Ltd.*, U.S. Department of Energy, Richland Operations Office, September 1998, Richland, Washington.

- Modification 10 (January 24, 2000) - see web reference http://www.hanford.gov/doe/contracts/de-ac06-96rl13308/index.html

DOE/ORP 2000a, *Maintenance Plan for the Hanford Immobilized Low-Activity Tank Waste Performance Assessment*, DOE/ORP-2000-01, Rev. 0, U.S. Department of Energy, Office of River Protection, Richland, Washington, February 2000. This plan was formally by the ORP Field Manager in a memorandum via French 2000b.

DOE/ORP 2000b, *Annual Summary of Immobilized Low-Activity Tank Waste (ILAWP Performance Assessment*, DOE/ORP-2000-19, U.S. Department of Energy, Office of River Protection, Richland, Washington, May 2000.

DOE/ORP 2000c, Contract with Bechtel, National, Inc., *Design, Construction, and Commissioning of the Hanford Tank Waste Treatment and Immobilization Plant*, Contract number DE-AC27-01RV141376, U.S. Department of Energy, Office of River Protection, Richland, Washington, December 2000. Web reference: http://www.hanford.gov/orp/contracts/de-ac27-01rv14136/index.html

DOE/RL 1991a, *Description of Codes and Models to Be Used in Risk Assessment*, DOE/RL-91-44, U.S. Department of Energy, Richland, Richland Operations Office, Washington, 1991.

DOE/RL 1992, *Annual Report for RCRA Groundwater Monitoring Projects at Hanford Site Facilities for 1991 - Progress Report*, DOE/RL-92-03, U.S. Department of Energy, Richland Operations Office, Richland, Washington.

DOE/RL 1993b, *Phase 1 Remedial Investigation Report for 200-BP-1 Operable Unit*, DOE/RL-92-70, U.S. Department of Energy, Richland Operations Office, Richland, Washington.

[1. p. 3-10]

DOE/RL 1993c, *200 East Groundwater Aggregate Area Management Study Report*, DOE/RL-92-19, U.S. Department of Energy, Richland Operations Office, Richland, Washington.

DOE/RL 1994a, *Remedial Investigation and Feasibility Study Report for the Environmental Restoration Facility*, DOE/RL-93-99, U.S. Department of Energy, Richland Operations Office, Richland, Washington, October 1994.

DOE/RL 1994b, *Hanford Site Background: Part 1, Soil Background for Nonradioactive Analytes*, DOE/RL-92-94, Revision 2, 2 volumes, U.S. Department of Energy, Richland Operations Office, Richland, Washington, March 1994.

DOE/RL 1995a, *Tank Waste Remediation System Integrated Technology Plan*, DOE/RL-92-61, Revision 2, U.S. Department of Energy, Richland Operations Office, Richland, Washington, February 1995.

[1. p. 1-6 contains figure for TWRS strategy.]

DOE/RL 1995b, *Hanford Site Background: Evaluation of Existing Soil Radionuclide Data*, DOE-RL-95-55, Rev. 0, U.S. Department of Energy, Richland Operations Office, Richland, Washington, July 1995.

DOE/RL 1995c, *Hanford Site Ground Water Protection Management Plan*, DOE-RL-89-12, Rev. 2, U.S. Department of Energy, Richland Operations Office, Richland, Washington, July 1995.

DOE/RL 1996, *Request for Proposals (RFP) No. DE-RP06-96RL13308*, letter from J.D. Wagoner to Prospective Offerors, Department of Energy, Richland Operations Office, Richland, Washington, February 20, 1996.

DOE/RL 1997, *Screening Assessment and Requirements for a Comprehensive Assessment: Columbia River Comprehensive Impact Assessment*, DOE/RL-96-16, Revision 0, U.S. Department of Energy, Richland Operations Office, Richland, Washington, 1997.

DOE/RL 2000, *Selection and Review of a Site-Wide Groundwater Model at the Hanford Site*, DOE/RL-2000-11, U.S. Department of Energy, Richland Operations Office, Richland, Washington, May 2000.

Ecology 1998, Washington State Department of Ecology, U. S. Environmental Protection Agency, U. S. Department of Energy, *Hanford Facility Agreement and Consent Order*, as amended through December 31, 1998, 89-10, Rev. 6. This document is available from any of the parties.

[1. Appendix D lists the activities and associated milestones. Activities 45 (closure of single-shell tanks), 50 (pretreatment processing), 60 (vitrification of Hanford low-level waste), and 90 (disposal of the immobilized low-activity waste) cover areas of concern for this performance assessment.]

EPA 1989b, *Risk Assessment Methodology: Environmental Impact Statement for NESHAPS Radionuclides. Volume I: Background Information Document*, EPA/520/1-89/005, U.S. Environmental Protection Agency, Washington, D.C., January 1989.

EPA 1993, External Exposure to Radionuclides in Air, Water, and Soil, EPA-402-R-93-081, U.S. Environmental Protection Agency, Washington, D.C., 1993.

ERDA 1975, *Final Environmental Statement Waste Management Operations, Hanford Reservation, Richland, Washington*, ERDA 1538, Vol. 1-2, U.S. Energy Research and Development Administration, Washington, D.C., December 1975.

Evans 2000, R. G. Evans, M. J. Hattendorf, and C. T. Kincaid, *Evaluation of the Potential for Agricultural Development at the Hanford Site*, PNNL-13125, Pacific Northwest National Laboratory, Richland, Washington, January 2000. Also Appendix P of Mann/Puigh 2000a.

Fayer 1995, M. J. Fayer and T. B. Walters, *Estimated Recharge Rate at the Hanford Site*, PNL-10285, Pacific Northwest Laboratory, Richland, Washington, March 1995.

Fayer 1999, M. J. Fayer, *Recharge Data Package for the Immobilized Low-Activity Waste 2001 Performance Assessment*, PNNL-13033, Pacific Northwest National Laboratory, Richland, Washington, December 1999. Also Appendix J of Mann/Puigh 2000a.

Fecht 1998, K. R. Fecht, K. A. Lindsey, B. N. Bjornstad, D. G. Horton, G. V. Last, and S. P. Reidel, *An Atlas of Clastic Injection Dikes of the Pasco Basin and Vicinity*. Bechtel Hanford Incorporated Report BHI-01103.

Finfrock 2000a, S. H. Finfrock, *Verification and Validation for VAM3DF, Version 1.00 (FFS Version 1.00)*, HNF-5636, Fluor Federal Services, Richland, Washington, January 2000. Also Appendix F of Mann/Puigh 2000a.

Finfrock 2000b, S. H. Finfrock, E. J. Freeman, R. Khaleel, and R. J. Puigh, *Near-Field, Far-Field, and Estimated Impact Calculations for the Hanford Immobilized Low-Activity Tank Waste Performance Assessment: 2001 Version*, RPP-7463, Fluor Federal Services, Richland, Washington, December 2000. This document forms part of Puigh 2001.

Freeze 1979, R. A. Freeze and J. A. Cherry, *Groundwater*, Prentice-Hall, Inc., Englewood Cliffs, New Jersey, 1979. [Section 2 discusses the principles of water flow.]

Farnsworth, R. K., M. K. W. Chan, and S. C. Slate. 1985. "The Effect of Radial Temperature Gradients on Glass Fracture in Simulated High-Level Waste Canisters." *Mat. Res. Soc. Symp. Proc.* **44**:831-838.

Frei 1996, M. W. Frei, "Issuance of Low-Level Waste Performance Assessment Guidance", letter from Mark W. Frei (Acting Associate Deputy Assistant Secretary for Waste Management, U.S. Department of Energy) dated November 1, 1996.

Frei 1997, M. W. Frei, "Conditional Acceptance of the Hanford 200 East Area Burial Ground Performance Assessment", letter from Mark W. Frei (Acting Deputy Assistant Secretary for Waste Management, U.S. Department of Energy) to Charles Hansen (Assistant Manager for Waste Management, U.S. Department of Energy, Richland Operations Office) dated June 30, 1997.

French 1999, R. T. French, "Disposal Authorization for the Hanford Site Low-Level Waste Disposal Facilities," memorandum to M. W. Frei (Deputy Assistant Secretary, Office of Project Completion), U.S. Department of Energy, Office of River Protection, December 29, 1999.

French 2000a, R. T. French, "Initial Data Package from the Tank Focus Area on 55 Test Glasses for Hanford Immobilized Low-Activity Waste (ILAW) Studies," memorandum to Mark W. Frei, 00-DPD-018, U.S. Department of Energy, Office of River Protection, Richland, Washington, March 10, 2000.

French 2000b, R. T. French, "U.S. Department of Energy (DOE), Office of River Protection (ORP) Approval of the Hanford Site Low-Level Waste (LLW) Disposal Facilities Maintenance Plan," memorandum to Mark W. Frei, U.S. Department of Energy, Office of Projection Completion, dated March 7, 2000, 00-DPD-015.

French 2000c, R. T. French, "Submittal of "Annual Summary of ILAW Performance Assessment," DOE/ORP-2000-19, Revision 0, memorandum to Carolyn L. Huntoon, Assistant Secretary for Environmental Management, U.S. Department of Energy, dated July 11, 2000.

Gee 1992, G. W. Gee, M. J. Fayer, M. L. Rockhold, and M. D. Campbell, "Variations in Recharge at the Hanford Site," *Northwest Science* 66(4):237-250.

Geomatrix Consultants, Inc. 1996, *Probablistic Seismic Hazard Analysis for DOE Hanford Site, Washington*, WHC-SD-W236A-TI-002, Revision 1, Westinghouse Hanford Company, Richland, Washington, 1996.

Gorelick 1999, S. Gorelick, C. Andrews, and J. Mercer, *Report of the Peer Review Panel on the Proposed Hanford Site-Wide Groundwater Model*, January 14, 1999. Available on the world-wide-web at http://www.bhi-erc.com/vadose/Peer/GW/GWmdlpr.pdf. Also Appendix E of DOE/RL 2000.

Graham 1981, M. J. Graham, M. D. Hall, S. R. Strait, and W. R. Brown, *Hydrology of the Separations Area*, RHO-ST-42, Rockwell Hanford Operations, Richland, Washington, July 1981.

Gramulich 1987, L. H. Gramulich, "Precipitation Variation in the Pacific Northwest (1675-1975) as Reconstructed from Tree Rings," *Annals of the Association of American Geographers*, 77:19-29.

Gupta 1987, S. K.Gupta, C. R. Cole, C. T. Kincaid, and A. M. Monti, *Coupled Fluid, Energy, and Solute Transport (CFEST) Model: Formulation and User's Manual*. BMI/ONWI-660, Battelle Memorial Institute, Columbus, Ohio, October 1987.

Hajek 1966, B.F. Hajek, *Soil Survey: Hanford Project in Benton County, Washington*, BNWL-243, Pacific Northwest Laboratory, Richland, Washington.

Hanlon 2000, B. M. Hanlon, *Waste Tank Summary Report for Month Ending June 30, 2000*, HNF-EP-0182-147, Lockheed Martin Hanford Company, Richland, Washington, August 2000 This report is issued monthly..

[1. Table A-1 summarizes the amount of waste in the tanks.]

[2. Appendix A provides the status of the tanks.]

Hartman 2000, M. J. Hartman, L. F. Morasch, and W. D. Webber (editors), *Hanford Site Groundwater Monitoring for Fiscal Year 1999*, PNNL-13116, Pacific Northwest National Laboratory, Richland, Washington, March 2000.

Hendrickson 1999, D. W. Hendrickson, D. E. Place, G. T. MacLean, S. L. Lambert, *Best-Basis Wash and Leach Factor Analysis*, HNF-3157, Rev. 0A, COGEMA Engineering, Richland, Washington, January 1999.

HFSUWG 1992a, *The Future for Hanford: Uses and Cleanup, Summary of the Final Report of the Hanford Future Site Uses Working Group*, 0026618, December 1992. This report is available through the Environmental Data Management Center, Lockheed Martin Services, Inc., Richland, Washington.

[1. Page 9 discusses use the central plateau wisely for waste management.]

[2. Page 23 discusses the future use options of the 200 Areas.]

[3. Page 25 discusses the cleanup scenario.]

HFSUWG 1992b, *The Future for Hanford: Uses and Cleanup, the Final Report of the Hanford Future Site Uses Working Group*, Document number 0026619, December 1992. This report is available through the Environmental Data Management Center, Lockheed Martin Services, Incorporated, Richland, Washington.

Hoitink 2000, D. J. Hoitink, K. W. Burk and J. V. Ramsdell, 2000, *Hanford Site Climatological Data Summary 1999 With Historical Data*, PNNL-13117, Pacific Northwest National Laboratory, Richland, Washington.

Horton 2000, D. G. Horton, S. P Reidel, Yi-Ju Chien, and R. M. Mitchell, *Remote-Handled Low-Activity Waste Disposal Facility Preoperational Monitoring Plan*, RPP-6877, Revision 0, prepared by Pacific Northwest National Laboratory for CH2M HILL Hanford Group, Inc., Richland, Washington, September 2000.

Huyakon 1999, P. S. Huyakon and S. Panday, *VAM3DF - Variably Saturated Analysis Model in Three Dimensions for the Data Fusion System: Documentation and User's Guide, Version 2.0*, HydroGeoLogic, Inc., Herndon, Virginia, 1999.

Johnson 1993, V. G. Johnson, *Groundwater Status Report*, WHC-EP-0595, Westinghouse Hanford Company, Richland, Washington, March 1993.

Kaplan 1999, D. L. Kaplan And R. J. Serne, *Geochemical Data Package For The Immobilized Low-Activity Waste Performance Assessment*, PNNL - 13037, Pacific Northwest National Laboratory, Richland, Washington, December 1999. Also Appendix N of Mann/Puigh 2000a.

Khaleel 1999, R. Khaleel, *Far-Field Hydrology Data Package For The Immobilized Low-Activity Waste Performance Assessment*, HNF-4769, Rev. 2, prepared by Fluor Federal Services for Fluor Daniel Hanford Company, Richland, Washington, December 1999. Also Appendix M of Mann/Puigh 2000a.

Kincaid 1995, C. T. Kincaid, J. W. Shade, G. A. Whyatt, M. G. Piepho, K. Rhoads, J. A. Voogd, J. H. Westsik, Jr., K. A. Blanchard, and B. G. Lauzon, *Performance Assessment of Grouted Double-Shell Tank Waste Disposal at Hanford*, WHC-SD-WM-EE-004, Revision 1, Westinghouse Hanford Company, Richland, Washington, May 1995.

[1. Section 1.5.1, page 1.15 explains the reason for the selection of 10,000 years as the general time of compliance and of 500 years as the time of inadvertent intruder compliance.]

[2. Sections 3.4.12 on page 3.69 and 3.4.13 starting on page 3.70 describe the vadose zone hydrologic parameters.]

[3. Section 3.3.6.6 on page 3.62 describes the effective diffusion constant for the vadose zone.]

[4. Section 2.6 describes the Grout Disposal Facility.]

[5. The population along the Columbia River is found as footnote f to Table 4-2 on page 4.12.]

[6. Appendix G.1 describes code selection.]

[7. Appendix H describes the benchmarking of PORFLOW 2.394gr against TRACR3D.]

[8. The footnote to Table 3-20 uses a screen depth of 4.6 m.]

Kincaid 1998, C. T. Kincaid, M. P. Bergeron, C. R. Cole, M. D. Freshley, N. L. Hassig, V. G. Johnson, D. I. Kaplan, R. J. Serne, G. P. Streile, D. L. Strenge, P. D. Thorne, L. W. Vail, G. A. Whyatt, S. K. Wurstner, *Composite Analysis for Low-Level Waste Disposal in the 200-Area Plateau of the Hanford Site*. PNNL-11800, Pacific Northwest National Laboratory, Richland, Washington, March 1998.

Kirkbride 1999, R. A. Kirkbride, *Tank Waste Remediation System Operational Utilization Plan*, HNF-SD-WM-SP-012, Rev. 1, Volume I and II, Numatec Hanford Company, Richland, Washington, May 1999.

Kozak 1989, M. W. Kozak, M. S. Y. Chu, C. P. Harlan, and P. A. Mattingly, *Background Information for the Development of a Low-Level Waste Performance Assessment Methodology*, NUREG/CR-5453 [SAND89-2509], Volume 4 (Section 2.0), U.S. Nuclear Regulatory Commission, Washington, D.C., 1989.

Kupfer 1999, M. J. Kupfer., A. L. Boldt, B. A. Higley, K. M. Hodgson, L. W. Shelton, B. C. Simpson, R. A. Watrous, M. D. LeClair, G. L. Borsheim, R. T. Winward, R. M. Orme, N. G. Colton, S. L. Lambert, D. E. Place, and W. W. Schulz, 1999, *Standard Inventories of Chemicals and Radionuclides in Hanford Site Tank Wastes*, HNF-SD-WM-TI-740, Rev. 0C, Lockheed Martin Hanford Corporation, Richland, Washington, February 1999.

Law 1996, A. Law, S. Panday, C. Denslow, K. Fetch, A. Knepp, *Hanford Sitewide Groundwater Flow and Transport Model Calibration Report*, BHI-00608, Rev. 0, Bechtel Hanford Inc., Richland, Washington, April 1996. Further work on calibration has been done and has been documented as Rev. 1, issued in September 1997.

Lindberg 1993, J. W. Lindberg, J. V. Borghese, B. N. Bjornstad, and M. P. Connelly, *Geology and Aquifer Characteristics of the Grout Treatment Facility.* WHC-SD-EN-TI-071, Westinghouse Hanford Company, Richland, Washington.

Lindberg 1997, J. W. Lindberg, B. A. Williams, and F. A. Spane, *Borehole Data Package For Well 299-E37-47A, PUREX Cribs*, PNNL-11515, Pacific Northwest National Laboratory, Richland, Washington.

Lindsey 1992, K. A. Lindsey, B. N. Bjornstad, J. W. Lindberg, and K. M. Hoffmann, *Geologic Setting of the 200 East Area: An Update*, WHC-SD-EN-TI-012, Rev. 0, Westinghouse Hanford Company, Richland, Washington, 1992.

Lindsey 1994a, K. A. Lindsey, S. P. Reidel, K. R. Fecht, J. L. Slate, A. G. Law, and A. M. Tallman, "Geohydrologic setting of the Hanford Site, South-Central Washington" in *Geologic Field Trips in the Pacific Northwest*, D. A. Swanson and R. A. Haugerud, eds., 1994 Annual Meeting, Geological Society of America, v. 1, p. 1C-1-16.

Lindsey 1994b, K. A. Lindsey, S. P. Reidel, G. K. Jaeger, K. J. Swett, and R. B. Mercer, *Geologic Setting of the Low-Level Burial Grounds*, WHC-SD-EN-TI-290, Rev. 0, Washington Hanford Company, Richland, Washington, October 1994.

Lindsey 1995, K. A. Lindsey, *Miocene- to Pliocene-Aged Suprabasalt Sediments of the Hanford Site, South-Central Washington*. BHI-00184, Rev. 0, Bechtel Hanford, Inc., Richland, Washington, 1995.

Lindsey 1996, K. A. Lindsey, *The Miocene to Pliocene Ringold Formation and Associated Deposits of the Ancestral Columbia River System, South-Central Washington, and North-Central Oregon*, Open-file Report 96-8, Washington Division of Geology and Earth Resources, Olympia, Washington.

Lu 1996, A.H. Lu, *Contaminant Transport in the Unconfined Aquifer, Input to the Low Level Tank Waste Interim PA*, WHC-SD-WM-RPT-241, Westinghouse Hanford Company, Richland, Washington, June 1996.

Lytle 1995, Headquarters Review of the *"Performance Assessment of Grouted Double-Shell Tank Waste at Hanford,"* memorandum from J. L. Lytle to J. Kinzer, U.S. Department of Energy, Washington, D.C., June 1, 1995.

Mann 1995a, F. M. Mann, *Data Packages for the Hanford Low-Level Tank Waste Interim Performance Assessment*, WHC-SD-WM-RPT-166, Revision 0, Westinghouse Hanford Company, Richland, Washington, July 1995.

Mann 1995b, F. M. Mann, C. R. Eiholzer, R. Khaleel, N. W. Kline, A. H. Lu, B. P. McGrail, P. D. Rittmann, and F. Schmittroth, *Definition of the Base Analysis Case of the Interim Performance Assessment*, WHC-SD-WM-RPT-200, Revision 0, Westinghouse Hanford Company, Richland, Washington, December 1995.

Mann 1995d, F. M. Mann, C. R. Eiholzer, N. W. Kline, B. P. McGrail, and M. G. Piepho, *Impacts of Disposal System Design Options on Low-Level Glass Waste Disposal System Performance*, WHC-EP-0810, Revision 1, Westinghouse Hanford Company, Richland, Washington, September 1995.

Mann 1996a, F. M. Mann, C. R. Eiholzer, A. H. Lu, P. D. Rittmann, N. W. Kline, Y. Chen, B. P. McGrail, G. F. Williamson, and N. R. Brown, *Hanford Low-Level Tank Waste Interim Performance Assessment*, WHC-EP-0884, Rev. 0,Westinghouse Hanford Company, Richland, Washington, September 1996.

Mann 1996b, F. M. Mann, I*NTEG: A Program to Calculate Groundwater Contamination and Human Doses*, WHC-SD-WM-RPT-219, Westinghouse Hanford Company, Richland, Washington, June 1996.

Mann 1997a, F. M. Mann, C. R. Eiholzer, A. H. Lu, P. D. Rittmann, N. W. Kline, Y. Chen, B. P. McGrail, G. F. Williamson, J. A. Voogd, N. R. Brown, and P. E. LaMont, *Hanford Low-Level Tank Waste Interim Performance Assessment*, HNF-EP-0884, Rev. 1, Fluor Daniel Hanford Company, Richland, Washington, September 1997.

Mann 1998a, F. M. Mann, R. J. Puigh II, P. D. Rittmann, N. W. Kline, J. A. Voogd, Y. Chen, C. R. Eiholzer, C. T. Kincaid, B. P. McGrail, A.H. Lu, G.F. Williamson, N. R. Brown, and P. E. LaMont, *Hanford Immobilized Low-Activity Tank Waste Performance Assessment*, DOE/RL-97-69, Rev. 0, U.S. Department of Energy, Richland Operations Office, Richland, Washington, March 1998.

Mann 1998b, F. M. Mann, and D. A. Myers, *Computer Code Selection Criteria for Flow and Transport Code(s) To be Used in Undisturbed Vadose Zone Calculations for TWRS Environmental Analyses*, HNF-1839, Lockheed Martin Hanford Corporation, Richland, Washington, January 1998.

Mann 1999a, F. M. Mann, *Performance Objectives for the Hanford Immobilized Low-Activity Waste (ILAW) Performance Assessment*, HNF-EP-0826, Revision 3, prepared by Fluor Daniel Northwest, Inc. for Fluor Daniel Hanford Company, Richland, Washington August 1999. Also Appendix A of Mann/Puigh 2000a.

Mann 1999b, F. M. Mann, *Scenarios for the Hanford Immobilized Low-Activity Waste (ILAW) Performance Assessment*, HNF-EP-0828, Rev. 3, Lockheed Martin Hanford Company, Richland, Washington, August 1999. Also Appendix B of Mann/Puigh 2000a.

Mann 1999c, F. M. Mann, C. T. Kincaid, W. J. McMahon, *Computer Code Selection Criteria for Flow and Transport Code(s) To Be Used in Vadose Zone Calculations for Environmental Analyses in the Hanford Site's Central Plateau*, HNF-5294, CH2M Hill Hanford Group, Inc. Richland, Washington, November 1999.

Mann/Puigh 2000a, F. M. Mann and R. J. Puigh II, *Data Packages for the Hanford Immobilized Low-Activity Tank Waste Performance Assessment: 2001 Version*, HNF-5636, prepared by Fluor Federal Services for Fluor Daniel Hanford Company, Richland, Washington, February 2000.

Mann/Puigh 2000b, F. M. Mann, S. H. Finfrock, E. J. Freeman, R. J. Puigh II, D. H. Bacon, M. P. Bergeron, B. P. McGrail, and S. K. Wurstner, *White Paper Updating the Conclusions of 1998 ILAW Performance Assessment*, DOE/ORP-2000-07, U.S. Department of Energy, Office of River Protection, Richland, Washington, April 2000.

Mann/Puigh 2000c, Annual Summary Of ILAW Performance Assessment, DOE/ORP-2000-19, U.S. Department of Energy, Office of River Protection, Richland, Washington, May 2000.

Mann/Puigh 2001, F. M. Mann and R. J. Puigh II, *Data Packages for the Hanford Immobilized Low-Activity Tank Waste Performance Assessment: 2001 Version*, HNF-5636, Rev. 2, prepared by Fluor Federal Services for Fluor Daniel Hanford Company, Richland, Washington, February 2001. {same as Mann/Puigh 2000a, except Appendix K updated.}

Mattigod 1994a, S. V. Mattigod, R. J. Serne, and H. Freeman, *100 Area Soil-Washing Bench-Scale Tests*, DOE/RL-93-107, U. S. Department of Energy, Richland Operations Office, Richland, Washington.

Mattigod 1994b , S. V., R. J. Serne, and H. Freeman, *100 Area Soil-Washing Bench-Scale Tests on 116-F-4 Pluto Crib Soil*, WHC-SD-EN-TI-268, Westinghouse Hanford Company. Richland, Washington.

Mattigod 2000, S. V. Mattigod, R. J. Serne, R. E. Clayton, T. Schaef, and D. McCready, *Mineralogy of Selected Sediment Samples from Borehole 299-E17-21*, Letter Report, Pacific Northwest National Laboratory, Richland, Washington, June 2000.

McGrail, 1997, B. P. McGrail, P. F. Martin, and C. W. Lindenmeier. "Accelerated Testing of Waste Forms Using a Novel Pressurized Unsaturated Flow (PUF) Method." *Mat. Res. Soc. Symp. Proc.* **465**:253-260.

McGrail 1998a, B. P. McGrail and D. H. Bacon, *Selection Of A Computer Code For Hanford Low-Level Waste Engineered-System Performance Assessment*, PNNL-10830 Rev. 1, Pacific Northwest National Laboratory, Richland, Washington, March 1998.

McGrail, 1998b, B. P. McGrail, W. L. Ebert, D. H. Bacon, and D. M. Strachan. *A Strategy to Conduct an Analysis of the Long-Term Performance of Low-Activity Waste Glass in a Shallow Subsurface Disposal System at Hanford*, PNNL-11834, Pacific Northwest National Laboratory, Richland, Washington.

McGrail 1999, B. P. McGrail, D. H. Bacon, J. P. Icenhower, W. L. Ebert, P. F. Martin, H. T. Schaef, and E. A. Rodriguez,, *Waste Form Release Data Package for the 2001 Immobilized Low-Activity Waste Performance Assessment*, PNNL-13043, Pacific Northwest National Laboratory, Richland, Washington, December 1999. Also Appendix K of Mann/Puigh 2000a. McGrail 2001 is an update of McGrail 2001.

McGrail 2001, B. P. McGrail, J. P. Icenhower, P. F. Martin, H. T. Schaef, M.J. O'Hara, E. A. Rodriguez, and J.L. Steele, *Waste Form Release Data Package for the 2001 Immobilized Low-Activity Waste Performance Assessment*, PNNL-13043, Rev. 2, Pacific Northwest National Laboratory, Richland, Washington, January 2001. Also Appendix K of Mann/Puigh 2001, Rev. 0A.

Meyer 1999, P. D. Meyer and R. J. Serne, *Near Field Hydrology Data Package for the Immobilized Low-Activity Waste 2001 Performance Assessment*, PNNL-13035, Revision 1, Pacific Northwest National Laboratory, Richland, Washington, December 1999. Also Appendix L of Mann/Puigh 2000a.

Millington-Quirk 1961, R. J. Millington and J. P. Quirk, "Permeability of Porous Solids," Trans Faraday Soc., **57:**1200-1207, 1961.

Mitchell 1995, *Immobilized Low Level Waste Disposal Options Configuration Study*, WHC-SD-WM-TI-686, Revision 0, Westinghouse Hanford Company, Richland, Washington, February 1995.

Mualem 1976, Y. Mualem, "A New Model for Predicting the Hydraulic Conductivity of Unsaturated Porous Media," *Water Resources Research*, 12 (1976) 513.

Myers 1979, C. W. Myers, S. M. Price, J. A. Caggiano, M. P. Cochran, W. J. Czimer, N. J. Davidson, R. C. Edwards, K. R. Fecht, G. E. Holmes, M. G. Jones, J. R. Kunk, R. D. Landon, R. K. Ledgerwood, J. T. Lillie, P. E. Long, T. H. Mitchell, E. H. Price, S. P. Reidel, and A. M. Tallman, *Geologic Studies of the Columbia Plateau: A Status Report*, RHO-BWI-ST-4, Rockwell Hanford Operations, Richland, Washington, October 1979.

Myers 1981, C. W. Myers and S. M. Price, "Bedrock Structure of the Cold Creek Syncline Area," in *Subsurface Geology of the Cold Creek Syncline*, RHO-BWI-ST-14 [see Tallman 1981], Rockwell Hanford Operations, Richland, Washington, July 1981.

Napier 1984, B. A. Napier, R. A. Peloquin, W. E. Kennedy Jr., and S. M. Neuder, *Intruder Dose Pathway Analysis for the Onsite Dispoal of Radioactive Wastes: The ONSITE/MAXI1 Computer Program*, NUREG/CR-3620, U.S. Nuclear Regulatory Commission, Washington, D.C., 1984.

Napier 1988, B. A. Napier, R. A. Peloquin, D. L. Strenge, and J. V. Ramsdell, *GENII – The Hanford Environmental Radiation Dosimetry Software System*, PNL-6584, Pacific Northwest Laboratory, Richland, Washington, December 1988.

NCRP 1987, *Ionizing Radiation Exposure of the Population of the United States*, Report No. 93, National Council on Radiation Protection, Bethesda, Maryland, 1987.

Neitzel 2000, D. A. Neitzel (editor), E. J. Antonio, C. J. Fosmire, R. A. Fowler, C. S. Glantz, S. M. Goodwin, D. W. Harvey, P. L. Hendrickson, D. G. Horton, T. M. Poston, A. C. Rohay, P. D. Thorne, M. K. Wright, *Hanford Site National Environmental Policy Act (NEPA) Characterization*, PNNL-64415, Rev. 12, Pacific Northwest National Laboratory, Richland, Washington, September 2000.

1. Section 4.6.3 presents demographic information.
2. Section 4.6 presents socioeconomic information
3. Section 4.1 presents climate and meteorology information.
4. Section 4.4 presents ecological information
5. Section 4.3.1.5 presents information on the potential of flooding

NLLWMP 1992, *Proceedings of the Department of Energy Performance Assessment Briefing, Denver, Colorado, October 29, 1991*, DOE/LLW-138, National Low-Level Waste Management Program, Idaho National Engineering Laboratory, Idaho Falls, Idaho, February 1992.

NRC/EPA 1987, NRC/EPA, 1987, *Joint NRC-EPA Guidance on a Conceptual Design Approach for Commercial Mixed Low-Level Radioactive and Hazardous Waste Disposal Facilities*, OSWER Directive 9487.00-8, August 3, 1987, U.S. Nuclear Regulatory Commission and the U.S. Environmental Protection Agency, Washington, D.C.

NRC, 1997, *Classification of Hanford Low-Activity Tank Waste Fraction*, letter from C. J. Paperiello, U.S. Nuclear Regulatory Commission, to J. J. Kinzer, U.S. Department of Energy, Richland Operations Office, dated June 9, 1997, U.S. Nuclear Regulatory Commission, Washington, D.C.

OFM 1999, *1999 Population Trends for Washington State*, Office of Financial Management, Forecasting Division, Olympia, Washington.

OFM 2000, *Washington State April 1 Population of Cities, Towns, and Counties, July 2000 Update*, Office of Financial Management, Forecasting Division, Olympia, Washington.

Orme 1996, R. M. Orme, *TWRS Privatization Process Technical Baseline*, WHC-SD-WM-TI-774, Rev. 0, Westinghouse Hanford Company, Richland, Washington.

Paperiello 1997, C. J. Paperiello (Director of Office of Nuclear Material Safety and Safeguards), letter dated June 1997 to Jackson Kinzer (Assistant Manager, Office of Tank Waste Remediation Systems) "Classification of Hanford Low-Activity Tank Waste Fraction", U.S. Nuclear Regulatory Commission, Washington, D.C.

{Letter is given in Appendix F.2.3 of Mann 1998a}.

Peters, R. D., and S. C. Slate. 1981. "Fracturing of Simulated High-Level Waste Canisters." *Nuc. Eng. Design* **67**:425-445.

Pickett 1998a, W. W. Pickett, *Immobilized Low-Activity Waste Interim Storage Facility, Project W-465 Conceptual Design Report*, HNF-1975, Rev. 1, prepared by Fluor Daniel Northwest, Inc. for Fluor Daniel Hanford, Inc., Richland, Washington.

Pickett 1998b, W. W. Pickett, *Immobilized Low-Activity Waste Disposal Facility, Project W-520 Conceptual Design Report [DRAFT]*, HNF-3013, Rev. B, dated September 21, 1998, prepared by Fluor Daniel Northwest, Inc. for Fluor Daniel Hanford, Inc., Richland, Washington.

PNL 1994, *Quality Assurance Plan*, PNL-MA-70, Pacific Northwest Laboratory, Richland, Washington, August 1994.

Power 1981, M. S. Power, K. J. Coppersmith, R. R. Youngs, D. P. Schwratz, and F.H. Swam III, *Final Safety Analysis Report WNP-2*, Amendment N.18, Appendix 2.5K, "Seismic Exposure Analysis for the WNP-2 and WNP-1/4 Site," Washington Public Power Supply System, Richland, Washington, 1981.

Pourbaix, 1974, M. Prourbaix, *Atlas of Electrochemical Equilibria in Aqueous Solutions*. English Translation of 1966 French version by J. A. Franklin (Ed.), National Association of Corrosion Engineers, Houston, Texas.

Puigh 1999, R. J. Puigh II, *Disposal Facility Data for the Hanford Immobilized Low-Activity Tank Waste*, HNF-4950, Rev. 1, prepared by Fluor Federal Services for Fluor Daniel Hanford Company, Richland, Washington, December 1999. Also Appendix I of Mann/Puigh 2000a.

Puigh 2000, R.J. Puigh II and F.M. Mann, *Statements of Work for FY 2001 to 2006 for the Hanford Low-Level Tank Waste Performance Assessment Project*, RPP-6702, Revision 0, CH2M Hill Hanford Group, Richland, Washington, June 2000.

Puigh 2001, R.J. Puigh and F. M. Mann, *Simulations for the Hanford Immobilized Low-Activity Tank Waste Performance Assessment: 2001 Version*, RPP-7464, Fluor Federal Services, Richland, Washington, February 2001.

Rawlins 1994, J. A. Rawlins, R. A. Karnesky, R. Khaleel, A. H. Lu, F. M. Mann, B. P. McGrail, W. J. McMahon, M. G. Piepho, P. D. Rittmann, and F. Schmittroth, *Impacts of Disposal System Design Options on Low-Level Glass Waste Disposal System Performance*, WHC-EP-0810, Revision 0, Westinghouse Hanford Company, Richland, Washington, September 1994.

RCRA, *Resource Conservation and Recovery Act of 1976*, 42 U.S.C. 6901, et seq.

Reidel 1998a, S. P. Reidel and K. D. Reynolds, *Characterization Plan For The Immobilized Low-Activity Waste Borehole*, PNNL-11802, Pacific Northwest National Laboratory, Richland, Washington.

Reidel 1998b, S. P. Reidel, D. G. Horton, and K. D. Reynolds, *Immobilized Low-Activity Waste Site Borehole 299-E17-21*, PNNL-11957, Pacific Northwest National Laboratory, Richland, Washington.

Reidel 1989, S. P. Reidel and P. R. Hooper, editors, "Volcanism and Tectonism in the Columbia River Flood-Basalt Province," Special Paper 239, Geological Society of America, Boulder, Colorado, p. 386, plate 1, 1989.

Reidel 1992, S.P. Reidel, K.A. Lindsey, and K.R. Fecht, *Field Trip Guide to the Hanford Site*, WHC-MR-0391, Westinghouse Hanford Company, Richland, Washington.

Reidel 1994a, S. P. Reidel and K. R. Fecht, *Geologic Map of the Richland 1:100,000 Quadrangle, Washington*, Open File Report 94-8, Washington State Department of Natural Resources, Olympia, Washington.

Reidel 1994b, S. P. Reidel and K. R. Fecht, *Geologic Map Of The Priest Rapids 1:100,000 Quadrangle, Washington*, Open File Report 94-13, Washington State Department of Natural Resources, Olympia, Washington.

Reidel 1999, S. P. Reidel and D. G. Horton , *Geologic Data Packages for 2001 Immobilized Low-Activity Waste Performance Assessment*, PNNL-12257, Rev. 2, Pacific Northwest National Laboratory, Richland, Washington, December 1999. Also Appendix G of Mann/Puigh 2000a.

Rhoads 1999, K. Rhoads, "HEDOP Review of Checklist", Pacific Northwest National Laboratory, Richland, Washington, published as last page of Rittmann 1999.

Richards 1931, L.A. Richards, "Capillary Conduction of Liquids Through Porous Mediums," *Physics*, 1 (1931) 318.

Rittmann 1993, P. D. Rittmann, *GRTPA - A Program to Calculate Human Dose from PORFLOW Output*, WHC-SD-WM-UM-018, Westinghouse Hanford Company, Richland, Washington, November 1993.

Rittmann 1994, P. D. Rittmann, *Dose Estimation for the Solid Waste Performance Assessment*, WHC-SD-WM-TI-616, Westinghouse Hanford Company, Richland, Washington, August 1994.

Rittmann 1999, P. D. Rittmann, *Exposure Scenarios And Unit Dose Factors For The Hanford Immobilized Low-Activity Tank Waste Performance Assessment*, HNF-SD-WM-TI-707, Rev. 1, prepared by Fluor Federal Services for Fluor Daniel Hanford Company, Richland, Washington, December 1999. Also Appendix O of Mann/Puigh 2000a.

Rockhold 1995, M. L. Rockhold, M. J. Fayer, C. T. Kincaid, and G. W. Gee, *Estimate of the Natural Ground Water Recharge for the Performance Assessment of a Low-Level Waste Disposal Facility at the Hanford Site*, PNL-10508, Pacific Northwest Laboratory, Richland, Washington, March 1995. [Also included as Appendix K in Mann 1995a.]

Rutherford 1997, W. A. Rutherford (Director, Site Infrastructure Division), letter 97-SID-285 to H. J. Hatch (President of Fluor Daniel Hanford, Inc.), "Contract DE-AC06-96RL113200 - Approval of Tank Waste Remediation System Complex Site Evaluation Report", dated July 10, 1997, U.S. Department of Energy, Richland Operations Office, Richland, Washington.

RWTSP 1994, *A Compilation of DOE Performance Assessment Peer Review Panel Review Comments and Recommendations*, DOE/LLW-216, Radioactive Waste Technical Support Program, Idaho National Engineering Laboratory, Idaho Falls, Idaho, 1994.

Schmittroth 1995, F. A. Schmittroth and T. H. DeLorenzo, *Consequence Ranking of Radionuclides in Hanford Tanks Waste*, WHC-SD-WM-RPT-163, Revision 0, Westinghouse Hanford Company, Richland, Washington, September 1995.

Schmittroth 1995a, F.A. Schmittroth, T.H. DeLorenzo, D.W. Wootan, and D.Y. Garbrick, *Inventories for Low-Level Tank Waste*, WHC-SD-WM-RPT-164, Revision 0, Westinghouse Hanford Company, Richland, Washington, June 1995. [Also included as Appendix J in Mann 1995a.]

Schramke 1988, J. A. Schramke, "Characterization of 200 Area Soil Samples," Letter Report. September 29, 1988, Pacific Northwest Laboratory, Richland, WA.

Schreckhise 1993, R. G. Schreckhise, K. Rhoads, J.S. Davis, B.A. Napier, and J.V. Ramsdell, *Recommended Environmental Dose Calculation Methods and Hanford Specific Parameters*, PNL-3777, Rev. 2, Pacific Northwest Laboratory, Richland, Washington, 1993.

Shade 1997, J. W. Shade, *TWRS Retrieval and Disposal Mission: Immobilized Low-Activity Waste Disposal Plan*, HNF-1517, Rev. 0, Fluor Daniel Hanford, Inc., Richland, Washington, December 1997.

Shord 1995, A. L. Shord, *Tank Waste Remediation System Complex Site Evaluation Report*, WHC-SD-WM-SE-021, Revision 0, Westinghouse Hanford Company, Richland, Washington, May 1995.

Skaggs 1981, R. L. Skaggs and W. H. Walters, *Flood Analysis of Cold Creek Near the Hanford Site*, RHO-BWI-C-120/PNL-4219, Rockwell Hanford Operations, Richland, Washington, 1981.

Smith 1990, R. M. Smith and W. R. Gorst, *RCRA Ground-Water Monitoring Projects for Hanford Facilities: Annual Progress Report for 1989*, PNL-7215, Pacific Northwest Laboratory, Richland, Washington, 1990.

Stewart 1987, G. H. Stewart, W. T. Farris, D. G. Huizenga, A. H. McMakin, G. P. Streile, and R. L. Treat, *Long-Term Performance Assessment of Grouted Phosphate/Sulfate Waste from N Reactor Operations*, PNL-6512, Pacific Northwest Laboratory, Richland, Washington, April 1987.

Tallman 1979, A. M. Tallman, K. R. Fecht, M. C. Marratt, and G. V. Last, *Geology of the Separation Areas Hanford Site, South Central Washington*, RHO-ST-23, Rockwell Hanford Operations, Richland, Washington, 1979.

Taylor 1999a, W. J. Taylor, *Contract No. DE-AC06-99RL14047 – Decision to Change the Immobilized Low-Activity Waste (ILAW) Disposal Baseline to Proceed with the Remote-Handled Trench Alternative*, letter 99-DPD-066 (correspondence control number 9958849), Department of Energy, Richland, Washington, December 1, 1999.

Taylor 1999b, W. J. Taylor, Contract N0. DE-AC06-96RL13200 Planning Guidance revisions for Development of Contract Deliverable Required by Performance Agreement TWR1.3.5, letter 99-AMPD-006 (correspondence control no. 9952261A), Department of Energy, Richland, Washington.

Thorne 1992, P. D. Thorne, P. D., and M. A. Chamness, *Status Report on the Development of a Three-Dimensional Conceptual Model for the Hanford Site Unconfined Aquifer System*. PNL-8332, Pacific Northwest Laboratory, Richland, Washington, 1992.

Thorne 1993, P. D. Thorne, M. A. Chamness, F. A. Spane Jr., V. R. Vermeul, and W. D. Webber, *Three-Dimensional Conceptual Model for the Hanford Site Unconfined Aquifer System, FY 93 Status Report.* PNL-8971, Pacific Northwest Laboratory, Richland, Washington, 1993.

Thorne 1994, P. D. Thorne, M. A. Chamness, V. R. Vermeul, Q. C. MacDonald, and S. E. Schubert, *Three-Dimensional Conceptual Model for the Hanford Site Unconfined Aquifer System, FY 1994 Status Report*. PNL-10195, Pacific Northwest Laboratory, Richland, Washington, 1994.

Vienna 2000, J. D. Vienna, A. Jiricka, B. P. McGrail, B. M. Jorgensen, D. E. Smith, B. R. Allen, J. C. Marra, D. K. Peeler, K. G. Brown, I. A. Reamer, and W. L. Ebert. 2000. *Hanford Immobilized LAW Product Acceptance Testing: Initial Data Package*. PNNL-13101, Pacific Northwest National Laboratory, Richland, Washington. [attachment to French 2000a]

Voogd 1998, J. A. Voogd, F. M. Mann, and A. J. Knepp, *Recommendations for Computer Code Selection of a Flow and Transport Code to be Used in Undisturbed Vadose Zone Calculations for TWRS Immobilized Wastes*, HNF-4356, Lockheed Martin Hanford Corporation, Inc., September 1998. Also Appendix E of Mann/Puigh 2000a.

WAC 173-200, "Water Quality Standards for Ground Waters of the State of Washington," *Washington State Administrative Code*, 173-200, Section 170, Washington State Department of Ecology, Olympia, Washington, December 1, 1990.

WAC 173-201A, "Water Quality Standards for Surface Waters of the State of Washington," *Washington State Administrative Code*, Washington State Department of Ecology, Olympia, Washington, December 22, 1992.

WAC 173-303, "Dangerous Waste Regulations", *Washington State Administrative Code*, Washington State Department of Ecology, March 3, 1991.

WAC 173-480, "Ambient Air Quality Standards and Emission Limits for Radionuclides," *Washington State Administrative Code*, Section 040, Washington State Department of Ecology, Olympia, Washington, July 7, 1986.

WAC 246-247, "Radiation Protection - Air Emissions," *Washington State Administrative Code*, Section 040, Washington State Department of Ecology, Olympia, Washington, January 31, 1991.

Walters 1994, W. H. Walters, M. C. Richmond, and B. G. Gilmore, *Reconstruction of Radionuclide Concentrations in the Columbia River from Hanford, Washington to Portland, Oregon, January 1950 - January 1971*. BNWD-2225 HEDR, Pacific Northwest Laboratory, Richland, Washington, 1994.

WCC 1989, *Evaluation of Seismic Hazard for N-Reactor Facilities, Hanford Reservation, Hanford, Washington*, WHC-MR-0023, prepared for Westinghouse Hanford Company by Woodward-Clyde Consultants, Oakland, California.

Westsik 1997, J. H. Westsik, Jr. and P. L. Miller, "Preliminary Product Acceptance Strategy for ILAW, IHLW, Intermediate Products, and Secondary Wastes," WIT-097-036, Pacific Northwest National Laboratory, Richland, Washington, January 1997.

WHC 1994a, *Overview of the Performance Objectives and Scenarios of the TWRS Low-Level Waste Disposal Program*, WHC-EP-0827, Revision 0, Westinghouse Hanford Company, Richland, Washington, October 1994.

[Based on comments on Revision 0, Revision 1 was issued in January 1995. Revision 1 is included as Appendix A in Mann 1995a.]

WHC 1994b, *Project W-025 Specifications: Section 02275 Geosynthetics*, WHC-S-045, Revision 3, Westinghouse Hanford Company, Richland, Washington.

WHC 1996, *Technical Basis for Classification of Low-Activity Waste Function from Hanford Site Tanks*, WHC-SD-WM-TI-699, Revision 1, Westinghouse Hanford Company, Richland, Washington, July 1996.

White 1996, M. D. White and M. Oostrom, *STOMP: Subsurface Transport Over Multiple Phases, Theory Guide*, PNNL-11217, Pacific Northwest National Laboratory, Richland, Washington.

Wiemers 1998, K. D. Wiemers, M. E. Lerchen, M. Miller, K. Meier, *Regulatory Data Quality Objectives Supporting Tank Waste Remediation System Privatization Project*, PNNL-12040, Rev. 0., Pacific Northwest National Laboratory, Richland, Washington.

Wilhite 1994, *Performance Assessment Peer Review Panel Recommendations on the "Performance Assessment of Grouted Double-Shell Tank Waste Disposal at Hanford" WHC-SD-WM-EE-004, Revision 0 (U)*, letter from E. L. Wilhite to J. A. Turi, SRT-WED-94-0112, Westinghouse Savannah River Company, Aiken, South Carolina, October 4, 1994.

Wood 1994, D. E. Wood (Chairman), R. U. Curl (Technical Secretary), D. R. Armstrong, J. R. Cook, M. R. Dolenc, D. C. Kochner, K. W. Owens, E. P. Regnier, G. W. Roles, R. R. Seitz, and M. I. Wood, *Performance Assessment Task Team Progress Report*, DOE/LLW-157, Revision 1, Idaho National Engineering Laboratory, Idaho Falls, Idaho, May, 1994.

Wood, 1995a, M. I. Wood, R. Khaleel, P. D. Rittmann, A. H. Lu, S. H. Finfrock, R. J. Serne, and K. J. Cantrell, *Performance Assessment for the Disposal of Low-Level Waste in the 200 West Area Burial Grounds*, WHC-EP-0645, Westinghouse Hanford Company, Richland, Washington, June 1995.

[1. Section 1.6 discusses the time of compliance.]
[2. P. 3-31 provides the discussion of the radon diffusivity coefficient.]
[3. Section 4.3.1 provides the calculation of the release of contaminants to air]

Wood 1995b, M. I. Wood, R. Khaleel, P. D. Rittmann, A. H. Lu, S. H. Finfrock, and T. H. DeLorenzo, *Environmental Remediation Disposal Facility Performance Assessment*, BHI-00169, Revision 00, Bechtel Hanford Company, Richland, Washington, August 1995.

Wood 1996, M. I. Wood, *Performance Assessment for the Disposal of Low-Level Waste in the 200 East Area Burial Grounds*, WHC-EP-0875, Westinghouse Hanford Company, Richland, Washington, September 1996.

[1. Section 1.6 discusses the time of compliance.]

Wootan 1999, D. W. Wootan, *Immobilized Low Activity Tank Waste Inventory Data Package*, HNF-4921, Rev. 0, prepared by Fluor Daniel Northwest, Inc., for Fluor Daniel Hanford Company, September 1999. Also Appendix H of Mann/Puigh 2000a.

WSRC 1992, *Radiological Performance Assessment for the Z-Area Saltstone Disposal Facility*, WSRC-RP-92-1360 (Appendix B.10), Westinghouse Savannah River Company, Aiken, South Carolina, December 1992.

Wurstner 1995, S. K. Wurstner, P. D. Thorne, M. A. Chamnes, M. D. Freshley, and M. D. Williams, *Development of a Three-Dimensional Ground-Water Model of the Hanford Site Unconfined Aquifer System: FY 1995 Status Report*, PNL-10886, Pacific Northwest National Laboratory, Richland, Washington, December 1995.

Wurstner 1997, S. K. Wurstner, P. D. Thorne, M. A. Chamness, M. D. Freshley, and M. D. Williams. *Development of a Three-dimensional Groundwater Model of the Hanford Site Unconfined Aquifer System*: FY 1995 Status Report. PNL-10886, Pacific Northwest Laboratory, Richland, Washington, December 1997.

Zhang 1996, Shengdong Zhang, Kingru Guo, Anshi Cui, Daming Li, Daming Liu, "Measurement of the Half Life of ^{126}Sn Using a Radiochemical Method", *Journal Radioanalytical and Nuclear Chemistry Letters*, 212 (1996) 93.

Appendix A

LFRG Comments on Performance Assessment for Hanford Immobilized Low-Activity Tank Waste, 7/27/99

Appendix A

Comments from
the Low-level Waste Disposal Facility Federal Review Group
(LFRG)
On the 1998 ILAW PA

(Table C-2 of DOE 1999c,
modified to show response for this PA)

LFRG Comments on Performance Assessment for Hanford Immobilized Low-Activity Tank Waste, 7/27/99.

Criteria	Criteria met?	Response	Issues	This Document
3.1.1 PA is Complete				
3.1.1.a. PA identifies the performance measures used in the PA and a justification of those performance measures as site-specific applications of the performance objectives.	Yes	Performance Measures are defined and reasonably justified in Section 1.6. The performance objective of 25 mrem/year was adopted as a performance measure. The location for compliance is the point of maximum exposure outside a 100-meter buffer zone surrounding the waste. The requirement to assess exposure to a hypothetical inadvertent intruder used the performance measures of 100 mrem/year for chronic exposure and 500 mrem for acute exposure. The time for compliance with these performance measures was taken to be 500 years after facility closure. This time, rather than the default time of 100 years, was justified on the basis of passive barriers and markers. The performance objective to protect water resources was interpreted to require protection of groundwater and surface water. For groundwater protection, the performance measure adopted was that concentrations of contaminants in groundwater not exceed Federal standards for drinking water. Thus, a dose of 4 mrem/year for beta/photon emitters and a concentration of 15 pCi/L for alpha emitters (including uranium) were used. These performance measures were applied to a hypothetical well located 100-meters down gradient from the disposal facility. For surface water, a performance measure of 1 mrem/year was adopted to be consistent with Washington State requirements. The point of compliance for surface water protection was assumed to be the point at which groundwater enters the Columbia river. The performance objective to restrict exposure of any member of the public to no more than 10 mrem/year via the air pathway was adopted as a performance measure. The performance objective to restrict emissions of radon to no more than 20 pCi/m^{2}s was also adopted as a performance measure.	No issues.	Same approach, see Section 1.6.

LFRG Comments on Performance Assessment for Hanford Immobilized Low-Activity Tank Waste, 7/27/99.

Criteria	Criteria met?	Response	Issues	This Document
3.1.1.b. PA presents information on the site geography, demography, land use plans, meteorology, ecology, geology, seismology, volcanology, surface water and groundwater hydrology, geochemistry, geologic resources, water resources, and natural background radiation sufficient to support the analysis presented in the performance assessment.	Yes	The PA presents information on the site geography, demography, land use plans, meteorology, ecology, and regional geology, geochemistry, seismology, volcanology, surface water and ground water resources, and natural background to the reasonable extent necessary. The general discussion on the near-field subsurface geology also seems reasonable; however more details should be presented in the PA. Borehole logs and well completion drawings of the three boreholes (Fig. 2-13) should present more details of the material types, geology, and subsurface hydrology. Tables should be included that list pertinent boreholes and monitor wells with total depth, top of casing, etc. Figure 2-10 poorly represents borehole locations. Consider using: a fold-out plate map, identify latitude and longitude coordinate system, and fence diagram to illustrate geology in area of disposal.	Need better traceability for many details and basic summaries of reference material. Note: Hanford disagreed with this comment based on the need for textual economy.	Figure 2-10 includes fence diagram for ILAW disposal site. New Figure 2-9 shows location of boreholes on ILAW site. Additional data on material types, geology, and subsurface hydrology provided in data packages.
3.1.1.c. PA presents information on the facility design features including elements of the design that address water infiltration disposal unit cover integrity, structural stability, and the inadvertent intruder barrier sufficient to support the analysis presented in the PA.	Yes	Section 2.4 describes the disposal technology. This section includes details of disposal vault construction, both for the existing vaults and for the additional vaults that will be constructed. Sections 2.4.1.4 and 2.4.1.5 discuss closure of the disposal units and the site. These sections discuss features of the closure designed to limit infiltration and those features that deter intrusion. The information presented is sufficient to support the analyses. However, the depiction of the cover design is confusing regarding the slope of the cover. The relationship of cover performance to potential contaminant transport in the vadose zone is not presented clearly. A no-slope cover could create greater deep percolation over the life of disposal. The cover design should consider ALARA concepts (sloping top cover to drain sheet flow in the event of 1000 year precipitation event).	Details regarding cover design are confusing. However, we recognize that conceptual designs were published after issuance of the PA.	Slope of current cover defined in Section 2.4.1. The relationship of cover performance to potential contaminant transport is discussed briefly.

LFRG Comments on Performance Assessment for Hanford Immobilized Low-Activity Tank Waste, 7/27/99.

Criteria	Criteria met?	Response	Issues	This Document
3.1.1.d. PA identifies Federal, state, and local statutes or regulations or agreements that impact site engineering, facility design, facility operations, and the relationship and/or impact of the results of the PA on site engineering, facility design, or facility operations because of these factors.	Yes	In Sections 1.5 and 1.6 all potentially applicable statutes, regulations or agreements are identified. In Section 1.5.2, *the Federal Facility Agreement and Consent Order* is discussed. Some of the legally enforceable milestones cover the Immobilized Waste Program. In Section 1.6.2.2, the *NRC Branch Technical Position on a Performance Assessment Methodology for Low-Level Radioactive Waste Disposal Facilities* is discussed. This document is pertinent because it lays out NRC PA requirements, namely the time of compliance which is 10,000 years. Hanford has adopted the longer time of compliance in order to fully comply with the Incidental Waste requirements of DOE 435.1. In Section 1.6.2.5, Federal and State requirements for drinking water are discussed and applied to the protection of groundwater resources. In Section 1.6.2.6, Federal and State requirements for surface water protection are discussed and applied to the ILAW PA. In Section 1.6.2.7, Federal and State requirements for air emission limits are discussed and applied to the ILAW PA. Section 2.4.1.1 discusses the RCRA design requirement for double containment under which the existing vaults were constructed.	No issues.	Same approach, see Sections 1.5 and 1.6.
3.1.1.e. PA identifies procedures and facility related documentation that may impact site engineering, facility design, or facility operations and the relationship and/or impact of the results of the performance assessment on the documents and site engineering, facility design, or facility operations.	Yes	The PA, in Sections 2.3 and 2.4 identifies documentation (e.g., TWRS record of decision, privatization specifications for immobilization) that may impact the site/facility. However, no evidence is provided that the assumed glass performance can actually be achieved.	No indication is provided that ~~t~~ assumed glass performance can be achieved. However, supplemental information provided by Hanford (see Appendix F) mitigated this issue.	The approach for estimating glass performance has changed. It now relies on experiment. See Section 3.4.4

LFRG Comments on Performance Assessment for Hanford Immobilized Low-Activity Tank Waste, 7/27/99.

Criteria	Criteria met?	Response	Issues	This Document
3.1.1.f. PA identifies and justifies key assumptions included in the analysis presented in the PA.	Yes	The PA identifies the key assumptions to be: 1) Inventory assumption that average values from modeling, corrected for credits, seems reasonable and justifiable. 2) Waste form performance assumption that short-term performance and long-term performance are equal is not justifiable without further information. No evidence is presented that the assumed glass performance can actually be achieved. 3) Disposal design, geotechnical considerations, and dose calculation assumptions seem reasonable and justifiable. 4) Recharge relationship to potential contaminant release assumptions needs more explanation in the next iteration of the PA.	1)No issues. 2) Issue is being addressed by Hanford's additional research activities. 3) No issues. 4) Hanford agrees that future Pa revisions will include these effects.	See Sections 1) 3.2 2) 3.4.4 and 7.8.2 3) 2.4, 3.4.3, and 4.3.6 4) 4.5.4
3.1.1.g. PA identifies the point of assessment for each performance measure, and justifies the selection of each point of assessment. *3.1.1.g.1.* The point of assessment for all-pathways, the air pathway excluding radon, and groundwater resource protection is justified based on future land use. If the future site boundary is uncertain, a reasonable point of assessment (e.g., point of maximum impact greater than 100-m from the edge of the disposal unit) is justified.	Yes	The PA, in Section 1.6.2.2 identifies the point of assessment for the all-pathways performance objective as being at the point of maximum exposure, but not less than 100-meters from the disposal facility. The 100-m well is also used for the groundwater protection performance objective as stated in section 1.6.2.5. The point of assessment is conservatively assumed to be the point of maximum exposure outside the 100-m buffer zone for the all pathways, air pathway (excluding radon), and the groundwater protection performance objectives.	No issues.	Same approach, see Section 1.6.

LFRG Comments on Performance Assessment for Hanford Immobilized Low-Activity Tank Waste, 7/27/99.

Criteria	Criteria met?	Response	Issues	This Document
3.1.1.g.2. The default point of assessment for the performance measure for radon exposure that is based on a limit on the average flux of radon of 20 pCi/m^2/s at the ground surface is the ground surface over the disposal unit.	Yes	The performance assessment demonstrates that radon fluxes will be below 20 pCi/m^2/s at the ground surface over the disposal unit. The calculations use appropriate models and assumptions. The deep burial of the waste significantly reduces the small amount of radon present by decay as a consequence of the short half life of radon. The analysis should state that the inventory does not contain sufficient radon precursors to generate significant radon during the time period of analysis. [See Table ES-6; Table 6-5; page 4-74 *et seq.*] Consequently, while the discussion could be improved, the analysis is complete for review purposes even in light of this oversight.	No issues.	Same approach (See Section 4.12).
3.1.1.g.3. The default point of assessment for the alternative performance measure for radon exposure that is based on a limit on air concentration of radioactive material of 0.5 pCi/L is 100-m from the edge of the disposal unit.	Yes	The default performance measure of 20 pCi/m^{2}s is used, thus, this criterion is not applicable	No issues.	Same approach (See Section 1.6.2.7).

LFRG Comments on Performance Assessment for Hanford Immobilized Low-Activity Tank Waste, 7/27/99.

Criteria	Criteria met?	Response	Issues	This Document
3.1.1.h. The performance assessment identifies and quantifies all radionuclides present in the low-level waste to be disposed of at the facility that could significantly contribute to dose for the all pathways analysis, the air pathway analysis, the groundwater analysis, and the intruder analysis. Technical justification is provided for those radionuclides considered in detail in the analyses, and conversely, those not considered in the analyses.	Yes	In Section 3.2.1, the radionuclides relevant to the PA are identified by means of a reasonable screening analysis. All radionuclides produced at Hanford were considered. The inventory of potentially important radionuclides, Section 3.2.2, was developed from generally reasonable assumptions regarding radionuclide production in reactors and partitioning in chemical processing and in the waste tanks. However, the estimate of ^{99}Tc inventory appears to be considerably over stated (see detailed comments by H. Babad).	The Tc-99 inventory appears to be considerably overstated.	Same approach, see Section 3.2. H. Babad's comments were based on a contract signed after 1998 ILAW PA was submitted and on results from short-term experiments. These experiments have been continued, but results still are not definitive.

LFRG Comments on Performance Assessment for Hanford Immobilized Low-Activity Tank Waste, 7/27/99.

Criteria	Criteria met?	Response	Issues	This Document
3.1.1.i. PA accounts for all relevant mechanisms for the release of radionuclides from the waste materials for environmental transport. The mechanisms analyzed are justified by references to relevant studies, available data, or supporting analyses in the PA.	No	The performance assessment presents a base case using a simplified model because the waste form had not been determined and only specifications for its short-term release rate are known (p. 3-8).The base case assumed the glass waste form released contaminants at a rate equivalent to the TWRS privatization RFP specification of $1.4x10^{-13}$ s^{-1} (p.3-39). It was assumed that this rate remained constant over time (however, the dimensions of the waste form decreased at a constant rate). Initially, the waste form was assumed to be a non-fractured monolith with dimensions of 1.2 x. 1.2 x. 1.8 m. No justification for the appropriateness of this assumption was provided. The preparers should have reviewed available data on glass leaching to put the assumed rate of glass corrosion into perspective. The contaminant release rates were independent of the infiltration rates used in the sensitivity study. This makes the infiltration sensitivity results less informative. The PA should discuss the vadose moisture relationship to contaminant release rate.	No evidence has been presented that the modeled performance has any relation to the actual performance which may reasonably be expected. Issue is being addressed by Hanford's additional research activities as noted in the supplemental information (see Appendix F). Need discussion of the relationship between vadose moisture and contaminant release rate.	Uses experimental data and calculations to simulate waste form performance, including the effect of varying recharge. See Section 4.6
3.1.1.j. PA provides a complete and clear description of the conceptual model of the environmental transport of the radionuclides from the waste materials to the points of compliance by air and water. The conceptual model is justified by referenced investigations, data, and supporting analyses that are representative of the site-specific conditions described.	Yes	With one exception, the conceptual model for the ground water pathway is complete, clearly described, and justified. See criterion 3.1.1.b for suggestions. The exception is the rate of contaminant release from the glass waste form. The specification in the privatization contract for waste immobilization is the short-term glass corrosion rate. No evidence is provided that the assumed rate can be achieved. The conceptual model for the air pathway is complete, clearly described, and justified.	Lack of evidence that assumed glass waste form performance can be achieved. Issue is being addressed by Hanford's additional research activities as noted in the supplemental information (see Appendix F).	Uses experimental data and calculations to simulate waste form performance. See Sections 3.5.3.1 and 3.5.4.1

LFRG Comments on Performance Assessment for Hanford Immobilized Low-Activity Tank Waste, 7/27/99.

Criteria	Criteria met?	Response	Issues	This Document
3.1.1.j.1. The conceptual model incorporates interpretations of available geochemical, geologic, meteorologic and hydrologic data, and the relevant mechanisms that have a significant effect on the transport of radionuclides at the disposal site.	Yes	Relevant mechanisms, supported by reasonable interpretations of available data are incorporated in the conceptual model for the air pathway. In general, the use of only two soil types in the vadose-zone model prevents evaluations of heterogeneities such as uncased, lost boreholes or preferential flow paths. The PA should more thoroughly present information on recharge rates and the relationship to contaminant concentrations and flux. The conceptual model for the base case does not incorporate mechanisms of glass corrosion. Rather, an assumed corrosion rate is used with no evidence provided to indicate whether the corrosion rate can actually be achieved.	Unsupported glass corrosion rate. Issue is being addressed by Hanford's additional research activities as noted in the supplemental information (see Appendix F).	Sensitivity cases for vadose zone added to address heterogeneity - clastic dyke, information on recharge rate and relationship to contaminant concentrations and flux. See Section 3.5.5. Glass corrosion mechanisms included in base analysis case (See Section 3.5.3.1).
3.1.1.j.2. Assumptions incorporated into the conceptual model to account for transport mechanisms lacking sufficient data or supporting analyses are identified and justified as reasonable representations of site behavior over the time period considered in the analysis.	No	Performance of glass waste form is assumed with no evidence that the assumption is credible.	No assurance that assumed glass performance can actually be achieved. .Issue is being addressed by Hanford's additional research activities as noted in the supplemental information (see Appendix F).	Uses experimental data and calculations to simulate waste form performance. See Sections 3.4.4 and Appendix E

LFRG Comments on Performance Assessment for Hanford Immobilized Low-Activity Tank Waste, 7/27/99.

Criteria	Criteria met?	Response	Issues	This Document
3.1.1.j.3. The conceptual model includes closure of the facility as justified based on referenced closure plans or reasonable assumptions of facility closure.	Yes	The conceptual model includes reasonable assumptions for facility closure. However, it is not clear exactly which closure design will be used (see pp. ES-xviii and 6.1). We recognize that conceptual designs were completed after completion of the PA.	No issues.	Closure based on issued Closure Plan (Burbank 2000) as approved by Boston 2000b. See Section 2.4.1
3.1.1.j.4. The conceptual model includes any credits to be taken in the analysis for the performance of engineered features. Credits for engineered features include a reasonable representation of the degradation of the engineered features that is justified by supporting investigations and data.	Yes	The analysis takes credit for the Hanford barrier to reduce infiltration. Increasing the infiltration rate to the natural rate after the first 1,000 years (the design life of the barrier) incorporated degradation of the barrier. A sensitivity case that used the natural recharge rate for the entire time provided information on the effect of a shorter life for the barrier than the design life. The analysis did not take credit for the waste packages. This is at least somewhat conservative. The analysis may be very conservative from the viewpoint that the waste containers will certainly be made of some sort of steel. Steel corrosion products are likely to be good at sorbing at least some radionuclides. This could have been investigated in a sensitivity case. The analysis takes credit for the concrete vaults, but only for 500 years. This is likely conservative. Sensitivity analyses were done with no credit for the vaults and with longer credit (i.e., 2,000 years) for the vaults.	No issues.	Near-field calculations involved full set of chemical reactions. Other work is similar to that in 1998 ILAW PA. See Sections 3.5.3.1 and 4.3.3.
3.1.1.j.5. The conceptual model includes natural processes that affect the transport of radionuclides (e.g., flooding, mass wasting, erosion, weathering) over the time period considered in the analysis, as justified based on referenced investigations and supporting analysis.	Yes	The conceptual model includes relevant natural processes and is consistent with other site PAs.	No issues.	Same approach. (See Sections 3.4 and 3.5)

LFRG Comments on Performance Assessment for Hanford Immobilized Low-Activity Tank Waste, 7/27/99.

Criteria	Criteria met?	Response	Issues	This Document
3.1.1.k. PA provides a clear description of the mathematical models used in the analyses. The mathematical models selected are justified and provide a reasonable representation of all of the elements of the conceptual model.	Yes	More clarification would add value to the analysis. For example, more information is required to describe the unit cell model used in some sensitivity analyses. What code is used (e.g., PORFLOW)? How many elements are used? What specific comparisons were made to the disposal facility model (e.g., moisture content, radionuclide transport, etc.) to ensure that these models are consistent?	Need additional information on unit cell model.	Unit cell no longer used. The combination of 1d and 2d calculations is discussed in Section 3.5.
3.1.1.k.1. The complexity of the mathematical models selected is commensurate with the available site data.	Yes	Mathematical models/computer code (AREST-CT for source release, PORFLOW for unsaturated zone, and VAM3D-CG for unsaturated flow and results) selections are commensurate with available data. Although, an observation regarding the difficulties and confusion due to many codes and models utilized in this PA, and to the non-integrated selection methodology to the codes/models in the CA (and other DOE disposal facilities) may lead to major inefficiencies.	No issues.	Updated codes were used (Section 3.5.2). Groundwater code/model is that used in CA.
3.1.1.k.2. Assumptions incorporated into the mathematical models are identified, justified, and consistent with the conceptual model	Yes	Assumptions are identified, justified, and consistent with the conceptual model.	No issues.	Same approach (See Section 3.5.2)
3.1.1.k.3. Mathematical models selected are documented and verified either in referenced publications or in the appendices of the performance assessment	Yes	Models are well documented.	No issues.	Same approach (See Section 3.5.2)

LFRG Comments on Performance Assessment for Hanford Immobilized Low-Activity Tank Waste, 7/27/99.

Criteria	Criteria met?	Response	Issues	This Document
3.1.1.l. PA provides a complete description of the important exposure pathways and scenarios for the specific disposal facility that are used in the evaluation of the potential doses to the hypothetical, individual member of the public and inadvertent intruder consistent with site-specific environmental conditions and local and regional practices. The exposure pathways and scenarios selected for detailed analysis are justified as conservative representations of the long-term performance of the LLW disposal facility.	Yes	The PA provides a sufficiently complete description of pathways and scenarios (Section 3.3). With the exception of glass performance (see criterion 3.1.2.b), pathways and scenarios are reasonable and conservative representations of long-term performance.	Insufficient justification for assumed glass performance. Issue is being addressed by Hanford's additional research activities as noted in the supplemental information (see Appendix F).	Uses experimental data and calculations to simulate waste form performance. See Sections 3.3.3. and 4.3.3.
3.1.1.l.1. Exposure pathways from the transport of contamination in groundwater that may be considered include potential exposures from the ingestion of contaminated groundwater, the use of contaminated groundwater for irrigation and livestock watering, and the biotic uptake and transport of contamination from groundwater and surface water. Potential exposure pathways from the transport of contamination in surface water include the ingestion of contaminated surface water and contaminated fish.	Yes	The exposure pathways from the transport of contamination in groundwater (Section 3.3.5) and include ingestion of contaminated groundwater, use of contaminated groundwater for irrigation of a small farm. Exposure comes from drinking contaminated water, ingesting contaminated food grown on the farm, ingesting and inhaling contaminated soil, and direct irradiation from the contaminated soil. Because the performance measure for surface water protection is a dose, assuming consumption of the surface water (Section 1.6.2.6), ingestion of contaminated fish was not considered.	No issues.	Same approach, see Section 3.3.5.

LFRG Comments on Performance Assessment for Hanford Immobilized Low-Activity Tank Waste, 7/27/99.

Criteria	Criteria met?	Response	Issues	This Document
3.1.1.l.2. If radiation dose is used as a measure of groundwater resource protection, the exposure scenarios consider the ingestion of water (at 2 liters per day or an alternative rate, if a justification is included) at the point of assessment, which represents the location of maximum exposure from a well constructed and developed using current practices typical for the local area	Yes	The groundwater protection scenario used a consumption rate of 2 L/day and assumed the well would be located to provide the maximum dose outside the 100-m buffer zone. Based on characterizations at numerous uranium mill tailings sites where inorganic contaminants were released decades ago and migrated into ground water, often in silty/sandy/gravely environments not unlike Hanford; vertical distribution of contaminant profile is often up to 20 meters. Based on these experiences, a 4.6-meter screen length seems reasonable and appropriate for the POC well 100-M down gradient of the disposal site (Section 3.4.7.2).	No issues.	Same approach. 4.6 m screen length justified based on local use (see Section 3.4.7)
3.1.1.l.3. Exposure scenarios from the transport of contamination in water for the all pathways analysis considers the use of groundwater and surface water consistent with local and regional practices. Exposure scenarios that may be considered include drinking water, crop irrigation and livestock watering, the ingestion of dairy products, livestock, fish, crops, and soil, the inhalation of resuspended particles, and external exposure.	Yes	The all pathways analysis considered groundwater uses consistent with local and regional practices. Exposure pathways (Section 3.3.4) include drinking contaminated water, ingesting contaminated food, ingesting and inhaling contaminated soil, and direct irradiation from the contaminated soil. The exposure pathways and scenarios are consistent with other Hanford performance assessments.	No issues.	Same approach (see Section 3.3.4)
3.1.1.l.4. Exposure pathways from the transport of contamination in the atmosphere that may be considered include potential exposure from immersion in air contaminated with volatile and nonvolatile radionuclides, deposition of volatile and nonvolatile radionuclides, and subsequent exposure from direct radiation, ingestion, and resuspension.	Yes	The analysis of potential exposure from the air pathway (Section 4.12) considered a limited set of radionuclides (^{3}H, ^{14}C, and ^{222}Rn) and a limited set of exposure pathways (inhalation and immersion). These assumptions are reasonable and are consistent with other Hanford PAs.	No issues.	Same approach (see Section 4.12)

LFRG Comments on Performance Assessment for Hanford Immobilized Low-Activity Tank Waste, 7/27/99.

Criteria	Criteria met?	Response	Issues	This Document
3.1.1.l.5. Exposure scenarios from the transport of contamination in air that may be considered include residential and gardening activities which include the direct inhalation of volatile and nonvolatile radionuclides, external exposure, ingestion of crops, soil, livestock, dairy products, and inhalation of resuspended particles.	Yes	Exposure scenarios for the transport of contamination in air are discussed in Section 4.12. Based on past performance assessments at Hanford, the analysis of airborne contamination is limited to three radionuclides (^{3}H, ^{14}C, and ^{222}Rn). The scenarios include inhalation and immersion in contaminated air.	No issues.	Same approach (see Section 4.12)
3.1.1.l.6. Exposure pathways from inadvertent intrusion into the waste disposal units identify the chronic and acute exposure pathways for each of the exposure scenarios considered. The exposure pathways include all relevant ingestion, external exposure, and inhalation pathways for each exposure scenario. [Direct ingestion of contaminated groundwater and exposures to radon should not be considered for inadvertent intrusion, because they are considered separately.]	Yes	The analysis of inadvertent intrusion (Section 5) identified the chronic and acute exposure pathways considered in the exposure scenarios. The chronic scenario was the homesteader scenario while for acute exposure, the well driller scenario was used. The exposure scenarios include all relevant pathways; direct ingestion of contaminated groundwater and exposures to radon are not considered.		Same approach (see Section 5)
3.1.1.l.7. Acute exposure scenarios for inadvertent intrusion considers direct intrusion into the disposal site and exhumation of accessible waste material. Relevant scenarios that may be considered include discovery, residential construction, and well drilling that incorporate external exposure, inhalation of resuspended particles, and ingestion of particles.	Yes	The acute scenario considered well drilling, direct intrusion into the disposal site and the exhumation of waste. The analysis properly rejected consideration of construction scenarios based on the depth of disposed waste. The drilling scenario analyzed included external exposure, inhalation of resuspended particles, and ingestion of particles.	No issues.	Same approach (see Section 5)

LFRG Comments on Performance Assessment for Hanford Immobilized Low-Activity Tank Waste, 7/27/99.

Criteria	Criteria met?	Response	Issues	This Document
3.1.1.l.8. Chronic exposure scenarios for inadvertent intrusion consider direct intrusion into the disposal site and exhumation of accessible waste material. Relevant scenarios that may be considered include residential use and post-construction, and post drilling agricultural use, that incorporate the ingestion of foodstuffs, ingestion of soil, external exposure, and inhalation of resuspended particles.	Yes	The chronic exposure scenario considered, the homesteader scenario (Section 5.2), includes direct intrusion into the disposal site and exhumation of waste. This scenario properly considered removal of waste by drilling rather than construction. The analysis included all relevant pathways and is consistent with other Hanford performance assessments.	No issues.	Same approach (see Section 5.3)
3.1.1.m. PA provides a coherent presentation of the relevant descriptive information concerning the site, the disposal facility, the waste characteristics that are reflected in the conceptual model, and the selection of the mathematical models used in the analysis. The descriptive information and the approach to modeling provide the necessary results to evaluate the exposure pathways and scenarios that are important to assess the performance of the disposal facility.	Yes	The description of the site, disposal facility, waste characteristics, and mathematical models are presented in a complete and coherent manner. The results are presented in a complete manner. However, no supporting information is provided to indicate that the assumed glass performance can actually be achieved.	No evidence that assumed glass performances can be expected to be achieved. Issue is being addressed by Hanford's additional research activities as noted in the supplemental information (see Appendix F).	Same approach, except for glass. This PA uses experimental data and calculations to simulate waste form performance (see Sections 3.3.3, 3.4.4, and 3.5.3.1. for glass.)

LFRG Comments on Performance Assessment for Hanford Immobilized Low-Activity Tank Waste, 7/27/99.

Criteria	Criteria met?	Response	Issues	This Document
3.1.1.n. The calculated results presented in the PA are consistent with the site characteristics, the waste characteristics, and the conceptual model of the facility. The demonstration of consistency is supported by available site monitoring data and supporting field investigations.	Yes	The calculated results are presented in a thorough and complete manner. (See sections 3, 4, and 5. The results are generally consistent with site and waste characteristics. However, no evidence is provided that the long term performance of the glass waste form can actually be achieved.	Insufficient justification for assumed glass performance. Issue is being addressed by Hanford's additional research activities as noted in the supplemental information (see Appendix F).	Same approach, except for glass. This PA uses experimental data and calculations to simulate waste form performance. See Sections 3.3.3, 3.4.4, and 3.5.3.1. for glass.
3.1.1.o. The models used for calculating the results presented in the PA are analyzed to identify the sensitive parameters in the analysis. The results of the sensitivity analysis are used to evaluate the uncertainty in the calculated results.	No	A deterministic base case was performed with a number of sensitivity analyses performed on a sub-system level (e.g., vadose-zone transport). However, some of the sensitivity analyses were performed with a different sub-system model (e.g., unit-cell model instead of the disposal facility model). The lack of consistency raises concern over the results and conclusions of the sensitivity analyses. No information was presented to relate the results of the unit cell model with the disposal facility model.	Lack of modeling consistency raises concern over the results and conclusions of the sensitivity analyses. In the factual accuracy review of the draft Review Team Report, Hanford disagreed with this comment.	No longer use unit cell model. Base case and sensitivity cases use same model. See Section 3.5.3.

LFRG Comments on Performance Assessment for Hanford Immobilized Low-Activity Tank Waste, 7/27/99.

Criteria	Criteria met?	Response	Issues	This Document
3.1.1.p. The results of the uncertainty analysis are interpreted as they relate to establishing reasonable assurance that the conclusions of the PA are correct.	Yes	The results of the uncertainty analysis are used in relation to reasonable assurance that conclusions are correct. However, no information is presented to indicate the assumed glass corrosion rate can actually be achieved.	Need assurance that assumed glass corrosion rates can actually be achieved. Issue is being addressed by Hanford's additional research activities as noted in the supplemental information (see Appendix F).	Same approach, except for glass. This PA uses experimental data and calculations to simulate waste form performance. See Sections 3.3.3, 3.4.4, and 3.5.3.1.
3.1.1.q. The PA integrates the results of the analysis, the uncertainty analysis, the performance measures, waste acceptance criteria, operating procedures, and applicable laws, regulations, policies and agreements to formulate conclusions.	No	The PA integrates the results of the analysis, the uncertainty analysis, the performance measures, etc. to formulate conclusions. However, the conclusions of the PA regarding compliance with the groundwater protection performance objective is not supported because no evidence is provided that the assumed glass waste form performance can actually be achieved.	No support for assumed glass waste form performance. Issue is being addressed by Hanford's additional research activities as noted in the supplemental information (see Appendix F).	Same approach, except for glass. This PA uses experimental data and calculations to simulate waste form performance. See Sections 3.3.3, 3.4.4, and 3.5.3.1.

LFRG Comments on Performance Assessment for Hanford Immobilized Low-Activity Tank Waste, 7/27/99.

Criteria	Criteria met?	Response	Issues	This Document
3.1.1.r. The PA includes an interpretation of the results that allows for a comparison to the performance measures used in the PA, and include any necessary limitations on facility design or operations that are required to meet the performance objectives.	Yes	The PA includes an interpretation of results compared to the Performance Objectives stated in Section 1.6. Section 6.3 discusses the requirements set by the results. Each performance objective discussion included the estimated impact compared to the base objective. Most discussions also included a list of key drivers or conditions that could affect the results.	No issues.	Same approach. See Section 7.2.
3.1.1.s. The PA discusses quality assurance measures applied to the preparation of the analysis and its documentation.	Yes	The description of quality assurance programs (Section 7) includes an overview description of the quality programs at various organizations that are involved in the ILAW project. In addition, the Hanford Environmental Dose Overview Panel reviewing approved dose calculations presented in the PA. Consequently, the discussion of quality programs is deemed complete.	No issues.	Same approach. See Appendix F
3.1.1.t. The PA includes an ALARA analysis, and if appropriate, the analytical methods for the ALARA assessment are described.	No	There is a minimal description of ALARA and similar activities in Section 4.11.	No issues.	Same approach. See Section 4.15
3.1.1.u. The PA included appendices or references to published documents and/or data that provide a basis for the discussions and analysis in the PA.	Yes	The appendices and references are complete to a fault. (See Section 9 and Appendices A-H).There is entirely too much reliance throughout the document on the references. For example, the general discussion on subsurface geology seems reasonable, however, details are vague. More traceable details should be present such as borehole logs and well completion drawings of the three new bore holes. Tables should be included that list pertinent boreholes and monitor wells with depth, toc, etc. Figure 2-10 poorly represents borehole locations. Consider using: a fold-out plate map, identify latitude and longitude coordinate system, fence diagram to illustrate geology in area of disposal.	Vagueness in the document as a result of over-reliance on reference material for important data that should be summarized in PA. In the factual accuracy review of the draft review team report, Hanford disagreed with this comment.	Same approach. However, we have included more details in main text.

LFRG Comments on Performance Assessment for Hanford Immobilized Low-Activity Tank Waste, 7/27/99.

Criteria	Criteria met?	Response	Issues	This Document
3.1.2. PA is Thorough and Technically Supported				
3.1.2.a. The PA presents an estimate of the radionuclide inventory of the radioactive waste disposed of and to be disposed of at the facility which is quantified and technically supported by records, data, studies and evaluations.	Yes	The waste being considered in this PA is from the Hanford high-level waste tanks. The waste was produced from chemical separation of fuel and target elements irradiated in the Hanford reactors. The inventory first considered all radionuclides produced at Hanford. Then, a simple and defensible screening methodology was employed to determine the most important radionuclides from the perspective of doses calculated in a PA. The resulting set of important radionuclides (p. 3-2) is consistent with previous Hanford PAs (i.e., those for the 200-E and 200-W burial grounds). The inventory of potentially important radionuclides was developed from generally reasonable assumptions regarding radionuclide production in reactors and partitioning in chemical processing and in the waste tanks. However, the estimate of ^{99}Tc inventory is likely to be considerably over stated (see detailed comments by H. Babad in Appendix).	No issues.	Same approach, see Section 3.2. H. Babad's comments were based on a contract signed by 1998 ILAW PA was submitted and on short-term experimental data. Although the experiments have been continued, the results are not definitive.
3.1.2.a.1. All of the radionuclides disposed and anticipated to be present in wastes to be disposed of are evaluated in the performance assessment. Any radionuclides screened from detailed analysis or having no inventory limit are identified, and the bases for these conclusions are supported and defensible	Yes	Same as Section 3.1.2.a response.	Same as Section 3.1.2.a issues.	See above

LFRG Comments on Performance Assessment for Hanford Immobilized Low-Activity Tank Waste, 7/27/99.

Criteria	Criteria met?	Response	Issues	This Document
3.1.2.a.2. Any estimates of the radionuclide inventory for past waste disposals are described and to the extent practical are based on past waste disposal records, a reasonable expectation of actual waste content based on a knowledge of the processes that generated the waste, calculations, sampling data, technical studies, and reasonable projections of waste to be disposed	Yes	Same as Section 3.1.2.a response..	Same as Section 3.1.2.a issues.	See above

LFRG Comments on Performance Assessment for Hanford Immobilized Low-Activity Tank Waste, 7/27/99.

Criteria	Criteria met?	Response	Issues	This Document
3.1.2.b. The physical and chemical characteristics of the waste disposed of in the past that affect the release and transport of radionuclides are identified. The physical and chemical characteristics of the waste form are quantified and supported by laboratory or field studies, or are based on referenced documentation.	No	The physical and chemical characteristics of the waste form were not quantified and do not seem to be supported by laboratory or field studies or referenced documentation. The base case simply assumed the glass waste form released contaminants at a rate equivalent to the TWRS privatization RFP specification of $1.4x10^{-13}$ s^{-1} (p.3-39). It was assumed that this rate remained constant over time (however, the dimensions of the waste form decreased at a constant rate). Initially, the waste form was assumed to be a non-fractured monolithic 1.2 x. 1.2 x. 1.8 m cube. No justification for the appropriateness of this assumption was provided. The preparers should have reviewed available data on glass leaching to put the assumed rate of glass corrosion into perspective. However, no attempt was made to relate the composition or properties of this glass with the glass that will be disposed in this disposal facility. The physical characteristics of the waste were taken into account in the release model, but it is not clear that they were conservatively simulated. The base case assumes that the glass is a monolith in the form of a cube (dimensions given above). A sensitivity case was analyzed where the waste form has the shape of a thin plate. The actual physical form of the waste will be highly dependent on conditions associated with pouring the glass into the container and handling of the filled containers. The glass may crack extensively. It is not clear that the cases analyzed bound the performance of an extensively cracked waste form. Sensitivity analyses consider a more mechanistic basis for performance of the waste form, assumed to be glass. Section 3.3.3 (page 3-20) contains a brief discussion of a scenario that would lead to release of radionuclides from a glass waste form. However, this scenario is not used in the analysis. Getter material (page 3-41) and waste conditioning layers (page 3-42) are mentioned but not used in the analysis.	The PA is only valid if the privatized contractor can demonstrate that the specified release rate can be met for both short and long time frames. There is no discussion of this aspect contained in the PA. Issue is being addressed by Hanford's additional research activities as noted in the supplemental information (see Appendix F).	This PA uses experimental data and calculations to simulate waste form performance. The ILAW program is committed to perform tests on the glass selected once the glass is selected. As noted in Section 7.5, it is highly likely that the glass selected will perform similarly to LAWABP1. Sensitivity case with high K_d for U and I provide insight into getter effect and water conditioning layer impact on waste form release is also discussed

LFRG Comments on Performance Assessment for Hanford Immobilized Low-Activity Tank Waste, 7/27/99.

Criteria	Criteria met?	Response	Issues	This Document
3.1.2.b. (continued) The physical and chemical characteristics of the waste disposed of in the past that affect the release and transport of radionuclides are identified. The physical and chemical characteristics of the waste form are quantified and supported by laboratory or field studies, or are based on referenced documentation.	No	Statements throughout the PA make clear that how release rate is controlled (i.e., the selection of waste forms and their performance) is the responsibility of the privatized contractor. Based on discussions with the PA analysts during the first Hanford site visit, the review team understood that the specific release rates in the waste form specification were derived from simple estimates of required disposal facility performance and not from capabilities of any specific waste forms. If this is true, then the base case analysis included in the PA does nothing more than confirm that the release rate selected for the contract specification was sufficiently small as to limit future doses to acceptable limits. This obviously circular argument leads to misleading statements, such as the one on page ES-ix. However, the authors recognize that more analysis must be done, as stated on page ES-xvii: The PA must show that these restrictions [e.g., release rates from waste forms] can be expected to be met. This task is attempted through the use of more mechanistic models contained in the sensitivity analyses. Some concerns related to the base case analysis include: The size assumed for the cubical waste form (page 3-42); The basis of equation 3.8 and its relationship to a cubic waste form (page 3-40; Basis for determining constant K4 (page 3-40); Basis for T=6.8E5 years (page 3-41); Concerns related to the sensitivity analysis include: Justification for spheres used as a waste form and their sizes (page C-3); Basis and justification for the release rate used in ARREST-CT (equation C.9); Basis and justification for the list of reactions used in the analysis (Table C.1); sensitivity analysis details that the fractional release rate will be met.	Same as Section 3.1.2.b. issues.	See above

LFRG Comments on Performance Assessment for Hanford Immobilized Low-Activity Tank Waste, 7/27/99.

Criteria	Criteria met?	Response	Issues	This Document
3.1.2.b. (continued) The physical and chemical characteristics of the waste disposed of in the past that affect the release and transport of radionuclides are identified. The physical and chemical characteristics of the waste form are quantified and supported by laboratory or field studies, or are based on referenced documentation.	No	In Appendix E (page E-42), a discussion is made claiming that use of computer models identified effects not seen in the laboratory (i.e., effects of ion exchange on pH). General concern that the model is giving correct information if it is not based on data derived from experimental sources. As a demonstration that the contract specification can be met, the PA is insufficient.	Same as Section 3.1.2.b. issues.	Note that the effect predicted has now been seen and measured (see Figure 3-8 in Section 3.4.4.3.)
3.1.2.c. Any inventory limits are developed from reasonable projections of waste to be disposed and analyses that consider the physical and chemical characteristics of the wastes if those characteristics affect the release and transport of the radionuclides.	No	Generally, the PA has identified significant parameters and has developed requirements for the facility and waste based on the analyses presented. Waste Acceptance Criteria (WAC) were developed from the analyses presented in the PA. However, as noted in criteria 3.1.1.i and 3.1.2.b, the assumed release rate of radionuclides from the glass waste form was that in the contract specification. No attempt was made to relate this assumed release rate to expected glass performance. In the analysis of compliance, the performance of glass LD6-5412 was assumed. There was no discussion of the performance of this glass in relation to that of glass expected to be produced.	No evidence is provided that the assumed glass waste form performance can be achieved. Thus, no assurance can be provided that performance objectives can reasonably be expected to not be exceeded. Issue is being addressed by Hanford's additional research activities as noted in the supplemental information (see Appendix F).	This PA uses experimental data and calculations to simulate waste form performance. See Sections 3.3.3, 3.4.4, and 3.5.3.1.

LFRG Comments on Performance Assessment for Hanford Immobilized Low-Activity Tank Waste, 7/27/99.

Criteria	Criteria met?	Response	Issues	This Document
3.1.2.d. The conceptual model is a reasonable interpretation of the existing geochemical geologic, meteorologic, hydrologic, and monitoring data for the site and disposal facility. The components of the conceptual model for the transport of radionuclides that are important to the conclusions relating to the long-term performance of the disposal facility are thoroughly analyzed. The assumptions incorporated into the conceptual model are consistent with the available data, related investigations, and theory related to the conceptual model. Any parameters included in the conceptual model are supported by data or related investigations relevant to the site and disposal facility.	Yes	Geochemical data is adequate (Table 3-8) and has adequate technical support. The sensitivity of this parameter has been adequately investigated for key radionuclides (e.g., page 4-50 *et seq.*). The geochemical data in the base case is adequately supported by data and investigations at the site, with appropriate references. The most mobile radionuclides (Sc, Tc) have been assigned a KD of O. Other radionuclides (U,I,C,S, and others) are assigned Kds less than 10 and at the bottom of the measured range for Hanford vadose zone soils. The sensitivity analysis examined both slight increases in the Kd for Se ad Tc and a decrease in the U and I Kd to zero. The sensitivity analysis for this parameter for these elements demonstrated that the dose from groundwater at 10,000 years is very dependent on this parameter for these elements. Finally, the long travel time of radionuclides in the groundwater results in significant radioactive decay of radionuclides with half lives less than 100 years. A table identifying calibration targets for recharge and head distributions for selected grids would be beneficial to the reader to better understand water balance, and observed vs. predicted fits. The water balance for the simulated post-Hanford conditions are provided in Chapter 3 (Section 3.5.3.3). Reference for the calibration fo the site-wdie model are provided in the same section.	No issues.	Same approach. Note that site-specific measurements indicate that I is mobile, while Se is not. See Section 3.4.3.3.

LFRG Comments on Performance Assessment for Hanford Immobilized Low-Activity Tank Waste, 7/27/99.

Criteria	Criteria met?	Response	Issues	This Document
3.1.2.e. The assumptions of the performance assessment related to the waste, site, and facility design and operations which are critical to the conclusions of the performance assessment are supported and the uncertainties associated with these assumptions are analyzed as part of the performance assessment. Credits for the performance of engineered features and site closure included in the conceptual model are based on data derived from field investigations, related investigations, or documented sources of information relevant to the site and disposal facility.	No	Assumptions related to the performance of the site and the facility are supported and uncertainties are analyzed. Credits for engineered features, including site closure, are derived from field investigations and other documented sources. However, as noted in criteria 3.1.1.i and 3.1.2.b, the assumed radionuclide release rate from the glass waste form is simply the contract specification for short-term release. There is no discussion of the relation of the assumed release rate and observed release rates of glass waste forms.	Noted in criteria 3.1.1.i and 3.1.2.b, the assumed radionuclide release rate from the glass waste form is simply the contract specification for short-term release. There is no discussion of the relation of the assumed release rate and observed release rates of glass waste forms. Issue is being addressed by Hanford's additional research activities as noted in the supplemental information (see Appendix F).	Same approach except for waste form. This PA uses experimental data and calculations to simulate waste form performance. See Sections 3.3.3, 3.4.4, and 3.5.3.1.
3.1.2.f. The conceptual model for the source term, groundwater flow, and radionuclide transport includes parameters for unsaturated and saturated flow, total and effective porosity, hydraulic conductivity, water retention, relative permeability relationships, volumetric water content, retardation, and diffusion that are based on data, related investigations, or documented references relevant to the site and disposal facility.	Yes	The vadose-zone parameters provided in Table 3-6 (p. 3-30) need further justification as to how they were obtained from Khaleel (1995). Were these parameters averaged over different soil types? See Section 3.1.2.d for geochemical discussions.		Same approach. The discussion in Section 3.4.3.2.2 has been expanded to address comment.

LFRG Comments on Performance Assessment for Hanford Immobilized Low-Activity Tank Waste, 7/27/99.

Criteria	Criteria met?	Response	Issues	This Document
3.1.2.g. The mathematical models used in the performance assessment for analyzing air and water transport of radionuclides are appropriate for the disposal facility and disposal site. The selected models provide a justified representation of the technically important mechanisms identified in the conceptual model, and provide calculated results that are a defensible basis for formulating conclusions.	Yes	Models used for the air pathways are appropriate and are consistent with the other Hanford performance assessments. PA should provide text on how radionuclide concentrations are transferred between the vadose and aquifer models. PA should consider that if the grid sizes are different, artificial dilution is occurring between the unsaturated- and saturated-zones.	Issues related to vadose zone modeling and interface between vadose and saturated zone matrix.	Same approach. Text added in Section 3.5.3.3.2.
3.1.2.g.1. The input data for the mathematical models are derived from field data from the site, laboratory data interpreted for field applications, or referenced literature sources which are applicable to the site. Assumptions which are used to formulate input data are justified and have a defensible technical basis.	Yes	The units on equations ES.3 & ES.4 (p. ES xv) are not consistent.		Units checked
3.1.2.g.2. Intermediate calculations are performed and results are presented that demonstrate, by comparison to site data or related investigations, the calculations of the mathematical models used in the performance assessment are representative of disposal site and facility behavior for important mechanisms represented in the mathematical models	Yes	The air pathway model is sufficiently simple that presentation of intermediate results is not appropriate. The unit cell model was used as a surrogate for the disposal facility model in many of the sensitivity analyses. However, there were no intermediate calculations to demonstrate that this simplified model correlates well with the disposal facility model. Therefore, sensitivity analyses may be providing results that are not consistent with the base case.	Correlation of unit cell model and disposal facility model is required to demonstrate that the sensitivity analyses are representative relative to the base case.	Same approach, except that unit cell is no longer used.

LFRG Comments on Performance Assessment for Hanford Immobilized Low-Activity Tank Waste, 7/27/99.

Criteria	Criteria met?	Response	Issues	This Document
3.1.2.g.3. Representations of groundwater well performance (e.g., construction, diameter, yield, depth of penetration, screen length) are reasonable reflections of regional practices and are justified.	No	Well completions might not be ideally suited to 3-d modeling. This potential data gap should be considered in future PA iterations.		Data covered in Section 3.4.7 based on tri-county survey.
3.1.2.g.4. The mathematical models are tested, by comparison to analytical calculations or other models, to demonstrate that the results are consistent with the conceptual model, physical and chemical processes represented in the models, and available site data. The models are evaluated for defensibility and are reasonable representations of the disposal site and facility performance by comparison to available site data, related technical investigations, or referenced documentation or literature.	Yes	The verification of mathematical models is discussed in Section 3.5. Models were verified versus other codes, analytical solutions, or site data, as appropriate. However, some questions regarding fundamental modeling assumptions remain. They are: Are vadose-zone moisture contents and water fluxes simulated at steady-state? If not, what are the initial conditions? If they are not steady, as the text seems to indicate, then how can the transport equations given in Eq. D.6 (p. D-3), which are based on steady-state flow, be used?	No issues.	Discused in Section 3.5.2.?
3.1.2.g.5. The initial conditions, the boundary conditions, and the changes of properties with time for the mathematical model are analytically correct (i.e., well posed), and derived from existing site data and information.	Yes	Boundary conditions of pumping model are taken from site-wide model, but these boundary conditions will change based on pumping rates used in the pumping model. Other boundary conditions are identified and reasonable.	No issues.	Same approach (See Section 3.5.3.3). Note pumping has small effect on aquifer.

LFRG Comments on Performance Assessment for Hanford Immobilized Low-Activity Tank Waste, 7/27/99.

Criteria	Criteria met?	Response	Issues	This Document
3.1.2.h. The dose analysis considers the exposure pathways and transfer factors and calculates the maximum dose using acceptable methodologies and parameters.	Yes	The dose analysis considers exposure pathways and transfer factors using acceptable methodologies. The dose analysis of radionuclides uses transfer coefficients that are well supported by data and references. (See Appendix B and Section 5) The dose analysis specifies consumption rates, inhalation rates, and external exposure rates (i.e., occupancy) and conditions. The sources of these rates are identified and are justified. Section 3.4.7.1 discusses dose conversion factors, and Table B-7 shows the ratio of dose factor differences between DOE and EPA dose factors for ingestion. In reality, the EPA dose factors should be used, since they are the more recent compilation and were intended for government-wide use (See Section 6.3.2.2). As shown in the text (page 3-49 *et seq.*), this does not make a significant difference in the results. While some dose factors (e.g., Tc-99) are somewhat higher, this does not affect the results of the dose calculations in a significant way, as demonstrated by Table B-7. Consequently, the analysis is complete, albeit not with the use of the most appropriate dose factors. The maximum dose was projected for 10,000 years, rather than 1000 years. This period of analysis was selected because of Nuclear Regulatory Commission licensing requirements for incidental waste as produced during high level waste activities. Consequently, the decision to examine a 10,000 year period rather than a 1000 year period after closure is acceptable.	No issues.	Same approach, except that EPA dose factors are now used (See Section 3.4.7).
3.1.2.h. (continued) The dose analysis considers the exposure pathways and transfer factors and calculates the maximum dose using acceptable methodologies and parameters.	Yes	The methodologies and Parameters used are reasonable and are consistent with other Hanford performance assessments and are justified by the literature and site-specific investigations. It is noteworthy that, in the ILAW PA, the size of the garden has been reduced from 2,500 m^2 to 500 m^2. In the reviews of the earlier Hanford PAs, the larger garden size was controversial. The smaller size is reasonable and may be conservative.	Same as Section 3.1.2.h. issues.	See above.

LFRG Comments on Performance Assessment for Hanford Immobilized Low-Activity Tank Waste, 7/27/99.

Criteria	Criteria met?	Response	Issues	This Document
3.1.2.h.1. The dose analysis for exposures to radionuclides identifies the transfer coefficients between media and justifies the parameters used in the analysis with supporting data or references to the literature	Yes	Same as Section 3.1.2.h response.	Same as Section 3.1.2.h. issues.	See above.
3.1.2.h.2. The dose analysis specifies the consumption of radioactively contaminated materials for the exposure pathways evaluated, the inhalation rates of contaminated materials, and the external exposure rates and conditions to radioactive materials. These parameters are justified using references to the literature or site-specific investigations	Yes	Same as Section 3.1.2.h response.	Same as Section 3.1.2.h. issues.	See above
3.1.2.h.3. The dose analysis is conducted using effective dose equivalents in accordance with ICRP-30 (1979) and uses dose conversion factors from recognized published sources.	Yes	Same as Section 3.1.2.h. response.	Same as Section 3.1.2.h. issues.	See above

LFRG Comments on Performance Assessment for Hanford Immobilized Low-Activity Tank Waste, 7/27/99.

Criteria	Criteria met?	Response	Issues	This Document
3.1.2.h.4. The maximum dose projected for 1000 years after facility closure at the point of compliance is used in the analysis for evaluating disposal of LLW or establishing waste acceptance criteria for future disposals	Yes	The PA used 10,000 years instead of 1,000 years for the time of compliance. This was justified on the basis of being necessary to obtain NRC concurrence in the incidental waste determination that will be required by DOE 435.1.	No issues.	1,000 years is used for the time of compliance, but comparisons at 10,000 years also are given for NRC. See Section 1.6. Requirements are based on 10,000 year comparison.
3.1.2.i. The sensitivity and uncertainty analysis considers those parameters and mechanisms that are important to the conclusions relating to the long-term performance of the disposal facility, including radionuclide inventory, radionuclide characteristics, release rates, site and facility characteristics, groundwater flow parameters, site meteorology, and radionuclide transport parameters. Parametric and mechanistic variations analyzed in the uncertainty analysis that are important to the conclusions are justified as reasonable for the site and facility using data or related field investigations.	No	A deterministic base case was performed with a number of sensitivity analyses performed on a sub-system level (e.g., vadose-zone transport). However, the sensitivity analyses were occasionally performed with a different sub-system model (e.g., unit-cell model vs. disposal facility model). The lack of consistency raises concern over the results and conclusions of the sensitivity analyses. Additional sensitivity studies on hydrologic properties and strata types are needed. Specifically, the inclusion of heterogeneities in the vadose zone can lead to fast flow paths and should be considered in sensitivity analyses.	Lack of consistency between models used for the facility and sensitivity cases. Additional sensitivity analyses are needed to provide robustness to the analysis (e.g., vadose zone heterogeneities, poorer waste form performance).	Same sub-system models used throughout. See Section 3.5.3. More sensitivity studies run. See Section 3.5.5.

LFRG Comments on Performance Assessment for Hanford Immobilized Low-Activity Tank Waste, 7/27/99.

Criteria	Criteria met?	Response	Issues	This Document
3.1.2.i.1. The parameters important to the components of the analysis are analyzed to identify the sensitive parameters, and the selection of sensitive parameters is quantitatively justified	No	Same as Section 3.1.2.i response.	Same as Section 3.1.2.i. issues.	See above
3.1.2.i.2. The sensitive parameters are analyzed for uncertainty in the results of the analysis to provide quantitative bounds for interpreting the results of the analysis.	No	Same as Section 3.1.2.i response.	Same as Section 3.1.2.i. issues.	See above
3.1.2.i.3. The results of the sensitivity analysis are determined using a prescribed methodology that is technically justified. The results of the analysis provide the necessary information to justify the assumptions and conclusions of the performance assessment.	No	Same as Section 3.1.2.i response.	Same as Section 3.1.2.i. issues.	See above
3.1.2.i.4. The maximum projected dose and time of occurrence is presented in the performance assessment to provide for understanding of the natural system being modeled and the behavior of the model.	No	Same as Section 3.1.2.i. response.	Same as Section 3.1.2.i. issues.	See above
3.1.2.j. The ALARA analysis provides a cost-benefit analysis that is an optimization of the collective or population dose based on the cost of dose reduction in the exposed population of $1,000 to $10,000 per person-rem averted. [ALARA analysis is not required if the projected individual or collective doses in the exposed population are trivial.]	No	Minimal ALARA discussion was presented. There is no explicit cost-benefit analysis relating to ALARA because conceptual facility designs were not available at the time of the report generation.	Minimal ALARA analysis.	Same approach, still do not have sufficient design information because of change to trench design.

LFRG Comments on Performance Assessment for Hanford Immobilized Low-Activity Tank Waste, 7/27/99.

Criteria	Criteria met?	Response	Issues	This Document
3.1.2.k. The inadvertent intruder analysis considers the natural and man-made processes that impact the possible exposure to an intruder and calculates the dose using acceptable methodologies and parameters.	Yes	The inadvertent intruder analysis has considered reasonable natural and man-made processes that impact the possible exposure to an intruder. The dose resulting from the scenarios was calculated using acceptable methodologies and parameters. The analysis considers reduction in radionuclide concentration by mixing with soil in a garden. It is noteworthy that the ILAW PA used a more conservative value for the size of the garden than the value used in previous performance assessments (the value used in previous assessments was considered too large by some reviewers).	No issues.	Same approach. (See Section 5.)
3.1.2.k.1. The inadvertent intruder analysis specifies the reductions in concentrations of radioactive material from mixing with uncontaminated material or the transport of radionuclides from the disposed waste mass, and justifies the parameters used in the analysis with site data, supporting analysis or referenced information.	Yes	Same as Section 3.1.2.k response.	Same as Section 3.1.2.k issues.	See above
3.1.2.k.2. The inadvertent intruder analysis accounts for naturally occurring processes (e.g., erosion, precipitation, flooding) and the degradation of engineered barriers in the calculation of results	Yes	Same as Section 3.1.2.k response.	Same as Section 3.1.2.k issues.	See above

LFRG Comments on Performance Assessment for Hanford Immobilized Low-Activity Tank Waste, 7/27/99.

Criteria	Criteria met?	Response	Issues	This Document
3.1.2.k.3. The inadvertent intruder analysis calculates the maximum dose from disposed materials during the period of 100–1000 years after site closure for waste acceptance criteria for wastes to be disposed of in the disposal facility using the recommendations of ICRP-30 (1979) and dose conversion factors from recognized published sources.	Yes	The inadvertent intruder analysis has assumed that the Hanford barrier used to cover the closed disposal facility remains intact for 1,000 years. The PA assumed that the concrete vaults would be degraded at 500 years. These assumptions are considered reasonable. The inadvertent intruder analysis presented the dose calculated over the 1,000 year period of compliance. The dose calculation used dose conversion factors from recognized published sources that are consistent with ICRP-30. The maximum dose is used to assess disposal facility performance and establish waste acceptance criteria.	No issues.	Same approach. See Section 5.
3.1.2.l. The results of the analyses for transport of radionuclides and the inadvertent intrusion into the disposal facility, and the sensitivity and uncertainty of the calculated results are comprehensive representations of the existing knowledge of the site and the disposal facility design and operations.	Yes	Based on the caveat of existing knowledge of the site and since building criteria into the facility design and waste form requirements, the results are a reasonable representation. Specific facility design criteria have not been fully defined such as: cover design, including the hydraulic diverter; getter usage; filler material, therefore leaving flexibility within the design to compensate for waste form deviations if necessary. This is not explicitly stated though implied and leads to concern since decisions have not been made.	Not all facility design factors have been selected.. If design criteria are different than the scenarios completed, PA changes will have to be made.	Same approach.

LFRG Comments on Performance Assessment for Hanford Immobilized Low-Activity Tank Waste, 7/27/99.

Criteria	Criteria met?	Response	Issues	This Document
3.1.3. PA Conclusions Are Valid and Acceptable				
3.1.3.a. The performance assessment presents valid conclusions that demonstrate that the all-pathways analysis, air pathway analysis, groundwater resource protection analysis, and inadvertent intruder analysis meet the performance objectives of DOE Order 5820.2A.	No	The performance assessment conclusions are not valid due to the incomplete information regarding waste form performance. See criterion 3.1.2.b.	Waste form performance not demonstrated. Issue is being addressed by Hanford's additional research activities as noted in the supplemental information (see Appendix F).	This PA uses experimental data and calculations to simulate waste form performance. Comparisons show increased margin over the 1998 ILAW PA. See Sections 3.3.3, 3.4.4, and 3.5.3.1.
3.1.3.a.1. The all pathways performance objective of 25 mrem/year effective dose equivalent is met over the performance period of 1000 years for all radionuclides disposed of in the disposal facility.	No	Same as Section 3.1.3.a. response.	Same as Section 3.1.3.a. issues.	See above
3.1.3.a.2. The air pathways performance objective of 10 mrem/year effective dose equivalent is met over the performance period of 1000 years for all radionuclides disposed of in the disposal facility.	Yes	The air pathways performance objective is met over the 10,000-year period justified for this analysis.	No issues.	Same approach and results. See Sections 4.12 and 7.2.5.

LFRG Comments on Performance Assessment for Hanford Immobilized Low-Activity Tank Waste, 7/27/99.

Criteria	Criteria met?	Response	Issues	This Document
3.1.3.a.3. The radon performance objective of an average flux of 20 pCi/m^2/s at the disposal surface or 0.5 pCi/L in air at the point of compliance is met over the performance period of 1000 years for all radionuclides disposed of in the disposal facility.	Yes	This measure is met by two entirely separate analytical approaches. First, there are insufficient radon precursors to generate significant radon. Second, the thick cover over the disposed waste reduces radon emissions by providing a thick cover that attenuates the diffusion of radon into the air. Consequently, the emissions of radon are trivial and the performance measure is met.	No issues	Same approach and results. See Sections 4.12 and 7.2.5.
3.1.3.a.4. The groundwater resource performance measures for all radionuclides to be disposed of in the disposal facility are met over the performance period of 1000 years at the prescribed point of compliance.	No	The conclusion that the groundwater protection performance objective is met is not valid because no evidence that the assumed glass waste form performance is likely to be realized is provided.	Glass waste form performance was not demonstrated. Issue is being addressed by Hanford's additional research activities as noted in the supplemental information (see Appendix F).	This PA uses experimental data and calculations to simulate waste form performance. Comparisons show increased margin over the 1998 ILAW PA. See Sections 3.3.3, 3.4.4, and 3.5.3.1. See Section 7.2 for comparison with performance objectives.

LFRG Comments on Performance Assessment for Hanford Immobilized Low-Activity Tank Waste, 7/27/99.

Criteria	Criteria met?	Response	Issues	This Document
3.1.3.a.5. The inadvertent intruder performance objectives of 100 mrem/year effective dose equivalent for chronic exposure and 500 mrem effective dose equivalent for acute exposure are met within the disposal facility over the performance period of 1000 years.	Yes	The inadvertent intruder performance objectives of 100 mrem/year for chronic exposure and 500 mrem for acute exposure are met for the period from about 200 years to 1,000 years and beyond. The results for the homesteader scenario exceed the 100 mrem/year performance objective at 100 years following closure. However, the assumption that inadvertent intrusion will be prohibited for 500 years following closure by passive means (markers, etc.) is reasonable.	No issues.	Same approach and similar results. See Sections 5 and 7.2.2.
3.1.3.a.6. The condition that doses from the disposal of waste are ALARA has been demonstrated and incorporated into the design and operations of the disposal facility.	Yes	An adequate ALARA discussion has been presented based on the level of available detailed planning. No summary of ALARA considerations was presented; instead this considerations relied heavily on references.	Minimal ALARA analysis.	Same approach.

LFRG Comments on Performance Assessment for Hanford Immobilized Low-Activity Tank Waste, 7/27/99.

Criteria	Criteria met?	Response	Issues	This Document
3.1.3.b. The performance assessment conclusions incorporate the findings of the calculated results for the all pathways analysis, air pathway analysis, groundwater resource protection analysis, inadvertent intruder analysis, and sensitivity and uncertainty analysis. The results are interpreted and integrated to formulate conclusions which are supported by the results and the uncertainties in the results.	No	The PA conclusions do not incorporate all results because the waste form performance is not demonstrated and therefore cannot be interpreted into facility design criteria. See discussion of 3.1.2.b. and 3.1.2.e.	Waste form performance not demonstrated. Issue is being addressed by Hanford's additional research activities as noted in the supplemental information (see Appendix F).	This PA uses experimental data and calculations to simulate waste form performance. Comparisons show increased margin over the 1998 ILAW PA. See Sections 3.3.3, 3.4.4, and 3.5.3.1. See Section 7.2 for comparison to performance objectives.

LFRG Comments on Performance Assessment for Hanford Immobilized Low-Activity Tank Waste, 7/27/99.

Criteria	Criteria met?	Response	Issues	This Document
3.1.3.c. The conclusions of the performance assessment are applied to the facility design and operations. The resulting design constraints and limitations on operations can be reasonably accomplished at the disposal facility.	No	The results of the performance assessment have been interpreted to derive requirements on facility design, waste form and facility operations. These requirements were then examined in comparison with expected waste inventories, possible designs, etc. The conclusion is that the constraints can be readily met. However, the conclusion regarding waste form performance is not valid because no support for the assumed performance is provided.	No evidence provided that assumed waste form performance is achievable. Issue is being addressed by Hanford's additional research activities as noted in the supplemental information (see Appendix F).	This PA uses experimental data and calculations to simulate waste form performance. Comparisons show increased margin over the 1998 ILAW PA See Sections 3.3.3, 3.4.4, and 3.5.3.1. See Section 7.6 for requirements.

LFRG Comments on Performance Assessment for Hanford Immobilized Low-Activity Tank Waste, 7/27/99.

Criteria	Criteria met?	Response	Issues	This Document
3.1.3.d. The conclusions of the performance assessment address and incorporate any constraints included in any Federal, state, and local statutes or regulations or agreements that impact the site design, facility design, or facility operations. The conclusions also address and incorporate any procedural or site documentation changes or constraints due to the results of the facility performance assessment. Reasonable assurance exists that these constraints and impacts are appropriately addressed in the performance assessment.	No	This criterion is met with the exception of the constraint of long-term glass performance. No evidence is provided that the assumed performance can be achieved.	Same as Section 3.1.3.c. issues.	This PA uses experimental data and calculations to simulate waste form performance. Comparisons show increased margin over the 1998 ILAW PA. See Sections 3.3.3, 3.4.4, and 3.5.3.1. Also see Section 7.5.

LFRG Comments on Performance Assessment for Hanford Immobilized Low-Activity Tank Waste, 7/27/99.

Criteria	Criteria met?	Response	Issues	This Document
3.1.3.e. The analysis, results, and conclusions of the performance assessment provide both a reasonable representation of the disposal facility=s long-term performance and a reasonable expectation that the disposal facility will remain in compliance with DOE Order 5820.2A	No	This criterion is met with the exception of the constraint of long-term glass performance. No evidence is provided that the assumed performance can be achieved.	Same as Section 3.1.3.c. issues.	This PA uses experimental data and calculations to simulate waste form performance. Comparisons show increased margin over the 1998 ILAW PA. See Sections 3.3.3, 3.4.4, and 3.5.3.1.Also see Section 7.5.

Appendix B

Dosimetry Dose Factors

Table B-1. Radionuclides to be Considered and Their Half Lives.

Nuclide	Half life (years)	Short-lived progeny in equilibrium with parent
H-3	12.33	
Be-10	1.600E+06	
C-14	5,730	
Na-22	2.6019	
Si-32+D	329.56	P-32
Cl-36	300,992	
K-40	1.277E+09	
Ti-44+D	47.30	Sc-44
V-49	0.92539 (338 d)	
Mn-54	0.85454 (312.12 d)	
Fe-55	2.7299	
Co-60	5.2713	
Ni-59	74,999	
Ni-63	100.10	
Se-79	805,000	
Rb-87	4.800E+10	
Sr-90+D	28.149	Y-90
Zr-93	1.530E+06	
Nb-91	680	
Nb-93m	16.13	
Nb-94	20,300	
Mo-93	3,500	
Tc-99	211,097	
Ru-106+D	1.01736 (371.59 d)	Rh-106
Pd-107	6.50E+06	
Ag-108m+D	127.00	Ag-108 (0.087)

Table B-1. Radionuclides to be Considered and Their Half Lives.

Nuclide	Half life (years)	Short-lived progeny in equilibrium with parent
Cd-109	1.26653 (462.6 d)	
Cd-113m	14.10	
In-115	4.410E+14	
Sn-121m+D	54.998	Sn-121 (0.776)
Sn-126+D	246,000	Sb-126m, Sb-126 (0.14)
Sb-125	2.7299	
Te-125m	0.15880 (58 d)	
I-129	1.570E+07	
Cs-134	2.0619	
Cs-135	2.30E+06	
Cs-137+D	29.999	Ba-137m (0.9443)
Ba-133	10.520	
Pm-147	2.6233	
Sm-147	1.060E+11	
Sm-151	89.997	
Eu-150	35.798	
Eu-152	13.330	
Eu-154	8.5919	
Eu-155	4.680	
Gd-152	1.080E+14	
Ho-166m	1,200	
Re-187	5.000E+10	
Tl-204	3.7801	
Pb-205	1.520E+07	
Pb-210+D	22.300	Bi-210
Bi-207	32.198	
Po-209	102.0	

Table B-1. Radionuclides to be Considered and Their Half Lives.

Nuclide	Half life (years)	Short-lived progeny in equilibrium with parent
Po-210	0.37886 (138.38 d)	
Ra-226+D	1,600	Rn-222, Po-218, Pb-214, Bi-214, Po-214(0.9998)
Ra-228+D	5.7498	Ac-228
Ac-227+D	21.769	Th-227(0.9862), Fr-223(0.0138), Ra-223, Rn-219, Po-215, Pb-211, Bi-211, Tl-207(.99725), Po-211(.00275)
Th-228+D	1.9129	Ra-224, Rn-220, Po-216, Pb-212, Bi-212, Po-212(0.6406), Tl-208(0.3594)
Th-229+D	7,340	Ra-225, Ac-225, Fr-221, At-217, Bi213, Po-213(0.9784), Tl-209(0.0216)
Th-230	75,380	
Th-232	1.405E+10	
Pa-231	32,759	
U-232	69.799	
U-233	159,198	
U-234	245,694	
U-235+D	7.037E+08	Th-231
U-236	2.342E+07	
U-238+D	4.468E+09	Th-234, Pa-234m, Pa-234 (0.0013)
Np-237+D	2.140E+06	Pa-233
Pu-236	2.8999	
Pu-238	87.697	
Pu-239	24,110	
Pu-240	6,563	
Pu-241+D	14.350	U-237 (2.39E-05)
Pu-242	373,507	
Pu-244+D	8.000E+07	U-240 (0.9988), Np-240m, Np-240 (0.0012)
Am-241	432.70	
Am-242m+D	141.00	Am-242(0.9955), Np-238(0.0045)
Am-243+D	7,370	Np-239

Table B-1. Radionuclides to be Considered and Their Half Lives.

Nuclide	Half life (years)	Short-lived progeny in equilibrium with parent
Cm-242	0.44611 (162.94 d)	
Cm-243	28.499	
Cm-244	18.100	
Cm-245	8,500	
Cm-246	4,730	
Cm-247+D	1.600E+07	Pu-243
Cm-248	339,981	
Cm-250+D	11,300	Pu-246(0.25), Am-246(0.25), Bk-250(0.14)
Bk-247	1,394	
Cf-248	0.91294 (333.45 d)	
Cf-249	350.60	
Cf-250	13.080	
Cf-251	897.98	
Cf-252	2.6449	

Note: Parentheses show (1) half-lives that are normally given in days, and (2) branching ratios that differ from 1.00.

Table B-2. Decay Chains Actually Computed.

Zr-93	→	Nb-93m				
Mo-93	→	Nb-93m				
Sb-125	→ .230	Te-125m				
Pm-147	→	Sm-147				
Eu-152	→ .2792	Gd-152				
Pb-210	→	Po-210				
Po-209	→ .9974	Pb-205				
Ra-226	→	Pb-210	→	Po-210		
Ra-228	→	Th-228				
Th-230	→	Ra-226	→	Pb-210	→	Po-210
Th-232	→	Ra-228	→	Th-228		
Pa-231	→	Ac-227				
U-232	→	Th-228				
U-233	→	Th-229				
U-234	→	Th-230	→	Ra-226	→	Pb-210
U-235	→	Pa-231	→	Ac-227		
Pu-236	→	U-232	→	Th-228		
Pu-238	→	U-234				
Pu-241	→	Am-241	→	Np-237		
Pu-244	→	Pu-240				
Am-241	→	Np-237				
Am-242m	→ .827 → .173	Cm-242 Pu-242	→	Pu-238	→	U-234
Am-243	→	Pu-239				
Cm-242	→	Pu-238	→	U-234		

Table B-2. Decay Chains Actually Computed.

Cm-243	→	Pu-239				
	→ .0024	Am-243				
Cm-244	→	Pu-240				
Cm-245	→	Pu-241	→	Am-241	→	Np-237
Cm-247	→	Am-243				
Cm-250	→	Cf-250				
	→ .14	Cm-246				
	.25					
Bk-247	→	Am-243				
Cf-248	→	Cm-244	→	Pu-240		
Cf-249	→	Cm-245	→	Pu-241	→	Am-241
Cf-250	→	Cm-246				
Cf-251	→	Cm-247				
Cf-252	→	Cm-248				

Notes:

1) Decay times are assumed to be less than 1000 years so that the ingrowth of progeny with long half-lives can be ignored.

2) There is a slight increase in the Pu-238 and U-234 for the Am-242m decay chain that is not shown. This is a result of the low-probability alpha decay of Am-242m. The complete chain is, Am-242m(0.00455)--->Np-238--->Pu-238--->U-234.

Table B-3. No Water Infiltration Case: Intruder.
Units are mrem per Ci exhumed.

Nuclide	External	Internal	Ingest	Inhale
H-3	0.00	1.44E-03	1.42E-03	2.05E-05
Be-10	2.15E-01	1.79E-01	1.04E-01	7.55E-02
C-14	2.73E-03	4.69E-02	4.64E-02	4.46E-04
Na-22	2.39E+03	2.57E-01	2.56E-01	1.63E-03
Si-32+D	2.28E+00	4.64E-01	2.44E-01	2.20E-01
Cl-36	4.64E-01	7.20E-02	6.73E-02	4.67E-03
K-40	1.73E+02	4.16E-01	4.13E-01	2.65E-03
Ti-44+D	2.40E+03	6.43E-01	5.47E-01	9.64E-02
V-49	0.00	1.44E-03	1.36E-03	7.36E-05
Mn-54	9.08E+02	6.30E-02	6.16E-02	1.43E-03
Fe-55	0.00	1.41E-02	1.35E-02	5.74E-04
Co-60	2.75E+03	6.44E-01	5.98E-01	4.67E-02
Ni-59	0.00	4.95E-03	4.67E-03	2.82E-04
Ni-63	0.00	1.35E-02	1.28E-02	6.61E-04
Se-79	3.78E-03	1.95E-01	1.93E-01	2.10E-03
Rb-87	2.85E-02	1.10E-01	1.09E-01	6.89E-04
Sr-90+D	4.68E+00	3.45E+00	3.40E+00	5.29E-02
Zr-93	0.00	1.05E-01	3.69E-02	6.85E-02
Nb-91	2.30E+00	1.78E-02	1.16E-02	6.23E-03
Nb-93m	2.11E-02	1.78E-02	1.16E-02	6.23E-03
Nb-94	1.72E+03	2.47E-01	1.59E-01	8.83E-02
Mo-93	1.20E-01	3.61E-02	3.00E-02	6.06E-03
Tc-99	2.54E-02	3.42E-02	3.24E-02	1.78E-03
Ru-106+D	2.33E+02	7.11E-01	6.09E-01	1.02E-01
Pd-107	0.00	6.04E-03	3.31E-03	2.73E-03
Ag-108m+D	1.75E+03	2.30E-01	1.69E-01	6.04E-02
Cd-109	2.99E+00	3.15E-01	2.91E-01	2.43E-02
Cd-113m	1.30E-01	3.90E+00	3.58E+00	3.26E-01
In-115	8.04E-02	4.31E+00	3.51E+00	7.98E-01
Sn-121m+D	4.28E-01	5.25E-02	5.00E-02	2.54E-03
Sn-126+D	2.14E+03	4.90E-01	4.69E-01	2.15E-02

Table B-3. No Water Infiltration Case: Intruder.
Units are mrem per Ci exhumed.

Nuclide	External	Internal	Ingest	Inhale
Sb-125	4.48E+02	6.50E-02	6.24E-02	2.60E-03
Te-125m	3.07E+00	8.31E-02	8.16E-02	1.56E-03
I-129	2.63E+00	6.17E+00	6.13E+00	3.71E-02
Cs-134	1.70E+03	1.64E+00	1.63E+00	9.88E-03
Cs-135	7.76E-03	1.58E-01	1.57E-01	9.71E-04
Cs-137+D	6.12E+02	1.12E+00	1.11E+00	6.81E-03
Ba-133	3.74E+02	7.72E-02	7.56E-02	1.67E-03
Pm-147	1.01E-02	3.17E-02	2.33E-02	8.36E-03
Sm-147	0.00	2.00E+01	4.11E+00	1.59E+01
Sm-151	2.00E-04	1.50E-02	8.64E-03	6.40E-03
Eu-150	1.58E+03	1.99E-01	1.41E-01	5.72E-02
Eu-152	1.22E+03	1.91E-01	1.44E-01	4.71E-02
Eu-154	1.34E+03	2.73E-01	2.12E-01	6.10E-02
Eu-155	3.70E+01	4.28E-02	3.40E-02	8.83E-03
Gd-152	0.00	5.54E+01	3.58E+00	5.18E+01
Ho-166m	1.86E+03	3.44E-01	1.79E-01	1.65E-01
Re-187	0.00	2.23E-04	2.11E-04	1.16E-05
Tl-204	8.16E-01	7.52E-02	7.47E-02	5.14E-04
Pb-205	1.43E-03	3.71E-02	3.62E-02	8.36E-04
Pb-210+D	1.20E+00	1.22E+02	1.19E+02	2.94E+00
Bi-207	1.64E+03	1.26E-01	1.22E-01	4.27E-03
Po-209	3.58E+00	5.54E+01	5.29E+01	2.52E+00
Po-210	9.28E-03	4.42E+01	4.22E+01	2.01E+00
Ra-226+D	1.91E+03	3.14E+01	2.96E+01	1.83E+00
Ra-228+D	1.05E+03	3.31E+01	3.20E+01	1.08E+00
Ac-227+D	3.84E+02	1.76E+03	3.29E+02	1.43E+03
Th-228+D	1.68E+03	9.16E+01	1.80E+01	7.36E+01
Th-229+D	2.99E+02	5.50E+02	8.96E+01	4.61E+02
Th-230	2.42E-01	8.17E+01	1.22E+01	6.95E+01
Th-232	1.05E-01	4.11E+02	6.07E+01	3.50E+02
Pa-231	3.64E+01	5.09E+02	2.36E+02	2.73E+02

Table B-3. No Water Infiltration Case: Intruder.
Units are mrem per Ci exhumed.

Nuclide	External	Internal	Ingest	Inhale
U-232	1.81E-01	1.70E+02	2.91E+01	1.41E+02
U-233	2.74E-01	3.52E+01	6.42E+00	2.88E+01
U-234	8.12E-02	3.44E+01	6.29E+00	2.82E+01
U-235+D	1.50E+02	3.22E+01	5.93E+00	2.62E+01
U-236	4.32E-02	3.26E+01	5.98E+00	2.67E+01
U-238+D	2.41E+01	3.11E+01	5.96E+00	2.52E+01
Np-237+D	2.11E+02	2.14E+02	9.87E+01	1.15E+02
Pu-236	4.56E-02	5.69E+01	2.60E+01	3.09E+01
Pu-238	3.06E-02	1.55E+02	7.11E+01	8.36E+01
Pu-239	5.76E-02	1.70E+02	7.87E+01	9.15E+01
Pu-240	2.97E-02	1.70E+02	7.87E+01	9.15E+01
Pu-241+D	3.78E-03	3.28E+00	1.52E+00	1.76E+00
Pu-242	2.60E-02	1.62E+02	7.47E+01	8.77E+01
Pu-244+D	3.62E+02	1.60E+02	7.38E+01	8.60E+01
Am-241	8.88E+00	1.76E+02	8.09E+01	9.47E+01
Am-242m+D	1.33E+01	1.69E+02	7.82E+01	9.09E+01
Am-243+D	1.77E+02	1.75E+02	8.07E+01	9.39E+01
Cm-242	3.44E-02	6.25E+00	2.56E+00	3.69E+00
Cm-243	1.14E+02	1.21E+02	5.58E+01	6.55E+01
Cm-244	2.56E-02	9.78E+01	4.49E+01	5.29E+01
Cm-245	6.84E+01	1.80E+02	8.31E+01	9.71E+01
Cm-246	2.36E-02	1.78E+02	8.22E+01	9.62E+01
Cm-247+D	3.50E+02	1.64E+02	7.60E+01	8.83E+01
Cm-248	1.78E-02	6.54E+02	3.02E+02	3.52E+02
Cm-250+D	3.42E+02	3.73E+03	1.73E+03	2.01E+03

The "Internal" column is the sum of the "Inhale" and "Ingest" columns. External and internal doses are separated because the glass waste matrix will prevent a portion of the exhumed activity from contributing to the internal dose.

Table B-4. No Water Infiltration Case: Post-Intrusion Resident.
Units are mrem per Ci exhumed.

Nuclide	External	Internal	Garden	Ingest	Inhale
H-3	0.00	1.46E+02	1.46E+02	2.37E-02	5.58E-04
Be-10	2.41E+00	1.65E+01	8.21E+00	3.78E+00	4.50E+00
C-14	3.00E-02	7.20E+02	7.19E+02	1.65E+00	2.60E-02
Na-22	2.36E+04	3.05E+02	2.97E+02	8.17E+00	8.54E-02
Si-32+D	2.55E+01	4.39E+02	4.17E+02	8.86E+00	1.30E+01
Cl-36	4.78E+00	9.96E+04	9.96E+04	2.25E+00	2.56E-01
K-40	1.93E+03	5.16E+03	5.15E+03	1.49E+01	1.56E-01
Ti-44+D	2.68E+04	8.57E+01	6.02E+01	1.98E+01	5.71E+00
V-49	0.00	1.54E-01	1.16E-01	3.50E-02	3.09E-03
Mn-54	6.98E+03	2.64E+02	2.62E+02	1.54E+00	5.83E-02
Fe-55	0.00	1.28E+00	8.15E-01	4.34E-01	3.02E-02
Co-60	2.89E+04	1.86E+02	1.63E+02	2.04E+01	2.61E+00
Ni-59	0.00	4.68E+00	4.49E+00	1.70E-01	1.68E-02
Ni-63	0.00	1.28E+01	1.23E+01	4.66E-01	3.93E-02
Se-79	4.24E-02	1.24E+02	1.16E+02	7.05E+00	1.25E-01
Rb-87	3.20E-01	1.83E+02	1.79E+02	3.98E+00	4.10E-02
Sr-90+D	5.15E+01	2.00E+04	1.98E+04	1.21E+02	3.09E+00
Zr-93	5.03E-03	7.48E+00	2.03E+00	1.36E+00	4.09E+00
Nb-91	2.58E+01	2.65E+00	1.86E+00	4.23E-01	3.71E-01
Nb-93m	2.32E-01	2.61E+00	1.83E+00	4.14E-01	3.64E-01
Nb-94	1.93E+04	3.64E+01	2.54E+01	5.79E+00	5.27E+00
Mo-93	1.33E+00	4.47E+01	4.33E+01	1.09E+00	3.64E-01
Tc-99	1.69E-01	7.93E+02	7.92E+02	7.01E-01	6.28E-02
Ru-106+D	1.90E+03	2.29E+02	2.08E+02	1.61E+01	4.39E+00
Pd-107	0.00	3.52E+00	3.24E+00	1.20E-01	1.62E-01
Ag-108m+D	1.96E+04	3.02E+02	2.92E+02	6.15E+00	3.59E+00
Cd-109	2.58E+01	8.55E+02	8.45E+02	8.16E+00	1.11E+00
Cd-113m	1.42E+00	1.26E+04	1.24E+04	1.27E+02	1.89E+01
In-115	9.04E-01	3.61E+02	1.85E+02	1.28E+02	4.76E+01
Sn-121m+D	4.78E+00	1.12E+01	9.24E+00	1.81E+00	1.50E-01
Sn-126+D	2.41E+04	1.05E+02	8.71E+01	1.71E+01	1.28E+00
Sb-125	4.44E+03	3.57E+01	3.31E+01	2.48E+00	1.52E-01
Te-125m	7.80E+00	3.40E+00	2.71E+00	6.73E-01	2.10E-02
I-129	2.58E+01	6.70E+03	6.50E+03	1.95E+02	1.93E+00
Cs-134	1.62E+04	1.60E+03	1.55E+03	5.05E+01	5.00E-01
Cs-135	8.72E-02	1.75E+02	1.69E+02	5.73E+00	5.79E-02
Cs-137+D	6.80E+03	1.23E+03	1.19E+03	4.01E+01	4.01E-01
Ba-133	4.06E+03	3.43E+01	3.16E+01	2.66E+00	9.59E-02
Pm-147	1.00E-01	4.04E+00	2.85E+00	7.48E-01	4.38E-01
Sm-147	0.00	1.65E+03	5.52E+02	1.50E+02	9.51E+02
Sm-151	2.24E-03	1.85E+00	1.16E+00	3.14E-01	3.80E-01

Table B-4. No Water Infiltration Case: Post-Intrusion Resident.
Units are mrem per Ci exhumed.

Nuclide	External	Internal	Garden	Ingest	Inhale
Eu-150	1.76E+04	2.73E+01	1.89E+01	5.11E+00	3.38E+00
Eu-152	1.34E+04	2.69E+01	1.90E+01	5.12E+00	2.74E+00
Eu-154	1.44E+04	3.87E+01	2.77E+01	7.44E+00	3.50E+00
Eu-155	3.86E+02	5.97E+00	4.33E+00	1.15E+00	4.90E-01
Gd-152	0.00	3.70E+03	4.81E+02	1.30E+02	3.09E+03
Ho-166m	2.09E+04	4.05E+01	2.41E+01	6.54E+00	9.83E+00
Re-187	0.00	1.75E+00	1.74E+00	7.62E-03	6.85E-04
Tl-204	8.38E+00	6.22E+00	3.71E+00	2.49E+00	2.80E-02
Pb-205	1.61E-02	6.82E+00	5.45E+00	1.32E+00	4.99E-02
Pb-210+D	1.33E+01	2.47E+04	1.94E+04	5.11E+03	2.37E+02
Bi-207	1.83E+04	2.46E+01	2.00E+01	4.39E+00	2.52E-01
Po-209	4.01E+01	6.40E+03	4.33E+03	1.92E+03	1.50E+02
Po-210	4.79E-02	2.61E+03	1.85E+03	7.07E+02	5.49E+01
Ra-226+D	2.15E+04	4.79E+03	3.52E+03	1.15E+03	1.13E+02
Ra-228+D	1.40E+04	5.48E+03	3.54E+03	1.20E+03	7.40E+02
Ac-227+D	4.25E+03	1.13E+05	1.68E+04	1.18E+04	8.42E+04
Th-228+D	1.59E+04	4.97E+03	7.37E+02	5.52E+02	3.69E+03
Th-229+D	3.35E+03	3.49E+04	4.13E+03	3.27E+03	2.75E+04
Th-230	7.38E+00	5.16E+03	5.62E+02	4.45E+02	4.15E+03
Th-232	8.06E+02	2.61E+04	2.94E+03	2.29E+03	2.09E+04
Pa-231	4.78E+02	3.81E+04	1.17E+04	8.78E+03	1.76E+04
U-232	3.01E+03	1.38E+04	3.73E+03	1.15E+03	8.96E+03
U-233	3.21E+00	2.74E+03	8.05E+02	2.32E+02	1.70E+03
U-234	9.04E-01	2.68E+03	7.88E+02	2.27E+02	1.66E+03
U-235+D	1.66E+03	2.51E+03	7.44E+02	2.14E+02	1.55E+03
U-236	4.81E-01	2.54E+03	7.49E+02	2.16E+02	1.57E+03
U-238+D	2.61E+02	2.45E+03	7.46E+02	2.15E+02	1.49E+03
Np-237+D	2.30E+03	2.39E+04	1.38E+04	3.49E+03	6.66E+03
Pu-236	1.02E+01	3.60E+03	1.07E+03	8.49E+02	1.68E+03
Pu-238	3.43E-01	1.07E+04	3.11E+03	2.58E+03	4.97E+03
Pu-239	6.48E-01	1.18E+04	3.45E+03	2.87E+03	5.46E+03
Pu-240	3.34E-01	1.18E+04	3.45E+03	2.87E+03	5.46E+03
Pu-241+D	1.19E-01	2.31E+02	6.77E+01	5.66E+01	1.07E+02
Pu-242	2.92E-01	1.12E+04	3.28E+03	2.72E+03	5.23E+03
Pu-244+D	4.07E+03	1.11E+04	3.24E+03	2.69E+03	5.13E+03
Am-241	9.98E+01	1.23E+04	3.69E+03	2.95E+03	5.65E+03
Am-242m+D	1.47E+02	1.20E+04	3.60E+03	2.89E+03	5.51E+03
Am-243+D	1.99E+03	1.22E+04	3.68E+03	2.94E+03	5.60E+03
Cm-242	1.97E-01	2.52E+02	7.39E+01	5.39E+01	1.24E+02
Cm-243	1.27E+03	8.30E+03	2.43E+03	2.01E+03	3.86E+03
Cm-244	2.82E-01	6.65E+03	1.94E+03	1.61E+03	3.10E+03
Cm-245	7.69E+02	1.25E+04	3.65E+03	3.03E+03	5.80E+03

Table B-4. No Water Infiltration Case: Post-Intrusion Resident.
Units are mrem per Ci exhumed.

Nuclide	External	Internal	Garden	Ingest	Inhale
Cm-246	2.65E-01	1.23E+04	3.60E+03	3.00E+03	5.74E+03
Cm-247+D	3.93E+03	1.14E+04	3.33E+03	2.77E+03	5.27E+03
Cm-248	2.00E-01	4.53E+04	1.33E+04	1.10E+04	2.10E+04
Cm-250+D	3.85E+03	2.58E+05	7.57E+04	6.30E+04	1.20E+05
Bk-247	9.63E+02	1.58E+04	4.66E+03	3.81E+03	7.31E+03
Cf-248	2.04E-01	1.95E+03	1.24E+03	2.14E+02	4.99E+02
Cf-249	3.91E+03	3.38E+04	2.27E+04	3.84E+03	7.34E+03
Cf-250	2.63E-01	1.49E+04	1.00E+04	1.68E+03	3.25E+03
Cf-251	1.18E+03	3.46E+04	2.32E+04	3.93E+03	7.48E+03
Cf-252	3.53E-01	7.23E+03	4.70E+03	7.70E+02	1.76E+03

The "Internal" column is the sum of the "Garden", "Inhale", and "Ingest" columns. External and internal doses are separated because the glass waste matrix will prevent a portion of the exhumed activity from contributing to the internal dose.

Table B-5. Low Water Infiltration Case: All Pathways Farmer.
Units are mrem per pCi/L in the ground water.

Nuclide	Total	Ingest (Drink)	Ingest (Other)	Inhale	External
H-3	4.58E-05	3.46E-05	7.04E-06	4.18E-06	0.00
Be-10	3.19E-03	2.52E-03	6.42E-04	3.03E-05	1.37E-06
C-14	4.67E-03	1.13E-03	3.54E-03	1.79E-07	1.71E-08
Na-22	5.21E-02	6.21E-03	3.22E-02	6.54E-07	1.37E-02
Si-32+D	7.42E-03	5.94E-03	1.38E-03	8.81E-05	1.44E-05
Cl-36	4.81E-02	1.64E-03	4.65E-02	1.87E-06	2.80E-06
K-40	2.83E-02	1.00E-02	1.72E-02	1.06E-06	1.10E-03
Ti-44+D	5.70E-02	1.33E-02	2.85E-02	3.87E-05	1.52E-02
V-49	4.26E-05	3.32E-05	9.42E-06	2.94E-08	0.00
Mn-54	6.19E-03	1.50E-03	4.11E-04	5.71E-07	4.28E-03
Fe-55	6.05E-04	3.28E-04	2.77E-04	2.30E-07	0.00
Co-60	4.57E-02	1.45E-02	1.46E-02	1.87E-05	1.66E-02
Ni-59	1.71E-04	1.13E-04	5.80E-05	1.13E-07	0.00
Ni-63	4.71E-04	3.12E-04	1.59E-04	2.65E-07	0.00
Se-79	1.15E-02	4.70E-03	6.80E-03	8.42E-07	2.40E-08
Rb-87	7.50E-03	2.66E-03	4.84E-03	2.76E-07	1.81E-07
Sr-90+D	1.19E-01	8.26E-02	3.59E-02	2.12E-05	2.93E-05
Zr-93	1.30E-03	8.96E-04	3.81E-04	2.75E-05	2.22E-09
Nb-91	3.06E-03	2.82E-04	2.76E-03	2.50E-06	1.46E-05
Nb-93m	3.01E-03	2.82E-04	2.73E-03	2.50E-06	1.32E-07
Nb-94	5.26E-02	3.86E-03	3.78E-02	3.54E-05	1.09E-02
Mo-93	1.19E-03	7.29E-04	4.62E-04	2.43E-06	7.55E-07
Tc-99	3.54E-03	7.88E-04	2.75E-03	7.09E-07	1.19E-07
Ru-106+D	1.98E-02	1.48E-02	3.78E-03	4.06E-05	1.15E-03
Pd-107	1.93E-04	8.05E-05	1.11E-04	1.10E-06	0.00
Ag-108m+D	2.51E-02	4.11E-03	9.89E-03	2.42E-05	1.11E-02
Cd-109	9.60E-03	7.07E-03	2.50E-03	9.72E-06	1.54E-05
Cd-113m	1.20E-01	8.69E-02	3.29E-02	1.31E-04	8.06E-07
In-115	1.27E-01	8.53E-02	4.17E-02	3.20E-04	5.11E-07
Sn-121m+D	4.54E-03	1.22E-03	3.32E-03	1.02E-06	2.71E-06
Sn-126+D	5.63E-02	1.14E-02	3.13E-02	8.64E-06	1.36E-02

Table B-5. Low Water Infiltration Case: All Pathways Farmer.
Units are mrem per pCi/L in the ground water.

Nuclide	Total	Ingest (Drink)	Ingest (Other)	Inhale	External
Sb-125	4.66E-03	1.52E-03	5.55E-04	1.04E-06	2.58E-03
Te-125m	2.77E-03	1.98E-03	7.86E-04	6.16E-07	5.68E-06
I-129	3.77E-01	1.49E-01	2.27E-01	1.49E-05	1.54E-05
Cs-134	1.10E-01	3.96E-02	6.07E-02	3.95E-06	9.49E-03
Cs-135	1.01E-02	3.82E-03	6.32E-03	3.89E-07	4.93E-08
Cs-137+D	7.53E-02	2.70E-02	4.44E-02	2.73E-06	3.85E-03
Ba-133	4.68E-03	1.84E-03	5.29E-04	6.68E-07	2.32E-03
Pm-147	7.70E-04	5.67E-04	2.00E-04	3.35E-06	5.81E-08
Sm-147	1.43E-01	9.99E-02	3.69E-02	6.39E-03	0.00
Sm-151	2.90E-04	2.10E-04	7.75E-05	2.57E-06	1.26E-09
Eu-150	1.47E-02	3.43E-03	1.26E-03	2.29E-05	9.99E-03
Eu-152	1.24E-02	3.50E-03	1.28E-03	1.89E-05	7.60E-03
Eu-154	1.53E-02	5.16E-03	1.88E-03	2.45E-05	8.23E-03
Eu-155	1.35E-03	8.26E-04	2.97E-04	3.54E-06	2.22E-04
Gd-152	1.36E-01	8.69E-02	2.82E-02	2.08E-02	0.00
Ho-166m	1.78E-02	4.36E-03	1.54E-03	6.61E-05	1.18E-02
Re-187	8.74E-06	5.14E-06	3.60E-06	4.65E-09	0.00
Tl-204	4.66E-03	1.81E-03	2.84E-03	2.06E-07	4.83E-06
Pb-205	1.12E-03	8.80E-04	2.39E-04	3.35E-07	9.10E-09
Pb-210+D	3.74E+00	2.90E+00	8.37E-01	1.19E-03	7.56E-06
Bi-207	1.42E-02	2.96E-03	8.82E-04	1.71E-06	1.04E-02
Po-209	1.83E+00	1.29E+00	5.41E-01	1.01E-03	2.27E-05
Po-210	1.41E+00	1.03E+00	3.81E-01	7.98E-04	3.17E-08
Ra-226+D	9.29E-01	7.18E-01	1.97E-01	7.36E-04	1.22E-02
Ra-228+D	9.97E-01	7.78E-01	2.11E-01	5.02E-04	7.68E-03
Ac-227+D	1.03E+01	7.99E+00	1.75E+00	5.75E-01	2.41E-03
Th-228+D	5.69E-01	4.38E-01	9.23E-02	2.95E-02	9.31E-03
Th-229+D	2.83E+00	2.18E+00	4.72E-01	1.85E-01	1.89E-03
Th-230	3.88E-01	2.96E-01	6.42E-02	2.79E-02	3.59E-06
Th-232	1.94E+00	1.47E+00	3.23E-01	1.40E-01	3.47E-04
Pa-231	7.08E+00	5.72E+00	1.25E+00	1.10E-01	2.62E-04
U-232	1.00E+00	7.07E-01	2.35E-01	5.65E-02	1.36E-03

Table B-5. Low Water Infiltration Case: All Pathways Farmer.
Units are mrem per pCi/L in the ground water.

Nuclide	Total	Ingest (Drink)	Ingest (Other)	Inhale	External
U-233	2.19E-01	1.56E-01	5.13E-02	1.16E-02	1.80E-06
U-234	2.14E-01	1.53E-01	5.03E-02	1.13E-02	5.13E-07
U-235+D	2.03E-01	1.44E-01	4.74E-02	1.05E-02	9.45E-04
U-236	2.04E-01	1.45E-01	4.78E-02	1.07E-02	2.73E-07
U-238+D	2.03E-01	1.45E-01	4.76E-02	1.01E-02	1.48E-04
Np-237+D	2.97E+00	2.40E+00	5.25E-01	4.62E-02	1.32E-03
Pu-236	7.79E-01	6.32E-01	1.34E-01	1.24E-02	3.79E-06
Pu-238	2.14E+00	1.73E+00	3.74E-01	3.35E-02	1.94E-07
Pu-239	2.36E+00	1.91E+00	4.13E-01	3.67E-02	3.66E-07
Pu-240	2.36E+00	1.91E+00	4.13E-01	3.67E-02	1.89E-07
Pu-241+D	4.57E-02	3.70E-02	8.02E-03	7.06E-04	5.79E-08
Pu-242	2.24E+00	1.81E+00	3.92E-01	3.52E-02	1.65E-07
Pu-244+D	2.22E+00	1.79E+00	3.88E-01	3.45E-02	2.30E-03
Am-241	2.43E+00	1.97E+00	4.25E-01	3.80E-02	5.64E-05
Am-242m+D	2.35E+00	1.90E+00	4.13E-01	3.65E-02	8.33E-05
Am-243+D	2.42E+00	1.96E+00	4.24E-01	3.77E-02	1.12E-03
Cm-242	7.58E-02	6.21E-02	1.23E-02	1.47E-03	1.28E-07
Cm-243	1.68E+00	1.36E+00	2.95E-01	2.63E-02	7.20E-04
Cm-244	1.35E+00	1.09E+00	2.37E-01	2.12E-02	1.60E-07
Cm-245	2.50E+00	2.02E+00	4.41E-01	3.89E-02	4.35E-04
Cm-246	2.47E+00	2.00E+00	4.36E-01	3.86E-02	1.50E-07
Cm-247+D	2.29E+00	1.85E+00	4.03E-01	3.54E-02	2.22E-03
Cm-248	9.09E+00	7.34E+00	1.60E+00	1.41E-01	1.13E-07
Cm-250+D	5.19E+01	4.20E+01	9.16E+00	8.04E-01	2.17E-03
Bk-247	3.14E+00	2.54E+00	5.49E-01	4.91E-02	5.44E-04
Cf-248	2.43E-01	1.80E-01	5.87E-02	4.32E-03	1.24E-07
Cf-249	3.55E+00	2.56E+00	9.41E-01	4.94E-02	2.21E-03
Cf-250	1.59E+00	1.15E+00	4.19E-01	2.24E-02	1.50E-07
Cf-251	3.63E+00	2.62E+00	9.63E-01	5.03E-02	6.66E-04
Cf-252	8.01E-01	5.83E-01	2.04E-01	1.34E-02	2.05E-07

Table B-6. No Water Infiltration Case: Intruder.
Units are mrem per Ci exhumed.

Nuclide	External	Internal	Ingest	Inhale
H-3	0.00	1.44E-03	1.42E-03	2.05E-05
Be-10	2.15E-01	1.79E-01	1.04E-01	7.55E-02
C-14	2.73E-03	4.69E-02	4.64E-02	4.46E-04
Na-22	2.39E+03	2.57E-01	2.56E-01	1.63E-03
Si-32+D	2.28E+00	4.64E-01	2.44E-01	2.20E-01
Cl-36	4.64E-01	7.20E-02	6.73E-02	4.67E-03
K-40	1.73E+02	4.16E-01	4.13E-01	2.65E-03
Ti-44+D	2.40E+03	6.43E-01	5.47E-01	9.64E-02
V-49	0.00	1.44E-03	1.36E-03	7.36E-05
Mn-54	9.08E+02	6.30E-02	6.16E-02	1.43E-03
Fe-55	0.00	1.41E-02	1.35E-02	5.74E-04
Co-60	2.75E+03	6.44E-01	5.98E-01	4.67E-02
Ni-59	0.00	4.95E-03	4.67E-03	2.82E-04
Ni-63	0.00	1.35E-02	1.28E-02	6.61E-04
Se-79	3.78E-03	1.95E-01	1.93E-01	2.10E-03
Rb-87	2.85E-02	1.10E-01	1.09E-01	6.89E-04
Sr-90+D	4.68E+00	3.45E+00	3.40E+00	5.29E-02
Zr-93	0.00	1.05E-01	3.69E-02	6.85E-02
Nb-91	2.30E+00	1.78E-02	1.16E-02	6.23E-03
Nb-93m	2.11E-02	1.78E-02	1.16E-02	6.23E-03
Nb-94	1.72E+03	2.47E-01	1.59E-01	8.83E-02
Mo-93	1.20E-01	3.61E-02	3.00E-02	6.06E-03
Tc-99	2.54E-02	3.42E-02	3.24E-02	1.78E-03
Ru-106+D	2.33E+02	7.11E-01	6.09E-01	1.02E-01
Pd-107	0.00	6.04E-03	3.31E-03	2.73E-03
Ag-108m+D	1.75E+03	2.30E-01	1.69E-01	6.04E-02
Cd-109	2.99E+00	3.15E-01	2.91E-01	2.43E-02
Cd-113m	1.30E-01	3.90E+00	3.58E+00	3.26E-01
In-115	8.04E-02	4.31E+00	3.51E+00	7.98E-01
Sn-121m+D	4.28E-01	5.25E-02	5.00E-02	2.54E-03
Sn-126+D	2.14E+03	4.90E-01	4.69E-01	2.15E-02
Sb-125	4.48E+02	6.50E-02	6.24E-02	2.60E-03
Te-125m	3.07E+00	8.31E-02	8.16E-02	1.56E-03
I-129	2.63E+00	6.17E+00	6.13E+00	3.71E-02
Cs-134	1.70E+03	1.64E+00	1.63E+00	9.88E-03
Cs-135	7.76E-03	1.58E-01	1.57E-01	9.71E-04
Cs-137+D	6.12E+02	1.12E+00	1.11E+00	6.81E-03
Ba-133	3.74E+02	7.72E-02	7.56E-02	1.67E-03
Pm-147	1.01E-02	3.17E-02	2.33E-02	8.36E-03
Sm-147	0.00	2.00E+01	4.11E+00	1.59E+01
Sm-151	2.00E-04	1.50E-02	8.64E-03	6.40E-03

Table B-6. No Water Infiltration Case: Intruder.
Units are mrem per Ci exhumed.

Nuclide	External	Internal	Ingest	Inhale
Eu-150	1.58E+03	1.99E-01	1.41E-01	5.72E-02
Eu-152	1.22E+03	1.91E-01	1.44E-01	4.71E-02
Eu-154	1.34E+03	2.73E-01	2.12E-01	6.10E-02
Eu-155	3.70E+01	4.28E-02	3.40E-02	8.83E-03
Gd-152	0.00	5.54E+01	3.58E+00	5.18E+01
Ho-166m	1.86E+03	3.44E-01	1.79E-01	1.65E-01
Re-187	0.00	2.23E-04	2.11E-04	1.16E-05
Tl-204	8.16E-01	7.52E-02	7.47E-02	5.14E-04
Pb-205	1.43E-03	3.71E-02	3.62E-02	8.36E-04
Pb-210+D	1.20E+00	1.22E+02	1.19E+02	2.94E+00
Bi-207	1.64E+03	1.26E-01	1.22E-01	4.27E-03
Po-209	3.58E+00	5.54E+01	5.29E+01	2.52E+00
Po-210	9.28E-03	4.42E+01	4.22E+01	2.01E+00
Ra-226+D	1.91E+03	3.14E+01	2.96E+01	1.83E+00
Ra-228+D	1.05E+03	3.31E+01	3.20E+01	1.08E+00
Ac-227+D	3.84E+02	1.76E+03	3.29E+02	1.43E+03
Th-228+D	1.68E+03	9.16E+01	1.80E+01	7.36E+01
Th-229+D	2.99E+02	5.50E+02	8.96E+01	4.61E+02
Th-230	2.42E-01	8.17E+01	1.22E+01	6.95E+01
Th-232	1.05E-01	4.11E+02	6.07E+01	3.50E+02
Pa-231	3.64E+01	5.09E+02	2.36E+02	2.73E+02
U-232	1.81E-01	1.70E+02	2.91E+01	1.41E+02
U-233	2.74E-01	3.52E+01	6.42E+00	2.88E+01
U-234	8.12E-02	3.44E+01	6.29E+00	2.82E+01
U-235+D	1.50E+02	3.22E+01	5.93E+00	2.62E+01
U-236	4.32E-02	3.26E+01	5.98E+00	2.67E+01
U-238+D	2.41E+01	3.11E+01	5.96E+00	2.52E+01
Np-237+D	2.11E+02	2.14E+02	9.87E+01	1.15E+02
Pu-236	4.56E-02	5.69E+01	2.60E+01	3.09E+01
Pu-238	3.06E-02	1.55E+02	7.11E+01	8.36E+01
Pu-239	5.76E-02	1.70E+02	7.87E+01	9.15E+01
Pu-240	2.97E-02	1.70E+02	7.87E+01	9.15E+01
Pu-241+D	3.78E-03	3.28E+00	1.52E+00	1.76E+00
Pu-242	2.60E-02	1.62E+02	7.47E+01	8.77E+01
Pu-244+D	3.62E+02	1.60E+02	7.38E+01	8.60E+01
Am-241	8.88E+00	1.76E+02	8.09E+01	9.47E+01
Am-242m+D	1.33E+01	1.69E+02	7.82E+01	9.09E+01
Am-243+D	1.77E+02	1.75E+02	8.07E+01	9.39E+01
Cm-242	3.44E-02	6.25E+00	2.56E+00	3.69E+00
Cm-243	1.14E+02	1.21E+02	5.58E+01	6.55E+01
Cm-244	2.56E-02	9.78E+01	4.49E+01	5.29E+01
Cm-245	6.84E+01	1.80E+02	8.31E+01	9.71E+01

Table B-6. No Water Infiltration Case: Intruder.
Units are mrem per Ci exhumed.

Nuclide	External	Internal	Ingest	Inhale
Cm-246	2.36E-02	1.78E+02	8.22E+01	9.62E+01
Cm-247+D	3.50E+02	1.64E+02	7.60E+01	8.83E+01
Cm-248	1.78E-02	6.54E+02	3.02E+02	3.52E+02
Cm-250+D	3.42E+02	3.73E+03	1.73E+03	2.01E+03
Bk-247	8.56E+01	2.27E+02	1.04E+02	1.22E+02
Cf-248	2.53E-02	1.82E+01	7.42E+00	1.08E+01
Cf-249	3.48E+02	2.28E+02	1.05E+02	1.23E+02
Cf-250	2.40E-02	1.03E+02	4.73E+01	5.59E+01
Cf-251	1.05E+02	2.33E+02	1.08E+02	1.25E+02
Cf-252	3.56E-02	5.75E+01	2.40E+01	3.35E+01

The "Internal" column is the sum of the "Inhale" and "Ingest" columns. External and internal doses are separated because the glass waste matrix will prevent a portion of the exhumed activity from contributing to the internal dose.

Table B-7. Low Water Infiltration Case: HSRAM Industrial.
Units are mrem per pCi/L in the ground water.

Nuclide	Total	Ingest	Inhale
H-3	1.62E-05	1.60E-05	2.02E-07
Be-10	1.17E-03	1.17E-03	7.43E-06
C-14	5.23E-04	5.23E-04	4.39E-08
Na-22	2.88E-03	2.88E-03	1.61E-07
Si-32+D	2.77E-03	2.75E-03	2.16E-05
Cl-36	7.58E-04	7.58E-04	4.60E-07
K-40	4.65E-03	4.65E-03	2.60E-07
Ti-44+D	6.16E-03	6.15E-03	9.49E-06
V-49	1.54E-05	1.54E-05	7.25E-09
Mn-54	6.93E-04	6.93E-04	1.41E-07
Fe-55	1.52E-04	1.52E-04	5.65E-08
Co-60	6.73E-03	6.73E-03	4.60E-06
Ni-59	5.25E-05	5.25E-05	2.77E-08
Ni-63	1.44E-04	1.44E-04	6.51E-08
Se-79	2.18E-03	2.18E-03	2.07E-07
Rb-87	1.23E-03	1.23E-03	6.78E-08
Sr-90+D	3.83E-02	3.83E-02	5.21E-06
Zr-93	4.22E-04	4.15E-04	6.74E-06
Nb-91	1.31E-04	1.31E-04	6.13E-07
Nb-93m	1.31E-04	1.31E-04	6.13E-07
Nb-94	1.79E-03	1.79E-03	8.69E-06
Mo-93	3.38E-04	3.38E-04	5.96E-07
Tc-99	3.65E-04	3.65E-04	1.75E-07
Ru-106+D	6.86E-03	6.85E-03	1.00E-05
Pd-107	3.75E-05	3.73E-05	2.69E-07
Ag-108m+D	1.91E-03	1.91E-03	5.94E-06
Cd-109	3.28E-03	3.28E-03	2.39E-06
Cd-113m	4.03E-02	4.03E-02	3.21E-05
In-115	3.96E-02	3.95E-02	7.85E-05
Sn-121m+D	5.63E-04	5.63E-04	2.50E-07
Sn-126+D	5.28E-03	5.28E-03	2.12E-06
Sb-125	7.03E-04	7.03E-04	2.56E-07
Te-125m	9.18E-04	9.18E-04	1.53E-07
I-129	6.90E-02	6.90E-02	3.65E-06
Cs-134	1.83E-02	1.83E-02	9.72E-07
Cs-135	1.77E-03	1.77E-03	9.56E-08
Cs-137+D	1.25E-02	1.25E-02	6.70E-07
Ba-133	8.50E-04	8.50E-04	1.64E-07
Pm-147	2.63E-04	2.63E-04	8.23E-07
Sm-147	4.78E-02	4.63E-02	1.57E-03
Sm-151	9.79E-05	9.73E-05	6.30E-07

Table B-7. Low Water Infiltration Case: HSRAM Industrial.
Units are mrem per pCi/L in the ground water.

Nuclide	Total	Ingest	Inhale
Eu-150	1.60E-03	1.59E-03	5.63E-06
Eu-152	1.62E-03	1.62E-03	4.64E-06
Eu-154	2.39E-03	2.39E-03	6.01E-06
Eu-155	3.83E-04	3.83E-04	8.69E-07
Gd-152	4.54E-02	4.03E-02	5.10E-03
Ho-166m	2.03E-03	2.02E-03	1.62E-05
Re-187	2.38E-06	2.38E-06	1.14E-09
Tl-204	8.40E-04	8.40E-04	5.06E-08
Pb-205	4.08E-04	4.08E-04	8.23E-08
Pb-210+D	1.34E+00	1.34E+00	2.90E-04
Bi-207	1.37E-03	1.37E-03	4.20E-07
Po-209	5.95E-01	5.95E-01	2.48E-04
Po-210	4.75E-01	4.75E-01	1.97E-04
Ra-226+D	3.33E-01	3.33E-01	1.81E-04
Ra-228+D	3.60E-01	3.60E-01	1.07E-04
Ac-227+D	3.84E+00	3.70E+00	1.41E-01
Th-228+D	2.10E-01	2.03E-01	7.25E-03
Th-229+D	1.05E+00	1.01E+00	4.54E-02
Th-230	1.44E-01	1.37E-01	6.85E-03
Th-232	7.17E-01	6.83E-01	3.44E-02
Pa-231	2.68E+00	2.65E+00	2.69E-02
U-232	3.41E-01	3.28E-01	1.38E-02
U-233	7.51E-02	7.23E-02	2.84E-03
U-234	7.35E-02	7.08E-02	2.77E-03
U-235+D	6.93E-02	6.68E-02	2.58E-03
U-236	6.99E-02	6.73E-02	2.63E-03
U-238+D	6.95E-02	6.70E-02	2.48E-03
Np-237+D	1.12E+00	1.11E+00	1.13E-02
Pu-236	2.96E-01	2.93E-01	3.05E-03
Pu-238	8.08E-01	8.00E-01	8.23E-03
Pu-239	8.94E-01	8.85E-01	9.01E-03
Pu-240	8.94E-01	8.85E-01	9.01E-03
Pu-241+D	1.73E-02	1.71E-02	1.73E-04
Pu-242	8.49E-01	8.40E-01	8.63E-03
Pu-244+D	8.38E-01	8.30E-01	8.46E-03
Am-241	9.19E-01	9.10E-01	9.32E-03
Am-242m+D	8.89E-01	8.80E-01	8.95E-03
Am-243+D	9.17E-01	9.08E-01	9.24E-03
Cm-242	2.91E-02	2.88E-02	3.63E-04
Cm-243	6.34E-01	6.28E-01	6.45E-03
Cm-244	5.10E-01	5.05E-01	5.21E-03
Cm-245	9.45E-01	9.35E-01	9.56E-03

Table B-7. Low Water Infiltration Case: HSRAM Industrial.
Units are mrem per pCi/L in the ground water.

Nuclide	Total	Ingest	Inhale
Cm-246	9.34E-01	9.25E-01	9.47E-03
Cm-247+D	8.64E-01	8.55E-01	8.69E-03
Cm-248	3.43E+00	3.40E+00	3.47E-02
Cm-250+D	1.96E+01	1.94E+01	1.97E-01
Bk-247	1.19E+00	1.18E+00	1.21E-02
Cf-248	8.46E-02	8.35E-02	1.06E-03
Cf-249	1.20E+00	1.19E+00	1.21E-02
Cf-250	5.38E-01	5.33E-01	5.50E-03
Cf-251	1.22E+00	1.21E+00	1.23E-02
Cf-252	2.73E-01	2.70E-01	3.30E-03

The "Total" column is the sum of the "Ingest" and "Inhale" columns.

Table B-8. Low Water Infiltration Case: HSRAM Residential.
Units are mrem per pCi/L in the ground water.

Nuclide	Total	Ingest (Drink)	Ingest (Other)	Inhale	External
H-3	4.92E-05	4.67E-05	2.13E-06	2.98E-07	0.00
Be-10	3.89E-03	3.40E-03	4.79E-04	1.13E-05	2.32E-06
C-14	1.84E-03	1.53E-03	3.14E-04	6.69E-08	2.91E-08
Na-22	3.29E-02	8.40E-03	1.20E-03	2.44E-07	2.33E-02
Si-32+D	9.27E-03	8.03E-03	1.18E-03	3.30E-05	2.46E-05
Cl-36	1.64E-02	2.21E-03	1.42E-02	7.00E-07	4.77E-06
K-40	1.81E-02	1.36E-02	2.62E-03	3.97E-07	1.86E-03
Ti-44+D	4.63E-02	1.80E-02	2.53E-03	1.45E-05	2.58E-02
V-49	5.08E-05	4.48E-05	5.96E-06	1.10E-08	0.00
Mn-54	9.61E-03	2.02E-03	3.01E-04	2.13E-07	7.29E-03
Fe-55	5.04E-04	4.43E-04	6.11E-05	8.58E-08	0.00
Co-60	5.06E-02	1.96E-02	2.75E-03	7.00E-06	2.82E-02
Ni-59	1.75E-04	1.53E-04	2.22E-05	4.22E-08	0.00
Ni-63	4.82E-04	4.21E-04	6.08E-05	9.92E-08	0.00
Se-79	7.26E-03	6.35E-03	9.08E-04	3.15E-07	4.08E-08
Rb-87	4.12E-03	3.59E-03	5.29E-04	1.03E-07	3.08E-07
Sr-90+D	1.30E-01	1.12E-01	1.83E-02	7.93E-06	4.98E-05
Zr-93	1.39E-03	1.21E-03	1.71E-04	1.03E-05	3.77E-09
Nb-91	4.61E-04	3.81E-04	5.38E-05	9.34E-07	2.48E-05
Nb-93m	4.36E-04	3.81E-04	5.36E-05	9.34E-07	2.24E-07
Nb-94	2.45E-02	5.21E-03	7.36E-04	1.32E-05	1.85E-02
Mo-93	1.13E-03	9.86E-04	1.45E-04	9.09E-07	1.28E-06
Tc-99	1.31E-03	1.07E-03	2.44E-04	2.64E-07	2.02E-07
Ru-106+D	2.47E-02	2.00E-02	2.69E-03	1.52E-05	1.96E-03
Pd-107	1.25E-04	1.09E-04	1.57E-05	4.10E-07	0.00
Ag-108m+D	2.52E-02	5.56E-03	8.19E-04	9.06E-06	1.88E-02
Cd-109	1.10E-02	9.56E-03	1.40E-03	3.63E-06	2.63E-05
Cd-113m	1.36E-01	1.18E-01	1.81E-02	4.89E-05	1.37E-06
In-115	1.32E-01	1.15E-01	1.62E-02	1.20E-04	8.69E-07
Sn-121m+D	1.88E-03	1.64E-03	2.32E-04	3.81E-07	4.60E-06
Sn-126+D	4.07E-02	1.54E-02	2.18E-03	3.23E-06	2.32E-02
Sb-125	6.76E-03	2.05E-03	3.08E-04	3.90E-07	4.40E-03
Te-125m	2.97E-03	2.68E-03	2.84E-04	2.28E-07	9.67E-06
I-129	2.31E-01	2.01E-01	2.92E-02	5.55E-06	2.62E-05
Cs-134	7.72E-02	5.35E-02	7.59E-03	1.48E-06	1.61E-02
Cs-135	5.92E-03	5.16E-03	7.54E-04	1.46E-07	8.39E-08
Cs-137+D	4.84E-02	3.65E-02	5.32E-03	1.02E-06	6.56E-03
Ba-133	6.77E-03	2.48E-03	3.51E-04	2.50E-07	3.94E-03
Pm-147	8.74E-04	7.67E-04	1.06E-04	1.25E-06	9.89E-08
Sm-147	1.56E-01	1.35E-01	1.90E-02	2.39E-03	0.00
Sm-151	3.25E-04	2.84E-04	4.00E-05	9.60E-07	2.15E-09

Table B-8. Low Water Infiltration Case: HSRAM Residential.
Units are mrem per pCi/L in the ground water.

Nuclide	Total	Ingest (Drink)	Ingest (Other)	Inhale	External
Eu-150	2.23E-02	4.64E-03	6.54E-04	8.57E-06	1.70E-02
Eu-152	1.83E-02	4.73E-03	6.64E-04	7.07E-06	1.29E-02
Eu-154	2.20E-02	6.97E-03	9.77E-04	9.14E-06	1.40E-02
Eu-155	1.65E-03	1.12E-03	1.56E-04	1.32E-06	3.77E-04
Gd-152	1.42E-01	1.18E-01	1.66E-02	7.78E-03	0.00
Ho-166m	2.68E-02	5.89E-03	8.31E-04	2.47E-05	2.01E-02
Re-187	8.16E-06	6.94E-06	1.21E-06	1.74E-09	0.00
Tl-204	2.80E-03	2.45E-03	3.40E-04	7.70E-08	8.22E-06
Pb-205	1.36E-03	1.19E-03	1.68E-04	1.25E-07	1.55E-08
Pb-210+D	4.50E+00	3.92E+00	5.76E-01	4.46E-04	1.29E-05
Bi-207	2.22E-02	4.00E-03	5.64E-04	6.40E-07	1.76E-02
Po-209	1.98E+00	1.74E+00	2.44E-01	3.78E-04	3.86E-05
Po-210	1.56E+00	1.39E+00	1.71E-01	2.96E-04	5.39E-08
Ra-226+D	1.13E+00	9.71E-01	1.38E-01	2.75E-04	2.07E-02
Ra-228+D	1.21E+00	1.05E+00	1.49E-01	2.05E-04	1.31E-02
Ac-227+D	1.25E+01	1.08E+01	1.52E+00	2.15E-01	4.10E-03
Th-228+D	7.00E-01	5.92E-01	8.10E-02	1.10E-02	1.58E-02
Th-229+D	3.43E+00	2.94E+00	4.14E-01	6.91E-02	3.22E-03
Th-230	4.67E-01	4.00E-01	5.63E-02	1.04E-02	6.10E-06
Th-232	2.33E+00	1.99E+00	2.82E-01	5.25E-02	5.91E-04
Pa-231	8.87E+00	7.74E+00	1.09E+00	4.10E-02	4.45E-04
U-232	1.12E+00	9.56E-01	1.37E-01	2.11E-02	2.31E-03
U-233	2.45E-01	2.11E-01	2.97E-02	4.32E-03	3.07E-06
U-234	2.40E-01	2.07E-01	2.91E-02	4.22E-03	8.72E-07
U-235+D	2.28E-01	1.95E-01	2.75E-02	3.94E-03	1.61E-03
U-236	2.28E-01	1.96E-01	2.77E-02	4.00E-03	4.64E-07
U-238+D	2.27E-01	1.96E-01	2.76E-02	3.78E-03	2.52E-04
Np-237+D	3.72E+00	3.24E+00	4.57E-01	1.73E-02	2.24E-03
Pu-236	9.77E-01	8.54E-01	1.18E-01	4.63E-03	6.45E-06
Pu-238	2.68E+00	2.34E+00	3.28E-01	1.25E-02	3.30E-07
Pu-239	2.96E+00	2.58E+00	3.63E-01	1.37E-02	6.23E-07
Pu-240	2.96E+00	2.58E+00	3.63E-01	1.37E-02	3.21E-07
Pu-241+D	5.73E-02	5.00E-02	7.05E-03	2.64E-04	9.84E-08
Pu-242	2.81E+00	2.45E+00	3.45E-01	1.32E-02	2.81E-07
Pu-244+D	2.78E+00	2.42E+00	3.41E-01	1.29E-02	3.91E-03
Am-241	3.05E+00	2.66E+00	3.74E-01	1.42E-02	9.60E-05
Am-242m+D	2.95E+00	2.57E+00	3.62E-01	1.36E-02	1.42E-04
Am-243+D	3.04E+00	2.65E+00	3.73E-01	1.41E-02	1.91E-03
Cm-242	9.52E-02	8.40E-02	1.07E-02	5.47E-04	2.18E-07
Cm-243	2.10E+00	1.83E+00	2.57E-01	9.82E-03	1.23E-03
Cm-244	1.69E+00	1.47E+00	2.07E-01	7.93E-03	2.72E-07
Cm-245	3.13E+00	2.73E+00	3.84E-01	1.46E-02	7.40E-04

Table B-8. Low Water Infiltration Case: HSRAM Residential.
Units are mrem per pCi/L in the ground water.

Nuclide	Total	Ingest (Drink)	Ingest (Other)	Inhale	External
Cm-246	3.10E+00	2.70E+00	3.80E-01	1.44E-02	2.55E-07
Cm-247+D	2.86E+00	2.50E+00	3.51E-01	1.32E-02	3.78E-03
Cm-248	1.14E+01	9.93E+00	1.40E+00	5.28E-02	1.92E-07
Cm-250+D	6.50E+01	5.67E+01	7.98E+00	3.01E-01	3.70E-03
Bk-247	3.93E+00	3.43E+00	4.83E-01	1.84E-02	9.25E-04
Cf-248	2.79E-01	2.44E-01	3.31E-02	1.61E-03	2.10E-07
Cf-249	3.97E+00	3.46E+00	4.89E-01	1.85E-02	3.76E-03
Cf-250	1.78E+00	1.55E+00	2.19E-01	8.38E-03	2.55E-07
Cf-251	4.06E+00	3.54E+00	5.00E-01	1.88E-02	1.13E-03
Cf-252	9.03E-01	7.88E-01	1.09E-01	5.01E-03	3.49E-07

Table B-9. Low Water Infiltration Case: HSRAM Agricultural.
Units are mrem per pCi/L in the ground water.

Nuclide	Total	Ingest (Drink)	Ingest (Other)	Inhale	External
H-3	5.73E-05	4.67E-05	1.03E-05	2.98E-07	0.00
Be-10	3.99E-03	3.40E-03	5.79E-04	1.13E-05	2.32E-06
C-14	6.44E-03	1.53E-03	4.92E-03	6.69E-08	2.91E-08
Na-22	8.82E-02	8.40E-03	5.65E-02	2.44E-07	2.33E-02
Si-32+D	9.30E-03	8.03E-03	1.22E-03	3.30E-05	2.46E-05
Cl-36	5.81E-02	2.21E-03	5.59E-02	7.00E-07	4.77E-06
K-40	4.09E-02	1.36E-02	2.55E-02	3.97E-07	1.86E-03
Ti-44+D	8.79E-02	1.80E-02	4.41E-02	1.45E-05	2.58E-02
V-49	5.31E-05	4.48E-05	8.25E-06	1.10E-08	0.00
Mn-54	9.73E-03	2.02E-03	4.18E-04	2.13E-07	7.29E-03
Fe-55	7.20E-04	4.43E-04	2.77E-04	8.58E-08	0.00
Co-60	6.57E-02	1.96E-02	1.79E-02	7.00E-06	2.82E-02
Ni-59	2.22E-04	1.53E-04	6.90E-05	4.22E-08	0.00
Ni-63	6.11E-04	4.21E-04	1.89E-04	9.92E-08	0.00
Se-79	1.44E-02	6.35E-03	8.10E-03	3.15E-07	4.08E-08
Rb-87	1.14E-02	3.59E-03	7.78E-03	1.03E-07	3.08E-07
Sr-90+D	1.60E-01	1.12E-01	4.81E-02	7.93E-06	4.98E-05
Zr-93	1.60E-03	1.21E-03	3.74E-04	1.03E-05	3.77E-09
Nb-91	3.91E-03	3.81E-04	3.50E-03	9.34E-07	2.48E-05
Nb-93m	3.84E-03	3.81E-04	3.46E-03	9.34E-07	2.24E-07
Nb-94	7.17E-02	5.21E-03	4.79E-02	1.32E-05	1.85E-02
Mo-93	1.56E-03	9.86E-04	5.72E-04	9.09E-07	1.28E-06
Tc-99	5.83E-03	1.07E-03	4.77E-03	2.64E-07	2.02E-07
Ru-106+D	2.54E-02	2.00E-02	3.44E-03	1.52E-05	1.95E-03
Pd-107	3.13E-04	1.09E-04	2.04E-04	4.10E-07	0.00
Ag-108m+D	4.37E-02	5.56E-03	1.93E-02	9.06E-06	1.88E-02
Cd-109	1.27E-02	9.56E-03	3.06E-03	3.63E-06	2.63E-05
Cd-113m	1.58E-01	1.18E-01	4.06E-02	4.89E-05	1.37E-06
In-115	1.55E-01	1.15E-01	4.00E-02	1.20E-04	8.69E-07
Sn-121m+D	5.19E-03	1.64E-03	3.54E-03	3.81E-07	4.60E-06
Sn-126+D	7.19E-02	1.54E-02	3.33E-02	3.23E-06	2.32E-02
Sb-125	6.99E-03	2.05E-03	5.35E-04	3.90E-07	4.40E-03
Te-125m	3.28E-03	2.68E-03	5.96E-04	2.28E-07	9.67E-06
I-129	5.92E-01	2.01E-01	3.90E-01	5.55E-06	2.62E-05
Cs-134	1.60E-01	5.35E-02	9.07E-02	1.48E-06	1.61E-02
Cs-135	1.46E-02	5.16E-03	9.42E-03	1.46E-07	8.39E-08
Cs-137+D	1.09E-01	3.65E-02	6.63E-02	1.02E-06	6.56E-03
Ba-133	6.92E-03	2.48E-03	5.00E-04	2.50E-07	3.94E-03
Pm-147	9.57E-04	7.67E-04	1.89E-04	1.25E-06	9.89E-08
Sm-147	1.73E-01	1.35E-01	3.51E-02	2.39E-03	0.00
Sm-151	3.59E-04	2.84E-04	7.38E-05	9.60E-07	2.15E-09

Table B-9. Low Water Infiltration Case: HSRAM Agricultural.
Units are mrem per pCi/L in the ground water.

Nuclide	Total	Ingest (Drink)	Ingest (Other)	Inhale	External
Eu-150	2.28E-02	4.64E-03	1.20E-03	8.57E-06	1.70E-02
Eu-152	1.89E-02	4.73E-03	1.22E-03	7.07E-06	1.29E-02
Eu-154	2.28E-02	6.97E-03	1.79E-03	9.14E-06	1.40E-02
Eu-155	1.78E-03	1.12E-03	2.84E-04	1.32E-06	3.77E-04
Gd-152	1.52E-01	1.18E-01	2.65E-02	7.78E-03	0.00
Ho-166m	2.74E-02	5.89E-03	1.46E-03	2.47E-05	2.01E-02
Re-187	1.13E-05	6.94E-06	4.39E-06	1.74E-09	0.00
Tl-204	5.72E-03	2.45E-03	3.26E-03	7.70E-08	8.22E-06
Pb-205	1.42E-03	1.19E-03	2.28E-04	1.25E-07	1.55E-08
Pb-210+D	4.72E+00	3.92E+00	8.00E-01	4.46E-04	1.29E-05
Bi-207	2.26E-02	4.00E-03	9.31E-04	6.40E-07	1.76E-02
Po-209	2.12E+00	1.74E+00	3.80E-01	3.78E-04	3.86E-05
Po-210	1.64E+00	1.39E+00	2.52E-01	2.96E-04	5.39E-08
Ra-226+D	1.21E+00	9.71E-01	2.17E-01	2.75E-04	2.07E-02
Ra-228+D	1.30E+00	1.05E+00	2.31E-01	2.05E-04	1.31E-02
Ac-227+D	1.26E+01	1.08E+01	1.56E+00	2.15E-01	4.10E-03
Th-228+D	7.00E-01	5.92E-01	8.15E-02	1.10E-02	1.58E-02
Th-229+D	3.43E+00	2.94E+00	4.17E-01	6.91E-02	3.22E-03
Th-230	4.67E-01	4.00E-01	5.67E-02	1.04E-02	6.10E-06
Th-232	2.33E+00	1.99E+00	2.86E-01	5.25E-02	5.91E-04
Pa-231	8.88E+00	7.74E+00	1.10E+00	4.10E-02	4.45E-04
U-232	1.23E+00	9.56E-01	2.52E-01	2.11E-02	2.31E-03
U-233	2.71E-01	2.11E-01	5.53E-02	4.32E-03	3.07E-06
U-234	2.65E-01	2.07E-01	5.41E-02	4.22E-03	8.72E-07
U-235+D	2.52E-01	1.95E-01	5.10E-02	3.94E-03	1.61E-03
U-236	2.52E-01	1.96E-01	5.14E-02	4.00E-03	4.64E-07
U-238+D	2.51E-01	1.96E-01	5.12E-02	3.78E-03	2.52E-04
Np-237+D	3.72E+00	3.24E+00	4.64E-01	1.73E-02	2.24E-03
Pu-236	9.77E-01	8.54E-01	1.18E-01	4.63E-03	6.45E-06
Pu-238	2.68E+00	2.34E+00	3.28E-01	1.25E-02	3.30E-07
Pu-239	2.96E+00	2.58E+00	3.64E-01	1.37E-02	6.23E-07
Pu-240	2.96E+00	2.58E+00	3.64E-01	1.37E-02	3.21E-07
Pu-241+D	5.73E-02	5.00E-02	7.05E-03	2.64E-04	9.84E-08
Pu-242	2.81E+00	2.45E+00	3.45E-01	1.32E-02	2.81E-07
Pu-244+D	2.78E+00	2.42E+00	3.41E-01	1.29E-02	3.91E-03
Am-241	3.05E+00	2.66E+00	3.74E-01	1.42E-02	9.60E-05
Am-242m+D	2.95E+00	2.57E+00	3.63E-01	1.36E-02	1.42E-04
Am-243+D	3.04E+00	2.65E+00	3.73E-01	1.41E-02	1.91E-03
Cm-242	9.54E-02	8.40E-02	1.09E-02	5.47E-04	2.18E-07
Cm-243	2.11E+00	1.83E+00	2.63E-01	9.82E-03	1.23E-03
Cm-244	1.69E+00	1.47E+00	2.12E-01	7.93E-03	2.72E-07
Cm-245	3.14E+00	2.73E+00	3.93E-01	1.46E-02	7.40E-04

Table B-9. Low Water Infiltration Case: HSRAM Agricultural.
Units are mrem per pCi/L in the ground water.

Nuclide	Total	Ingest (Drink)	Ingest (Other)	Inhale	External
Cm-246	3.10E+00	2.70E+00	3.89E-01	1.44E-02	2.55E-07
Cm-247+D	2.87E+00	2.50E+00	3.60E-01	1.32E-02	3.78E-03
Cm-248	1.14E+01	9.93E+00	1.43E+00	5.28E-02	1.92E-07
Cm-250+D	6.52E+01	5.67E+01	8.17E+00	3.01E-01	3.70E-03
Bk-247	3.93E+00	3.43E+00	4.83E-01	1.84E-02	9.25E-04
Cf-248	3.01E-01	2.44E-01	5.51E-02	1.61E-03	2.10E-07
Cf-249	4.37E+00	3.46E+00	8.90E-01	1.85E-02	3.76E-03
Cf-250	1.96E+00	1.55E+00	3.96E-01	8.38E-03	2.55E-07
Cf-251	4.47E+00	3.54E+00	9.11E-01	1.88E-02	1.13E-03
Cf-252	9.86E-01	7.88E-01	1.93E-01	5.01E-03	3.49E-07

Table B-10. Low Water Infiltration Case: Native American Subsistence Resident.
Units are mrem per pCi/L in the ground water.

Nuclide	Total	Ingest (Drink)	Ingest (Other)	Inhale	External
H-3	1.03E-04	7.01E-05	2.79E-05	5.09E-06	0.00
Be-10	8.25E-03	5.10E-03	3.08E-03	6.44E-05	2.32E-06
C-14	1.34E-02	2.29E-03	1.11E-02	3.80E-07	2.91E-08
Na-22	1.52E-01	1.26E-02	1.17E-01	1.39E-06	2.33E-02
Si-32+D	1.95E-02	1.20E-02	7.21E-03	1.87E-04	2.46E-05
Cl-36	1.80E-01	3.32E-03	1.76E-01	3.98E-06	4.77E-06
K-40	8.37E-02	2.04E-02	6.15E-02	2.26E-06	1.86E-03
Ti-44+D	1.50E-01	2.69E-02	9.70E-02	8.23E-05	2.58E-02
V-49	1.09E-04	6.72E-05	4.12E-05	6.25E-08	0.00
Mn-54	1.24E-02	3.03E-03	2.08E-03	1.21E-06	7.28E-03
Fe-55	1.47E-03	6.65E-04	8.01E-04	4.89E-07	0.00
Co-60	1.04E-01	2.95E-02	4.61E-02	3.98E-05	2.82E-02
Ni-59	4.56E-04	2.30E-04	2.25E-04	2.40E-07	0.00
Ni-63	1.25E-03	6.32E-04	6.18E-04	5.64E-07	0.00
Se-79	3.10E-02	9.53E-03	2.15E-02	1.79E-06	4.08E-08
Rb-87	2.33E-02	5.39E-03	1.79E-02	5.88E-07	3.08E-07
Sr-90+D	3.38E-01	1.68E-01	1.71E-01	4.51E-05	4.98E-05
Zr-93	3.29E-03	1.82E-03	1.42E-03	5.84E-05	3.77E-09
Nb-91	7.63E-03	5.72E-04	7.03E-03	5.31E-06	2.48E-05
Nb-93m	7.52E-03	5.72E-04	6.95E-03	5.31E-06	2.24E-07
Nb-94	1.23E-01	7.82E-03	9.62E-02	7.53E-05	1.85E-02
Mo-93	3.22E-03	1.48E-03	1.73E-03	5.17E-06	1.28E-06
Tc-99	1.23E-02	1.60E-03	1.07E-02	1.51E-06	2.02E-07
Ru-106+D	4.96E-02	3.00E-02	1.76E-02	8.65E-05	1.96E-03
Pd-107	6.34E-04	1.63E-04	4.69E-04	2.33E-06	0.00
Ag-108m+D	6.91E-02	8.34E-03	4.19E-02	5.15E-05	1.88E-02
Cd-109	2.62E-02	1.43E-02	1.18E-02	2.07E-05	2.63E-05
Cd-113m	3.32E-01	1.76E-01	1.55E-01	2.78E-04	1.37E-06
In-115	3.20E-01	1.73E-01	1.46E-01	6.81E-04	8.69E-07
Sn-121m+D	1.03E-02	2.46E-03	7.80E-03	2.17E-06	4.60E-06
Sn-126+D	1.20E-01	2.31E-02	7.34E-02	1.84E-05	2.32E-02
Sb-125	9.78E-03	3.08E-03	2.31E-03	2.22E-06	4.39E-03
Te-125m	6.70E-03	4.02E-03	2.67E-03	1.31E-06	9.67E-06
I-129	1.21E+00	3.02E-01	9.10E-01	3.16E-05	2.62E-05
Cs-134	3.06E-01	8.03E-02	2.10E-01	8.41E-06	1.61E-02
Cs-135	2.94E-02	7.74E-03	2.17E-02	8.28E-07	8.39E-08
Cs-137+D	2.14E-01	5.48E-02	1.53E-01	5.81E-06	6.56E-03
Ba-133	1.02E-02	3.72E-03	2.52E-03	1.42E-06	3.94E-03
Pm-147	1.95E-03	1.15E-03	7.97E-04	7.12E-06	9.89E-08
Sm-147	3.62E-01	2.03E-01	1.45E-01	1.36E-02	0.00
Sm-151	7.37E-04	4.26E-04	3.06E-04	5.46E-06	2.15E-09

Table B-10. Low Water Infiltration Case: Native American Subsistence Resident.
Units are mrem per pCi/L in the ground water.

Nuclide	Total	Ingest (Drink)	Ingest (Other)	Inhale	External
Eu-150	2.90E-02	6.96E-03	4.99E-03	4.88E-05	1.70E-02
Eu-152	2.51E-02	7.10E-03	5.06E-03	4.02E-05	1.29E-02
Eu-154	3.19E-02	1.05E-02	7.43E-03	5.20E-05	1.40E-02
Eu-155	3.24E-03	1.68E-03	1.18E-03	7.53E-06	3.77E-04
Gd-152	3.39E-01	1.76E-01	1.19E-01	4.42E-02	0.00
Ho-166m	3.53E-02	8.84E-03	6.22E-03	1.41E-04	2.01E-02
Re-187	2.42E-05	1.04E-05	1.37E-05	9.90E-09	0.00
Tl-204	1.14E-02	3.68E-03	7.75E-03	4.38E-07	8.22E-06
Pb-205	2.94E-03	1.78E-03	1.16E-03	7.13E-07	1.55E-08
Pb-210+D	9.91E+00	5.88E+00	4.03E+00	2.52E-03	1.29E-05
Bi-207	2.78E-02	6.00E-03	4.22E-03	3.64E-06	1.76E-02
Po-209	4.72E+00	2.61E+00	2.12E+00	2.15E-03	3.86E-05
Po-210	3.55E+00	2.08E+00	1.47E+00	1.70E-03	5.39E-08
Ra-226+D	2.47E+00	1.46E+00	9.88E-01	1.57E-03	2.07E-02
Ra-228+D	2.65E+00	1.58E+00	1.06E+00	1.05E-03	1.31E-02
Ac-227+D	2.66E+01	1.62E+01	9.20E+00	1.22E+00	4.10E-03
Th-228+D	1.45E+00	8.88E-01	4.87E-01	6.27E-02	1.58E-02
Th-229+D	7.30E+00	4.41E+00	2.49E+00	3.93E-01	3.22E-03
Th-230	9.99E-01	6.00E-01	3.39E-01	5.93E-02	6.10E-06
Th-232	4.99E+00	2.99E+00	1.70E+00	2.98E-01	5.91E-04
Pa-231	1.84E+01	1.16E+01	6.59E+00	2.33E-01	4.45E-04
U-232	2.64E+00	1.43E+00	1.08E+00	1.20E-01	2.31E-03
U-233	5.77E-01	3.16E-01	2.36E-01	2.46E-02	3.07E-06
U-234	5.65E-01	3.10E-01	2.31E-01	2.40E-02	8.72E-07
U-235+D	5.34E-01	2.92E-01	2.18E-01	2.24E-02	1.61E-03
U-236	5.37E-01	2.95E-01	2.20E-01	2.27E-02	4.64E-07
U-238+D	5.34E-01	2.93E-01	2.19E-01	2.15E-02	2.52E-04
Np-237+D	7.73E+00	4.86E+00	2.76E+00	9.83E-02	2.24E-03
Pu-236	2.02E+00	1.28E+00	7.10E-01	2.64E-02	6.45E-06
Pu-238	5.55E+00	3.50E+00	1.98E+00	7.13E-02	3.30E-07
Pu-239	6.14E+00	3.88E+00	2.19E+00	7.81E-02	6.23E-07
Pu-240	6.14E+00	3.88E+00	2.19E+00	7.81E-02	3.21E-07
Pu-241+D	1.19E-01	7.50E-02	4.24E-02	1.50E-03	9.84E-08
Pu-242	5.83E+00	3.68E+00	2.08E+00	7.48E-02	2.81E-07
Pu-244+D	5.76E+00	3.64E+00	2.05E+00	7.33E-02	3.91E-03
Am-241	6.32E+00	3.99E+00	2.25E+00	8.08E-02	9.60E-05
Am-242m+D	6.11E+00	3.85E+00	2.18E+00	7.75E-02	1.42E-04
Am-243+D	6.30E+00	3.97E+00	2.24E+00	8.01E-02	1.91E-03
Cm-242	1.94E-01	1.26E-01	6.45E-02	3.13E-03	2.18E-07
Cm-243	4.36E+00	2.75E+00	1.56E+00	5.59E-02	1.23E-03
Cm-244	3.51E+00	2.21E+00	1.25E+00	4.51E-02	2.72E-07
Cm-245	6.51E+00	4.10E+00	2.33E+00	8.28E-02	7.40E-04

Table B-10. Low Water Infiltration Case: Native American Subsistence Resident.
Units are mrem per pCi/L in the ground water.

Nuclide	Total	Ingest (Drink)	Ingest (Other)	Inhale	External
Cm-246	6.44E+00	4.05E+00	2.30E+00	8.21E-02	2.55E-07
Cm-247+D	5.95E+00	3.74E+00	2.13E+00	7.53E-02	3.78E-03
Cm-248	2.37E+01	1.49E+01	8.46E+00	3.00E-01	1.92E-07
Cm-250+D	1.35E+02	8.51E+01	4.84E+01	1.71E+00	3.70E-03
Bk-247	8.16E+00	5.15E+00	2.90E+00	1.04E-01	9.25E-04
Cf-248	6.16E-01	3.66E-01	2.41E-01	9.20E-03	2.10E-07
Cf-249	9.01E+00	5.19E+00	3.71E+00	1.05E-01	3.76E-03
Cf-250	4.04E+00	2.33E+00	1.66E+00	4.77E-02	2.55E-07
Cf-251	9.22E+00	5.31E+00	3.80E+00	1.07E-01	1.13E-03
Cf-252	2.03E+00	1.18E+00	8.17E-01	2.85E-02	3.49E-07

Table B-11. Low Water Infiltration Case: Columbia River Population.
Units are person-rem per pCi/L in the Columbia River.

Nuclide	Total	Ingest (Drink)	Ingest (Other)	Inhale	External
H-3	2.29E-01	1.73E-01	3.48E-02	2.09E-02	0.00
Be-10	1.52E+01	1.26E+01	2.48E+00	1.50E-01	5.60E-03
C-14	1.95E+01	5.64E+00	1.39E+01	8.87E-04	7.02E-05
Na-22	2.14E+02	3.11E+01	1.26E+02	3.25E-03	5.63E+01
Si-32+D	3.55E+01	2.97E+01	5.33E+00	4.37E-01	5.92E-02
Cl-36	1.88E+02	8.18E+00	1.80E+02	9.29E-03	1.15E-02
K-40	1.22E+02	5.02E+01	6.72E+01	5.26E-03	4.49E+00
Ti-44+D	2.40E+02	6.64E+01	1.12E+02	1.92E-01	6.23E+01
V-49	2.03E-01	1.66E-01	3.66E-02	1.46E-04	0.00
Mn-54	2.66E+01	7.48E+00	1.59E+00	2.84E-03	1.76E+01
Fe-55	2.72E+00	1.64E+00	1.08E+00	1.14E-03	0.00
Co-60	1.98E+02	7.26E+01	5.72E+01	9.29E-02	6.81E+01
Ni-59	7.93E-01	5.67E-01	2.26E-01	5.60E-04	0.00
Ni-63	2.18E+00	1.56E+00	6.20E-01	1.32E-03	0.00
Se-79	5.03E+01	2.35E+01	2.68E+01	4.18E-03	9.85E-05
Rb-87	3.23E+01	1.33E+01	1.90E+01	1.37E-03	7.43E-04
Sr-90+D	5.53E+02	4.13E+02	1.39E+02	1.05E-01	1.20E-01
Zr-93	6.10E+00	4.48E+00	1.48E+00	1.36E-01	9.10E-06
Nb-91	1.23E+01	1.41E+00	1.08E+01	1.24E-02	5.98E-02
Nb-93m	1.21E+01	1.41E+00	1.07E+01	1.24E-02	5.42E-04
Nb-94	2.13E+02	1.93E+01	1.48E+02	1.76E-01	4.47E+01
Mo-93	5.46E+00	3.65E+00	1.80E+00	1.21E-02	3.10E-03
Tc-99	1.46E+01	3.94E+00	1.07E+01	3.53E-03	4.87E-04
Ru-106+D	9.36E+01	7.40E+01	1.47E+01	2.02E-01	4.72E+00
Pd-107	8.43E-01	4.02E-01	4.35E-01	5.43E-03	0.00
Ag-108m+D	1.05E+02	2.06E+01	3.87E+01	1.20E-01	4.55E+01
Cd-109	4.52E+01	3.54E+01	9.74E+00	4.83E-02	6.34E-02
Cd-113m	5.63E+02	4.35E+02	1.28E+02	6.49E-01	3.31E-03
In-115	5.91E+02	4.27E+02	1.63E+02	1.59E+00	2.10E-03
Sn-121m+D	1.91E+01	6.08E+00	1.31E+01	5.05E-03	1.11E-02
Sn-126+D	2.36E+02	5.70E+01	1.23E+02	4.29E-02	5.59E+01

Table B-11. Low Water Infiltration Case: Columbia River Population.
Units are person-rem per pCi/L in the Columbia River.

Nuclide	Total	Ingest (Drink)	Ingest (Other)	Inhale	External
Sb-125	2.03E+01	7.59E+00	2.15E+00	5.18E-03	1.06E+01
Te-125m	1.30E+01	9.91E+00	3.11E+00	3.07E-03	2.33E-02
I-129	1.64E+03	7.45E+02	8.91E+02	7.38E-02	6.32E-02
Cs-134	4.75E+02	1.98E+02	2.38E+02	1.96E-02	3.89E+01
Cs-135	4.39E+01	1.91E+01	2.48E+01	1.93E-03	2.02E-04
Cs-137+D	3.25E+02	1.35E+02	1.74E+02	1.35E-02	1.58E+01
Ba-133	2.07E+01	9.18E+00	2.06E+00	3.31E-03	9.51E+00
Pm-147	3.63E+00	2.84E+00	7.76E-01	1.66E-02	2.39E-04
Sm-147	6.75E+02	5.00E+02	1.43E+02	3.17E+01	0.00
Sm-151	1.36E+00	1.05E+00	3.01E-01	1.27E-02	5.19E-06
Eu-150	6.32E+01	1.72E+01	4.91E+00	1.14E-01	4.10E+01
Eu-152	5.38E+01	1.75E+01	4.98E+00	9.38E-02	3.12E+01
Eu-154	6.70E+01	2.58E+01	7.29E+00	1.21E-01	3.38E+01
Eu-155	6.21E+00	4.13E+00	1.15E+00	1.76E-02	9.11E-01
Gd-152	6.47E+02	4.35E+02	1.09E+02	1.03E+02	0.00
Ho-166m	7.65E+01	2.18E+01	6.00E+00	3.28E-01	4.84E+01
Re-187	3.97E-02	2.57E-02	1.40E-02	2.31E-05	0.00
Tl-204	2.02E+01	9.07E+00	1.11E+01	1.02E-03	1.98E-02
Pb-205	5.33E+00	4.40E+00	9.28E-01	1.66E-03	3.74E-05
Pb-210+D	1.78E+04	1.45E+04	3.25E+03	5.87E+00	3.10E-02
Bi-207	6.07E+01	1.48E+01	3.43E+00	8.49E-03	4.25E+01
Po-209	8.56E+03	6.43E+03	2.13E+03	5.01E+00	9.31E-02
Po-210	6.63E+03	5.13E+03	1.50E+03	3.97E+00	1.30E-04
Ra-226+D	4.41E+03	3.59E+03	7.64E+02	3.65E+00	4.99E+01
Ra-228+D	4.74E+03	3.89E+03	8.16E+02	2.34E+00	3.15E+01
Ac-227+D	4.96E+04	4.00E+04	6.74E+03	2.85E+03	9.90E+00
Th-228+D	2.73E+03	2.19E+03	3.56E+02	1.46E+02	3.82E+01
Th-229+D	1.36E+04	1.09E+04	1.82E+03	9.17E+02	7.78E+00
Th-230	1.87E+03	1.48E+03	2.48E+02	1.38E+02	1.47E-02
Th-232	9.31E+03	7.37E+03	1.24E+03	6.96E+02	1.42E+00
Pa-231	3.40E+04	2.86E+04	4.81E+03	5.44E+02	1.07E+00

Table B-11. Low Water Infiltration Case: Columbia River Population.
Units are person-rem per pCi/L in the Columbia River.

Nuclide	Total	Ingest (Drink)	Ingest (Other)	Inhale	External
U-232	4.74E+03	3.54E+03	9.16E+02	2.80E+02	5.58E+00
U-233	1.04E+03	7.80E+02	2.00E+02	5.73E+01	7.40E-03
U-234	1.02E+03	7.64E+02	1.96E+02	5.60E+01	2.11E-03
U-235+D	9.62E+02	7.21E+02	1.85E+02	5.22E+01	3.88E+00
U-236	9.65E+02	7.26E+02	1.86E+02	5.30E+01	1.12E-03
U-238+D	9.60E+02	7.24E+02	1.85E+02	5.01E+01	6.09E-01
Np-237+D	1.42E+04	1.20E+04	2.03E+03	2.29E+02	5.41E+00
Pu-236	3.74E+03	3.16E+03	5.18E+02	6.15E+01	1.56E-02
Pu-238	1.02E+04	8.64E+03	1.44E+03	1.66E+02	7.96E-04
Pu-239	1.13E+04	9.56E+03	1.60E+03	1.82E+02	1.50E-03
Pu-240	1.13E+04	9.56E+03	1.60E+03	1.82E+02	7.75E-04
Pu-241+D	2.19E+02	1.85E+02	3.10E+01	3.50E+00	2.38E-04
Pu-242	1.08E+04	9.07E+03	1.51E+03	1.74E+02	6.77E-04
Pu-244+D	1.06E+04	8.96E+03	1.50E+03	1.71E+02	9.43E+00
Am-241	1.17E+04	9.83E+03	1.64E+03	1.88E+02	2.32E-01
Am-242m+D	1.13E+04	9.50E+03	1.59E+03	1.81E+02	3.42E-01
Am-243+D	1.16E+04	9.80E+03	1.64E+03	1.87E+02	4.61E+00
Cm-242	3.65E+02	3.11E+02	4.73E+01	7.31E+00	5.25E-04
Cm-243	8.05E+03	6.78E+03	1.14E+03	1.30E+02	2.96E+00
Cm-244	6.48E+03	5.45E+03	9.16E+02	1.05E+02	6.57E-04
Cm-245	1.20E+04	1.01E+04	1.70E+03	1.93E+02	1.78E+00
Cm-246	1.19E+04	9.99E+03	1.68E+03	1.91E+02	6.15E-04
Cm-247+D	1.10E+04	9.23E+03	1.56E+03	1.76E+02	9.12E+00
Cm-248	4.36E+04	3.67E+04	6.19E+03	7.00E+02	4.64E-04
Cm-250+D	2.49E+05	2.10E+05	3.54E+04	3.99E+03	8.92E+00
Bk-247	1.51E+04	1.27E+04	2.12E+03	2.44E+02	2.23E+00
Cf-248	1.15E+03	9.02E+02	2.28E+02	2.15E+01	5.07E-04
Cf-249	1.67E+04	1.28E+04	3.66E+03	2.45E+02	9.08E+00
Cf-250	7.49E+03	5.75E+03	1.63E+03	1.11E+02	6.14E-04
Cf-251	1.71E+04	1.31E+04	3.74E+03	2.50E+02	2.73E+00

Table B-12. Ratio of Total Dose to Drinking Water Dose.

Nuclide	Residential	Agricultural	All Pathways	NASR	Population
H-3	1.05	1.23	1.32	1.47	1.32
Be-10	1.14	1.17	1.27	1.62	1.21
C-14	1.21	4.22	4.14	5.87	3.46
Na-22	3.92	10.51	8.39	12.11	6.88
Si-32+D	1.15	1.16	1.25	1.62	1.20
Cl-36	7.42	26.27	29.41	54.13	22.98
K-40	1.33	3.01	2.82	4.11	2.43
Ti-44+D	2.58	4.89	4.29	5.56	3.62
V-49	1.13	1.18	1.29	1.61	1.22
Mn-54	4.75	4.81	4.14	4.09	3.56
Fe-55	1.14	1.63	1.84	2.21	1.66
Co-60	2.58	3.35	3.15	3.52	2.73
Ni-59	1.14	1.45	1.51	1.98	1.40
Ni-63	1.14	1.45	1.51	1.98	1.40
Se-79	1.14	2.27	2.45	3.25	2.14
Rb-87	1.15	3.17	2.82	4.32	2.43
Sr-90+D	1.16	1.43	1.43	2.02	1.34
Zr-93	1.15	1.32	1.46	1.81	1.36
Nb-91	1.21	10.26	10.86	13.35	8.75
Nb-93m	1.14	10.08	10.68	13.16	8.61
Nb-94	4.70	13.76	13.64	15.68	11.03
Mo-93	1.15	1.58	1.64	2.18	1.50
Tc-99	1.23	5.47	4.49	7.66	3.71
Ru-106+D	1.23	1.27	1.34	1.65	1.26
Pd-107	1.15	2.88	2.40	3.89	2.10
Ag-108m+D	4.54	7.86	6.10	8.29	5.10
Cd-109	1.15	1.32	1.36	1.83	1.28
Cd-113m	1.15	1.35	1.38	1.88	1.30
In-115	1.14	1.35	1.49	1.85	1.39
Sn-121m+D	1.14	3.16	3.74	4.17	3.15
Sn-126+D	2.65	4.67	4.94	5.18	4.14

Table B-12. Ratio of Total Dose to Drinking Water Dose.

Nuclide	Residential	Agricultural	All Pathways	NASR	Population
Sb-125	3.29	3.40	3.07	3.18	2.68
Te-125m	1.11	1.23	1.40	1.67	1.32
I-129	1.15	2.94	2.53	4.01	2.20
Cs-134	1.44	3.00	2.77	3.82	2.40
Cs-135	1.15	2.83	2.65	3.80	2.30
Cs-137+D	1.33	3.00	2.79	3.91	2.41
Ba-133	2.73	2.79	2.55	2.74	2.26
Pm-147	1.14	1.25	1.36	1.70	1.28
Sm-147	1.16	1.28	1.43	1.79	1.35
Sm-151	1.14	1.26	1.38	1.73	1.30
Eu-150	4.80	4.92	4.28	4.16	3.68
Eu-152	3.87	3.99	3.54	3.54	3.07
Eu-154	3.15	3.27	2.96	3.05	2.60
Eu-155	1.48	1.59	1.63	1.93	1.50
Gd-152	1.21	1.29	1.56	1.92	1.49
Ho-166m	4.55	4.66	4.08	3.99	3.51
Re-187	1.17	1.63	1.70	2.32	1.55
Tl-204	1.14	2.33	2.57	3.11	2.23
Pb-205	1.14	1.19	1.27	1.65	1.21
Pb-210+D	1.15	1.20	1.29	1.69	1.22
Bi-207	5.54	5.64	4.80	4.64	4.10
Po-209	1.14	1.22	1.42	1.81	1.33
Po-210	1.12	1.18	1.37	1.71	1.29
Ra-226+D	1.16	1.25	1.29	1.69	1.23
Ra-228+D	1.15	1.23	1.28	1.68	1.22
Ac-227+D	1.16	1.16	1.29	1.64	1.24
Th-228+D	1.18	1.18	1.30	1.64	1.25
Th-229+D	1.17	1.17	1.30	1.66	1.25
Th-230	1.17	1.17	1.31	1.66	1.26
Th-232	1.17	1.17	1.31	1.67	1.26
Pa-231	1.15	1.15	1.24	1.59	1.19

Table B-12. Ratio of Total Dose to Drinking Water Dose.

Nuclide	Residential	Agricultural	All Pathways	NASR	Population
U-232	1.17	1.29	1.41	1.84	1.34
U-233	1.16	1.28	1.40	1.82	1.33
U-234	1.16	1.28	1.40	1.82	1.33
U-235+D	1.17	1.29	1.41	1.83	1.33
U-236	1.16	1.28	1.40	1.82	1.33
U-238+D	1.16	1.28	1.40	1.82	1.33
Np-237+D	1.15	1.15	1.24	1.59	1.19
Pu-236	1.14	1.14	1.23	1.57	1.18
Pu-238	1.15	1.15	1.24	1.58	1.19
Pu-239	1.15	1.15	1.24	1.58	1.19
Pu-240	1.15	1.15	1.24	1.58	1.19
Pu-241+D	1.15	1.15	1.24	1.59	1.19
Pu-242	1.15	1.15	1.24	1.58	1.19
Pu-244+D	1.15	1.15	1.24	1.59	1.19
Am-241	1.15	1.15	1.24	1.58	1.19
Am-242m+D	1.15	1.15	1.24	1.59	1.19
Am-243+D	1.15	1.15	1.24	1.58	1.19
Cm-242	1.13	1.14	1.22	1.54	1.18
Cm-243	1.15	1.15	1.24	1.59	1.19
Cm-244	1.15	1.15	1.24	1.59	1.19
Cm-245	1.15	1.15	1.24	1.59	1.19
Cm-246	1.15	1.15	1.24	1.59	1.19
Cm-247+D	1.15	1.15	1.24	1.59	1.19
Cm-248	1.15	1.15	1.24	1.59	1.19
Cm-250+D	1.15	1.15	1.24	1.59	1.19
Bk-247	1.15	1.15	1.24	1.58	1.19
Cf-248	1.14	1.23	1.35	1.68	1.28
Cf-249	1.15	1.26	1.39	1.74	1.31
Cf-250	1.15	1.26	1.38	1.73	1.30
Cf-251	1.15	1.26	1.39	1.74	1.31
Cf-252	1.14	1.25	1.37	1.71	1.30

Table B-13. Ingestion Dose Factors.
Units are mrem/pCi Ingested.

Nuclide	f1	GENII	EPA	DOE	GENII/EPA	DOE/EPA
H-3	1	6.12E-08	6.40E-08	6.30E-08		
Be-10	0.005	4.70E-06	4.66E-06	4.20E-06		0.90
C-14	1	2.06E-06	2.09E-06	2.10E-06		
Na-22	1	1.06E-05	1.15E-05	1.20E-05	0.92	
Si-32+D	0.01	1.11E-05	1.10E-05	9.40E-06		0.85
Cl-36	1	2.95E-06	3.03E-06	3.00E-06		
K-40	1	1.79E-05	1.86E-05	1.90E-05		
Ti-44+D	0.01	2.35E-05	2.46E-05	1.91E-05		0.78
V-49	0.01	6.04E-08	6.14E-08	5.40E-08		0.88
Mn-54	0.1	2.76E-06	2.77E-06	2.70E-06		
Fe-55	0.1	6.15E-07	6.07E-07	5.80E-07		
Co-60	0.3	2.65E-05	2.69E-05	2.60E-05		
Ni-59	0.05	2.05E-07	2.10E-07	2.00E-07		
Ni-63	0.05	5.72E-07	5.77E-07	5.40E-07		0.94
Se-79	0.8	8.33E-06	8.70E-06	8.30E-06		
Rb-87	1	4.73E-06	4.92E-06	4.80E-06		
Sr-90+D	0.3	1.31E-04	1.53E-04	1.40E-04	0.86	0.92
Zr-93	0.002	1.64E-06	1.66E-06	1.60E-06		
Nb-91	0.01	5.05E-07	5.22E-07	5.30E-07		
Nb-93m	0.01	5.05E-07	5.22E-07	5.30E-07		
Nb-94	0.01	7.25E-06	7.14E-06	5.10E-06		0.71
Mo-93	0.8	1.21E-06	1.35E-06	1.30E-06	0.90	
Tc-99	0.8	2.23E-06	1.46E-06	1.30E-06	1.53	0.89
Ru-106+D	0.05	2.73E-05	2.74E-05	2.10E-05		0.77
Pd-107	0.005	1.50E-07	1.49E-07	1.40E-07		0.94
Ag-108m+D	0.05	7.58E-06	7.62E-06	7.50E-06		
Cd-109	0.05	1.32E-05	1.31E-05	1.20E-05		0.92
Cd-113m	0.05	1.62E-04	1.61E-04	1.50E-04		0.93
In-115	0.02	8.68E-05	1.58E-04	1.40E-04	0.55	0.89
Sn-121m+D	0.02	2.24E-06	2.25E-06	1.99E-06		0.88
Sn-126+D	0.02	2.08E-05	2.11E-05	1.83E-05		0.87

Table B-13. Ingestion Dose Factors.
Units are mrem/pCi Ingested.

Nuclide	f1	GENII	EPA	DOE	GENII/EPA	DOE/EPA
Sb-125+D	0.1	2.83E-06	2.81E-06	2.60E-06		0.93
Te-125m	0.2	3.72E-06	3.67E-06	3.40E-06		0.93
I-129	1	2.49E-04	2.76E-04	2.80E-04	0.90	
Cs-134	1	6.82E-05	7.33E-05	7.40E-05	0.93	
Cs-135	1	6.86E-06	7.07E-06	7.10E-06		
Cs-137+D	1	4.74E-05	5.00E-05	5.00E-05	0.95	
Ba-133	0.1	3.05E-06	3.40E-06	3.20E-06	0.90	0.94
Pm-147	0.0003	1.06E-06	1.05E-06	9.50E-07		0.90
Sm-147	0.0003	1.86E-04	1.85E-04	1.80E-04		
Sm-151	0.0003	3.87E-07	3.89E-07	3.40E-07		0.87
Eu-150	0.001	6.34E-06	6.36E-06	6.20E-06		
Eu-152	0.001	6.48E-06	6.48E-06	6.00E-06		0.93
Eu-154	0.001	9.61E-06	9.55E-06	9.10E-06		
Eu-155	0.001	1.53E-06	1.53E-06	1.30E-06		0.85
Gd-152	0.0003	1.61E-04	1.61E-04	1.50E-04		0.93
Ho-166m	0.0003	8.13E-06	8.07E-06	7.80E-06		
Re-187	0.8	1.45E-08	9.51E-09	8.30E-09	1.52	0.87
Tl-204	1	3.46E-06	3.36E-06	3.20E-06		
Pb-205	0.2	1.64E-06	1.63E-06	1.50E-06		0.92
Pb-210+D	0.2	5.40E-03	5.37E-03	5.11E-03		
Bi-207	0.05	5.49E-06	5.48E-06	4.90E-06		0.89
Po-209	0.1	2.39E-03	2.38E-03	2.00E-03		0.84
Po-210	0.1	1.90E-03	1.90E-03	1.60E-03		0.84
Ra-226+D	0.2	9.51E-04	1.33E-03	1.10E-03	0.72	0.83
Ra-228+D	0.2	8.44E-04	1.44E-03	1.20E-03	0.59	0.83
Ac-227+D	0.001	1.44E-02	1.48E-02	1.46E-02		
Th-228+D	0.0002	5.79E-04	8.11E-04	7.54E-04	0.71	0.93
Th-229+D	0.0002	3.87E-03	4.03E-03	3.91E-03		
Th-230	0.0002	5.48E-04	5.48E-04	5.30E-04		
Th-232	0.0002	2.73E-03	2.73E-03	2.80E-03		
Pa-231	0.001	1.06E-02	1.06E-02	1.10E-02		

Table B-13. Ingestion Dose Factors.
Units are mrem/pCi Ingested.

Nuclide	f1	GENII	EPA	DOE	GENII/EPA	DOE/EPA
U-232	0.05	1.31E-03	1.31E-03	1.30E-03		
U-233	0.05	2.90E-04	2.89E-04	2.70E-04		0.93
U-234	0.05	2.84E-04	2.83E-04	2.60E-04		0.92
U-235+D	0.05	2.67E-04	2.67E-04	2.51E-04		0.94
U-236	0.05	2.69E-04	2.69E-04	2.50E-04		0.93
U-238+D	0.05	2.70E-04	2.68E-04	2.43E-04		0.91
Np-237+D	0.001	5.22E-03	4.44E-03	3.90E-03	1.18	0.88
Pu-236	0.001	1.16E-03	1.17E-03	1.30E-03		1.11
Pu-238	0.001	3.19E-03	3.20E-03	3.80E-03		1.19
Pu-239	0.001	3.53E-03	3.54E-03	4.30E-03		1.21
Pu-240	0.001	3.53E-03	3.54E-03	4.30E-03		1.21
Pu-241+D	0.001	6.79E-05	6.85E-05	8.60E-05		1.26
Pu-242	0.001	3.35E-03	3.36E-03	4.10E-03		1.22
Pu-244+D	0.001	3.32E-03	3.32E-03	4.00E-03		1.20
Am-241	0.001	3.62E-03	3.64E-03	4.50E-03		1.24
Am-242m+D	0.001	3.50E-03	3.52E-03	4.20E-03		1.19
Am-243+D	0.001	3.62E-03	3.63E-03	4.50E-03		1.24
Cm-242	0.001	1.15E-04	1.15E-04	1.10E-04		
Cm-243	0.001	2.50E-03	2.51E-03	2.90E-03		1.16
Cm-244	0.001	2.01E-03	2.02E-03	2.30E-03		1.14
Cm-245	0.001	3.73E-03	3.74E-03	4.50E-03		1.20
Cm-246	0.001	3.70E-03	3.70E-03	4.50E-03		1.22
Cm-247+D	0.001	3.40E-03	3.42E-03	4.10E-03		1.20
Cm-248	0.001	1.36E-02	1.36E-02	1.60E-02		1.18
Cm-250+D	0.001	7.76E-02	7.77E-02	7.77E-02		
Bk-247	0.001	3.81E-03	4.70E-03	2.30E-03	0.81	0.49
Cf-248	0.001	3.39E-04	3.34E-04	2.80E-04		0.84
Cf-249	0.001	4.75E-03	4.74E-03	4.60E-03		
Cf-250	0.001	2.13E-03	2.13E-03	1.90E-03		0.89
Cf-251	0.001	4.82E-03	4.85E-03	4.60E-03		0.95
Cf-252	0.001	1.09E-03	1.08E-03	9.40E-04		0.87

Table B-13. Ingestion Dose Factors.
Units are mrem/pCi Ingested.

Nuclide	f1	GENII	EPA	DOE	GENII/EPA	DOE/EPA

Notes:

(1) GENII Internal DF are from the July 1999 library revision by PDR. EPA Inhalation & Ingestion dose factors from Federal Guidance Report Number 11, EPA-520/1-88-020, Sept 1988. DOE Ingestion & Inhalation dose factors from DOE/EH-0071, (DE88-014297), July 1988. All are 50 year committed EDE.

(2) "DF" means dose factor. "f1" is the fraction of ingested activity reaching body fluids.

(3) The short-lived radioactive progeny shown on Table B-1 are assumed to be in secular equilibrium with their parent nuclide. The dose factors for implicit daughters have been added to the parent dose factor to give the values shown.

(4) The last two columns show ratios of GENII and DOE ingestion dose factors to the EPA dose factors. Ratios of dose factors within 5% of the EPA value are not shown.

Table B-14. Inhalation Dose Factors
Units are mrem/pCi Inhaled.

Nuclide	Lung Model	GENII	EPA	DOE	GENII/EPA	DOE/EPA
H-3	H2O	9.02E-08	9.60E-08	9.45E-08	0.94	
Be-10	Y	3.54E-04	3.54E-04	3.50E-04		
C-14	Organic	2.06E-06	2.09E-06	2.10E-06		
Na-22	D	7.11E-06	7.66E-06	8.00E-06	0.93	
Si-32+D	Y	1.02E-03	1.03E-03	1.01E-03		
Cl-36	W	2.21E-05	2.19E-05	2.00E-05		0.91
K-40	D	1.19E-05	1.24E-05	1.20E-05		
Ti-44+D	D	4.18E-04	4.52E-04	4.50E-04	0.92	
V-49	W	3.46E-07	3.45E-07	2.80E-07		0.81
Mn-54	W	6.36E-06	6.70E-06	6.40E-06	0.95	
Fe-55	D	2.74E-06	2.69E-06	2.60E-06		
Co-60	Y	2.00E-04	2.19E-04	1.50E-04	0.91	0.68
Ni-59	D	1.28E-06	1.32E-06	1.30E-06		
Ni-63	D	3.06E-06	3.10E-06	3.00E-06		
Se-79	W	9.49E-06	9.84E-06	8.90E-06		0.9
Rb-87	D	3.18E-06	3.23E-06	3.30E-06		
Sr-90+D	D	2.10E-04	2.48E-04	2.37E-04	0.85	
Zr-93	D	3.16E-04	3.21E-04	3.20E-04		
Nb-91	Y	2.94E-05	2.92E-05	2.80E-05		
Nb-93m	Y	2.94E-05	2.92E-05	2.80E-05		
Nb-94	Y	3.91E-04	4.14E-04	3.30E-04	0.94	0.8
Mo-93	Y	2.80E-05	2.84E-05	2.80E-05		
Tc-99	W	9.00E-06	8.33E-06	7.50E-06	1.08	0.9
Ru-106+D	Y	4.75E-04	4.77E-04	4.40E-04		0.92
Pd-107	Y	1.29E-05	1.28E-05	1.30E-05		
Ag-108m+D	Y	2.58E-04	2.83E-04	2.00E-04	0.91	0.71
Cd-109	D	1.15E-04	1.14E-04	1.00E-04		0.88
Cd-113m	D	1.54E-03	1.53E-03	1.40E-03		0.92
In-115	D	2.02E-03	3.74E-03	3.40E-03	0.54	0.91
Sn-121m+D	W	1.18E-05	1.19E-05	9.26E-06		0.78
Sn-126+D	W	1.00E-04	1.01E-04	7.54E-05		0.75
Sb-125+D	W	1.23E-05	1.22E-05	9.80E-06		0.8
Te-125m	W	7.18E-06	7.29E-06	6.70E-06		0.92
I-129	D	1.51E-04	1.74E-04	1.80E-04	0.87	
Cs-134	D	4.28E-05	4.63E-05	4.70E-05	0.92	
Cs-135	D	4.49E-06	4.55E-06	4.50E-06		
Cs-137+D	D	2.98E-05	3.19E-05	3.20E-05	0.93	
Ba-133	D	6.00E-06	7.81E-06	6.90E-06	0.77	0.88
Pm-147	Y	3.92E-05	3.92E-05	3.40E-05		0.87

Table B-14. Inhalation Dose Factors
Units are mrem/pCi Inhaled.

Nuclide	Lung Model	GENII	EPA	DOE	GENII/EPA	DOE/EPA
Sm-147	W	7.48E-02	7.47E-02	7.10E-02		
Sm-151	W	3.01E-05	3.00E-05	2.90E-05		
Eu-150	W	2.50E-04	2.68E-04	2.70E-04	0.93	
Eu-152	W	2.11E-04	2.21E-04	2.20E-04		
Eu-154	W	2.78E-04	2.86E-04	2.60E-04		0.91
Eu-155	W	4.12E-05	4.14E-05	3.90E-05		0.94
Gd-152	D	2.44E-01	2.43E-01	2.40E-01		
Ho-166m	W	7.46E-04	7.73E-04	7.20E-04		0.93
Re-187	W	5.86E-08	5.44E-08	4.90E-08	1.08	0.9
Tl-204	D	2.46E-06	2.41E-06	2.30E-06		
Pb-205	D	3.97E-06	3.92E-06	3.70E-06		0.94
Pb-210+D	D	1.39E-02	1.38E-02	1.32E-02		
Bi-207	W	1.96E-05	2.00E-05	1.40E-05		0.7
Po-209	D	1.19E-02	1.18E-02	1.01E-02		0.86
Po-210	D	9.65E-03	9.40E-03	8.10E-03		0.86
Ra-226+D	W	8.22E-03	8.60E-03	7.91E-03		0.92
Ra-228+D	W	4.40E-03	5.08E-03	4.49E-03	0.87	0.88
Ac-227+D	D	6.71E+00	6.72E+00	6.72E+00		
Th-228+D	W	3.47E-01	3.45E-01	3.13E-01		0.91
Th-229+D	W	2.16E+00	2.16E+00	2.02E+00		0.94
Th-230	W	3.27E-01	3.26E-01	3.20E-01		
Th-232	W	1.64E+00	1.64E+00	1.60E+00		
Pa-231	W	1.29E+00	1.28E+00	1.30E+00		
U-232	Y	6.56E-01	6.59E-01	6.70E-01		
U-233	Y	1.35E-01	1.35E-01	1.30E-01		
U-234	Y	1.32E-01	1.32E-01	1.30E-01		
U-235+D	Y	1.24E-01	1.23E-01	1.20E-01		
U-236	Y	1.26E-01	1.25E-01	1.20E-01		
U-238+D	Y	1.18E-01	1.18E-01	1.20E-01		
Np-237+D	W	6.32E-01	5.40E-01	4.90E-01	1.17	0.91
Pu-236	W	1.45E-01	1.45E-01	1.60E-01		1.1
Pu-238	W	3.90E-01	3.92E-01	4.60E-01		1.17
Pu-239	W	4.30E-01	4.29E-01	5.10E-01		1.19
Pu-240	W	4.30E-01	4.29E-01	5.10E-01		1.19
Pu-241+D	W	8.17E-03	8.25E-03	1.00E-02		1.21
Pu-242	W	4.08E-01	4.11E-01	4.80E-01		1.17
Pu-244+D	W	4.03E-01	4.03E-01	4.80E-01		1.19
Am-241	W	4.41E-01	4.44E-01	5.20E-01		1.17
Am-242m+D	W	4.24E-01	4.26E-01	5.10E-01		1.2
Am-243+D	W	4.41E-01	4.40E-01	5.20E-01		1.18

Table B-14. Inhalation Dose Factors

Units are mrem/pCi Inhaled.

Nuclide	Lung Model	GENII	EPA	DOE	GENII/EPA	DOE/EPA
Cm-242	W	1.75E-02	1.73E-02	1.70E-04		
Cm-243	W	3.07E-01	3.07E-01	3.50E-01		1.14
Cm-244	W	2.48E-01	2.48E-01	2.70E-01		1.09
Cm-245	W	4.55E-01	4.55E-01	5.40E-01		1.19
Cm-246	W	4.51E-01	4.51E-01	5.40E-01		1.2
Cm-247+D	W	4.15E-01	4.14E-01	4.90E-01		1.18
Cm-248	W	1.65E+00	1.65E+00	1.90E+00		1.15
Cm-250+D	W	9.43E+00	9.40E+00	9.40E+00		
Bk-247	W	4.65E-01	5.74E-01	5.50E-01	0.81	
Cf-248	Y	5.11E-02	5.07E-02	4.30E-02		0.85
Cf-249	W	5.77E-01	5.77E-01	5.50E-01		
Cf-250	W	2.63E-01	2.62E-01	2.20E-01		0.84
Cf-251	W	5.87E-01	5.88E-01	5.60E-01		
Cf-252	Y	1.55E-01	1.57E-01	1.30E-01		0.83

Notes:

(1) GENII Internal DF are from the July 1999 library revision by PDR. EPA Inhalation & Ingestion dose factors from Federal Guidance Report Number 11, EPA-520/1-88-020, Sept 1988. DOE Ingestion & Inhalation dose factors from DOE/EH-0071, (DE88-014297), July 1988. All are 50 year committed EDE.

(2) "DF" means dose factor. "Lung" refers to the ICRP lung model classification, "H2O" is tritium vapor (which includes skin absorption), "Organic" means organic carbon, "D" is days, "W" is weeks, and "Y" is years.

(3) The short-lived radioactive progeny shown on Table B-1 are assumed to be in secular equilibrium with their parent nuclide. The dose factors for implicit daughters have been added to the parent dose factor to give the values shown.

(4) The last two columns show ratios of GENII and DOE inhalation dose factors to the EPA dose factors. Ratios of dose factors within 5% of the EPA value are not shown.

Table B-15. External Dose Rate Factors.
Units are mrem/h per Ci/m^2.

Nuclide	GENII	EPA	DOE	GENII/EPA	DOE/EPA
H-3	3.49E-08	0	0	EPA=0	
Be-10	4.33E-01	5.37E-01	0	0.806	DOE=0
C-14	7.51E-03	6.82E-03	0		DOE=0
Na-22	6.75E+03	5.98E+03	2.40E+04	1.13	4.01
Si-32+D	9.62E+00	5.70E+00	0	1.69	DOE=0
Cl-36	8.58E-01	1.16E+00	5.32E-04	0.74	0.000459
K-40	4.87E+02	4.33E+02	1.56E+03	1.12	3.6
Ti-44+D	7.10E+03	6.00E+03	2.57E+04	1.18	4.28
V-49	0	0	8.60E-01		EPA=0
Mn-54	2.53E+03	2.27E+03	9.59E+03	1.11	4.22
Fe-55	1.07E-01	0	2.52E+00	EPA=0	EPA=0
Co-60	7.51E+03	6.87E+03	2.59E+04		3.77
Ni-59	1.31E-01	0	4.75E+00	EPA=0	EPA=0
Ni-63	1.91E-04	0	0	EPA=0	
Se-79	5.37E-03	9.44E-03	0	0.569	DOE=0
Rb-87	4.02E-02	7.13E-02	0	0.564	DOE=0
Sr-90+D	1.97E+01	1.17E+01	0	1.68	DOE=0
Zr-93	1.34E-04	0	0	EPA=0	
Nb-91	5.74E+00	5.74E+00	8.36E+01		14.6
Nb-93m	4.33E-02	5.28E-02	1.17E+01	0.82	222
Nb-94	4.67E+03	4.29E+03	1.81E+04		4.22
Mo-93	2.43E-01	2.99E-01	6.59E+01	0.813	220
Tc-99	5.04E-02	6.35E-02	7.14E-03	0.794	0.112
Ru-106+D	7.32E+02	5.83E+02	2.40E+03	1.26	4.12
Pd-107	4.16E-06	0	0	EPA=0	
Ag-108m+D	5.37E+03	4.37E+03	1.90E+04	1.23	4.35
Cd-109	2.61E+00	7.47E+00	1.08E+02	0.349	14.5
Cd-113m	4.28E-01	3.24E-01	0	1.32	DOE=0
In-115	2.56E-01	2.01E-01	0	1.27	DOE=0
Sn-121m+D	5.15E+00	1.07E+00	0	4.81	DOE=0
Sn-126+D	6.56E+03	5.36E+03	2.37E+04	1.22	4.42
Sb-125+D	1.49E+03	1.12E+03	5.05E+03	1.33	4.51
Te-125m	8.78E+00	7.67E+00	2.40E+02	1.14	31.3
I-129	5.54E+00	6.57E+00	2.51E+02	0.843	38.2
Cs-134	5.23E+03	4.24E+03	1.80E+04	1.23	4.25
Cs-135	1.46E-02	1.94E-02	0	0.753	DOE=0
Cs-137+D	1.82E+03	1.53E+03	6.59E+03	1.19	4.31
Ba-133	1.10E+03	9.36E+02	4.78E+03	1.18	5.11

Table B-15. External Dose Rate Factors.
Units are mrem/h per Ci/m^2.

Nuclide	GENII	EPA	DOE	GENII/EPA	DOE/EPA
Pm-147	2.74E-02	2.53E-02	4.68E-02		1.85
Sm-147	0	0	0		
Sm-151	1.95E-03	4.99E-04	5.93E-02	3.91	119
Eu-150	5.04E+03	3.96E+03	0	1.27	DOE=0
Eu-152	3.60E+03	3.05E+03	1.27E+04	1.18	4.16
Eu-154	3.74E+03	3.34E+03	1.38E+04	1.12	4.13
Eu-155	8.98E+01	9.24E+01	8.16E+02		8.83
Gd-152	0	0	0		
Ho-166m	4.67E+03	4.64E+03	1.88E+04		4.05
Re-187	0	0	0		
Tl-204	1.93E+00	2.04E+00	1.48E+01		7.25
Pb-205	8.75E-02	3.58E-03	8.61E+00	24.4	2410
Pb-210+D	3.85E+00	3.00E+00	3.42E+01	1.28	11.4
Bi-207	4.92E+03	4.11E+03	1.72E+04	1.2	4.18
Po-209	8.95E+00	8.95E+00	4.10E+01		4.58
Po-210	2.68E-02	2.32E-02	9.81E-02	1.16	4.23
Ra-226+D	5.61E+03	4.78E+03	1.92E+04	1.17	4.02
Ra-228+D	3.04E+03	2.62E+03	1.04E+04	1.16	3.97
Ac-227+D	1.08E+03	9.61E+02	5.00E+03	1.12	5.2
Th-228+D	4.92E+03	4.20E+03	1.66E+04	1.17	3.95
Th-229+D	9.04E+02	7.45E+02	4.09E+03	1.21	5.49
Th-230	4.11E-01	6.05E-01	1.03E+01	0.679	17
Th-232	2.13E-01	2.63E-01	7.60E+00	0.81	28.9
Pa-231	9.09E+01	9.11E+01	4.08E+02		4.48
U-232	3.10E-01	4.52E-01	1.17E+01	0.686	25.9
U-233	4.81E-01	6.86E-01	5.70E+00	0.701	8.31
U-234	1.89E-01	2.03E-01	9.21E+00		45.4
U-235+D	2.52E+02	3.74E+02	2.17E+03	0.674	5.8
U-236	9.85E-02	1.08E-01	8.36E+00		77.4
U-238+D	7.10E+01	5.87E+01	2.81E+02	1.21	4.79
Np-237+D	7.13E+02	5.28E+02	3.06E+03	1.35	5.8
Pu-236	9.45E-02	1.14E-01	1.13E+01	0.829	99.1
Pu-238	1.06E-01	7.65E-02	9.79E+00	1.39	128
Pu-239	1.59E-01	1.44E-01	4.31E+00	1.1	29.9
Pu-240	7.29E-02	7.43E-02	9.35E+00		126
Pu-241+D	9.43E-03	9.29E-03	4.40E-02		4.74
Pu-242	9.57E-02	6.49E-02	7.78E+00	1.47	120
Pu-244+D	1.17E+03	9.04E+02	3.86E+03	1.29	4.27
Am-241	1.45E+01	2.22E+01	3.41E+02	0.653	15.4
Am-242m+D	3.58E+01	3.28E+01	2.66E+02		8.11

Table B-15. External Dose Rate Factors.
Units are mrem/h per Ci/m^2.

Nuclide	GENII	EPA	DOE	GENII/EPA	DOE/EPA
Am-243+D	4.49E+02	4.42E+02	2.94E+03		6.65
Cm-242	5.97E-02	8.59E-02	1.07E+01	0.695	125
Cm-243	2.90E+02	2.86E+02	1.67E+03		5.84
Cm-244	5.09E-02	6.39E-02	9.46E+00	0.797	148
Cm-245	1.32E+02	1.71E+02	9.74E+02	0.772	5.7
Cm-246	4.19E-02	5.89E-02	8.37E+00	0.711	142
Cm-247+D	1.30E+03	8.74E+02	4.16E+03	1.49	4.76
Cm-248	3.83E-02	4.45E-02	6.71E+00	0.861	151
Cm-250+D	1.20E+03	8.55E+02	4.40E+03	1.4	5.15
Bk-247	2.32E+02	2.14E+02	0		DOE=0
Cf-248	3.43E-02	6.32E-02	7.68E+00	0.543	122
Cf-249	9.82E+02	8.71E+02	4.02E+03	1.13	4.62
Cf-250	5.37E-02	6.01E-02	7.81E+00	0.894	130
Cf-251	2.40E+02	2.62E+02	1.55E+03		5.92
Cf-252	4.25E-02	8.91E-02	7.23E+00	0.477	81.1

Notes:

(1) GENII external DRF were computed using the EXTDF program. EPA external DRF are from Federal Guidance Report Number 12, EPA 402-R-93-081 (Sept 1993). DOE external DRF are from DOE/EH-0070 (July 1988).

(2) Short-lived radioactive progeny included in the "+D" nuclides are in secular equilibrium with their parent nuclide.

(3) The conversion to area units from volume units assumes a thickness of 0.15 meters. The density correction applied to the EPA (1993) dose rate factors is 1.067. Because Nb-91 and Po-209 are not part of the EPA compilation, the GENII values were used.

(4) The last two columns show ratios of GENII and DOE external dose rate factors to the EPA dose rate factors. Ratios within 10% of the EPA value are not shown.

Appendix C

Equations Used in Major Codes

C. GOVERNING EQUATIONS USED IN MAJOR CODES

C.1 INTRODUCTION

This section briefly summarizes the equations used in the major computer codes. More information can be found in the user's manual for each of the codes:

- CFEST Gupta 1987
- STORM Bacon 2000
- VAM3DF Huyakorn 1999.

C.2 FLOW AND TRANSPORT

C.2.1 Overview

This section discusses the equations important in calculating moisture flow and contaminant transport. All three major codes use the same basic equations. The first section presents the equations on which the water flow calculations are based. The next section discusses contaminant transport associated with moisture flow. The final section describes moisture movement under diffusive conditions.

C.2.2 Moisture Flow

Two distinct moisture content regimes are present during contaminant transport: the unconfined aquifer and the disposal facility/vadose zone. In the unconfined aquifer all the pore spaces are filled with water; that is, the medium is saturated with water. In the disposal facility/ vadose zone the pore spaces between the soil particles are only partially filled with water. These zones are unsaturated.

Water flow through a saturated porous medium, such as the unconfined aquifer, is governed by the empirical relationship known as Darcy's Law (Freeze 1979) and by the conservation of mass. Darcy's law can be expressed as

$$\vec{v} = -\overleftrightarrow{K}\,\vec{\nabla} h \qquad \text{(C.1)}$$

where v is the velocity vector (m/year)
K is the hydraulic conductivity tensor (m/year)
h is the hydraulic head vector (m).

By using the conservation of water entering and leaving a volume and by using Darcy's law to relate the hydraulic gradient to the rate at which water enters and leaves the same volume, transient water flow in a saturated porous media can be expressed as

$$\nabla\left[\overset{\Leftrightarrow}{K}\nabla h\right] = \frac{Sh}{t} + Q \tag{C.2}$$

where S is the specific storage (m^{-1})

Q is the source or sink of moisture (y^{-1}).

Darcy's law defines the discharge of water through a cross section of porous media. However, in contamination transport, the average velocity of water flowing through the medium is important. This is because contaminants that are not geochemically retarded move with the water. The average velocity of the pore water is determined by dividing the velocity of the water by the porosity of the medium. Porosity is defined as the ratio of void space to total volume.

In an unsaturated medium, the pores are not completely filled with water. Capillary forces and the dependence of hydraulic conductivity on moisture content also must be considered. Richards equation (Richards 1931) becomes the governing equation:

$$\nabla[K(\psi)\nabla\psi\,] + \partial K_{zz}(\psi)/\partial z = (d\theta/d\psi)\,(\partial\psi/\partial t) + Q \tag{C.3}$$

where K is again the hydraulic conductivity tensor (m/year), but now depends on the pressure head

ψ is the pressure head (m), which depends on the moisture content

θ is the moisture content (dimensionless)

z is the vertical column of moisture (m).

The relationship between the pressure head and the hydraulic head is simply

$$h = \psi + z. \tag{C.4}$$

For the performance assessment calculations, the hydraulic conductivity tensor is reduced to a single function, with

$$K_{ij} = K, \text{ for } i = j \text{ and} \tag{C.5}$$

$$K_{ij} = 0, \text{ for } i \neq j.$$

The functional dependence of the pressure head on moisture content and of the hydraulic conductivity on pressure head and ultimately on moisture content is discussed in Section 3.4.3.2.

For extremely dry conditions, vapor diffusion may be important. In such conditions, water does not move as a collective body, but rather as single molecules. Such diffusion can be described by Fick's equation,

$$\frac{dm}{dt} = -\,Dv\,A\,\frac{dC}{dx} \tag{C.6}$$

where dm/dt is the mass rate of water vapor diffusion (g/year)

D_v is the effective vapor diffusion coefficient (m^2/year)

A is the cross section area (m^2)

C is the water vapor mass concentration in the gas phase (g/m^3)

dC/dx is the water vapor mass concentration gradient (g/m^4).

C.2.3 Advective and Diffusive Transport

The equation for the advective and diffusive transport of contaminants can be viewed as a mass balance on a differential volume. The advective-dispersive equation for solute movement through a porous medium with a constant, steady-state flow velocity was developed (Codell 1982) for the limiting case of unidirectional advective transport with three-dimensional dispersion in a homogeneous, saturated aquifer,

$$n_e \frac{\partial C}{\partial t} + (n - ne)\frac{\partial G}{\partial t} + (1-n)\frac{\partial P}{\partial t} + n_e u \frac{\partial C}{\partial x} =$$

$$n_e\left[E_x \frac{\partial^2 C}{\partial x^2} + E_y \frac{\partial^2 C}{\partial y^2} + E_z \frac{\partial^2 C}{\partial z^2}\right] +$$

$$(n - n_e)\left[E_x^1 \frac{\partial^2 G}{\partial x^2} + E_y^1 \frac{\partial^2 G}{\partial y^2} + E_z^1 \frac{\partial^2 G}{\partial z^2}\right] -$$

$$n_e \lambda C - (1-n)\lambda P - (n - n_e)\lambda G \qquad \text{(C.7)}$$

where C is the dissolved concentration in the liquid phase in voids that are interconnected and allow flow [flowing voids] (g/m^3 or Ci/m^3)

G is the dissolved concentration in the liquid phase in voids that are not interconnected and do not allow flow [non-flowing voids] (g/m^3 or Ci/m^3)

P is the particulate concentrations on the solid phase (g/g or Ci/g)

n is the total porosity (dimensionless)

n_e is the effective porosity (dimensionless)

t is the time (year)

u is the x-component of groundwater or pore water velocity (m/year)

E_i is the dispersion coefficient in the flowing voids in the i-th (where i = x, y, or z) direction (m^2/year)

E_i' is the diffusion coefficient in the non-flowing voids in the i-th direction (m^2/year)

λ is the decay constant [= (ln 2)/half life] (y^{-1}).

Each term in the equation represents some aspect of the solute movement through the porous medium. The first term on the left of the equal sign is the accumulation (storage) of the

solute in the liquid phase in the flowing void. The second term is the accumulation in the liquid phase in the nonflowing void. The third term is the accumulation in the solid phase; and the term to the left of the equal sign is x-direction advective transport in the flowing voids in the liquid phase. The first term to the right of the equal sign represents the dispersive transport in the flowing voids in the liquid phase in each direction. The second term represents the diffusive transport in the nonflowing voids in the liquid phase in each direction. The last terms are the chemical degradation or radioactive decay in the liquid phase in the flowing void, in the solid phase, and in the liquid phase in the nonflowing void respectively.

Using the following assumptions:

- The dissolved concentration in the nonflowing voids (G) equals the dissolved concentration in the flowing voids (C) for each time and position
- The contaminant absorption process can be described by a constant, ($K = \rho^* K_d/(1 - n)$), representing the ratio between the contaminant absorbed to the soil matrix (P) and the contaminant dissolved in solution (C)
- The diffusion in the nonflowing void (E'_i) is comparable with the dispersion in the flowing void (E_i),the equation (D.7) can be simplified to

$$\frac{\partial C}{\partial t} + \frac{u}{R_f}\frac{\partial C}{\partial x} = \frac{D_x}{R_f}\frac{\partial^2 C}{\partial x^2} + \frac{D_y}{R_f}\frac{\partial^2 C}{\partial y^2} + \frac{D_z}{R_f}\frac{\partial^2 C}{\partial z^2} - \lambda C \qquad \text{(C.8)}$$

in which $$D_i = n\, E_i / n_e \qquad \text{(C.9)}$$

and $$R_f = n / n_e + (\rho^* K_d) / n_e \qquad \text{(C.10)}$$

and where

D_i is the pseudodispersion coefficient (m^2/year)

R_f is the retardation factor (dimensionless)

ρ is the bulk density (g/m^3)

K_d is the equilibrium (partition or distribution) coefficient (m^3/g).

The retardation factor (R_f) is used as a measure of the mobility of constituents in a porous medium.

By making the following substitutions,

$$u^* = u / R_f \qquad \text{(C.11)}$$

and $$D_i^* = D_i / R_f ,$$

the contaminant transport equation can be written as

$$\frac{\partial C}{\partial t} + u^* \frac{\partial C}{\partial x} = D_x^* \frac{\partial^2 C}{\partial x^2} + D_y^* \frac{\partial^2 C}{\partial y^2} + D_z^* \frac{\partial^2 C}{\partial z^2} - \lambda C \qquad \text{(C.12)}$$

The first equation of this section [equation (D.1)] specifically addresses the general conditions for saturated flow and solute movement. However, with the following minor modifications, it also can be applied to the unsaturated zone:

- The porosities (n and n_e) are assumed to be equal to the soil matrix moisture content
- The one-dimensional flow is in the vertical direction.
- For this case, the retardation factor is defined by

$$R_f = 1 + (\rho^* K_d) / \theta \qquad \text{(C.13)}$$

where θ is the moisture content of the partially saturated zone and dispersion is considered only in the flow direction.

C.2.4 Vapor Transport

Some contaminants may move upward from the disposal facility to the surface because they are in the vapor phase. Such movement is governed by Fick's second law,

$$D \frac{\partial^2 C}{\partial z^2} = \frac{\partial C}{\partial t} \qquad \text{(C.14)}$$

where

C	is the concentration (g/m^3 or Ci/m^3)
z	is the distance (m)
t	is time (year)
D	is the diffusion coefficient (m^2/year).

The solution for concentration C in the z direction over time t is given by:

$$\frac{C}{C_0} = erfc\left(\frac{z}{2\sqrt{Dt}}\right) \qquad \text{(C.15)}$$

where erfc is the complimentary error function and C/C_o is the relative concentration. The mass transport across the surface becomes

$$\frac{\partial C}{\partial t} = \frac{C_0}{2\sqrt{\pi DT}} \frac{z}{t} \exp\left(\frac{-z^2}{4Dt}\right) \qquad \text{(C.16)}$$

C.3 WASTE FORM

C.3.1 Mass Conservation of Aqueous Solutes

Based on the continuum theory, the model can be represented by a set of partial differential equations (PDE) that describe the mass conservation of solutes in pore fluids. Assuming that the rock matrix does not deform, the mass conservation law of solutes can be written as

$$\frac{\partial(\phi S_w \rho_w C_i)}{\partial t} = -\vec{\nabla} \cdot \vec{J} + \sum_{j=1}^{N_r} v_{ij} W_j, i = 1,2,... \tag{C.17}$$

where ϕ is the porosity

S_w is the water saturation

ρ_w the density of the aqueous solution

C_i is the molal concentration of solute i

J_i is the flux of species i

v_{ij} is the stoichiometric coefficient of species i in reaction j

N_r is the number of total reactions

W_j is the rate of reaction j.

In general, the reaction rate is a nonlinear function of the concentrations. Through the term W_j, one solute species is nonlinearly coupled with other species. The nonlinear partial differential equation [equation (C.1)] simply states that the time rate of change of aqueous species concentrations consists of two parts; one is the contribution of transport and the other is the contribution of all reactions. Assuming the phenomenon of hydrodynamic dispersion can be represented by a Fickian-type law, the first term on the right-hand side can be expanded into

$$-\vec{\nabla} \cdot \vec{J}_i = -\vec{\nabla} \cdot \left(\phi S_w \rho_w D_i \vec{\nabla} C_i + \vec{u} \phi S_w \rho_w C_i\right) \tag{C.18}$$

where D_i is the dispersion coefficient of i
u is the velocity of pore fluid.

The second term at the right-hand side of equation (C.18) represents all types of reactions, including aqueous speciation, redox reactions, solid precipitation and dissolution, and adsorption. In general, chemical reactions can be treated as either equilibrium-controlled or kinetic-controlled. Several of the available reaction-transport models can only treat equilibrium reactions (Mangold 1991). In this case, the nonlinear equation (C.18) can be transformed into a linear equation, making it numerically easier to solve. However, many reactions are kinetically controlled, especially solid dissolution and precipitation reactions. Consequently, both equilibrium and kinetic reactions are included in the model used here. To emphasize this, the reaction term in equation (C.18) is split into two parts: one represents the contributions from equilibrium reactions, the other represents contributions from kinetic reactions

$$\sum_{j=1}^{N_r} v_{ij} W_j = \sum_{j=1}^{Ne} v_{ij}^e W_j^e + \sum_{j=1}^{N_k} v_{ij}^k W_j^k \tag{C.19}$$

where v_{ij}^e and v_{ij}^k are the stoichiometric coefficients in equilibrium reactions and kinetic reactions, respectively, while W_j^e and W_j^k are the rates of equilibrium and kinetic reactions, respectively.

To define the mathematical form of the *W's*, note that for any kinetic reaction *j* involving aqueous and solid species *m* with the form

$$\sum v_{mj} B_m = 0 \tag{C.20}$$

using the law of mass-action, with activity corrections, the rate can be expressed as

$$W_j^k = A_j k_j \left[\prod_{v_{ij}<0} (\gamma_i C_i)^{-v_{ij}} - \prod_{v_{ij}>0} \frac{(\gamma_i C_i)^{v_{ij}}}{K_j^{eq}} \right] \tag{C.21}$$

where A_j is a factor

k_j is the rate constant

γ_i is the activity coefficient, which is a function of the concentrations of all species.

For aqueous reactions, $A_j = 1$. For solid dissolution and precipitation reactions, A_j is the effective reaction surface in unit volume of the porous medium. If we further assume that all solids are spherical grains or can be represented as equivalent spherical grains with radii of $R_{l(j)}$, and that the effective reaction surface is proportional to water saturation, then

$$W_j^k = 4\pi R_{l(j)}^2 n_{l(j)} S_w k_j \left[\prod_{v_{ij}<0} (\gamma_i C_i)^{-v_{ij}} - \prod_{v_{ij}>0} \frac{(\gamma_i C_i)^{v_{ij}}}{K_j^{eq}} \right], \tag{C.22}$$

where n_l is the number of grains in unit volume of porous medium.

Several formulas, such as Davies equation, B-dot equation, and Pitzer's model, can be used to calculate γ_i. The B-dot equation with modifications for neutral species adopted by Wolery (1992) is computationally economic and stable, and can handle moderate salinity; making it the most suitable for reaction-transport problems. Although Pitzer's model can handle high ionic strength, computationally it is not feasible for reaction-transport simulations because of its complicated structure and the lack of Pitzer constants for all but a few aqueous species.

C.3.2 Texture Dynamics

Dissolution and precipitation reactions can change the volume fractions of solids as a function of time. For spherical grains, the change rate is

$$\frac{\partial V_l}{\partial t} = 4\pi R_l^2 n_l \frac{\partial R_l}{\partial t}, \tag{C.23}$$

while

$$\frac{\partial R_l}{\partial t} = \sum_j k_j \left[\prod_{v_{ij}<0} (\gamma_i C_i)^{-v_{ij}} - \prod_{v_{ij}>0} \frac{(\gamma_i C_i)^{v_{ij}}}{K_j^{eq}} \right] / \rho_j , \tag{C.24}$$

where V_l is the volume fraction of solid l

R_l is the change rate in radius of solid l

ρ_l is the molar density of l.

Equation (C.24) serves as the bridge between the aqueous phase and solid phases so the whole system is mass-conserved.

C.3.3 Contaminant Release Rate From Glass

The equation for the contaminant release rate from glass is taken as

$$J_i = v_i a_{H^+}^{-\eta(T)} k_o e^{\frac{E_a}{RT}} \left[1 - \left(\frac{Q}{K} \right)^{\sigma} \right], \tag{C.25}$$

where J_i is the flux of element i

v_i is the stoichmetric coefficient of element i

a_{H+} is the activity of H^+

η is the pH power law coefficient

T is the temperature

k_o is the intrinsic rate constant

E_a is the activation energy

R is the gas constant

Q is the ion activity product

K is the pseudoequilibrium constant

σ is the average stoichiometric parameter for the overall reaction.

Appendix D

Detailed Results For Estimated Impacts

D. Detailed Results For Estimated Impacts

D.1 Introduction

This appendix summarizes the detailed results from the waste form, vadose zone, groundwater, and INTEG calculations to estimate the impacts for the different sensitivity cases investigated in this performance assessment. The details for the waste form calculations are provided in Bacon 2000. The details for the near-field, far field, and INTEG results can be found in Finfrock 2000. The details for the groundwater results can be found in Bergeron 2000. This appendix also includes a description of the detailed files that are included with this performance assessment on a compact disc that is available on request.

D.2 Waste Form Calculations

The contaminant fluxes for the base analysis case and all sensitivity cases have been provided and discussed in Section 4.5. Table 4-12 also provides a relative comparison of the results at 1,000 and 10,000 years after facility closure for the technetium flux compared to the base analysis case for all waste form sensitivity cases investigated. For additional details on the waste form calculation results, see Bacon 2000.

For completeness, output files from the waste form calculations that have been processed as input files to the far field VAM3D calculations are provided. See Section D.6 for a description of these files.

D.3 Vadose Zone Calculation

The contaminant fluxes to the aquifer for the base analysis case and the best estimate case have been provided and discussed in Section 4.3. The time dependence of the contaminant flux to the aquifer is shown in Figures 4-3 and 4-10 for the mobile (K_d = 0 mL/g) and less mobile (K_d = 0.6, 4.0 and 10. mL/g). This time dependence is reflected in the time dependence of the "vad-casename.bat" files for each sensitivity case see Section D.6).

D.4 Groundwater Calculations

Discussion of the base case flow and transport calculations of the define (WIF) are provided in Section 4.3 and the associated WIFs are summarized in Table 4.2. Discussion of the sensitivity cases are provided in Section 4.7 and the resulting ratios of the sensitivity case WIFs with the base case WIFs are summarized in Table 4.16.

Additional details of the underlying assumptions and supporting groundwater flow and transport calculations for both the base and sensitivity cases are presented in Bergeron 2000.

D.5 Estimated Impacts

Table D-1 summarizes the results for the estimated impacts to the beta-photon drinking water dose, the alpha concentration, and the all-pathway dose for the all-pathway farmer scenario except where noted. The estimated impacts are associated with a downgradient well located 100 m below the ILAW site except where noted. The estimated impacts are provided for 1,000 and 10,000 years after facility closure. The maximum estimated impacts also are provided. In general the maximum estimated impacts for the alpha concentration and all-pathway dose occurs for the maximum time calculated (typically 20,000 years after facility closure [except for the base analysis case where it is 100,000 years after facility closure]). Also included in Table D-1 are the file names for the INTEG calculations.

Table D-1. Summary of Estimated Impacts for 2001 ILAW PA.

INTEG Filename	Case Designation	Estimated Impact at 1,000 y after Facility Closure (1)			Estimated Impact at10,000 y after Facility Closure (1)			Maximum Estimated Impact (1) [peak time or max time for calculation]		
		B/γ dose (mrem/y)	alpha concen. (pCi/L)	all-pathways dose (mrem/y)	B/γ dose (mrem/y)	alpha concen. (pCi/L)	all-pathways dose (mrem/y)	B/γ dose (mrem/y)	alpha concen. (pCi/L)	all-pathways dose (mrem/y)
42base	Base analysis case	2.13E-05	1.02E-16	7.78E-05	1.02E-02	3.39E-02	7.00E-02	1.25E-02 [76,500 y]	5.42E-01 [100,000 y]	5.88E-01 [100,000 y]
42break	Best estimate case	4.67E-11	2.25E-22	1.71E-10	3.46E-07	5.01E-08	1.31E-06	1.85E-06 [20,000 y]	9.29E-07 [20,000 y]	7.63E-06 [20,000 y]
Facility Cases										
42break	Full barrier	4.67E-11	2.25E-22	1.71E-10	3.46E-07	5.01E-08	1.31E-06	1.85E-06 [20,000 y]	9.29E-07 [20,000 y]	7.63E-06 [20,000 y]
50break	Full barrier - 50 mm/y	2.09E-09	9.64E-21	7.33E-09	7.92E-07	8.94E-07	3.76E-06	3.03E-06 [20,000 y]	5.43E-06 [20,000 y]	1.63E-05 [20,000 y]
42vert	Vertical barrier	0.00E+00	0.00E+00	0.00E+00	2.03E-07	8.97E-09	7.51E-07	1.2E-06 [20,000 y]	3.14E-07 [20,000 y]	4.68E-06 [20,000 y]
42short	Shorter capillary break	8.53E-10	4.10E-21	3.12E-09	1.05E-06	6.03E-07	4.41E-06	3.94E-06 [20,000 y]	5.24E-06 [20,000 y]	1.94E-05 [20,000 y]
42vault	Concrete vault - base	6.05E-03	9.19E-10	2.21E-02	1.81E-02	6.94E-01	7.38E-01	1.85E-02 [20,000 y]	7.41E-01 [20,000 y]	7.90E-01 [20,000 y]
42all	No sideslope	1.10E-06	5.28E-18	4.01E-06	9.98E-03	8.61E-03	4.48E-02	1.21E-02 [17,400 y]	2.76E-01 [20,000 y]	3.13E-01 [20,000 y]
Waste Form Release										
42for	Forward rate	2.08E-04	9.98E-16	7.59E-04	9.08E-02	3.32E-01	6.54E-01	9.89E-02 [20,000 y]	3.13E+00 [20,000 y]	3.41E+00 [20,000 y]
42noion	No ion exchange	1.68E-05	8.06E-17	6.13E-05	8.41E-03	2.72E-02	5.71E-02	1.04E-02 [20,000 y]	2.91E-01 [20,000 y]	3.21E-01 [20,000 y]
42highion	Forward rate + 5X ion exchange	2.18E-04	1.05E-15	7.97E-04	1.00E-01	3.92E-01	7.46E-01	1.09E-01 [18,700 y]	3.45E+00 [20,000 y]	3.77E+00 [20,000 y]
42nosec	No secondary phase	1.06E-05	5.08E-17	3.86E-05	5.39E-03	1.75E-02	3.67E-02	6.60E-03 [20,000 y]	1.86E-01 [20,000 y]	2.05E-01 [20,000 y]
01	Recharge = 0.1 mm/y	6.95E-12	3.34E-23	2.54E-11	7.16E-07	1.84E-08	2.64E-06	3.23E-06 [20,000 y]	6.30E-07 [20,000 y]	1.24E-05 [20,000 y]

Table D-1. Summary of Estimated Impacts for 2001 ILAW PA.

INTEG Filename	Case Designation	Estimated Impact at 1,000 y after Facility Closure (1)			Estimated Impact at10,000 y after Facility Closure (1)			Maximum Estimated Impact (1) [peak time or max time for calculation]		
		B/γ dose (mrem/y)	alpha concen. (pCi/L)	all-pathways dose (mrem/y)	B/γ dose (mrem/y)	alpha concen. (pCi/L)	all-pathways dose (mrem/y)	B/γ dose (mrem/y)	alpha concen. (pCi/L)	all-pathways dose (mrem/y)
09	Recharge = 0.9 mm/y	3.76E-09	1.81E-20	1.38E-08	1.41E-04	5.18E-06	5.22E-04	1.81E-04 [20,000 y]	2.57E-04 [20,000 y]	9.10E-04 [20,000 y]
50	Recharge = 50 mm/y	4.00E-2	2.63E-01	3.99E-01	3.76E-02	1.52E+00	1.61E+00	7.62E-02 [300 y]	1.56E+00 [3,400 y]	1.65e+00 [3,400 y]
42sandfill	Sand backfill	4.48E-04	2.15E-15	1.64E-03	1.77E-02	1.76E-01	2.35E-01	1.80E-02 [4,700 y]	6.65E-01 [20,000 y]	7.11E-01 [20,000 y]
42sdiff	10X WF aqueous diffusion	4.03E-06	1.94E-17	1.47E-05	1.20E-04	1.21E-03	1.61E-03	1.31E-04 [20,000 y]	4.52E-03 [20,000 y]	4.89E-03 [20,000 y]
42steel	Steel included	2.18E-05	1.05E-16	7.96E-05	1.01E-02	3.39E-02	6.98E-02	1.49E-02 [20,000 y]	3.75E-01 [20,000 y]	4.02E-01 [20,000 y]
42condlayr	Top conditioning Layer	2.11E-05	1.02E-16	7.72E-05	9.44E-03	3.31E-02	6.66E-02	1.10E-02 [20,000 y]	3.26E-01 [20,000 y]	3.58E-01 [20,000 y]
42altglass	HLP-31 glass	2.57E-03	1.24E-14	9.41E-03	6.77E-01	3.87E+00	6.23E+00	6.78E-01 [9,200 y]	2.40E+01 [20,000 y]	2.56E+01 [20,000 y]
Vadose Zone Cases										
42iso	Isotropic field flow	1.32E-05	6.35E-17	4.83E-05	1.02E-02	1.26E-02	4.96E-02	1.22E-02 @ 20,000 y	3.02E-01 @ 20,000 y	3.39E-01 @ 20,000 y
42sand	All sand	5.37E-06	2.58E-17	1.96E-05	1.00E-02	2.54E-03	3.91E-02	1.24E-02 [52,500 y]	5.36E-01 [100,000 y]	5.85E-01 [100,000 y]
42grav	All gravel	1.04E-04	1.84E-09	3.80E-04	1.05E-02	3.60E-01	3.87E-01	1.24E-02 [52,000 y]	5.43E-01 [100,000 y]	5.92E-01 [100,000 y]
42deep	VZ - 3 m thicker	1.78E-05	8.56E-17	6.51E-05	1.02E-02	3.24E-02	6.86E-02	1.24E-02 [52,000 y]	5.37E-01 [100,000 y]	5.86E-01 [100,000 y]
42dike	Clastic dike	1.91E-05	9.16E-17	6.96E-05	1.01E-02	2.81E-02	6.42E-02	1.22E-02 [20,000 y]	3.32E-01 [20,000 y]	3.68E-01 [20,000 y]
42ukd0	U K_d = 0	2.13E-05	6.12E-04	2.09E-04	1.02E-02	3.07E-01	1.29E-01	1.24E-02 [52,500 y]	5.41E-01 [100,000 y]	5.87E-01 [100,000 y]

Table D-1. Summary of Estimated Impacts for 2001 ILAW PA.

INTEG Filename	Case Designation	Estimated Impact at 1,000 y after Facility Closure [1]			Estimated Impact at10,000 y after Facility Closure [1]			Maximum Estimated Impact [1] [peak time or max time for calculation]		
		B/γ dose (mrem/y)	alpha concen. (pCi/L)	all-pathways dose (mrem/y)	B/γ dose (mrem/y)	alpha concen. (pCi/L)	all-pathways dose (mrem/y)	B/γ dose (mrem/y)	alpha concen. (pCi/L)	all-pathways dose (mrem/y)
42kd0	K_d = 0 for all radionuclides [2]	3.11E-05	1.6E-02 (3.78E-06)	3.68E-02	1.49E-02	4.34e+00 (5.95E-03)	8.69E+00	1.82E-02 [54,500 y]	4.70e+00 [15,000 y] (5.15E-02 [100,000 y])	9.05E+00 [13,000 y]
42diff	10X increase in Difusion	3.17E-05	1.52E-16	1.16E-04	1.02E-02	4.46E-02	8.05E-02	1.22E-02 [20,000 y]	3.57E-01 [20,000 y]	3.93E-01 [20,000 y]
42disp	2X increase in dispersion	3.76E-05	1.81E-16	1.37E-04	1.02E-02	5.17E-02	8.73E-02	1.22E-02 [20,000 y]	3.50E-01 [20,000 y]	3.86E-01 [20,000 y]
Groundwater Cases										
42base[4]	Well intercept. = 1000m	1.58E-05	7.58E-17	5.78E-05	7.58E-03	2.52E-02	5.20E-02	9.29E-03 [76,500 y]	4.03E-01 [100,000 y]	4.37E-01 [100,000 y]
42base[4]	Well intercept. = CR	1.99E-06	9.52E-18	7.26E-06	9.52E-04	3.16E-03	6.53E-03	1.17E-03 [76,500 y]	5.06E-02 [100,000 y]	5.49E-02 [100,000 y]
42base[4]	Trench at south end	3.20E-05	1.53E-16	1.17E-04	1.53E-02	5.09E-02	1.05E-01	1.88E-02 [76,500 y]	8.13E-01 [100,000 y]	8.82E-01 [100,000 y]
42base[4]	90° rotation	4.07E-05	1.95E-16	1.49E-04	1.95E-02	6.47E-02	1.34E-01	2.39E-02 [76,500 y]	1.04E+00 [100,000 y]	1.12E+00 [100,000 y]
42base[4]	Smaller layout	5.75E-06	2.75E-17	2.10E-05	2.75E-03	9.15E-03	1.89E-02	3.38E-03 [76,500 y]	1.46E-01 [100,000 y]	1.59E-01 [100,000 y]
42base[4]	Larger layout	2.56E-05	1.22E-16	9.34E-05	1.22E-02	4.07E-02	8.40E-02	1.50E-02 [76,500 y]	6.50E-01 [100,000 y]	7.06E-01 [100,000 y]
42vault[5]	Existing vault site	2.60E-03	3.95E-10	9.50E-03	7.78E-03	2.98E-01	3.17E-01	7.74E-03 [20,000 y]	3.19E-01 [100,000 y]	3.40E-01 [100,000 y]
42base[4]	30 L/d pumping	2.13E-05	1.02E-16	7.78E-05	1.02E-02	3.39E-02	7.00E-02	1.25E-02 [76,500 y]	5.42E-01 [100,000 y]	5.88E-01 [100,000 y]
42base[4]	100 L/d pumping	2.13E-05	1.02E-16	7.78E-05	1.02E-02	3.39E-02	7.00E-02	1.25E-02 [76,500 y]	5.42E-01 [100,000 y]	5.88E-01 [100,000 y]
42base[4]	300 L/d pumping	2.13E-05	1.02E-16	7.78E-05	1.02E-02	3.39E-02	7.00E-02	1.25E-02 [76,500 y]	5.42E-01 [100,000 y]	5.88E-01 [100,000 y]

Table D-1. Summary of Estimated Impacts for 2001 ILAW PA.

INTEG Filename	Case Designation	Estimated Impact at 1,000 y after Facility Closure (1)			Estimated Impact at10,000 y after Facility Closure (1)			Maximum Estimated Impact (1) [peak time or max time for calculation]		
		B/γ dose (mrem/y)	alpha concen. (pCi/L)	all-pathways dose (mrem/y)	B/γ dose (mrem/y)	alpha concen. (pCi/L)	all-pathways dose (mrem/y)	B/γ dose (mrem/y)	alpha concen. (pCi/L)	all-pathways dose (mrem/y)
42base(4)	1000 L/d pumping	2.13E-05	1.02E-16	7.78E-05	1.02E-02	3.39E-02	7.00E-02	1.25E-02 [76,500 y]	5.42E-01 [100,000 y]	5.88E-01 [100,000 y]
42base(4)	Reduced hyd. Cond (3X)	2.55E-04	1.22E-15	9.32E-04	1.22E-01	4.06E-01	8.39E-01	1.50E-01 [76,500 y]	6.49E+00 [100,000 y]	7.04E+00 [100,000 y]
42base(4)	Regional recharge increase (3X)	1.96E-05	9.38E-17	7.16E-05	9.38E-03	3.12E-02	6.44E-02	1.15E-02 [76,500 y]	4.99E-01 [100,000 y]	5.41E-01 [100,000 y]
42base(4)	Regional recharge decrease (3X)	1.45E-05	6.94E-17	5.29E-05	6.94E-03	2.31E-02	4.76E-02	8.50E-03 [76,500 y]	3.69E-01 [100,000 y]	4.00E-01 [100,000 y]
42base(4)	Decrease regional upgradient boundaries (2X)	1.79E-05	8.57E-17	6.54E-05	8.57E-03	2.85E-02	5.88E-02	1.05E-02 [76,500 y]	4.55E-01 [100,000 y]	4.94E-01 [100,000 y]
Inventory Cases										
42maxTc	Increase Tc inventory 5X	7.03E-05	1.02E-16	2.98E-04	3.35E-02	3.39E-02	1.75E-01	3.99E-02 [20,000 y]	5.37E-01 [100,000 y]	6.95E-01 [100,000 y]
42noTc	Reduce Tc to 0	9.00E-06	1.02E-16	2.26E-05	4.33E-03	3.39E-02	4.38E-02	6.05E-03 [100,000 y]	5.37E-01 [100,000 y]	5.59E-01 [100,000 y]
42-2i	Double I inventory	3.01E-05	1.02E-16	1.00E-04	1.45E-02	3.39E-02	8.10E-02	1.82E-02 [80,000 y]	5.37E-01 [100,000 y]	6.01E-01 [100,000 y]
42-2u	Double U inventory	2.13E-05	1.02E-16	7.78E-05	1.02E-02	5.82E-02	7.55E-02	1.24E-02 [52,000 y]	8.72E-01 [96,000 y]	6.77E-01 [100,000 y]
42ub	All inventory at bounding	5.52E-05	4.83E-16	1.73E-04	2.66E-02	1.86E-01	3.11E-01	3.47E-02 [100,000 y]	2.76E+00 [100,000 y]	2.95E+00 [100,000 y]
42ubmaxTc	Bounding value + max Tc	1.02E-04	4.83E-16	3.85E-04	4.90E-02	1.86E-01	4.12E-01	5.96E-02 [50,000 y]	2.76E+00 [100,000 y]	3.07E+00 [32,000 y]

Table D-1. Summary of Estimated Impacts for 2001 ILAW PA.

INTEG Filename	Case Designation	Estimated Impact at 1,000 y after Facility Closure (1)			Estimated Impact at10,000 y after Facility Closure (1)			Maximum Estimated Impact (1) [peak time or max time for calculation]		
		B/γ dose (mrem/y)	alpha concen. (pCi/L)	all-pathways dose (mrem/y)	B/γ dose (mrem/y)	alpha concen. (pCi/L)	all-pathways dose (mrem/y)	B/γ dose (mrem/y)	alpha concen. (pCi/L)	all-pathways dose (mrem/y)
Dosimetry Cases										
ind-100m	Industrial	9.86E-06	1.02E-16	9.86E-06	4.71E-03	3.39E-02	1.69E-02	5.71E-03 [53,000 y]	5.37E-01 [100,000 y]	2.08E-01 [100,000 y]
res-100m	Residential	2.88E-05	1.02E-16	3.44E-05	1.38E-02	3.39E-02	5.68E-02	1.68E-02 [53,000 y]	5.37E-01 [100,000 y]	6.89E-01 [100,000 y]
agr-100m	Agricultural	2.88E-05	1.02E-16	1.26E-04	1.38E-02	3.39E-02	1.01E-01	1.68E-02 [53,000 y]	5.37E-01 [100,000 y]	7.48E-01 [100,000 y]
nat-CR	Native American (3)	4.52E-06	1.07E-17	2.77E-05	2.16E-03	3.55E-03	2.22E-02	2.63E-03 [52,500 y]	5.62E-02 [100,000 y]	1.64E-01 [100,000 y]
CRPop-CR	CR population (3)	1.12E-02	1.07E-17	3.42E-02	5.33E+00	3.55E-03	3.28E+02	6.49E+0 [53,000 y]	5.62E-02 [100,000y]	2.91E+02 [100,000 y]
DOE-100m	DOE dose parameters	1.87E-05	9.55E-17	6.67E-05	8.96E-03	3.16E-02	5.93E-02	1.10E-02 [58,000 y]	5.01E-01 [100,000 y]	4.91E-01 [100,000 y]
Other Sensitivity Cases										
42sub	Cap break subsidence	5.33E-09	2.56E-20	1.95E-08	3.97E-03	2.35E-05	1.45E-02	5.22E-03 [19,000 y]	1.28E-02 [20,000 y]	3.15E-02 [20,000 y]
Pulse42	Pulse	7.41E+00	3.56E-11	2.71E+01	5.18E-12	6.50E+01	6.29E+01	1.69E+01 [1,385 y]	6.93E+01 [11,100 y]	6.72E+01 [11,200 y]
42instant (2)	Instantaneous VZ transport	2.87E-03	1.48E+0 (3.49E-04)	3.39E+00	1.61E-02	4.68E+00 (6.4E-03)	9.36E+00	7.96E-01 [33 y]	4.83E+00 [13,100 y] (5.16E-02 [100,000 y])	9.43E+00 [11,100 y]
42conc	Concrete K_ds	1.37E-05	1.02E-16	5.87E-05	9.98E-03	5.56E-04	3.73E-02	1.24E-02 [53,000 y]	4.74E-01 [100,000 y]	5.22E-01 [100,000 y]

Table D-1. Summary of Estimated Impacts for 2001 ILAW PA.

INTEG Filename	Case Designation	Estimated Impact at 1,000 y after Facility Closure (1)			Estimated Impact at10,000 y after Facility Closure (1)			Maximum Estimated Impact (1) [peak time or max time for calculation]		
		B/γ dose (mrem/y)	alpha concen. (pCi/L)	all-pathways dose (mrem/y)	B/γ dose (mrem/y)	alpha concen. (pCi/L)	all-pathways dose (mrem/y)	B/γ dose (mrem/y)	alpha concen. (pCi/L)	all-pathways dose (mrem/y)

(1) The estimated impacts are associated with a well located 100 meters downgradient form the ILAW site

(2) The numbers in parentheses are the estimated radium concentrations

(3) The estimated impacts are calculated for a well just before the aquifer flows into the Columbia River

(4) The estimated impacts use the WIFs provided in Tables 4-2 and 4-16 with the Base Analysis Case

(5) The estimated impact use the existing vault WIF provided in Table 4-16 with the Base Analysis Case WIF from Table 4-2

D.6 Outline for Compact Disk Files

The output files for each sensitivity case have been copied onto a compact disk (CD) that is available on request. Table D-2 provides a cross-reference between the sensitivity case descriptions and the summary output files for the waste form, vadose zone, and dose estimate (INTEG) results.

All files on the CD are stored under a directory structure that defines the type of files and case names. The top directory is named 'ILAW;' beneath it are two directories named 'Waste Form' and 'Integration.' The 'Waste Form' directory contains subdirectories corresponding to different waste form cases, which in turn contain the data files used in the calculations. The 'Integration' directory contains subdirectories corresponding to the INTEG cases, which in turn contain the input and output files for each INTEG calculation.

The waste form case subdirectory names begin with the name of the STORM case (e.g., case WFA is in directory WFA-base-42) identified in Table D-2. Each subdirectory contains two files: 'storm2vam.out' and 'storm2vam.g17.' Some subdirectories may contain multiple versions of each file, with a suffix indicating which near-field flow calculation they are associated with. The '.out' files contain excerpted data from the STORM output data. These data are in three columns, corresponding to time (year), release rate (micromols/m^2/secomd), and release rate (Ci/m^2/year). The '.g17' files contain the release rate data (converted to Ci/year for each node) in the format required for input to the far-field transport calculations. The integration subdirectory names correspond to the INTEG cases identified in Tables D-1 and D-2. Each subdirectory contains four files: named 'run.bat,' 'vad casename.bac,' 'casename.out,' and 'casename.dat' (where 'casename' is replaced with the case name). The 'run.bat' file contains some of the input parameters required for the INTEG run, including the well intercept factor (WIF), recharge rate, and the names of the data files used in the INTEG calculation (all the data files are in the 'lib' subdirectory under the integration directory). The 'vad-casename.bac' file contains the data from the corresponding far-field transport calculations. These data are the release rate (in Ci/year) from the vadose zone into the groundwater with the first column being time (in years) and the subsequent columns each corresponding to a different K_d (typically only the first two K_d columns are used, with the remainder being filled with 0s). The 'casename.out' file contains the general results of the INTEG calculation and the 'casename.dat' file contains the detailed results for each nuclide.

Table D-2. Cross-reference for Sensitivity Cases and Output Files from Waste Form, Vadose Zone, and INTEG Calculations for the 2001 ILAW PA.

Case	Description	Waste Form Filename	Far Field Transport Filename	INTEG Case Filename
1	**Reference Cases:**			
1-1	Base analysis case	wfa	42base-t	42base
1-2	Best estimate case	wfd	42break-t	42break
2	**Scenario Cases:**			
2-1	Irrigation	wfa	42base-t	50 [(a)]
2-2	Well locations	wfa	42base-t	42base [(a)]
2-3	Pumping rates	wfa	42base-t	42base [(a)]
3	**Inventory Cases:**			
3-1	Upper bound inventory.	wfa	42base-t	42ub
3-2	Maximum ^{99}Tc inventory	wfa	42base-t	42maxtc
3-3	No Tc inventory	wfa	42base-t	42notc
3-4	Double I inventory	wfa	42base-t	42-2I
3-5	Double U inventory	wfa	42base-t	42-2u
3-6	Upper bound + maximum Tc inventory	wfa	42base-t	42ubmaxtc
4	**Recharge Cases:**			
4-1	Rupert sand	wf4	09-t	09
4-2	High recharge	wf6	50-t	50
4-3	Low recharge	wfd	01-t	01
4-4	Low recharge for 500 years, then 4.2mm/year	wfa [(b)]	42base-t [(b)]	42base [(b)]
5	**Geology Cases:**			
5-1	Entire formation - sandy	wfa	42sand-t	42sand
5-2	Entire formation - gravelly	wfa	42grav-t	42grav
5-3	Clastic dikes	wfa	42dike-t	42dike
5-4	Deep water table	wfa	42deep-t	42deep
5-5	Instantaneous vadose zone transport	wfa	na [(c)]	42instant
6	**Facility Cases:**			
6-1	Capillary break (best estimate case)	Same as case 1-2		
6-2	Side slope	wfa	42all-t	42all
6-3	Vertical capillary break	wfa	42vert-t	42vert
6-4	Short break	wfa	42short-t	42short
6-5	Sand backfill	wf11	42sandfill-t	42sandfill
6-6	Alternative facility design (vault)	wf16	42vault-t	42vault

Table D-2. Cross-reference for Sensitivity Cases and Output Files from Waste Form, Vadose Zone, and INTEG Calculations for the 2001 ILAW PA.

Case	Description	Waste Form Filename	Far Field Transport Filename	INTEG Case Filename
7	**Degradation Cases:**			
7-1	Surface barrier	no barrier = base case		
7-2	Degraded capillary break (subsidence)	wfa		42sub
7-3	Bathtub effect	(d)	(d)	(d)
8	**Hydrologic Parameter Cases:**			
8-1	Isotropic conductivity	wfa	42iso-t	42iso
8-2	Sand backfill	Same as case 6-5		
8-3	Entire formation - sandy	Same as case 5-1		
8-4	Entire formation - gravelly	Same as case 5-2		
9	**Waste Form Cases:**			
9-1	Forward rate	wfb	42for-t	42for
9-2	No ion exchange	wf1	42noion-t	42noion
9-3	No secondary product	wf2	42nosec-t	42nosec
9-4	Infiltration rate = 0.1 mm/y	Same as case 4-3		
9-4	Infiltration rate = 0.5 mm/y	wf3	nc [(e)]	nc [(e)]
9-5	Infiltration rate = 0.9 mm/y	Same as case 4-1		
9-6	Infiltration rate = 4.2 mm/y	Same as case 1-1		
9-7	Infiltration rate = 10 mm/y	wf5	nc [(e)]	nc [(e)]
9-8	Infiltration rate = 50 mm/y	Same as case 4-2		
9-9	Sand backfill	Same as case 6-5		
9-10	Steel containers	wf25	42steel-t	42steel
9-11	Chemical conditioning layer	wf10	42cond-t	42condlayr
9-12	Alternative facility (vault)	Same as case 6-6		
9-13	Alternative glass	wf28	42altglass-t	42altglass
9-14	Diffusion parameter	wf29	42sdiff-t	42sdiff
9-15	Uranium	wf26	nc [(e)]	nc [(e)]
9-16	Two-dimensional waste form model	wf9	nc [(e)]	nc [(e)]
9-17	Pulse	na [(c)]	pulse-t	pulse42
10	**Geochemical Cases:**			
10-1	Uranium trapping	wfa	42base-t, 42conc-t	42conc
10-2	Uranium k_d = 0.0 mL/g	wfa	42base-t	42ukd0
10-3	All k_d = 0.0 mL/g	wfa	42base-t	42kd0
11	**Exposure**			
11-1	Alternative dose factors (DOE)	wfa	42base-t	DOE-100m
11-2	Industrial scenario - 100 m	wfa	42base-t	ind-100m

Table D-2. Cross-reference for Sensitivity Cases and Output Files from Waste Form, Vadose Zone, and INTEG Calculations for the 2001 ILAW PA.

Case	Description	Waste Form Filename	Far Field Transport Filename	INTEG Case Filename
11-3	Residential scenario - 100 m	wfa	42base-t	res-100m
11-4	Agricultural scenario - 100 m	wfa	42base-t	agr-100m
11-5	Native American - CR	wfa	42base-t	nat-CR
11-6	CR population - CR	wfa	42base-t	CRPop-CR
12	**Location/Layout of Facility**			
12-1	Trench layouts	wfa	42base-t	42base [(a)]
12-2	Existing vaults	wf16	42vault-t	42vault [(f)]

(a) Use results from base analysis case and normalize INTEG results to appropriate WIFs provided in Table 4-2 and 4-16

(b) Estimated from base analysis case @ 500 years earlier (e.g., at 500 and 9,500 years after facility closure)

(c) na = not applicable

(d) See Bacon 2001 and Finfrock 2000b for details

(e) nc = not calculated

(f) Use results from vault calculation and WIF for existing vault site (Table 4-16)

DOE/ORP-2000-24, Rev. 0
Based on PNNL-11834, with revisions

Appendix E

A Strategy to Conduct an Analysis of the Long-Term Performance of Low-Activity Waste Glass in a Shallow Subsurface Disposal System at Hanford

B. P. McGrail
W. L. Ebert[(a)]
D. H. Bacon
D. M. Strachan

February 1998
Revised for 2001 ILAW PA: November 2000

Prepared for
the U.S. Department of Energy
under Contract DE-AC06-76RLO 1830

Pacific Northwest National Laboratory
Richland, Washington 99352

[(a)] Argonne National Laboratory, Argonne, IL 60439

DOE/ORP-2000-24, Rev. 0
Based on PNNL-11834, with revisions

DISCLAIMER

This report was prepared as an account of work sponsored by an agency of the United States Government. Neither the United States Government nor any agency thereof, nor Battelle Memorial Institute, nor any of their employees, makes **any warranty, expressed or implied, or assumes any legal liability or responsibility for the accuracy, completeness, or usefulness of any information, apparatus, product, or process disclosed, or represents that its use would not infringe privately owned rights.** Reference herein to any specific commercial product, process, or service by trade name, trademark, manufacturer, or otherwise does not necessarily constitute or imply its endorsement, recommendation, or favoring by the United States Government or any agency thereof, or Battelle Memorial Institute. The views and opinions of authors expressed herein do not necessarily state or reflect those of the United States Government or any agency thereof.

PACIFIC NORTHWEST NATIONAL LABORATORY
operated by
BATTELLE MEMORIAL INSTITUTE
for the
UNITED STATES DEPARTMENT OF ENERGY
under Contract DE-AC06-76RLO 1830

Printed in the United States of America

Available to DOE and DOE contractors from the
Office of Scientific and Technical Information, P.O. Box 62, Oak Ridge, TN 37831;
prices available from (615) 576-8401.

Available to the public from the National Technical Information Service,
U.S. Department of Commerce, 5285 Port Royal Rd., Springfield, VA 22161

SUMMARY

Treatment services are being procured to vitrify low-activity tank waste for eventual disposal in a shallow subsurface facility at the Hanford Site. Over 500,000 metric tons of low-activity waste glass will be generated, which is among the largest volumes of waste within the U.S. Department of Energy (DOE) complex and is one of the largest inventories of long-lived radionuclides planned for disposal in a low-level waste facility. Before immobilized waste can be disposed of, DOE must approve a "performance assessment," which is a document that describes the impacts of the disposal facility on public health and environmental resources. Because the release rate of radionuclides from the glass waste form is a key factor determining these impacts, a sound scientific basis for determining their long-term release rates must be developed if this disposal action is to be accepted by regulatory agencies, stakeholders, and the public. In part, the scientific basis is determined from a sound testing strategy.

The foundation of the proposed testing strategy is a well-accepted mechanistic model that is being used to calculate the glass corrosion behavior over the geologic time scales required for performance assessment. This model requires that six parameters be determined, and the testing program is defined by an appropriate set of laboratory experiments to determine these parameters, and is combined with a set of field experiments to validate the model as a whole.

Three general classes of laboratory tests are proposed in this strategy: 1) characterization, 2) accelerated, and 3) service condition. Characterization tests isolate and provide specific information about processes or parameters in theoretical models. Accelerated tests investigate corrosion behavior that will be important over the regulated service life of a disposal system within a laboratory time frame of a few years or less. Service condition tests verify that the techniques used in accelerated tests do not change the alteration mechanisms. The recommended characterization tests are single-pass flow-through tests using a batch reactor design. Accelerated and service conditions tests include product consistency and pressurized unsaturated flow (PUF) tests. Nonradioactive glasses will be used for the majority of the laboratory testing (~80%), with the remainder performed with glasses containing a selected set of key radionuclides. Additionally, a series of PUF experiments with a natural analog of basaltic glass is recommended to confirm that the alteration products observed under accelerated conditions in the PUF tests are similar to those found associated with the natural analog. This will provide additional confidence in using the PUF test results to infer long-term corrosion behavior.

Field tests are proposed as a unique way to validate the glass corrosion and contaminant transport models being used in the performance assessment. To better control the test conditions, the field tests are to be performed in lysimeters (corrugated steel containers buried flush with the ground surface). Lysimeters provide a way to combine a glass, Hanford formation soil, and perhaps other engineered materials in a well-controlled test, but on a scale that is not practicable in the laboratory. The recommended field tests include some experiments where a steady flow rate of water is artificially applied. These tests use a glass designed to have a high corrosion rate, making monitoring contaminant release and transport easier. Either existing lysimeters at the Hanford Site or new lysimeters that have been equipped with the latest in monitoring equipment and located near the proposed disposal site can be used for these experiments.

CONTENTS

E-1.0 INTRODUCTION E-1
E-2.0 DISPOSAL SYSTEM DESCRIPTION E-3
E-2.1 WATER INFILTRATION E-3
E-2.2 FACILITY DESCRIPTION E-4
E-3.0 MODELING APPROACH E-6
E-3.1 GLASS CORROSION PROCESS E-6
E-3.1.1 Importance of Secondary Phases E-6
E-3.1.2 Effect of Ion Exchange E-7
E-3.2 GLASS CORROSION MODEL E-8
E-3.2.1 Rate Law for Hydrolysis and Dissolution E-8
E-3.2.1.1 Experiments for Kinetic Rate Law Parameters. E-9
E-3.2.1.2 Experiments for Affinity Term Parameters. E-10
E-3.2.2 Rate Law for Ion Exchange E-11
E-4.0 LABORATORY TESTING E-13
E-4.1 SINGLE-PASS FLOW-THROUGH TEST E-14
E-4.1.1 Well-Mixed Batch Reactor E-14
E-4.1.2 Packed Bed Reactor E-14
E-4.1.3 Fluidized Bed Reactor E-15
E-4.1.4 SPFT Testing Strategy E-15
E-4.2 VAPOR HYDRATION TEST E-16
E-4.3 PRODUCT CONSISTENCY TEST E-17
E-4.4 PRESSURIZED UNSATURATED FLOW TEST E-19
E-4.5 OTHER TEST METHODS E-22
E-4.5.1 Soxhlet Tests E-22
E-4.5.2 MCC-1 Test E-22
E-4.5.3 MCC-3 Solubility Test E-23
E-4.5.4 Periodic Replenishment Tests E-23
E-4.5.5 Unsaturated or “Drip” Test E-24
E-4.5.6 Accelerated Dissolution Test E-25
E-4.6 REQUIRED TESTS WITH RADIOACTIVE GLASSES E-25
E-4.7 MATERIALS INTERACTION TESTS E-26
E-4.8 ROLE OF NATURAL ANALOGS E-27
E-4.9 LABORATORY TESTING STRATEGY SUMMARY E-29
E-5.0 FIELD TESTING E-30
E-6.0 MODELING THE DISPOSAL SYSTEM E-32
E-6.1 SUBPROCESS MODEL DEVELOPMENT E-33
E-6.1.1 Adaptive Reaction Network E-33
E-6.1.2 Composition-Dependent Hydraulic Property Model E-33
E-6.2 NUMERICAL METHODS E-34
E-6.3 DISPOSAL SYSTEM SIMULATIONS FOR THE PERFORMANCE ASSESSMENT E-35
E-7.0 CONCLUSION E-38
E-8.0 REFERENCES E-39

LIST OF FIGURES

Figure E-2.1. Schematic of ILAW Disposal System. E-4
Figure E-3.1. Links Among Glass Tests and Modeling. E-8
Figure E-3.2. Excess Sodium Release via Ion Exchange as a function of Temperature for LAWABP1 Glass at pH(25 ^{o}C)=9. ..... E-12
Figure E-4.1. Schematic of a Typical Batch Flow Through Cell. E-14
Figure E-4.2. SPFT Test Results for Various ILAW Glasses. E-16
Figure E-4.3. Schematic of VHT Test. E-16
Figure E-4.4. PUF Apparatus. E-19
Figure E-4.5. Normalized Release Rates in PUF Tests with LAWABP1 Glass. E-21
Figure E-6.1 Modeling Strategy for Assessing ILAW Disposal System. E-37

LIST OF TABLES

Table E-4.1. Master Test Matrix for Long Term Performance Evaluation of a Glass. E-29

GLOSSARY

ADT	accelerated dissolution test
ALT	accelerated leach test
ANL	Argonne National Laboratory
AREST-CT	Analyzer of RadionuclidE Source Term with Chemical Transport
ASTM	American Society for Testing and Materials
CPU	central processing unit
DLT	dynamic leach test
DOE	U.S. Department of Energy
EMSP	Environmental Management Science Program
GFLOPS	giga floating point operations per second
HLW	high-level waste
ILAW	immobilized low-activity waste
ISO	International Standards Organization
LAW	low-activity waste
MIIT	Materials Interface Interaction Test
PCT	product consistency test
PNNL	Pacific Northwest National Laboratory
PUF	pressurized unsaturated flow
RH	relative humidity
SPFT	single-pass flow-through test
STOMP	a nonisothermal, multiphase flow simulator
STORM	Subsurface Transport Over Reactive Multiphases
S/V	surface area-to-solution volume ratio
VHT	vapor hydration test
WIPP	Waste Isolation Pilot Plant

E-1.0 INTRODUCTION

The Hanford Site in southeastern Washington State has been used extensively to produce nuclear materials for the U.S. strategic defense arsenal by the U.S. Department of Energy (DOE) and its predecessors, the U.S. Atomic Energy Commission and the U.S. Energy Research and Development Administration. A large inventory of radioactive and mixed waste has accumulated in 177 buried single- and double-shell tanks. The DOE is proceeding with plans to permanently dispose of this waste (Ecology 1996; 62 FR 8693). Liquid waste recovered from the tanks will be pretreated to separate the low-activity fraction from the high-level and transuranic waste. The small volume of high-level immobilized waste and the much larger volume of low-activity waste (LAW) will be disposed of in different locations. The high-level waste (HLW) will be stored on the Hanford Site until sent to a federal geologic repository. The immobilized low-activity waste (ILAW) will be placed in a near-surface disposal system on the Hanford Site.

Services are being procured for treating and immobilizing the tank waste. The leading processing option for waste immobilization is vitrification. Vitrifying the LAW is expected to generate over 500,000 metric tons or 200,000 m^3 (6,000,000 ft^3) of ILAW glass that will be disposed of under this plan. This is among the largest volumes of waste within the DOE complex and is one of the largest inventories of long-lived radionuclides planned for disposal in a low-level waste facility.

Before the immobilized waste can be disposed of, DOE must approve a “performance assessment,” which is a document that describes the long-term impacts of the disposal facility on public health and environmental resources. The first ILAW performance assessment was published in 1998 (Mann 1998a), and DOE conditionally approved this performance assessment (DOE 1999d), issuing a disposal authorization statement (DOE 1999a). A major conclusion from the performance assessment is that the release rate of radionuclides from the glass waste form by reaction with water is one of the key parameters that determines the impacts of the disposal action and is the most uncertain. Consequently, a sound scientific basis for determining the long-term release rates of radionuclides from these glasses must be developed if this disposal action is to be accepted by regulatory agencies, stakeholders, Native American Tribes, and the public.

A general approach for the evaluation of materials behavior in a disposal site has been developed that outlines logical steps to validate and confirm the corrosion behavior of materials whose life expectancies must greatly exceed the length of time over which experimental data can be obtained (ASTM 1991). These steps include determining the likely range of environmental factors in the disposal system, identifying and characterizing materials that are likely to be present in the disposal system, performing tests under site-relevant conditions to determine important alteration processes for those materials, developing models for key alteration processes, and performing tests that accelerate those processes. The ASTM protocol also recommends tests to confirm the corrosion model and to use information provided by analog materials or systems. Many steps in this approach relevant to waste glass behavior in general

have been completed in studies conducted for deep geologic disposal systems and can be directly applied to the Hanford Site disposal system. For example, the processes that control glass corrosion are well understood, and rate expressions have been developed and tested. What remains is primarily to characterize the specific corrosion behavior of actual ILAW glasses. This includes identifying (or confirming) the corrosion processes that will control the long-term behavior of the glasses and release of radionuclides, measuring parameters needed to perform model calculations for performance assessment, and conducting accelerated and service condition tests to confirm and provide confidence in those calculations.

The purpose of this report is to document a technical strategy developed by Pacific Northwest National Laboratory (PNNL)[a] and Argonne National Laboratory that the ILAW disposal program will pursue over the next several years to evaluate the long-term radionuclide release behavior of the ILAW glass(es) under development by the private contractors. As such, this document is intended to serve as the technical basis for the glass testing program that is needed to complete the performance assessment for the ILAW disposal facility. Specific matrices of tests will not be developed in this report; these are to be provided in separate test plans for each test method. However, this document will define the general classes of tests for which test plans will need to be developed and provide a general range of appropriate conditions for these tests. We begin the discussion of the technical strategy with a brief overview of the disposal system design and expected environmental conditions at the site.

[a]Pacific Northwest National Laboratory is operated for the U.S. Department of Energy by Battelle under Contract DE-AC06-76RLO 1830.

E-2.0 DISPOSAL SYSTEM DESCRIPTION

The Hanford Site is a 1450 km^2 area of semi-arid land located in southeastern Washington state. Average annual precipitation is 16 cm, with 44% of this total occurring during November, December, and January. Daytime high temperatures in summer can exceed 40°C, while outbreaks of arctic air masses in winter can cause temperatures to drop below -18°C. Plans call for the disposal system to include a protective surface barrier with design elements to minimize root intrusion, animal intrusion, and water infiltration. The use of silt-loam soils, when combined with a representative community of shrub-steppe vegetation, has been shown to cause most precipitation falling on the region to be lost through evapotranspiration. Consequently, the disposal facility is to be located in relatively dry, unsaturated soil, and performance assessment models must be applicable to the specific physics and chemistry of this type of system.

E-2.1 WATER INFILTRATION

Water flow in the near-surface unsaturated zone is transient because of intermittent precipitation events. Transient water flow begins when water enters at the ground surface and infiltrates downward into the soil column. At some distance from the ground surface transient effects will dampen out and the downward flowing water will reach a steady infiltration rate. The distance at which steady infiltration occurs is sometimes referred to as the penetration depth (Eagleson 1978; Salvucci 1993). Thus, the unsaturated zone essentially comprises two regions: an unsteady-flow region between the ground surface and penetration depth, and a steady-flow region between the penetration depth and the saturated zone water table. The steady flux in the lower unsaturated region is equal to the annual rate of groundwater recharge and therefore is composed of contributions not only from the most recent pulse, but from previous precipitation events as well.

The ILAW disposal facility will be situated below the penetration depth in the region of steady flow. The natural rate of moisture infiltration is approximately 4.2 mm/year (Fayer 1999). However, the natural rate of moisture infiltration cannot be relied upon because construction of the disposal system will destroy the natural soil-sediment profile and remove surface vegetation. Consequently, a protective surface barrier will be engineered with sediment layers and a capillary barrier to prevent or minimize infiltration. The design basis for the Hanford barrier (Myers and Duranceau 1994) specifies that less than 0.5 mm/year will pass through the barrier for the first 1,000 years. Infiltration beyond the root zone is controlled at the soil/atmosphere interface where surface soils and sediments and vegetation interact with the climate. The frequency, duration, and magnitude of precipitation and runoff events determine the infiltration rate. Infiltration into the disposal facility will be controlled by the physics described above, the unsaturated hydraulic properties of the surface and subsurface barriers to infiltration, the vault and surrounding soil, and the matric and gravity potential gradients.

E-2.2 FACILITY DESCRIPTION

A detailed design for the ILAW disposal facility is not yet available. However, the current designs (Puigh 1998) have the disposal facility as a series of large, covered trenches. The present plans are that the ILAW packages will be 1.22 m in diameter by 2.3 m high. A layer of ILAW packages will be laid down and covered with dirt. Across the center of the facility, packages would be arranged in three layers, with only one or two layers along the outer edges. Figure E-2.1 shows a schematic for the disposal facility, using a slightly earlier design.

All the concepts include backfilled soil around and on top of the waste containers in the facility. The soil was included in these concepts 1) for structural support, 2) to wick moisture away from the waste containers, and 3) to provide radiation shielding for the facility workers. These concepts also have a similar barrier philosophy. The uppermost barrier is the surface barrier, which consists of sand-gravel layers to work as a capillary break, a layer (that may or may not be included in the final design) for conditioning the chemistry of the water to help minimize the rate of glass corrosion and/or radionuclide release, and a layer of basalt riprap to deter burrowing animals, plant root intrusion, and inadvertent intruders. Beneath the surface barrier, another sand-gravel capillary break will divert moisture coming through the surface barrier away from the vault. This barrier combination minimizes the amount of water that enters the vault.

Figure E-2.1. Schematic of ILAW Disposal System. (This is for the design from early 2000).

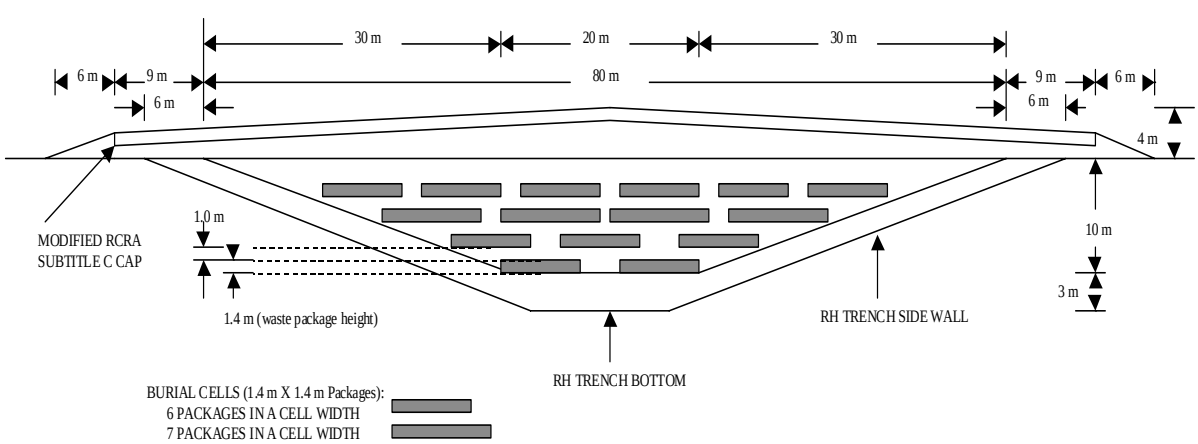

The disposal vaults are to be located approximately 15 m below the top of the surface barrier. At this depth, the ambient temperature is approximately 15°C, and temperature fluctuations are less than 2°C. Also, because the ILAW generates a small amount of heat from radioactive decay (McGrail and Mahoney 1995), the disposal system can be treated adequately as an isothermal system. The waste packages are expected to consist of a rectangular steel container that holds the glass and possibly a filler material. The glass will likely not be annealed and thus will be thermally stress fractured to some extent. The extent of fracturing is important because it increases the available surface area for possible contact by water and thus can potentially increase the radionuclide release rate from the disposal system.

Based on this disposal system concept, small amounts of water are expected to percolate through the disposal system and eventually penetrate the steel containers and contact the glass. The goal of the glass testing program then, is to provide the necessary supporting data so that the radionuclide release behavior of this system can be modeled with sufficient confidence to support an overall performance assessment for disposal of ILAW at the Hanford Site.

E-3.0 MODELING APPROACH

Because it is impossible to formulate a rationale and a defensible testing program without understanding the physical and chemical processes that govern glass corrosion and radionuclide release as well as the conceptual models that describe these processes, we briefly review these concepts below.

E-3.1 GLASS CORROSION PROCESS

Fortunately, much is known about glass-water reaction processes. Glass forms ranging from simple binary and ternary silicate glasses to complex waste glasses with 30 or more components have been studied for 35 years. Much of this work relevant to silicate waste glasses has recently been compiled and critically reviewed (Bates et al. 1994). A general picture of the glass corrosion process in water has emerged that can be summarized as follows: on initial contact by water, alkali is extracted by ion exchange in what is thought to be a diffusion-controlled process. Simultaneously, hydrolysis and dissolution of the glass network occurs. In unsaturated disposal systems where water content and flow rate are expected to be very low, the rate of ion exchange and dissolution decrease, but for different reasons. The ion-exchange rate slows in accordance with a diffusion-controlled process as a reaction layer builds up on the glass over time. A reaction layer builds up as a result of silanol condensation reactions that reform Si-O bonds. The dissolution rate of the glass network slows because of the common ion effect (i.e., as the solution becomes more concentrated in glass components, the difference in chemical potential between the glass and aqueous phase decreases, which decreases the dissolution rate). The dissolution rate cannot become zero because silicate glasses are thermodynamically unstable in water.

E-3.1.1 Importance of Secondary Phases

As a solution in contact with a dissolving glass becomes more and more concentrated in glass components, solubility limits for alteration phases begin to be exceeded. Although no generally accepted theory has been proposed to describe the factors controlling nucleation and growth, ultimately, the glass transforms into a paragenetic assemblage of alteration products or minerals. Also, no generally accepted theory exists that can be used to predict which specific phases should form or the sequence of their formation. However, from the Simplexity Principle (Goldsmith 1953), we know that the most disordered phase should form from a random system of components first. We know from the Ostwald Step Rule (Ostwald 1897) that subsequent transformations to more stable phases should occur in steps where the reaction products obtained at each step lay near the previous state in free energy. These governing principles have extremely important implications for the testing strategy because at the low temperatures (15°C) relevant for the ILAW disposal system, metastable and/or amorphous phases may persist for long periods of time. Consequently, a means must be found for accelerating the transformation process during laboratory testing without altering the fundamental transformation process itself.

The secondary phases that form from the glass-water reaction process are expected to depend principally on the composition of the glass and not on other components in the disposal system because the glass supplies the majority of the elements to the fluid from which the secondary phases precipitate. However, the water conditioning layer, filler material in and/or between waste packages, and the concrete used in vault construction also may affect the formation of secondary phases, especially in localized regions. Glasses that are stable with respect to the formation of alteration products will maintain a slow but finite rate of network hydrolysis and dissolution indefinitely. Many existing natural glasses exhibit these characteristics, having withstood weathering over geologic time scales. Laboratory tests have generally reproduced the same types of alteration products that have been found on these glasses (Grambow et al. 1986, Luo et al. 1997), confirming their long-term stability with respect to forming alteration phases. However, glasses that are unstable with respect to alteration product formation exhibit autocatalytic reactivity, i.e., a very rapid increase in dissolution rate that is limited only by the availability of water or the forward reaction rate of the glass, whichever is the rate limiting process. High-level waste glasses (Van Iseghem and Grambow 1988 have exhibited this phenomenon and so has a representative ILAW glass, LD6-5412 (McGrail et al. 1997a). Consequently, the laboratory testing program must ensure that the ILAW glass(es) being produced by the private vendors fall into the former, stable category. If not, then the tests should provide guidance for modifying the glass composition into a region with known long-term stability.

E-3.1.2 Effect of Ion Exchange

Because of the large effect that secondary phase formation has on glass dissolution rates, recent work on glass-water interactions has focused on understanding this process and incorporating it into models (Ebert and Bates 1993). The ion-exchange process has been largely ignored because it has been thought to be a short-duration, secondary, or tertiary process that had little or no bearing on long-term corrosion or radionuclide release rates from glasses. The only significant effect identified in the literature that is attributed to alkali ion exchange is an increase in solution pH in static laboratory tests conducted at high surface-area-to-volume ratios (Strachan et al. 1990; Bourcier and Feng 1993).

The discovery of the significance of ion exchange to long-term radionuclide release rates was only very recently made possible by the development of computational tools that can simulate the coupled processes of glass dissolution, mass transport, and chemical reactions in a complex disposal system (Chen, McGrail, and Engel 1997). By comparing simulations where Na ion exchange was included versus those where it was excluded, Chen, McGrail, and Engel (1997) showed that the ion-exchange reaction increased the pH in a conceptual design for an ILAW disposal vault from approximately 9.8 to over 12.5, which increased the radionuclide release rate by over 3 orders of magnitude. Thus, the overall performance of the disposal system can be significantly improved if improved glasses are developed that minimize alkali ion exchange. Formulation of such glasses can be rationally accomplished only through development of a fundamental scientific understanding of the ion-exchange process. Such a study is currently

being supported under DOE's Environmental Management Science Program (EMSP), and the results and conclusions from this work will be closely coordinated with the testing program described in this report.

E-3.2 GLASS CORROSION MODEL

It is impossible to develop a rationale testing program without thoroughly understanding the model that is being used to calculate the glass corrosion behavior over the geologic time scales required for performance assessment. In fact, the testing program is directly linked and derived from the data requirements of this model. Figure E-3.1 illustrates the basic link between modeling and testing. At the top of the pyramid is the conceptual model that describes the glass corrosion process. The parameters that make up this model are abstracted at the mid-level of the pyramid. Once the parameter set is known, the testing program is determined by the appropriate experiments needed to obtain each parameter in the set. This strategy is consistent with American Society for Testing and Materials guidelines (ASTM 1991), but we emphasize the "model driven" approach here because, ultimately, the credibility of the performance assessment rests on the credibility of the models and supporting data, not on a specific test. Following this approach, the conceptual model for glass corrosion planned for use in the performance assessment is discussed in the next section.

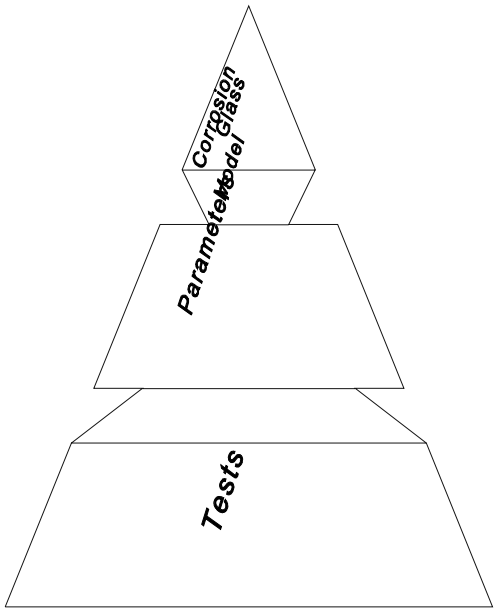

Figure E-3.1. Links Among Glass Tests and Modeling.

E-3.2.1 Rate Law for Hydrolysis and Dissolution

The literature on modeling glass dissolution is extensive. However, Strachan, Bourcier, and McGrail (Strachan et al.1994) published a review of the subject. An interested reader should consult this paper and the references cited therein for additional details. The conclusion from this study was that of all the models that have been developed to describe glass dissolution behavior, the general kinetic rate law proposed by Aagaard and Helgeson (Aagaard and Helgeson 1982) and later adapted by Grambow (Grambow 1985), best describes the majority of the experimental data that has been gathered over 35 years of studying glass-water reaction processes. Consequently, this model has been selected for use on the ILAW disposal project. The corrosion of silicate glasses in water can be represented as a special type of irreversible dissolution reaction. The reaction is irreversible because the glass cannot be reformed by precipitation from aqueous solution.

A conventional transition state kinetic rate equation can be used to compute the flux of any element *i* released from the glass into the aqueous phase and is given by

$$J_i^a = \nu_i k e^{-\frac{E_a}{RT}} \left[1 - \left(\frac{Q}{K} \right)^{\sigma} \right] \prod_{j=1...M} a_j^{-\eta_j} \quad i1,2,...N \tag{E.1}$$

where

a_j	=	activity of *j*th aqueous species
k	=	intrinsic rate constant, g/m^2•s
E_a	=	activation energy, J/mol
J_i^a	=	flux of element *i* to the aqueous phase, g/m^2•s
K	=	equilibrium constant of rate controlling reaction
M	=	number of species directly affecting the rate
N	=	number of elements
Q	=	ion-activity product of rate controlling reaction
R	=	gas constant, 8.314 J/mol•K
T	=	temperature, K
v_i	=	stoichiometric coefficient of element *i* in the glass
σ	=	net reaction order
η_j	=	stoichiometric coefficient for the *j*th reactant species.

Equation (E.1) is a constitutive relationship that relates temperature and the composition of water contacting the glass to the corrosion rate. Currently, H^+ is the only aqueous species that has been found to directly influence the rate via the activity product term (Bourcier et al. 1992). Consequently, Equation (E.1) can be simplified to

$$J_i^a = \nu_i k e^{-\frac{E_a}{RT}} a_{H^+}^{-\eta} \left[1 - \left(\frac{Q}{K} \right)^{\sigma} \right], \qquad i = 1,2,...N \tag{E.2}$$

where a_{H^+} is the hydrogen ion activity. Because the temperature is assumed to be a known constant, and v_i values are determined from the glass composition, application of Equation (E.2) for modeling glass corrosion in a disposal system requires the determination of six parameters; k, E_a, η, σ, *K*, and *Q*. In accordance with the strategy illustrated in Figure E-3.1 and the ASTM 1174 approach, the testing program is then defined by an appropriate set of experiments that determines these parameters.

E-3.2.1.1 Experiments for Kinetic Rate Law Parameters. If a glass is placed in a dilute solution that is refreshed at an infinite rate, the chemical affinity term $[1-(Q/K)^{\sigma}]$ in Equation (G.2) equals 1, and the corrosion rate of the glass is determined only by the three traditional kinetic rate law parameters, k, E_a, and η. Experimentally, the single-pass flow-through (SPFT) test is used to approximate these conditions. By adjusting glass surface area and flow rate, the solution remains dilute, but not so dilute that the solution concentrations cannot be determined with standard analytical techniques. The SPFT test has been used to measure reaction rates of

minerals (Knauss and Wolery 1986; Dove and Crerar 1990) and glasses (Knauss et al. 1990; McGrail and Olson 1992; McGrail et al. 1997c). By monitoring the change in dissolution rate over a sufficient range of temperature and pH values, k, E_a, and η can be easily obtained by applying standard nonlinear regression techniques to Equation (E.2). Details of the recommended experimental procedure and tests are given in Section E-4.1.

E-3.2.1.2 Experiments for Affinity Term Parameters. By definition, σ and K are the *parameters* of the chemical affinity term $[1-(Q/K)^{\sigma}]$ and so are usually obtained from laboratory experiments. The ion activity product (Q) is a *variable* and must be computed as a function of time and space for the disposal system (McGrail and Mahoney 1995; Bacon and McGrail 1997). Computation of Q is complex and depends on physical properties of the system, such as flow rate and glass surface area, and chemical properties, such as solubility products and the amounts and types of alteration products formed (see Section E-3.1.1). Because transport and chemical processes interact, or more precisely are coupled, a special type of computational model, called a reactive chemical transport model, is required for simulations.[(a)] The key inputs to this model derived from the glass testing program are the parameters σ and K, and the identification of glass alteration products. These data are extremely important because they can affect the calculated long-term corrosion rate of the glass by 3 to 4 orders of magnitude.

The pseudoequilibrium constant (K) and reaction order parameter (σ) probably are the most difficult parameters to obtain in the rate law, and, unfortunately, also are the most poorly documented in terms of experimental techniques and methods for obtaining them. Unlike for a crystalline or amorphous phase, the assignment of K for a glass is ambiguous, because by definition, equilibrium between the glass and water does not exist. Assigning K to a hypothetical phase including all the glass elements has not proven successful in modeling laboratory test data (Bourcier 1989; Advocat et al. 1990). Consequently, an approximation is used where K is associated with a reversible microscopic reaction that is rate limiting and not the macroscopic glass-water reaction itself. Good agreement with laboratory test data for most glasses has been obtained by assigning K to a simple SiO_2 polymorph, such as chalcedony, or mixtures of simple hydroxides and silicate phases (Bourcier et al. 1990; Gin 1996).

Unfortunately, the “agreement” typically reported in the literature lacks a statistical basis and usually is just trial and error reckoning of batch test data to calculated curves (Bourcier et al. 1990). The situation for determining the parameter σ is even poorer with most studies of silicate mineral and glass dissolution simply assuming $\sigma=1$. In other cases (Bourcier et al. 1994), σ and/or K have been regressed using data from batch tests. Batch tests introduce additional difficulties in accurately obtaining these parameters because pH and solution concentrations change continuously throughout the test, requiring “corrections” derived from the rate law itself. This introduces the possibility of inseparable causality errors. In a recent paper, McGrail et al. (1997c) illustrated how the SPFT test can be used to obtain σ and K by varying the flow rate over a sufficiently wide range. Their technique has the advantage of being performed at fixed pH and steady-state solution concentrations and does not require data “corrections” derived from the rate

---

[(a)]The interested reader should consult McGrail and Mahoney (1995), Chen et al. (1997), and Bacon and McGrail (1997) for details.

law. Consequently, the experimental techniques and formal mathematics developed by McGrail et al. will be used to obtain these parameters (see Section E-4.1).

Because there is no single test that can reliably evaluate the effects of secondary phases on the long-term corrosion rate of a glass, our approach is to employ a range of accelerated experimental techniques. By doing so, a range of physical and environmental factors can be examined that affect the rate and type of secondary phases formed. The use of different tests to accelerate glass corrosion provides added confidence that the artifacts associated with each test method are understood and properly taken into account and that long-term corrosion behavior of the glass is understood. Three types of long-term experiments are recommended for the majority of the testing: 1) vapor hydration tests, 2) product consistency tests (PCTs), and 3) pressurized unsaturated flow (PUF) tests. Each of these tests and the alternative tests are discussed in detail in Section E-4.0.

E-3.2.2 Rate Law for Ion Exchange

Although ion exchange has been largely ignored in the recent literature on the glass-water reactions, the process has been the subject of numerous early studies. In fact, the traditional idea of glass "leaching" involves the basic mechanism of ion exchange in which an H^+ or H_3O^+ ion exchanges for an alkali ion (M^+) in the glass, thereby generating a hydrated layer on the glass surface. The overall chemical reaction describing the process can be written as:

$$\equiv\text{Si-O-M} + H^+ \rightarrow \equiv\text{Si-OH} + M^+ \qquad \text{(E.3)}$$

or

$$\equiv\text{Si-O-M} + H_3O^+ \rightarrow \equiv\text{Si-OH} + M^+ + H_2O. \qquad \text{(E.4)}$$

Rana and Douglas (Rana and Douglas 1961a and 1961b) were among the first to report on this mechanism. Boksay, Bouquet, and Dobos (Boksay 1968) and Doremus (Doremus 1975; Doremus 1977; Lanford et al. 1979) pioneered the idea that ion counter-diffusion or interdiffusion is the rate limiting process for the exchange reaction. Recent data on a representative ILAW glass, LD6-5412, is also consistent with a diffusion-controlled release mechanism. Figure E-3.2 shows that Na is being released, presumably by ion exchange, at a linear rate with respect to $t^{1/2}$ in excess of the rate of matrix dissolution.

Detailed studies of the ion exchange process(es) are being conducted under the EMSP program. Once these studies are complete, an appropriate rate equation for ion exchange will be developed. The parameters that make up this model (possibly diffusion coefficients) will need to be determined from laboratory tests on the vendor glass compositions. However, until the EMSP studies are further along, it is premature to identify specific test methods and conditions.

Figure E-3.2. Excess Sodium Release via Ion Exchange as a function of Temperature for LAWABP1 Glass at pH(25 °C)=9.

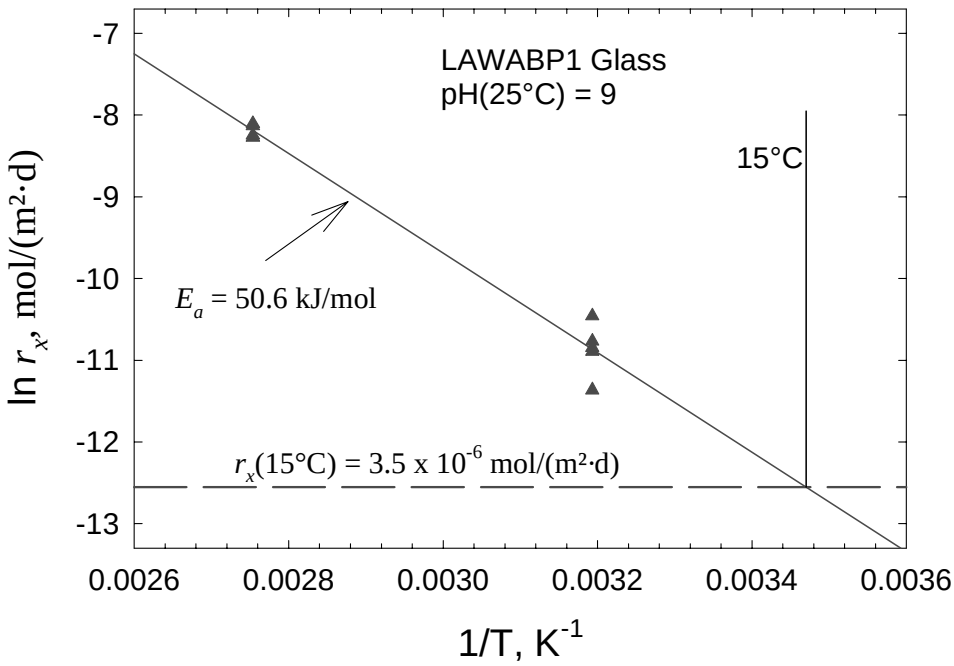

E-4.0 LABORATORY TESTING

Waste glasses are laboratory tested to identify important corrosion processes under site-relevant conditions and to measure parameter values needed to model long-term behavior (see Section E-3.0). Three general classes of tests are proposed in this strategy: 1) characterization, 2) accelerated, and 3) service condition. Characterization tests are used to isolate and provide specific information about processes or parameters in theoretical models. Test conditions are usually very different from expected service conditions to highlight a particular process and minimize or hold constant other effects. Examples of such tests include measuring basic material properties, such as density and compressive strength. Characterization tests proposed in this plan related to glass corrosion are SPFT tests used to measure kinetic rate law parameters.

Accelerated tests are used to investigate corrosion behavior that will be important over the regulated service life of a disposal system within a laboratory time frame of a few years or less. Therefore, it is important to know likely site conditions over long times to determine what aspects of glass corrosion need to be considered in the performance assessment. Elevated temperatures and high glass surface area-to-solution volume ratio (S/V) often are used to accelerate the reactions and processes that lead to glass dissolution. It is important to verify that the technique used to accelerate a reaction or process does not cause a change in the rate-limiting step or mechanism of the process or, if it does, the change must be taken into account. For example, water diffusion, ion exchange, and hydrolysis will be affected to a different degree by changes in the temperature, and the overall temperature dependence of glass corrosion will include contributions from all three processes, although it may be dominated by one process under particular test conditions. Accelerated test methods that will be used to study the advanced stages of glass dissolution include the PCT, the vapor hydration test (VHT), and the PUF test. Tests will be conducted over a range of conditions to link the dissolution behavior under disposal conditions with that under accelerating test conditions.

Service condition tests are conducted to verify that the techniques used in accelerated tests do not change the alteration mechanisms. They are designed to approximate, to the extent possible in the laboratory, the physical and chemical environment of the disposal system. Because of the low temperature of the ILAW disposal system and the very slow rate of moisture flow expected in the disposal facility, laboratory tests approximating these conditions are unlikely to yield meaningful data in reasonable time periods. Consequently, no specific service condition tests are proposed in this plan. Rather, the parameter values for some tests are selected so as to reflect service conditions. For example, some PUF experiments may be performed with fractured glass monoliths instead of ground glass to provide service condition information on water flow paths and glass alteration processes in fractures. However, solution flow rate and temperature adopted for these tests will likely be higher than the expected conditions. Again, the purpose of the testing program is to demonstrate a scientific understanding of the processes controlling long-term glass corrosion so that the *models* describing these processes can be used with confidence in extrapolating to the expected service conditions.

Having described the general types of tests to be performed, the specific characterization and accelerated tests proposed under this plan are discussed in Sections E-4.1 through E-4.9.

E-4.1 SINGLE-PASS FLOW-THROUGH TEST

The SPFT test is an open system test where a solution at a known flow rate and constant temperature flows through a reaction cell that contains the sample. The configuration precludes recirculation of a portion of the effluent and so makes a "single-pass" through the reaction cell. Many different SPFT apparatuses have been developed, but these all can be classified under three basic types: 1) well-mixed batch, 2) packed bed, and 3) fluidized bed. The advantages and disadvantages of each design are discussed below.

E-4.1.1 Well-Mixed Batch Reactor

Figure E-4.1 shows a schematic of a typical batch flow through cell. Fluid and, optionally, a gas or gas mixture is pumped into the cell. Fluid exits the cell and is collected in a separate container for later chemical analysis. Mixing is accomplished by convection from the solution flow and (optionally) gas flow into the reactor. Some researchers have used a mechanical stirrer as well. The key advantages to using this type of reactor include the ability to use powdered or monolithic samples, use and control a gas or gas mixture during the test, and eliminate the need to control bubble formation in the fluid inlet, as is necessary with a packed bed reactor (see below). The only disadvantage to using a batch reactor is the need to ensure that when using powdered samples, sufficient mixing occurs to prevent agglomeration of the particles or formation of a stagnant solution around the sample.

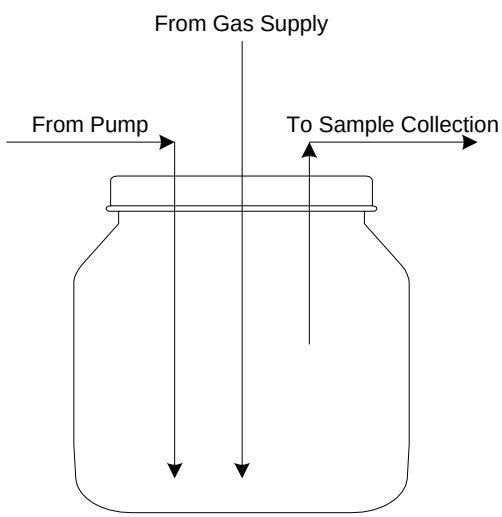

Figure E-4.1. Schematic of a Typical Batch Flow Through Cell.

E-4.1.2 Packed Bed Reactor

In a typical packed-bed type reactor, a porous bed of the test material is packed between two frits that have a nominal pore size smaller than the particle size of the sample. Solution flows through the porous bed and is collected in the same manner as with the batch reactor. The key advantage to using this type of reactor is that it eliminates the possibility of a stagnant solution layer as is possible with a batch reactor. However, this design has several important disadvantages. Care must be exercised to ensure that gas bubbles do not form in the inlet lines, which can become entrained in the porous bed. Entrained bubbles could exclude part of the

sample surface from contact with the fluid. McGrail and Olson (1992) reported that it was impossible to prevent bubble formation in their fluid inlet lines at 90°C, despite vigorous attempts to degas the solution. This limited the effective operating temperature to 70°C or less. The second disadvantage is that by the nature of the design, a concentration gradient will exist across the bed. However, depending on the specifics of the corrosion mechanism, this may or may not be of concern. Finally, the option of imposing a fixed gas partial pressure in the reaction cell is not available as it is with the batch-type reactor.

E-4.1.3 Fluidized Bed Reactor

The fluidized bed reactor is similar to the packed bed reactor except that much less sample is used so that, when sufficiently high flow rates are used, the sample particles are suspended or "fluidized" in the cell. The advantages of this design are that it eliminates the concentration gradient inherent with the packed bed reactor and ensures complete exposure of the entire particle surface area to the fluid. However, this test configuration has numerous disadvantages. First, depending on the particle size and density difference between the sample and the fluid, a relatively high flow rate is required to fluidize the bed. The flow rate required often can be sufficiently high that the solution exiting the reactor does not differ enough from background concentrations to be statistically significant. This is particularly problematic at lower temperatures because the flow rate required to fluidize the bed will change only slightly with temperature, but the dissolution rate of the test material may decrease by 2 to 3 orders of magnitude over the temperature range of 90 to 20°C, thus compounding detection limit problems. Second, the high flow rates required generate large volumes of effluent. This can present an expensive waste disposal problem, especially when testing radioactive materials. Third, because the particles are in motion and collide with one another, particle abrasion may cause a change in surface area during the test, which may be difficult to quantify. Fourth, the reactor must be carefully engineered and tested to prevent particles from settling in quiescent pockets and from transporting out of the reactor to the collection system.

E-4.1.4 SPFT Testing Strategy

Based on the discussion of SPFT testing methods in Sections E-4.1.1 through E-4.1.3, the advantages of the batch reactor are sufficient to select it as the preferred test apparatus design. Testing must then be performed over an appropriate range of conditions. The pH of the water percolating through an ILAW disposal system will almost certainly be between pH 6 and 13, so the pH dependence of the rate must be determined over this range. Collecting SPFT data over the acidic pH range is not required. The activation energy (E_a) is another important parameter in the model, and SPFT tests must be run over a sufficient range of temperatures to accurately determine this parameter. A typical data set that provides the three parameters, k, E_a, and η, is shown in Figure E-4.2.

The procedures outlined in McGrail et al. (1997c) should also be followed in running SPFT tests over a sufficient range of flow rates to evaluate the parameters σ and K. Although K

should be independent of pH and perhaps σ as well, at least one additional experiment at another pH should be performed for confirmation. Finally, test results (McGrail et al. 1997c) on LD6-5412 glass indicated the possibility that an additional element (besides Si), such as Al, may need to be included in the affinity term. If a similar conclusion is reached based on the SPFT test results for the vendor glass compositions, then a series of tests should be performed where the concentrations of the test element(s) are varied independently. An analytical solution for a mixed Si-Al kinetic rate ILAW model was developed by McGrail et al. (1997c) and can be used to develop a statistical design for these tests.

Figure E-4.2. SPFT Test Results for Various ILAW Glasses.

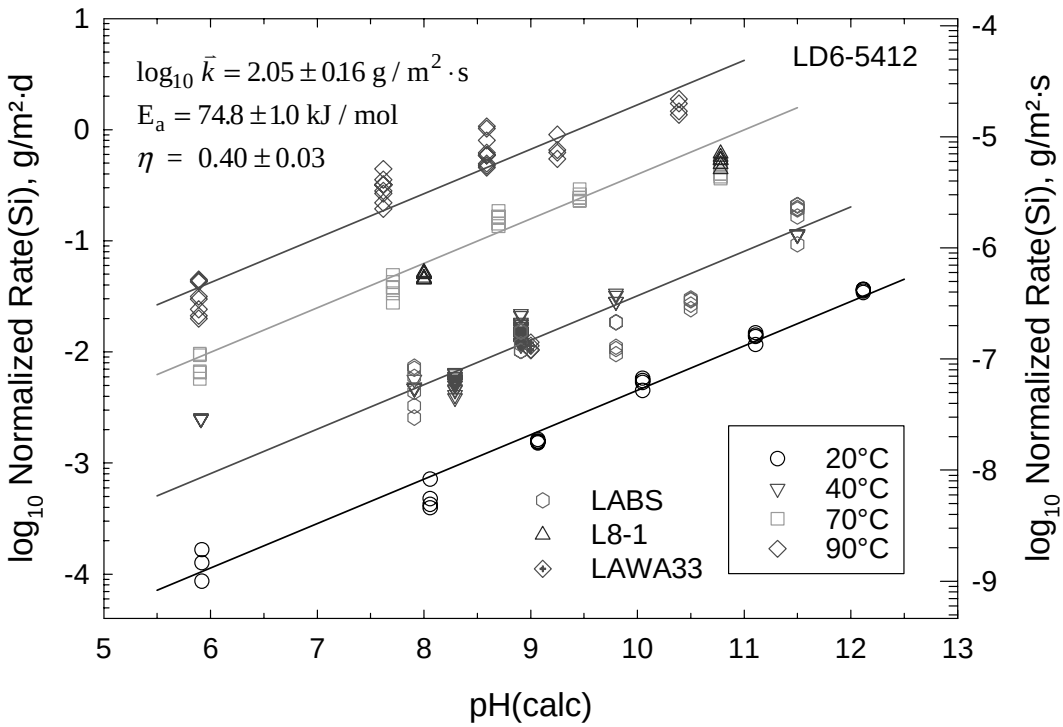

E-4.2 VAPOR HYDRATION TEST

Figure E-4.3. Schematic of VHT Test.

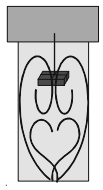

The VHT is the simplest accelerated test to be used in the recommended testing strategy because there is only one degree of freedom in test parameters that can be varied, temperature, excluding test duration and humidity. The principle use of the test is as a convenient means of generating alteration phases for analysis within a short period, but it also is

useful as a qualitative measure of the effect of alteration phase formation on the corrosion rate. The VHT is a static test in which a monolithic sample is exposed to water vapor in a sealed vessel, as illustrated in Figure E-4.3. At relative humidity (RH) above about 80%, a thin film of water condenses on the sample. The thickness of the film increases with the RH, and it is in this film that the glass corrodes. The thickness of the film determines the effective S/V ratio of the system; for a uniform layer, the S/V ratio is simply the inverse of the thickness of the film. Most VHTs have been performed in 100% relative humidity at temperatures above 100°C, although tests have been conducted at lower humidities and temperatures. At the completion of a test, the sample is removed from the vessel, and the reacted surface is analyzed with high-resolution electron microscopy. Discrete precipitated crystalline phases usually form when the sample corrodes. The solution evaporates from the sample when the test is terminated and is not available for analysis. This precludes using the test to evaluate and test models of glass corrosion behavior, which require detailed measurements of the solution composition in contact with the glass.

Vapor hydration has been used by archaeologists to replicate the weathering observed on obsidian artifacts recovered from terrestrial sites (Friedman and Long 1976). The method has also been used to simulate the long-term weathering of tektite (Mazer et al. 1992) and basaltic glasses (Byers et al. 1986). Because the test method produces the same alteration phases that form during the weathering of natural glasses over long periods, the test has also been used to accelerate the corrosion of waste glasses. High-level waste glasses commonly form clay layers in VHTs. Glasses having compositions relevant to anticipated ILAW for Hanford formation zeolite phases similar to analcime, gobbinsite, and phillipsite.

To extract kinetic information, VHTs will be run over a minimum of four temperatures, all at 100% RH. However, it is important to recognize that the rate measured in VHTs is not the glass dissolution rate, but the rate at which alteration phases are formed. It is presumed that precipitation rates of the alteration phases are much faster than the glass dissolution rate. Tests with radioactive glasses will be used to measure the distribution of radionuclides between alteration phases and residual phases (see Section E-4.6).

E-4.3 PRODUCT CONSISTENCY TEST

The PCT has been standardized as an ASTM standard procedure (ASTM 1994). The ASTM standard includes two methods: PCT Method A was developed specifically for verifying process control of vitrified HLW forms and is conducted with specific values of test parameters; PCT Method B does not specify the values of test parameters. Because the PCT Method B encompasses commonly used variations of test parameters, we refer to all static dissolution tests with crushed glass generically as PCTs.

The PCTs are conducted by reacting an aliquot of crushed glass that has been sieved to isolate the desired size fraction with an aliquot of a solution in a sealed vessel at the desired temperature. The glass S/V can be calculated from the glass-solution mass ratio and the specific

surface area of the crushed glass to determine the average dissolution rate during the test. Tests are conducted as batch tests wherein a separate test is run for each duration. At the end of the test, the solution is analyzed for pH and the concentrations of dissolved glass components. The latter are used to calculate the amount of glass that has reacted and the dissolution rate. The reacted glass surface also can be analyzed to help characterize the reaction mechanism, such as when an alkali-depleted layer or alteration phases form.

Because the test conditions in PCTs are water-saturated and static (closed-system), which are not consistent with expected disposal system conditions, including a significant number of PCTs in this plan requires explanation. Traditionally, PCTs are used as a means to study advanced stages of corrosion at high glass-solution mass ratio (or S/V), high temperature, and long test duration. It is argued that the reaction conditions in the PCTs are similar in several regards to the conditions expected in a disposal site. Although waste glasses will not be crushed, the S/V values commonly used in PCTs are similar to the effective S/V values when a small volume of water contacts a glass. The static conditions of the PCTs are also probably not too different from the very low water infiltration rates anticipated. Therefore, PCTs probably provide a fair simulation of the corrosion behavior after a small amount of water has contacted a waste package and reveal key reaction processes. While each of these statements is true to some extent, they provide insufficient justification for running PCTs as they establish only heuristic connections with modeling.

Consistent with the model-centered approach used in this plan, the PCT is used to calibrate the substantial set of supporting geochemical data that are required for modeling the dynamic evolution in solution chemistry that occurs as a consequence of glass-water reactions. The term “calibration” in this context refers to a complex iterative process whereby the evolution in solution composition and secondary phase formation observed in PCTs is reproduced, with a reasonable level of uncertainty, in a geochemical model of the system. The process is complex because during a closed-system test, like the PCT, changes in the concentrations of dissolved glass components, the solution pH, and, in some cases, dissolved air components must be modeled simultaneously. Fortunately, the geochemical simulator selected for modeling this system, the EQ3/6 code (Wolery and Daveler 1992), has capabilities for handling these complexities.

The calibration process requires, among other things, estimating solubility product values for secondary minerals that are identified in the PCTs, but for which thermodynamic data are not available. These values can be generated by fitting to the PCT data or by using empirical methods, such as with a polymer model (Mattigod and McGrail 1998). However, if a particular phase is found to have an important effect on long-term glass corrosion rates, it is recommended that independent measurements of its solubility product be performed. Once the geochemical model has been calibrated against the PCT data, the significant aqueous speciation and dissolution-precipitation reactions in the model can be identified. This reaction set and supporting thermodynamic data then make up the reaction network that is used in the reactive transport model to compute radionuclide release from the disposal system (Bacon and McGrail 1997).

Because the dissolution behavior of glasses in PCTs are usually strongly affected by the affinity term, PCT results can also be used to measure of the values of the saturation concentration (K) and the net reaction order variable (σ). However, the effect of a changing pH and solution composition complicates the extraction of these values. Instead, the results of PCTs conducted for long durations can be used to confirm the values of K and σ that are derived from the SPFT tests (see Section E-4.1.4).

There are two degrees of freedom for parameter variation in PCTs, temperature and S/V, excluding test duration. It is recommended that PCTs be performed at a minimum of four separate temperatures between 20 and 90°C and at two S/V ratios. Tests at elevated temperatures are needed to measure the trends in the corrosion behavior as a function of temperature and to determine if the corrosion mechanism changes with temperature. Use of higher S/V ratios provides another means of accelerating the extent of reaction. However, there are limits to the values of S/V that are practicable. At S/V ratios >20,000 m^{-1}, test artifacts become important. Initial alkali ion exchange and dissolution of fines can increase leachate ionic strength and pH to values that are unrealistic for a disposal system subject to open-system mass transport. In PCTs conducted in containers impermeable to air, the available CO_2(g) can also be consumed, which compounds the pH excursion from the ion-exchange and limits the formation of important carbonate minerals. Consumption of water from hydrolysis of the glass becomes an important consideration, as the S/V could be a steeply time-varying function. This makes interpretation of the test data much more difficult. Consequently, it is recommended that the S/V be limited to a maximum of 20,000 m^{-1}.

E-4.4 PRESSURIZED UNSATURATED FLOW TEST

Figure E-4.4. PUF Apparatus.

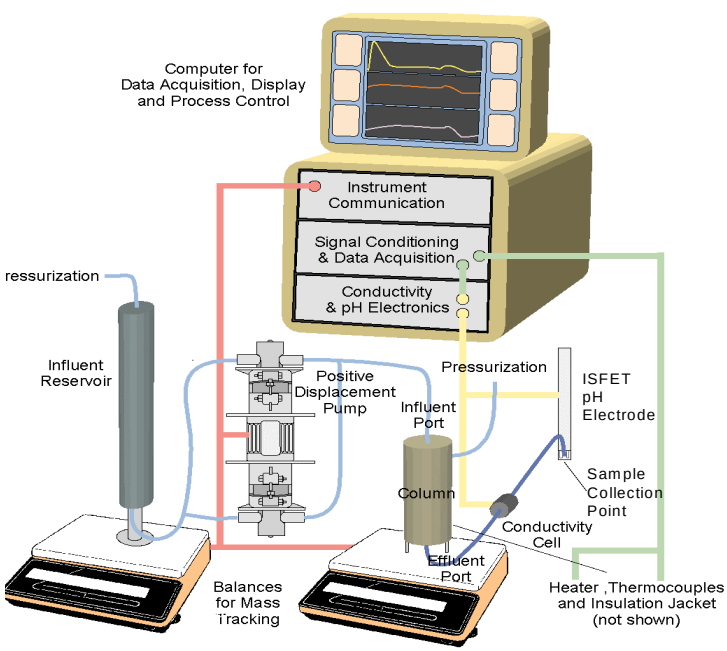

The PUF test is a new technique developed at PNNL for testing waste forms (McGrail et al. 1997a and 1997b). The experimental design provides a novel way to study waste form corrosion behavior under unsaturated conditions, subject to open-system flow and transport. Like the SPFT test, the PUF test provides three degrees of freedom for parameter variation: temperature, glass surface area, and flow rate.

The basic test apparatus consists of a column packed with glass particles (or other material) of a known size and density, and a computer data acquisition and control system (see Figure E-4.4). The

column is fabricated from a chemically inert material so that dissolution reactions are not influenced by interaction with the column. A porous titanium plate of proprietary design is sealed in the bottom of the column to ensure an adequate pressure differential for the conductance of fluid while operating under unsaturated conditions (Wierenga et al. 1993). Titanium was chosen because it is highly corrosion resistant and has excellent wetting properties. When water saturated, the porous plate allows water but not air to flow through it, as long as the applied pressure differential does not exceed the air entry relief pressure or "bubble pressure" of the plate. The computer control system runs LabVIEW™ (National Instruments Corporation) software for logging test data to disk from several thermocouples, pressure sensors, inline sensors for effluent pH and conductivity, and column weight from an electronic balance to accurately track water mass balance and saturation level.

Several important findings have resulted from PUF experiments that have been performed on LD6-5412 glass and SRL-202 glass, a reference HLW glass for the Defense Waste Processing Facility. With LD6-5412 glass, precipitation of zeolitic secondary phases was correlated with an acceleration of the glass reaction rate, exactly as was found in PCTs conducted at a high surface area-to-volume ratio (S/V) of 20,000 m^{-1} and the same 90°C temperature. However, in the PCTs, the accelerated reaction stage did not occur before about 120 to 240 days. In the PUF test, the accelerated reaction stage was reached after only about 12 days. This is an acceleration factor of about 10 to 20, even though the specific surface area of the glass used in the PUF test was about 10 times smaller than the specific surface area of the glass used in the PCTs. In the PUF test with SRL-202 glass, precipitation of an aluminosilicate phase, pianlinite [$Al_2Si_2O_6(OH)_2$], was correlated with a 50% decrease in volumetric water content, indicating a change in the hydraulic properties of the sample. This is the first evidence ever reported that corrosion and secondary phase precipitation can induce changes in the unsaturated hydraulic properties of a glass waste form. Experiments with Pu-containing glass packed in a thin layer between two layers of SRL-202 glass (not containing Pu) have also shown that >90% of the Pu, brought into solution from corrosion of the Pu glass, exits the column as a colloid. This is important because to exit the column as a colloid in this experiment, the colloids must have been transported approximately half the column length through a layer of crushed SRL-202 glass. Consequently, the PUF test provides a means to study the formation and transport of radiocolloids under unsaturated flow conditions.

Based on the findings from the PUF experiments that have been run to date, the test will play an important role in the overall testing strategy. First, because the test combines glass corrosion, unsaturated flow, and mass transport processes under controlled conditions, it is ideally suited to provide data for validation of the reactive transport model being used for long-term performance calculations for the disposal system (Bacon and McGrail 1997). Second, the demonstrated ability to accelerate the transformation of the glass into alteration products means that the test will provide critical information on these phases, and the stability of the glass with respect to the formation of these phases, in relatively short periods of time. Third, aged samples from the test can be independently evaluated for changes in unsaturated hydraulic properties, thereby providing critical data for modeling fluid flow through the disposal system. Fourth, the flow-through configuration allows for different engineered-barrier materials to be tested in

combination to evaluate interactive effects on glass corrosion rates and/or radionuclide release (see Section E-4.7).

Although the PUF test is assigned a key role in the overall testing strategy for the ILAW program, it must be recognized that because of the complex apparatus required, the number of PUF experiments that can be performed is constrained by relatively high costs per test, equipment availability, and access to skilled technicians to run the test. Consequently, it is recommended that PUF tests be performed at three different temperatures only. Also, because very little information currently exists on the effect of flow rate on the PUF test results, a series of tests should be performed on one vendor glass formulation that covers a range of flow rates. These experiments should be designed to examine whether the corrosion rates can be correlated with a reduced parameter, such as the ratio of volumetric flow rate to glass surface area, a well-defined correlating parameter in SPFT tests (McGrail et al. 1997c). Finally, tests are recommended with radioactive glasses (see Section E-4.6) and a series of materials interaction experiments with at least cement and glass combinations, but perhaps including iron or iron corrosion products as well (see Section E-4.7).

Typical results from the PUF test are shown in Figure E-4.5.

Figure E-4.5. Normalized Release Rates in PUF Tests with LAWABP1 Glass.

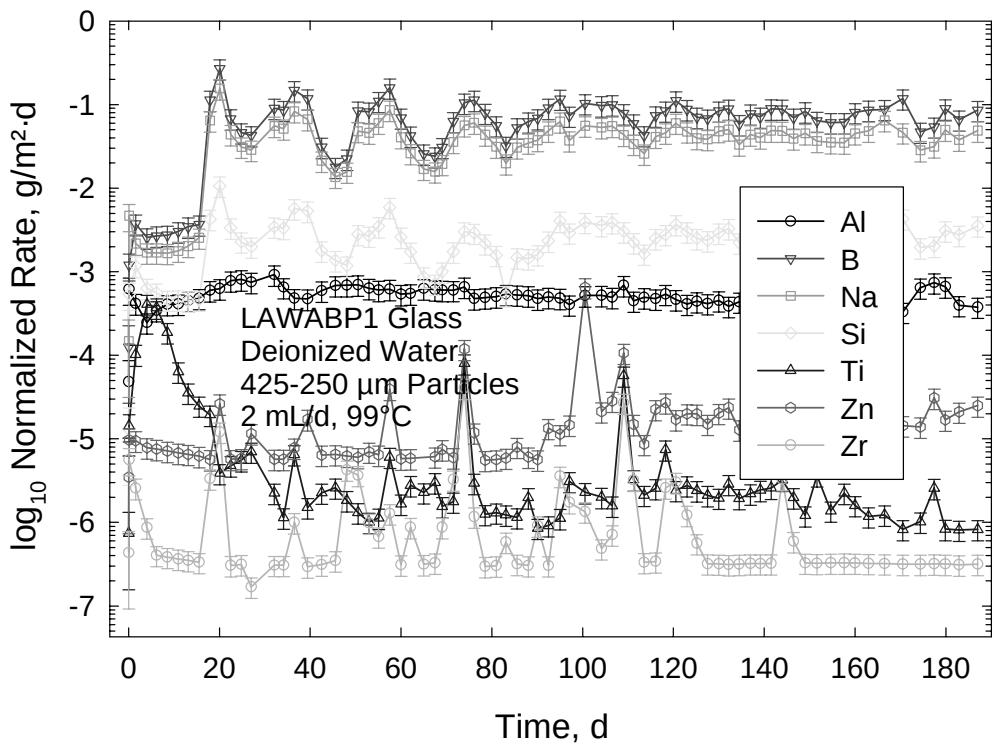

E-4.5 OTHER TEST METHODS

Other test methods have been used to measure the values of model parameters and to study glass corrosion behavior under site-relevant conditions. Some of the more commonly used test methods are described below. The reasons why these tests are not included in the testing strategy for Hanford Site ILAW are also discussed. Basically, the other test methods described below provide little or no additional relevant information when compared with the tests proposed in Sections E-4.1 through E-4.4.

E-4.5.1 Soxhlet Tests

Soxhlet tests provide a method for measuring the glass corrosion rates under highly dilute conditions. Soxhlet tests are performed by reacting a sample with condensed fluid in a refluxing apparatus. Water is boiled from a reservoir, condensed in a reflux tube, then allowed to drip into a small cup that contains the sample. The solution in the sample cup is refreshed as condensate drips into the sample cup. Complete volume replacement of the fluid in the cup typically occurs every few minutes but the precise replenishment time depends on the sample cup volume and refluxing conditions. The refluxing action provides an effective flow rate that can be varied by controlling the applied heat flux to the device. Tests are usually run to attain a flow rate sufficiently high that the solution in the sample cup remains highly dilute. The corrosion rate can be measured by periodically removing a sample of the solution in the reservoir for analysis. The Materials Characterization Center Soxhlet test (MCC-5) specifies the use of a monolithic sample and an all-Teflon apparatus (Strachan et al. 1981), although crushed samples and stainless steel apparatuses have also been used.

Soxhlet tests have been used to measure the initial corrosion rate of glasses as a function of the temperature, particularly for European HLW glasses (Delage and Dussossoy 1991; Tovena et al. 1994). Unfortunately, because the system operates with condensed vapor, the dissolution rate can only be easily measured at the pH of distilled water at the test temperature. Because the dissolution rate is required over a pH range of 6 to 13, the SPFT technique (see Section E-4.1) is preferred for these measurements.

E-4.5.2 MCC-1 Test

The MCC-1 static leach test method was developed to compare the durabilities of candidate waste forms developed to stabilize high-level nuclear waste (DOE 1982). The test procedure has been standardized by the ASTM (ASTM 1992). The method calls for placing a monolithic specimen of known geometric surface area into a volume of solution such that the S/V is 10 m^{-1}. The test may be performed with demineralized water, a reference silicate solution, or a reference brine. The reference temperature and time are 90°C and 28 days, although

temperatures of 40 or 70°C and other durations can be used.[a] The MCC-1 test typically provides a solution-dominated system in that the leachate remains dilute as the glass dissolves. However, tests conducted for long time periods may be affected by changes in solution chemistry. Samples corroded in MCC-1 tests show details of the chemical and physical alteration of the glass surface and have provided insight into mechanisms controlling the initial stages of corrosion (Bates et al. 1991; Oversby and Phinney 1992).

While the MCC-1 method was originally designed to compare the relative chemical durabilities of candidate waste forms, the test can be used to characterize several aspects of the corrosion process in conjunction with a corrosion mechanism. Tests conducted for short time periods provide a simple means of measuring the glass corrosion rate under dilute conditions. Tests have been performed in buffer solutions or solutions spiked with various glass components to determine the effects of the leachate chemistry on the glass corrosion rate (Advocat et al. 1991). Longer term tests can be run to monitor the alteration of the glass surface during corrosion to investigate the corrosion mechanism (Strachan 1983; Bates et al. 1991). However, because each of these processes is covered in greater depth using SPFT and PCTs, there is no compelling need to include MCC-1 tests in the testing strategy for ILAW glass.

E-4.5.3 MCC-3 Solubility Test

The MCC-3 test was designed to measure the maximum solubility of a waste form in the solution of interest (MCC 1984). This test method formed the basis of the PCT. Tests were to be conducted until the solution composition did not vary with the reaction time (i.e., until the glass “saturated” the solution). However, application (Shade and Strachan 1986) of the test method showed that 1) constant solution compositions were not achieved within a few weeks, and 2) the solution composition depended on the particle size of the glass used. The first observation is a direct result of the glass reactivity, while the second is due to the different S/V that results from the different total surface areas of different sieve fractions. Tests conducted at higher S/Vs usually generate more concentrated solutions. The MCC-3 procedure was subsequently modified such that 1) a single size fraction is specified, and 2) the test vessel is continuously agitated during the test, usually by placing the vessel on a roller. The PCT has effectively replaced the MCC-3 test in most laboratories, although all of the complications associated with the use of crushed glass found during development of the MCC-3 tests are common to the PCT procedure.

E-4.5.4 Periodic Replenishment Tests

Several test methods have been developed in which leachate solution is periodically removed from an ongoing static test and replaced with an equal volume of fresh solution. Such replacement tests have been used to simulate very low flow rates that cannot be attained using

---

[a]The MCC-2 test procedure is a variation of the MCC-1 procedure that permits reaction temperatures of 110, 150, and 190°C.

mechanical pumps (Barkatt et al. 1983 and 1984). Either monolithic or crushed samples can be used, and different starting solution compositions can be used. Specific test methods have different replacement schedules and replace different fractions of the total solution volume. For example, the test designated by the International Standardization Organization (ISO) calls for replacing the entire solution volume daily for the first week, every week for eight weeks, monthly for six months, and twice yearly thereafter (Hespe 1971). The American Nuclear Society test method ANS 16.1 and variations of the ANS 16.1, such as the Dynamic Leach Test (DLT) and the Accelerated Leach Test (ALT), are similar total volume exchange tests. They differ primarily in the replacement schedules. These tests were developed to characterize materials from which contaminants are assumed, a priori, to be released by a diffusion-controlled process, such as with grouts and cements. Although the ANS 16.1 test is required for ILAW in the Phase 1 Hanford Privatization Contracts, this type of test provides little insight to the long-term corrosion behavior of glass waste forms. This is because concentrations of the waste form components and solution pH change over time in the fluid contacting the waste form until the fresh fluid is injected, which then causes a sudden and abrupt change in the solution chemistry. Such conditions are extremely difficult to interpret and cannot be treated adequately with conventional geochemical computer codes. Consequently, no periodic replenishment tests are proposed in this plan.

E-4.5.5 Unsaturated or "Drip" Test

The Unsaturated Test or "drip test" was developed at ANL to simulate the corrosion of a waste glass that is intermittently contacted by transient water in an unsaturated geologic environment, such as that at Yucca Mountain (Bates and Gerding 1986). A sample of the waste form and possibly other engineering or geologic materials is placed in the center of a reaction cell. A small amount of liquid water is injected through a septum and allowed to drip from the feed tube onto the upper surface of the sample. Initial aliquots of added water are vaporized until the air is saturated; subsequent aliquots drip onto the sample. Solution that drips from the sample during the test and collects in the bottom of the test vessel can be analyzed to quantify the amount of glass that has dissolved and been transported away from the waste form. The corroded glass can also be analyzed to assess the corrosion mechanism, study materials interactions, and identify any alteration phases that form (Woodland et al. 1991). Unsaturated tests are being used as one of the primary sources of radionuclide release data in a total system performance assessment for the Yucca Mountain Site (Stout and Leider 1996).

Unfortunately, the "drip test" has several drawbacks with respect to evaluating ILAW glass behavior relevant to disposal at the Hanford Site. First, the drip test is a quasi-static method, similar to the periodic replenishment tests discussed in Section E-4.5.4. Consequently, the same difficulties exist in applying conventional modeling tools for modeling the experiment as were previously described for these tests. Second, the exact amount of fluid in contact with the sample at any given time is not known (and likely variable), so the effective S/V, a key parameter needed in modeling, is poorly defined. Finally, the drip test was originally designed as a service condition test corresponding to a particular scenario at the Yucca Mountain Site where fluid may periodically drip on the waste packages from fluid-filled fractures. This "drip" scenario does not represent a possible hydrodynamic condition for the ILAW disposal system,

which is located in a shallow, sandy soil. The PUF method is preferred for unsaturated testing because it applies a steady unsaturated hydraulic condition on the sample, and the total amount of water in contact with the sample is continuously monitored.[a] These features make the PUF test amenable to modeling using standard computational methods and tools.

E-4.5.6 Accelerated Dissolution Test

The accelerated dissolution test (ADT) was designed to measure the dissolution rate of a glass in the presence of its alteration phases and in a solution that is in near equilibrium with those phases. The alteration phases are generated by vapor hydration of a sample of the glass being evaluated, and the nearly saturated solution is generated in a PCT conducted at high S/V and at the temperature at which the dissolution rate is to be measured. The dissolution rate is measured by mass loss of a fresh monolithic sample. To date, the ADT has only been applied to measure the dissolution rate of the LD6-5412 glass (Ebert et al. 1996). The rate measured with ADTs was consistent with that estimated from long-term PCTs and that extrapolated from VHTs. However, an inoculation period existed in which the dissolution rate was at first very low and then increased because of the effects of the alteration phases. The occurrence of this period, which was of different durations in replicate tests, is not fully understood, but may be related to time needed for the solution and alteration phases to equilibrate. A specific role for the ADT has not been identified in this plan, but the test will likely continue to be used periodically to confirm long-term dissolution rates measured in VHTs and PCTs.

E-4.6 REQUIRED TESTS WITH RADIOACTIVE GLASSES

In Sections E-4.1 through E-4.5, no distinction was made with regards to testing “cold” or fully radioactive glasses. Because the ultimate goal of the testing program is to evaluate long-term radionuclide release rates, and not glass corrosion rates per se, some testing must obviously be performed with radionuclide-containing materials. However, it is not required that all testing be performed with radioactive materials. This is because the radionuclides found to be of most concern in the performance assessment (Mann et al. 1997) for the ILAW disposal system are ^{99}Tc, ^{79}Se, and ^{129}I. These radionuclides are extremely soluble under the oxidizing conditions that are expected at the site. Consequently, the rate of glass corrosion ultimately determines the rate of release for these important elements. However, at very long times, Pu and U isotopes also contribute to the computed doses from the groundwater pathway (Mann et al. 1997). These elements are expected to form sparingly soluble precipitates in the disposal vault and also may be transported as colloids, so the release rates will not depend directly on the corrosion rate of the glass. For these elements, experiments with radioactive glasses are needed to identify the solubility-controlling phases. Release rates of the soluble radionuclides also need to be checked

---

[a]The capability to monitor spatial variations in moisture distribution during a PUF test will be available shortly at PNNL with the installation of an X-ray computed microtomography system.

for congruency with the rate of glass corrosion to eliminate the possibility of a mechanism, such as ion exchange, that could selectively enhance release rates.

Because only very limited data have been obtained with a single ILAW glass (LD6-5412) doped with ^{99}Tc, it is difficult at this time to define what amount of testing with radioactive glasses is required. The level of testing also depends strongly on future funding levels for the ILAW disposal program. A reasonable conjecture includes a reduced set of VHT, PCT, and PUF tests with a fully radioactive glass containing each radionuclide of interest. The reduced set may include VHTs at one temperature, PCTs at two temperatures but only the highest S/V, and PUF experiments, also at two temperatures, but at two flow rates and one glass surface area. Concentrations of the radionuclides in the test glasses likely should not reflect the expected activity levels in the actual glass product. Consideration should be given to doping the test glasses at significantly higher levels than expected so that it is easier to identify secondary solids containing the radionuclides. Because the radionuclide concentrations and radioactivity levels of ILAW glass are very low, there is little or no concern regarding radiolysis-induced experimental artifacts or having the radioactive glasses exhibit different long-term corrosion behavior when compared with nonradioactive glasses.

E-4.7 MATERIALS INTERACTION TESTS

The ILAW disposal system will include the following additional materials, besides glass, that are used in construction or as part of the waste package: 1) concrete used in the vault walls, ceiling, and floor; 2) carbon or stainless steel containers used to hold the glass; and 3) filler material used inside the containers to consume void space. Of these materials, the concrete is of the most interest because of the anticipated volume required, approximately 320,000 metric tons (Burbank 1997), and the chemical effect of the concrete in increasing pH and Ca, Na, and K concentrations. Corrosion of the metal containers will generate iron oxyhydroxides that are known to adsorb or coprecipitate with Si (Harder 1978). This can act as an additional sink for Si, resulting in enhanced rates of glass corrosion (McVay and Buckwalter 1983; McGrail 1986). However, iron hydroxide precipitates also may have a beneficial effect in that they are well known adsorbents for a wide variety of metals, and so could lower release rates for some radionuclides. No specific filler material has been identified, so the significance of this material to glass corrosion behavior cannot be assessed at this time.

Because the concrete is used exclusively on the exterior of the vaults, the interactive effects of the concrete on the glass (if any) will most likely be confined to a region at the "interface" between the two materials. This is because diffusion and/or advection limit the total mass flux of OH^-, Ca^{2+}, etc. from the concrete that is available for reaction with the glass. To properly test this mass-transport rate-limited process in the laboratory, a technique is required where mass transport by diffusion and/or advection from the concrete into the glass can be controlled. Batch experimental methods, such as the VHT or PCT, are intentionally designed to be well-mixed systems to avoid mass transport constraints on the reaction processes. Consequently, these methods are unsuited for this materials interaction study. Fortunately, the

PUF technique provides a means to control mass transfer and transport rates by the particle size and flow rate used in the test. The concrete and glass can be configured sequentially, such that the water can "equilibrate" with the concrete before entering the porous glass bed. By comparing differences in corrosion rates and radionuclide release, with and without the concrete, and by examining the alteration products formed, especially at the interface between the two materials, a good understanding of the interactions between the materials can be developed.

Interactive effects with the container or iron corrosion products are more difficult to assess because the material will be distributed throughout the disposal system, including the interior region of each vault. In this case, the mass transport limitations discussed above for the concrete do not apply, at least on a scale larger than a single waste package. A highly localized assessment of the interactive effect could be obtained by running a VHT where the container material and glass are "sandwiched" together. An alternative would be to run PCT or PUF experiments where the glass and container material particles are mixed together in volume percentages equivalent to what is expected in the current disposal system design. Glass corrosion rates would then be directly compared with and without the metal present to obtain a direct assessment of the interactive effects, if any. Care must be exercised in these tests to ensure that the available O_2 is not consumed from oxidation of the steel.

E-4.8 ROLE OF NATURAL ANALOGS

Analogy is a scientific method that uses inference from certain resemblances to imply a probable further similarity (Ewing and Jercinovic 1987; Petit 1992). The term natural analog refers to a material or process that resembles those expected in a waste disposal system or the methodology used to study and assess them. The analysis of analog materials has been used to enhance confidence in the validity of long-term predictions made with mechanistic models, as well as assisting in the development of those models (ASTM 1991). By studying the alteration of natural materials that has occurred over millions of years due to weathering in a range of terrestrial environments, insight has been gained into the long-term corrosion behavior of waste glasses in a disposal environment. This is done by characterizing the natural alteration of the analog material and comparing it to alteration produced in laboratory tests with naturally occurring or chemically identical synthetic materials. In addition to studying the natural alteration of a material, it is also important to identify the alteration mode(s) that controls corrosion of the analog material and to verify that the same process that controls the rate in the short-term testing also controls the long-term behavior that is being modeled. Applications of natural analogs include

- comparing alteration products generated during long-term corrosion of natural glasses to those generated in accelerated laboratory tests to verify experimental methods of accelerating glass corrosion

- studying specific reaction processes that are important in waste glass corrosion and are highlighted in the corrosion mechanism of a natural material

- studying the relationship between the kinetics of natural glass corrosion measured in short-term laboratory tests and the known long-term durability of the glass to verify that the appropriate reactions and processes are modeled for long-term calculations

- calibrating the degree to which a laboratory test accelerates a corrosion mode.

The use of natural analogs to extract kinetic information is usually limited to bounding estimates because of the uncertain and changing conditions to which the analog material has been subjected, including wet-dry cycling, variations in temperature and water composition, etc., and uncertainty regarding the age of the sample itself. In most cases, kinetic information must be extracted by examining reacted solids that are usually incomplete assemblages of alteration phases. Nevertheless, corroded natural glasses provide valuable insight regarding corrosion processes that are important to long-term corrosion and confidence in the accelerating properties of laboratory tests.

Geologists have studied samples of basaltic glasses recovered from marine, geothermal, and subglacial environments. Corrosion of basaltic glasses results in the formation of palagonite, which is a generic term for an assemblage of alteration phases that includes clays and zeolites. The same phases have been observed to form in nature and in laboratory tests (Lutze 1985; Byers et al. 1985). In both natural settings and in laboratory tests, the amounts and in some cases the identities of phases that are formed depend both on the glass composition and the environmental conditions (e.g., the temperature, chemistry, and volume of the solution contacting the glass). Waste glasses have been shown to react similarly to basalt glasses in laboratory tests and to transform to many of the same phases. This provides evidence that 1) the laboratory test accelerates the corrosion behavior of basalt glasses and leads to the same phases formed in nature over very long time periods and 2) the same processes that control long-term basalt glass corrosion in terrestrial sites (and under terrestrial conditions) also control the long-term corrosion of waste glasses.

Long-term testing of natural analog glasses using VHT and PCT methods is being funded at ANL through separate DOE programs. Consequently, there are no current plans to support additional VHT and PCT testing of natural analogs through the ILAW disposal project. However, the PUF method has only recently been developed, and no natural materials have been examined using this test method. Consequently, a small number of long-term PUF tests should be performed using a selected natural analog. The preferred material would have a much higher alkali content than is typical of rhyolitic or basaltic glasses and would have been subjected to environmental weathering conditions analogous to those expected for the disposal system. One possible site for such samples is the obsidian flows at Newberry Crater, Oregon (25 miles south of Bend, Oregon), which range in age from 1,200 to about 6,700 years B.P. This area has an arid environment similar to that of the Hanford Site and potentially provides similar analogs at different ages within a short distance of each other. Regardless, the selected natural analog sample for study must be as well-characterized as possible in terms of the sample age and weathering conditions if it is to be useful for comparing against data from PUF experiments.

E-4.9 LABORATORY TESTING STRATEGY SUMMARY

Table E-4.1 represents a compilation of the recommended testing discussed in Sections E-4.1 through E-4.6. To the best of the authors' current knowledge, this is the minimum matrix of laboratory tests required to fully characterize the long-term corrosion and radionuclide release behavior of a glass waste form for disposal at the Hanford Site. A duration limit of 2000 days was selected because the major decisions regarding acceptable glass compositions and disposal system design need to be made in approximately the next 5 years. Consequently, tests beyond this time frame will have little impact on the overall program.

A key issue not discussed in the strategy up to this point is variability. Variability in the waste stream delivered to the private vendors will result in variability in the composition of the glass product; i.e., no single glass composition represents the entire inventory of glasses to be produced during the vitrification campaigns. Glass compositional variability must also be addressed in evaluating the long-term performance of the disposal system. One approach is to identify a selected set of glasses that represent compositional extremes and then perform a reduced set of experiments on these glasses. The results from these tests can then be used to bound the release rate behavior for entire compositional space. Once data are available on the reference vendor glass compositions and the variability expected during processing is quantified, specific compositions and tests can be proposed.

Table E-4.1. Master Test Matrix for Long Term Performance Evaluation of a Glass.

Test Method	Temp	pH	Flow Rate	Surf. Area	Sol. Vol.	Duration Range (days)
SPFT(k, E_a, η)	4	6	Var.[1]	1		14-30
SPFT(K, σ)	1	2	15	1		14-30
VHT	4					1-2000
PCT	4			2[2]	1[2]	30-2000
PUF	3		3	2		30-2000
Rad. Glasses						
VHT	1					1-365
PCT	2			1[2]	1[2]	30-2000
PUF	2		2	1		30-2000

[1]Flow rate sufficiently high so that $Q/K \approx 0$.
[2]Varied as S/V.

E-5.0 FIELD TESTING

Field testing provides a unique opportunity to obtain site-relevant data on the corrosion behavior of waste forms under conditions that more closely approximate service conditions than is possible in the laboratory. Recognizing this fact, several burial studies with glass waste forms have been conducted in the United States and abroad. One of the first studies involving glasses was carried out in the early 1980's at the Stripa Site in Sweden. The Stripa Site is an abandoned iron mine located in a granitic formation approximately 350 m below the surface. Specimens were fabricated in a "pineapple slice" geometry and stacked into assemblies that were either heated to 90ºC or maintained at ambient mine temperatures (8 to 10ºC). Samples were extracted at predetermined intervals (0.25, 0.5, 1, and 2 years) for extensive characterization using surface spectroscopic and microscopic analytical techniques. In the United States, a comprehensive field test involving HLW glasses was performed for the Materials Interface Interaction Tests (MIITs) at the Waste Isolation Pilot Plant (WIPP) in Carlsbad, New Mexico. Located approximately 650 m below the surface in the Salvo salt formation, a wide array of glasses and waste package materials was tested for 5 years. Pineapple slices of test samples were stacked on heated Teflon assemblies in such a manner as to test a variety of interfacial reactions. The United States also has participated in burial studies conducted at the Mol Site in Belgium (clay geology) and Ballidon Site in the United Kingdom (limestone) in an effort to test the performance of a simulated HLW glass (SRL-165) in other geologies.

At the Hanford Site, grout waste forms have been field tested in lysimeters at the Grout Waste Test Facility located in the 300 Area (Last et al. 1995). A lysimeter essentially consists of a corrugated steel container buried flush with the ground surface. Lysimeters can range in size from small soil-filled cans, a few centimeters in diameter and a few centimeters deep, to large caissons that are several meters wide and tens of meters deep. Lysimeters can be simply designed with little or no peripheral instrumentation, or they can be designed with extensive monitoring features, including devices for monitoring temperature, water content and matric potential and devices for extracting samples of water for chemical analysis. Lysimeters have been built and used at the Hanford Site for a variety of reasons, including the assessment of recharge rates, biointrusion studies, radionuclide transport studies, evapotranspiration studies, and field-scale waste-form performance tests (Gee and Jones 1985; Rockhold et al. 1995).

Although lysimeters have several disadvantages, they are a logical choice for field testing of the glass corrosion and contaminant transport models being developed for the ILAW disposal system. The devices provide a way to combine an ILAW glass, Hanford formation soil, and perhaps other engineered materials in a well-controlled test, but on a scale that is not practicable in the laboratory. The test is controlled because the walls of the lysimeter form a physical boundary in the system being studied that defines a fixed volume for calculating water storage and tracer mass balance and restricting the geometry of flow within the lysimeter to essentially one dimension. Interpretation of complex temporal variations in tracer release and transport is much simpler in one spatial dimension. The field scale affords the opportunity to monitor contaminant release and transport in time and space that is not possible in laboratory experiments, such as with the PUF test (see Section E-4.4). This is especially true when

operating under low-moisture-content conditions where the volume of solution available per cubic meter for collection of samples is small.

Lysimeter experiments should be used as a tool to confirm the coupled glass corrosion and contaminant transport model described in Section E-3.0. For this purpose, there is no need to exclusively test glasses similar in composition to the vendor's formulation or to simulate natural conditions as much as possible. Instead, some experiments should be run with an applied steady flow rate of water and with a glass designed to have high corrosion rate so that it is easier to monitor contaminant release and transport during the test. It is also important that these experiments be designed and instrumented appropriately so that data can be collected to support validation studies of other key models being used on the ILAW disposal program, such as a multiphase flow simulator.

E-6.0 MODELING THE DISPOSAL SYSTEM

The previous discussion of the testing strategy would not be complete without a discussion of the link to modeling the disposal system, as this is the ultimate use of the data generated by the testing program. The fundamental objective of the performance assessment for disposing of ILAW is to calculate the radiation dose to a future population as a result of any release and transport of radionuclides to the unconfined aquifer located approximately 70 m below the disposal facility. Computer models will be used to simulate the processes controlling the release and transport of radionuclides to the unconfined aquifer. The computer codes must perform three major simulation functions: 1) release of contaminants from the vitrified waste, 2) transport of those contaminants through the engineered system, and 3) transport through the vadose zone to the groundwater. In Section E-3.2, we presented the kinetic rate law for glass corrosion:

$$J_i^a = \nu_i k e^{-\frac{E_a}{RT}} a_{H^+}^{-\eta} \left[1 - \left(\frac{Q}{K} \right)^{\sigma} \right], \qquad i = 1,2,...N$$

Assuming that k, E_a, η, *K*, and σ are all known parameters developed from the laboratory testing program, to determine the mass flux of any component *i* released from the glass to the aqueous phase, it is necessary to calculate the pH and ion activity product, *Q*. Because the calculation of these chemical variables depends on both the physical properties of the system, such as flow rate and glass surface area, and chemical properties, such as solubility products and the amounts and types of alteration products formed, functions (1) and (2) discussed above cannot be decoupled. A special type of computational model, called a reactive chemical transport model, is required for simulations.

In 1995, the Hanford Low-Activity Waste Disposal Project selected a reactive transport code to calculate contaminant release rates from the engineered components of the disposal system (McGrail and Mahoney 1995). The **A**nalyzer of **R**adionuclid**E** **S**ource **T**erm with **C**hemical **T**ransport (AREST-CT) code describes multicomponent reactive transport in an isothermal, partially saturated, porous medium. The model includes chemical reactions between aqueous, gaseous, and solid phases. Reactions involving minerals are described through appropriate kinetic rate laws, along with a special option for treating irreversible reactions (such as glass corrosion) via the kinetic rate, Equation (G.2). Homogeneous reactions within the aqueous phase are assumed to be reversible with their reaction rates controlled by transport and local equilibrium mass action relations. Local equilibrium between a gas or gas mixture and the aqueous phase is treated through Henry's Law. Solute transport includes contributions from advection, diffusion, dispersion, and radioactive decay.

Because of evidence from PUF experiments that significant changes in hydraulic properties may occur as a result of precipitation of secondary phases, it was decided in 1997 to incorporate a multiphase flow and transport capability into AREST-CT so that these property

changes could be coupled to the flow field. The specific mechanisms incorporated in the code are changes in porosity, and hence hydraulic conductivity, caused by mineral precipitation-dissolution and changes in water saturation caused by water consumption-production in chemical reactions. This was accomplished by coupling AREST-CT with STOMP, a nonisothermal, multiphase flow simulator (White and Oostrom 1996). The new coupled code is called STORM, **S**ubsurface **T**ransport **O**ver **R**eactive **M**ultiphases.

As it is currently configured, the STORM code represents a relatively complete model of the physical and reactive chemical transport processes that are required for simulating radionuclide release rates from the disposal system. However, several improvements to the code are needed to support long-term performance calculations, especially in more than one spatial dimension. These improvements can be classified in terms of 1) subprocess models and 2) numerical methods.

E-6.1 SUBPROCESS MODEL DEVELOPMENT

STORM has two subprocess models requiring further development: 1) adaptive reaction network and 2) composition-dependent hydraulic property model.

E-6.1.1 Adaptive Reaction Network

The set of reactions to be considered in a single STORM run, the reaction network, is fixed as specified in the input file. Consequently, careful consideration must be given to including all important solid and solution species that may be important in the system. This is extremely difficult because the system being modeled is usually changing chemically in time and space, often in ways that cannot be predicted a priori. Consequently, solid and solution species that were important at the start of a run can become unimportant components in the reaction network and vice versa. A subprocess model is needed in STORM that adapts the reaction network periodically. This can be accomplished by conducting a phase boundary search at each node. The phase boundary search is a numerical implementation of the mineralogic phase rule. It operates by querying a general thermodynamic database and computing an ion activity product for each solid that could exist in the current system based on the elements being considered. Supersaturated phases are added to the reaction network, and undersaturated phases can be deleted. However, because the dissolution rate of a phase is finite, deletion of the phase from the network is constrained until the total mass falls below some specified value.

E-6.1.2 Composition-Dependent Hydraulic Property Model

Unsaturated flow experiments with glass waste forms have shown that the dissolution of the glass and subsequent formation of secondary minerals, such as zeolites and clays, can change the unsaturated flow properties of the glass (McGrail et al. 1997c.). Constitutive equations are

used in computational modeling of multiphase flow to relate changes in flow properties, such as hydraulic conductivity and permeability, to changes in primary variables, such as matric potential or volumetric water content (Tietje and Tapkenhinrichs 1993). For example, a water-retention function developed by van Genuchten (1980) is commonly used in modeling unsaturated flow in porous media

$$\theta = \theta_r + (\theta_s - \theta_r)/[1+(\alpha\psi)^n]^m$$

where θ, θ_r, and θ_s are water content, residual water content, and saturated water content, respectively, ψ is matric potential, and α, n, and m are fitted parameters that are related to the physical properties of the porous medium. Physical properties, such as porosity, tortuosity, air entry matric potential, residual moisture content, etc., are typically assumed as invariant properties of the matrix, and so α, n, and m are assumed to be constant as well. Such assumptions are invalid in chemically reactive systems where macroscopic changes in physical and chemical properties can be induced by interphase mass transfer reactions that affect the pore scale. In general, the most important mass-transfer reactions involve dissolution of primary solid phases and concomitant precipitation of secondary solid phases.

A fundamental physicochemical basis for modifying the empirical fitting coefficients used in constitutive relationships, like the van Genuchten function, for multiphase flow through a system containing fractured glass should be developed. One possible approach to develop an appropriate model is to conduct experiments where hydraulic and physicochemical property data are obtained on uncorroded and corroded glass samples, possibly obtained from PCT and PUF experiments. This data set will form the basis for developing physicochemical constitutive relationships for unsaturated flow. These relationships can then be tested by comparing computer simulations with measurements of the solid phase and moisture distribution during PUF tests (see Section E-4.4).

E-6.2 NUMERICAL METHODS

The vitrified waste may be in the form of large glass blocks riddled with stress fractures. Berkowitz, Bear, and Braester (1988) suggested that solute transport in fractured media can be considered at a number of different scales. A near-field scale would include a few discrete fractures near the source. At a far-field scale, the fractured media could be treated as a continuum that is representative of an equivalent porous medium in which the repeating fractures behave as large pores. Their work focused on a contaminant source surrounded by a fractured porous medium. The fractured glass waste packages emplaced in a vault (Figure E-2.1) presents a different situation; the contaminants are already distributed within the glass matrix and are released as the glass dissolves. Given the low flow rates through the vault, the contaminants will be mixed by diffusion within each fracture. If stress fractures in the glass waste form are numerous and closely spaced, a continuum approach to modeling flow and transport through the vault will likely be adequate. Consequently, developing a model capable of handling flow and transport in discrete fractures is not warranted at this time.

Currently, STORM executes on a fixed, two-dimensional cartesian finite grid. This makes the code inefficient when handling sharp concentration fronts that commonly develop in reactive transport simulations. Consequently, implementing an adaptive gridding algorithm is recommended. Adaptive gridding provides a means to increase the number of computational cells in regions where sharp concentration fronts exist and coarsens the grid where concentrations are uniform. This refinement better captures the movement of these fronts with less numerical dispersion and increases execution speed by putting extra grids at only those locations where they are needed.

Two-dimensional simulations of coupled unsaturated flow and reactive transport with STORM require significant computing resources. A two-dimensional simulation with 22 aqueous species, 9 solid species, 10 equilibrium reactions, and 10 kinetic reactions on a 30 by 35 grid requires 1 week to reach a simulation time of 20,000 years running on a Sun Ultra 1. A sensitivity analysis consisting of multiple two-dimensional runs would therefore take years to complete.

Several alternatives exist for decreasing the execution time of the code. The simplest is to execute the simulations on a workstation with a faster scalar central processing unit (CPU). Workstations are available that are several times faster than a Sun Ultra 1; within 5 years, workstations will be available that are 10 to 100 times faster than a Sun Ultra 1. A second alternative is to adapt STORM for execution on a machine with multiple, parallel processors. Currently, an effort is underway at PNNL to develop a parallel multiphase flow and reactive transport code, targeted for execution on an IBM NWMPP1 computer, capable of 247 GFLOPS. However, the reactive transport algorithm used in this code, operator-splitting, is likely to be restricted to much smaller time steps than the global-implicit algorithm used in STORM. Once this new code is available, testing will be performed to determine the relative efficiency of two codes in running an actual ILAW disposal system simulation. If significant improvements in execution time are demonstrated on a realistic simulation, then the techniques and algorithms developed from the research program on parallel multiphase flow and reactive transport codes may be implemented in a parallel version of the STORM code so that it may be used to solve the larger problems required for the ILAW disposal system performance assessment.

E-6.3 DISPOSAL SYSTEM SIMULATIONS FOR THE PERFORMANCE ASSESSMENT

The ultimate objective of the laboratory and field testing, and model development activities discussed in the previous sections of this report is to provide technically credible calculations of radionuclide release and transport in support of a formal performance assessment for the ILAW disposal system. The general methodology (Mann et al. 1998) is to divide the problem into logical parts that correspond to the computer simulation tools that will be applied in different parts of the problem domain. Figure E-6.1 illustrates the recommended overall computational strategy. The very-near-surface infiltration rate provides a key boundary condition for the remainder of the simulations. The coupled unsaturated flow, chemical reactions, and

contaminant transport simulator (see Section E-6.0) is applied from just below the root zone to some distance into the soil (probably several meters) below the floor of the disposal vault. This region is defined as the near field. Water exiting the region near the vault is expected to be of high ionic strength and pH and this plume will migrate down into the soil column for some distance until dispersion and chemical interactions with the soil components attenuate it. Beyond this depth, the chemical composition of the migrating fluid will likely change very little. Consequently, it is possible to limit the domain over which computationally intensive reactive chemical transport simulations must be performed by switching to a relatively simple vadose zone flow and transport simulation in the far-field domain. The radionuclide flux exiting the vadose zone to the unconfined aquifer is computed with this model and is used as a boundary condition for the unconfined aquifer flow and transport simulator. The final step in the methodology is to compute the impacts, if any, from ingestion, inhalation, and external radiation to humans exposed to the contaminants by withdrawing water from the aquifer and using it for drinking, farming, and other purposes.

The methodology outlined in Figure E-6.1 is remarkably robust for conducting a performance assessment. Each simulation tool is based on basic principles of physics, chemistry, and thermodynamics. No ad hoc assumptions are made about the performance of the waste form or other components of the engineered and natural system. Consequently, changes in boundary conditions, such as infiltration rate, or scenarios, such as an assumed failure of the capillary break, can be quantitatively assessed in terms of their overall impacts on system performance. Of course, the database needed to support the mechanistic models used in the selected simulation tools is substantial. In this report, we have attempted to define the minimum required data set to support the coupled unsaturated flow, chemical reactions, and contaminant transport simulator (see Section E-4.0). Although a considerable amount of testing is required, it is not intractable. Similar statements can be made about the other parts of the methodology. Consequently, the approach outlined in Figure E-6.1, and especially the laboratory and field testing required to support it, are not unreasonable or unrealistic, assuming current programmatic funding levels and schedule are maintained.

Figure E-6.1 Modeling Strategy for Assessing ILAW Disposal System.

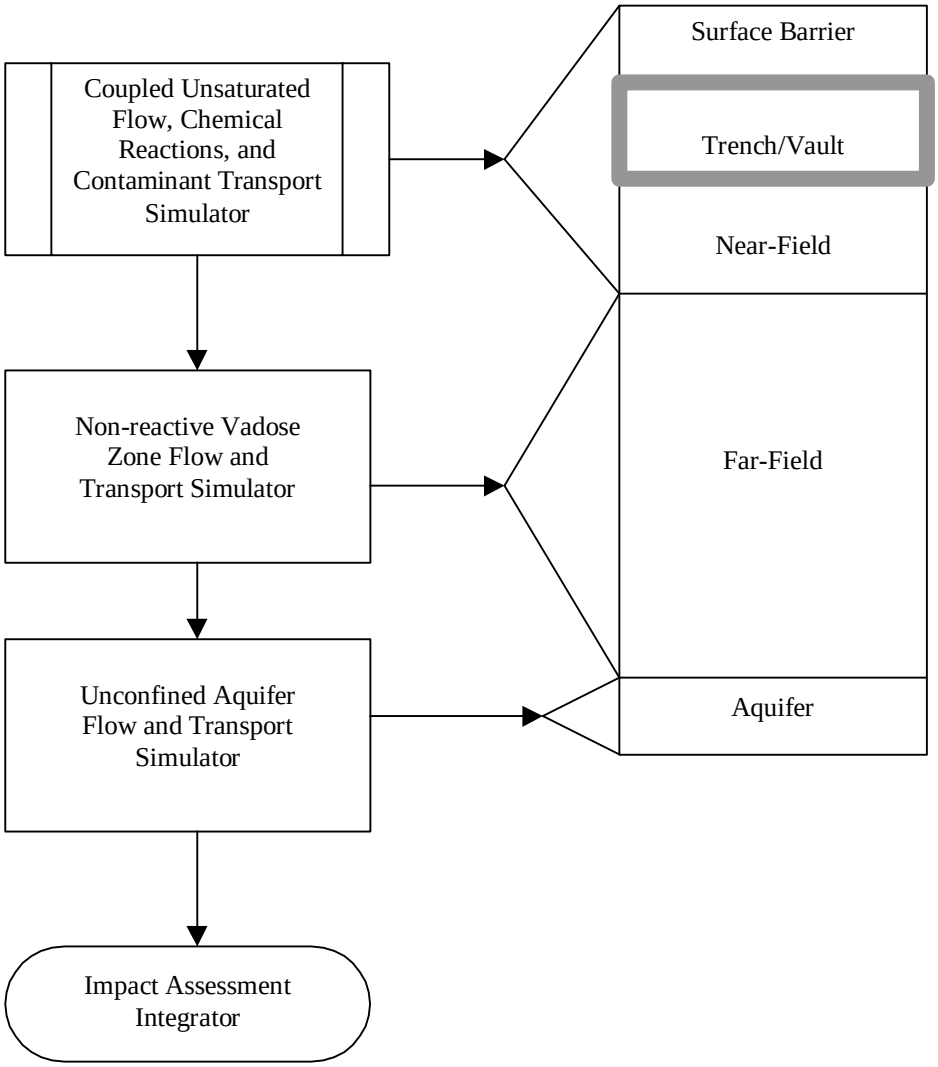

E-7.0 CONCLUSION

An overall strategy for evaluating the long-term performance of a low-activity waste glass at the Hanford Site has been presented. The strategy combines laboratory testing and field testing into an overall plan for demonstrating a scientific understanding of the processes controlling long-term glass corrosion. Models describing these processes can then be used with confidence in extrapolating to the disposal system conditions and calculating radionuclide release rates in a formal performance assessment.

The recommended laboratory testing includes single-pass flow-through (SPFT), product consistency (PCT), and pressurized unsaturated flow (PUF) tests. The majority of the laboratory testing (~80%) is to be conducted using nonradioactive glasses, with the remainder performed with glasses containing a selected set of key radionuclides. Additionally, a series of PUF experiments with a natural analog of basaltic glass are recommended to confirm that the alteration products observed under accelerated conditions in the PUF tests are similar to those found associated with the natural analog. This will provide additional confidence in using the PUF test results to infer long-term corrosion behavior.

The final component of the strategy is a set of field experiments using both vendor glasses and specially formulated highly reactive glasses. The purpose of these experiments is to validate the models for glass corrosion and reactive chemical transport that form the technical basis for calculating radionuclide release rates in the disposal system. These experiments can be performed in existing lysimeters at the Hanford Site, or in new lysimeters that have been equipped with the latest in monitoring equipment and located near the proposed disposal site. The field tests will be closely coordinated with other tasks in the ILAW performance assessment activity, so that may serve to validate other key model inputs to the performance assessment.

E-8.0 REFERENCES

Aagaard, P., and H. C. Helgeson. 1982. "Thermodynamic and Kinetic Constraints on Reaction Rates Among Minerals and Aqueous Solutions. I. Theoretical Considerations." *Am. J. Sci.* **282**:237-285.

Advocat, T., J. L. Crovisier, B. Fritz, and E. Vernaz. 1990. "Thermokinetic Model of Borosilicate Glass Dissolution." *Mat. Res. Soc. Symp. Proc.* **176**:241-248.

Advocat, T., J. L. Crovisier, E. Vernaz, G. Ehret, and H. Charpentier. 1991. "Hydrolysis of R7T7 Nuclear Waste Glass in Dilute Media: Mechanisms and Rate as a Function of pH." *Mat. Res. Soc. Symp. Proc.* **212**:57-64.

American Society for Testing and Materials (ASTM). 1991. *Standard Practice for Prediction of the Long-Term Behavior of Waste Package Materials Including Waste Forms Used in Geologic Disposal of High-Level Nuclear Waste*. ASTM C1174, Philadelphia, Pennsylvania.

American Society for Testing and Materials (ASTM). 1992. *Test Method for Static Leaching of Monolithic Waste Forms for Disposal of Radioactive Waste*. ASTM Standard C1220-92, American Society for Testing and Materials, Philadelphia, Pennsylvania.

American Society for Testing and Materials (ASTM). 1994. *Standard Test Methods for Determining Chemical Durability of Nuclear Waste Glasses: The Product Consistency Test (PCT)*. ASTM C1285, Philadelphia, Pennsylvania.

Bacon, D. H., and B. P. McGrail. 1997. "Source Term Analysis for Hanford Low-Activity Tank Waste Using the STORM Code: A Coupled Unsaturated Flow And Reactive Transport Model." *Am. Chem. Soc. Proc.* (in press).

Barkatt, Aa., P. B. Macedo, W. Sousanpour, A. Barkatt, M. A. Boroomand, C. F. Fisher, J. J. Shirron, P. Szoke, and V.L. Rogers. 1983. "The Use of a Flow Test and a Flow Model in Evaluating the Durability of Various Nuclear Waste-Form Materials." *Nucl. Chem. Waste Mgmt*. **4**:153-169.

Barkatt, Aa., W. Sousanpour, Al. Barkatt, M. A. Boroomand, and P. B. Macedo. 1984. "Leach Behavior of SRL TDS-131 Defense Waste Glass in Water at High/Low Flow Rates." *Mat. Res. Soc. Symp. Proc.* **26**:643-653.

Bates, J. K. C. R. Bradley, E. C. Buck, J. C. Cunnane, W. L. Ebert, X. Feng, J. J. Mazer, D. J. Wronkiewicz, J. Sproull, W. L. Bourcier, B. P. McGrail, and M. K. Altenhofen. 1994. *High-Level Waste Borosilicate Glass: A Compendium of Corrosion Characteristics*. DOE-EM-0177, U.S. Department of Energy, Office of Waste Management, Washington, D.C.

Bates, J. K., and T. J. Gerding. 1986. *One-Year Results of the NNWSI Unsaturated Test Procedure: SRL 165 Glass Application*. ANL-85-41, Argonne National Laboratory, Argonne, Illinois.

Bates, J. K., W. L. Ebert, J. J. Mazer, J. P. Bradley, C. R. Bradley, and N. L. Dietz. 1991. "The Role of Surface Layers in Glass Leaching Performance." *Mat. Res. Soc. Symp. Proc*. **212**:77-87.

Berkowitz, B., J. Bear, and C. Braester. 1988. "Continuum Models for Contaminant Transport in Fractured Porous Formations." *Water Resour. Res*. **24**(8):1225-1236.

Boksay, Z., G. Bouquet, and S. Dobos. 1968. "The Kinetics of the Formation of Leached Layers on Glass Surfaces." *Phys. Chem. Glasses* **9**(2):69-71.

Bourcier, W. L. 1989. *Geochemical Modeling of Radioactive Waste Glass Dissolution Using EQ3/6: Preliminary Results and Data Needs*. UCID-21869, Lawrence Livermore National Laboratory, Livermore, California.

Bourcier, W. L., D. W. Peiffer, K. G. Knauss, K. D. McKeegan, and D. K. Smith. 1990. A Kinetic Model for Borosilicate Glass Dissolution Based on the Dissolution Affinity of a Surface Alteration Layer." *Mat. Res. Soc. Symp. Proc*. **176**:209-216.

Bourcier, W. L., H. C. Weed, S. N. Nguyen, J. K. Nielsen, L. Morgan, L. Newton, and K. G. Knauss. 1992. *Proc. Seventh Annual Water-Rock Interaction Conf.*, Balkema, Rotterdam, pp. 81-84.

Bourcier, W. L., S. A. Carroll, and B. L. Phillips. 1994. "Constraints on the Affinity Term for Modeling Long-Term Glass Dissolution Rates." *Mat. Res. Soc. Symp. Proc*. **333**:507-512.

Bourcier, W. L., W. L. Ebert, and X. Feng. 1993. "Modeling Surface Area to Volume Effects on Borosilicate Glass Dissolution." *Mat. Res. Soc. Symp. Proc.* **294**:577-582.

Burbank, D. A., Jr. 1997. *Analysis of Alternatives for Immobilized Low-Activity Waste Disposal*. HNF-SD-TWR-AGA-004, Rev. 0, SGN Eurisys Services Corporation, Richland, Washington.

Byers, C. D., M. J. Jercinovic, and R. C. Ewing. 1986. *A Study of Natural Glass Analogues as Applied to Alteration of Nuclear Waste Glass*. NUREG/CR-4842, Nuclear Regulatory Commission,

Byers, C. D., M. J. Jercinovic, R. C. Ewing, and K. Keil. 1985. "Basalt Glass: An Analogue for the Evaluation of the Long-Term Stability of Nuclear Waste Form Borosilicate Glasses." *Mat. Res. Soc. Symp. Proc*. **44**:583-590.

Chen, Y., B. P. McGrail, and D. W. Engel. 1997. "Source-Term Analysis for Hanford Low-Activity Tank Waste Using the Reaction-Transport Code AREST-CT." *Mat. Res. Soc. Symp. Proc.* **465**:1051-1058.

Delage, F., and J. L. Dussossoy. 1991. "R7T7 Glass Initial Dissolution Rate Measurements Using a High-Temperature Soxhlet Device." *Mat. Res. Soc. Symp. Proc.* **212**:41-47.

DOE 1982 (see U.S. Department of Energy 1982)

DOE 1997 (see U.S. Department of Energy 1997)

Doremus, R. H. 1975. "Interdiffusion of Hydrogen and Alkali Ions in a Glass Surface." *J. Noncrystalline Solids* **19**(2):137-44.

Doremus, R. H. 1977. "Diffusion in Glasses and Melts." *J. Noncrystalline Solids* **25**:261-292.

Dove, P. M., and D. A. Crerar. 1990. "Kinetics of Quartz Dissolution in Electrolyte Solutions Using a Hydrothermal Mixed Flow Reactor." *Geochim. Cosmochim. Acta* **54**:955-969.

Eagleson, P. S. 1978. "Climate, Soil and Vegetation, A Simplified Model of Soil Moisture Movement in the Liquid Phase." *Water Resour. Res.* **14**(5):722-730.

Ebert, W. L., A. J. Bakel, and N. R. Brown. 1996. "Measurement of the Glass Dissolution Rate in the Presence of Alteration Phases." *Proceedings International Topical Meeting on Nuclear and Hazardous Waste Management*, Spectrum '96, Seattle, Washington, pp. 569-575.

Ebert, W. L., and J. K. Bates. 1993. "A Comparison of Glass Reaction at High and Low Glass Surface/Solution Volume." *Nuc. Tech.* **104**:372-384.

Ecology. 1996. Washington State Department of Ecology, United States Environmental Protection Agency, United States Department of Energy. *Hanford Facility Agreement and Consent Order*, Sixth Amendment, February 1996.

Ewing, R. C., and M. J. Jercinovic. 1987. "Natural Analogues: Their Applications to the Prediction of the Long-Term Behavior of Nuclear Waste Forms." *Mat. Res. Symp. Proc.* **84**:67-83.

Fayer 1999, M. J. Fayer, *Recharge Data Package for the Immobilized Low-Activity Waste 2001 Performance Assessment*, PNNL-13033, Pacific Northwest National Laboratory, Richland, Washington, December 1999.

Friedman, I., and W. Long. 1976. "Hydration Rate of Obsidian." *Science* **191**:347-352.

Gee, G. W., and T. L. Jones. 1985. *Lysimeters at the Hanford Site: Present and Future Needs*. PNL-5578, Pacific Northwest National Laboratory, Richland, Washington.

Gin, S. 1996. "Control of R7T7 Nuclear Glass Alteration Kinetics Under Saturation Conditions." *Mat. Res. Soc. Symp. Proc*. **412**:189-196.

Goldsmith, J. R. 1953. "A 'Simplexity Principle' and Its Relation to 'Ease' of Crystallization." *J. Geol.* **61**:439-451.

Grambow, B. E. 1985. "A General Rate Equation for Nuclear Waste Glass Corrosion." *Mat. Res. Soc. Symp. Proc.* **44**:15-27.

Grambow, B., M. J. Jercinovic, R. C. Ewing, and C. D. Byers. 1986. "Weathered Basalt Glass: A Natural Analogue for the Effects of Reaction Progress on Nuclear Waste Glass Alteration." *Mat. Res. Soc. Symp. Proc.* **50**:263-272.

Harder, H. 1978. "Synthesis of Iron Layer Silicate Minerals under Natural Conditions." *Clays and Clay Minerals* **26**(1):65-72.

Hespe, E. D. 1971. "Leach Testing of Immobilized Radioactive Waste Solids: A Proposal for a Standard Method." In *Atomic Energy Review* **9**(1):195-207, International Atomic Energy Agency, Vienna.

Knauss, K. G., and T. J. Wolery. 1986. "Dependence of Albite Dissolution Kinetics on pH and Time at 25°C and 70°C." *Geochim. Cosmochim. Acta* **50**:2481-2497.

Knauss, K. G., W. L. Bourcier, K. D. McKeegan, C. I. Merzbacher, S. N. Nguyen, F. J. Ryerson, D. K. Smith, H. C. Weed, L. Newton. 1990. "Dissolution Kinetics of a Simple Analogue Nuclear Waste Glass as a Function of pH, Time and Temperature." *Mat. Res. Soc. Symp. Proc.* **176**:371-381.

Lanford, W. A., K. Davis, P. Lamarche, T. Laursen, R. Groleau, and R. H. Doremus. "Hydration of Soda-Lime Glass." 1979. *J. Noncrystalline Solids* **33**(2):249-266.

Last, G. V., R. J. Serne, and V. L. LeGore. 1995. *Field Lysimeter Studies for Performance Evaluation of Grouted Hanford Defense Wastes*. PNL-10166, Pacific Northwest National Laboratory, Richland, Washington.

Luo, J. S., W. L. Ebert, J. J. Mazer, and J. K. Bates. 1997. "Simulation of Natural Corrosion by Vapor Hydration Test: Seven-Year Results." *Mat. Res. Soc. Symp. Proc.* **465**:157-163.

Lutze, W., and G. G. Malow. 1985. "Alteration of Basalt Glasses: Implications for Modeling the Long-Term Stability of Nuclear Waste Glasses." *Nature* **314**(21):252-255.

Mann 1998a, F. M. Mann, R. J. Puigh II, P. D. Rittmann, N. W. Kline, J. A. Voogd, Y. Chen, C. R. Eiholzer, C. T. Kincaid, B. P. McGrail, A.H. Lu, G.F. Williamson, N. R. Brown, and P. E. LaMont, *Hanford Immobilized Low-Activity Tank Waste Performance Assessment*, DOE/RL-97-69, Rev. 0, U.S. Department of Energy, Richland Operations Office, Richland, Washington, March 1998.

Materials Characterization Center. 1984. *MCC-3 Agitated Powder Leach Test*. PNL-3990, Pacific Northwest Laboratory, Richland, Washington.

Mattigod, S. V. and B. P. McGrail. 1998. "Estimating the Standard Free Energy of Formation of Zeolites Using the Polymer Model." *Zeolites* (in press).

Mazer, J. J., J. K. Bates, C. M. Stevenson, and C. R. Bradley. 1992. "Obsidians and Tektites: Natural Analogues for Water Diffusion in Nuclear Waste Glasses." *Mat. Res. Soc. Symp. Proc*. **257**:513-520.

McGrail, B. P. 1986. "Waste Package Component Interactions with Savannah River Defense Waste Glass in a Low-Magnesium Salt Brine." *Nuc. Tech*. **75**(2):168-186.

McGrail, B. P., and K. M Olson. 1992. *Evaluating Long-term Performance of In-situ Vitrified Waste Forms: Methodology and Results*. PNL-8358, Pacific Northwest Laboratory, Richland, Washington.

McGrail, B. P., and L. A. Mahoney. 1995. *Selection of a Computer Code for Hanford Low-Level Waste Engineered-System Performance Assessment*. PNL-10830, Pacific Northwest Laboratory, Richland, Washington.

McGrail, B. P., C. W. Lindenmeier, P. F. Martin, and G. W. Gee. 1997a. "The Pressurized Unsaturated Flow (PUF) Test: A New Method for Engineered-Barrier Materials Evaluation." In *Transactions of the American Ceramic Society Vol. 72*, eds. V. Jain and D. K. Peeler, Columbus, Ohio.

McGrail, B. P., P. F. Martin, and C. W. Lindenmeier. 1997b. "Accelerated Testing of Waste Forms Using a Novel Pressurized Unsaturated Flow (PUF) Method." *Mat. Res. Soc. Symp. Proc.* **465**:253-260.

McGrail, B. P., W. L. Ebert, A. J. Bakel, and D. K. Peeler. 1997c. "Measurement of Kinetic Rate Law Parameters on a Na-Ca-Al Borosilicate Glass for Low-Activity Waste." *J. Nuc. Mat.* **249**:175-189.

McVay, G. L., and C. Q. Buckwalter. 1983. "Effect of Iron on Waste Glass Leaching." *J. Am. Ceram. Soc*. **66**(3):170-174.

Myers, D. R., and D. A. Duranceau. 1994. *Prototype Hanford Surface Barrier: Design Bases Document*. BHI-007, Bechtel Hanford Company, Richland, Washington.

Ostwald, W. Z. 1897. "Studien über die Bildung und Umwaldung fester Korper. 1. Abhandlung: Ubersattigung and Uberkaltung." *Zeitschr. Physik Chemie* **22**:289-330.

Oversby, V. L., and D. L. Phinney. 1992. "The Development of Surface Alteration Layers on SRL-165 Nuclear Waste Glass." *J. Nuc. Mat.* 190:247-268.

Petit, J. C. 1992. "Reasoning by Analogy: Rational Foundation of Natural Analogue Studies." *Appl. Geochem., Suppl. Issue* **1**:9-11.

Rana, M. A., and R. W. Douglas. 1961a. "The Reaction Between Glass and Water. Part 1. Experimental Methods and Observations." *Phys. Chem. Glasses* **2**(6):179-195.

Rana, M. A., and R. W. Douglas. 1961b. "The Reaction Between Glass and Water. Part 2. Discussion of the Results." *Phys. Chem. Glasses* **2**(6):196-204.

Rockhold, M. L., M. J. Fayer, C. T. Kincaid, and G. W. Gee. 1995. *Estimation of Natural Ground Water Recharge for the Performance Assessment of a Low-Level Waste Disposal Facility at the Hanford Site.* PNL-10508, Pacific Northwest National Laboratory, Richland, Washington.

Salvucci, G. D. 1993. "An Approximate Solution for Steady Vertical Flux of Moisture Through an Unsaturated Homogeneous Soil." *Water Resour. Res.* **29**(11):3749-3753.

Shade, J. W., and D. M. Strachan. 1986. "Effect of High Surface Area to Solution Volume Ratios on Waste Glass Leaching." *Am. Ceram. Soc. Bull*. **65**(12):1568-1573.

Stout, R. B., and H. Leider. 1996. *Waste Form Characteristics Report, Version 1.2*. UCRL-ID-108314, Rev. 1.2, Lawrence Livermore National Laboratory, Livermore, California.

Strachan, D. M., B. P. McGrail, M. J. Apted, D. W. Engel, and P. W. Eslinger. 1990. *Preliminary Assessment of the Controlled Release of Radionuclides from Waste Packages Containing Borosilicate Waste Glass*. PNL-7591, Pacific Northwest Laboratory, Richland, Washington.

Strachan, D. M., W. L. Bourcier, and B. P. McGrail. 1994. "Toward a Consistent Model for Glass Dissolution." *Radioactive Waste Management and Environmental Restoration* **19**:129-145.

Strachan, D.M. 1983. "Results from Long-Term Use of the MCC-1 Static Leach Test Method." *Nucl. Chem. Waste Mgmt*. **4**:177-188.

Strachan, D.M., B.O. Barnes, and R.P. Turcotte. 1981. "Standard Leach Tests for Nuclear Waste Materials." *Mat. Res. Soc. Symp. Proc.* **3**:347-354.

Tietje, O., and M. Tapkenhinrichs. 1993. "Evaluation of Pedo-Transfer Functions." *Soil Sci. Soc. Am. J.* **57**:1088-1095.

Tovena, I., T. Advocat, D. Ghaleb, E. Vernaz, and F. Larche. 1994. "Thermodynamic and Structural Models Compared with the Initial Dissolution Rates of "SON" Glass Samples." *Mat. Res. Soc. Symp. Proc.* **333**:595-602.

U.S. Department of Energy (DOE). 1982. *Nuclear Waste Materials Handbook: Test Methods*. Technical Information Center report, DOE/TIC-11400.

U.S. Department of Energy (DOE). 1997. *Record of Decision for the Tank Waste Remediation System, Hanford Site, Richland, Washington*. Federal Register, Volume 62, page 8693, February 26, 1997.

van Genuchten. 1980. "A Closed-Form Equation for Predicting the Hydraulic Conductivity of Unsaturated Soils." *Soil Sci. Soc. Am. J.* **44**:892-898.

Van Iseghem, P. and B. Grambow. 1988. "The Long-Term Corrosion and Modelling of Two Simulated Belgian Reference High-Level Waste Glasses." *Mat. Res. Soc. Symp. Proc.* **112**:631-639.

White, M. D., and M. Oostrom. 1996. *STOMP: Subsurface Transport Over Multiple Phases, Theory Guide*. PNNL-11217, Pacific Northwest National Laboratory, Richland, Washington.

Wierenga, P. J., M. H. Young, G. W. Gee, R. G. Hills, C. T. Kincaid, T. J. Nicholson, and R. E. Cady. 1993. *Soil Characterization Methods for Unsaturated Low-Level Waste Sites*. PNL-8480, Pacific Northwest National Laboratory, Richland, Washington.

Wolery, T. J., and S. A. Daveler. 1992. *EQ6, A Computer Program for Reaction Path Modeling of Aqueous Geochemical Systems: Theoretical Manual, User's Guide and Related Documentation*. UCRL-MA-110662 PT IV, Lawrence Livermore Laboratory, Livermore, California.

Woodland, A. B., J. K. Bates, and T. J. Gerding. 1991. *Parametric Effects on Glass Reaction in the Unsaturated Test Method*. ANL-91-36, Argonne National Laboratory, Argonne, Illinois.

Appendix F

Quality Assurance

F. QUALITY ASSURANCE

F.1 OVERVIEW

This section describes the quality assurance activities associated with the performance assessment activity. The quality assurance activities involve reviewing the Performance Assessment by recognized subject matter experts and knowledgeable stakeholders. Three separate areas are covered: experimental data collection, computer code use, and analyses. The following sections are arranged according to which organization performs the activity being discussed.

F.2 CH2M HILL HANFORD GROUP, INC.

The River Protection Project (RPP) Immobilized Waste Program quality assurance activities are covered by the RPP Quality Assurance Program Description (CHG 2000) and associated implementing procedures. This program addresses the requirements of the *Quality Assurance Program Description* of the Tank Farms Contractor, which is based on Title 10 *Code of Federal Regulations* (CFR) Part 830.120 and U.S. Department of Energy (DOE) Order 5700.6C (DOE 1991).

CH2M HILL Hanford Group, Inc. (CHG) is responsible for the quality aspects of all work discussed in this performance assessment.

F.3 PACIFIC NORTHWEST NATIONAL LABORATORY

Pacific Northwest National Laboratory personnel conducted their work for the performance assessment according to the appropriate portions of the laboratory's quality assurance (QA) program. This program conforms to 10 CFR 830.120, "Quality Assurance" through implementation of its Subject Based Management System (SBMS). The SBMS (http://sbms.pnl.gov) includes a set of administrative procedures that define how the requirements of 10 CFR 830.120 are implemented. The administrative procedures define controls, policies, and established methods for managing and conducting all aspects of work that affect quality.

A key aspect of the QA program involves technical and peer reviews of procedures, test plans, data, calculations, and test results. The reviews range from verifying that calculations or data reduction have been performed correctly to evaluating the test methodology described in a proposed test plan.

Records generated from all activities are indexed and managed according to QA program requirements. Record-holding facilities are used for long-term records retention and storage.

F.4 OTHER CONTRACTORS

Other organizations, such as Argonne National Laboratory and Fluor Federal Services worked on this activity. Their work was performed under either the quality assurance plans of CHG or the Pacific Northwest National Laboratory.

F.5 HANFORD ENVIRONMENTAL DOSE OVERVIEW PANEL

The DOE, Richland Operations Office, established the Hanford Environmental Dose Oversight Panel (HEDOP) (Schreckhise 1993) to perform the following:

- Ensure that appropriate radiological and nonradiological environmental and health dose assessment methods are used at the Hanford Site
- Ensure that all Hanford Site-related environmental and health dose assessments are technically consistent
- Foster communications among Hanford Site contractors regarding environmental and health dose assessments.

All dose calculations used in this performance assessment have been reviewed and approved for publication by a HEDOP reviewer (Rhoads 1999).

F.6 TECHNICAL REVIEWS OF SUPPORTING DOCUMENTS

External technical reviews by outside experts are being held on specialized topics because of the large amount of technical data used in performance assessments. These reviews are done to ensure that the proper methods, techniques, and resources are used in obtaining the data.

Hanford Site experts reviewed each data package. In addition, experts from outside the Hanford Site reviewed the waste form and geotechnical data packages. The list of external reviewers is given in Table F-1.

F.7 REVIEW OF THE PERFORMANCE ASSESSMENT

DOE's Low-Level Waste Disposal Facility Federal Review Group (LFRG) (DOE 1999c) formally reviewed the 1998 ILAW Performance Assessment (Mann 1998a). Based on this review, the DOE issued the Disposal Authorization Statement (DOE 1999d) accepting the ILAW Performance Assessment . This acceptance is contingent on the following actions being accomplished:

- Providing the LFRG with documentation of the near-term glass test results to provide confidence that the glass performance assumed in the performance assessment can actually be achieved

Table F-1. Data Package External Reviewers.

Area	Reviewer	Affiliation
Geology	Dr. Ann Tallman Newell P. Campbell	Independent (formally Smith College and Westinghouse Hanford Company) Independent (formally Professor of Geology, Yakima Valley College).
Recharge	John Robert Nimmo Bridget R. Scanlon	United States Geological Survey, Menlo Park, CA University of Texas at Austin
Near-Field Hydrology	John Robert Nimmo Bridget R. Scanlon	United States Geological Survey, Menlo Park, CA University of Texas at Austin
Far-Field Hydrology	Lynn W. Gelhar	Civil & Environmental Engineering, Massachusetts Institute of Technology
Geochemistry	Dr. Tjalle (Chuck) Vandergraaf Dr. Steve Serkiz Dr. Patrick Brady	Atomic Energy of Canada Limited, Whiteshell Research Laboratory in Pinawa, Manitoba Savannah River Technology Center Department of Geochemistry, Sandia National Laboratory

- Addressing the secondary issues identified by the review team in future revisions to the performance assessment.

Documentation on relevant glass performance has been provided to the LFRG for their review (French 1999 and French 2000a) and the LFRG has determined that the condition has been met (DOE 2000). The secondary issues identified by the LFRG are addressed in this version of the ILAW Performance Assessment (see Appendix A).

The 1998 ILAW Performance Assessment also was reviewed by the Washington State Department of Ecology (Appendix F of Mann 1998a) and by staff of the U.S. Nuclear Regulatory Commission.

This document was reviewed by the immobilized low-activity waste performance assessment team, as well as by program management of the Immobilized Waste Storage and Disposal Program (K.C. Burgard) and of DOE's Office of River Protection (N.R. Brown, P.E. LaMont, and others). In addition, the lead authors of other Hanford Site performance assessments (C.T. Kincaid [Grout Performance Assessment and Hanford Site Composite Analysis] and M.I. Wood [200 East Area Solid Waste Performance Assessment and 200 West Area Solid Waste Performance Assessment]) performed an overall technical review of this report.

Comments on the draft version of this report by the review team of the Low-Level Waste Disposal Facility Federal Review Group have been incorporated.

Distribution List

U.S. Department of Energy, Office of River Protection (26h)
H.L. Boston
Carol A. Babel (25h) H6-60
Philip E. LaMont (h) H6-60

U.S. Department of Energy, Richland Operations (1h)
R.D. Hildebrand (h) A5-13
G.H. Sanders

Bechtel Hanford Incorporated (2h)
B.H. Ford (h) H0-21
M.J. Graham (h) H0-21

CH2M Hill Hanford Group (9h)
D.A. Burbank (h) L6-75
K.C. Burgard (h) L6-75
J.O. Honeyman
A.J. Knepp
F.M. Mann (7) H0-22
G.L. Parsons
R.W. Root
P.S. Schaus
J.A. Voogd

Fluor Federal Services (3h)
S. H. Finfrock
R. Khaleel
R.J. Puigh (3) B4-43
P.D. Rittmann

Fluor Hanford, Inc. (1h)
M.I. Wood (h) H8-44

Lockheed Martin Services, Inc. (4h)
Central Files (h)
Document Clearance (h)
DOE Reading Room (h)
Hanford Technical Library (h)

Oregon State Department of Energy (1h)
Nuclear Safety Division
625 Marion St. NE
Salem Oregon 97310

Dirk Dunning (h)

Pacific Northwest National Laboratory (7h)
D. H. Bacon (h) K9-33
M.P. Bergeron (h) K9-33
M.J. Fayer (h) K9-33
C.T. Kincaid (h) K9-33
B.P. McGrail (h) K6-81
S. Reidel (h) K6-81
R.J. Serne (h) K6-81

54 hard copies